Hiromi Hirata · Atsuo Iida *Editors*

Zebrafish, Medaka, and Other Small Fishes

New Model Animals in Biology, Medicine, and Beyond

Springer

Zebrafish, Medaka, and Other Small Fishes

Hiromi Hirata • Atsuo Iida
Editors

Zebrafish, Medaka, and Other Small Fishes

New Model Animals in Biology, Medicine, and Beyond

Springer

Editors
Hiromi Hirata
College of Science and Engineering
Aoyama Gakuin University
Sagamihara, Japan

Atsuo Iida
Institute for Frontier Life
and Medical Sciences
Kyoto University
Kyoto, Japan

ISBN 978-981-13-1878-8 ISBN 978-981-13-1879-5 (eBook)
https://doi.org/10.1007/978-981-13-1879-5

Library of Congress Control Number: 2018956132

This Springer imprint is published by the registered company Springer Nature Singapore Pte Ltd.
The registered company address is: 152 Beach Road, #21-01/04 Gateway East, Singapore 189721, Singapore

Foreword

This book, *Zebrafish, Medaka, and Other Small Fishes: New Model Animals in Biology, Medicine, and Beyond*, offers readers advanced research topics in small fish biology. These aquatic animals have come to the forefront of biomedical research as simple genetic models for biological studies that retain molecular, cellular, and physiological similarities with humans. Consequently, the majority of disease-causing genes have orthologs in fish, and genetic models can be used advantageously for drug screening. Small fish thus offer great hopes for biology and medicine.

The first two parts of the book describe common elements that are essential for the development, homeostasis, and reproduction of zebrafish and medaka. The developmental topics covered are molecular signaling in development and cancer (Ishitani and Zou), the ontology of blood vessels (Phng), hematopoietic stem cells (Kobayashi), and the development of sensory neurons (Ogino and Hirata). The second part deals with homeostasis related to gravity (Chatani and Kudo), reproduction (Kanda), and secondary sex characteristics (Ogino).

The third part focuses on the development of human disease models in zebrafish and medaka and their use in clinical studies, including angiogenesis (Katraki-Pavlou and Beis), myopathies (Baxter and Bryson-Richardson), dystrophies (Mitsuhashi), scoliosis (Guo, Ikegawa, and Shukunami), and Parkinson's disease (Uemura and Takahashi).

The last part describes challenging studies that utilize several fish species possessing special, unique traits, such as blind cavefish (Rohner), viviparous fish (Iida), electric fish (Kohashi), and catfish, which have an excellent sense of taste (Ikenaga and Kiyohara).

Collectively, these reviews encompass the broad range of studies currently under way in a variety of fish species, from cavefish to fish in space. The thought-provoking chapters are of general interest to a broad readership, as you will likely find a topic of direct pertinence to your own interests in biology, biotechnology, or drug discovery and at the same time discover new and fascinating subjects that can be uniquely studied in fish. This book thus nicely illustrates the usefulness and pertinence of modern fish biology. Quoting the concluding sentence from Neil Shubin's book

Your Inner Fish (Pantheon Press, 2008): “I can imagine few things more beautiful or intellectually profound than finding the basis for our humanity, and remedies for many of the ills we suffer, nestled inside some part of the most humble creatures that have ever lived on our planet.” We hope this book will help convey our enthusiasm for fish models pertinent to drier vertebrates as well.

Department of Neurosciences
University of Montréal,
Montréal, Canada

Pierre Drapeau

Preface

Small fish such as zebrafish and medaka are now among the major model organisms employed in the life sciences. As model organisms, small fish owe their use in the life sciences to the remarkable extent of species variation that commonly presents researchers with complementary characteristics for studies ranging from development and regeneration to complex behaviors such as learning and memory.

Zebrafish (*Danio rerio*) was first introduced as a vertebrate model organism in the 1970s by Prof. George Streisinger at the University of Oregon. Originating from India, the zebrafish was chosen as a result of its ease of laboratory maintenance and diurnal driven ability to produce hundreds of embryos each day that displayed a rapid rate of external development. These attributes contributed to the use of zebrafish in two large-scale mutagenesis projects in Germany and the United States in the 1990s. These and other mutagenesis projects, coupled with the development of transgenic techniques and fluorescent proteins for live-cell imaging, solidified the use of zebrafish in the life sciences and thereby caused an expansion of the zebrafish research community.

By comparison, medaka (*Oryzias latipes*) has been a popular pet fish in Japan since the mid-1800s. In the late 1900s, the isolation of two genetically distinct lines and several temperature-sensitive mutants promoted the use of medaka in the life sciences. In addition, several genetically divergent populations of medaka have been identified. While the method of sex determination has remained enigmatic in zebrafish, a sex chromosome and a sex-determination gene have been identified in medaka. These and other genetic attributes have rendered medaka the second most popular fish model in the life sciences.

Over the last decade, development of cutting-edge technologies such as next-generation sequencing, CRISPR/Cas9-mediated genome editing, high-resolution imaging, and a cellular-level connectome have further fostered the use of zebrafish and medaka in the life sciences. As many of these techniques are translatable to other small fishes, we expect that additional fish models will be developed enabling scientists to address research topics that are not readily assessable in zebrafish and medaka.

Zebrafish, Medaka, and Other Small Fishes: New Model Animals in Biology, Medicine, and Beyond introduces readers to research topics in small fish biology currently being investigated by a group of young and ambitious scientists. This special book includes not only basic biology to investigate common mechanisms in animals, but also clinical models as translational research for human diseases using zebrafish and medaka. In addition, the other chapters deal with eccentric small fish with highly unique traits seemingly uncommon in other species. We suggest these are forthcoming vertebrate models to provide novel insights and significance for basic and applied research.

It will be a great pleasure to the authors if this book aids readers in their understanding of small fish and the ongoing studies that utilize them, with the hope that it encourages participation in the large and fantastic world of small fish.

Kyoto, Japan — Atsuo Iida
Sagamihara, Japan — Hiromi Hirata

Contents

Part I
Development and Cell Biology

Chapter 1
Zebrafish Wnt/β-Catenin Signaling Reporters Facilitate Understanding of In Vivo Dynamic Regulation and Discovery of Therapeutic Agents

Tohru Ishitani and Juqi Zou

Abstract Wnt/β-catenin signaling plays multiple roles in embryogenesis, organogenesis, and adult tissue homeostasis, and its dysregulation is linked to numerous human diseases such as cancer. Although strict spatiotemporal regulation must support the multi-functionality of Wnt/β-catenin signaling, detailed mechanisms remain unclear. In addition, Wnt/β-catenin signaling is a potential drug target candidate and several inhibitors have been identified by in vitro screening, but none have yet been incorporated into clinical practice. Recent studies using reporter zebrafish lines have gradually improved our understanding of in vivo dynamic regulation of Wnt/β-catenin signaling and have facilitated the discovery of new chemicals that can reduce Wnt/β-catenin signaling and cancer cell viability with few side effects. Here, we describe several new mechanisms supporting the spatiotemporal regulation of Wnt/β-catenin signaling and new small molecule inhibitors, discovered using zebrafish reporters. In addition, we discuss the potential of zebrafish signaling reporters in both developmental biology and pharmaceutical sciences.

Keywords Wnt/β-catenin signaling · reporter · modifier · chemical inhibitor · anti-cancer drug

1.1 Introduction

Wnt/β-catenin signaling is an evolutionarily conserved system that controls cell proliferation, fate specification, differentiation, survival, and death during embryogenesis, organogenesis, and adult tissue homeostasis (Clevers 2006; Clevers and Nusse 2012; Logan and Nusse 2004). Dysregulation of this signaling system is

T. Ishitani (✉) · J. Zou
Lab of Integrated Signaling Systems, Department of Molecular Medicine, Institute for Molecular & Cellular Regulation, Gunma University, Maebashi, Gunma, Japan
e-mail: ishitani@gunma-u.ac.jp

H. Hirata, A. Iida (eds.), *Zebrafish, Medaka, and Other Small Fishes*,
https://doi.org/10.1007/978-981-13-1879-5_1

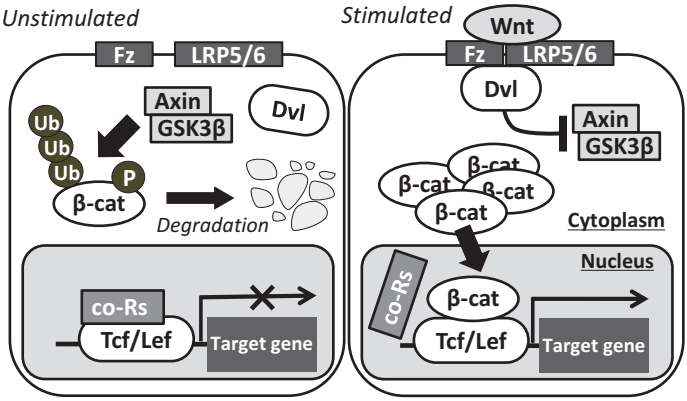

Fig. 1.1 The Wnt/β-catenin signaling pathway. In unstimulated conditions, levels of cytoplasmic β-catenin are kept low by a destruction complex including GSK3β and Axin. Tcf/Lef represses the expression of target genes by interacting with transcriptional co-repressors (co-Rs). Binding of Wnt to the receptor Frizzled (Fz) and its co-receptor LRP5/6 activates Dvl, and then Dvl promotes dissociation of the β-catenin destruction complex and consequently stabilizes cytoplasmic β-catenin. As a result, β-catenin accumulates and enters the nucleus, where it forms complexes with Tcf/Lef that activate gene expression. *Ub* ubiquitin, *P* phosphorylation, *β-cat* β-catenin

linked to various human diseases, including cancer, obesity, diabetes, osteoporosis, schizophrenia, and autism (Clevers 2006; Clevers and Nusse 2012; De Ferrari and Moon 2006; Logan and Nusse 2004). This system transduces its signal by controlling the levels of cytoplasmic β-catenin protein (Fig. 1.1). In unstimulated cells, cytoplasmic β-catenin are maintained at low levels by a destruction complex that includes glycogen synthase kinase 3β (GSK3β) and Axin. GSK3β phosphorylates β-catenin at the N-terminal region, thereby promoting its ubiquitination by the E3 Ub ligase β-TrCP and the subsequent proteasomal degradation (Clevers 2006; Clevers and Nusse 2012; Logan and Nusse 2004). The Tcf/Lef family of transcription factors represses the expression of Wnt/β-catenin target genes by interacting with transcriptional co-repressors, such as histone deacetylase 1 (HDAC1) and Groucho (Arce et al. 2009). Wnt/β-catenin signaling is activated when the secreted glycoprotein Wnt binds to the cell surface receptor Frizzled (Fz) and its co-receptor LRP5/6. This Wnt-bound receptor complex then recruits the cytoplasmic protein Dishevelled (Dvl), which in turn promotes the dissociation of the β-catenin degradation complex. This series of events results in the stabilization of cytoplasmic β-catenin. The increased β-catenin concentration drives its migration into the nucleus where it forms complexes with Tcf/Lef, which activates gene expression. This core Wnt/β-catenin signaling process has been revealed through extensive investigation using invertebrate models, mammalian cell culture, and *Xenopus* early embryos over the past three to four decades. In addition, knockout mouse analyses have contributed to our understanding of the role Wnt/β-catenin signaling plays in animal development and disease. However, the spatiotemporal dynamics of Wnt/β--catenin signaling and its regulatory mechanisms in living animals remains unclear though recent studies using Wnt/β-catenin signaling reporter zebrafish lines have

gradually improved our understanding. Here, we introduce Wnt/β-catenin signaling reporter zebrafish lines and review several studies in which new mechanisms supporting the spatiotemporal regulation of Wnt/β-catenin signaling were revealed using these reporter lines. Furthermore, we also demonstrate how reporter lines may be useful in the exploration of new anti-cancer drugs.

1.2 Wnt/β-Catenin Signaling Reporter Zebrafish Lines and Their Properties

Zebrafish are one of the most suitable animals for live imaging because of their optical clarity and rapid development. A transgenic zebrafish line carrying the Wnt/β--catenin signaling reporter top:GFP (original name: TOPdGFP)—which contains four copies of consensus Tcf/Lef binding sites, a *c-fos* minimal promoter, and a d2EGFP reporter gene (Fig. 1.2; Dorsky et al. 2002)—has proved to be a useful tool for understanding the regulation of in vivo Wnt/β-catenin signaling. In fact, new domains in which Wnt/β-catenin signaling is activated and new mechanisms that regulate Wnt/β-catenin signaling have been discovered using this reporter (some of which are described in Sect. 1.3). However, given that fine reporter activity has only been observed in some Wnt/β-catenin signaling-active sites in living top:GFP-transgenic fish using a fluorescence stereomicroscope (Fig. 1.2), attempts have been made to improve Wnt/β-catenin signaling reporters. We generated OTM:d2EGFP (original name: Tcf/Lef-miniP:dGFP), which comprises a destabilized green fluorescent protein (d2EGFP) driven by a promoter containing six copies of Tcf/Lef binding sites and a minimal promoter (miniP) derived from Promega pGL4 (Fig. 1.2; Shimizu et al. 2012). Moro et al. (2012) also generated two new reporters, 7xTCF-Xla.Siam:GFP and 7xTCF-Xla.Siam:nlsmCherry, which express GFP or monomeric Cherry proteins with nuclear localization signals (nlsmCherry) under the control of seven multimerized TCF responsive elements upstream of the minimal promoter of the *Xenopus* direct β-catenin target gene, *siamois* (Fig. 1.2). Results showed that both reporters were activated in almost all cells in which Wnt/β-catenin signaling is known to be active in zebrafish, and they also revealed further new developmental roles of Wnt/β-catenin signaling, including in the formation of the brain-blood vessel network and gill filaments (Moro et al. 2012; Shimizu et al. 2012). These reporters are useful but should be used separately. 7xTCF-Xla.Siam:GFP and 7xTCF-Xla.Siam:nlsmCherry are suitable for searching for new Wnt/β-catenin signaling-active cells/areas because they express fluorescence strongly; the half-lives of GFP and mCherry are very long (more than 24 h), so fluorescence of 7xTCF-Xla.Siam:GFP and 7xTCF-Xla.Siam:nlsmCherry can be detected in cells where Wnt/β-catenin signaling was activated in the past. On the other hand, OTM:d2EGFP is suitable for the detection of dynamic changes during Wnt/β-catenin signaling in vivo as the half-life of the d2EGFP protein, the fluorescent reporter in OTM:d2EGFP, is relatively short (approximately 2 h). In addition, to detect “highly” dynamic signaling changes, we recently generated “the third

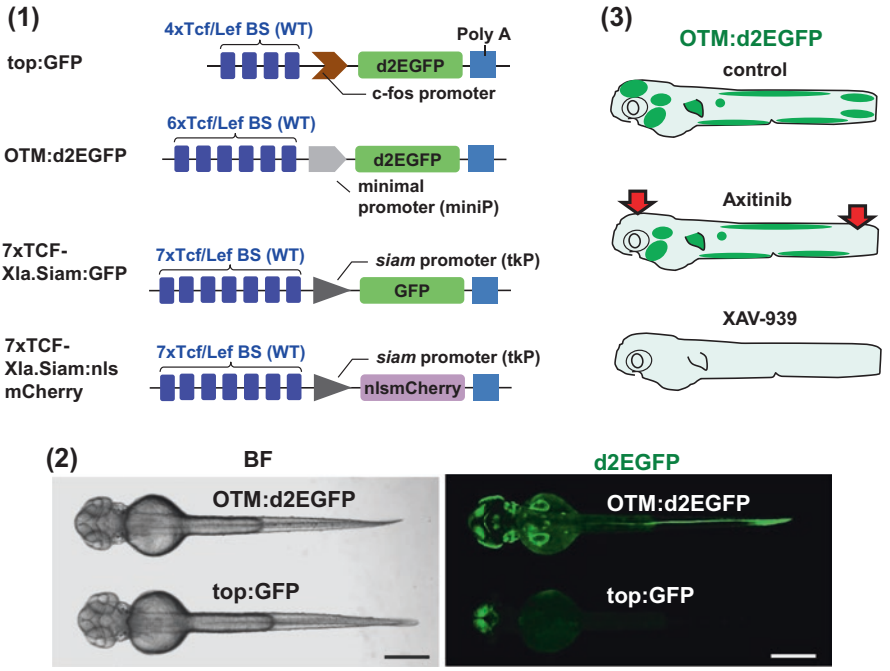

Fig. 1.2 Zebrafish Wnt/β-catenin signaling reporters. (1) Schematic diagrams of Wnt/β-catenin signaling-reporter constructs. Tcf/Lef BS: consensus sequence of the Tcf/Lef-binding site; PolyA: polyadenylation sequence. (2) Comparison of reporter activity in OTM:d2EGFP- and top:GFP transgenic zebrafish embryos. Dorsal views of transgenic embryos, with the anterior side to the left. Cells expressing d2EGFP were visualized by fluorescence microscopy (right panel). Bright-field (BF) images are shown in the left panel. Scale bar, 200 μm. (3) Effects of chemical inhibitors on OTM:d2EGFP reporters. Reporter activity was shown as green. Axitinib reduces OTM:d2EGFP expression in the midbrain and tail (red arrows), while XAV-939 completely blocks it in whole embryos

generation of *in vivo* Wnt/β-catenin signaling reporter"—OTM:Eluc-CP—which expresses destabilized emerald luciferase in response to Wnt/β-catenin activation. Using this, we can detect the dynamic change of Wnt/β-catenin signaling activity during brain anterior-posterior patterning (Akieda et al. in preparation). OTM:Eluc-CP will facilitate rigorous analysis of the spatiotemporal dynamics of Wnt/β-catenin signaling.

1.3 Studies Using the Reporter Zebrafish Revealed New Regulatory Mechanisms of Wnt/β-Catenin Signaling

Mechanisms supporting the spatiotemporal dynamics of Wnt/β-catenin signaling in living animals remain unclear, but recent studies with reporter zebrafish, described within this section, have gradually improved our understanding.

1.3.1 Reck: A New Wnt Regulator in Plasma Membrane

The G protein-coupled receptor Gpr124 promotes Wnt7-mediated β-catenin signaling and controls central nervous system (CNS) angiogenesis (Posokhova et al. 2015; Zhou and Nathans 2014). Vanhollebeke et al. (2015) discovered that Reck (reversion-inducing-cysteine-rich protein with Kazal motifs), a GPI-anchored extracellular protein, cooperates with Gpr124 to activate Wnt/β-catenin signaling in zebrafish CNS angiogenesis. Knockdown of Gpr124 and Reck using morpholino antisense oligonucleotides (MO) reduced 7xTCF-Xla.Siam: GFP reporter activity in zebrafish CNS endothelial cells and induced identical CNS-specific vascular defects. Reck interacted with Gpr124 in the plasma membrane and synergistically promoted Wnt7-mediated β-catenin signaling. In addition, live imaging analyses of genetically mosaic zebrafish revealed that Gpr124- and Reck-dependent Wnt/β--catenin signaling is specifically required for endothelial tip cells during sprouting angiogenesis in the CNS. Interestingly, knockdown of Reck and Gpr124 specifically affected CNS angiogenesis but did not produce gross morphological phenotypes, indicating that Gpr124 and Reck are Wnt/β-catenin signaling modulators specifically required for CNS angiogenesis.

1.3.2 Hipk2 and Nephrocystin-4: New Dvl Modulators

Homeodomain-interacting protein kinase 2 (Hipk2) was identified as a positive regulator of Wnt/β-catenin signaling using biochemistry and *Drosophila* genetics (Lee et al. 2009). However, the mechanism by which Hipk2 promotes Wnt/β-catenin signaling and its physiological significance was unclear but is explained by our recent study using OTM:d2EGFP. MO-mediated knockdown of Hipk2 reduced OTM:d2EGFP activity and the protein levels of Dvl, which is a core regulator of Wnt/β-catenin signaling. Consequently, Wnt/β-catenin signaling-mediated brain anterior-posterior (AP) patterning and tail development in zebrafish embryos were disturbed. Interestingly, these defects were rescued by injection of Hipk2 wild-type or kinase-negative mutant mRNA (Shimizu et al. 2014), suggesting that Hipk2 promotes Dvl protein levels and Wnt/β-catenin signaling in a kinase activity-independent manner, and this regulation contributes to brain and tail development. Biochemical analyses revealed that Hipk2 promotes the binding of protein phosphatase 1c (PP1c) to Dvl and thus the consequent dephosphorylation of Dvl, which prevents Itch ubiquitin E3 ligase-mediated Dvl ubiquitination and degradation to stabilize Dvl (Fig. 1.3; Shimizu et al. 2014). Consistent with this, knockdown of PP1c also reduced OTM:d2EGFP activity; Hipk2 MO-induced reduction of OTM:d2EGFP activity was rescued by injection of the Dvl 3A mutant, in which PP1c-dephosphorylation sites were substituted to alanine (Shimizu et al. 2014). Thus, a new post-translational modification of Dvl and its roles in Wnt signal transduction and embryogenesis were revealed by the reporter zebrafish studies.

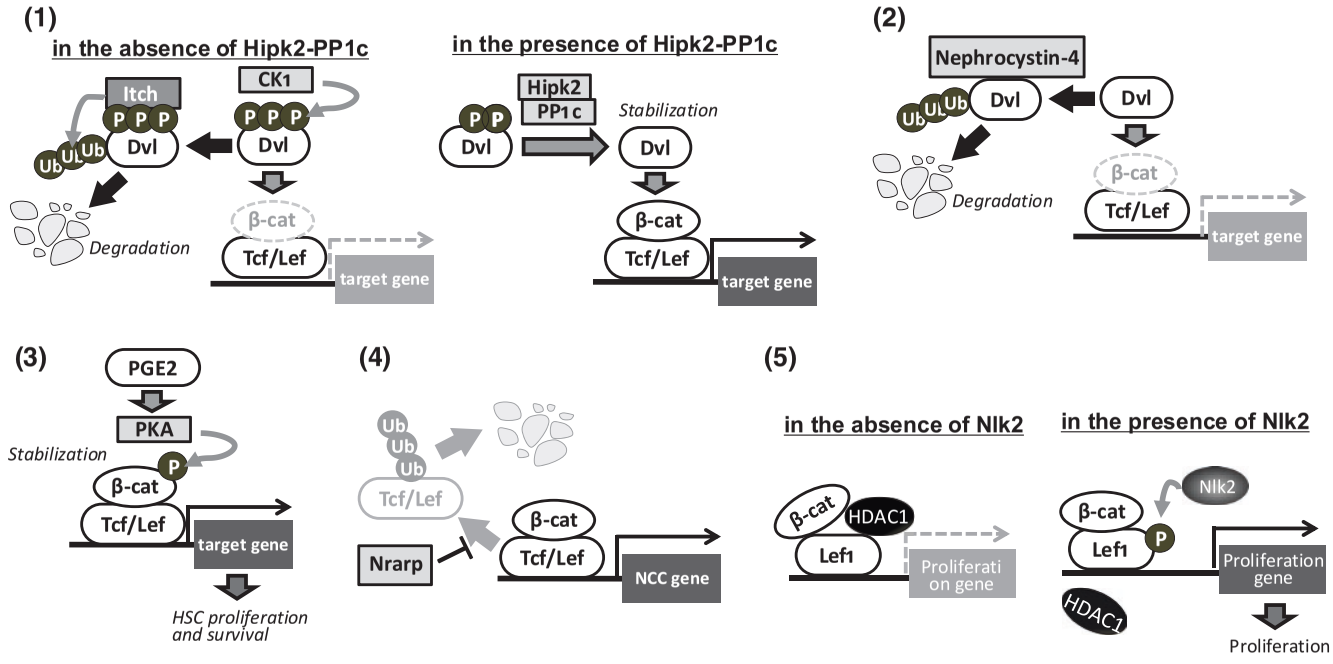

Fig. 1.3 New regulatory mechanisms of Wnt/β-catenin signaling revealed using the reporter zebrafish. (1) In the absence of Hipk2-PP1c activity, Dvl is phosphorylated by CK1 and consequently ubiquitinated by Itch and then degraded via proteasome. As a result, the Wnt/β-catenin target gene is inactivated. In the presence of Hipk2-PP1c activity, Hipk2 promotes the binding of PP1c to Dvl and PP1c-mediated Dvl dephosphorylation and consequently stabilizes Dvl. Stabilized Dvl efficiently transduces Wnt signaling and induces target gene expression. (2) Nephrocystin-4 binds to and promotes the ubiquitination and degradation of Dvl. (3) PGE2 promotes PKA-mediated phosphorylation and stabilization of β-catenin and thereby stimulates HSC proliferation and survival. (4) Nrarp blocks the ubiquitination of Lef1 and consequently promotes Lef1 stabilization and Lef1-mediated Wnt/β-catenin signaling. (5) In the absence of Nlk2 activity, HDAC1 binds to Lef1 and inhibits Lef1-mediated transcription. When Nlk2 is activated, Nlk2 phosphorylates Lef1 thereby preventing HDAC1-mediated Lef1 inhibition and allowing NPCs to proliferate

The *NPHP4* gene encoding nephrocystin-4 is associated with nephronophthisis, which is a hereditary nephropathy characterized by interstitial fibrosis and cyst formation. Burckle et al. (2011) examined the molecular and cellular functions of Nephrocystin-4 using zebrafish as a model. Injection of Nephrocystin-4 MO enhanced top:GFP activity in the pronephric duct and produced pronephric cysts; Nephrocystin-4 MO-mediated pronephric cyst formation was enhanced by co-injection with the MO against prickle2 gene encoding a negative regulator of Dvl. In the mammalian kidney cell line (MDCK), exogenous Nephrocystin bound to Dvl and reduced its protein level and Wnt/β-catenin reporter activity (Burckle et al. 2011). Based on these findings, it was concluded that Nephrocystin-4 represses the Wnt-β-catenin pathway via Dvl degradation (Fig. 1.3) and contributes to morphogenesis of zebrafish pronephros.

1.3.3 Simplet and PGE-PKA Axis: New β-Catenin Modulators

Simplet was first isolated as a gene expressed in the developing CNS of medaka fish (Deyts et al. 2005) although molecular function is unclear. Using reporter fish, Kizil et al. (2014) showed that Simplet is required for Wnt/β-catenin signaling as it positively regulates β-catenin nuclear localization; injection of *simplet* MO prevented nuclear accumulation of β-catenin. Activation of top:GFP and 7xTCF-Xla.Siam:nlsmCherry activities and expression of Wnt/β-catenin target genes, *cdx4*, *tbx6*, and *gbx1*, were also prevented in the tail bud stage of zebrafish embryos but not in 85% epiboly stage embryos; loss of Wnt/β-catenin signaling also produced axial defects (Kizil et al. 2014). Simplet localized into the nucleus. Overexpression of Simplet promoted β-catenin nuclear localization but not in nuclear-localization-signal (NLS)-deleted mutant SimpletΔNLS positive cells; overexpression of this mutant blocked β-catenin nuclear localization and transcriptional activity. Biochemical analyses revealed that Simplet proteins interact directly with β-catenin (Kizil et al. 2014). These results suggest that Simplet associates with β-catenin to promote its nuclear localization and transcriptional activity and plays an essential role in zebrafish axial development.

Wnt/β-catenin signaling has been implicated in the regulation of hematopoietic stem cells (HSCs); the bioactive lipid prostaglandin E2 (PGE2) also regulates the induction and engraftment of HSCs (Reya et al. 2003; Trowbridge et al. 2006). Therefore, Goessling et al. (2009) focused on the relationship between PGE2 and HSCs and discovered that PGE2 promotes Wnt/β-catenin signaling in HSC regulation. Treatment of zebrafish embryos with PGE2 enhanced top:GFP activity in HSCs and Wnt/β-catenin signaling-mediated HSC proliferation and survival, while treatment with indomethacin, which suppresses PGE2 production, reduced them. This suggests that PGE2 positively regulates Wnt/β-catenin signaling in HSCs. Furthermore, treatment with the PKA chemical activator forskolin reversed indomethacin-induced HSC reduction, while treatment with the PKA chemical inhibitor H89 blocked PGE2-induced HSC formation, suggesting that PGE2 regu-

lates HSCs via PKA. By carrying out assays using hematopoietic mouse ES cells, Goessling et al. (2009) confirmed that the relationship between PGE2, PKA, and Wnt/β-catenin signaling is also conserved in mammals. In addition, it was found that PGE treatment promoted the phosphorylation of β-catenin at Ser-675, which is mediated by PKA, and stabilizes β-catenin in mouse ES cells; indomethacin reduced this phosphorylation and β-catenin protein levels (Goessling et al. 2009). Thus, PGE2-PKA axis stimulates β-catenin stability and the consequent Wnt/β-catenin signaling activity through β-catenin phosphorylation to promote HSC formation (Fig. 1.3).

1.3.4 Nrarp and NLK: New Tcf/Lef Modifiers

We discovered the essential roles of Lef1 post-translational modification in embryogenesis using top:GFP reporter zebrafish and showed that proper control of Lef1 ubiquitination is involved in the development of neural crest cells (NCCs) (Fig. 1.3; Ishitani et al. 2005). NCCs are pluripotent progenitors induced within the neuroepithelium in vertebrate embryos. They migrate to target destinations throughout the embryo and differentiate into diverse cell types, including sensory neurons, glia, smooth muscle, cranial cartilage, bone cells, endocrine cells, and pigment cells. Wnt/β-catenin signaling is known to regulate induction, migration, and differentiation of NCCs (Yanfeng et al. 2003) and furthermore, Ishitani et al. (2005) found that Nrarp (Notch-regulated ankyrin repeat protein), a small protein containing two ankyrin repeats, promotes Wnt/β-catenin signaling activity in NCCs by blocking Lef1 ubiquitination. Nrarp was expressed in migrating neural crest cells; Nrarp knockdown, using MO, reduced top:GFP reporter activity in migrating NCCs and induced defects in NCC migration and differentiation (Ishitani et al. 2005), which suggests that Nrarp contributes to NCC development through positive regulation of Wnt/β-catenin signaling in migrating NCCs. Biochemical analyses also showed that Nrarp blocks the ubiquitination-proteasome-dependent degradation of Lef1 and consequently stabilizes it, which promotes Wnt/β-catenin signaling in migrating NCCs (Ishitani et al. 2005). This was the first discovery of ubiquitination of Tcf/Lef family proteins.

Lef1 phosphorylation is also essential for midbrain development (Fig. 1.3). Previous reports showed that MAP kinase-related nemo-like kinase (NLK) phosphorylates the Tcf/Lef family of transcription factors and activates Wnt/β-catenin signaling in *Caenorhabditis elegans* (Ishitani et al. 1999; Meneghini et al. 1999) though the physiological role of NLK-mediated Tcf/Lef regulation in vertebrates was not explained. We found that knockdown of zebrafish NLK (Nlk2) reduced top:GFP reporter activity and proliferation of neural progenitor cells in the developing midbrain, without gross morphological defects (Ota et al. 2012). This suggests that Nlk2 acts as a midbrain-specific Wnt/β-catenin activator and promotes cell proliferation in the midbrain of zebrafish. Biochemical studies revealed that Nlk2 phosphorylates Lef1 at the conserved Thr residue, which promotes Lef1 tran-

scriptional activity by blocking the interaction of Lef1 with HDAC1(Ota et al. 2012). Consistent with this finding, the Nlk2 knockdown-induced reduction in top:GFP activity was reversed by co-knockdown of HDAC1 (Ota et al. 2012). Thus, the midbrain-specific regulation of Wnt/β-catenin signaling was revealed using reporter fish.

It is noteworthy that inhibition of Reck, Gpr124, Nephrocystin-4, PGE2, Nrarp, and/or Nlk2 induces defects in specific tissues, which suggests they are cell/tissue type-specific Wnt/β-catenin signaling modifiers, but not general Wnt/β-catenin signaling regulators. Such cell/tissue type-specific modifiers should support the spatiotemporal dynamics of Wnt/β-catenin signaling, which enables Wnt/β-catenin signaling to play diverse roles in animal development and homeostasis.

1.4 Utility of the Wnt/β-Catenin Signaling Reporter Zebrafish for Drug Discovery

Wnt/β-catenin signaling regulates stem cell fates, and dysregulation of Wnt/β-catenin signaling causes various human diseases, including cancer, mental disorders, osteoporosis, and obesity. Therefore, chemical inhibitors against Wnt/β-catenin signaling have potential as regenerative medicines and therapeutic agents; several chemical inhibitors of Wnt/β-catenin signaling, such as XAV-939, IWR-1, IWP-2, and ICG-001, have already been identified. XAV-939 and IWR-1 reduce β-catenin protein levels by promoting Axin protein stabilization, and IWP-2 also blocks Wnt secretion (Chen et al. 2009). ICG-001 blocks β-catenin binding to a histone acetyltransferase CREB-binding protein (CBP) and consequently prevents CREB-mediated β-catenin activation (Teo et al. 2005). Importantly, treatment with these chemical inhibitors eliminates not only Wnt/β-catenin signaling activity in mammalian cells but also the activities of Wnt/β-catenin signaling reporters (7xTCF-Xla.Siam:GFP and OTM:d2EGFP) in zebrafish (Moro et al. 2012; Shimizu et al. 2012). Therefore, reporter fish were used for identification of new chemicals that can inhibit Wnt/β-catenin signaling in vivo. In this section, we describe three chemicals, the in vivo activities of which were characterized using Wnt/β-catenin signaling reporter fish.

1.4.1 9-Hydroxycanthin-6-one Promotes β-Catenin Degradation by Activating GSK3β

Ohishi et al. (2015) screened plant extracts using reporter assays in HEK293 cells and identified the β-carboline alkaloid 9-hydroxycanthin-6-one as a new Wnt/β-catenin inhibitor. Although the direct target molecules of 9-hydroxycanthin-6-one

remain unclear, treatment with 9-hydroxycanthin-6-one activated GSK3β-mediated phosphorylation and the consequent degradation of β-catenin. To confirm in vivo activity of this inhibitor, Ohishi et al. (2015) used top:GFP Wnt/β-catenin reporter fish. Treatment with 9-hydroxycanthin-6-one reduced top:GFP activity and expression of endogenous Wnt/β-catenin target genes, including *mitf* and *zic2a*, and partially rescued the eyeless phenotype induced by treatment with BIO, a GSK3β specific inhibitor (Ohishi et al. 2015), which suggests that this inhibitor can block Wnt/β-catenin signaling via GSK3β regulation in vivo.

1.4.2 PMED-1 Blocks β-Catenin Binding to CREB

Because XAV-939, IWR-1, and 9-hydroxycanthin-6-one affect the activity of the Wnt/β-catenin core signaling system, which contributes to the homeostasis of various tissues, these inhibitors may not only affect abnormal tissues but may also damage healthy ones. In contrast, pharmacological inhibition of the cell type-specific modulators may enable cell type-specific Wnt/β-catenin signaling regulation and contribute to disease treatment with few side effects. Two histone acetyltransferases, CREB and p300, interact with β-catenin to activate β-catenin-mediated transcription although the binding of each results in distinct effects. CBP-β-catenin complexes positively regulate the expression of genes promoting cell proliferation while p300-β-catenin complexes are not involved in cell proliferation (Teo and Kahn 2010). Interestingly, ICG-001 specifically inhibits β-catenin binding to CBP, but not to p300, and blocks β-catenin-mediated cell proliferation. In addition, ICG-001 is selectively cytotoxic to colon carcinoma cells because treatment with ICG-001 kills SW480 and HCT116 colon cancer cells, while it has no effect on CCD-841Co normal colonic epithelial cells (Teo et al. 2005). Therefore, ICG-001 is thought to be usable for cancer treatment with few side effects. Delgado et al. (2014) searched for chemicals that possess similar activity to ICG-001 by using in silico analysis and zebrafish reporter assays. To identify compounds structurally similar to ICG-001, they screened the ZINC 10 database (http://zinc.docking.org/subsets/lead-like) and identified PMED-1 as the lead compound, with ≥70% similarity to ICG-001. Similar to ICG-001, PMED-1 blocked the interaction of β-catenin with CBP, but not with p300, and reduced the viability of hepatocellular carcinoma (HCC) cells; it has no toxicity in human normal hepatocytes (Fig. 1.4; Delgado et al. 2014). Results also showed that PMED-1 can block Wnt/β-catenin signaling in vivo using OTM:d2EGFP reporter zebrafish. Interestingly, the OTM:d2EGFP activity in PMED-1-treated zebrafish embryos was strongly inhibited from 5 to 15 h after treatment but restored after 24 h; OTM:d2EGFP activity still continued to be suppressed 24 h after treatment in XAV939-treated zebrafish embryos, which indicates that the half-life of Wnt/β-catenin inhibitory activity of PMED-1 is shorter than that of XAV939. Thus, it is possible to evaluate the effect on Wnt/β-catenin signaling activity and its duration in vivo of a new Wnt/β-catenin inhibitor using reporter fish.

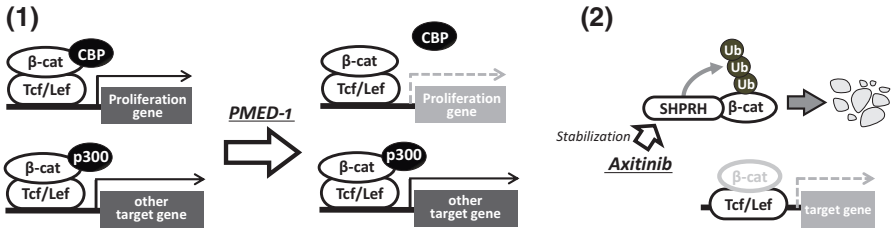

Fig. 1.4 Chemical inhibitors against Wnt/β-catenin signaling, which were characterized by reporter fish analyses. (1) PMED-1 blocked the interaction of β-catenin with CBP but not with p300. (2) Axitinib binds to and stabilizes the E3 ubiquitin ligase, SHPRH. Axitinib-stabilized SHPRH promoted the ubiquitination and degradation of nuclear β-catenin

1.4.3 Axitinib Promotes β-Catenin Degradation in Nucleus

Most Wnt/β-catenin pathway mutations in cancer patients are observed in the β-catenin gene and the APC gene, which encodes a component of the β-catenin destruction complex. Therefore, it is important to develop drugs that target downstream of the destruction complex. Recently, Qu et al. (2016) identified axitinib as such a drug; 460 Food and Drug Administration (FDA)-approved drugs were screened to find chemicals capable of inhibiting Wnt/β-catenin signaling activation induced by treatment with BIO, a GSK3β specific inhibitor, in HEK293 cells. Qu et al. (2016) also confirmed that axitinib inhibits in vivo Wnt/β-catenin signaling in OTM:d2EGFP zebrafish. Interestingly, axitinib reduced OTM:d2EGFP activity in the developing midbrain and tail but not in the developing ear, lateral line primordia, pectoral fin, fin fold, or cranial NCCs (Fig. 1.2; Qu et al. 2016); XAV-939 completely eliminated OTM:d2EGFP activity in the whole body (Fig. 1.2; Shimizu et al. 2012). Results suggest that axitinib inhibits Wnt/β-catenin signaling in specific cells but not in all cells. Consistent with this idea, axitinib reduced the activities of Wnt/β-catenin signaling and proliferation in colon cancer cells but not in normal intestinal tissues (Qu et al. 2016), indicating that axitinib may be usable for colon cancer treatment with few side effects. Furthermore, biochemical analyses revealed that axitinib binds to and stabilizes the E3 ubiquitin ligase SHPRH (SNF2, histone-linker, PHD and RING finger domain-containing helicase). Axitinib-stabilized SHPRH promoted the ubiquitination and degradation of nuclear β-catenin, which was independent of the β-catenin destruction complex including APC and GSK3β (Fig. 1.4; Qu et al. 2016). Thus, a new Wnt/β-catenin signaling inhibitor and its mechanism of action were elucidated.

1.5 Conclusions

Numerous molecules that regulate Wnt/β-catenin signaling have been discovered previously using invertebrate models, mammalian cell culture, and *Xenopus* early embryos. It was believed that most were “general regulators” that participate in the

control of Wnt/β-catenin signaling in all cells/tissues, but their physiological roles in vertebrates were unclear. However, recent studies using reporter zebrafish lines have revealed cell/tissue-type specific Wnt/β-catenin signaling modifiers, such as Reck, Gpr124, Nephrocystin-4, Nrarp, and Nlk2, which must complicate the spatio-temporal pattern of Wnt/β-catenin signaling activity in order to play multiple roles in animal development and homeostasis. It is also possible that parts of previously identified regulators may also be cell/tissue-type-specific modifiers. Future studies on previously and newly identified Wnt regulators using reporter fish will facilitate further understanding of cell/tissue type-specific Wnt/β-catenin signaling regulation and thereby make clear the whole picture of Wnt/β-catenin signaling regulation in living animals.

Reporter zebrafish lines will also help the discovery of new anti-cancer drugs that have few side effects. The chemicals that control the activity of Wnt/β-catenin core signaling systems may affect the homeostasis of healthy tissues, while chemical inhibitors against cell/tissue-specific modulators may enable cancer tissue-specific regulation. It is worth noting that axitinib inhibits OTM:d2EGFP reporter activity in a part of Wnt/β-catenin-active cells in zebrafish embryos and also reduces the activity of Wnt/β-catenin signaling and proliferation in colon cancer cells but not in normal intestinal tissues (Qu et al. 2016). This indicates that axitinib acts as a Wnt/β-catenin inhibitor in specific cells and may be able to reduce colon cancer cell activity without causing severe side effects. It also suggests that such cell/tissue-specific reporter inhibition could be used as an index for safe Wnt/β-catenin inhibitors that can be employed for cancer therapy in anti-cancer drug screening.

In addition to Wnt/β-catenin signaling, other cell signaling pathways, including TGF-β/BMP and Shh, are activated repeatedly and play multiple roles in animal development and homeostasis, and dysregulation of these pathways is involved in tumorigenesis. In addition, reporter fish lines that visualize various signaling pathways have been generated (Casari et al. 2014; Laux et al. 2011; Schwend et al. 2010). Therefore, a similar strategy can be implemented to investigate the in vivo regulatory mechanisms of other cell signaling pathways and their control agents. Thus, cell signaling reporter zebrafish are a useful tool for both investigating the mechanisms of dynamic signaling regulation and for identifying new drugs controlling particular signaling pathways in specific cells/tissues.

References

Arce L, Pate KT, Waterman ML (2009) Groucho binds two conserved regions of LEF-1 for HDAC-dependent repression. BMC Cancer 9:159

Burcklé C, Gaudé HM, Vesque C et al (2011) Control of the Wnt pathways by nephrocystin-4 is required for morphogenesis of the zebrafish pronephros. Hum Mol Genet 20(13):2611–2627

Casari A, Schiavone M, Facchinello N et al (2014) A Smad3 transgenic reporter reveals TGF-beta control of zebrafish spinal cord development. Dev Biol 396(1):81–93

Chen B, Dodge ME, Tang W et al (2009) Small molecule-mediated disruption of Wnt-de pendent signaling in tissue regeneration and cancer. Nat Chem Biol 5(2):100–107

Clevers H (2006) Wnt/β-catenin signaling in development and disease. Cell 127(3):469–480
Clevers H, Nusse R (2012) Wnt/β-catenin signaling in development and disease. Cell 149(6):1192–1205
De Ferrari GV, Moon RT (2006) The ups and downs of Wnt signaling in prevalent neurological disorders. Oncogene 25(57):7545–7553
Delgado ER, Yang J, So J et al (2014) Identification and characterization of a novel small molecule inhibitor of β-catenin signaling. Am J Pathol 184(7):2111–2122
Deyts C, Candal E, Joly JS, Bourrat F (2005) An automated in situ hybridization screen in the Medaka to identify unknown neural genes. Dev Dyn 234(3):698–708
Dorsky RI, Scheldahl LC, Moon RT (2002) A transgenic Lef1/β-catenin-dependent reporter is expressed in spatially restricted domains throughout zebrafish development. Dev Biol 241(2):229–237
Goessling W, North TE, Loewer S et al (2009) Genetic interaction of PGE2 and Wnt signaling regulates developmental specification of stem cells and regeneration. Cell 136(6):1136–1147
Ishitani T, Ninomiya-Tsuji J, Nagai S et al (1999) The TAK1-NLK-MAPK-related pathway antagonizes signalling between beta-catenin and transcription factor TCF. Nature 399(6738):798–802
Ishitani T, Matsumoto K, Chitnis AB, Itoh M (2005) Nrarp functions to modulate neural-crest-cell differentiation by regulating LEF1 protein stability. Nat Cell Biol 27(11):1106–1112
Kizil C, Küchler B, Yan JJ et al (2014) Simplet/Fam53b is required for Wnt signal trans- duction by regulating β-catenin nuclear localization. Development 141(18):3529–3539
Laux DW, Febbo JA, Roman BL (2011) Dynamic analysis of BMP-responsive smad activ- ity in live zebrafish embryos. Dev Dyn 240(3):682–694
Lee W, Swarup S, Chen J, Ishitani T, Verheyen EM (2009) Homeodomain-interacting pro- tein kinases (Hipks) promote Wnt/Wg signaling through stabilization of beta-catenin/Arm and stimulation of target gene expression. Development 136(2):241–252
Logan CY, Nusse R (2004) The Wnt signaling pathway in development and disease. Annu Rev Cell Dev Biol 20:781–810
Meneghini MD, Ishitani T, Carter JC et al (1999) MAP kinase and Wnt pathways converge to down-regulate an HMG-domain repressor in Caenorhabditis elegans. Nature 399(6738):793–797
Moro E, Ozhan-Kizil G, Mongera A et al (2012) In vivo Wnt signaling tracing through a transgenic biosensor fish reveals novel activity domains. Dev Biol 366(2):327–340
Ohishi K, Toume K, Arai MA et al (2015) 9-Hydroxycanthin-6-one, a β-Carboline alkaloid from Eurycoma longifolia, is the first Wnt signal inhibitor through activation of glycogen synthase kinase 3β without depending on casein kinase 1α. J Nat Prod 78(5):1139–1146
Ota S, Ishitani S, Shimizu N et al (2012) NLK positively regulates Wnt/β-catenin signalling by phosphorylating LEF1 in neural progenitor cells. EMBO J 31(8):1904–1915
Posokhova E, Shukla A, Seaman S et al (2015) GPR124 functions as a WNT7-specific co- activator of canonical β-catenin signaling. Cell Rep 10(2):123–130
Qu Y, Gharbi N, Yuan X et al (2016) Axitinib blocks Wnt/β-catenin signaling and directs asymmetric cell division in cancer. Proc Natl Acad Sci U S A 113(33):9339–9344
Reya T, Duncan AW, Ailles L et al (2003) A role for Wnt signalling in self-renewal of haematopoietic stem cells. Nature 423(6938):409–414
Schwend T, Loucks EJ, Ahlgren SC (2010) Visualization of Gli activity in craniofacial tissues of hedgehog-pathway reporter transgenic zebrafish. PLoS One 5(12):e14396
Shimizu N, Kawakami K, Ishitani T (2012) Visualization and exploration of Tcf/Lef func- tion using a highly responsive Wnt/β-catenin signaling-reporter transgenic zebrafish. Dev Biol 370(1):71–85
Shimizu N, Ishitani S, Sato A, Shibuya H, Ishitani T (2014) Hipk2 and PP1c cooperate to maintain Dvl protein levels required for Wnt signal transduction. Cell Rep 8(5):1391–1404
Teo JL, Kahn M (2010) The Wnt signaling pathway in cellular proliferation and differentiation: a tale of two coactivators. Adv Drug Deliv Rev 62(12):1149–1155

Teo JL, Ma H, Nguyen C, Lam C, Kahn M (2005) Specific inhibition of CBP/beta-catenin interaction rescues defects in neuronal differentiation caused by a presenilin-1 mutation. Proc Natl Acad Sci U S A 102(34):12171–12176

Trowbridge JJ, Xenocostas A, Moon RT, Bhatia M (2006) Glycogen synthase kinase-3 is an in vivo regulator of hematopoietic stem cell repopulation. Nat Med 12(1):89–98

Vanhollebeke B, Stone OA, Bostaille N et al (2015) Tip cell-specific requirement for an atypical Gpr124- and Reck-dependent Wnt/β-catenin pathway during brain angiogenesis. elife 4:e06489

Yanfeng W, Saint-Jeannet JP, Klein PS (2003) Wnt-frizzled signaling in the induction and differentiation of the neural crest. BioEssays 25:317–325

Zhou Y, Nathans J (2014) Gpr124 controls CNS angiogenesis and blood-brain barrier in- tegrity by promoting ligand-specific canonical wnt signaling. Dev Cell 31(2):248–256

Chapter 2
Endothelial Cell Dynamics during Blood Vessel Morphogenesis

Li-Kun Phng

Abstract Blood vessels, together with the heart, have a fundamental role in supporting the metabolic demands of tissues not only during development but also in adults. New blood vessels are frequently generated through angiogenesis when new vessels emerge from pre-existing ones (Fig. 2.1a). Initially, endothelial cells (ECs) lining an existing vessel are selected to become tip cells to spearhead the formation of new vascular sprouts. New sprouts grow through EC proliferation and the polarized collective migration of both tip and trailing stalk cells into the avascular tissue. In order to generate a network of interconnecting vessel segments, tip cells anastomose with neighboring tip cells to establish new vascular loops. Importantly, vascular sprouts develop into tubes through which oxygen, metabolites, cells, and waste products can circulate around the body. Finally, the tubular network of blood vessels are either maintained or, depending on the tissue requirements in which the vessels pervade, remodeled through pruning into a more refined vascular network that carries blood flow optimally to tissues (Fig. 2.1b).

Over the past few decades, many key signaling pathways that regulate blood vessel development have been identified using primarily the mouse as the model organism. These include the Neuropilin (NRP)/Vascular Endothelial Growth Factor (VEGF)/Vascular Endothelial Growth Factor Receptor (VEGFR), Jagged/Delta-like/Notch, Transforming Growth Factor β (TGFβ)/Bone Morphogenic Protein (BMP) and EphrinB/EphB signaling cascades (Adams RH, Alitalo K. Nat Rev Mol Cell Biol 8:464–478, 2007; Potente M, Makinen T. Nat Rev Mol Cell Biol 18:477, 2017). Although these studies have uncovered the fundamental principles of angiogenesis, temporal information on the cellular dynamics of angiogenesis has been lacking due to difficulties in performing live imaging in mouse embryos and tissues. These challenges are alleviated by the use of zebrafish, whose embryos develop *ex utero,* are optically transparent and are therefore highly suited for live imaging. Combined with recent advances in imaging techniques and the development of fluorescent biosensors or reporters, it is now possible to observe the dynamics of ECs at cellular and

L.-K. Phng (✉)
Laboratory for Vascular Morphogenesis, RIKEN Center for Biosystems Dynamics Research, Kobe, Japan
e-mail: likun.phng@riken.jp

H. Hirata, A. Iida (eds.), *Zebrafish, Medaka, and Other Small Fishes*,
https://doi.org/10.1007/978-981-13-1879-5_2

subcellular resolution as blood vessel morphogenesis takes place. Imaging vascular morphogenesis in the zebrafish embryo has been indispensable in the identification of morphogenetic events such as apical membrane invagination and the elucidation of the cellular mechanisms of anastomosis and vessel pruning, which are dynamic processes that are difficult to visualize and investigate in mouse models.

In this chapter, I will summarize recent findings from zebrafish studies that highlight the dynamic nature of ECs during angiogenesis and vessel remodeling and focus on how the actin cytoskeleton regulates EC morphogenesis and behavior.

Keywords Angiogenesis · vascular morphogenesis · endothelial cells · actin cytoskeleton · membrane · junction · zebrafish · live imaging

2.1 Endothelial Morphogenetic Behaviors During Vessel Development and Remodeling

ECs display great plasticity with the ability to generate extensive cell shape changes necessary to drive diverse cellular behaviors. Although they are individually heterogeneous in behavior during development, ECs collectively coordinate their cellular processes to generate a hierarchical, well-patterned network of tubular blood vessels (Fig. 2.1).

2.1.1 Endothelial Cell Migration and Elongation

Angiogenic vessels are characterized by vascular sprouts that are headed by endothelial tip cells, which are recognized by their long filopodia, and trailing stalk cells (Kurz et al. 1996; Lawson and Weinstein 2002; Gerhardt et al. 2003). As tip cells have higher VEGFR2 and VEGFR3 activities and lower Notch and TGFβ/BMP signaling (Potente and Makinen 2017), they are highly migratory and have a

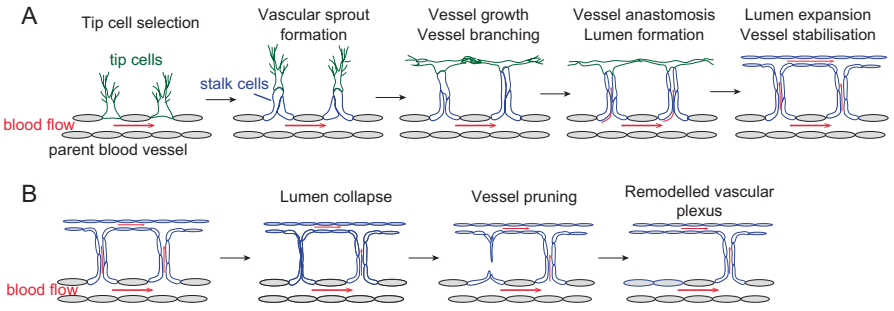

Fig. 2.1 (**a**) New blood vessel formation through angiogenesis. (**b**) Remodeling of a primitive vascular plexus through vessel pruning

competitive advantage over stalk cells to take the leading position in the vessel sprout. The growth or extension of the new vessel sprout requires the coordinated migration of both tip and stalk cells into the avascular tissue as well as stalk cell elongation (Sauteur et al. 2014).

2.1.2 Endothelial Cell Proliferation

Vessel growth also depends on the proliferation of endothelial tip and stalk cells (Siekmann and Lawson 2007; Costa et al. 2016). During this process, ECs undergo rounding and furrowing at anaphase (Phng et al. 2013; Aydogan et al. 2015). Cytokinesis of daughter cells can be symmetrical or asymmetrical, depending on the presence or absence of a lumen within the vessel during proliferation (Aydogan et al. 2015; Costa et al. 2016). Asymmetric EC division influences EC behavior since it leads to a higher distribution of mRNA and proteins from the VEGFR signaling pathway in one daughter cell (Costa et al. 2016). As a consequence, the daughter cell with higher VEGFR signaling migrates faster to take the leading tip cell position.

2.1.3 Endothelial Cell Branching and Anastomosis

To expand the vascular network, new branch points are made by either the selection of new tip cells to form new vascular sprouts or by the bifurcation of a tip cell. During bifurcation, the cell transforms into a T-shaped cell by generating two protrusions from the cell body to make a new branch point. Vessel branching is followed by anastomosis whereby a new cell-cell contact is created between two tip cells or between a tip cell and a functional blood vessel (Herwig et al. 2011; Lenard et al. 2013) so to establish a closed vascular loop.

2.1.4 Endothelial Cell Rearrangements

ECs do not remain static within blood vessels. In growing vascular sprouts, dynamic shuffling between tip and stalk cells for the leading position occurs (Jakobsson et al. 2010) and, upon ablation of tip cells of the zebrafish intersegmental vessel (ISV), stalk cells rapidly transform into new tip cells during sprouting angiogenesis (Sauteur et al. 2014), demonstrating that tip and stalk cell fates are interchangeable. In developing blood vessels that are initially unicellular in organization (such as that of ISVs, see Fig. 2.2a), cell rearrangements drive the conversion of the vessel to a multicellular organization. Here, cell rearrangement is coupled with extensive cell morphogenesis. Among these, cell splitting occurs when a single EC surrounding a

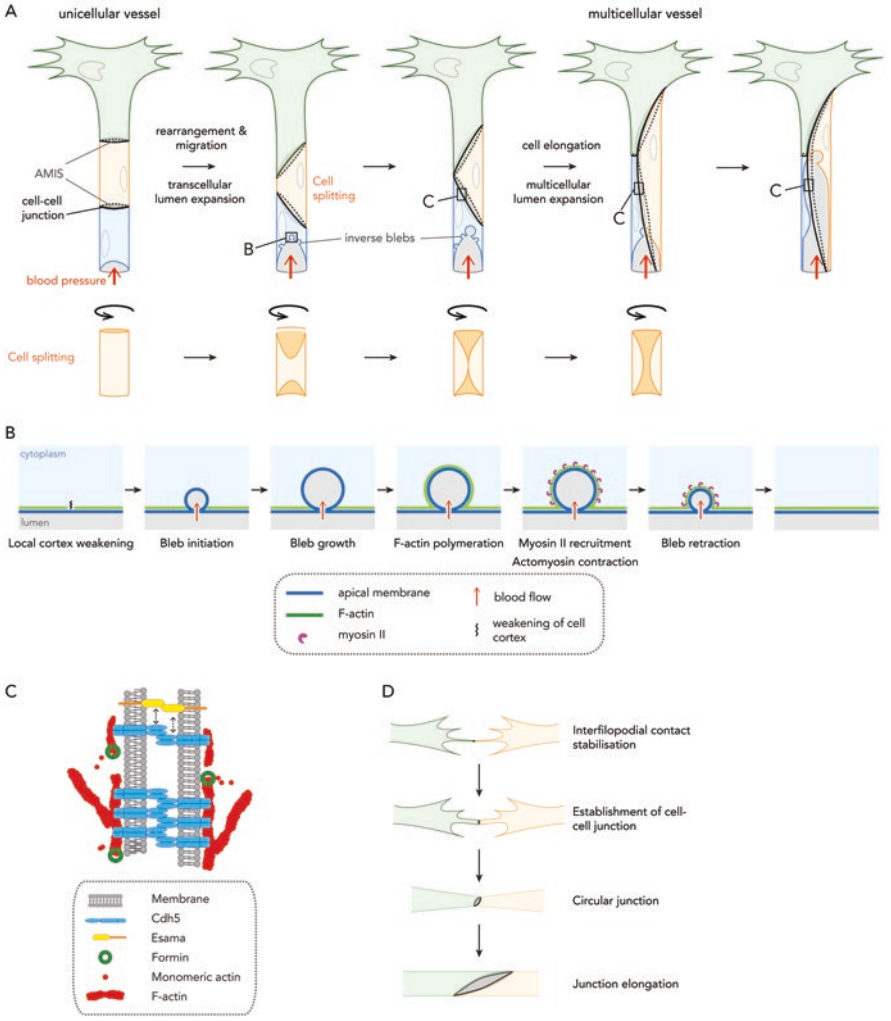

Fig. 2.2 (**a**) Membrane dynamics and junction remodeling during the formation of tubular blood vessels. AMIS, apical membrane initiation site. (**b**) Inverse blebbing during lumen expansion is controlled by local and transient actomyosin activity. (Figure adapted from Gebala et al. 2016). (**c**) Endothelial cell-cell junction elongation and maintenance requires formin-mediated actin polymerization, Cdh5 (VE-cadherin) and Esama. (**d**) Anastomosis between two tip cells requires the stabilization of interfilopodial contacts and the assembly and remodeling of endothelial cell-cell junction

lumen splits on one side (Fig. 2.2a, Lenard et al. 2013). In developed vessels, ECs rearrange their positions relative to each other to make new neighbors. For example, single-labeled cells are observed to translocate from one ISV to another (Blum et al. 2008; Yu et al. 2015) and vein-derived endothelial tip cells change their forward course of migration to move backwards into the vascular plexus to contribute to artery formation in a Cxcr4a–dependent manner (Xu et al. 2014). These observations highlight the dynamic nature of ECs not only during the migratory phase of angiogenesis but also during the reorganization of ECs in tubules and in vessel remodeling.

2.1.5 Apical Membrane Invagination

ECs undergo extensive morphological changes in order to expand its apical compartment during lumen formation. In transcellular lumen formation, the apical membrane invaginates into the cell body to form a luminal space, or hollow cell (Figs. 2.2a and 2.4c), and compresses the cytoplasm at the same time so that the EC becomes squeezed between the basal and apical membranes (Herwig et al. 2011; Gebala et al. 2016).

2.1.6 Vessel Pruning

During the remodeling of a vascular plexus, segments of blood vessels are pruned from the network (Fig. 2.3). ECs rearrange in the vessel segment to be pruned and migrate into a neighboring vessel, transforming the vessel from a multicellular to a unicellular vessel (Lenard et al. 2015). In some vessels, EC self-fusion can occur to generate unicellular tubes (Lenard et al. 2015). Interestingly, cell self-fusion does not give rise to an autocellular junction.

2.2 Endothelial Membrane Dynamics During Vessel Morphogenesis

As described in the previous section, ECs frequently transform its shape to match its function during vascular morphogenesis. In this section, I will discuss local shape changes in the endothelial apical and basal membranes that drive EC morphogenesis and how membrane dynamics are regulated during angiogenesis.

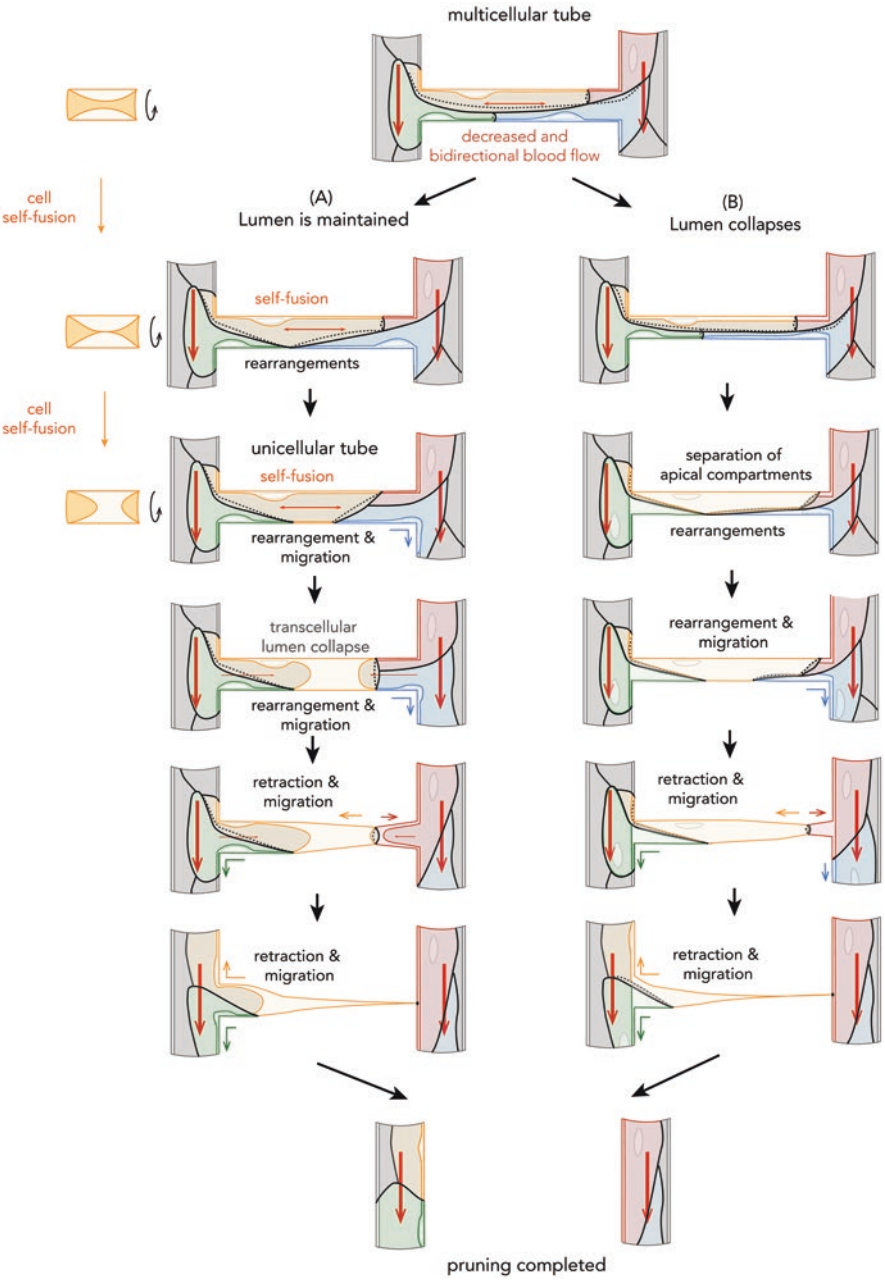

Fig. 2.3 Decreased blood flow and changes in flow direction trigger vessel pruning. The lumen of the vessel segment can either be maintained (**a**) or can collapse (**b**). If the lumen is maintained, EC junction remodeling, cell rearrangements, cell self-fusion and cell migration convert the multicellular tube into a unicellular tube. Eventually, the transcellular lumen collapses, resulting in two separate luminal compartments. If the lumen collapses, cell rearrangements and migration lead to unicellular organization of the vessel segment. In both mechanisms, the process of vessel pruning is completed by the migration of the final cell in the pruned vessel to one of the major branches and the resolution of the last cell-cell contact. (Figure adapted from Lenard et al. 2015)

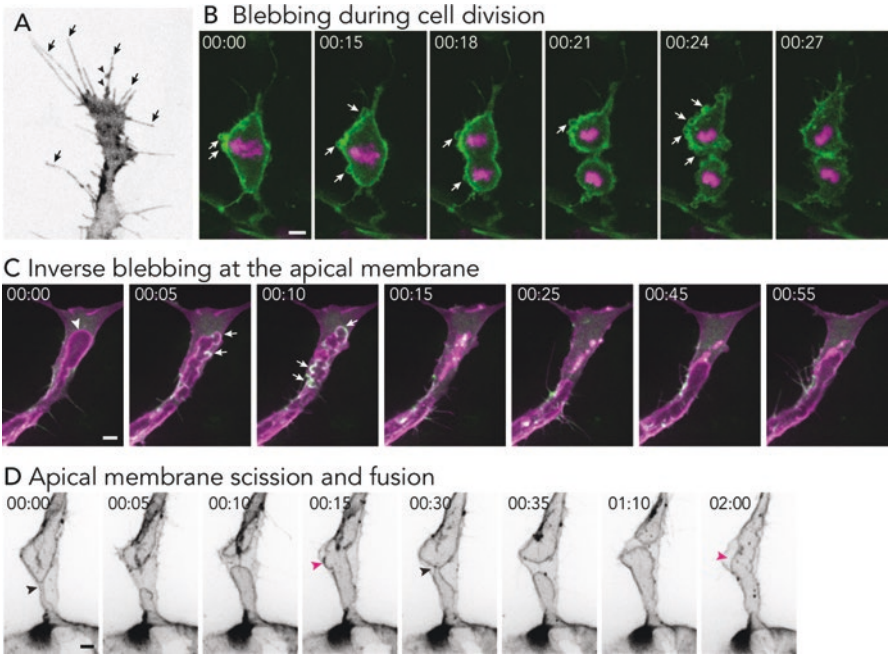

Fig. 2.4 Endothelial membrane dynamics during blood vessel morphogenesis. (**a**) Endothelial tip cells generate extensive filopodia (arrows) during migration. Arrowheads, lamellipodia-like protrusions. (**b**) Blebs (arrows) during EC division. Green, membrane; magenta, H2B. (**c**) Inverse blebbing drives lumen expansion into an endothelial tip cell during ISV formation. Arrowhead, apical membrane. Arrows, retracting blebs. 00:15, lumen collapse. 00:25–00:55, fusion and integration of collapsed apical membranes into the invaginating lumen. Green, F-actin (Lifeact); magenta, membrane. (**d**) Black arrowhead, site of apical membrane scission. Magenta arrowhead, fusion of two opposing apical membranes to form a continuous lumen. Scale bars, 5 μm. 00:00, hours:minutes

2.2.1 Endothelial Cell Membrane Plasticity

Migrating cells exhibit front-rear polarity whereby they generate membrane protrusions at the leading edge to drive forward movement (Ridley 2011). During angiogenesis, F-actin-rich filopodia are the most prominent protrusions formed at the leading edge of migrating endothelial tip cells (Fig. 2.4a, Gerhardt et al. 2003; Fraccaroli et al. 2012; Phng et al. 2013). Tip cells also use filopodia to facilitate contact with other ECs with which to anastomose to create new vessel connections (Phng et al. 2013). ECs can additionally generate lamellipodia and blebs. Lamellipodia protrude from filopodia and likely facilitate the growth and expansion of vascular sprouts (Phng et al. 2013) while blebs are generated during EC division (Fig. 2.4b, Phng et al. 2013; Aydogan et al. 2015) and in the apical membrane during lumen expansion (Figs. 2.2a and 2.4c, Gebala et al. 2016).

Blebs are spherical membrane protrusions that are recognized as another form of leading edge protrusion that drives the migration of cells such as zebrafish progenitor germ cells (Paluch and Raz 2013). However, the blebs observed in the apical membrane of expanding lumen protrude into the EC cytoplasm. They are therefore referred to as inverse blebs. Interestingly, two classes of inverse blebs are observed. In one class, the inverse blebs resolved soon after forming while in the second class, the blebs persisted. The second class of blebs is often observed at the front of the expanding apical membrane and drives the expansion of new lumens in the vessel (Gebala et al. 2016).

Other apical membrane behaviors have also been reported during lumen formation of angiogenic vessels. The formation and fusion of intracellular vesicles in single ECs to form bigger vacuolar compartments have been proposed to initiate transcellular lumenization of angiogenic vessels (Kamei et al. 2006; Wang et al. 2010; Yu et al. 2015). Intracellular vesicles can also arise from the collapse and scission of an expanding lumen (Fig. 2.4c, Gebala et al. 2016). These vesicles subsequently re-fuse with and contribute to the expanding lumen. After lumen expansion, the apical membrane continues to exhibit dynamic behavior, going through cycles of luminal membrane scission and fusion before establishing a stable lumen (Fig. 2.4d, Lenard et al. 2013; Gebala et al. 2016). During vessel regression, apical membrane scission occurs before the lumen collapses (Lenard et al. 2015).

2.2.2 Regulation of Membrane Dynamics by Actomyosin Activity

The actin cytoskeleton is integral in providing cells with mechanical support, regulating cell shape, and generating the driving forces for cell movement (Pollard and Cooper 2009). By assembling distinct cellular structures, such as filopodia and lamellipodia, the actin cytoskeleton confers the cell the capacity to change its morphology and generate movement. During angiogenesis, diverse actin cytoskeleton structures of different subcellular localization and dynamics are generated in ECs at distinct phases of vessel morphogenesis (Phng et al. 2013). Furthermore, by following the dynamics of these actin structures, it was possible to determine that some actin-based structures such as that in filopodia and apical compartment during lumen expansion are transient while others such as the actin cables in EC junctions are more stable.

It has long been assumed that endothelial tip cells use filopodia for guided cell migration and vessel patterning. Interestingly, the depletion of filopodia formation in vivo by using low concentrations of Latrunculin B, an actin polymerization inhibitor, does not inhibit EC migration during ISV formation (Phng et al. 2013). Instead, tip cells generate lamellipodia at the leading edge that are sufficient to drive the cell forward albeit at a reduced speed. Furthermore, tip cell guidance is unaffected since

normal ISV patterning persisted, indicating that filopodia are dispensable for tip cell guidance (Phng et al. 2013). These observations highlight the plasticity of ECs in generating different membrane protrusions that cooperate to promote efficient polarized migration during vessel formation.

Recent publications have revealed some molecular insights on the regulation of EC protrusions in vivo. The bone morphogenetic protein (BMP) regulates the formation of zebrafish caudal vein plexus (CVP) (Wiley et al. 2011) by inducing Arghef9b-mediated Cdc42 activation, which in turn activates Formin-like 3 (Fmnl3) to assemble linear F-actin cables that generate filopodia (Wakayama et al. 2015). The failure to generate filopodia leads to incomplete CVP formation due to defects in ECs migration (Wakayama et al. 2015). Additionally, the loss of filopodia by ECs can prevent vessel anastomosis that is required for ventral CVP formation (Phng et al. 2013). Interestingly, inhibition of Fmnl3 activity does not completely abolish filopodia formation in ISVs (Phng et al. 2015; Wakayama et al. 2015), indicating differences in the molecular regulation of filopodia of ECs from different vascular beds.

Unlike filopodia and lamellipodia, the formation of blebs is not generated by actin polymerization. Instead, bleb formation is initiated by the local detachment of the plasma membrane from the cell cortex or the local rupture of the cortex. While intracellular pressure and cytoplasmic flow propel classical bleb expansion (Blaser et al. 2006; Charras 2008; Paluch and Raz 2013), blood flow drive the expansion of inverse blebs at the apical membrane of ECs (Fig. 2.2b, Gebala et al. 2016). In both types of blebs, the cortex is initially free of F-actin. However, actin assembly and non-muscle myosin II activity at the bleb cortex subsequently promote the retraction of both classical (Charras 2008) and inverse blebs (Figs. 2.2b and 2.4c, Gebala et al. 2016). In ECs, misregulation of myosin II activity results in uncontrolled blebbing at the apical membrane due to decreased bleb retraction and consequently prevents proper transcellular lumen formation in angiogenic vessels (Gebala et al. 2016). This finding indicates that inverse blebbing at the apical membrane needs to be actively suppressed for controlled, unidirectional lumen expansion.

2.3 Endothelial Cell–Cell Junction Dynamics During Vessel Morphogenesis

The generation of vascular tubes requires the coordinated activity of many ECs that are connected through cell-cell junctions, which dynamically remodel to allow cell shape changes and rearrangement. Notably, while tubulogenesis requires the formation, expansion, and stabilization of cell-cell junctions, vessel pruning entails junction disassembly.

2.3.1 Cell-Cell Junction Remodeling During Sprout Extension

During sprouting angiogenesis, ECs are initially arranged in a serial manner within the vascular sprout (unicellular vessel, Fig. 2.2a). In this arrangement, cell-cell junctions are circular in shape but are subsequently transformed to an elliptical shape (Fig. 2.2a, Sauteur et al. 2014). Such junction morphogenesis is required to drive EC elongation that is observed during sprout growth or extension and to allow the formation of multicellular tubes (Sauteur et al. 2014).

2.3.2 Formation of New Junctions During Anastomosis

The de novo formation of new EC junctions in vivo can be conveniently studied during the process of anastomosis. Anastomosis is facilitated by filopodial contacts, although ECs can still anastomose in the absence of filopodia through lamellipodia (Phng et al. 2013) or when endothelial cell bodies come to direct contact (Sauteur et al. 2017). Upon stabilization of filopodia contacts, new junctions form and expand into rings (Fig. 2.2d, Herwig et al. 2011). As in the case of growing vascular sprouts, the circular junctional rings become elliptical to allow EC elongation and the formation of multicellular tube.

2.3.3 Cell-Cell Junction Organization During Blood Vessel Tubulogenesis

Different mechanisms exist to make lumens in angiogenic vessels. In one mechanism called *cord hollowing*, cell rearrangements drive lumen formation. From a unicellular junction conformation, cells converge toward each other, leading to new contacts and junction formation (Herwig et al. 2011; Lenard et al. 2013). As apical membranes form de novo at intercellular junctions (Herwig et al. 2011; Pelton et al. 2014), the two membrane compartments merge into one, resulting in the formation of a continuous lumen space. In another mechanism that is observed in vessels where cell rearrangements is initially limited, transcellular lumen formation occurs. Here, the lumen is formed by apical membrane invagination and internal apical membrane fusion to form a hollow cell and unicellular tube. Transcellular lumen formation is highly dependent on blood pressure as its cessation prevents apical membrane invagination (Herwig et al. 2011; Lenard et al. 2013; Gebala et al. 2016). Often, unicellular tubes are transformed into multicellular tubes, which are characterized by two (or more) longitudinal junctions along the vascular axis, by junction elongation and cell rearrangements (Sauteur et al. 2014).

It is likely, however, that ECs employ several mechanisms to make tubes. Live imaging experiments show that cell rearrangements can simultaneously occur to

align the apical membranes of different ECs as transcellular lumen formation takes place at the region of the vessel that is connected to a patent vessel (personal observation). As the invaginating lumen reaches a cell-cell junction, inter-cellular apical membrane fusion occurs to allow a rapid expansion of the lumen (see Fig. 2.2a).

2.3.4 *Reorganization of Cell-Cell Junctions during Vessel Pruning*

Once formed, the primitive vascular network remodels to give rise to a network with efficient blood flow. Vascular remodeling is greatly influenced by local changes of hemodynamic forces (see Sect. 2.4.4) and comprises of vessel pruning or regression that occurs in a step-wise manner (Fig. 2.3, Chen et al. 2012; Kochhan et al. 2013; Lenard et al. 2015). In vessel segments that are selected for pruning, junction remodeling transforms the vessels from that of a multicellular to a unicellular vessel. Furthermore, regressing vessels frequently display lumen collapse or stenosis before cell rearrangements. Here, the vessel goes through a transient non-lumenized state as a multicellular cord with continuous junctional connections. However, in 30% of pruning events in the subintestinal vessels of the zebrafish, the lumen does not collapse prior to or during junction rearrangements (Lenard et al. 2015). Instead, regressing vessels become unicellular tubes with transcellular lumens that eventually collapse towards the end of pruning. In both scenarios, ECs in the regressing segment migrate away from each other, with cells displaying axial polarity towards their direction of migration (Franco et al. 2015). Through active migration, cell contacts that were previously established within the vessel segment resolve and cells integrate into the neighboring vessels (Chen et al. 2012; Franco et al. 2015; Lenard et al. 2015). Interesting, Lenard et al also observed a different mechanism of vessel remodeling, collateral fusion (Lenard et al. 2015), which is also likely induced by low blood flow.

2.3.5 *Molecular Regulation of Endothelial Cell-Cell Junctions*

Immunohistochemistry staining and live-imaging of fluorescently labeled proteins demonstrate that vascular endothelial-cadherin (VE-cadherin or Cdh5) (Lenard et al. 2013), zonula occludens 1 (Herwig et al. 2011) and endothelial cell-selective adhesion molecule a (Esama) (Sauteur et al. 2014) localize at newly formed endothelial cell-cell junctions. During vessel extension, Cdh5 is required for stalk cell elongation and motility by driving the transformation of junctions from circular to elliptical (Fig. 2.2c, Sauteur et al. 2014). Additionally, Cdh5 regulates the process of anastomosis by facilitating the formation of interfilopodial contacts since endothelial tip cells deficient in Cdh5 require more filopodial interactions to establish firm

contacts (Lenard et al. 2013; Sauteur et al. 2017). Although *Esama* zebrafish mutants do not display any overt vascular phenotype, loss of *Esama* function in ECs worsens the vascular defects in *Cdh5* mutants to decrease the ability of ECs to recognize each other and maintain cell-cell contacts during vessel sprout extension and dorsal longitudinal anastomotic vessel (DLAV) formation (Fig. 2.2c, Sauteur et al. 2017).

2.3.6 Regulation of Endothelial Cell-Cell Junctions by the Actin Cytoskeleton

The interaction between cell-cell junction molecules and the actin cytoskeleton is important in junction remodeling. The transformation of ring-shaped to elliptical-shaped junctions in stalk cells during sprout outgrowth is mediated by the interactions between the C-terminus β–catenin binding domain of Cdh5 and the F-actin cytoskeleton (Sauteur et al. 2014). In *cdh5* mutants, junction elongation failed to occur so that vessels are mostly in the unicellular arrangement. Furthermore, the organization of F-actin cytoskeleton in the cortex is disrupted in the mutants and appeared as puncta with areas devoid of F-actin cables (Sauteur et al. 2014). The VE-cadherin/F-actin interaction is probably required to transmit the deforming force to elongate the endothelial cell junctions (Heinz-Georg Belting, personal communication).

The establishment of actin cables at cell-cell junctions is crucial for the remodeling of junctions. Fluorescence recovery after photobleaching (FRAP) of EGFP-Actin revealed a mobile pool of F-actin with high turnover at endothelial cell-cell junctions of the DA and PCV whose polymerization is dependent on the formin family of actin nucleators (Phng et al. 2015). In developing ISVs, Formin-like 3 (Fmnl3) translocates to endothelial junctions. A reduction in formin activity decreases F-actin cable formation at junctions to inhibit cell rearrangement and the formation of multicellular tubes. Like *cdh5* mutants, Fmnl3 morphants and embryos treated with the pan-formin inhibitor, SMIFH2, display an increase in discontinuous junctions in ISVs and the DLAV, which often fail to lumenize or, if it occurred, lumen continuity becomes disrupted due to weakened junction integrity. Furthermore, the maintenance of vessels as multicellular tubes requires formin activity, highlighting the role of F-actin polymerization in supporting the remodeling and maintenance of junctions and consequently, lumen integrity (Fig. 2.2c, Phng et al. 2015).

In recent years, several molecules that link membrane receptors to the actin cytoskeleton have been implicated in vessel morphogenesis. These include members of the Ezrin/Radixin/Moesin (ERM) family, which, when activated, can associate with both actin and membranes. In the zebrafish, moesin 1 localizes to endothelial cell-cell junctions during ISV formation, and its knockdown by antisense morpholino prevents ISV tubulogenesis in a cell autonomous manner (Wang et al. 2010). The scaffold protein AmotL2, a member of the Angiomotin family, couples Cdh5 to

F-actin (Hultin et al. 2014). Its inactivation dissociates Cdh5 from actin cytoskeletal tensile forces that affected EC shape and ultimately, aortic lumen expansion and formation in both mouse and zebrafish (Hultin et al. 2014). However, it is uncertain whether AmotL2 also has a role in regulating lumen formation of angiogenic vessels since the disruption of DA formation has an adverse effect on ISV formation.

2.4 Influence of Hemodynamic Forces on Blood Vessel Morphogenesis

Once blood vessels become lumenized, ECs become exposed to increasing hemodynamic forces in the form of shear stress and blood pressure. Such forces subsequently regulate EC signaling, cell polarity, vessel remodeling, and the mechanical phenotype and stiffness of blood vessels (Nicoli et al. 2010; Collins et al. 2014; Baeyens et al. 2016). Because of the ability to manipulate blood flow while performing live imaging, the use of zebrafish has been instrumental in aiding the understanding of how ECs temporally respond to hemodynamic forces to modulate vessel morphogenesis.

2.4.1 Modulation of Endothelial Cell Polarity by Blood Flow

ECs exhibit a front-rear polarity during migration whereby the Golgi apparatus is positioned ahead of the nucleus (Franco et al. 2015; Kwon et al. 2016). However, this polarity shifts upon the onset of blood flow. Live imaging of ECs of zebrafish ISVs, DA, and PCV revealed that the Golgi shifts its position so that it is downstream of or against the flow direction (Franco et al. 2015; Kwon et al. 2016). Interestingly, EC polarity is less prominent in vessels of venous origin, probably because of lower blood flow (Kwon et al. 2016).

2.4.2 Lumen Formation and Maintenance Depends on Blood Flow

The expansion of apical membranes by inverse blebbing during lumen formation is highly dependent on blood flow. When blood flow in the lumenizing vessel segment is decreased by slowing the heart rate or disrupted by ablating its connection to the parental vessel carrying blood flow, apical membrane blebbing ceases and lumen expansion stalls (Gebala et al. 2016). Furthermore, the continued presence of blood flow or pressure is critical in keeping the lumen open (Kochhan et al. 2013).

Blood flow additionally regulates endothelial gene expression profiles that contribute to the maintenance of vessel lumen. It negatively regulates the expression of the pro-angiogenic chemokine, *cxcr4a*, to convert ECs from an active to a more quiescent phenotype (Bussmann et al. 2011) and induces cytoplasmic to nuclear localization of Yes-Activated Protein 1 (Yap1), a transcriptional co-regulator that binds to enhancer elements through TEA domain (TEAD) factors downstream of Hippo signaling (Panciera et al. 2017) to promote transcriptional activity of genes that contribute to the maintenance of lumenized blood vessels (Nakajima et al. 2017). The localization of Yap1 is regulated by its association with angiomotins which, upon the onset of blood flow, preferentially binds to actin cytoskeleton and releases YAP. In zebrafish mutants that lack *yap1* expression, there is increased vessel stenosis and retraction in several vessel plexi including the DLAV and cerebellar central artery (Nakajima et al. 2017). However, it remains unclear which genes operate downstream of Yap1 to stabilize perfused blood vessels.

2.4.3 Hemodynamic Forces Regulate Vessel Diameter and Size

During development, the DA and PCV of the zebrafish display a biphasic response to increases in blood flow (Sugden et al. 2017). Between 24 and 48 hours post fertilization (hpf), the increase in cardiac output induces outward remodeling of the axial vessels so that their diameter increases. This is supported by the findings that decreases in blood flow by pharmacological inhibition of heart contraction reduces the diameter of the DA (Baeyens et al. 2015). Between 48 and 72 hpf, a second phase of remodeling occurs with the constriction of the DA, a process that is dependent on EC shape changes whereby ECs transform from a rounded to a more elongated shape while keeping the surface area and perimeter constant (Sugden et al. 2017). Such shape changes within a tube would induce a narrower tube. The flow-induced shape change is dependent on the activity of endoglin, a receptor involved in the TGFβbeta/BMP pathway (Sugden et al. 2017). ECs deficient in *endoglin* expression fail to respond to increases in hemodynamic forces so that vessels become enlarged, leading to patterning defects such as arterial-venous shunts. Another molecule that regulates vessel diameter is Flt4 (or Vegfr3). Progressive decrease in *Flt4* expression reduces the diameter of the DA in a Vegfc-independent manner (Baeyens et al. 2015).

2.4.4 Role of Hemodynamic Forces on Vessel Formation and Remodeling

Although EC differentiation and the initial vascular patterning of many tissues are largely independent on blood flow, the onset of circulation is required for the subsequent remodeling of primitive vascular plexi and the development of some blood vessels.

In the zebrafish, the fifth and sixth aortic arches (AA) connects the aortic sac to the lateral dorsal aorta to transport blood from the heart to the trunk and tail (Anderson et al. 2008). The formation of the fifth AA is dependent on blood flow-induced expression of *klf2a*, which in turn activates endothelial-specific microRNA, *mir-126*, to activate Vegf signaling that is essential for AA development (Nicoli et al. 2010). Hemodynamic forces are also required for the proper development of the CVP, a process that entails EC sprouting. The inhibition of blood flow and lowering of blood viscosity at the primitive heart stage impair the morphogenesis of the CVP by decreasing EC number, sprouting and vascular loops so that the plexus remains immature (Goetz et al. 2014).

Once formed, a primitive vascular plexus can become remodeled by vessel pruning into a more refined network that permits efficient blood flow. It is becoming increasing evident that hemodynamic forces determine which vessel segments should undergo pruning. Chen et al described the process of pruning to begin with vessel thinning, followed by vessel collapse and finally, elimination of the vessel segment (Chen et al. 2012). By carefully quantifying blood flow in many vessel segments of the zebrafish midbrain vasculature, they found that vessels that become pruned display decreased blood flow velocity and shear stress as well as bi-directional blood flow prior to pruning and have different flow characteristics from unpruned segments. Pharmacological elevation or suppression of blood flow decreases or increases the frequency of vessel pruning, respectively (Chen et al. 2012; Kochhan et al. 2013). Notably, single-cell imaging revealed that vessel pruning is driven by Rac1-mediated EC migration (Chen et al. 2012). These experiments suggest that increasing flow asymmetry between juxtaposed vessel segments triggers vessel regression. While the vessel segment experiencing high flow becomes stabilized, the segment with the lowest flow regresses (Chen et al. 2012; Kochhan et al. 2013) to finally shape a hierarchical and efficient vascular network.

2.4.5 Mechanosensors of Hemodynamic Forces

How are hemodynamic forces in the vessel lumen sensed and transduced into biochemical signals and cellular responses in ECs? In the zebrafish, the primary cilia has been demonstrated to transduce subtle changes in blood flow and viscosity into differential calcium levels in ECs through the calcium-permeable channel PKD2 (Goetz et al. 2014). However, the role of cilia as a mechanotranducer of hemodynamic forces may be limited to early phases of blood vessel development or regions with low shear forces since high shear stress can disassemble cilia (Iomini et al. 2004) and cilia are almost absent in the caudal artery and vein by 48 hpf (Goetz et al. 2014). Given that ECs must still be able to respond to changes in hemodynamic forces, it is likely that other cellular structures or molecules serve as mechanosensors or machanotransducers of blood flow to regulate blood vessel homeostasis. One such candidate is the calcium channel, Piezo1, which in the mouse has been reported to sense shear stress and to induce calcium influx in ECs to drive blood

vessel remodeling (Li et al. 2014). However, its function in EC mechanobiology in the zebrafish has yet to be revealed. Additionally, the receptors, VEGFR2 and VEGFR3, the junctional molecules, VE-cadherin, PECAM-1 and vinculin, the transmembrane proteins, heparin sulfate proteoglycan and syndecan 4, and the intermediate filament, vimentin, have been reported to transduce hemodynamic forces to biochemical and cell morphological changes in ECs in culture (Tzima et al. 2005; Grashoff et al. 2010; Conway et al. 2013; Baeyens et al. 2014; Coon et al. 2015). In particular, VEGFR3 has been shown to monitor endothelial fluid shear stress set point to mediate outward or inward remodeling of blood vessels to adjust lumen diameter in the zebrafish (Baeyens et al. 2015). However, it remains elusive how these mechanosensory complexes sense alterations in blood flow to modulate EC responses.

2.5 Conclusions

In recent years, the zebrafish has been invaluable in providing insights into the dynamics of EC behavior during blood vessel formation and remodeling. Although we have gained a better understanding of the cellular principles of blood vessel morphogenesis, it still unclear how ECs communicate with each other to coordinate their actions. Another challenge is to understand how endothelial membrane and junction plasticity are molecularly regulated at distinct steps of vessel morphogenesis. Given that these are dynamic events that are spatially and temporally regulated, the zebrafish will continue to be instrumental in understanding the molecular and mechanical regulation of blood vessel morphogenesis.

Acknowledgments I would like to thank Henry Belting for critical reading of the manuscript. I apologize to authors whose work in this research area was not cited due to space restrictions.

References

Adams RH, Alitalo K (2007) Molecular regulation of angiogenesis and lymphangiogenesis. Nat Rev Mol Cell Biol 8:464–478

Anderson MJ, Pham VN, Vogel AM, Weinstein BM, Roman BL (2008) Loss of unc45a precipitates arteriovenous shunting in the aortic arches. Dev Biol 318:258

Aydogan V, Lenard A, Denes AS, Sauteur L, Belting H-G, Affolter M (2015) Endothelial cell division in angiogenic sprouts of differing cellular architecture. Biol Open 4:1259

Baeyens N, Mulligan-Kehoe MJ, Corti F, Simon DD, Ross TD, Rhodes JM, Wang TZ, Mejean CO, Simons M, Humphrey J, Schwartz MA (2014) Syndecan 4 is required for endothelial alignment in flow and atheroprotective signaling. Proc Natl Acad Sci 111:17308

Baeyens N, Nicoli S, Coon BG, Ross TD, Van den Dries K, Han J, Lauridsen HM, Mejean CO, Eichmann A, Thomas J-L, Humphrey JD, Schwartz MA (2015) Vascular remodeling is governed by a VEGFR3-dependent fluid shear stress set point. elife 4:1

Baeyens N, Bandyopadhyay C, Coon BG, Yun S, Schwartz MA (2016) Endothelial fluid shear stress sensing in vascular health and disease. J Clin Invest 126:821

Blaser H, Reichman-Fried M, Castanon I, Dumstrei K, Marlow FL, Kawakami K, Solnica-Krezel L, Heisenberg C-P, Raz E (2006) Migration of zebrafish primordial germ cells: a role for myosin contraction and cytoplasmic flow. Dev Cell 11:613

Blum Y, Belting H-G, Ellertsdottir E, Herwig L, Lüders F, Affolter M (2008) Complex cell rearrangements during intersegmental vessel sprouting and vessel fusion in the zebrafish embryo. Dev Biol 316:312

Bussmann J, Wolfe SA, Siekmann AF (2011) Arterial-venous network formation during brain vascularization involves hemodynamic regulation of chemokine signaling. Development 138:1717

Charras GT (2008) A short history of blebbing. J Microsc 231:466

Chen Q, Jiang L, Li C, Hu D, J-w B, Cai D, J-l D (2012) Haemodynamics-driven developmental pruning of brain vasculature in zebrafish. PLoS Biol 10:e1001374

Collins C, Osborne LD, Guilluy C, Chen Z, O'Brien ET, Reader JS, Burridge K, Superfine R, Tzima E (2014) Haemodynamic and extracellular matrix cues regulate the mechanical phenotype and stiffness of aortic endothelial cells. Nat Commun 5:3984

Conway DE, Breckenridge MT, Hinde E, Gratton E, Chen CS, Schwartz MA (2013) Fluid shear stress on endothelial cells modulates mechanical tension across VE-cadherin and PECAM-1. Curr Biol 23(11):1024–1030

Coon BG, Baeyens N, Han J, Budatha M, Ross TD, Fang JS, Yun S, Thomas J-L, Schwartz MA (2015) Intramembrane binding of VE-cadherin to VEGFR2 and VEGFR3 assembles the endothelial mechanosensory complex. J Cell Biol 208:975

Costa G, Harrington KI, Lovegrove HE, Page DJ, Chakravartula S, Bentley K, Herbert SP (2016) Asymmetric division coordinates collective cell migration in angiogenesis. Nat Cell Biol 18:1292

Fraccaroli A, Franco CA, Rognoni E, Neto F, Rehberg M, Aszodi A, Wedlich-Söldner R, Pohl U, Gerhardt H, Montanez E (2012) Visualization of endothelial actin cytoskeleton in the mouse retina. PLoS One 7:e47488

Franco CA, Jones ML, Bernabeu MO, Geudens I, Mathivet T, Rosa A, Lopes FM, Lima AP, Ragab A, Collins RT, Phng L-K, Coveney PV, Gerhardt H (2015) Dynamic endothelial cell rearrangements drive developmental vessel regression. PLoS Biol 13:e1002125

Gebala V, Collins R, Geudens I, Phng L-K, Gerhardt H (2016) Blood flow drives lumen formation by inverse membrane blebbing during angiogenesis in vivo. Nat Cell Biol 18:443

Gerhardt H, Golding M, Fruttiger M, Ruhrberg C, Lundkvist A, Abramsson A, Jeltsch M, Mitchell C, Alitalo K, Shima D, Betsholtz C (2003) VEGF guides angiogenic sprouting utilizing endothelial tip cell filopodia. J Cell Biol 161:1163

Goetz JG, Steed E, Ferreira RR, Roth S, Ramspacher C, Boselli F, Charvin G, Liebling M, Wyart C, Schwab Y, Vermot J (2014) Endothelial cilia mediate low flow sensing during zebrafish vascular development. Cell Rep 6:799

Grashoff C, Hoffman BD, Brenner MD, Zhou R, Parsons M, Yang MT, McLean MA, Sligar SG, Chen CS, Ha T, Schwartz MA (2010) Measuring mechanical tension across vinculin reveals regulation of focal adhesion dynamics. Nature 466:263. Nature Publishing Group

Herwig L, Blum Y, Krudewig A, Ellertsdottir E, Lenard A, Belting H-G, Affolter M (2011) Distinct cellular mechanisms of blood vessel fusion in the zebrafish embryo. Current Biology: CB 21:1942

Hultin S, Zheng Y, Mojallal M, Vertuani S, Gentili C, Balland M, Milloud R, Belting H-G, Affolter M, Helker CSM, Adams RH, Herzog W, Uhlén P, Majumdar A, Holmgren L (2014) AmotL2 links VE-cadherin to contractile actin fibres necessary for aortic lumen expansion. Nat Commun 5:3743

Iomini C, Tejada K, Mo W, Vaananen H, Piperno G (2004) Primary cilia of human endothelial cells disassemble under laminar shear stress. J Cell Biol 164:811

Jakobsson L, Franco CA, Bentley K, Collins RT, Ponsioen B, Aspalter IM, Rosewell I, Busse M, Thurston G, Medvinsky A, Schulte-Merker S, Gerhardt H (2010) Endothelial cells dynamically

compete for the tip cell position during angiogenic sprouting. Nat Cell Biol 12(10):943–953. Nature Publishing Group
Kamei M, Brian Saunders W, Bayless KJ, Dye L, Davis GE, Weinstein BM (2006) Endothelial tubes assemble from intracellular vacuoles in vivo. Nat Cell Biol 442:453
Kochhan E, Lenard A, Ellertsdottir E, Herwig L, Affolter M, Belting H-G, Siekmann AF (2013) Blood flow changes coincide with cellular rearrangements during blood vessel pruning in zebrafish embryos. PLoS One 8:e75060
Kurz H, Gärtner T, Eggli PS, Christ B (1996) First blood vessels in the avian neural tube are formed by a combination of dorsal angioblast immigration and ventral sprouting of endothelial cells. Dev Biol 173:133
Kwon H-B, Wang S, Helker CSM, Rasouli SJ, Maischein H-M, Offermanns S, Herzog W, Stainier DYR (2016) In vivo modulation of endothelial polarization by Apelin receptor signalling. Nat Commun 7:11805
Lawson ND, Weinstein BM (2002) In vivo imaging of embryonic vascular development using transgenic zebrafish. Dev Biol 248:307
Lenard A, Ellertsdottir E, Herwig L, Krudewig A, Sauteur L, Belting H-G, Affolter M (2013) In vivo analysis reveals a highly stereotypic morphogenetic pathway of vascular anastomosis. Dev Cell 25:492
Lenard A, Daetwyler S, Betz C, Ellertsdottir E, Belting H-G, Huisken J, Affolter M (2015) Endothelial cell self-fusion during vascular pruning. PLoS Biol 13:e1002126
Li J, Hou B, Tumova S, Muraki K, Bruns A, Ludlow MJ, Sedo A, Hyman AJ, McKeown L, Young RS, Yuldasheva NY, Majeed Y, Wilson LA, Rode B, Bailey MA, Kim HR, Fu Z, Carter DAL, Bilton J, Imrie H, Ajuh P, Dear TN, Cubbon RM, Kearney MT, Prasad RK, Evans PC, Ainscough JFX, Beech DJ (2014) Piezo1 integration of vascular architecture with physiological force. Nature 515(7526):279–282. Nature Publishing Group
Nakajima H, Yamamoto K, Agarwala S, Terai K, Fukui H, Fukuhara S, Ando K, Miyazaki T, Yokota Y, Schmelzer E, Belting H-G, Affolter M, Lecaudey V, Mochizuki N (2017) Flow-dependent endothelial YAP regulation contributes to vessel maintenance. Dev Cell 40:523. Elsevier Inc
Nicoli S, Standley C, Walker P, Hurlstone A, Fogarty KE, Lawson ND (2010) MicroRNA-mediated integration of haemodynamics and Vegf signalling during angiogenesis. Nature 464:1196
Paluch EK, Raz E (2013) The role and regulation of blebs in cell migration. Curr Opin Cell Biol 25:582
Panciera T, Azzolin L, Cordenonsi M, Piccolo S (2017) Mechanobiology of YAP and TAZ in physiology and disease. Nat Rev Mol Cell Biol 18:758
Pelton JC, Wright CE, Leitges M, Bautch VL (2014) Multiple endothelial cells constitute the tip of developing blood vessels and polarize to promote lumen formation. Development 141:4121
Phng LK, Stanchi F, Gerhardt H (2013) Filopodia are dispensable for endothelial tip cell guidance. Development 140:4031
Phng L-K, Gebala V, Bentley K, Philippides A, Wacker A, Mathivet T, Sauteur L, Stanchi F, Belting H-G, Affolter M, Gerhardt H (2015) Formin-mediated actin polymerization at endothelial junctions is required for vessel lumen formation and stabilization. Dev Cell 32:123
Pollard TD, Cooper JA (2009) Actin, a central player in cell shape and movement. Science 326:1208
Potente M, Makinen T (2017) Vascular heterogeneity and specialization in development and disease. Nat Rev Mol Cell Biol 18:477. Nature Publishing Group
Ridley AJ (2011) Life at the leading edge. Cell 145:1012. Elsevier Inc
Sauteur L, Krudewig A, Herwig L, Ehrenfeuchter N, Lenard A, Affolter M, Belting H-G (2014) Cdh5/VE-cadherin promotes endothelial cell Interface elongation via cortical actin polymerization during Angiogenic sprouting. Cell Rep 9:504. The Authors
Sauteur L, Affolter M, Belting H-G (2017) Distinct and redundant functions of Esama and VE-cadherin during vascular morphogenesis. Development 144:1554

Siekmann AF, Lawson ND (2007) Notch signalling limits angiogenic cell behaviour in developing zebrafish arteries. Nature 445:781

Sugden WW, Meissner R, Aegerter-Wilmsen T, Tsaryk R, Leonard EV, Bussmann J, Hamm MJ, Herzog W, Jin Y, Jakobsson L, Denz C, Siekmann AF (2017) Endoglin controls blood vessel diameter through endothelial cell shape changes in response to haemodynamic cues. Nat Cell Biol 19:653

Tzima E, Irani-Tehrani M, Kiosses WB, Dejana E, Schultz DA, Engelhardt B, Cao G, DeLisser H, Schwartz MA (2005) A mechanosensory complex that mediates the endothelial cell response to fluid shear stress. Nature 437:426

Wakayama Y, Fukuhara S, Ando K, Matsuda M, Mochizuki N (2015) Cdc42 mediates bmp-induced sprouting angiogenesis through Fmnl3-driven assembly of endothelial Filopodia in zebrafish. Dev Cell 32:109. Elsevier Inc

Wang Y, Kaiser MS, Larson JD, Nasevicius A, Clark KJ, Wadman SA, Roberg-Perez SE, Ekker SC, Hackett PB, McGrail M, Essner JJ (2010) Moesin1 and Ve-cadherin are required in endothelial cells during in vivo tubulogenesis. Development 137:3119

Wiley DM, Kim J-D, Hao J, Hong CC, Bautch VL, Jin S-W (2011) Distinct signalling pathways regulate sprouting angiogenesis from the dorsal aorta and the axial vein. Nat Cell Biol 13:686

Xu C, Hasan SS, Schmidt I, Rocha SF, Pitulescu ME, Bussmann J, Meyen D, Raz E, Adams RH, Siekmann AF (2014) Arteries are formed by vein-derived endothelial tip cells. Nat Commun 5:5758

Yu JA, Castranova D, Pham VN, Weinstein BM (2015) Single-cell analysis of endothelial morphogenesis in vivo. Development 142:2951

Chapter 3
Development of Hematopoietic Stem Cells in Zebrafish

Isao Kobayashi

Abstract Hematopoietic stem cells (HSCs) are a rare population of cells with the remarkable abilities to both self-renew and differentiate into all types of mature blood cells. Understanding of the developmental mechanisms of HSCs is of great importance to instruct and expand HSCs from pluripotent precursors, such as induced pluripotent stem cells (iPSCs). The zebrafish is a unique vertebrate model in which numerous elegant experimental approaches can be applied to the study of HSC development, including live-imaging, chemical and genetic screening, and genome editing. HSCs are specified from a shared vascular precursor, the angioblast, and arise directly from the ventral floor of the dorsal aorta. HSCs then migrate to a transient hematopoietic organ, the caudal hematopoietic tissue, where microenvironmental niche cells promote the expansion of HSCs prior to the colonization of the kidney, the final adult hematopoietic organ in zebrafish. Over the past decade, a number of intrinsic and extrinsic signaling molecules involved in the specification, maintenance, migration, and proliferation of HSCs have been identified in the zebrafish embryo. Importantly, despite evolutional divergence, the genetic programs governing HSC development are highly conserved among vertebrates, indicating that studies in zebrafish may be translated to regenerative medicine using human iPSCs. This chapter highlights the current knowledge and recent advances regarding the cellular origin and molecular regulation of HSC development in zebrafish.

Keywords Hematopoietic stem cell · Hemogenic endothelium · Angioblast · Dorsal aorta · Caudal hematopoietic tissue · Definitive hematopoiesis

I. Kobayashi (✉)
Faculty of Biological Science and Technology, Institute of Science and Engineering, Kanazawa University, Kakumamachi, Kanazawa, Ishikawa, Japan
e-mail: ikobayashi@se.kanazawa-u.ac.jp

H. Hirata, A. Iida (eds.), *Zebrafish, Medaka, and Other Small Fishes*,
https://doi.org/10.1007/978-981-13-1879-5_3

3.1 Introduction

3.1.1 General

Hematopoietic stem cells (HSCs) are self-renewing multipotent cells that can generate all mature blood cells throughout the lifespan of an individual (Weissman 2000). Due to the limited lifespan of mature blood cells, HSCs must be continually available to replace cells lost in circulation. Despite this demand, most adult HSCs present in the bone marrow are quiescent and divide rarely under homeostatic conditions. This is probably to prevent the depletion of the stem cell pool or to protect HSCs from myelotoxic injury. Instead, hematopoietic progenitor cells (HPCs), which are the progeny of HSCs that have the limited or no self-renewal ability, rapidly proliferate and differentiate to satisfy the requirements for new mature blood cells (Cheshier et al. 1999; Walkley et al. 2005). HSCs in the bone marrow interact with other cell types known as niche cells such as osteoblasts, endothelial cells, and stromal cells. These niche cells tightly regulate the balance between the quiescence, self-renewal, and differentiation of HSCs through essential signaling molecules called "niche factors" (Ehninger and Trumpp 2011; Hoggatt et al. 2016; Yu and Scadden 2016; Beerman et al. 2017). A timely response to blood cell requirements is thus largely dependent on the function of the niche under normal physiological conditions and during hematopoietic crises such as loss of blood, hemolysis, or infection.

HSCs present within adult bone marrow or newborn cord blood are by far the most widely utilized stem cells in the clinic. It is always difficult, however, to find immune-matched donors or to obtain sufficient numbers of HSCs for transplantation therapies to treat blood-related disorders (e.g., anemia, leukopenia, leukemia, etc.). Generation of HSCs from pluripotent precursors, including induced pluripotent stem cells (iPSCs), is therefore a key therapeutic aim. It is of great interest to better understand the developmental mechanisms of HSCs in the embryo because elucidation of this developmental process might provide insight into the cellular and molecular cues needed to instruct and expand HSCs from pluripotent precursors (Murry and Keller 2008).

3.1.2 Zebrafish as a Model for the Study of HSC Development

Almost two decades ago, the zebrafish emerged as a new genetic model to analyze hematopoietic development as well as human hematopoietic diseases (Zhu and Zon 2002; Bradbury 2004). Its embryos are externally fertilized and transparent, enabling in vivo live-imaging analysis, which can capture the dynamics of HSC development, including HSC birth, migration, and cell division. The high fecundity and rapid generation time of zebrafish make phenotype-based forward genetic screening feasible, permitting the discovery of novel signaling pathways that control

hematopoietic development (de Jong and Zon 2005). Moreover, the recent advent of genome-editing technologies by the CRISPR/Cas9 system will further promote the investigation of the spatial and temporal regulatory mechanisms within the specific cell types (Jao et al. 2013; Gagnon et al. 2014; Hisano et al. 2015; Shah et al. 2015; Kawahara et al. 2016). Importantly, despite the evolutional divergence, the genetic programs governing hematopoiesis are highly conserved between mammals and fish. Our understanding of the regulatory mechanisms of HSC development has been greatly improved by the zebrafish system within the last decade. This chapter discusses this conservation and highlights the current knowledge and recent advances regarding the cellular origin and molecular regulation of HSC development in the zebrafish embryo.

3.2 Comparison of Hematopoietic Development between the Mouse and Zebrafish

3.2.1 Hematopoietic Development in the Mouse

Hematopoietic development in vertebrates can be characterized by two waves of hematopoiesis: the primitive and definitive waves. In the mouse, the primitive wave is initiated in the extra-embryonic yolk sac (YS), where primitive erythrocytes are generated from unipotent hematopoietic precursors at day 7.5 post-coitum (E7.5) (Dzierzak and Medvinsky 1995; Palis et al. 1999). These blood islands consist of nucleated erythrocytes expressing embryonic globin genes (Stamatoyannopoulos 2005). Macrophages and megakaryocytes are also generated in the YS during the primitive wave (Shepard and Zon 2000; Tober et al. 2007). Primitive hematopoiesis is transient and replaced by the definitive wave during embryonic stages.

Multilineage definitive hematopoiesis is first initiated by erythro-myeloid progenitors (EMPs), which emerge in the YS and placenta at E9.5 and have the potential to differentiate into both erythroid and myeloid lineages but not the lymphoid lineage (Palis et al. 1999; Bertrand et al. 2005). Erythrocytes derived from EMPs are enucleated and express adult globin genes, while the embryonic globin gene is weakly expressed (McGrath et al. 2011). The intra-embryonic aorta-gonad-mesonephros (AGM) region gives rise to HSCs with the potential to generate all blood lineages including the lymphoid lineage (Müller et al. 1994; Cumano et al. 1996; Godin and Cumano 2002; Medvinsky and Dzierzak 1996). Lineage-tracing studies revealed that HSCs arise from a subset of specialized endothelial cells present in the ventral floor of the dorsal aorta (DA), termed hemogenic endothelial cells (HECs), via the endothelial-to-hematopoietic transition (EHT) (Zovein et al. 2008; Boisset et al. 2010). HSC formation also occurs in the umbilical and vitelline arteries, placenta, and YS (de Bruijn et al. 2000; Gekas et al. 2005; Ottersbach and Dzierzak 2005; Samokhvalov et al. 2007). Hematopoietic stem/progenitor cells (HSPCs) arising from the DA at E10.5 initially form the intra-aortic hematopoietic

clusters (IAHCs), which contain cells expressing both hematopoietic (CD41 and CD45) and endothelial (CD31 and VE-cadherin) markers (Fraser et al. 2002; de Bruijn et al. 2002; North et al. 2002). HSPCs isolated at E10.5 cannot reconstitute adult hematopoiesis without ex vivo organ culture, whereas HSPCs present at E11.5 can engraft the adult niche (Taoudi et al. 2008; Rybtsov et al. 2011). Thus, developing HSCs within IAHCs (pre-HSCs) require further maturation that potentiates their engraftment and survival in future hematopoietic niches. After leaving the IAHCs, HSCs migrate to the fetal liver (FL), the main hematopoietic organ in mid-late gestation. In contrast to adult HSCs in the bone marrow, HSCs in the FL are largely cycling and frequently undergo symmetric cell divisions, in which both daughter cells retain self-renewal capacity and multipotency, resulting in a marked expansion of the HSC pool (Ema and Nakauchi 2000; Lessard et al. 2004; Khan et al. 2016). Shortly before birth (E17), HSCs finally seed the bone marrow, which becomes the major site of hematopoiesis in the adult stage.

3.2.2 Hematopoietic Development in the Zebrafish

Hematopoiesis in zebrafish also occurs in two waves, but these waves occur in distinct locations compared to mammals. The primitive wave in the zebrafish embryo is initiated in the intra-embryonic lateral plate mesoderm (LPM), which is the bilateral stripes that flank the somite during early somitogenesis (Liao et al. 1998; Thompson et al. 1998). The anterior LPM (ALPM) is the major site of primitive myelopoiesis, whereas the posterior LPM (PLPM) contains mostly erythroid precursors and a few myeloid precursors (Detrich et al. 1995; Warga et al. 2009; Galloway and Zon 2003). The PLPM also gives rise to angioblasts, a common precursor of endothelial cells and definitive HSPCs (Dooley et al. 2005; Patterson et al. 2005). At around 15 h post-fertilization (hpf), cells in the PLPM begin to migrate axially along the ventral domain of the somite and reach the midline to form the intermediate cell mass (ICM). The ICM is the major site of primitive erythropoiesis and has a similar cellular architecture to the mammalian YS blood islands (Davidson and Zon 2004; Hsia and Zon 2005; de Jong and Zon 2005). Around the same time, angioblasts also reach the midline and form the vascular cord, which subsequently develops into the lumenal DA and posterior cardinal vein (PCV) (Jin et al. 2005).

As in mammals, definitive hematopoiesis in the zebrafish embryo is initiated by EMPs (Bertrand et al. 2007). EMPs can be detected as *lmo2*$^{+}$ *gata1*$^{+}$ cells at around 24 hpf in the posterior blood island (PBI), which is located in the anterior-ventral tail. Shortly before the initiation of blood circulation (23 hpf), specified HECs can be observed in the ventral floor of the DA (Wilkinson et al. 2009), the AGM equivalent in zebrafish. In vivo live-imaging has directly shown a number of HSPCs to bud off from the ventral floor of the DA and enter the circulation at around 30–54 hpf (Bertrand et al. 2010; Kissa and Herbomel 2010). These nascent HSPCs express both hematopoietic (*cmyb* and *cd41*) and endothelial (*kdrl*) markers (Bertrand et al. 2010), similar to pre-HSCs in the mouse embryo (Fraser et al. 2002; de Bruijn et al. 2002;

North et al. 2002). After arising from the DA, HSCs migrate via the circulation to the caudal hematopoietic tissue (CHT), which is a transient hematopoietic organ that is equivalent to the FL in mammals (Murayama et al. 2006; Jin et al. 2007; Blaser et al. 2017). HSPCs in the CHT actively proliferate and differentiate (Tamplin et al. 2015). Very recently, a clonal fate mapping study using *drl:CreER*^{T2}; *ubi:Zebrabow* double-transgenic animals, which allow the labeling of individual HSCs and their progeny with a unique color, demonstrated that approximately 21 HSCs arise from the DA in the zebrafish embryo. These initial cells expand to 30 HSCs during the embryonic stage (Henninger et al. 2017). Expanded HSCs then move to the kidney marrow to sustain lifelong hematopoiesis or to the thymus, where some HSCs differentiate into T lymphocytes (Davidson and Zon 2004; de Jong and Zon 2005).

3.3 Molecular Regulation of HSC Specification in the Zebrafish Embryo

3.3.1 Transcriptional Regulation of HSC Specification

HSCs originate from a shared vascular precursor, the angioblast. Although angioblasts emerge in both the ALPM and PLPM, HSCs are specified only from endothelial cells of the trunk DA, suggesting that angioblasts in the PLPM are pre-patterned to respond to specification signals, or that HSC specification signals are spatially restricted to the trunk area of the embryo. A number of intrinsic and extrinsic signaling molecules that are required to establish HSC fate have been identified in the zebrafish embryo (Clements and Traver 2013). The transcription factor Runx1 (also known as AML1) is required for definitive but not primitive, hematopoiesis in both mammals and zebrafish (Chen et al. 2009; Kalev-Zylinska et al. 2002; Gering and Patient 2005). The expression of *runx1* is detected in the ventral floor of the DA as early as 23 hpf in the zebrafish embryo (Burns et al. 2002; Wilkinson et al. 2009). Loss of *runx1* in the zebrafish embryo resulted in the burst of HECs in the ventral floor of the DA and loss of definitive HSPCs (Kissa and Herbomel 2010), indicating that Runx1 plays an essential role in the initiation of EHT. Since *runx1* expression is very specific to HECs/HSPCs within the DA, *runx1* is widely utilized as a marker to distinguish HECs/HSPCs from other endothelial cells or differentiated blood cells in the zebrafish embryo.

The basic helix-loop-helix transcription factor stem-cell leukemia (Scl, also known as Tal1) is essential for both primitive and definitive hematopoiesis as well as the vascular formation (Patterson et al. 2005; Dooley et al. 2005). In zebrafish, two distinct isoforms of Scl, Scl-α and Scl-β, are produced based on an alternative promoter site (Qian et al. 2007). Although these two isoforms are functionally redundant in primitive erythropoiesis, their roles in definitive hematopoiesis are divergent. The full-length isoform, *scl-α*, is expressed by primitive erythroid precursors in the ICM and in HECs after 36 hpf, whereas the N-terminal-truncated

isoform, *scl-β*, is expressed in HECs at an earlier stage, probably before 22 hpf. Morpholino knockdown of *scl-β* resulted in the reduction of *runx1* expression in the DA, while loss of *runx1* did not affect the expression of *scl-β* in the DA, suggesting that Scl-β acts as upstream of Runx1 in HECs. In contrast, loss of Scl-α did not affect the expression of *runx1* in the DA although the number of HSPCs in the CHT was largely reduced at 3 days post-fertilization (dpf). These data suggest that Scl-β is required for HSC specification via the regulation of *runx1* expression in HECs, whereas Scl-α plays an essential role in the maintenance of HSCs after the specification process (Qian et al. 2007; Zhen et al. 2013).

Ets variant 2 (Etv2, also known as Etsrp) is a critical regulator of vascular development and primitive myelopoiesis in zebrafish (Sumanas and Lin 2006; Sumanas et al. 2008). The expression of *etv2* is first detected in both the ALPM and PLPM as early as 11 hpf and later in the whole vasculature (Sumanas and Lin 2006). Morpholino knockdown of *etv2* induced down-regulation of *scl-α*, *scl-β*, and *fli1*, an ETS domain transcription factor expressed in the LPM and vascular endothelium (Thompson et al. 1998; Lawson and Weinstein 2002), resulting in defective blood vessel formation and the complete loss of definitive HSPCs (Sumanas and Lin 2006; Ren et al. 2010). The vascular defect of *etv2* morphants could be rescued by injection of *fli1* mRNA. In addition, injection of *scl-β* mRNA along with *fli1* mRNA rescued *runx1* expression in the DA in *etv2* morphants, suggesting that Etv2 activates the expression of both *fli1* and *scl-β* to establish HSC fate in the angioblast (Ren et al. 2010). Surprisingly, injection of *scl-α* mRNA alone partially restored both the vasculature and *runx1* expression in *etv2* morphants (Ren et al. 2010), despite the dispensable role of Scl-α in HSC specification (Zhen et al. 2013). One possible explanation is that the specification of angioblasts, which occurs prior to HSC specification, requires a specific level of Scl-α expression, and this requirement can be partially compensated for by Scl-β. Scl-α overexpression may also be able to compensate for the loss of Scl-β, restoring the HSC fate in the angioblast. Taken together, these studies demonstrate that Etv2 plays an essential role in both the angioblast specification and HSC specification via the regulation of Scl-α, Scl-β, and Fli1.

Gata2 plays an important role in HSC development, proliferation, and survival as well as the vascular formation in mammals (Tsai et al. 1994; Tsai and Orkin 1997; Lim et al. 2012; Johnson et al. 2012; de Pater et al. 2013; Gao et al. 2013). Due to genome duplication, two paralogues of *gata2* exist in the zebrafish: *gata2a* and *gata2b*. In embryonic stages, *gata2a* is expressed in the LPM and the trunk vasculature, whereas the expression of *gata2b* is more restricted to HECs/HSPCs (Detrich et al. 1995; Brown et al. 2000; Butko et al. 2015). While vascular formation was intact, loss of Gata2b led to the down-regulation of *runx1* and *cmyb*, a downstream target gene of Runx1 that is essential for the maintenance of HSCs (Soza-Ried et al. 2010; Zhang et al. 2011). Enforced expression of *runx1* in Gata2b-deficient embryos rescued the expression of *cmyb* in the DA (Butko et al. 2015), indicating that Gata2b is required for HSC specification through the regulation of Runx1. In contrast, deficiency in *gata2a* led to severe defects in vascular formation

and circulation (Zhu et al. 2011; Butko et al. 2015). Although it remains unclear if zebrafish Gata2 proteins also play a role in HSC proliferation and survival as has been shown in the mouse (Tsai and Orkin 1997; de Pater et al. 2013), it is tempting to speculate that duplication of the *gata2* locus in zebrafish might have led to a functional separation between the roles of Gata2 in vasculogenesis and hematopoiesis.

3.3.2 Regulation of HSC Specification by Notch Signaling

Notch signaling is involved in the patterning of the trunk vasculature and HECs. Canonical Notch signaling is initiated when a membrane-bound Notch ligand (Delta or Jagged) on the signal-sending cell interacts directly with a Notch receptor on the signal-receiving cell. After binding to a Notch ligand, the Notch receptor is cleaved first by ADAM TACE metalloproteases at the S2 site, then by γ-secretase at the S3 site, which releases the Notch intracellular domain (NICD) that translocates to the nucleus and modulates transcription of Notch target genes (Brou et al. 2000; Bozkulak and Weinmaster 2009; Mumm et al. 2000; Kopan and Ilagan. 2009). Mutation or deletion of *Mindbomb* (*Mib*), which encodes a ubiquitin ligase required for Notch signal transduction (Itoh et al. 2003; Chen and Casey Corliss 2004), resulted in the loss of HECs in both the mouse and zebrafish (Burns et al. 2005; Yoon et al. 2008). Chimeric mice generated from both wild-type and Notch1-deficient cells showed no contribution of Notch1-deficient cells to adult hematopoiesis, indicating that signaling through Notch1 is required for HSC specification in a cell autonomous manner (Hadland et al. 2004).

In zebrafish, four Notch receptor genes, *notch1a*, *1b*, *2*, and *3*, have been identified. A recent study revealed that three of these receptors, Notch1a, 1b, and 3, are independently required for HSC specification (Kim et al. 2014). All of these three *notch* genes (*notch1a*, *1b*, and *3*) are expressed in the PLPM and somite during somitogenesis and the vascular endothelium after 24 hpf. Loss of *notch1a* resulted in loss of *runx1* and *efnb2a*, a marker of the aortic endothelium, revealing the requirement for Notch1a in both HSC and aortic specification, similar to Notch1 in the mouse (Kreb et al. 2000). In contrast, loss of *notch1b* or *notch3* resulted in loss of *runx1* but did not affect *efnb2a* expression. These data suggest that Notch1b and Notch3 are required for HSC specification but are dispensable for aortic specification. Aortic *notch1b* expression is regulated in part by a zinc finger transcription factor, ecotropic viral integration site-1 (Evi1), through the phosphorylation of AKT. The Evi1–pAKT–Notch1b signaling pathway has been shown to be required cell-autonomously for HSC specification (Konantz et al. 2016). Interestingly, however, Notch3 is required non-cell autonomously for HSC specification. In Notch3-deficient embryos, enforced expression of NICD in the somite rescued the expression of *runx1* in the DA, whereas enforced expression in the vascular endothelium did not. Thus, while its target gene is still unclear, Notch3-dependent sig-

naling within the somite regulates HSC specification indirectly in the zebrafish embryo (Kim et al. 2014).

The requirement for somitic Notch ligands, Delta-C (Dlc) and Dld, in HSC specification has been shown in zebrafish (Clements et al. 2011; Kobayashi et al. 2014; Lee et al. 2014). A β-catenin-independent (non-canonical) Wnt ligand, Wnt16, is expressed within the somite during somitogenesis. Morpholino knockdown of *wnt16* reduced both *dlc* and *dld* in the somite and led to a loss of definitive HSPCs, but left aortic specification was intact. Injection of both *dlc* and *dld* mRNA along with *wnt16* morpholino was sufficient to rescue the expression of *runx1* in the DA (Clements et al. 2011). The expression of *dlc*, but not *dld*, in the somite is mediated by fibroblast growth factor (FGF) signaling. Loss of FGF signaling or *fgfr4*, which is regulated by Wnt16, inhibited the formation of HSPCs in the DA, while the defect in HSPCs in these embryos was rescuable by injection of *dlc* mRNA (Lee et al. 2014). These data suggest that Wnt16 regulates the expression of *dlc* through FGF signaling (Clements et al. 2011; Lee et al. 2014). To establish an HSC fate, angioblasts directly receive Dlc and Dld signaling from the somite (Kobayashi et al. 2014). During somitogenesis, angioblasts migrate axially along the ventral domain of the somite to reach the midline. Migrating angioblasts tightly adhere to the somite based on the interaction of two different cell adhesion molecules, junctional adhesion molecule 1a (Jam1a), and Jam2a. Loss of either Jam1a or Jam2a led to a delay in angioblast migration and reduction of *runx1* in the DA. Jam1a-deficiency had no effect on the expression of Notch receptor or ligand genes, but *runx1* expression could be restored in the absence of Jam1a through enforced expression of *dlc* or *dld*. These data suggest that the intimate contact between the angioblast and the somite by Jam1a–Jam2a binding promotes efficient Notch signal transduction from the somite to the angioblast (Kobayashi et al. 2014). Taken together, these studies suggest that the somite regulates HSC specification through the presentation of requisite Notch ligands Dlc and Dld to the angioblasts during axial migration.

A Notch ligand Jagged1 (Jag1) expressed by the aortic endothelium also plays an important role in HSC specification in both the mouse and zebrafish (Robert-Moreno et al. 2008; Espín-Palazón et al. 2014; Monteiro et al. 2016). In mice, Jag1 is required for definitive hematopoiesis through the regulation of *Gata2* expression in AGM cells, but it is not required for the establishment of arterial fate (Robert-Moreno et al. 2008). Similar to murine Jag1, zebrafish Jag1a is involved in HSC specification but not arterial specification (Espín-Palazón et al. 2014; Monteiro et al. 2016). The expression of *jag1a* in the DA is regulated in part by tumor necrosis factor α (TNF-α) and TNF receptor 2 (TNFR2) signaling (Espín-Palazón et al. 2014), a signaling pathway that is associated with the regulation of inflammation and immunity. Loss of TNFR2 led to a reduction in *jag1a* expression and loss of HSPCs in the DA (Espín-Palazón et al. 2014). In addition to TNF-α, transforming growth factor-β (TGF-β) is also involved in the regulation of aortic *jag1a* (Monteiro et al. 2016). TGF-β1a and TGF-β1b are produced in aortic endothelial cells, while TGF-β3 is expressed in the notochord. All these autocrine and paracrine inputs of TGF-β contribute to the expression of *jag1a* in the aortic endothelium through the activation of TGF-β receptor 2 (TGFβR2) (Monteiro et al. 2016). These data indi-

cate that Notch signal transduction within the aortic endothelium via Jag1a is also necessary for HSC specification.

In summary, angioblasts require at least two distinct inputs of Notch signaling to establish HSC fate in the zebrafish embryo: (1) Dlc and Dld from the somite and (2) Jag1a from the aortic endothelium. It remains unclear, however, whether these distinct Notch signaling events activate different downstream targets in HSC precursors and which receptor mediates each signaling event.

3.3.3 Regulatory Signaling Pathways Required for HSC Specification

The hedgehog (Hh) signaling pathway is a major regulator of cell differentiation, proliferation, and tissue polarity. Murine embryonic stem (ES) cell studies have suggested a role for Hh signaling in hematopoiesis (Maye et al. 2000; Dyer et al. 2001; Byrd et al. 2002). In zebrafish, Sonic-hedgehog (Shh) regulates the expression of vascular endothelial growth factor A (*vegfa*) in the somite (Lawson et al. 2002), and the Shh–Vegfa signaling axis has been implicated in the regulation of definitive but not primitive, hematopoiesis (Gering and Patient 2005). Treatment with an Hh inhibitor (cyclopamine) or mutation of Hh-related genes, such as *shh* or *smoothened* (*smo*), resulted in defective angioblast migration, arterial specification, and HSC specification. Similarly, inhibition of Vegf signaling also led to a reduction in *efnb2a*, *notch3*, and *runx1* expression in the DA (Gering and Patient 2005). These results suggest a model in which Shh expressed by the notochord and/or floorplate induces the expression of Vegfa in the somite, which then regulates arterial and HSC programs through the Notch signaling.

In vertebrates, multiple isoforms of Vegfa are expressed in the somite. In *Xenopus*, a short Vegfa isoform, Vegfa-122, is responsible for the expression of arterial marker genes; an intermediate isoform, Vegfa-170, is required for HSC specification (Leung et al. 2013). A recent study showed similar divergent roles for Vegfa isoforms in zebrafish (Genthe and Clements 2017). An extracellular protein R-spondin 1 (Rspo1), which is implicated in the enhancement of Wnt/β-catenin signaling, controls HSC specification through the regulation of *vegfa* and *wnt16* expression in the somite. Loss of *rspo1* resulted in the reduction of both *vegfa* and *wnt16* in the somite and loss of HSPCs. The effect of HSPCs in Rspo1-deficient embryos was rescued by injection of an intermediate isoform, *vegfa-165*, but not the short isoform, *vegfa-121* (Genthe and Clements 2017). Since somitic Vegfa controls the expression of *tgfb1a* and *tgfb1b* in the DA (Monteiro et al. 2016), it is likely that Vefga-165 regulates HSC specification through the activation of the TGF-β1/Jag1a signaling pathway.

Bone morphogenetic protein (BMP) signaling is essential for patterning the ventroposterior mesoderm of the developing embryo cooperatively with the Wnt signaling. It has been shown in zebrafish that BMP4 signaling regulates HSC specification

independently from the Vegfa and Notch signaling pathways (Wilkinson et al. 2009; Pouget et al. 2014). The expression of *bmp4* is detected in the pronephros and the ventral mesenchyme underlying the DA at around 24 hpf (Chin et al. 1997). Loss of *bmp4* led to a reduction of HECs in the DA without affecting aortic specification (Wilkinson et al. 2009). Recently, it was revealed that the expression of *bmp4* in the ventral mesenchyme is negatively regulated by FGF signaling and is involved in HSC specification (Pouget et al. 2014). When FGF signaling was inhibited by heat-induction of dominant-negative (DN) Fgfr1 at around 20 hpf, the expression of *bmp4* in the ventral mesenchyme was increased, resulting in the enhanced expression of *runx1* in the DA. Conversely, when FGF signaling was enforced by heat-induction of constitutively active Fgfr1 at around 20 hpf, the expression of *bmp4* was reduced in the ventral mesenchyme, leading to a reduction in *runx1* expression in the DA. These studies also showed that FGF signaling represses *bmp4* expression directly and indirectly via the induction of BMP antagonists Noggin2 and Gremlin1a expressed by the neighboring somite (Pouget et al. 2014).

Recently, proinflammatory signaling has been implicated in the regulation of HSC specification in both the mouse and zebrafish (Espín-Palazón et al. 2014; Sawamiphak et al. 2014; Li et al. 2014; He et al. 2015). As described in Sect. 3.3.2, TNF-α acts as upstream of the Notch ligand Jag1a to regulate HSC specification (Espín-Palazón et al. 2014). In contrast, the proinflammatory cytokine interferon-γ (IFN-γ) acts downstream of Notch and regulates HSC specification (Sawamiphak et al. 2014). Deficiency in IFN-γ or its receptor Crfb17 led to reduced *runx1* expression in the DA, while enforced expression of IFN-γ increased the number of HSPCs. Furthermore, HSPC defects caused by the inhibition of Notch signaling could be rescued by enforced production of IFN-γ. It has also been shown that IFN-γ/Crfb17 signaling activates Stat3, an atypical transducer of IFN-γ that is required for HSC development. These studies suggest that IFN-γ, controlled by Notch signaling, regulates HSC specification through the activation of Stat3 (Sawamiphak et al. 2014).

In addition to regulating many diverse functions such as cell proliferation and differentiation, adenosine signaling has recently been demonstrated to be required for HSC specification (Jing et al. 2015). The adenosine receptor A_{2b} is expressed on endothelial cells prior to HSC emergence. Loss of adenosine signaling or A_{2b} led to a reduction in *scl-β* and *runx1* expression without affecting vascular formation, while elevated adenosine signaling enhanced the production of HSPCs. Adenosine signaling activates the cyclic AMP (cAMP)–protein kinase A (PKA) pathway to promote the production of Cxcl8, a chemokine expressed by endothelial cells. Injection of *cxcl8* mRNA was sufficient to rescue defective HSPC formation in A_{2b}–deficient embryos. These results suggest that adenosine signaling in endothelial cells regulates HSC specification via the production of Cxcl8 (Jing et al. 2015).

As shown in Fig. 3.1, although a number of extrinsic signaling molecules that regulate HSC specification have been identified in the zebrafish embryo, only Notch (through Dlc, Dld, and Jag1a) and BMP4 regulate HSC programs directly in angioblasts/HECs. While the possible presence of other direct signaling molecules still cannot be excluded, the precisely timed and tuned coordination of Notch and BMP4

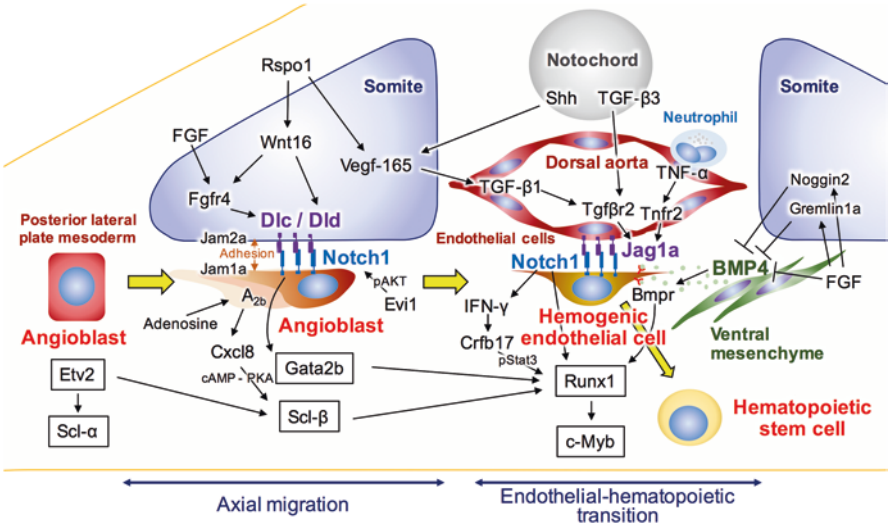

Fig. 3.1 The process of hematopoietic stem cell specification
Hematopoietic stem cells (HSCs) are specified from the angioblast, which arises in the posterior lateral plate mesoderm. Angioblasts expressing Etv2 and Scl-α axially migrate along the ventral domain of the somite to reach the midline. Angioblasts experience an initial Notch signaling event via the interaction with somitic cells during axial migration, leading to the expression of Gata2b. Angioblasts also begin to express Scl-β through the adenosine signaling to become the hemogenic endothelial cells (HECs). Within the aortic floor, HECs receive a second Notch signal from the aortic endothelial cells to drive the expression of Runx1. At almost the same time, BMP4 signaling from the ventral mesenchyme also induces Runx1 expression. Nascent Runx1^{+} HSCs then enter maturation and proliferation steps within the dorsal aorta and begin to express c-Myb. All boxed transcription factors (Etv2, Scl-α, Scl-β, Gata2b, Runx1, and c-Myb) are essential for HSC development. Among them, *scl-β*, *gata2b*, *runx1*, and *cmyb* are used as the marker for HSCs in zebrafish embryos

signaling may be one of the most important factors necessary to establish the HSC fate in angioblasts.

3.4 Maintenance and Expansion of HSCs in the Zebrafish Embryo

3.4.1 Maintenance and Expansion of HSCs Within the Dorsal Aorta

After specification, nascent HSCs require extrinsic signals for their maturation, maintenance, and proliferation within the DA and CHT. The effects of blood flow and the shear stress on the endothelium have important roles in the maintenance of developing HSCs in the DA (North et al. 2009; Wang et al. 2011). Mutation of the

cardiac troponin T2a (*tnnt2a*) gene, which results in a lack of heartbeat, led to a drastic reduction of HSPCs in the DA at 36 hpf although initial *runx1* expression (24 hpf) in the DA was normal in these embryos (North et al. 2009; Wang et al. 2011). This indicates that blood flow is necessary for HSC maintenance/proliferation but not specification. Shear stress on blood vessel walls associated with blood flow induces the production of nitric oxide (NO) through nitric oxide synthases (NOS) (Moncada and Higgs 2006). Inhibition of NOS led to decreased numbers of HSPCs, and chemical production of NO caused a significant increase in HSPCs. In *tnnt2a* mutant embryos, defective HSPCs with reduced expression of a NOS gene (*nos1*) could be rescued by enforced production of NO. Moreover, *nos1*-deficient transplanted cells failed to contribute to HSPCs. These results indicate that NO signaling mediated by shear stress regulates the maintenance/proliferation of HSPCs cell-autonomously (North et al. 2009; Wang et al. 2011).

As described in Sect. 3.3.2., Notch signaling pathways are required for HSC specification cell-autonomously and non-cell autonomously. It has been reported, however, that Notch signaling must be down-regulated in HECs during the maturation of HSCs in both the mouse and zebrafish (Richard et al. 2013; Lizama et al. 2015; Zhang et al. 2015). G protein-coupled receptor 183 (Gpr183, also known as Ebi2; Epstein-Barr virus-induced gene 2) is activated by its ligand 7α-25-OHC and promotes the degradation of Notch1 through the proteasome pathway. Mutation of *gpr183* in zebrafish embryos resulted in the increased expression of Notch target genes (*efnb2a*, *her6*, and *her9*) in the DA and loss of HSPCs, without affecting HSC specification (Zhang et al. 2015). The requirement for Notch down-regulation was further confirmed by enforced expression of heat-inducible NICD and DN-mastermind-like (MAML), which can promote and inhibit the activation of Notch target genes, respectively. Enforced expression of NICD at an early stage (20 hpf) led to an increased number of HSPCs in the DA; DN-MAML expression at the same stage resulted in the loss of HSPCs. By contrast, enforced expression of NICD at a later stage (26 hpf) led to a reduction of HSPCs, whereas DN-MAML expression increased HSPC numbers (Zhang et al. 2015). Thus, Notch signaling is not continuously required during HSC development, and down-regulation of Notch is necessary for the final maturation of HSCs.

A chemical genetic screen in zebrafish embryos has identified the role of prostaglandin in the HSC proliferation. Prostaglandin E2 (PGE2) is the main effector of prostanoid and is regulated by both cyclooxygenase 1 (Cox1, also known as Ptgs1) and Cox2 (also known as Ptgs2a). While treatment of zebrafish embryos with PGE2 increased the number of HSPCs, Cox inhibition decreased HSPC numbers (North et al. 2007). PGE2 regulates the Wnt signaling pathway through the stabilization of β-catenin (Goessling et al. 2009). β-catenin-dependent (canonical) Wnt signaling is crucial for the development, maintenance, and proliferation of HSCs (Ruiz-Herguido et al. 2012; Luis et al. 2009). Wnt signaling is induced when a Wnt ligand binds to a Frizzled family receptor. Upon activation of the receptor, β-catenin becomes stabilized and enters the nucleus, where it interacts with a transcription factor T-cell factor (TCF, also known as LEF; lymphoid enhancer binding factor) to drive the expression of Wnt target genes. In zebrafish embryos, induction of a

membrane-level Wnt antagonist, *dickkopf1* (*dkk1*), led to the reduction of HSPCs in the DA, an effect that could be rescued by treatment with PGE2. In contrast, induction of *axin1*, which encodes a protein that promotes the destruction of β-catenin, also led to a reduction of HSPCs, but this effect could not be rescued by PGE2 treatment. These data suggest that PGE2 interacts with Wnt signaling pathway to block the degradation of β-catenin (Goessling et al. 2009). Recently, the requirement for a canonical Wnt ligand, Wnt9a, in HSC proliferation has been shown in zebrafish (Grainger et al. 2016). Wnt9a is expressed by the somite and acts as a paracrine signal to induce the expression of the cell cycle regulator c-Myc in angioblasts during angioblast migration. When Wnt signaling was inhibited by enforced expression of DN-*tcf* or injection of *wnt9a* morpholino, the expression of *cmyb* in the DA was normal until 30 hpf but reduced after 31 hpf. This effect was rescued by enforced expression of *cmyc*, suggesting that the Wnt9a/c-Myc signaling pathway is not necessary for initial HSC specification but is required for the proliferation of HSPCs in the DA (Grainger et al. 2016). Together, canonical Wnt signaling promotes the proliferation of HSCs in the DA through the regulation of c-Myc, and this signaling pathway is stabilized by PGE2 during somitogenesis.

Hypoxic stress during the developmental stage is also important factor for proliferation of HSPCs (Kwan et al. 2016). Hypoxic stress activates the hypothalamic-pituitary-adrenal/interrenal (HPA/I) stress response axis, which is regulated by the neurotransmitter serotonin within the central nerve system (CNS). Exposure to serotonin or a hypoxia mimetic cobalt chloride ($CoCl_2$) induced the production of cortisol and increased HSPC numbers in the DA. Inhibition of neuronal tryptophan hydroxlyase (Tph), a synthesizer of serotonin, led to reduced HSPC numbers. Mutation of the *nr3c1* gene, which encodes a receptor that can bind to cortisol (glucocorticoid receptor, GR), also resulted in the reduction of HSPCs. Selective induction of *nr3c1* under the *runx1* promoter rescued the number of HSPCs in *nr3cl* mutant embryos, indicating that hypoxia-induced stress signaling directly stimulates the proliferation of HSPCs within the DA (Kwan et al. 2016).

Vitamin D is also a positive regulator of HSC proliferation during the developmental stage (Cortes et al. 2016). Vitamin D synthesis begins with the transformation of 7-dehydrocholesterol to the non-active vitamin D precursor cholecalciferol (D3) by UV radiation in the skin. D3 is then modified by the cytochrome P450 enzymes 2R1 (Cyp2r1) and 27B1 (Cyp27b1) to generate 1, 25-hydroxy vitamin D (1,25(OH)D3), the active form of vitamin D. Treatment of zebrafish embryos with 1,25(OH)D3 resulted in an increase in HSPCs in the DA. In contrast, loss of vitamin D receptor a (*vdra*) or *cyp27b1* caused a reduction in HSPCs. Increased numbers of HSPCs were also observed when embryos were treated with calcipotriol, a vitamin D3 analog that has been shown to be 100-fold less calcemic than 1,25(OH)D3, indicating that vitamin D regulates HSC proliferation independently of Ca^{2+} regulation. Taken together, vitamin D3 acts directly on HSPCs, independent of calcium regulation, to increase proliferation in the DA (Cortes et al. 2016).

The extracellular matrix (ECM) is an important component of the hematopoietic microenvironment that can sequester cytokines and regulate signal transduction (Davis and Senger 2005). The ECM structure is dynamic and actively remodeled by

degrading proteases known as matrix metalloproteinases (MMPs) (Heissig et al. 2003). In zebrafish embryos, Mmp2 is expressed in the trunk vasculature and mesenchyme and is involved in the egress of HSPCs from the DA. Inhibition of Mmp2 led to the accumulation of an ECM component fibronectin, resulting in the retention of HSPCs and formation of an abnormal pattern of hematopoietic clusters in the DA. Inhibition of Mmp2 also led to the delay of HSPC colonization in the CHT. These data suggest that Mmp2 facilitates the process of EHT by remodeling ECM in the DA (Theodore et al. 2017).

3.4.2 Proliferation of HSCs Within the Caudal Hematopoietic Tissue

The CHT contains a sinusoidal structure of the vascular endothelium and is equivalent to the FL in mammals (Murayama et al. 2006; Jin et al. 2007). Live-imaging analysis of HSPCs in the CHT revealed the specific interaction of HSPCs with vascular endothelial cells and mesenchymal stromal cells. When HSPCs reach the CHT, they are enwrapped in endothelial cells (described as"endothelial cuddling"). This interaction induces and maintains contact between an HSC and a single mesenchymal stromal cell, which can induce and orient the cell division of the HSC (Tamplin et al. 2015). Chemical inhibition of Cxcl12/Cxcr4 signaling, which is known to play a role in the homing and mobilization of HSCs (Lapidot et al. 2005; Sugiyama et al. 2006), led to a reduction of HSPCs in the CHT. In contrast, inhibition of TGF-β expanded the HSPC population, which is consistent with mouse studies that showed that TGF-β signaling negatively regulates HSPC proliferation (Soma et al. 1996; Yamazaki et al. 2011). These data suggest that the expansion of HSCs is largely dependent on vascular and/or perivascular niches in the CHT (Tamplin et al. 2015).

The Cxcl8/Cxcr1 signaling regulates HSPC colonization and proliferation in the CHT (Blaser et al. 2017). Heat-shock induction of Cxcl8 or Cxcr1 after 36 hpf increased HSPC numbers in the CHT (Blaser et al. 2017). In contrast, loss of Cxcl8 led to the reduction of HSPCs in both the DA and CHT, due to defects in HSPC specification and probably also due to impaired HSPC colonization of the CHT (Jing et al. 2015; Blaser et al. 2017). Interestingly, neither *cxcl8* nor *cxcr1* was expressed in HSPCs at 72 hpf when HSPCs are proliferating in the CHT, indicating that Cxcl8/Cxcr1 signaling regulates HSPC proliferation non-cell autonomously. Enhanced Cxcl8/Cxcr1 signaling increased CHT volume and the expression level of *cxcl12a* within the endothelium, suggesting that Cxcl8/Cxcr1 signaling promotes the proliferation of HSPCs by remodeling of environmental niche cells in the CHT (Blaser et al. 2017).

Endothelial cells within the CHT produce an essential cytokine to promote HSPC proliferation. A basic helix–loop–helix transcription factor Tfec (transcription factor EC) is expressed by endothelial cells present within the CHT. Enforced expression of *tfec* led to increased numbers of HSPCs, while *tfec* mutants exhibited reduced definitive hematopoiesis (Mahony et al. 2016). Tfec mediates the expression of kit ligand b (*kitlgb*, also known as *scf*; stem cell factor), which encodes a cytokine that can bind to c-Kit and plays an important role in HSC proliferation and maintenance (Ding et al. 2012). Injection of *kitlgb* mRNA in *tfec* mutant embryos rescued HSPC numbers, suggesting that Tfec expressed by endothelial cells regulates HSPC proliferation via the production of Kitlgb in the CHT (Mahony et al. 2016). Thus, endothelial cells within the CHT play an essential role in the expansion of HSPCs.

Mmp9 is an ECM remodeling protein that is expressed by primitive neutrophils present within the CHT. Inhibition of Mmp9 increased the number of HSPCs in the CHT but decreased them in the thymus. Interestingly, the total number of HSPCs in the whole embryo was unchanged in these embryos, suggesting that Mmp9 is

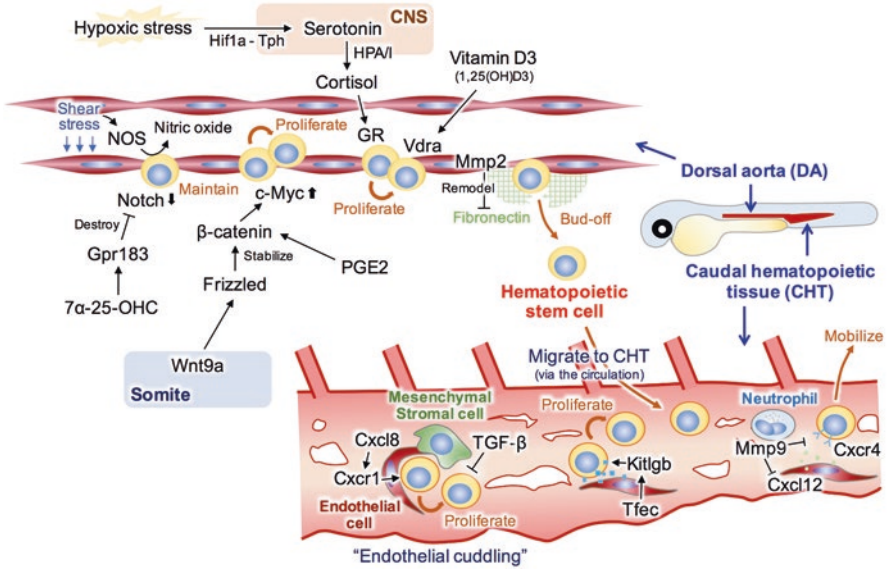

Fig. 3.2 Maintenance and proliferation of hematopoietic stem cells
The maintenance of hematopoietic stem cells (HSCs) within the ventral floor of the dorsal aorta (DA) requires shear stress associated with the blood flow, leading to the production of nitric oxide through nitric oxide synthases (NOS). While Notch signaling is up-regulated in the specification process, it is, in turn, down-regulated via the Gpr183 signaling pathway in the maturation process of HSCs. Wnt9a signaling from the somite induces the expression of c-Myc, which promotes the proliferation of HSCs in the DA. In addition, cortisol and vitamin D3 also directly influence the HSC proliferation in the DA. After budding from the DA, HSCs migrate via the circulation to the caudal hematopoietic tissue (CHT), where environmental niche cells (endothelial cells, mesenchymal stromal cells, etc.) produce cytokine signals that accelerate HSC proliferation. Cxcl8-Cxcr1 signaling and Kitlgb positively regulate and TGF-β signaling negatively regulates the expansion of the HSC pool. Cxcl12-Cxcr4 signaling is involved in the homing and mobilization of HSCs

involved in the mobilization of HSPCs from the CHT. Similar phenotypes were also observed when *cxcl12b* was overexpressed in the endothelium. In addition, the accumulation of HSPCs by Mmp9 inhibition was ameliorated by knockdown of *cxcl12a*, raising the possibility that Mmp9 expressed by primitive neutrophils controls HSPC mobilization through the repression of Cxcl12/Cxcr4 signaling (Theodore et al. 2017).

Taken together, the maintenance and proliferation of HSCs are very dependent on environmental factors, such as blood flow, hypoxia, and niche cell functions. This suggests that although early hematopoiesis occurs in a transient hematopoietic organ, the signaling cascades that can respond to blood cell requirements are mostly established during embryonic stages. Signaling molecules involved in the maturation, maintenance, and proliferation of HSCs are summarized in Fig. 3.2.

3.5 Conclusion

Our understanding of the molecular mechanisms of vertebrate HSC development has been largely improved by the zebrafish system over the past decade. This contribution could not be possible without the unique and wide variety of experimental approaches available to the zebrafish model. These include innovative approaches as well as well-established tools and methodologies, including transgenic/mutant animals, live-imaging, microinjection, transplantation, cell culture systems, chemical and forward genetic screens, and genome editing systems. In summary, the zebrafish represents an ideal system to dissect the fundamental mechanisms of HSC development and will continue to be leveraged for its unique attributes in order to make new discoveries regarding the molecular cues needed to instruct and expand HSCs from pluripotent precursors.

References

Beerman I, Luis TC, Singbrant S, Lo Celso C, Méndez-Ferrer S (2017) The evolving view of the hematopoietic stem cell niche. Exp Hematol 50:22e6

Bertrand JY, Giroux S, Golub R et al (2005) Characterization of purified intraembryonic hematopoietic stem cells as a tool to define their site of origin. Proc Natl Acad Sci U S A 102:134–139

Bertrand JY, Kim AD, Violette EP, Stachura DL, Cisson JL, Traver D (2007) Definitive hematopoiesis initiates through a committed erythromyeloid progenitor in the zebrafish embryo. Development 134:4147–4156

Bertrand JY, Chi NC, Santoso B, Teng S, Stainier DY, Traver D (2010) Haematopoietic stem cells derive directly from aortic endothelium during development. Nature 464:108–111

Blaser BW, Moore JL, Hagedorn EJ et al (2017) CXCR1 remodels the vascular niche to promote hematopoietic stem and progenitor cell engraftment. J Exp Med 214:1011–1027

Boisset JC, van Cappellen W, Andrieu-Soler C, Galjart N, Dzierzak E, Robin C (2010) In vivo imaging of haematopoietic cells emerging from the mouse aortic endothelium. Nature 464:116–120

Bozkulak EC, Weinmaster G (2009) Selective use of ADAM10 and ADAM17 in activation of Notch1 signaling. Mol Cell Biol 29:5679–5695

Bradbury J (2004) Small fish, big science. PLoS Biol 2:E148
Brou C, Logeat F, Gupta N et al (2000) A novel proteolytic cleavage involved in notch signaling: the role of the disintegrin-metalloprotease TACE. Mol Cell 5:207–216
Brown LA, Rodaway AR, Schilling TF et al (2000) Insights into early vasculogenesis revealed by expression of the ETS-domain transcription factor Fli-1 in wild-type and mutant zebrafish embryos. Mech Dev 90:237–252
Burns CE, DeBlasio T, Zhou Y, Zhang J, Zon L, Nimer SD (2002) Isolation and characterization of runxa and runxb, zebrafish members of the runt family of transcriptional regulators. Exp Hematol 30:1381–1389
Burns CE, Traver D, Mayhall E, Shepard JL, Zon LI (2005) Hematopoietic stem cell fate is established by the notch-Runx pathway. Genes Dev 19:2331–2342
Butko E, Distel M, Pouget C et al (2015) Gata2b is a restricted early regulator of hemogenic endothelium in the zebrafish embryo. Development 142:1050–1061
Byrd N, Becker S, Maye P et al (2002) Hedgehog is required for murine yolk sac angiogenesis. Development 129:361–372
Chen W, Casey Corliss D (2004) Three modules of zebrafish mind bomb work cooperatively to promote Delta ubiquitination and endocytosis. Dev Biol 267:361–373
Chen MJ, Yokomizo T, Zeigler BM, Dzierzak E, Speck NA (2009) Runx1 is required for the endothelial to haematopoietic cell transition but not thereafter. Nature 457:887–891
Cheshier SH, Morrison SJ, Liao X, Weissman IL (1999) In vivo proliferation and cell cycle kinetics of long-term self-renewing hematopoietic stem cells. Proc Natl Acad Sci U S A 96:3120–3125
Chin AJ, Chen JN, Weinberg ES (1997) Bone morphogenetic protein-4 expression characterizes inductive boundaries in organs of developing zebrafish. Dev Genes Evol 207:107–114
Clements WK, Traver D (2013) Signalling pathways that control vertebrate haematopoietic stem cell specification. Nat Rev Immunol 13:336–348
Clements WK, Kim AD, Ong KG, Moore JC, Lawson ND, Traver D (2011) A somitic Wnt16/notch pathway specifies haematopoietic stem cells. Nature 474:220–224
Cortes M, Chen MJ, Stachura DL et al (2016) Developmental vitamin D availability impacts hematopoietic stem cell production. Cell Rep 17:458–468
Cumano A, Dieterlen-Lievre F, Godin I (1996) Lymphoid potential, probed before circulation in mouse, is restricted to caudal intraembryonic splanchnopleura. Cell 86:907–916
Davidson AJ, Zon LI (2004) The 'definitive' (and 'primitive') guide to zebrafish hematopoiesis. Oncogene 23:7233–7246
Davis GE, Senger DR (2005) Endothelial extracellular matrix: biosynthesis, remodeling, and functions during vascular morphogenesis and neovessel stabilization. Circ Res 97:1093–1107
de Bruijn MF, Speck NA, Peeters MC, Dzierzak E (2000) Definitive hematopoietic stem cells first develop within the major arterial regions of the mouse embryo. EMBO J 19:2465–2474
de Bruijn MF, Ma X, Robin C, Ottersbach K, Sanchez MJ, Dzierzak E (2002) Hematopoietic stem cells localize to the endothelial cell layer in the midgestation mouse aorta. Immunity 16:673–683
de Jong JL, Zon LI (2005) Use of the zebrafish system to study primitive and definitive hematopoiesis. Annu Rev Genet 39:481–501
de Pater E, Kaimakis P, Vink CS et al (2013) Gata2 is required for HSC generation and survival. J Exp Med 210:2843–2850
Detrich HW, Kieran MW, Chan FY et al (1995) Intraembryonic hematopoietic cell migration during vertebrate development. Proc Natl Acad Sci U S A 92:10713–10717
Ding L, Saunders TL, Enikolopov G, Morrison SJ (2012) Endothelial and perivascular cells maintain haematopoietic stem cells. Nature 481:457–462
Dooley KA, Davidson AJ, Zon LI (2005) Zebrafish scl functions independently in hematopoietic and endothelial development. Dev Biol 277:522–536
Dyer MA, Farrington SM, Mohn D, Munday JR, Baron MH (2001) Indian hedgehog activates hematopoiesis and vasculogenesis and can respecify prospective neurectodermal cell fate in the mouse embryo. Development 128:1717–1730

Dzierzak E, Medvinsky A (1995) Mouse embryonic hematopoiesis. Trends Genet 11:359–366
Ehninger A, Trumpp A (2011) The bone marrow stem cell niche grows up: mesenchymal stem cells and macrophages move in. J Exp Med 208:421–428
Ema H, Nakauchi H (2000) Expansion of hematopoietic stem cells in the developing liver of a mouse embryo. Blood 95:2284–2288
Espín-Palazón R, Stachura DL, Campbell CA et al (2014) Proinflammatory signaling regulates hematopoietic stem cell emergence. Cell 159:1070–1085
Fraser ST, Ogawa M, Yu RT, Nishikawa S, Yoder MC (2002) Definitive hematopoietic commitment within the embryonic vascular endothelial-cadherin(+) population. Exp Hematol 30:1070–1078
Gagnon JA, Valen E, Thyme SB et al (2014) Efficient mutagenesis by Cas9 protein-mediated oligonucleotide insertion and large-scale assessment of single-guide RNAs. PLoS One 9:e98186
Galloway JL, Zon LI (2003) Ontogeny of hematopoiesis: examining the emergence of hematopoietic cells in the vertebrate embryo. Curr Top Dev Biol 53:139–158
Gao X, Johnson KD, Chang YI et al (2013) Gata2 cis-element is required for hematopoietic stem cell generation in the mammalian embryo. J Exp Med 210:2833–2842
Gekas C, Dieterlen-Lièvre F, Orkin SH, Mikkola HK (2005) The placenta is a niche for hematopoietic stem cells. Dev Cell 8:365–375
Genthe JR, Clements WK (2017) R-spondin 1 is required for specification of hematopoietic stem cells through Wnt16 and Vegfa signaling pathways. Development 144:590–600
Gering M, Patient R (2005) Hedgehog signaling is required for adult blood stem cell formation in zebrafish embryos. Dev Cell 8:389–400
Godin I, Cumano A (2002) The hare and the tortoise: an embryonic haematopoietic race. Nat Rev Immunol 2:593–604
Goessling W, North TE, Loewer S et al (2009) Genetic interaction of PGE2 and Wnt signaling regulates developmental specification of stem cells and regeneration. Cell 136:1136–1147
Grainger S, Richter J, Palazón RE et al (2016) Wnt9a is required for the aortic amplification of nascent hematopoietic stem cells. Cell Rep 17:1595–1606
Hadland BK, Huppert SS, Kanungo J et al (2004) A requirement for Notch1 distinguishes 2 phases of definitive hematopoiesis during development. Blood 104:3097–3105
He Q, Zhang C, Wang L et al (2015) Inflammatory signaling regulates hematopoietic stem and progenitor cell emergence in vertebrates. Blood 125:1098–1106
Heissig B, Hattori K, Friedrich M, Rafii S, Werb Z (2003) Angiogenesis: vascular remodeling of the extracellular matrix involves metalloproteinases. Curr Opin Hematol 10:136–141
Henninger J, Santoso B, Hans S et al (2017) Clonal fate mapping quantifies the number of haematopoietic stem cells that arise during development. Nat Cell Biol 19:17–27
Hisano Y, Sakuma T, Nakade S et al (2015) Precise in-frame integration of exogenous DNA mediated by CRISPR/Cas9 system in zebrafish. Sci Rep 5:8841
Hoggatt J, Kfoury Y, Scadden DT (2016) Hematopoietic stem cell niche in health and disease. Annu Rev Pathol 11:555–581
Hsia N, Zon LI (2005) Transcriptional regulation of hematopoietic stem cell development in zebrafish. Exp Hematol 33:1007–1014
Itoh M, Kim CH, Palardy G et al (2003) Mind bomb is a ubiquitin ligase that is essential for efficient activation of notch signaling by Delta. Dev Cell 4:67–82
Jao LE, Wente SR, Chen W (2013) Efficient multiplex biallelic zebrafish genome editing using a CRISPR nuclease system. Proc Natl Acad Sci U S A 110:13904–13909
Jin SW, Beis D, Mitchell T, Chen JN, Stainier DY (2005) Cellular and molecular analyses of vascular tube and lumen formation in zebrafish. Development 132:5199–5209
Jin H, Xu J, Wen Z (2007) Migratory path of definitive hematopoietic stem/progenitor cells during zebrafish development. Blood 109:5208–5214
Jing L, Tamplin OJ, Chen MJ et al (2015) Adenosine signaling promotes hematopoietic stem and progenitor cell emergence. J Exp Med 212:649–663
Johnson KD, Hsu AP, Ryu MJ et al (2012) Cis-element mutated in GATA2-dependent immunodeficiency governs hematopoiesis and vascular integrity. J Clin Invest 122:3692–3704

Kalev-Zylinska ML, Horsfield JA, Flores MV et al (2002) Runx1 is required for zebrafish blood and vessel development and expression of a human RUNX1-CBF2T1 transgene advances a model for studies of leukemogenesis. Development 129:2015–2030
Kawahara A, Hisano Y, Ota S, Taimatsu K (2016) Site-specific integration of exogenous genes using genome editing technologies in zebrafish. Int J Mol Sci 17:727
Khan JA, Mendelson A, Kunisaki Y et al (2016) Fetal liver hematopoietic stem cell niches associate with portal vessels. Science 351:176–180
Kim AD, Melick CH, Clements WK et al (2014) Discrete notch signaling requirements in the specification of hematopoietic stem cells. EMBO J 33:2363–2373
Kissa K, Herbomel P (2010) Blood stem cells emerge from aortic endothelium by a novel type of cell transition. Nature 464:112–115
Kobayashi I, Kobayashi-Sun J, Kim AD et al (2014) Jam1a-Jam2a interactions regulate haematopoietic stem cell fate through notch signalling. Nature 512:319–323
Konantz M, Alghisi E, Müller JS et al (2016) Evi1 regulates notch activation to induce zebrafish hematopoietic stem cell emergence. EMBO J 35:2315–2331
Kopan R, Ilagan MX (2009) The canonical notch signaling pathway: unfolding the activation mechanism. Cell 137:216–233
Krebs LT, Xue Y, Norton CR et al (2000) Notch signaling is essential for vascular morphogenesis in mice. Genes Dev 14:1343–1352
Kwan W, Cortes M, Frost I et al (2016) The central nervous system regulates embryonic HSPC production via stress-responsive glucocorticoid receptor signaling. Cell Stem Cell 19:370–382
Lapidot T, Dar A, Kollet O (2005) How do stem cells find their way home? Blood 106:1901–1910
Lawson ND, Weinstein BM (2002) In vivo imaging of embryonic vascular development using transgenic zebrafish. Dev Biol 248:307–318
Lawson ND, Vogel AM, Weinstein BM (2002) Sonic hedgehog and vascular endothelial growth factor act upstream of the notch pathway during arterial endothelial differentiation. Dev Cell 3:127–136
Lee Y, Manegold JE, Kim AD et al (2014) FGF signalling specifies haematopoietic stem cells through its regulation of somitic notch signalling. Nat Commun 5:5583
Lessard J, Faubert A, Sauvageau G (2004) Genetic programs regulating HSC specification, maintenance and expansion. Oncogene 23:7199–7209
Leung A, Ciau-Uitz A, Pinheiro P et al (2013) Uncoupling VEGFA functions in arteriogenesis and hematopoietic stem cell specification. Dev Cell 24:144–158
Li Y, Esain V, Teng L et al (2014) Inflammatory signaling regulates embryonic hematopoietic stem and progenitor cell production. Genes Dev 28:2597–2612
Liao EC, Paw BH, Oates AC, Pratt SJ, Postlethwait JH, Zon LI (1998) SCL/Tal-1 transcription factor acts downstream of cloche to specify hematopoietic and vascular progenitors in zebrafish. Genes Dev 12:621–626
Lim KC, Hosoya T, Brandt W et al (2012) Conditional Gata2 inactivation results in HSC loss and lymphatic mispatterning. J Clin Invest 122:3705–3717
Lizama CO, Hawkins JS, Schmitt CE et al (2015) Repression of arterial genes in hemogenic endothelium is sufficient for haematopoietic fate acquisition. Nat Commun 6:7739
Luis TC, Weerkamp F, Naber BA et al (2009) Wnt3a deficiency irreversibly impairs hematopoietic stem cell self-renewal and leads to defects in progenitor cell differentiation. Blood 113:546–554
Mahony CB, Fish RJ, Pasche C, Bertrand JY (2016) tfec controls the hematopoietic stem cell vascular niche during zebrafish embryogenesis. Blood 128:1336–1345
Maye P, Becker S, Kasameyer E, Byrd N, Grabel L (2000) Indian hedgehog signaling in extraembryonic endoderm and ectoderm differentiation in ES embryoid bodies. Mech Dev 94:117–132
McGrath KE, Frame JM, Fromm GJ et al (2011) A transient definitive erythroid lineage with unique regulation of the β-globin locus in the mammalian embryo. Blood 117:4600–4608
Medvinsky A, Dzierzak E (1996) Definitive hematopoiesis is autonomously initiated by the AGM region. Cell 86:897–906
Moncada S, Higgs EA (2006) Nitric oxide and the vascular endothelium. Handb Exp Pharmacol 176:213–254

Monteiro R, Pinheiro P, Joseph N et al (2016) Transforming growth factor β drives Hemogenic endothelium programming and the transition to hematopoietic stem cells. Dev Cell 38:358–370
Müller AM, Medvinsky A, Strouboulis J, Grosveld F, Dzierzak E (1994) Development of hematopoietic stem cell activity in the mouse embryo. Immunity 1:291–301
Mumm JS, Schroeter EH, Saxena MT et al (2000) A ligand-induced extracellular cleavage regulates gamma-secretase-like proteolytic activation of Notch1. Mol Cell 5:197–206
Murayama E, Kissa K, Zapata A et al (2006) Tracing hematopoietic precursor migration to successive hematopoietic organs during zebrafish development. Immunity 25:963–975
Murry CE, Keller G (2008) Differentiation of embryonic stem cells to clinically relevant populations: lessons from embryonic development. Cell 132:661–680
North TE, de Bruijn MF, Stacy T et al (2002) Runx1 expression marks long-term repopulating hematopoietic stem cells in the midgestation mouse embryo. Immunity 16:661–672
North TE, Goessling W, Walkley CR et al (2007) Prostaglandin E2 regulates vertebrate haematopoietic stem cell homeostasis. Nature 447:1007–1011
North TE, Goessling W, Peeters M et al (2009) Hematopoietic stem cell development is dependent on blood flow. Cell 137:736–748
Ottersbach K, Dzierzak E (2005) The murine placenta contains hematopoietic stem cells within the vascular labyrinth region. Dev Cell 8:377–387
Palis J, Robertson S, Kennedy M, Wall C, Keller G (1999) Development of erythroid and myeloid progenitors in the yolk sac and embryo proper of the mouse. Development 126:5073–5084
Patterson LJ, Gering M, Patient R (2005) Scl is required for dorsal aorta as well as blood formation in zebrafish embryos. Blood 105:3502–3511
Pouget C, Peterkin T, Simões FC, Lee Y, Traver D, Patient R (2014) FGF signalling restricts haematopoietic stem cell specification via modulation of the BMP pathway. Nat Commun 5:5588
Qian F, Zhen F, Xu J, Huang M, Li W, Wen Z (2007) Distinct functions for different scl isoforms in zebrafish primitive and definitive hematopoiesis. PLoS Biol 5:e132
Ren X, Gomez GA, Zhang B, Lin S (2010) Scl isoforms act downstream of etsrp to specify angioblasts and definitive hematopoietic stem cells. Blood 115:5338–5346
Richard C, Drevon C, Canto PY et al (2013) Endothelio-mesenchymal interaction controls runx1 expression and modulates the notch pathway to initiate aortic hematopoiesis. Dev Cell 24:600–611
Robert-Moreno A, Guiu J, Ruiz-Herguido C et al (2008) Impaired embryonic haematopoiesis yet normal arterial development in the absence of the notch ligand Jagged1. EMBO J 27:1886–1895
Ruiz-Herguido C, Guiu J, D'Altri T et al (2012) Hematopoietic stem cell development requires transient Wnt/β-catenin activity. J Exp Med 209:1457–1468
Rybtsov S, Sobiesiak M, Taoudi S et al (2011) Hierarchical organization and early hematopoietic specification of the developing HSC lineage in the AGM region. J Exp Med 208:1305–1315
Samokhvalov IM, Samokhvalova NI, Nishikawa S (2007) Cell tracing shows the contribution of the yolk sac to adult haematopoiesis. Nature 446:1056–1061
Sawamiphak S, Kontarakis Z, Stainier DY (2014) Interferon gamma signaling positively regulates hematopoietic stem cell emergence. Dev Cell 31:640–653
Shah AN, Davey CF, Whitebirch AC, Miller AC, Moens CB (2015) Rapid reverse genetic screening using CRISPR in zebrafish. Nat Methods 12:535–540
Shepard JL, Zon LI (2000) Developmental derivation of embryonic and adult macrophages. Curr Opin Hematol 7:3–8
Soma T, Yu JM, Dunbar CE (1996) Maintenance of murine long-term repopulating stem cells in ex vivo culture is affected by modulation of transforming growth factor-beta but not macrophage inflammatory protein-1 alpha activities. Blood 87:4561–4567
Soza-Ried C, Hess I, Netuschil N, Schorpp M, Boehm T (2010) Essential role of c-myb in definitive hematopoiesis is evolutionarily conserved. Proc Natl Acad Sci U S A 107:17304–17308
Stamatoyannopoulos G (2005) Control of globin gene expression during development and erythroid differentiation. Exp Hematol 33:259–271

Sugiyama T, Kohara H, Noda M, Nagasawa T (2006) Maintenance of the hematopoietic stem cell pool by CXCL12-CXCR4 chemokine signaling in bone marrow stromal cell niches. Immunity 25:977–988

Sumanas S, Lin S (2006) Ets1-related protein is a key regulator of vasculogenesis in zebrafish. PLoS Biol 4:e10

Sumanas S, Gomez G, Zhao Y, Park C, Choi K, Lin S (2008) Interplay among Etsrp/ER71, Scl, and Alk8 signaling controls endothelial and myeloid cell formation. Blood 111:4500–4510

Tamplin OJ, Durand EM, Carr LA et al (2015) Hematopoietic stem cell arrival triggers dynamic remodeling of the perivascular niche. Cell 160:241–252

Taoudi S, Gonneau C, Moore K et al (2008) Extensive hematopoietic stem cell generation in the AGM region via maturation of VE-cadherin+CD45+ pre-definitive HSCs. Cell Stem Cell 3:99–108

Theodore LN, Hagedorn EJ, Cortes M et al (2017) Distinct roles for matrix Metalloproteinases 2 and 9 in embryonic hematopoietic stem cell emergence, migration, and niche colonization. Stem Cell Rep 8:1226–1241

Thompson MA, Ransom DG, Pratt SJ et al (1998) The cloche and spadetail genes differentially affect hematopoiesis and vasculogenesis. Dev Biol 197:248–269

Tober J, Koniski A, McGrath KE et al (2007) The megakaryocyte lineage originates from hemangioblast precursors and is an integral component both of primitive and of definitive hematopoiesis. Blood 109:1433–1441

Tsai FY, Orkin SH (1997) Transcription factor GATA-2 is required for proliferation/survival of early hematopoietic cells and mast cell formation, but not for erythroid and myeloid terminal differentiation. Blood 89:3636–3643

Tsai FY, Keller G, Kuo FC et al (1994) An early haematopoietic defect in mice lacking the transcription factor GATA-2. Nature 371:221–226

Walkley CR, McArthur GA, Purton LE (2005) Cell division and hematopoietic stem cells: not always exhausting. Cell Cycle 4:893–896

Wang L, Zhang P, Wei Y, Gao Y, Patient R, Liu F (2011) A blood flow-dependent klf2a-NO signaling cascade is required for stabilization of hematopoietic stem cell programming in zebrafish embryos. Blood 118:4102–4110

Warga RM, Kane DA, Ho RK (2009) Fate mapping embryonic blood in zebrafish: multi- and unipotential lineages are segregated at gastrulation. Dev Cell 16:744–755

Weissman IL (2000) Stem cells: units of development, units of regeneration, and units in evolution. Cell 100:157–168

Wilkinson RN, Pouget C, Gering M et al (2009) Hedgehog and Bmp polarize hematopoietic stem cell emergence in the zebrafish dorsal aorta. Dev Cell 16:909–916

Yamazaki S, Ema H, Karlsson G et al (2011) Nonmyelinating Schwann cells maintain hematopoietic stem cell hibernation in the bone marrow niche. Cell 147:1146–1158

Yoon MJ, Koo BK, Song R et al (2008) Mind bomb-1 is essential for intraembryonic hematopoiesis in the aortic endothelium and the subaortic patches. Mol Cell Biol 28:4794–4804

Yu VW, Scadden DT (2016) Heterogeneity of the bone marrow niche. Curr Opin Hematol 23:331–338

Zhang Y, Jin H, Li L, Qin FX, Wen Z (2011) cMyb regulates hematopoietic stem/progenitor cell mobilization during zebrafish hematopoiesis. Blood 118:4093–4101

Zhang P, He Q, Chen D et al (2015) G protein-coupled receptor 183 facilitates endothelial-to-hematopoietic transition via Notch1 inhibition. Cell Res 25:1093–1107

Zhen F, Lan Y, Yan B, Zhang W, Wen Z (2013) Hemogenic endothelium specification and hematopoietic stem cell maintenance employ distinct Scl isoforms. Development 140:3977–3985

Zhu H, Zon LI (2002) Use of zebrafish models for the analysis of human disease. Curr Protoc Hum Genet Chapter 15: unit 15.13

Zhu C, Smith T, McNulty J et al (2011) Evaluation and application of modularly assembled zinc-finger nucleases in zebrafish. Development 138:4555–4564

Zovein AC, Hofmann JJ, Lynch M et al (2008) Fate tracing reveals the endothelial origin of hematopoietic stem cells. Cell Stem Cell 3:625–636

Chapter 4
Rohon-Beard Neuron in Zebrafish

Kazutoyo Ogino and Hiromi Hirata

Abstract We experience various sensations through our skin. The sensations are received by distinct sensory channels that are expressed in the trigeminal ganglion (TG) or the dorsal root ganglion (DRG). TG neurons innervate the head skin, whereas DRG neurons innervate the skin of the trunk and limbs. In addition to these neuronal populations, larvae of anamniote vertebrates (lampreys, teleosts, and amphibians) have an additional sensory neuronal population that develops prior to functional maturation of DRG neurons, termed Rohon-Beard (RB) neurons. RB neurons innervate the trunk skin; thus, the TG and RB neurons are responsible for larval somatosensation. After the maturation of DRG neurons, the physiological roles of the RB neurons are replaced progressively by the DRG neurons. Studies of somatosensation in zebrafish have suggested that the transition from RB neurons to DRG neurons is completed within 5 days post fertilization. During this transition, the RB neurons undergo programmed cell death; thus, RB neurons have been considered to be a transient neuronal population. However, recent studies using zebrafish have indicated that some RB neurons survive for at least 2 weeks post-fertilization. These long-lived RBs are distinguished by Protein Kinase C-α (PKCα) expression and comprise <40% of the RB population although their physiological significance remains to be elucidated. Furthermore, RB neurons show diversity in gene expression other than the PKCα gene, implying that there are several different cell types in RB neurons. However, the physiological significance of this diversity also remains unclear. Visualization of the neural activity and functional manipulation could contribute to greater insight into RB neuron physiology. Many genetic tools that enable the visualization and manipulation of cell activity have been introduced to zebrafish biology. In addition, some enhancer or promoter sequences that induce gene expression in specific subtypes of RB neurons have been isolated. Using these molecular tools, researchers can investigate the physiology of distinct RB neurons. Here, We focus on RB neurons, presenting a current understanding of their development, diversity, and function and methods for their manipulation and visualization.

K. Ogino · H. Hirata (✉)
Department of Chemistry and Biological Science, College of Science and Engineering, Aoyama Gakuin University, Sagamihara, Japan
e-mail: kogino@chem.aoyama.ac.jp; hihirata@chem.aoyama.ac.jp

H. Hirata, A. Iida (eds.), *Zebrafish, Medaka, and Other Small Fishes*,
https://doi.org/10.1007/978-981-13-1879-5_4

Keywords Zebrafish · Rohon-Beard neuron · Somatosensory · Touch-evoked response · Reticulospinal neuron · Mauthner cell

4.1 What Is the RB Neuron?

Our skin allows for the perception of various sensations, including thermal, chemical, and mechanical sensations, via the activity of sensory neurons that project peripheral terminals into the skin. In vertebrates, cell bodies of somatosensory neurons are found in either the trigeminal ganglion (TG) or the dorsal root ganglion (DRG). The TG sensory neurons innervate the head skin, whereas the DRG sensory neurons are involved in the reception of stimulation to the rest of the body, such as the trunk and limbs. Both the TG and DRG neurons express many types of sensory receptor channels that receive stimulus information, such as thermosensitive, chemosensitive, and mechanosensitive channels (McKemy et al. 2002; Lumpkin and Caterina 2007; Coste et al. 2010; Geffeney and Goodman 2012; Li et al. 2016).

In addition to these sensory neuronal populations, the larvae of anamniote vertebrates (lampreys, teleosts, and amphibians) have an additional population of sensory neurons, termed Rohon-Beard (RB) neurons after the scientists who first described them in the nineteenth century. RB neurons are pseudo-unipolar neurons which have two types of axons, namely, central and peripheral axons (Bernhardt et al. 1990; Metcalfe et al. 1990) (Fig. 4.1a). The RB neurons share following morphological features between the anamniote vertebrates (Roberts 2000). Large spherical cell

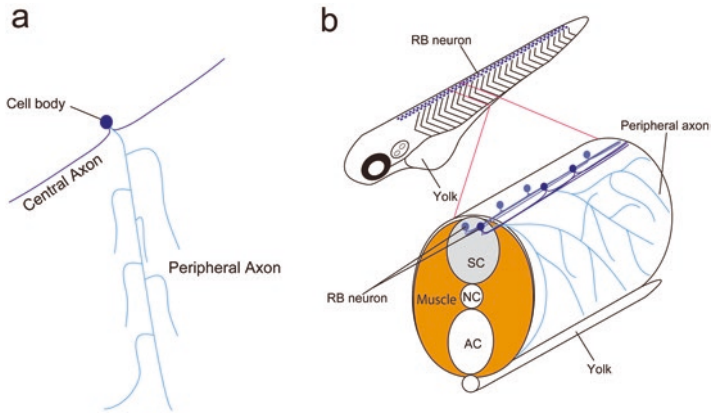

Fig. 4.1 Schematic diagram of RB neuron
(a) Morphology of RB neuron. Central axon bifurcate and extend in both the rostral and caudal directions, whereas the peripheral axon is highly branched to innervate skin broadly. (**b**) The cell bodies of RB neurons are arranged as two lines of longitudinal columns in the dorsal spinal cord. Both the central and peripheral axons grow only in the ipsilateral side. The central axons elongate in the rostral or caudal direction in the spinal cord, whereas the peripheral axons elongate to the outside of the spinal cord and innervate the skin
SC spinal cord, *NC* notochord, *AC* abdominal cavity

bodies of RB neurons (diameter 10–20 μm) reside in the dorsal spinal cord as longitudinal columns. From the cell body, the central axon extends in the rostral-caudal direction, and the ascending branch extends to the hindbrain, whereas the peripheral axon projects toward the skin to innervate dermal sensory structures or terminate as free endings in the dermis or epidermis (Fig. 4.1b). These axons never cross the midline, thus the elongation is restricted to the ipsilateral side (Bernhardt et al. 1990; Metcalfe et al. 1990; Halloran et al. 1999). The sensory input from RB neurons to the CNS activates a neural network that triggers an escape response to move away from the stimulus (Metcalfe et al. 1990). The stereotyped dorsal position and morphological features including large spherical cell body help us to identify RB neurons in the spinal cord. In addition, the large cell body makes electrophysiological recording of neural activity easier.

4.2 Why Zebrafish Is Widely Used for Investigation of RB Neuron

Using zebrafish embryo as experimental model, many papers according RB neuron have been published. Zebrafish (*Danio rerio*) has been widely used as an excellent vertebrate model to study biological science, including developmental biology and neuroscience. Zebrafish is a small tropical fish; therefore, we can easily breed them in laboratory. Adult female lay 100–200 eggs during mating with adult male twice a week throughout the year. The fertilized egg rapidly develops to larva whose body is optically transparent. In optimum temperature, 28.5 °C, the larvae hatch out in 3 days after fertilization (dpf), and they start to swim and take food in 4–5 dpf (Kimmel et al. 1995). The rapid development and the optical transparency allow us to observe developmental morphological changes that occur in the larval body. Zebrafish typically attain sexual maturity approximately 3 months post fertilization. This short generation time is advantageous for genetic analysis and manipulation, and many transgenic lines and mutants including gene knockout lines have been established. Transgenic lines that express fluorescent protein in specific cell type help the developmental observation. To label RB neurons, many transgenic zebrafish that express fluorescent proteins in RB neurons have been established (Asakawa et al. 2008; Palanca et al. 2013). These advantages also facilitate neuroscience study using electrophysiological recording of neuronal activity in fluorescence protein labeled neuron and manipulation of neuronal activity by optogenetic methods in developing zebrafish embryos in either wild-type background or mutant background. In addition to the genetic labeling, RB neuron cell body can also be labeled by immunostaining (Table 4.1). The immunostaining method allows us to investigate subcellular distribution of proteins in RB neuron. Consequently, zebrafish have come to be broadly used as an animal model to investigate RB neurons. In addition to zebrafish, Medaka (*Oryzias latipes*), Japanese small fresh water fish, has also been used as a model vertebrate for biological investigations. Medaka has similar advantages to zebrafish, short generation time (2–3 months), rapid development,

Table 4.1 Antibodies that can label the cell body of RB neuron

Name	Antigen	Subclass (Manufacture)	Dilution	Refs.
SC-208	PKC alpha	Rabbit polyclonal antibody (Santa Cruz biotechnologies)	1:500	Slatter et al. (2005)
				Palanca et al. (2013)
SP19	Alpha subunit of all Na_vs	Rabbit polyclonal IgG (LifeSpan BioScience)	1:500	Nakano et al. (2010)
				Ogino et al. (2015)
zn12	L2/HNK-1	Mouse monoclonal, IgG1 (Zebrafish International Resource Center)	1:4000	Metcalfe et al. (1990)
				Reyes et al. (2004)
16A11	HuC/HuD	Mouse monoclonal, IgG2b (Molecular Probes)	1:500 to 1:1000	Marusich et al. (1994)
				Pineda et al. (2006)
				Nakano et al. (2010)
				Ogino et al. (2015)
39.4D5	Islet1 and Islet2	Mouse monoclonal, IgG2b (Developmental Studies Hybridoma Bank)	1:500	Pineda et al. (2006)
40.2D6	Islet1	Mouse monoclonal, IgG1 (Developmental studies Hybridoma bank)	1:100	Low et al. (2012)

and optical transparency of larval body (Wittbrodt et al. 2002). However, the Medaka model has not been used to RB neuron study, unlike zebrafish.

Larvae of lamprey and amphibian have also RB neuron. However, lamprey and *Xenopus* are less advantageous compared to zebrafish. In lamprey, it is very difficult to correct the embryos, because breeding procedure for lamprey has not been established. In addition, generation time of lamprey is 5–7 years (McCauley et al. 2015). On the other hand, *Xenopus laevis* are easily maintained in laboratory. However, this frog has some undesirable features for genetic manipulation. The generation time is longer than 1 year and furthermore the genome is allotetraploid (Hirsch et al. 2002). These features hamper generation of genetically engineered frogs, because all four alleles have to be mutated to generate homozygous mutants through time-consuming crossbreeding programs. In addition, body of their larvae is opacity, because each cell contains yolk. In spite of these disadvantages, some studies have examined the development of RB neurons in *Xenopus laevis* (Patterson and Krieg 1999; Fujita et al. 2000; Coen et al. 2001; Rossi et al. 2008; Park et al. 2012). To overcome the disadvantages in *Xenopus laevis*, *Xenopus tropicalis* has been introduced as a new model amphibian (Hirsch et al. 2002). This frog has a smaller diploid genome than *Xenopus laevis*, and the generation time of 4–6 month, which

is shorter than that of *Xenopus laevis*. These features help to generate transgenic or gene knockout animal. In fact, a high efficient transgenesis method and a CRISPR/Cas9 mediated targeted mutagenesis method have been applicated to *Xenopus tropicalis* (Ogino et al. 2006; Nakayama et al. 2013). The new model frog might contribute to RB neuron study as a useful model animal.

4.3 Development of the RB Cell

Zebrafish develop rapidly at 28.5 °C. During the developmental process, a fish-shaped embryo with a distinguishable head, trunk, and tail is formed within the first 24 hours post-fertilization (hpf). During early development, zebrafish larvae begin to display two touch-evoked escape responses, contraction and swimming (Saint-Amant and Drapeau 1998). The touch-evoked contractions are rapid, alternating contractions of the trunk, which begin by 21 hpf. On the other hand, the touch-evoked swimming begins by 28 hpf. This tactile sensitivity of larval zebrafish is conferred by two sensory neuron populations, TG and RB neurons, as mentioned above. Thus, these sensory neurons are becoming functional and are incorporated into the neural pathway that induces the escape response by 21 hpf.

CNS development begins with the formation of the neural plate, an ectoderm derivative on the dorsal side of the embryo. In zebrafish, the formation of the neural plate begins as dorsal epiblast thickening at 9 hpf (Kimmel et al. 1995). By 19 hpf, the neural plate is progressively transformed into the neural tube, i.e., the precursor of the vertebrate CNS, through dynamic cellular movement. During this process, the medial region of the neural plate forms the ventral side of the neural tube, whereas the lateral region forms the dorsal side of the neural tube. The process of neural tube formation involves two intermediate stages termed the neural keel and neural rod that are present at 13 hpf and 16 hpf, respectively. During neural tube formation, primary spinal neurons begin to extend axons toward neuronal and muscle targets and the larval zebrafish develop locomotion.

RB neurons and trunk neural crest cells (NCCs) are derived from the same region of the lateral neural plate (Blader et al. 1997; Lewis and Eisen 2003). Defective mutations in BMP signaling lead to a loss or dramatic reduction in both RB neurons and NCCs (Nguyen et al. 1998; Nguyen et al. 2000). In addition, the development of RB neuron and NCCs were impaired also in zebrafish lacking functional *prdm1*, transcription factor expressing at the lateral neural plate where RB neuron and NCCs are being specified (Hernandez-Lagunas et al. 2005). These data suggest that RB neuron and NCCs share some developmental molecular mechanisms. The segregation of RB neurons and NCCs is dependent on Delta-Notch signaling. At around 12 hpf, some of the progenitor cells express several *delta* homologs that activate Notch receptors on adjacent cells, which then differentiate into NCCs (Haddon et al. 1998; Cornell and Eisen 2000). Stimulation of Notch signaling reduces neural plate expression of *ngn1* (Blader et al. 1997). Expression of *ngn1* is detected in the neural plate from the 3-somite stage (10-11 hpf), and then the hign-level ngn1

expressing cells form solid clusters that are srrounded by low-level *ngn1* expressing cells. Functional analysis by over-expression or knockdown of the *ngn1* gene demonstrated that *ngn1* is necessary for RB neuron development (Blader et al. 1997; Andermann et al. 2002). Ngn1 induces expression of downstream basic helix-loop-helix (bHLH) genes, such as *neuroD*, to promote neural differentiation from proliferative neural precursor cells to post-mitotic neurons (Kanungo et al. 2009).

RB neurons begin to extend their central axons in both the rostral and the caudal direction at 16 hpf (Kuwada et al. 1990; Liu and Halloran 2005). The two central axons initiate outgrowth simultaneously from opposite ends at the basal (ventral) side of the cell body and then elongate to the opposite direction (Andersen et al. 2011). These central axons from RB neurons of the ipsilateral side grow longitudinally together in the spinal cord, forming the dorsal longitudinal fasciculus (DLF), which is a relatively loose fascicle (Liu and Halloran 2005). Similarly, the peripheral axons begin to extend from the cell body and either emerge as a branch from one of the central axons or directly emerge from the cell body at 17–18 hpf. After the emergence, the peripheral axon extends toward the outside of the spinal cord to innervate the skin (Kuwada et al. 1990; Liu and Halloran 2005; Andersen et al. 2011). After leaving the spinal cord, the peripheral axons bifurcate several times to form a highly branched structure that densely covers the surface of the skin. Thus, the central axon elongation is fascicular, whereas the peripheral axon elongation is repulsive. The differences in the projection patterns suggest that different mechanisms guide RB neuron processes.

LIM homeodomain transcription factors (LIM-HD) and their cofactors (CLIMs) are required for the elongation and branching of the peripheral axon (Segawa et al. 2001; Becker et al. 2002; Andersen et al. 2011; Tanaka et al. 2011). In contrast to the peripheral axon, the growth rate of the central axon is increased in LIM-HD activity disrupted RB neuron. The opposite effect of the LIM-HD activity indicates that the growth of the central and the peripheral axon is differentially regulated. Recently, it was reported that Calsyntenin-1 (Clstn-1) is a critical regulator for growth and branching of the peripheral axons (Ponomareva et al. 2014). Clstn-1 is a kinesin adaptor and is required for rapid movement of Rab5 containing endosomes along axons. Ponomareva et al. suggested that the Rab5-containing endosomes may deliver important molecules for the peripheral axon branching process to the branching point in the axon. Dpysl3 and PlexinA4 are downstream genes of Isl1 and Isl2a, respectively (Miyashita et al. 2004; Tanaka et al. 2011). Dpysl3 is a member of cytosolic phosphoproteins that mediate semaphorin signaling. Knockdown experiments using antisense morpholino for Dpysl3 or Sema3D indicate that Dpysl3 cooperates with Sema3D for RB neuron peripheral axon outgrowth (Tanaka et al. 2011). After leaving the spinal cord, peripheral axons are attracted to molecular cues from the skin. This axon guidance requires the leukocyte antigen-related (LAR) family of receptor tyrosine phosphatases *ptprfa* and *ptprfb* (Wang et al. 2012). LAR receptors are expressed in RB neurons, and LAR-deficient neurons show a defect in peripheral axon guidance. In addition, heparin sulfate proteoglycans (HSPGs), a direct ligand for LAR receptors, are enriched in the skin; thus, HSPGs may be involved in the attraction of peripheral axons to the skin. The

branching of peripheral axons requires Slit2 and PlexinA4, which are commonly known as the receptors for semaphorins.

RB neurons normally innervate ipsilateral skin, as the peripheral axons do not cross the dorsal midline, in which Sema3D is expressed (Halloran et al. 1999). Sema3D deficiency or knockdown studies show that Sema3D propels elongating peripheral axons. More specifically, Sema3D propels the peripheral axons away from the spinal cord through repulsion process. However, the Sema3D does not influence central axon extension. In contrast to Sema3D, transient axonal glycoprotein-1 (TAG-1) affects central axon projection but not peripheral axon projection. TAG-1 is a glycosyl-phosphatidylinositol-linked (GPI-linked) membrane protein that is expressed in RB neurons during axon elongation and promotes the extension of the central axons of RB neurons (Warren et al. 1999; Liu and Halloran 2005). In this manner, central and peripheral axons elongate to different directions and follow different guidance cues.

4.4 Escape Response Evoked by RB Neuron Activation

After the 21 hpf stage, tactile stimulations on the trunk and tail are received by RB neurons and transmitted to the CNS to induce the touch-evoked response (Saint-Amant and Drapeau 1998; Low et al. 2012). Although tactile sensitivity has been well-established in vertebrates, the mechanosensory molecules for the sensation were not identified until recently. To identify the mechanically activated channel, Coste et al. screened several mouse and rat cell lines by applying force to the cell surface while patch-clamp recording, they identified two mechanically activated cation channels, Piezo1 and Piezo2, in mouse neuroblastoma cell line Neuro2A (Coste et al. 2010). Both Piezo1 and 2 are expressed in some mechano-sensitive tissues related to visceral pain, such as the bladder, colon, and lung. In the aspect of cutaneous sensation, Piezo2 was required for mechanically activated currents in subset of DRG neurons, whereas the expression levels of Piezo1 in DRG neurons were very low. A part of the Piezo2 expressing DRG neurons also expresses transient receptor potential cation channel subfamily V member (TRPV1) channels, which are activated by heating and exposure to capsaicin, suggesting a potential role of Piezo2 in noxious mechanosensation (Coste et al. 2010). Coste et al. also showed that piezo proteins are conserved in many animals, plants, and single cell organisms, such as mycetozoa and ciliophoran (Coste et al. 2010). The zebrafish genome has three piezo homologs, *piezo1*, *piezo2a*, and *piezo2b*. The expression of *piezo2b* is specific to TG and RB neurons in larvae at 24 hpf, whereas *piezo1* and *piezo2a* are not expressed in these neurons (Faucherre et al. 2013). Morpholino oligonucleotide-mediated *piezo2b* knockdown shows that *piezo2b* is essential for tactile sensation in zebrafish larvae (Faucherre et al. 2013). A subset of the Piezo2b expressing RB neurons also express TRPA1b, which is activated by exposure to mustard oil, a noxious stimulating compound. The gene expression profile is comparable with mouse

DRG neurons. It is generally considered that the touch-evoked response is mediated by reticulospinal (RS) neurons in the hindbrain.

Reticulospinal (RS) neurons in the hindbrain are involved in the initiation and regulation of C-start escape from various stimuli, including sound, visual, and tactile stimulation (O'Malley et al. 1996; Liu and Fetcho 1999; Weiss et al. 2006). Among RS neurons, Mauthner cells and two of its serial homologs, MiD2cm and MiD3cm, have been well-studied for their involvement in the initiation and regulation of the escape response (Lee et al. 1991; O'Malley et al. 1996; Nakayama and Oda 2004; Korn and Faber 2005). These neurons are thought to constitute a parallel pathway that is collectively termed the "Mauthner series (M-series)" (Lee et al. 1991). Mauthner cells are a pair of giant RS neurons located in rhombomere 4 of the hindbrain in teleosts and amphibians. This neuron projects large diameter axons toward the contralateral spinal motor neurons. Following stimulation, the excited Mauthner cell emits a single action potential which is sufficient to evoke a C-start escape response via contraction of the contralateral skeletal muscle. On the other hand, MiD2cm and MiD3cm reside in rhombomeres 5 and 6, respectively. Similar to Mauthner cells, these Mauthner homologs extend axons to the contralateral side of spinal cord and make synaptic contact with contralateral motor neurons. These Mauthner homologs can initiate the escape response with similar kinetics to that initiated by Mauthner cell. However, the latency of the Mauthner homolog-initiated escape is longer than Mauthner cell-initiated escape (Kohashi and Oda 2008). Tactile stimulation of the head induces the largest amount of bending, and the turning angle reduces as the stimulated position moves toward a posterior region (Saint-Amant and Drapeau 1998; Umeda et al. 2016). A correlation between the stimulated position and the bending angle is required for survival in response to a threat in the environment. For forward-facing threats, fish should substantially change the direction of their swimming in the opposite direction. In contrast, for rear-facing threats, fish should rapidly move forward but not in the opposite direction. The combination of activated M-series neurons probably affects C-bend turning angles for the escape. When only Mauthner cells are activated by electrical stimulation, C-start escape with small turn angle is initiated (Nissanov et al. 1990). Similarly, caudal tactile stimuli activate only the Mauthner cell, leading to the induction of a small turning angle, whereas stimulation to the rostral trunk region activates Mauthner cells and the homologous M-series neurons and then an escape response with larger turn angle is initiated (O'Malley et al. 1996). How is A-P information transmitted to higher brain regions and processed to regulate escape behavior? The cell bodies of RB neurons are arranged in a pair of longitudinal columns on the dorsal side of the spinal cord. The longitudinal arrangement of RB neurons is suitable for detecting the anterior-posterior (A-P) positional information of stimuli. The A-P positional information of stimuli affects the bending angle. Although all RB neurons have an ascending central axon, most of the ascending axons terminate in the spinal cord, while a few RB axons enter the hindbrain. Interestingly, Mauthner dendrite-contacting RB neurons are more abundant in the rostral spinal cord, whereas many of the central axon of caudal RB neurons does not reach the hindbrain (Umeda et al. 2016). The sensory information from the caudal RB neuron may be relayed by

Commissural Primary Ascending (CoPA) neurons. CoPA neurons reside in the dorsal spinal cord, and their dendrites receive glutamatergic synaptic input from RB neurons (Gleason et al. 2003; Pietri et al. 2009). In addition, the axon of CoPA neurons ascends in the contralateral dorsal spinal cord to the diencephalon, thus the M-series neurons could be activated by this RB-CoPA pathway (Hale et al. 2001; Pietri et al. 2009; Umeda and Shoji 2017). Meanwhile, the escape response could also be initiated via an intra-spinal circuit but not M-series neurons. Previous studies show that disconnecting the spinal cord and hindbrain at somite 2 did not interfere with the touch response. In contrast, disconnection at somite-10 completely abolishes the touch response; thus, the neural circuitry that is sufficient to generate the touch response resides in the spinal cord between somites 2 and 10 (Downes and Granato 2006; Pietri et al. 2009). Anatomical data suggest that the CoPA neurons also contact descending interneurons, such as the circumferential ipsilateral descending (CiD) neurons and ipsilateral projecting (IC) neurons in the rostral spinal cord (Pietri et al. 2009). These interneurons provide excitatory input to motor neurons through both glutamatergic synapses and gap junction mediated electrical synapses (Saint-Amant and Drapeau 2001; Knogler and Drapeau 2014). However, additional functional studies using electrophysiology or ablation experiments are necessary to verify that CoPA neurons make functional synaptic contact with CiD and IC neurons. The larval zebrafish reflex arc for the touch response has been thought to consist of RB neurons, RS neurons, and motor neurons. However, this circuit could be more complex, and the details have not been elucidated.

4.5 Other Sensations Received by RB Neurons

In addition to mechanical stimulus, it has been suggested that RB neurons are also activated by thermal or chemical stimulus (Prober et al. 2008; Low et al. 2010a; Gau et al. 2013; Ogino et al. 2015).

Previous studies have identified five heat-activated channels (TRPV1-4, TRPM3) and two cold-activated channels (TRPM8 and TRPA1) in the rodent genome. These seven thermosensitive TRPs are expressed in sensory neurons in the TG and DRG and are activated at different temperatures (Dhaka et al. 2006; Vriens et al. 2011). TRPV1 and 2 respond to painful heating, activating at temperatures >42 °C and >52 °C, respectively. In contrast, TRPV3 and 4 are activated by non-painful warming (TRPV3: >33 °C; TRPV4: <27 °C to 42 °C). TRPM3 responds to noxious heating (>42 °C), similar to TRPV1. TRPV1 is also activated by capsaicin, a pungent compound from chili peppers, therefore capsaicin gives us burning sensation when the compound contacts to mucous membrane, such as in the oral cavity, that are innervated by TRPV1-expressing sensory neurons. Similarly, menthol provides a cooling sensation due to activation of the cool-activated channel TRPM8 (Bautista et al. 2007). In human sensory system, TRPM8 is activated at <25 °C, whereas another cool-activated channel, TRPA1, is activated at <17 °C. In addition to cooling stimuli, TRPA1 is also activated in response to chemical stimulants such as allyl

isothiocyanate (mustard oil), cinnamaldehyde (a pungent component in cinnamon), diallyl disulfide (a pungent component in garlic), acrolein (a toxic component in tear gas and vehicle exhaust), and 4-hydroxynonenal (an endogenous compound that is produced in response to tissue injury, inflammation, and oxidative stress) (Prober et al. 2008).

Zebrafish is a freshwater tropical fish that is broadly distributed across parts of India, Bangladesh, Nepal, Burma, and Pakistan (Lawrence 2007). Based on the habitat condition, 28.5 °C is recommended as optimum temperature for rearing in laboratory (Kimmel et al. 1995). As expected from their preference temperature, larval zebrafish robustly avoid noxious hot (36 °C) or cold (10 °C) temperatures (Prober et al. 2008; Gau et al. 2013). Gau et al. conducted a gene knockdown experiment using antisense morpholino for the *trpv1* gene and revealed that TRPV1 is required for the heat avoiding response but not required for the response to cold stimulus. The heat avoiding behavior is probably evoked by TG and RB neurons activation, which express transient receptor potential (TRP) channels, *trpv1* and *trpa1b* (Prober et al. 2008; Gau et al. 2013). In contrast to TRPV1, TRPA1b is not a thermal sensing channel but a chemical sensing channel that is activated by mustard oil (Prober et al. 2008). The activation of RB neurons by mustard oil evokes an escape response (Low et al. 2010a; Ogino et al. 2015). The TRP1b expressing RB neurons also express Piezo2b which is required for a tactile stimulus-evoked escape response (Faucherre et al. 2013). On the other hand, piezo2b-positive/trpa1b-negative RB neurons have also been observed, thus *trpa1b* is expressed in a subset of *piezo2b* expressing RB neurons (Faucherre et al. 2013). Gene expression analysis revealed that some subunits of P2X, ATP-gated ion channel, are expressed in RB neurons (Kucenas et al. 2003; Palanca et al. 2013). The zebrafish genome contains nine genes encoding a subunit of P2X. Among them, four genes, *p2rx3a*, *p2rx3b*, *p2rx4.1,* and *p2rx514*, were expressed in RB neurons. The expression of the *p2rx3a* and *p2rx3b* genes were detected in the majority of RB neurons, whereas the expression of *p2rx4.1* and *p2rx514* were detected only in a small proportion of RB neurons in 24 hpf larvae (Kucenas et al. 2003). The *p2rx3a* and *p2rx3b* genes are homologous to the mammalian *p2rx3* gene, which is expressed in sensory neurons for pain sensation. The P2X channel function has both homomeric and heteromeric channels of the subunits with different kinetics (Kucenas et al. 2003; Roberts et al. 2006). The diversities of the P2X subunits may provide a physiological diversity to RB neurons. Above data of gene expression pattern suggests that RB neurons are a much-diverged population. In addition, an RB neuron subtype that simultaneously expresses *trpa1b*, *p2rx3a,* protein kinase C alpha (PKCα) was identified by gene expression analysis (Slatter et al. 2005; Palanca et al. 2013). The simultaneous expression of different modal receptors in the RB neuron indicates that RB neurons are multimodal sensory neurons. Physiological analysis of the touché mutant, a light-touch unresponsiveness mutant, revealed that RB neurons can be classified into two groups based on their electrical responses to subthreshold tactile stimuli (Low et al. 2010a, 2011). That is, subthreshold tactile stimuli induce generator potentials in type I but not in type II RB neurons. The voltage of the generator potentials increases with the intensity of the subthreshold tactile stimuli. When the

voltage reaches a sufficient amplitude, the generator potentials trigger action potentials. In the touché mutant, type II RB neurons have completely disappeared. Investigation of the touché mutant suggests that type II RB neurons transmit light-touch sensations (Low et al. 2010a).

Unlike the heat-sensing TRP channels, the equivalent cold-sensing TRPs have not been identified in zebrafish RB neurons. As mentioned above, two cold-activated TRP channels, TRPA1 and TRPM8, were identified in mammalian genomes. In zebrafish, TRPA1 is required for chemical sensations although *trpa1* knockout larvae responded to cooling stimuli in a manner similar to that of wildtype larvae (Prober et al. 2008). No homolog of *trpm8* has been identified in comprehensive genome-wide studies in zebrafish (Saito and Shingai 2006). Genome analysis has also revealed the absence of TRPM8 in other teleost from 10 different orders (Gracheva and Bagriantsev 2015); thus, the loss of the *trpm8* gene may have occurred in the common ancestor of the teleost. In the zebrafish genome, 28 homologs of TRP channels have been identified, 3 *trpv* homologs, 2 *trpa1* homologs, 12 *trpc* homologs, and 11 *trpm* homologs (Saito and Shingai 2006; Kastenhuber et al. 2013; Von Niederhausern et al. 2013). The physiological function of the TRP channels can be diverse among teleosts and mammals. For example, mammalian TRPV1 is not only activated in response to heat at >42 °C but also in response to a low pH and capsaicin. In contrast, the zebrafish TRPV1 is activated at 32 °C or in response to low pH but not in response to capsaicin (Gau et al. 2013). Further research with new genetic techniques such as genome editing or new in vivo imaging techniques could contribute to the discovery of the genes for cold sensation. In addition to above TRP channels, the transcripts of *trpm7* and *trpc4* have been detected in RB neurons (Prober et al. 2008; Gau et al. 2013; Low et al. 2011; Von Niederhausern et al. 2013). However, the functional investigation thereto has not been conducted. Future investigations may also possibly shed light on the physiological significance of the RB neurons.

4.6 Apoptosis of RB Cells

RB neurons have been considered to be almost completely removed via caspase activity-dependent programmed cell death (apoptosis), and then the primary sensory function of RB neurons is replaced by DRG neurons (Williams et al. 2000; Svoboda et al. 2001; Reyes et al. 2004). The apoptotic RB neurons in larval zebrafish can be detected using transferase-mediated dUTP nick end-labeling (TUNEL) (Cole and Ross 2001). The apoptosis is first observed at 24 hpf in the rostral region of the spinal cord. During development, the region of apoptotic RB neurons moves caudally toward the end of the spinal cord. By 48 hpf, most apoptotic RB neurons are concentrated in the caudal region. Simultaneously with the active apoptosis of RB neurons, the peripheral processes of DRG neurons form. Apoptotic activity peaks between 36 and 48 hpf and rapidly decrease by 72 hpf. This correlation suggests a link between the death of RB neurons and the birth of DRG neurons.

However, RB cell degeneration occurs normally in mutants lacking DRG (*colorless* mutant). Thus, RB apoptosis and DRG development may be separate processes.

TrkC1, a receptor for the neurotrophin NT-3, is expressed in subpopulations of RB neurons. RB neuronal apoptosis is initiated only in TrkC1-negative neurons, suggesting that TrkC1 and NT-3 protect RB neurons from apoptosis (Williams et al. 2000). In support of this hypothesis, antibodies that deplete NT-3 induce RB neuronal apoptosis, while exogenous application of NT-3 reduces RB neuronal apoptosis. In addition to TrKC1-signaling, cyclin-dependent kinase 5 (Cdk5) may be involved in the regulation of RB neuronal apoptosis. SiRNA-mediated knockdown of Cdk5 promotes RB neuronal cell death, whereas overexpression of Cdk5 decreases RB neuronal cell death (Kanungo et al. 2006). One of the major apoptosis regulating mechanism is the mitochondrial pathway in which cytochrome c that released from mitochondria promote caspase activation (Czabotar et al. 2014). This process is regulated by bcl-2 proteins. In *Xenopus laevis*, RB neuron survival rate was significantly increased by overexpression of Bcl-X_L, one of the anti-apoptotic bcl-2 protein, in the nervous system (Coen et al. 2001). In cultured mammalian cell, the expression level of Bcl-X_L was reduced by depression of cdk5 activity (Brinkkoetter et al. 2009). Thus, the apoptosis of RB neuron might be regulated by the cdk5-Bcl-X_L regulated mitochondria pathway.

Voltage-gated sodium channel (Nav) mediated electrical activity is also likely required for the initiation of RB neuronal apoptosis, because pharmacological blockade of the Nav current reduced RB neuron death (Svoboda et al. 2001). This hypothesis is supported by the observation that RB neuron death was also reduced in a mutant whose RB neurons cannot generate action potential due to loss of Nav on the surface (Nakano et al. 2010). Nav is a large protein (~260 kDa) with 24 transmembrane domains and is responsible for the rising phase of the action potential in all neurons and muscles (Cantrell and Catterall 2001). Among nine Nav subtypes (Nav1.1–1.9), RB neuron express Nav1.1 and Nav1.6 (Novak et al. 2006). The Nav1.6 encoded by the *scn8aa* gene is the dominant subtype in RB neurons, as the morphants and mutants of *scn8aa* show a significant reduction in the peak amplitude of Nav in RB neurons and are unresponsive to tactile stimuli (Pineda et al. 2006; Low et al. 2010b). Antisense morpholino-mediated knockdown of the Nav1.6 also reduced the RB neuron death (Pineda et al. 2006). However, the relationship between the mitochondria pathway and Nav1.6 mediated electrical activity has not been elucidated yet.

Many studies including the above-mentioned have argued that most, if not all, RB neurons are lost by 4 dpf. However, recent studies revealed that 30–40% of RB neurons that express PKCα persist until at least 16 dpf (Slatter et al. 2005; Patten et al. 2007; Palanca et al. 2013). The existence of the long-lived RB neurons suggests that the removing of RB neurons in zebrafish may be much more of a restricted phenomenon than previously thought.

4.7 Mutants That Contributed to Investigate Nav Synthesis and Transport Mechanisms

As mentioned above, RB neurons require Nav to generate action potential. In excitable cells, such as neuron and muscle, Navs are transported to the specific regions of the cell membrane to form clusters, after the synthesis in the endoplasmic reticulum (ER). The Nav clusters have been identified in the axon initial segment and nodes of Ranvier of neurons. These clusters are molecular machinery for the generation and propagation of action potentials. Although the molecular basis of the Nav clustering at these sites has been extensively investigated (Rasband 2010), the molecular mechanisms that govern synthesis and transport of Nav has been less explored.

Six mutant zebrafish with reduced touch response have been identified in a large mutagenesis screening (Granato et al. 1996). RB neurons of four mutants of them (*alligator*, *macho*, *steiffer*, *crocodile*) showed reduction in Nav current amplitude, leading to a defect in the generation of action potentials and becoming touch-insensitive (Ribera and Nüsslein-Volhard 1998; Carmean and Ribera 2010). At present, responsible genes of *alligator* and *macho* have been identified (Carmean et al. 2015) (Ogino et al. 2015). Detailed analysis of these mutant provided insights into the molecular mechanisms of Nav synthesis and transport.

The mutation responsible for the *alligator* mutant is a nonsense mutation at leucine 39 (L39X) in a gene encoding the really interesting new gene (RING), finger protein 121 (RNF121) (Ogino et al. 2015). The nonsense mutation resulted in premature stop codon before the first transmembrane domain, thus the mutated gene appeared to be a null allele. RNF 121 is an E3-ubiquitin ligase with 6-transmembrane domain present in the endoplasmic reticulum (ER) and *cis*-Golgi compartments, and the catalytic activity is involved in ER-associated degradation (ERAD) (Darom et al. 2010; Araki and Nagata 2011). Some of the nascent protein that is synthesized in the ER would be misfolded or unfolded. In healthy cells, the inadequately folded proteins are removed by ERAD to prevent accumulation of the aberrant protein. In RB neurons of the mutant *alligator*, Navs accumulated in ER and cis-Golgi, instead of being transported to the cell surface, thus, RNF121 activity is essential for the proper intracellular trafficking of Nav in RB neurons, probably through removing of the misfolded Nav. Therefore, the study in *alligator* mutant indicated that RNF121 participates in the quality control of Nav during their synthesis (Ogino et al. 2015).

A missense mutation in the start codon of the *pigk* gene has been identified as the mutation responsible for *macho* mutant (Carmean et al. 2015). The missense mutation would result in a loss of function of the PigK protein, which is involved in addition of glycophospatidylinositol (GPI) to immature protein in ER. The GPI residue serves as an anchor for protein to bind to the cell membrane; thus, hypofunction of the complex that catalyzes GPI attachment leads to the mislocalization of GPI-anchored proteins. In addition to the *macho* mutant, the reduction of Nav current in RB neurons was recorded in a novel touch-insensitive mutant, *mi310* (Nakano et al. 2010). In RB neurons of a *mi310* mutant, the responsible mutation

was identified in a gene encoding the PigU subunit of the GPI transamidase complex. This mutation was a missense mutation that abolishes the enzyme activity of PigU. These studies revealed that RB neurons require GPI transamidase activity for the proper Nav current and also for touch sensitivity. However, it remains to be elucidated how GPI transamidase affects to the Nav current, because Nav is not GPI-anchored protein. Unidentified GPI-anchored protein possibly participates to establish the proper Nav current.

4.8 Tools for Manipulating RB Neurons

Many genetic encoding tools have been introduced to zebrafish biology. As aforementioned, zebrafish embryos are suitable for in vivo imaging and manipulation of neural activity due to the transparency of their body.

Intracellular Ca^{2+} concentration transiently increases during the generation of action potential via Ca^{2+} influx through voltage-gated Ca^{2+} channels. The Ca^{2+} transients in electrically stimulated RB neurons were visualized in cameleon-expressing zebrafish as the first successfully genetically encoded calcium indicator (GECI) (Higashijima et al. 2003). Cameleon is a FRET (fluorescence resonance energy transfer)-based GECI in which two different fluorescent proteins are linked by calmodulin (CaM) and CaM binding M13 peptide (Miyawaki et al. 1997). Binding of Ca^{2+} to CaM induces conformational change that increases the FRET efficiency between the fluorescent proteins. Thus, increases in intracellular Ca^{2+} concentration are visualized as a change in the ratio of fluorescence intensities between these fluorescent proteins. Therefore, cameleon serves as a ratiometric calcium indicator. After the development of cameleon, Nakai et al. produced a high Ca^{2+} affinity GECI composed of a single GFP, named GCaMP (Nakai et al. 2001). GCaMPs are circularly permuted (cp) EGFP that are fused to CaM at its C terminus and the M13 peptide at its N terminus (Nakai et al. 2001). Their fluorescence intensity is enhanced through the conformational change that is induced by Ca^{2+} binding to the calmodulin domain; therefore, GCaMPs visualize the Ca^{2+} transient as an alteration of the fluorescent intensity. In many model animals including zebrafish, GCaMPs were widely used for measuring neuronal activity in large populations of neurons because of their high Ca^{2+} affinity, which results in a high signal to noise ratio (Akerboom et al. 2012; Muto et al. 2011; Muto et al. 2013; Marsden and Granato 2015; Warp et al. 2012). After their development, to improve sensitivity, GCaMP was mutated to produce variants (Ohkura et al. 2005; Tallini et al. 2006; Tian et al. 2009; Akerboom et al. 2012; Chen et al. 2013; Muto et al. 2011). Fluorescence changes in GCaMP7a, the latest version of GCaMP, are approximately 3.2-fold greater than those of GCaMP-HS (Muto et al. 2013). Using the improved GCaMP expressing zebrafish larvae, spontaneous neuronal activities were visualized in the tectum, habenula, and hindbrain at single-cell resolution (Muto et al. 2013). To expand the GFP-based single color palette, blue fluorescent GECI (B-GECO) and red fluorescent GECI (R-GECO) were developed through mutating the cpGFP and replacing

the cpGFP with cpRFP, respectively (Zhao et al. 2011). These GECIs enabled multicolor Ca^{2+} imaging in zebrafish (Walker et al. 2013). Subcellular localization of GECIs can be modulated with the addition of a signal peptide or a protein that is localized to a relevant subcellular domain. Presynaptic terminal localized GCaMPs (SyGCaMPs) and SyRGECO were developed via fusion with synaptophysin, a transmembrane protein in synaptic vesicles (Dreosti et al. 2009; Nikolaou et al. 2012; Akerboom et al. 2012; Walker et al. 2013). Similarly, following the development of targeted GCaMPs, postsynaptic targeted GCaMP was developed via fusion of the postsynaptic matrix protein homer to the N terminus of GCaMP (Pech et al. 2015), and cell membrane targeted GCaMP was developed via fusion of the CAAX peptide to the C terminus of GCaMP (Tsai et al. 2014) or fusion of the LCK peptide to the N terminus of GCaMP (Shigetomi et al. 2010). In addition, mitochondrion-targeted GCaMP was developed via fusion of cytochrome C oxidase 4 to the N terminus of GCaMP (Park et al. 2010), and nuclear localized GCaMP was developed via fusion of histone H2B to the N terminus of GCaMP (Freeman et al. 2014) or fusion of a nuclear localization signal to the N terminus or C terminus of GCaMP (Kim et al. 2014). The combination of these targeting techniques and the multicolor palette enable multi-color Ca^{2+} imaging in a single cell.

Channelrhodopsin-2 (ChR2) and halorhodopsin (NpHR) enabled light-stimulated non-invasive manipulation of neural activity in zebrafish larvae. ChR2 is a light-gated channel that permeates a wide range of mono- and divalent cations, upon blue-light absorption. This cation flow depolarizes the membrane potential with high temporal precision, as the ChR2-mediated depolarizing currents reach a maximal rise rate within 2.3 ± 1.1 m sec after a blue-light pulse onset (Boyden et al. 2005). Single action potentials are reliably elicited in ChR2 expressing neurons after the light emission (Boyden et al. 2005). The first application of ChR2 in zebrafish was an experiment in which ChR2 was expressed in trigeminal and RB neurons under the control of the *isl1* promoter (Douglass et al. 2008). After stimulating the somatosensory neurons using a standard dissecting microscope and light pulses, single spikes from a single somatosensory neuron could drive escape behavior. Recently, Umeda et al. (2016) identified a novel escape response that is induced after single RB neuron excitation using an improved ChR2, ChRWR (channelrhodopsin-wide receiver), and laser microscopy to perform more precise single cell stimulation (Umeda et al. 2016). ChRWR is a chimeric protein of ChR1 and ChR2, and this improved ChR2 has a higher efficiency in plasma-membrane expression and photocurrents with little desensitization (Wang et al. 2009). NpHR is a fast light-activated chloride pump, thus NpHR can reversibly silence neural firing, contrast to ChR2. For reliable silencing, substantial membrane expression of NpHR is required. However, NpHR forms aggregates that are toxic to cells at high expression levels. This toxicity may result from the retention of NpHR in the ER (Gradinaru et al. 2007; Zhao et al. 2008). In addition, analysis of the amino acid sequence of NpHR revealed that it does not contain a typical signal peptide sequence (Zhao et al. 2008). To overcome this problem, the membrane expression efficiency of NpHR was improved through replacing the first 27 amino acids of NpHR with the signal peptide of the β subunit of nAchR and adding an ER export

signal from Kir2.1 to the C terminus of NpHR (Gradinaru et al. 2007; Zhao et al. 2008). The new enhanced NpHR (eNpHR) does not form aggregates and its membrane expression level is dramatically increased (Gradinaru et al. 2007; Zhao et al. 2008). An eNpHR expressing transgenic zebrafish line has been established, and neural firing in this model is effectively suppressed by light stimulation (Arrenberg et al. 2009). In addition, using this transgenic line in combination with ChR2 identified swim command neurons in the zebrafish hindbrain. The swimming behaviors that were induced in response to stimulating ChR2 expressing hindbrain neurons were blocked via the activation of NpHR in the same hindbrain neurons (Arrenberg et al. 2009).

Kaede is a photo-convertible fluorescent protein that changes from green to red after irradiation with ultra violet (UV) or violet light (Ando et al. 2002). Therefore, specific Kaede-expressing cells can be labeled after photo-conversion. Additionally, cells can be labeled with different colors after differentiation. UV irradiation to Kaede expressing cells at early stages of development labels early differentiated cells with red fluorescence, while only more recently differentiated cells are green.

4.9 Conclusion

Genetic manipulation using forward-genetics approaches have generated many mutant zebrafish lines, some of which are useful as human disease models. In zebrafish larvae, RB neurons are easily identifiable, and their relatively large cell body is suitable for electrophysiological recording of neural activity. Moreover, RB neurons are an attractive model for investigating the molecular mechanisms of axonal elongation. Many enhancer/promoter sequences that drive gene expression in all or a subset of RB neurons have been isolated (Table 4.1). With these enhancer/promoter sequences, any gene of interest can be expressed in RB neurons to investigate its function. Moreover, the function of the genes of interest can be investigated in human disease models. Zebrafish are a highly fertile animal and their larvae are easily drug-treatable via the addition of a compound into the breeding media. In this manner, experiments can be performed to investigate interactions among a diseased state and gene activity, the pharmacological effects of drugs, or new therapeutic agents using high throughput screening. The activation of RB neurons evokes a stereotyped escape response; thus, RB neuronal activity can be explored as a behavioral response. As a result, the RB neurons of zebrafish are an attractive experimental model. However, by 4 dpf, most RB neurons undergo apoptosis; therefore, their short lifespan may be disadvantageous for some experiments. However, long-lived RB neurons that express PKCα may be investigated to overcome this disadvantage. Experiments using the RB neurons of mutant zebrafish have revealed the molecular mechanisms that are essential for the proper intracellular trafficking of nascent protein. The RB neuron experimental model will continue to contribute insight for both basic and applied science.

References

Akerboom J, Chen TW, Wardill TJ, Tian L, Marvin JS, Mutlu S, Calderon NC, Esposti F, Borghuis BG, Sun XR, Gordus A, Orger MB, Portugues R, Engert F, Macklin JJ, Filosa A, Aggarwal A, Kerr RA, Takagi R, Kracun S, Shigetomi E, Khakh BS, Baier H, Lagnado L, Wang SS, Bargmann CI, Kimmel BE, Jayaraman V, Svoboda K, Kim DS, Schreiter ER, Looger LL (2012) Optimization of a GCaMP calcium indicator for neural activity imaging. J Neurosci 32(40):13819–13840. https://doi.org/10.1523/JNEUROSCI.2601-12.2012

Andermann P, Ungos J, Raible DW (2002) Neurogenin1 defines zebrafish cranial sensory ganglia precursors. Dev Biol 251(1):45–58

Andersen EF, Asuri NS, Halloran MC (2011) In vivo imaging of cell behaviors and F-actin reveals LIM-HD transcription factor regulation of peripheral versus central sensory axon development. Neural Dev 6(1):27

Ando R, Hama H, Yamamoto-Hino M, Mizuno H, Miyawaki A (2002) An optical marker based on the UV-induced green-to-red photoconversion of a fluorescent protein. Proc Natl Acad Sci 99(20):12651–12656

Araki K, Nagata K (2011) Protein folding and quality control in the ER. Cold Spring Harb Perspect Biol 3(11):a007526

Arrenberg AB, Del Bene F, Baier H (2009) Optical control of zebrafish behavior with halorhodopsin. Proc Natl Acad Sci 106(42):17968–17973

Asakawa K, Suster ML, Mizusawa K, Nagayoshi S, Kotani T, Urasaki A, Kishimoto Y, Hibi M, Kawakami K (2008) Genetic dissection of neural circuits by Tol2 transposon-mediated Gal4 gene and enhancer trapping in zebrafish. Proc Natl Acad Sci 105(4):1255–1260

Bautista DM, Siemens J, Glazer JM, Tsuruda PR, Basbaum AI, Stucky CL, Jordt SE, Julius D (2007) The menthol receptor TRPM8 is the principal detector of environmental cold. Nature 448(7150):204–208. https://doi.org/10.1038/nature05910

Becker T, Ostendorff HP, Bossenz M, Schlüter A, Becker CG, Peirano RI, Bach I (2002) Multiple functions of LIM domain-binding CLIM/NLI/Ldb cofactors during zebrafish development. Mech Dev 117(1):75–85

Bernhardt RR, Chitnis AB, Lindamer L, Kuwada JY (1990) Identification of spinal neurons in the embryonic and larval zebrafish. J Comp Neurol 302(3):603–616

Blader P, Fischer N, Gradwohl G, Guillemont F, Strahle U (1997) The activity of neurogenin1 is controlled by local cues in the zebrafish embryo. Development 124(22):4557–4569

Boyden ES, Zhang F, Bamberg E, Nagel G, Deisseroth K (2005) Millisecond-timescale, genetically targeted optical control of neural activity. Nat Neurosci 8(9):1263–1268. https://doi.org/10.1038/nn1525

Brinkkoetter PT, Olivier P, Wu JS, Henderson S, Krofft RD, Pippin JW, Hockenbery D, Roberts JM, Shankland SJ (2009) Cyclin I activates Cdk5 and regulates expression of Bcl-2 and Bcl-XL in postmitotic mouse cells. J Clin Invest 119(10):3089–3101

Cantrell AR, Catterall WA (2001) Neuromodulation of Na+ channels: an unexpected form of cellular platicity. Nat Rev Neurosci 2(6):397

Carmean V, Ribera AB (2010) Genetic analysis of the touch response in zebrafish (Danio rerio). Int J Comp Psychol/ISCP Int Soc Comp Psychol Univ Calabria 23(1):91

Carmean V, Yonkers MA, Tellez MB, Willer JR, Willer GB, Gregg RG, Geisler R, Neuhauss SC, Ribera AB (2015) Pigk mutation underlies macho behavior and affects Rohon-beard cell excitability. J Neurophysiol 114(2):1146–1157. https://doi.org/10.1152/jn.00355.2015

Chen TW, Wardill TJ, Sun Y, Pulver SR, Renninger SL, Baohan A, Schreiter ER, Kerr RA, Orger MB, Jayaraman V, Looger LL, Svoboda K, Kim DS (2013) Ultrasensitive fluorescent proteins for imaging neuronal activity. Nature 499(7458):295–300. https://doi.org/10.1038/nature12354

Coen L, du Pasquier D, Le Mevel S, Brown S, Tata J, Mazabraud A, Demeneix BA (2001) Xenopus Bcl-XL selectively protects Rohon-beard neurons from metamorphic degeneration. Proc Natl Acad Sci 98(14):7869–7874

Cole LK, Ross LS (2001) Apoptosis in the developing zebrafish embryo. Dev Biol 240(1):123–142. https://doi.org/10.1006/dbio.2001.0432

Cornell RA, Eisen JS (2000) Delta signaling mediates segregation of neural crest and spinal sensory neurons from zebrafish lateral neural plate. Development 127(13):2873–2882

Coste B, Mathur J, Schmidt M, Earley TJ, Ranade S, Petrus MJ, Dubin AE, Patapoutian A (2010) Piezo1 and Piezo2 are essential components of distinct mechanically activated cation channels. Science 330(6000):55–60

Czabotar PE, Lessene G, Strasser A, Adams JM (2014) Control of apoptosis by the BCL-2 protein family: implications for physiology and therapy. Nat Rev Mol Cell Biol 15(1):49

Darom A, Bening-Abu-Shach U, Broday L (2010) RNF-121 is an endoplasmic reticulum-membrane E3 ubiquitin ligase involved in the regulation of β-integrin. Mol Biol Cell 21(11):1788–1798

Dhaka A, Viswanath V, Patapoutian A (2006) Trp ion channels and temperature sensation. Annu Rev Neurosci 29:135–161. https://doi.org/10.1146/annurev.neuro.29.051605.112958

Douglass AD, Kraves S, Deisseroth K, Schier AF, Engert F (2008) Escape behavior elicited by single, channelrhodopsin-2-evoked spikes in zebrafish somatosensory neurons. Curr Biol 18(15):1133–1137. https://doi.org/10.1016/j.cub.2008.06.077

Downes GB, Granato M (2006) Supraspinal input is dispensable to generate glycine-mediated locomotive behaviors in the zebrafish embryo. J Neurobiol 66(5):437–451. https://doi.org/10.1002/neu.20226

Dreosti E, Odermatt B, Dorostkar MM, Lagnado L (2009) A genetically encoded reporter of synaptic activity in vivo. Nat Methods 6(12):883–889. https://doi.org/10.1038/nmeth.1399

Faucherre A, Nargeot J, Mangoni ME, Jopling C (2013) piezo2b regulates vertebrate light touch response. J Neurosci 33(43):17089–17094. https://doi.org/10.1523/JNEUROSCI.0522-13.2013

Freeman J, Vladimirov N, Kawashima T, Mu Y, Sofroniew NJ, Bennett DV, Rosen J, Yang CT, Looger LL, Ahrens MB (2014) Mapping brain activity at scale with cluster computing. Nat Methods 11(9):941–950. https://doi.org/10.1038/nmeth.3041

Fujita N, Saito R, Watanabe K, Nagata S (2000) An essential role of the neuronal cell adhesion molecule contactin in development of the Xenopus primary sensory system. Dev Biol 221(2):308–320

Gau P, Poon J, Ufret-Vincenty C, Snelson CD, Gordon SE, Raible DW, Dhaka A (2013) The zebrafish ortholog of TRPV1 is required for heat-induced locomotion. J Neurosci 33(12):5249–5260. https://doi.org/10.1523/JNEUROSCI.5403-12.2013

Geffeney SL, Goodman MB (2012) How we feel: ion channel partnerships that detect mechanical inputs and give rise to touch and pain perception. Neuron 74(4):609–619. https://doi.org/10.1016/j.neuron.2012.04.023

Gleason MR, Higashijima S-i, Dallman J, Liu K, Mandel G, Fetcho JR (2003) Translocation of CaM kinase II to synaptic sites in vivo. Nat Neurosci 6(3):217–218

Gracheva EO, Bagriantsev SN (2015) Evolutionary adaptation to thermosensation. Curr Opin Neurobiol 34:67–73

Gradinaru V, Thompson KR, Zhang F, Mogri M, Kay K, Schneider MB, Deisseroth K (2007) Targeting and readout strategies for fast optical neural control in vitro and in vivo. J Neurosci 27(52):14231–14238. https://doi.org/10.1523/JNEUROSCI.3578-07.2007

Granato M, Van Eeden F, Schach U, Trowe T, Brand M, Furutani-Seiki M, Haffter P, Hammerschmidt M, Heisenberg C-P, Jiang Y-J (1996) Genes controlling and mediating locomotion behavior of the zebrafish embryo and larva. Development 123(1):399–413

Haddon C, Smithers L, Schneider-Maunoury S, Coche T, Henrique D, Lewis J (1998) Multiple delta genes and lateral inhibition in zebrafish primary neurogenesis. Development 125(3):359–370

Hale ME, Ritter DA, Fetcho JR (2001) A confocal study of spinal interneurons in living larval zebrafish. J Comp Neurol 437(1):1–16

Halloran MC, Severance SM, Yee CS, Gemza DL, Raper JA, Kuwada JY (1999) Analysis of a zebrafish semaphorin reveals potential functions in vivo. Dev Dyn 214(1):13–25

Hernandez-Lagunas L, Choi IF, Kaji T, Simpson P, Hershey C, Zhou Y, Zon L, Mercola M, Artinger KB (2005) Zebrafish narrowminded disrupts the transcription factor prdm1 and is required for neural crest and sensory neuron specification. Dev Biol 278(2):347–357

Hirsch N, Zimmerman LB, Grainger RM (2002) Xenopus, the next generation: X. tropicalis genetics and genomics. Dev Dyn 225(4):422–433

Kanungo J, Li BS, Zheng Y, Pant HC (2006) Cyclin-dependent kinase 5 influences Rohon-beard neuron survival in zebrafish. J Neurochem 99(1):251–259. https://doi.org/10.1111/j.1471-4159.2006.04114.x

Kanungo J, Zheng YL, Mishra B, Pant HC (2009) Zebrafish Rohon-beard neuron development: cdk5 in the midst. Neurochem Res 34(6):1129–1137. https://doi.org/10.1007/s11064-008-9885-4

Kastenhuber E, Gesemann M, Mickoleit M, Neuhauss SC (2013) Phylogenetic analysis and expression of zebrafish transient receptor potential melastatin family genes. Dev Dyn 242(11):1236–1249

Kim CK, Miri A, Leung LC, Berndt A, Mourrain P, Tank DW, Burdine RD (2014) Prolonged, brain-wide expression of nuclear-localized GCaMP3 for functional circuit mapping. Front Neural Circuits 8:138. https://doi.org/10.3389/fncir.2014.00138

Kimmel CB, Ballard WW, Kimmel SR, Ullmann B, Schilling TF (1995) Stages of embryonic development of the zebrafish. Dev Dyn 203(3):253–310

Knogler LD, Drapeau P (2014) Sensory gating of an embryonic zebrafish interneuron during spontaneous motor behaviors. Front Neural Circuits 8:121. https://doi.org/10.3389/fncir.2014.00121

Kohashi T, Oda Y (2008) Initiation of Mauthner-or non-Mauthner-mediated fast escape evoked by different modes of sensory input. J Neurosci 28(42):10641–10653

Korn H, Faber DS (2005) The Mauthner cell half a century later: a neurobiological model for decision-making? Neuron 47(1):13–28. https://doi.org/10.1016/j.neuron.2005.05.019

Kucenas S, Li Z, Cox JA, Egan TM, Voigt MM (2003) Molecular characterization of the zebrafish P2X receptor subunit gene family. Neuroscience 121(4):935–945. https://doi.org/10.1016/s0306-4522(03)00566-9

Kuwada JY, Bernhardt RR, Nguyen N (1990) Development of spinal neurons and tracts in the zebrafish embryo. J Comp Neurol 302(3):617–628

Lawrence C (2007) The husbandry of zebrafish (Danio rerio): a review. Aquaculture 269(1):1–20

Lee K, Robert K, Eaton RC (1991) Identifiable reticulospinal neurons of the adult zebrafish, Brachydanio rerio. J Comp Neurol 304(1):34–52

Lewis KE, Eisen JS (2003) From cells to circuits: development of the zebrafish spinal cord. Prog Neurobiol 69(6):419–449. https://doi.org/10.1016/s0301-0082(03)00052-2

Li CL, Li KC, Wu D, Chen Y, Luo H, Zhao JR, Wang SS, Sun MM, Lu YJ, Zhong YQ, Hu XY, Hou R, Zhou BB, Bao L, Xiao HS, Zhang X (2016) Somatosensory neuron types identified by high-coverage single-cell RNA-sequencing and functional heterogeneity. Cell Res 26(1):83–102. https://doi.org/10.1038/cr.2015.149

Liu KS, Fetcho JR (1999) Laser ablations reveal functional relationships of segmental hindbrain neurons in zebrafish. Neuron 23(2):325–335

Liu Y, Halloran MC (2005) Central and peripheral axon branches from one neuron are guided differentially by Semaphorin3D and transient axonal glycoprotein-1. J Neurosci 25(45):10556–10563. https://doi.org/10.1523/JNEUROSCI.2710-05.2005

Low SE, Ryan J, Sprague SM, Hirata H, Cui WW, Zhou W, Hume RI, Kuwada JY, Saint-Amant L (2010a) Touche is required for touch-evoked generator potentials within vertebrate sensory neurons. J Neurosci 30(28):9359–9367. https://doi.org/10.1523/JNEUROSCI.1639-10.2010

Low SE, Zhou W, Choong I, Saint-Amant L, Sprague SM, Hirata H, Cui WW, Hume RI, Kuwada JY (2010b) Na(v)1.6a is required for normal activation of motor circuits normally excited by tactile stimulation. Dev Neurobiol 70(7):508–522. https://doi.org/10.1002/dneu.20791

Low SE, Amburgey K, Horstick E, Linsley J, Sprague SM, Cui WW, Zhou W, Hirata H, Saint-Amant L, Hume RI, Kuwada JY (2011) TRPM7 is required within zebrafish sensory neurons

for the activation of touch-evoked escape behaviors. J Neurosci 31(32):11633–11644. https://doi.org/10.1523/JNEUROSCI.4950-10.2011
Low SE, Woods IG, Lachance M, Ryan J, Schier AF, Saint-Amant L (2012) Touch responsiveness in zebrafish requires voltage-gated calcium channel 2.1b. J Neurophysiol 108(1):148–159. https://doi.org/10.1152/jn.00839.2011
Lumpkin EA, Caterina MJ (2007) Mechanisms of sensory transduction in the skin. Nature 445(7130):858–865. https://doi.org/10.1038/nature05662
Marsden KC, Granato M (2015) In vivo ca(2+) imaging reveals that decreased dendritic excitability drives startle habituation. Cell Rep 13(9):1733–1740. https://doi.org/10.1016/j.celrep.2015.10.060
Marusich MF, Furneaux HM, Henion PD, Weston JA (1994) Hu neuronal proteins are expressed in proliferating neurogenic cells. Dev Neurobiol 25(2):143–155
McCauley DW, Docker MF, Whyard S, Li W (2015) Lampreys as diverse model organisms in the genomics era. Bioscience 65(11):1046–1056
McKemy DD, Neuhausser WM, Julius D (2002) Identification of a cold receptor reveals a general role for TRP channels in thermosensation. Nature 416(6876):52
Metcalfe WK, Myers PZ, Trevarrow B, Bass MB, Kimmel CB (1990) Primary neurons that express the L2/HNK-1 carbohydrate during early development in the zebrafish. Development 110(2):491–504
Miyashita T, Yeo SY, Hirate Y, Segawa H, Wada H, Little MH, Yamada T, Takahashi N, Okamoto H (2004) PlexinA4 is necessary as a downstream target of Islet2 to mediate slit signaling for promotion of sensory axon branching. Development 131(15):3705–3715. https://doi.org/10.1242/dev.01228
Miyawaki A, Llopis J, Heim R, McCaffery JM, Adams JA, Ikura M, Tsien RY (1997) Fluorescent indicators for Ca2+ based on green fluorescent proteins and calmodulin. Nature 388(6645):882–887
Muto A, Ohkura M, Kotani T, Higashijima S, Nakai J, Kawakami K (2011) Genetic visualization with an improved GCaMP calcium indicator reveals spatiotemporal activation of the spinal motor neurons in zebrafish. Proc Natl Acad Sci U S A 108(13):5425–5430. https://doi.org/10.1073/pnas.1000887108
Muto A, Ohkura M, Abe G, Nakai J, Kawakami K (2013) Real-time visualization of neuronal activity during perception. Curr Biol 23(4):307–311. https://doi.org/10.1016/j.cub.2012.12.040
Nakai J, Ohkura M, Imoto K (2001) A high signal-to-noise Ca2+ probe composed of a single green fluorescent protein. Nat Biotechnol 19(2):137
Nakano Y, Fujita M, Ogino K, Saint-Amant L, Kinoshita T, Oda Y, Hirata H (2010) Biogenesis of GPI-anchored proteins is essential for surface expression of sodium channels in zebrafish Rohon-Beard neurons to respond to mechanosensory stimulation. Development 137(10):1689–1698. https://doi.org/10.1242/dev.047464
Nakayama H, Oda Y (2004) Common sensory inputs and differential excitability of segmentally homologous reticulospinal neurons in the hindbrain. J Neurosci 24(13):3199–3209. https://doi.org/10.1523/JNEUROSCI.4419-03.2004
Nakayama T, Fish MB, Fisher M, Oomen-Hajagos J, Thomsen GH, Grainger RM (2013) Simple and efficient CRISPR/Cas9-mediated targeted mutagenesis in Xenopus tropicalis. Genesis 51(12):835–843
Nguyen VH, Schmid B, Trout J, Connors SA, Ekker M, Mullins MC (1998) Ventral and lateral regions of the zebrafish gastrula, including the neural crest progenitors, are established by abmp2b/swirlPathway of genes. Dev Biol 199(1):93–110
Nguyen VH, Trout J, Connors SA, Andermann P, Weinberg E, Mullins MC (2000) Dorsal and intermediate neuronal cell types of the spinal cord are established by a BMP signaling pathway. Development 127(6):1209–1220
Nikolaou N, Lowe AS, Walker AS, Abbas F, Hunter PR, Thompson ID, Meyer MP (2012) Parametric functional maps of visual inputs to the tectum. Neuron 76(2):317–324. https://doi.org/10.1016/j.neuron.2012.08.040

Nissanov J, Eaton RC, DiDomenico R (1990) The motor output of the Mauthner cell, a reticulospinal command neuron. Brain Res 517(1):88–98

Novak AE, Taylor AD, Pineda RH, Lasda EL, Wright MA, Ribera AB (2006) Embryonic and larval expression of zebrafish voltage-gated sodium channel alpha-subunit genes. Dev Dyn 235(7):1962–1973. https://doi.org/10.1002/dvdy.20811

Ogino H, McConnell WB, Grainger RM (2006) Highly efficient transgenesis in Xenopus tropicalis using I-SceI meganuclease. Mech Dev 123(2):103–113

Ogino K, Low SE, Yamada K, Saint-Amant L, Zhou W, Muto A, Asakawa K, Nakai J, Kawakami K, Kuwada JY, Hirata H (2015) RING finger protein 121 facilitates the degradation and membrane localization of voltage-gated sodium channels. Proc Natl Acad Sci U S A 112(9):2859–2864. https://doi.org/10.1073/pnas.1414002112

Ohkura M, Matsuzaki M, Kasai H, Imoto K, Nakai J (2005) Genetically encoded bright Ca2+ probe applicable for dynamic Ca2+ imaging of dendritic spines. Anal Chem 77(18):5861–5869

O'Malley DM, Kao Y-H, Fetcho JR (1996) Imaging the functional organization of zebrafish hindbrain segments during escape behaviors. Neuron 17(6):1145–1155

Palanca AM, Lee SL, Yee LE, Joe-Wong C, Trinh le A, Hiroyasu E, Husain M, Fraser SE, Pellegrini M, Sagasti A (2013) New transgenic reporters identify somatosensory neuron subtypes in larval zebrafish. Dev Neurobiol 73(2):152–167. https://doi.org/10.1002/dneu.22049

Park YU, Jeong J, Lee H, Mun JY, Kim JH, Lee JS, Nguyen MD, Han SS, Suh PG, Park SK (2010) Disrupted-in-schizophrenia 1 (DISC1) plays essential roles in mitochondria in collaboration with Mitofilin. Proc Natl Acad Sci U S A 107(41):17785–17790. https://doi.org/10.1073/pnas.1004361107

Park B-Y, Hong C-S, Weaver JR, Rosocha EM, Saint-Jeannet J-P (2012) Xaml1/Runx1 is required for the specification of Rohon-beard sensory neurons in Xenopus. Dev Biol 362(1):65–75

Patten SA, Sihra RK, Dhami KS, Coutts CA, Ali DW (2007) Differential expression of PKC isoforms in developing zebrafish. Int J Dev Neurosci 25(3):155–164. https://doi.org/10.1016/j.ijdevneu.2007.02.003

Patterson KD, Krieg PA (1999) Hox11-family genes XHox11 and XHox11L2 in Xenopus: XHox11L2 expression is restricted to a subset of the primary sensory neurons. Dev Dyn 214(1):34–43

Pech U, Revelo NH, Seitz KJ, Rizzoli SO, Fiala A (2015) Optical dissection of experience-dependent pre- and postsynaptic plasticity in the Drosophila brain. Cell Rep 10(12):2083–2095. https://doi.org/10.1016/j.celrep.2015.02.065

Pietri T, Manalo E, Ryan J, Saint-Amant L, Washbourne P (2009) Glutamate drives the touch response through a rostral loop in the spinal cord of zebrafish embryos. Dev Neurobiol 69(12):780–795. https://doi.org/10.1002/dneu.20741

Pineda RH, Svoboda KR, Wright MA, Taylor AD, Novak AE, Gamse JT, Eisen JS, Ribera AB (2006) Knockdown of Nav1.6a Na+ channels affects zebrafish motoneuron development. Development 133(19):3827–3836. https://doi.org/10.1242/dev.02559

Ponomareva OY, Holmen IC, Sperry AJ, Eliceiri KW, Halloran MC (2014) Calsyntenin-1 regulates axon branching and endosomal trafficking during sensory neuron development in vivo. J Neurosci 34(28):9235–9248. https://doi.org/10.1523/JNEUROSCI.0561-14.2014

Prober DA, Zimmerman S, Myers BR, McDermott BM Jr, Kim SH, Caron S, Rihel J, Solnica-Krezel L, Julius D, Hudspeth AJ, Schier AF (2008) Zebrafish TRPA1 channels are required for chemosensation but not for thermosensation or mechanosensory hair cell function. J Neurosci 28(40):10102–10110. https://doi.org/10.1523/JNEUROSCI.2740-08.2008

Rasband MN (2010) The axon initial segment and the maintenance of neuronal polarity. Nat Rev Neurosci 11(8):552

Reyes R, Haendel M, Grant D, Melancon E, Eisen JS (2004) Slow degeneration of zebrafish Rohon-beard neurons during programmed cell death. Dev Dyn 229(1):30–41. https://doi.org/10.1002/dvdy.10488

Ribera AB, Nüsslein-Volhard C (1998) Zebrafish touch-insensitive mutants reveal an essential role for the developmental regulation of sodium current. J Neurosci 18(22):9181–9191

Roberts A (2000) Early functional organization of spinal neurons in developing lower vertebrates. Brain Res Bull 53(5):585–593

Roberts JA, Vial C, Digby HR, Agboh KC, Wen H, Atterbury-Thomas A, Evans RJ (2006) Molecular properties of P2X receptors. Pflugers Arch 452(5):486–500. https://doi.org/10.1007/s00424-006-0073-6

Rossi CC, Hernandez-Lagunas L, Zhang C, Choi IF, Kwok L, Klymkowsky M, Artinger KB (2008) Rohon-beard sensory neurons are induced by BMP4 expressing non-neural ectoderm in Xenopus laevis. Dev Biol 314(2):351–361

Saint-Amant L, Drapeau P (1998) Time course of the development of motor behaviors in the zebrafish embryo. J Neurobiol 37(4):622–632

Saint-Amant L, Drapeau P (2001) Synchronization of an embryonic network of identified spinal interneurons solely by electrical coupling. Neuron 31(6):1035–1046

Saito S, Shingai R (2006) Evolution of thermoTRP ion channel homologs in vertebrates. Physiol Genomics 27(3):219–230

Segawa H, Miyashita T, Hirate Y, Higashijima S-i, Chino N, Uyemura K, Kikuchi Y, Okamoto H (2001) Functional repression of Islet-2 by disruption of complex with Ldb impairs peripheral axonal outgrowth in embryonic zebrafish. Neuron 30(2):423–436

Shigetomi E, Kracun S, Sofroniew MV, Khakh BS (2010) A genetically targeted optical sensor to monitor calcium signals in astrocyte processes. Nat Neurosci 13(6):759–766. https://doi.org/10.1038/nn.2557

Higashijima S-i, Masino MA, Mandel G, Fetcho JR (2003) Imaging neuronal activity during zebrafish behavior with a genetically encoded calcium indicator. J Neurophysiol 90(6):3986–3997

Slatter CA, Kanji H, Coutts CA, Ali DW (2005) Expression of PKC in the developing zebrafish, Danio rerio. J Neurobiol 62(4):425–438. https://doi.org/10.1002/neu.20110

Svoboda KR, Linares AE, Ribera AB (2001) Activity regulates programmed cell death of zebrafish Rohon-beard neurons. Development 128(18):3511–3520

Tallini YN, Ohkura M, Choi B-R, Ji G, Imoto K, Doran R, Lee J, Plan P, Wilson J, Xin H-B (2006) Imaging cellular signals in the heart in vivo: cardiac expression of the high-signal Ca2+ indicator GCaMP2. Proc Natl Acad Sci U S A 103(12):4753–4758

Tanaka H, Nojima Y, Shoji W, Sato M, Nakayama R, Ohshima T, Okamoto H (2011) Islet1 selectively promotes peripheral axon outgrowth in Rohon-Beard primary sensory neurons. Dev Dyn 240(1):9–22

Tian L, Hires SA, Mao T, Huber D, Chiappe ME, Chalasani SH, Petreanu L, Akerboom J, McKinney SA, Schreiter ER (2009) Imaging neural activity in worms, flies and mice with improved GCaMP calcium indicators. Nat Methods 6(12):875–881

Tsai FC, Seki A, Yang HW, Hayer A, Carrasco S, Malmersjo S, Meyer T (2014) A polarized Ca2+, diacylglycerol and STIM1 signalling system regulates directed cell migration. Nat Cell Biol 16(2):133–144. https://doi.org/10.1038/ncb2906

Umeda K, Shoji W (2017) From neuron to behavior: sensory-motor coordination of zebrafish turning behavior. Develop Growth Differ 59(3):107–114. https://doi.org/10.1111/dgd.12345

Umeda K, Ishizuka T, Yawo H, Shoji W (2016) Position- and quantity-dependent responses in zebrafish turning behavior. Sci Rep 6:27888. https://doi.org/10.1038/srep27888

Von Niederhausern V, Kastenhuber E, Stauble A, Gesemann M, Neuhauss SC (2013) Phylogeny and expression of canonical transient receptor potential (TRPC) genes in developing zebrafish. Dev Dyn 242(12):1427–1441. https://doi.org/10.1002/dvdy.24041

Vriens J, Owsianik G, Hofmann T, Philipp SE, Stab J, Chen X, Benoit M, Xue F, Janssens A, Kerselaers S, Oberwinkler J, Vennekens R, Gudermann T, Nilius B, Voets T (2011) TRPM3 is a nociceptor channel involved in the detection of noxious heat. Neuron 70(3):482–494. https://doi.org/10.1016/j.neuron.2011.02.051

Walker AS, Burrone J, Meyer MP (2013) Functional imaging in the zebrafish retinotectal system using RGECO. Front Neural Circuits 7:34. https://doi.org/10.3389/fncir.2013.00034

Wang H, Sugiyama Y, Hikima T, Sugano E, Tomita H, Takahashi T, Ishizuka T, Yawo H (2009) Molecular determinants differentiating photocurrent properties of two channelrhodopsins from chlamydomonas. J Biol Chem 284(9):5685–5696

Wang F, Wolfson SN, Gharib A, Sagasti A (2012) LAR receptor tyrosine phosphatases and HSPGs guide peripheral sensory axons to the skin. Curr Biol 22(5):373–382. https://doi.org/10.1016/j.cub.2012.01.040

Warp E, Agarwal G, Wyart C, Friedmann D, Oldfield CS, Conner A, Del Bene F, Arrenberg AB, Baier H, Isacoff EY (2012) Emergence of patterned activity in the developing zebrafish spinal cord. Curr Biol 22(2):93–102. https://doi.org/10.1016/j.cub.2011.12.002

Warren JT, Chandrasekhar A, Kanki JP, Rangarajan R, Furley AJ, Kuwada JY (1999) Molecular cloning and developmental expression of a zebrafish axonal glycoprotein similar to TAG-1. Mech Dev 80(2):197–201

Weiss SA, Zottoli SJ, Do SC, Faber DS, Preuss T (2006) Correlation of C-start behaviors with neural activity recorded from the hindbrain in free-swimming goldfish (Carassius auratus). J Exp Biol 209(23):4788–4801

Williams JA, Barrios A, Gatchalian C, Rubin L, Wilson SW, Holder N (2000) Programmed cell death in zebrafish rohon beard neurons is influenced by TrkC1/NT-3 signaling. Dev Biol 226(2):220–230. https://doi.org/10.1006/dbio.2000.9860

Wittbrodt J, Shima A, Schartl M (2002) Medaka—a model organism from the far east. Nat Rev Genet 3(1):53

Zhao S, Cunha C, Zhang F, Liu Q, Gloss B, Deisseroth K, Augustine GJ, Feng G (2008) Improved expression of halorhodopsin for light-induced silencing of neuronal activity. Brain Cell Biol 36(1–4):141–154. https://doi.org/10.1007/s11068-008-9034-7

Zhao Y, Araki S, Wu J, Teramoto T, Chang YF, Nakano M, Abdelfattah AS, Fujiwara M, Ishihara T, Nagai T, Campbell RE (2011) An expanded palette of genetically encoded ca(2)(+) indicators. Science 333(6051):1888–1891. https://doi.org/10.1126/science.1208592

Part II
Homeostasis and Reproduction

Chapter 5
Fish in Space Shedding Light on Gravitational Biology

Masahiro Chatani and Akira Kudo

Abstract Space flight in an environment with reduced gravity has severe effects on the body. Astronauts suffer from a significant decrease in bone mineral density during space missions, but the molecular mechanisms responsible for such changes in bone density are unclear. To identify these mechanisms, unique experiments on medaka fish were performed twice at the International Space Station (ISS). One was a two-month long experiment for the analysis of bone growth, which revealed a decrease in the mineral density of pharyngeal bones. Another was a short-term experiment for live imaging of transgenic medaka lines and transcriptome analysis during 8 days, which revealed an increase in the expression levels of five genes. Overall, these studies on medaka fish provided an initial explanation of the process.

Keywords Medaka · Bone · Gravity · International Space Station · Osteoclast · Osteoblast

M. Chatani (✉)
Department of Pharmacology, School of Dentistry, Showa University, Shinagawa-ku, Tokyo, Japan
e-mail: chatani@dent.showa-u.ac.jp

A. Kudo
Department of Pharmacology, School of Dentistry, Showa University, Shinagawa-ku, Tokyo, Japan

Tokyo Institute of Technology, Meguro-ku, Tokyo, Japan
e-mail: akudo@bio.titech.ac.jp

H. Hirata, A. Iida (eds.), *Zebrafish, Medaka, and Other Small Fishes*,
https://doi.org/10.1007/978-981-13-1879-5_5

5.1 Effect of Gravity on Life

5.1.1 Consideration of the Effect of Gravity on Life Before the Space Exploration Era

How has the effect of gravity on life been considered? In 1897, Crookes remarked that forms as well as behaviors of our bodies are totally regulated by the strength of gravity on Earth (Crookes 1987). In 1917, Thompson published *On Growth and Form* and discussed whether doubling the force of gravity would lead to the failure of our bipedal form, and suggested that the majority of terrestrial animals would resemble short-legged saurians or serpents under such conditions. However, halving the force of gravity would result in a lighter, slenderer, and more active body, requiring less energy and heat and smaller sizes of heart and lungs (Thompson 1917). Given these hypotheses, gravity has been considered as a factor affecting the living body.

5.2 History of Bone Loss Under Microgravity

5.2.1 Astronauts Under Microgravity

Microgravity has been thought to induce osteoporosis. Physiological studies in spaceflight have been performed using various animals (Table 5.1). The first evidence of the undesirable changes produced in bones during spaceflight was an increase in urinary calcium excretion by the cosmonauts on board Vostok 2 and 3 (David 1963). However, until now, little data is available on its precise nature in the course of flight time (Rambaut and Goode 1985). In 2000, the study of bone mineral density at the distal radius and tibia of 15 cosmonauts, who sojourned in space for one, two, or 6 months in the Russian MIR space station, was reported. This study suggested that the level of decrease in bone mineral density differs between weight-bearing and non-weight-bearing bones (Vico et al. 2000). In the weight-bearing tibial site, cancellous BMD loss was already evident after the first month and deteriorated with mission duration. In tibial cortices, bone mineral loss was noted after a two-month flight. In contrast, the BMD in radial cortices were not significantly changed at any of the time points, whereas cancellous BMD loss was relatively weak and insignificant.

5.2.2 Animal Experiments in Space for Bone Study

Many animals have been utilized in space environments for studying the effect of microgravity. The first animal that revealed a decreased bone volume in space was a dog. The dogs on the 22-day flight in Cosmos 110 suffered from 11.5–12.3% reduction in heel bone density, resulting in a rise of serum calcium and double urinary and

Table 5.1 History of bone study in space (selected experiments)

Year	Ship	Species	Duration	Principal findings	References
1961–1962	Vostok	Human	1–4 days	Increase of urinary calcium excretion	David (1963)
1966	Cosmos	Dog	22 days	Reduction of heel bone density	Parin et al. (1968)
1973–1974	Skylab	Human	84 days	Increase of urinary calcium excretion	Rambaut and Goode (1985)
				Reduction of heel bone density	
				Lower level of serum PTH	
1975	Vostok	Juvenile rat	19.5 days	Decrease of bone formation in tibia	Morey and Baylink (1978)
1979	Cosmos	Juvenile rat	18.5 days	Decrease of remodeling activity in alveolar bone	Simmons et al. (1983)
1983	Cosmos	Pregnant rat	5 days	Increased osteoclast number and decreased bone mass via excess resorption	Vico et al. (1987)
1992	Space Shuttle (*Endeavor*)	Chicken embryo	7–10 days	Little effect on bone metabolism in lambs	Kawashima et al. (1995)
1992	Cosmos	Newts	12 days	Reduction of osteoclast number in tail regeneration	Berezovska et al. (1998)
1994	Space Shuttle (*Columbia*)	Juvenile OVX rat	14 days	Reduction of bone mineral density in femur and lumbar vertebra	Keune et al. (2016)
1994	Mir	Human	1, 2, 6 months	Reduction of bone mineral density in tibia	Vico et al. (2000)
2009	International Space Station	Mouse	3 months	Decrease of trabecular number in femur	Tavella et al. (2012)
2010, 2011	Space Shuttle (*Discovery*)	Juvenile mouse	13, 15 days	Reduction of bone volume in mandible. Reduction of distance between CEJ and AC	Ghosh et al. (2016)
2012	International Space Station	Juvenile medaka	58 days	Decrease of mineral density in pharyngeal bones	Chatani et al. (2015)
2014	International Space Station	Medaka embryo	8 days	Upregulation of bone-related gene expression	Chatani et al. (2016)

PTH parathyroid hormone, *OVX* ovariectomized, *CEJ* cemento-enamel junction, *AC* alveolar crest

fecal calcium excretion (Parin et al. 1968). The mammalian animal models rats and mice have often been applied for space experiments. The results showed the reduction of BMD in tibia, femur, or lumbar vertebrae (Morey and Baylink 1978; Vico et al. 1987; Keune et al. 2016; Tavella et al. 2012). Interestingly, the effect of microgravity appeared on non-weight-bearing bones (Simmons et al. 1983; Ghosh et al. 2016). In addition, unique studies were performed in space using chickens for embryogenesis (Kawashima et al. 1995) and newts for regeneration (Berezovska et al. 1998).

5.2.3 *Discussion on Changes in Bone Formation and Resorption in Space*

Abnormal skeletons have been found in numerous species under microgravity. Two hypotheses can be generalized from data obtained in spaceflight. First, the inhibition of bone formation during spaceflight, including complete cessation of periosteal bone formation, as observed in rats (Morey and Baylink 1978). Second, the increase in bone resorption during spaceflight was indicated by an increased number of osteoclasts in pregnant rats and a decreased bone mass due to excess resorption when subjected to weightlessness for 5 days (Vico et al. 1987). These reports indicate that it is necessary to examine the bone metabolism in various parts of several animal models to estimate the effect of gravity on life accurately.

5.3 Advantages of Studying Bone Development in Medaka

5.3.1 *Bone Growth and Modeling*

During skeletal development, bone is altered in size dramatically without any significant change in its complex architecture. This alteration is achieved by the formation of new bones at one site by osteoblasts and resorption of old bones by osteoclasts at another site within the same bone (Bard 1990; Frost 1990; Seeman 2003). It has been postulated that osteoblasts and osteoclasts act in separate sites in an uncoupled manner (Teti 2011). However, an interaction between osteoblasts and osteoclasts is possible, because bone formation and resorption occurs in a coordinated manner in mammals, as revealed by bone modeling during skull growth for enveloping brain tissues (Fong et al. 2003). Furthermore, the growth of long bones is controlled by bone modeling that involves a complex pattern of bone formation and resorption, which is achieved by a balanced activity of osteoblasts and osteoclasts along the periosteal or endosteal surface of the cortical bones (Schenk et al. 1973).

5.3.2 *Pharyngeal Bone in Medaka*

The pharyngeal bone, where osteoclasts emerge in the earliest stage of development in medaka, is a good candidate for an in vivo analysis of bone modeling. Pharyngeal bones consist of several hundreds of teeth called pharyngeal teeth and supporting bones. There are many TRAP (tartrate resistant acid phosphatase)-positive multinuclear osteoclasts having ruffled border in supporting bones of the adult medaka (Nemoto et al. 2007). It was reported that sequential tooth regeneration occurs throughout the life of medaka (Abduweli et al. 2014), suggesting the possibility that pharyngeal bones would show frequent bone modeling.

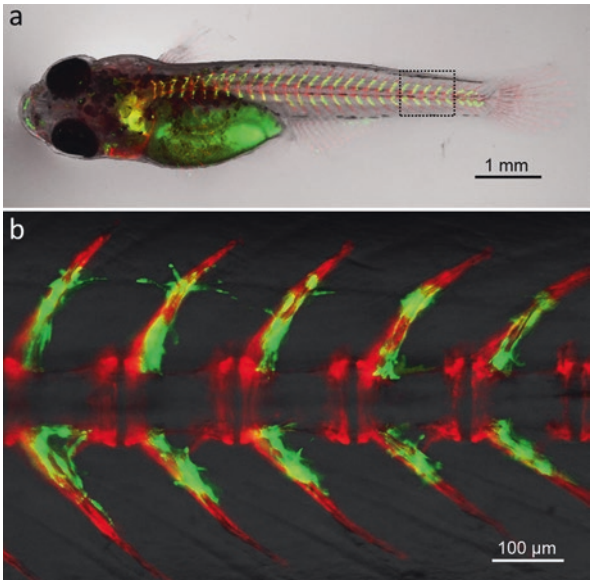

Fig. 5.1 Fluorescence imaging of medaka osteoclasts and osteoblasts (**a**) Whole image of *osterix* promoter-DsRed/*TRAP* promoter-GFP double transgenic medaka larva, which visualizes osteoblasts (red) and osteoclasts (green). (**b**) The vertebral region. Enlarged image of dotted box in "a"

To visualize osteoblasts and osteoclasts in vivo, medaka *osterix* promoter-DsRed transgenic line for osteoblasts (Inohaya et al. 2007) and the medaka *TRAP* promoter-GFP transgenic line for osteoclasts were previously developed (Chatani et al. 2011). Finally, a double transgenic line of *osterix*-DsRed and *TRAP*-GFP (Chatani et al. 2015) was generated to examine the cooperation between osteoblasts and osteoclasts in the same animal in vivo (Fig. 5.1). Osteoclasts, which are differentiated from c-fms$^+$ osteoclast progenitors, are exclusively localized in the developed supporting bones, and osteoblasts are mainly localized in immature supporting bones (Mantoku et al. 2016). Osteoblast ablation-induced osteoclast apoptosis is a new finding that shows the communication between osteoblasts and osteoclasts in bone modeling (Fig. 5.2).

5.4 Fish as the Favored Animal Model in Space

5.4.1 The First Medaka Fish in Space

In the 1990s, Dr. Ijiri's group tried to see whether fish can mate successfully in the absence of gravity on the space shuttle *Columbia* and provided the first example of a successful vertebrate mating in space (Ijiri 1995). Before performing this experiment, they observed the behavior of medaka as a preliminary step in the parabolic flight.

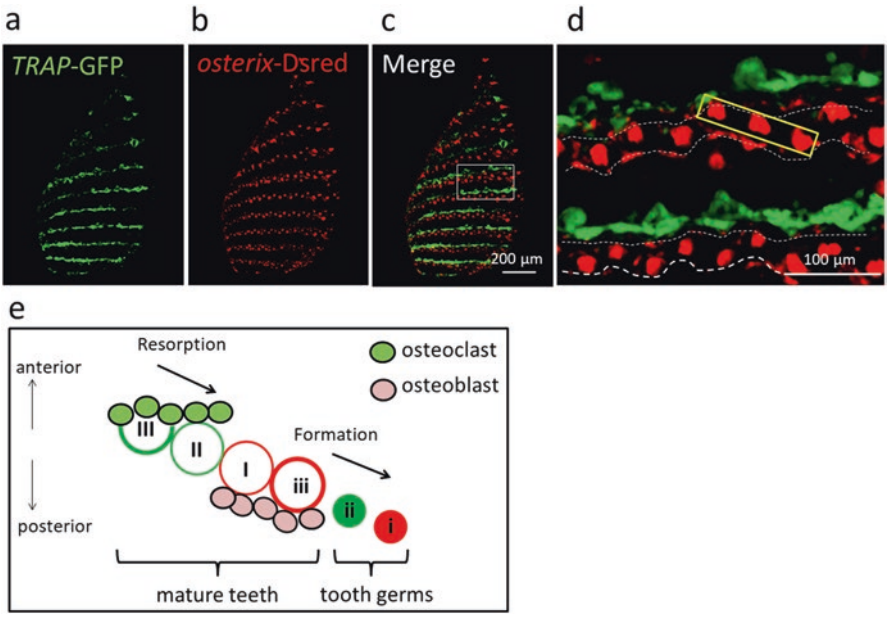

Fig. 5.2 Distinctive localization of osteoclasts and osteoblasts (**a**, **b**) *TRAP* promoter-GFP (**a**) *osterix* promoter-DsRed signals (**b**) at right upper pharyngeal bone. (**c**) Merge image of "a" and "b." (**d**) Enlarged image of white square in "c." Yellow square shows tooth family. (**e**) Model of the role for tooth change mediated by bone resorption and formation. (Mantoku et al. 2016)

5.4.2 Facilities for Rearing Fish in the ISS

The aquatic habitat was developed by JAXA (Japan Aerospace Exploration Agency), which was based on the aquatic animal facilities used in Space Shuttle (Masukawa et al. 2003; Uchida et al. 2002; Sakimura and Suzuki 1999). This aquatic habitat is used for rearing small freshwater fish, such as medaka or zebrafish, for up to 90 days in space. The habitat is composed of the closed water circulation system that includes a water circulation unit, the gas exchanger for exchange of dissolved gas in the circulating water, the biological filter for water purification, and two aquariums as habitats for fish (Fig. 5.3). The water circulation unit includes water pumps, flow sensors, a temperature controller, and an accumulator to control the environment for fish habitation. The total water volume of the water circulation system is 3.2 L, and the water volume of each aquarium is 0.7 L. The aquarium has an automatic feeder to supply artificial powdery food to fish. Each aquarium is equipped with an LED (light emitting diode) light for producing day and night cycles and a CCD (charge-coupled device) camera for observation of fish. Outlines of the aquatic habitat and a flow scheme are shown in the JAXA homepage (JAXA 2017). These components were performed in the Multi-purpose Small Payload Rack (MSPR) at the Japanese Experiment Module (JEM) in ISS. During fish habitation in the aquatic habitat, the

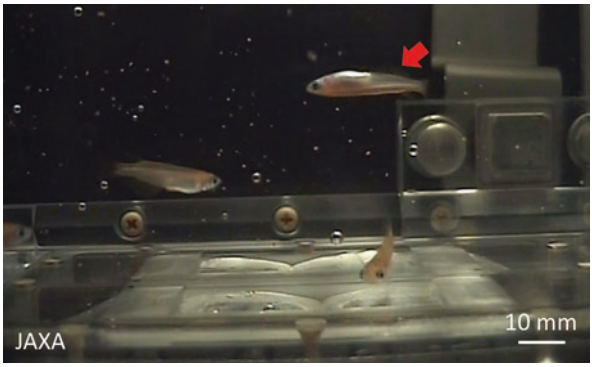

Fig. 5.3 Behaviors of reared fish in AQH in ISS Medaka (red arrow) is floating and swimming upside down in AQH. (Chatani et al. 2015)

water temperature was maintained at 25.5–26 °C, and the water flow rate was controlled at 0.1 L per minute for each aquarium. The dissolved oxygen was maintained at over 90% saturation by gas exchange with the cabin and the water quality was controlled by using a biological filter of nitrifying bacteria. The water quality was checked by the astronauts once or twice a week with test strips, and there was no accumulation of either ammonia or nitrite during the experiments. The day and night cycle, obtained by use of a white LED light, was controlled to provide 14 h of light (380 lux) and 10 h of dim light (10 lux; this dim light was used for dorsal light response of fish). Three kinds of powdery food, Otohime B-1 (Marubeni Nisshin Feed) and Kyowa N250 and N400 (Kyowa Hakko Bio), were supplied to the fish by the automatic feeder in the aquarium twice or thrice a day.

5.4.3 Two Kinds of Fish Reared at the Aquarium in Space

To examine the physiological changes in space, medaka and zebrafish were reared at the aquarium in the ISS. The effects on bone of medaka and skeletal muscles of zebrafish in space were studied. Sixteen medaka were launched and reared for approximately 2 months in 2012, (Chatani et al. 2015) whereas 18 zebrafish were reared for 1.5 months in 2015.

5.5 Long-Term Experiment in the ISS

Patients on bed rest and those with age-related osteoporosis suffer from loss of bone density. Results from the experiment in space can provide the data that may be used to develop new drugs and treatments for these patients. During long stays in space, the bone volume of astronauts decreases remarkably. However, the molecular mechanism of bone loss remains unknown. Enhancement of the osteoclast (cells responsible for bone resorption) is assumed to cause decrease in bone mineral density in

space. To investigate the molecular mechanism, the osteoblast- and osteoclast-specific double transgenic medaka fish were developed, because medaka is a model animal for organogenesis.

Medaka is a vertebrate fish commonly used for scientific research, because they have a smaller genome size than zebrafish have, can live in a much smaller area, and consume less food, water, and oxygen. Medaka have mated successfully in space, indicating that medaka is an ideal fish suitable for raising all life stages from juveniles to adults in the AQH system under the microgravity environment of the ISS.

To investigate the effect of microgravity on osteoclasts in space, a long-term experiment on medaka was performed in 2012 (Chatani et al. 2015). It specifically aimed to examine the alteration of osteoclast activity under microgravity by performing histological and gene expression analysis (Aquarium-AQH 1). The molecular mechanisms that activate osteoclasts in microgravity are under investigation. In the Aquarium AQH 2, medaka living in microgravity were examined; these genetically modified fish have translucent bodies, with fluorescent proteins to allow clearer observation of their cellular and genetic changes during space flight.

The cellular activities of bone formation and resorption have been studied in the gravity-sensitive pharyngeal region of medaka, which contains hundreds of teeth and many osteoclasts in the adult fish. Observations revealed that the fish became accustomed to microgravity by displaying unique behaviors, such as upside down, vertical, and tight-circle swimming (Fig. 5.3). In addition, it was found that the mating behavior at day 33 under microgravity is not different from that on Earth. Interestingly, they tended to become motionless at day 47, suggesting reduced muscle force. Tooth germ formation during tooth development was normal in the flight group. During 56 days in microgravity, the mineral density of the upper pharyngeal bone and the tooth region decreased approximately 24% and the osteoclast volume increased compared to those of the ground control fish (Fig. 5.4). Using an electron microscope, the abnormal structure of osteoclast mitochondria was observed. Moreover, transcriptome analysis revealed a significant increase in the activity of two genes that may be involved in mitochondrial function, suggesting that osteoclast activation might be linked to the sensitivity of mitochondria to microgravity. Overall, the results indicated the impaired physiological function and reduced mechanical use of the body under microgravity, in addition to osteoclast activation, induce stress owing to weightlessness.

Further, other studies examined the ovary, intestine, testis, liver, brain, and eyes, and focused on observing the biological impact of microgravity on these organs (Murata et al. 2015). The analysis of 5345 genes from the six tissues, mentioned earlier, revealed similar but highly tissue-specific changes. Eleven genes were upregulated (the process by which a cell increases the quantity of a cellular component, such as RNA or protein, in response to an external stimulus; i.e., the action opposite to downregulation) in more than four of the tissues examined, indicating the presence of a common immune and stress response system to spaceflight. A few genes in the brain and eyes responded to the space environment. By contrast, more than 2500 genes altered their expression levels in the caudal (near the tail) part of the intestine, suggesting that this organ is highly sensitive to stress induced by

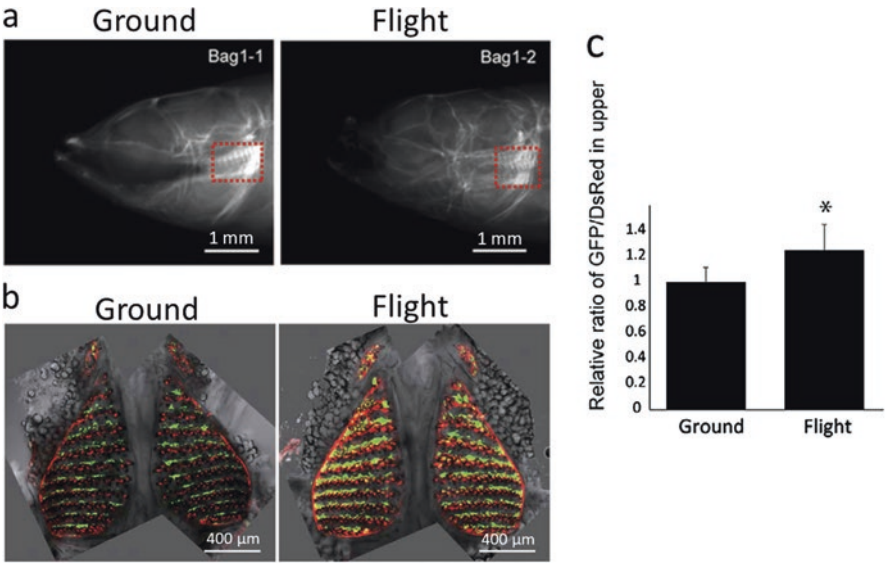

Fig. 5.4 Changes of medaka bone under microgravity
(**a**) Soft X-ray analysis. Lateral views of the heads of ground (left) and flight medaka (right) reared for 56 days. The red-dotted box shows the pharyngeal bone region. (**b**) Upper pharyngeal bones and teeth of *osterix* promoter-DsRed/*TRAP* promoter-GFP double transgenic medaka at day 56. (**c**) Graph shows the relative value of GFP volume divided by DsRed volume. (Chatani et al. 2015)

microgravity. Many genes were downregulated in the liver without accompanying tissue abnormalities. No significant alterations in the gene expression levels ("significant" refers to more than two-fold difference) were detected in the ovary. However, the expression levels of genes for egg envelope proteins were suppressed in the ovary, and egg development became slightly abnormal in space fish, even though body growth and maturation were not delayed. In the testis, spermatocytes, spermatids, and spermatozoa were comparable between the flight and ground groups, suggesting that normal spermatogenesis is maintained during spaceflight.

These results shed light on the mechanism underlying the regulation of bone physiology and organ tissue changes under microgravity.

5.6 Short-Term Experiment in the ISS

To investigate the mechanism of bone loss during spaceflight, it is important to study the initial response immediately after exposure to microgravity, because this response triggers for bone loss. To examine the early effects of microgravity on bone cells, transgenic medaka larvae were embedded in a gel (Fig. 5.5) and sent to the ISS for a live-imaging study in space in 2014 (Chatani et al. 2016), and the

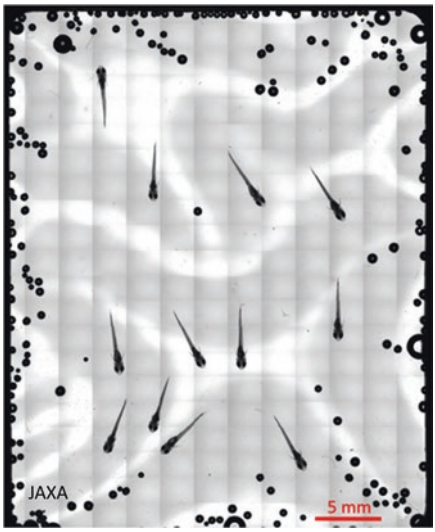

Fig. 5.5 Overall picture of the medaka chamber captured at the ISS Totally, 273 images captured by 5x objective lens were integrated by Tiling method, showing an overall picture of the medaka chamber. This figure shows suitable localization of medaka fish for observation by 20x objective lens

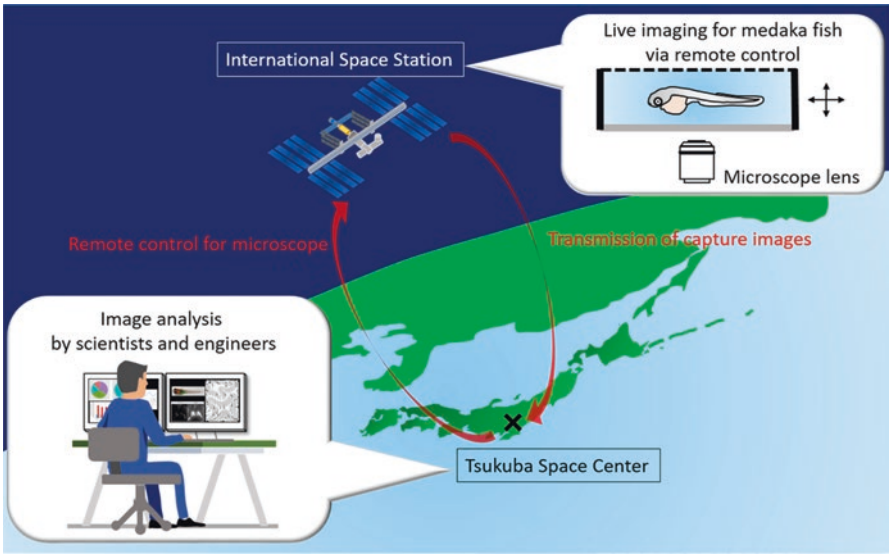

Fig. 5.6 Scheme of live-imaging method under microgravity
During the experiment at the ISS, the crew set up medaka samples, and remote observations and operations were conducted by command from Earth via the ELT (Experiment Laptop Terminal). The recorded image files were transferred back to Earth

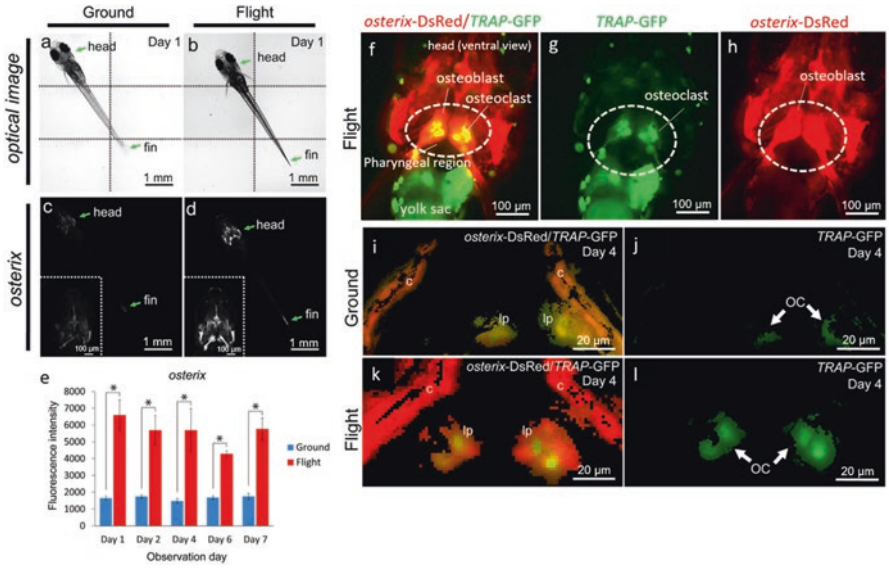

Fig. 5.7 Bone metabolism under microgravity: Increase of fluorescent signals of osteoblasts and osteoclasts in medaka
(**a**–**d**) Whole body imaging of the *osterix*-DsRed transgenic line. (**e**) The fluorescent intensity from day 1 to 7 of observation constantly increased in the flight group. (**f**–**h**) The representative visualizing data for *osterix*-DsRed/*TRAP*-GFP in the flight group. (**i**–**l**) The merged images were captured in 3D view for *osterix*-DsRed and *TRAP*-GFP in the pharyngeal bone region of the double transgenic line
Lp: lower pharyngeal bone; c: cleithrum. GFP signals identify osteoclasts (OC). (Chatani et al. 2016)

signals produced in the ISS by fluorescence microscopy via remote operation from Tsukuba Space Center were observed (Fig. 5.6). For this experiment, four different double medaka transgenic lines were utilized. Particularly, upregulation of fluorescent signals of osteoblasts and osteoclasts in these double transgenic lines was investigated to focus on osteoblast-osteoclast interaction under microgravity. In the live imaging of osteoblasts, intensity of *osterix*- and *osteocalcin*-DsRed in pharyngeal bones was significantly enhanced a day after launch, and this enhancement continued for 8 and 5 days, respectively. In osteoclasts, the signals of *TRAP*-GFP and *MMP9*-DsRed were highly increased at day 4 and 6 in flight after launch (Fig. 5.7).

In addition, HiSeq from pharyngeal bones of juvenile fish at day 2 after launch showed upregulation of two osteoblast- and three osteoclast-related genes. The pattern of gene expression in these transgenic fish was examined by transcriptome analysis. HiSeq analysis of the pharyngeal bones showed the enhanced expression of osteoblast- and osteoclast-related genes. Furthermore, gene ontology analysis via RNA-Seq from the whole body showed that nuclear transcription was significantly enhanced; particularly, transcription regulators were more upregulated at day 2 than

at day 6. Finally, five genes—*c-fos, jun-b, pai-1*, *ddit4*, and *tsc22d3*—were identified, which were upregulated commonly in the whole body at days 2 and 6 and in the pharyngeal bone at day 2. Our results suggested that exposure to microgravity immediately induced dynamic alteration of gene expressions. In summary, our results from live imaging and transcriptome analysis may prompt the establishment of a new field in gravitational biology.

5.7 Conclusion and Future Perspectives

In a study on medaka fish under microgravity, changes appeared in the activities of bone cells. Thus, the highly valued fish models could be more conveniently used for elucidating the effects of microgravity on bones in comparison to traditional rodent models. The past rodent models and our fish data show that there are drastic changes at the sites of active bone metabolism. These studies provide a better understanding of the response of bone to reduced gravity and shed light on the mechanism underlying the regulation of bone physiology under microgravity.

Acknowledgment This work was supported by a grant-in-aid for scientific research from the Ministry of Education, Culture, Sports, Science, and Technology of Japan (Grant No. JP16K15778, JP16H01635 (Group No. A01), JP18H04986 (Group No. A01)).

References

Abduweli D, Baba O, Tabata MJ et al (2014) Tooth replacement and putative odontogenic stem cell niches in pharyngeal dentition of medaka (Oryzias latipes). Microscopy (Oxf) 63:141–153

Bard J (1990) Morphogenesis. Cambridge University Press, Cambridge, p 260

Berezovska OP, Rodionova NV, Grigoryan EN et al (1998) Changes in the numbers of osteoclasts in newts under conditions of microgravity. Adv Space Res 21:1059–1063

Chatani M, Takano Y, Kudo A (2011) Osteoclasts in bone modeling, as revealed by in vivo imaging, are essential for organogenesis in fish. Dev Biol 360:96–109

Chatani M, Mantoku A, Takeyama K et al (2015) Microgravity promotes osteoclast activity in medaka fish reared at the international space station. Sci Rep 5:14172

Chatani M, Morimoto H, Takeyama K et al (2016) Acute transcriptional up-regulation specific to osteoblasts/osteoclats in medaka fish immediately after exposure to microgravity. Sci Rep 6:39545

Crookes W (1987) Address by the president. Proc Soc Psych Res 12:338–355

David H (1963) Russians discuss space radiation in conference. Missiles and Rockets 21:34

Fong KD, Warren SM, Loboa EG et al (2003) Mechanical strain affects dura mater biological processes: implications for immature calvarial healing. Plast Reconstr Surg 112:1312–1327

Frost HM (1990) Skeletal structural adaptations to mechanical usage (SATMU): 1. Redefining Wolff's law: the bone modeling problem. Anat Rec 226:403–413

Ghosh P, Stabley JN, Behnke BJ et al (2016) Effects of spaceflight on the murine mandible: possible factors mediating skeletal changes in non-weight bearing bones of the head. Bone 83:156–161

Ijiri K (1995) Fish mating experiment in space -what it aimed at and how it was prepared. Biol Sci Space 9:3–16
Inohaya K, Takano Y, Kudo A (2007) The teleost intervertebral region acts as a growth center of the centrum: in vivo visualization of osteoblasts and their progenitors in transgenic fish. Dev Dyn 236:3031–3046
JAXA homepage. http://iss.jaxa.jp/en/kiboexp/pm/aqh/. Accessed 23 Apr 2017
Kawashima K, Yamaguchi A, Shinki T et al (1995) Microgravity generated by space flight has little effect on the growth and development of chick embryonic bone. Biol Sci Space 9:82–94
Keune JA, Branscum AJ, Iwaniec UT et al (2016) Effects of spaceflight on bone microarchitecture in the axial and appendicular skeleton in growing ovariectomized rats. Sci Rep 5:18671
Mantoku A, Chatani M, Aono K et al (2016) Osteoblast and osteoclast behaviors in the turnover of attachment bones during medaka tooth replacement. Dev Biol 409:370–381
Masukawa M, Ochiai T, Kamigaichi S et al (2003) NASDA next generation aquatic habitat for space shuttle and ISS. Adv Space Res 32:1541–1546
Morey ER, Baylink DJ (1978) Inhibition of bone formation during space flight. Science 201:1138–1141
Murata Y, Yasuda T, Watanabe-Asaka T et al (2015) Histological and transcriptomic analysis of adult Japanese medaka sampled onboard the international space station. PLoS One 10:e0138799
Nemoto Y, Higuchi K, Baba O et al (2007) Multinucleate osteoclasts in medaka as evidence of active bone remodeling. Bone 40:399–408
Parin VV, Pravetskiy VN, Gurovskiy NN et al (1968) Some biomedical results of the experiment performed onboard the COSMOS-110 biosatellite. Space biology 2:7–14
Rambaut PC, Goode AW (1985) Skeletal changes during space flight. Lancet 2:1050–1052
Sakimura T, Suzuki T, Matsubara et al (1999) NASDA aquatic animal experiment facilities for space shuttle. Biol Sci Space 13:314–320
Schenk R, Merz WA, Muhlbauer R et al (1973) Effect of ethane-1-hydroxy-1,1-diphosphonate (EHDP) and dichloromethylene diphosphonate (cl 2 MDP) on the calcification and resorption of cartilage and bone in the tibial epiphysis and metaphysis of rats. Calcif Tissue Res 11:196–214
Seeman E (2003) Periosteal bone formation--a neglected determinant of bone strength. N Engl J Med 349:320–323
Simmons DJ, Ruffell JE, Winter F et al (1983) Effect of spaceflight on the non-weight-bearing bones of rat skeleton. Am J Phys 244:319–326
Tavella S, Ruggiu A, Giuliani A et al (2012) Bone turnover in wild type and pleiotrophin-transgenic mice housed for three months in the international space station (ISS). PLoS One 7:e33179
Teti A (2011) Bone development: overview of bone cells and signaling. Curr Osteoporos Rep 9:264–273
Thompson D (1917) In: Bonner JT (ed) On growth and form. Cambridge University, Cambridge, pp 32–37
Uchida S, Masukawa M, Kamigaichi S (2002) NASDA aquatic animal experiment facilities for space shuttle and ISS. Adv Sp Res 30:797–802
Vico L, Chappard D, Alexandre C et al (1987) Effects of weightlessness on bone mass and osteoclast number in pregnant rats after a five-day spaceflight (Cosmos 1514). Bone 8:95–103
Vico L, Collet P, Guignandon A et al (2000) Effects of long-term microgravity exposure on cancellous and cortical weight-bearing bones of cosmonauts. Lancet 355:1607–1611

Chapter 6
Small Teleosts Provide Hints Toward Understanding the Evolution of the Central Regulatory Mechanisms of Reproduction

Shinji Kanda

Abstract Reproduction is one of the most important characteristics of all living organisms. In vertebrates, interactions among the hypothalamus, pituitary, and gonad are important for the regulation of reproduction. In spite of the wide variety of reproductive traits among species, the current knowledge regarding the central regulation of reproduction has mainly been acquired from mammalian studies until recently. This approach does not provide the information what is and is not common in vertebrates. Recently, molecular genetic tools became available that can be rather easily applied to the model teleost species, medaka and zebrafish. In particular, when these techniques are combined with classical surgeries developed in the twentieth century, medaka became one of the most powerful models for understanding the neuroendocrine regulation of reproduction in vertebrates. Moreover, single-cell physiological approaches, such as patch-clamp electrophysiology and Ca^{2+} imaging, can be performed in established transgenic lines to unveil the regulatory mechanisms at the cellular level. By combining such physiological results and results from recently developed genome editing techniques, mechanism of central regulation of reproduction has been getting clear in teleosts. In this chapter, I will discuss recent developments in understanding the central regulatory mechanisms of reproduction in teleosts in comparison with the knowledge in mammals. By comparing these two classes, a broader picture of the evolution of reproductive regulation in vertebrates will emerge.

Keywords GnRH · Reproduction · Hypothalamus · Pituitary · Kisspeptin · Estrogen · LH · FSH

S. Kanda (✉)
Department of Biological Sciences, Graduate School of Science, University of Tokyo, Bunkyo, Tokyo, Japan
e-mail: shinji@bs.s.u-tokyo.ac.jp

H. Hirata, A. Iida (eds.), *Zebrafish, Medaka, and Other Small Fishes*,
https://doi.org/10.1007/978-981-13-1879-5_6

Abbreviations

ARC	Arcuate nucleus
AVPV	Anteroventral periventricular
cmlc2	Cardiac myosin light chain 2
CRISPR	Clustered regularly interspaced short palindromic repeats
FSH	Follicle-stimulating hormone
FSHB	Follicle-stimulating hormone β
GnRH	Gonadotropin-releasing hormone
GPA	Glycoprotein α
HPG axis	Hypothalamic-pituitary-gonadal axis
LH	Luteinizing hormone
LHB	Luteinizing hormone β
OVX	Ovariectomy
PMSG	Pregnant mare serum gonadotropin
POA	Preoptic area
TALEN	Transcription activator-like effector nuclease

6.1 Neuroendocrinological Studies in Small Fishes:Advantages and Disadvantages

Vertebrates use hormones to maintain homeostasis as well as to initiate special events in their lives, such as reproduction, when the conditions inside and outside of the body become appropriate. Neuroendocrinology is the study that examines how such hormone release is regulated and how these hormones work. Until recently, most fish endocrinologists have used fish species such as sea bass, goldfish, and salmon, because their large size allows the administration of hormones and the measurement of serum hormone concentrations by radioimmunoassay, which directly indicates the identity of the hormones. Such studies have provided immeasurable information for hormonal functions and have contributed to applications such as aquaculture. However, most of the hormonal functions are determined by the experimental results using whole bodies. Thus, the mechanisms at the cellular level is often remain to be elucidated.

On the other hand, mammalian studies have utilized various molecular genetic tools, such as transgenic technique and homologous recombination, and have revealed the mechanisms of neuroendocrinological regulation in the brain and pituitary. In other words, most of our understanding of the neuroendocrinological regulation at the cellular level is limited to mammals, posing a great disadvantage for biological interests for the following reasons. First, mammals are one class of species, and many nonmammalian studies, including ours, have shown that mammals have special characteristics not observed in other classes. Second, to understand the neuroendocrinological systems from a biological point of view, evolution should be considered. Without knowledge of nonmammals, we cannot understand the

Table 6.1 Advantages and disadvantages of small or larger fish

	Larger fish	Smaller fish
Morphological studies	One can detail the anatomy of peripheral organs and the central nervous system	One can observe whole sections of a whole brain in a single slide
Generation time	Generally long (often over 1 year)	Generally short (2–3 months in shortest)
Maintenance	Large tanks for individual fish lines occupy much space, limiting the scale of fish maintenance	One can raise many fish lines in a laboratory scale
Transgenic/KO	△	○
Physiological studies in the CNS	Recording from slice preparations with larger cells	Recording from whole brain in vitro preparation with intact neural circuits, ideally

principles in vertebrates. Finally, yet importantly, there are several special techniques that take advantage of the unique central nervous system of teleosts.

We have been studying the neuroendocrinological regulation of reproduction by taking advantage of medaka. Using medaka, we can apply molecular genetic tools that specifically label or artificially induce gene expression in target cells, allowing subsequent single-cellular physiological experiments. The hurdle to producing transgenic animals is much lower than that in larger fishes, because medaka has a short life cycle and produces many fertilized eggs daily. Moreover, medaka provides additional advantages over other fishes for the neuroendocrinological study of reproduction. They are not only seasonal breeders, but they can also switch between reproductive and nonreproductive states based solely on the day length. Many creatures are seasonal breeders, but most of them require temperature changes to induce changes in their breeding conditions. These temperature changes also alter metabolic rates and make it difficult to identify breeding state-specific phenomena. Because the most frequently used laboratory animals, such as mice and rats, have lost their seasonality, medaka studies may provide needed insight in the area of seasonal breeding.

The advantages of medaka and zebrafish as experimental animals for neuroendocrinological studies compared to larger fish are summarized in Table 6.1.

6.2 Mechanism of Hypothalamic-Pituitary-Gonadal (HPG) Axis Regulation Revealed by Studies in Medaka

6.2.1 HPG Axis Regulation in Mammals

Before discussing fish reproduction, I would like to describe the central regulation of reproduction in mammals because they are the best studied. Since their discovery in 1977, gonadotropin-releasing hormone (GnRH) neurons in the hypothalamus

have been known to form the final common pathway for reproduction. GnRH neurons project to the median eminence and release the peptide GnRH from their nerve terminals into the hypophyseal portal vessels. The released GnRH stimulates gonadotrophs in the pituitary, causing the release of follicle-stimulating hormone (FSH) and luteinizing hormone (LH) into the general circulation. FSH and LH play distinct roles in the gonads (ovaries in females). FSH is responsible for the initial phase of folliculogenesis, whereas the pulsatile release of LH is required for the late phase of folliculogenesis. Because their release occurs only when the sex steroid level is low, steroids are considered to provide negative feedback. After the follicles are fully developed and thus the serum estrogen level is elevated, a surge like GnRH release occurs, which evokes an LH surge. The LH surge, which depends on the positive feedback of estrogen, causes ovulation in females. These positive and negative feedback actions of sex steroids do not occur through direct action on GnRH neurons. On the contrary, the recently discovered kisspeptin neurons, located in the arcuate and anteroventral periventricular (AVPV) nucleus, are sensitive to estrogen and inhibit and stimulate the release of GnRH in response to low and high estrogen concentrations, respectively (Fig. 6.1a). In contrast to the situation in mammals, the central regulatory mechanisms of reproduction in nonmammalian vertebrates are poorly understood. One can speculate that the knowledge of mechanisms in mammals cannot be applied to nonmammals because there are many obvious differences between them. For instance, mammals produce a small number of offspring, while fish produce many eggs. Moreover, during late folliculogenesis, there has been no clear evidence for the existence of the LH pulse in any nonmammalian species. Thus, to elucidate the vertebrate neuroendocrine regulation of reproduction, nonmammalian studies are necessary. Here, I will mainly focus on recent studies using small teleosts, and medaka in particular.

Fig. 6.1 (continued) hormone (FSH)-producing cells. Second, in mammals, LH and FSH are secreted from a single type of gonadotroph, while in teleosts, LH and FSH are secreted from separate LH- or FSH-producing cells. (**a**) Schematic illustration of the regulatory mechanisms of the hypothalamic-pituitary-gonadal (HPG) axis in mammals. The release of Kiss1 from kisspeptin neurons (Kiss) in the arcuate nucleus (ARC) is negatively regulated by ovarian estrogen and promotes folliculogenesis by inducing pulsatile GnRH and LH release. On the other hand, the release of kisspeptin in the anteroventral periventricular (AVPV) nucleus is positively regulated by estrogen and induces ovulation by stimulating the GnRH and LH surge. FSH is thought to be involved in the initial phase of folliculogenesis. (**b**) Schematic illustration of the regulatory mechanisms of the HPG axis in teleosts. In teleosts, kisspeptin neurons, which have been demonstrated to be estrogen sensitive, do not regulate GnRH neurons. Negative and positive feedbacks are conserved, but their mechanisms are largely unknown. Unlike in mammals, in teleosts, FSH is the gonadotropin responsible for folliculogenesis, and GnRH neurons and LH are dispensable for it. Hypophysiotropic GnRH neurons, which induce LH release, and LH itself are required only for final oocyte maturation and ovulation

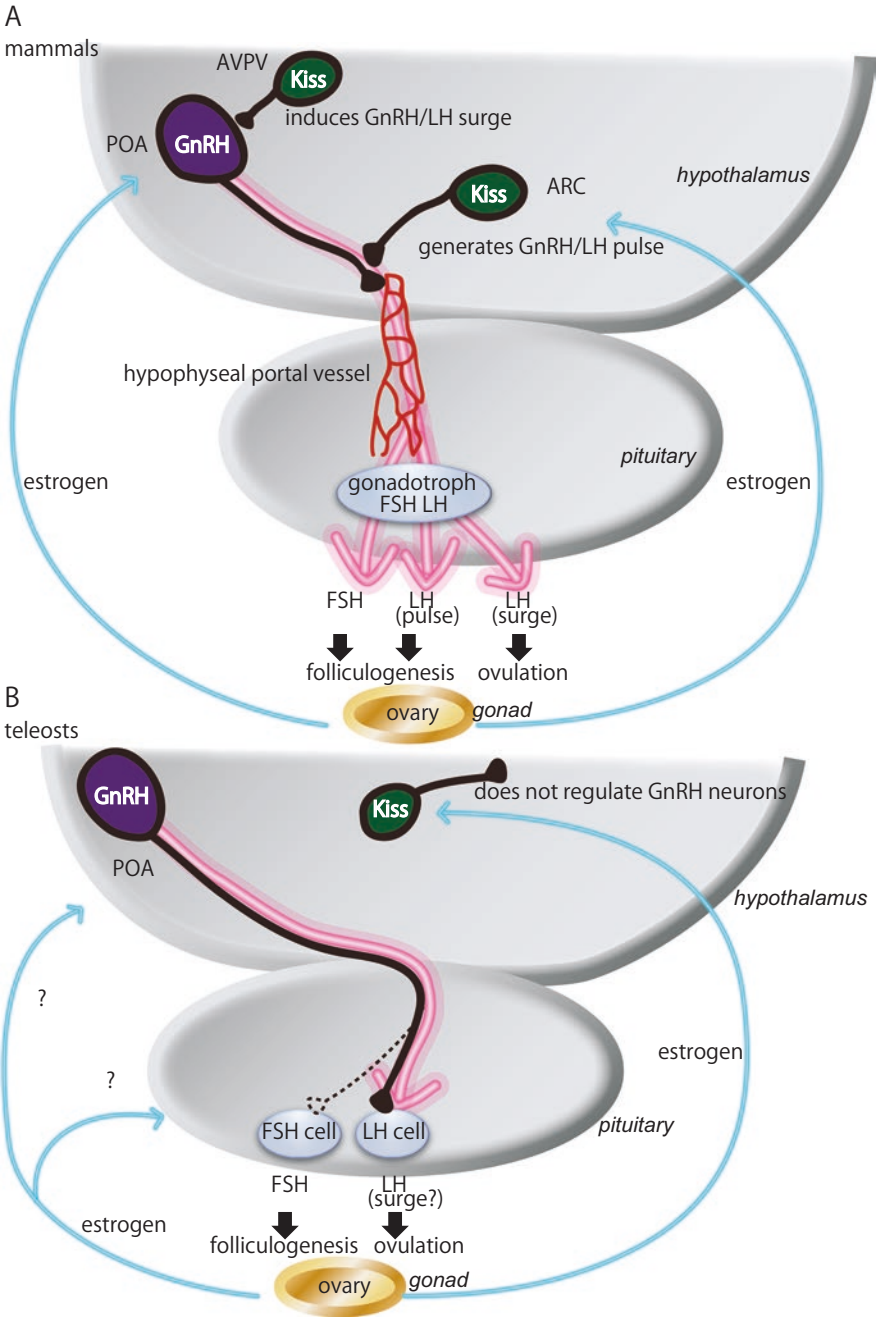

Fig. 6.1 Commonalities and differences in the central regulatory mechanisms of reproduction between mammals and teleosts. In both groups, preoptic area (POA) gonadotropin-releasing hormone (GnRH) neurons that regulate pituitary function are important for the regulation of luteinizing hormone (LH) release from the pituitary. Morphologically, there are two major differences. First, in mammals, GnRH neurons release GnRH into the hypophyseal portal vessels, whereas in teleosts, they directly project to the pituitary and release GnRH in the vicinity of LH- and follicle-stimulating

6.2.2 *Advantages of Medaka for the Study of HPG Axis Regulation*

To understand the common principles of vertebrate HPG axis regulation, medaka is the primary species that should be investigated. Two common small teleosts, zebrafish and medaka, are used as models. It is favorable that these two species are very distinct species within teleost lineage: teleosts emerged around 283 mya, and the ancestors of zebrafish and medaka branched around 211 mya (Betancur et al. 2013). Therefore, common findings in zebrafish and medaka should be similar to the principles found in all teleosts. Actually, many studies have reported differences between zebrafish and medaka. Thus, parallel studies in these two small fish species provide insight into the principles of reproductive regulation.

Compared to zebrafish, medaka offers some advantages for studying the central regulation of reproduction. As described earlier, medaka is a seasonal breeder, whereas zebrafish is a continuous breeder. In addition, we can perform ovariectomy (OVX, removal of the ovary) surgeries in medaka (Kanda et al. 2011). In our experience, more than 90% of medaka survive and are healthy after the surgery. We can also administer hydrophobic hormones such as estrogen, and its inhibitors, simply by exposing fish to the water containing the reagents (Hiraki et al. 2014) or feeding them foods containing the reagents (Kanda et al. 2011). The ease of hormonal treatment and inhibition using hydrophobic compounds is very useful because hydrophobic sex steroid hormones are strongly involved in reproductive regulation.

I will review recent results from studies in medaka and compare them to studies in zebrafish and other species. These studies provide hints toward understanding the principles of HPG axis regulation in teleosts.

6.2.3 *The Gene Knockout (KO) Technique Indicated Essential Components of Reproduction in the Brain and the Pituitary*

Following the recent development of genome-editing tools, medaka became one of the easiest animals in which to generate knockouts. Transcription Activator-Like Effector Nuclease (TALEN) and Clustered Regularly Interspaced Short Palindromic Repeats (CRISPR) techniques have provided several knockout lines for key regulators of the HPG axis.

6.2.3.1 Pituitary Hormones

FSH and LH are members of the heterodimeric glycoprotein hormone family; FSH consists of a glycoprotein α (GPA) subunit and a follicle-stimulating hormone β (FSHB) subunit, whereas LH consists of a GPA subunit and a luteinizing hormone

β (LHB) subunit. Therefore, for the analysis of FSH, the *fshb* gene was deleted, and for LH, the *lhb* gene was deleted. In medaka, both the FSH knockout and LH knockout females are infertile. However, their phenotypes are quite different. FSH homozygous knockouts show a very small yolk accumulation compared to that of the heterozygous knockouts. On the other hand, the LH knockout medaka show fully developed ovaries with oocytes after yolk accumulation (Takahashi et al. 2016b). In fact, a single intraperitoneal injection of recombinant LH (Ogiwara et al. 2013) or pregnant mare serum gonadotropin (PMSG), which is an LH but not FSH receptor agonist, could induce ovulation in the LH knockout medaka. The ligand knockouts and the receptor knockouts showed similar results (Murozumi et al. 2014). The FSH receptor knockout cannot undergo yolk accumulation, whereas the LH receptor knockout showed a failure in ovulation. Therefore, FSH is required for folliculogenesis, while LH is required for final oocyte maturation and subsequent ovulation in medaka.

In zebrafish, there are several reports of knockouts for LH, FSH, the LH receptor, and the FSH receptor (Chu et al. 2015, 2014; Zhang et al. 2015a, b). The LH KO zebrafish showed similar results as the LH KO medaka. On the other hand, the female FSH KO zebrafish was fertile, unlike the FSH KO medaka. This discrepancy can be explained by the fact that LH can bind to both FSH and LH receptors in both species, and LH may compensate for the loss of FSH in zebrafish. In fact, FSH receptor KO zebrafish cannot reproduce. Taken together, the evidence from the ligand and receptor knockouts of both zebrafish and medaka indicates that the FSH system is required for folliculogenesis, while the LH system is required for final oocyte maturation and subsequent ovulation as a basic principle in teleosts. This principle is quite different from that in mammals, which require pulsatile LH release for folliculogenesis, while teleosts require only FSH.

6.2.3.2 GnRH Is One of the Most Important Regulators of Ovulation in Vertebrates

We also generated *gnrh1* knockout medaka to understand the function of GnRH1 (Takahashi et al. 2016b). Our GnRH1 knockout showed a similar phenotype as the LH knockout. We also demonstrated that an LH analog can rescue the deficiency in ovulation in this knockout. As the *gnrh1* knockout showed reduced *lhb* expression and normal *fshb* expression in the pituitary. GnRH can be considered essential for ovulation because it is required for the stimulation of LH release from the pituitary, which has been demonstrated using physiological experiments.

The GnRH Knockout Zebrafish Is Fertile, Which Does Not Deny the Importance of GnRH in Cyprinids

In zebrafish, multiple research groups have shown that *gnrh* knockouts are fertile (Spicer et al. 2016; Liu et al. 2017). Additionally, the double knockout, in which both GnRH paralogues were eliminated from the genome, is also fertile. Thus, in

contrast to medaka, zebrafish does not require GnRH for ovulation. However, these results do not deny the importance of GnRH in zebrafish. One important observation was that in goldfish, which belong to the same Cyprinidae family, artificial ovulation was induced by the coinjection of a GnRH analog and dopamine inhibitor in long-day and low-temperature conditions, in which endogenous FSH but not LH is functional (Chang and Peter 1983). Importantly, since artificial ovulation was not induced when either one of the reagents was absent, both the existence of GnRH and the disinhibition of dopamine are necessary for LH surge induction and subsequent ovulation in goldfish. Although there is still a discrepancy between goldfish and zebrafish, the requirement for dopamine inhibition in addition to GnRH in cyprinids (Fontaine et al. 2013) might explain the difference in phenotype between GnRH knockout zebrafish and medaka.

In light of the previous intraperitoneal injection studies in various fishes and tetrapods, it can be inferred that dopamine inhibition of LH release was acquired during the early teleost lineage and became weakened at some point during the long evolutionary history of teleosts. In sturgeons, which emerged prior to the teleost-specific 3R whole-genome duplication, GnRH can induce ovulation in the absence of dopamine inhibition. Likewise, many studies in perciform fishes, which emerged relatively recently (~133 mya), demonstrated ovulation after the injection of GnRH analog only. On the other hand, species that emerged relatively early after the 3R duplication are likely to exhibit dopamine inhibition (e.g., eel and cyprinids).

Comparison of Results of Multiple Species Leads to a Conclusion Which Widely can Be Applied to Teleosts

Knockout studies in both zebrafish and medaka and previous injection studies strongly suggest that GnRH is nearly essential for ovulation in teleosts, and zebrafish are the exception. Given similar reports in tetrapods, GnRH may be generally important for vertebrate reproduction, at least in bony vertebrates.

Interestingly, there may be a tendency for medaka to experience more severe dysfunction from a single gene knockout in comparison to zebrafish, at least in the case of the gonadotropin and GnRH genes. The period after the 3R whole-genome duplication preceding the emergence of Beloniformes (medaka) is longer than preceding the emergence of Cypriniformes (zebrafish). I speculate that dispensable genes involved in compensatory pathways were lost during this longer period. Thus, medaka may display critical phenotypes after gene knockouts.

It is evident that comparative studies of zebrafish and medaka are necessary for understanding the general function of GnRH and gonadotropins in teleosts. The discrepancies and their explanations introduced here indicate that parallel studies using at least two distinct species, such as zebrafish and medaka (Betancur et al. 2013), are important for understanding the general principles of the central regulatory mechanisms of reproduction in teleosts.

6.2.3.3 Kisspeptin May Be a Mammalian-Specific Regulator of Reproduction

Kisspeptin is an essential regulator of reproduction in mammals. Since its discovery in 2003, kisspeptin and kisspeptin neurons have been one of the hottest topics in neuroendocrinology. Many researchers have examined the effects of intraperitoneal injection of synthetic kisspeptin peptides, and studies have shown that kisspeptin increases the serum concentration of LH in some fish. However, I do not believe that kisspeptin is a regulator of reproduction in teleosts based on our results in medaka and on studies performed by others and us in other fish species. I would like to introduce lines of evidence from medaka.

Several experimental results contradict the involvement of kisspeptin in reproductive regulation. First, GnRH neurons, which are the targets of kisspeptin, do not express either subtype of kisspeptin receptors in medaka (Kanda et al. 2013). This negative result may deny the possibility that kisspeptin regulation of the HPG axis is similar to that in mammals. This result was replicated in seabass (Escobar et al. 2013b). Second, both male and female kisspeptin knockout medaka reproduce normally (Nakajo et al. 2017). A similar result was reported in zebrafish. Third, kisspeptin administration did not alter the serum LH concentration in goldfish (Nakajo et al. 2017). It was also demonstrated that kisspeptin peptide did not alter the firing activity of GnRH neurons (Nakajo et al. 2017). Several reports showed that kisspeptin administration induced an increase in LH in some fish species, in spite of the absence of kisspeptin receptor in GnRH neurons generally in teleosts. Although there is a possibility that unknown mechanism other than GnRH neuron regulation could work, I have no idea about that partly because we could not replicate at least one of the reports in goldfish. Therefore, from the evidence derived from a combination of morphological, knockout, and electrophysiological studies, kisspeptin in teleosts does not have the same function as observed in mammals, in which kisspeptin acts directly on the GnRH and modulate LH release.

In spite of the controversy regarding the function of kisspeptin, we found that the steroid sensitivity of kisspeptin neurons is widely conserved in bony vertebrates, including teleosts and mammals. We showed that kisspeptin neurons in medaka hypothalamus as well as in the goldfish preoptic area express estrogen receptors, and estrogen alters the expression of the kisspeptin gene (Kanda et al. 2008, 2012; Mitani et al. 2010) and kisspeptin neuronal firing activity (Hasebe et al. 2014). The evolutionary scenario of steroid-sensitive kisspeptin neurons has been described earlier (Kanda and Oka 2012).

From these observations, I hypothesize that kisspeptin neurons play an unknown role in the response to serum sex steroid changes. During the long evolutionary history, mammalian species may have begun to express kisspeptin receptors on GnRH neurons to generate the pulsatile mode of GnRH and LH secretion. This speculation is consistent with the observation that LH pulses are found only in mammals.

6.2.4 *Physiological Analysis of GnRH1 Neurons and Their Regulation of LH and FSH Release*

I have described the importance of GnRH1 and its possible essentiality in vertebrates. To my knowledge, none of the vertebrate species lack the hypophysiotropic GnRH system. Here, I will review recent developments in understanding the hypophysiotropic GnRH system by using physiological analyses in medaka.

In medaka, transgenic lines have been generated that express GFP-labeled *gnrh1, 2*, or *3* neurons (Okubo et al. 2006; Kanda et al. 2010; Takahashi et al. 2016a). It is very difficult to select GFP-positive individuals when GFP is expressed only in the adult brain. This situation sometimes occurs in the labeling of neurons involved in reproductive regulation, which are not necessarily expressed in larvae. To solve this problem, we are using a double-promoter technique. There are two preferred enhancers that induce the expression of fluorescent proteins in larvae and are easy to recognize. One is cardiac myosin light chain 2 (*cmlc2*), which induces fluorescent protein expression in the heart muscles. Interestingly, because the *cmlc2* enhancer works on the promoters located in both the 5′ and 3′ direction, we only have to insert one fluorescent protein gene for both the enhancer of interest and *cmlc2* (see Fig. 1a of Takahashi et al. 2016a). The other is globin β4, which induces expression in the red blood cells in the larval stages, but not in adulthood (Maruyama et al. 2012). Flowing blood cells are easy to identify, which makes screening easier. By using this double-promoter strategy, we efficiently generated several transgenic lines.

GnRH1 transgenic medaka has provided morphological and physiological information on the hypophysiotropic GnRH neurons. Because GnRH1 neurons were shown to project to the pituitary (Takahashi et al. 2016a), we analyzed their spontaneous firing activity using a loose-patch recording technique, a relatively easy extracellular technique for recording from a single target neuron. It was found that GnRH1 neurons generally fire in an irregular pattern (Karigo et al. 2012). Interestingly, their firing activity increases during the time that the LH surge is supposed to occur (Takahashi et al. 2013). Moreover, Ca^{2+} imaging showed that GnRH peptide administration increases the intracellular Ca^{2+} of LH and FSH cells in the pituitary (Karigo et al. 2014). The expression of *lhb* and *fshb* mRNA in isolated pituitary preparations also showed an increase in response to GnRH peptide exposure. These data indicate that the GnRH system stimulates both FSH and LH release, although its essentiality is limited to LH release.

Interestingly, we also demonstrated that the firing activity of GnRH1 neurons is suppressed specifically in females when there is a shortage of glucose (Hasebe et al. 2016). In the future, medaka will provide a very good experimental model for elucidation of the relationship between reproduction and nutrition. Unfortunately, because the size of most medaka neurons is too small to perform whole cell patch-clamp

recordings with a low access resistance, it will be difficult to elucidate intracellular mechanisms that involve ion channels. In such cases, perhaps, electrophysiology studies in larger fish may solve this problem, although the generation of GFP transgenic fish in larger species generally takes a long time.

6.2.5 GFP Labeling of Receptor-Expressing Neurons May Provide New Insights on Specific Neuronal Systems

So far, the function of kisspeptin in species other than mammals is unclear, although the steroid sensitivity of kisspeptin neurons is conserved in bony vertebrates. As this steroid sensitivity is the common feature of the vertebrate kisspeptin system, we began to detect the conserved kisspeptin functions in vertebrates. Dozens of double in situ hybridization studies resulted in the discovery of some of the neurotransmitters that are regulated by kisspeptin system (Escobar et al. 2013a; Kanda et al. 2013), but all the neurons that express the kisspeptin receptor were not identified. Thus, we established a transgenic line in which the kisspeptin-receptor-expressing neurons were labeled by GFP. Using this transgenic line, we performed single-cell RNA-seq to identify the neurotransmitters whose release is regulated by kisspeptin. We also performed patch-clamp recordings to elucidate the effects of kisspeptin on kisspeptin-receptor-expressing neurons, guided by their GFP expression. We have identified some neurotransmitters using this method. If this method is applied to other neuronal systems in the future, novel functions of neurotransmitters will be efficiently detected using the combination of transgenic medaka and next-generation sequencing.

6.3 Conclusion

From the study of the neuroendocrinological regulation of reproduction, it can be concluded that the mechanisms discovered in mammals are not always applicable to teleosts, and vice versa, because fish are not an ancestor of mammals. Rather, they have proceeded through a long evolutionary history after diverging from their common ancestors. Thus, by searching for the commonalities and differences, we can identify the common principles as well as the differences that have contributed to the adaptation of each species. Using the advantages of medaka, only some of which are mentioned in this chapter, will contribute to a more complete understanding of vertebrate neuroendocrine systems.

References

Betancur RR, Broughton RE, Wiley EO, Carpenter K, Lopez JA, Li C, Holcroft NI, Arcila D, Sanciangco M, Cureton Ii JC, Zhang F, Buser T, Campbell MA, Ballesteros JA, Roa-Varon A, Willis S, Borden WC, Rowley T, Reneau PC, Hough DJ, Lu G, Grande T, Arratia G, Orti G (2013) The tree of life and a new classification of bony fishes. PLoS Curr 5. https://doi.org/10.1371/currents.tol.53ba26640df0ccaee75bb165c8c26288

Chang JP, Peter RE (1983) Effects of pimozide and des Gly10,[D-Ala6]luteinizing hormone-releasing hormone ethylamide on serum gonadotropin concentrations, germinal vesicle migration, and ovulation in female goldfish, Carassius auratus. Gen Comp Endocrinol 52(1):30–37

Chu L, Li J, Liu Y, Hu W, Cheng CH (2014) Targeted gene disruption in zebrafish reveals noncanonical functions of LH signaling in reproduction. Mol Endocrinol 28(11):1785–1795. https://doi.org/10.1210/me.2014-1061

Chu L, Li J, Liu Y, Cheng CH (2015) Gonadotropin signaling in Zebrafish ovary and testis development: Insights from gene knockout study. Mol Endocrinol 29(12):1743–1758. https://doi.org/10.1210/me.2015-1126

Escobar S, Felip A, Gueguen MM, Zanuy S, Carrillo M, Kah O, Servili A (2013a) Expression of kisspeptins in the brain and pituitary of the European sea bass (Dicentrarchus labrax). J Comp Neurol 521(4):933–948. https://doi.org/10.1002/cne.23211

Escobar S, Servili A, Espigares F, Gueguen MM, Brocal I, Felip A, Gomez A, Carrillo M, Zanuy S, Kah O (2013b) Expression of kisspeptins and kiss receptors suggests a large range of functions for kisspeptin systems in the brain of the European sea bass. PLoS One 8(7):e70177. https://doi.org/10.1371/journal.pone.0070177

Fontaine R, Affaticati P, Yamamoto K, Jolly C, Bureau C, Baloche S, Gonnet F, Vernier P, Dufour S, Pasqualini C (2013) Dopamine inhibits reproduction in female zebrafish (Danio rerio) via three pituitary D2 receptor subtypes. Endocrinology 154(2):807–818. https://doi.org/10.1210/en.2012-1759

Hasebe M, Kanda S, Shimada H, Akazome Y, Abe H, Oka Y (2014) Kiss1 neurons drastically change their firing activity in accordance with the reproductive state: insights from a seasonal breeder. Endocrinology 155(12):4868–4880. https://doi.org/10.1210/en.2014-1472

Hasebe M, Kanda S, Oka Y (2016) Female-Specific Glucose Sensitivity of GnRH1 Neurons Leads to Sexually Dimorphic Inhibition of Reproduction in Medaka. Endocrinology 157(11):4318–4329. https://doi.org/10.1210/en.2016-1352

Hiraki T, Nakasone K, Hosono K, Kawabata Y, Nagahama Y, Okubo K (2014) Neuropeptide B is female-specifically expressed in the telencephalic and preoptic nuclei of the medaka brain. Endocrinology 155(3):1021–1032. https://doi.org/10.1210/en.2013-1806

Kanda S, Oka Y (2012) Evolutionary insights into the steroid sensitive *kiss1* and *kiss2* neurons in the vertebrate brain. Front Endocrinol 3(28). https://doi.org/10.3389/fendo.2012.00028

Kanda S, Akazome Y, Matsunaga T, Yamamoto N, Yamada S, Tsukamura H, Maeda K, Oka Y (2008) Identification of KiSS-1 product kisspeptin and steroid-sensitive sexually dimorphic kisspeptin neurons in medaka (*Oryzias latipes*). Endocrinology 149(5):2467–2476. https://doi.org/10.1210/en.2007-1503

Kanda S, Nishikawa K, Karigo T, Okubo K, Isomae S, Abe H, Kobayashi D, Oka Y (2010) Regular pacemaker activity characterizes gonadotropin-releasing hormone 2 neurons recorded from green fluorescent protein-transgenic medaka. Endocrinology 151(2):695–701. https://doi.org/10.1210/en.2009-0842

Kanda S, Okubo K, Oka Y (2011) Differential regulation of the luteinizing hormone genes in teleosts and tetrapods due to their distinct genomic environments - Insights into gonadotropin beta subunit evolution. Gen Comp Endocrinol 173(2):253–258. https://doi.org/10.1016/j.ygcen.2011.05.015

Kanda S, Karigo T, Oka Y (2012) Steroid sensitive kiss2 neurones in the goldfish: evolutionary insights into the duplicate kisspeptin gene-expressing neurones. J Neuroendocrinol 24(6):897–906. https://doi.org/10.1111/j.1365-2826.2012.02296.x

Kanda S, Akazome Y, Mitani Y, Okubo K, Oka Y (2013) Neuroanatomical evidence that kisspeptin directly regulates isotocin and vasotocin neurons. PLoS One 8(4):e62776. https://doi.org/10.1371/journal.pone.0062776

Karigo T, Kanda S, Takahashi A, Abe H, Okubo K, Oka Y (2012) Time-of-Day-Dependent changes in GnRH1 neuronal activities and Gonadotropin mRNA expression in a daily spawning fish, Medaka. Endocrinology 153(7):3394–3404. https://doi.org/10.1210/en.2011-2022

Karigo T, Aikawa M, Kondo C, Abe H, Kanda S, Oka Y (2014) Whole brain-pituitary in vitro preparation of the transgenic medaka (Oryzias latipes) as a tool for analyzing the differential regulatory mechanisms of LH and FSH release. Endocrinology 155(2):536–547. https://doi.org/10.1210/en.2013-1642

Liu Y, Tang H, Xie R, Li S, Liu X, Lin H, Zhang Y, Cheng CH (2017) Genetic Evidence for Multifactorial Control of the Reproductive Axis in Zebrafish. Endocrinology 158(3):604–611. https://doi.org/10.1210/en.2016-1540

Maruyama K, Wang B, Ishikawa Y, Yasumasu S, Iuchi I (2012) 1kbp 5' upstream sequence enables developmental stage-specific expressions of globin genes in the fish, medaka Oryzias latipes. Gene 492(1):212–219. https://doi.org/10.1016/j.gene.2011.10.026

Mitani Y, Kanda S, Akazome Y, Zempo B, Oka Y (2010) Hypothalamic Kiss1 but not Kiss2 neurons are involved in estrogen feedback in medaka (Oryzias latipes). Endocrinology 151(4):1751–1759. https://doi.org/10.1210/en.2009-1174

Murozumi N, Nakashima R, Hirai T, Kamei Y, Ishikawa-Fujiwara T, Todo T, Kitano T (2014) Loss of follicle-stimulating hormone receptor function causes masculinization and suppression of ovarian development in genetically female medaka. Endocrinology 155(8):3136–3145. https://doi.org/10.1210/en.2013-2060

Nakajo M, Kanda S, Karigo T, Takahashi A, Akazome Y, Uenoyama Y, Kobayashi M, Oka Y (2017) Evolutionally conserved function of kisspeptin neuronal system is non-reproductive regulation as revealed by non-mammalian study. Endocrinology 159(1):163-183. https://doi.org/10.1210/en.2017-00808

Ogiwara K, Fujimori C, Rajapakse S, Takahashi T (2013) Characterization of luteinizing hormone and luteinizing hormone receptor and their indispensable role in the ovulatory process of the medaka. PLoS One 8(1):e54482. https://doi.org/10.1371/journal.pone.0054482

Okubo K, Sakai F, Lau EL, Yoshizaki G, Takeuchi Y, Naruse K, Aida K, Nagahama Y (2006) Forebrain gonadotropin-releasing hormone neuronal development: insights from transgenic medaka and the relevance to X-linked Kallmann syndrome. Endocrinology 147(3):1076–1084. https://doi.org/10.1210/en.2005-0468

Spicer OS, Wong TT, Zmora N, Zohar Y (2016) Targeted Mutagenesis of the Hypophysiotropic Gnrh3 in Zebrafish (Danio rerio) Reveals No Effects on Reproductive Performance. PLoS One 11(6):e0158141. https://doi.org/10.1371/journal.pone.0158141

Takahashi T, Fujimori C, Hagiwara A, Ogiwara K (2013) Recent advances in the understanding of teleost medaka ovulation: the roles of proteases and prostaglandins. Zool Sci 30(4):239–247. https://doi.org/10.2108/zsj.30.239

Takahashi A, Islam MS, Abe H, Okubo K, Akazome Y, Kaneko T, Hioki H, Oka Y (2016a) Morphological analysis of the early development of telencephalic and diencephalic gonadotropin-releasing hormone neuronal systems in enhanced green fluorescent protein-expressing transgenic medaka lines. J Comp Neurol 524(4):896–913. https://doi.org/10.1002/cne.23883

Takahashi A, Kanda S, Abe T, Oka Y (2016b) Evolution of the hypothalamic-pituitary-gonadal axis regulation in vertebrates revealed by Knockout Medaka. Endocrinology 157(10):3994–4002. https://doi.org/10.1210/en.2016-1356

Zhang Z, Lau SW, Zhang L, Ge W (2015a) Disruption of zebrafish Follicle-Stimulating Hormone Receptor (fshr) but not Luteinizing Hormone Receptor (lhcgr) gene by TALEN leads to failed follicle activation in females followed by sexual reversal to males. Endocrinology 156(10):3747–3762. https://doi.org/10.1210/en.2015-1039

Zhang Z, Zhu B, Ge W (2015b) Genetic analysis of zebrafish gonadotropin (FSH and LH) functions by TALEN-mediated gene disruption. Mol Endocrinol 29(1):76–98. https://doi.org/10.1210/me.2014-1256

Chapter 7
Diversified Sex Characteristics Developments in Teleost Fishes: Implication for Evolution of Androgen Receptor (AR) Gene Function

Yukiko Ogino, Gen Yamada, and Taisen Iguchi

Abstract Gene duplication is a dominant driving force of evolution. The steroid hormone receptor (SR) gene family is thought to have arisen from gene duplication. However, the molecular events which produce new protein functions after genome duplication have not been fully understood. Teleost fishes present an excellent model to investigate an accurate evolutionary history of protein function after whole genome duplication (WGD), because the teleost-specific WGD (TSGD) 350 million years ago (Ma) resulted in a variety of duplicated genes that exist in modern fishes. We focused on the androgen receptor (AR) gene, since two different subtype genes, ARα and ARβ, were generated in the TSGD. It was previously shown that ARβ has retained the ancestral function, whereas ARα has evolved as a hyperactive form of AR in the teleost lineage. Such evolutionary novelty of protein function in AR genes might facilitate the emergence of divergent sex characteristics in the teleost lineage. Results of the combined functional and 3D analyses of medaka ARs identified the substitutions that led to changes in protein structure and function between medaka ARα and ARβ. By tracing evolutionary changes in protein function of ARs in teleost lineage, we recently revealed that the substitutions generating a new functionality of teleost ARα were fixed in the teleost genome after the divergence of the Elopomorpha lineage. Such findings would provide an historical explanation for the retention of the duplicated AR copies in the euteleost genome. We also highlighted the molecular mechanisms of secondary sex characteristics development in teleost fishes, using Western mosquitofish and medaka as models.

Y. Ogino (✉)
Attached Promotive Centre for International Education and Research of Agriculture, Faculty of Agriculture, Kyushu University, Fukuoka, Japan
e-mail: ogino@agr.kyushu-u.ac.jp

G. Yamada
Department of Developmental Genetics, Institute of Advanced Medicine, Wakayama Medical University, Wakayama, Wakayama, Japan
e-mail: transg8@wakayama-med.ac.jp

T. Iguchi
Graduate School of Nanobioscience, Yokohama City University, Yokohama, Japan

H. Hirata, A. Iida (eds.), *Zebrafish, Medaka, and Other Small Fishes*,
https://doi.org/10.1007/978-981-13-1879-5_7

Keywords Androgen · Sex characteristics · Gonopodium · Papillary processes · Androgen receptor · Whole genome duplication

7.1 Introduction

Vertebrates show diverse sexual characters in sexually attractive and reproductive organs, which are regulated by steroid hormones, particularly androgens. The sex characteristics specify male characters that bring reproductive diversity leading to biodiversity. Physiological and morphological responses to androgens are thought to occur predominantly through binding to the androgen receptor (AR), a member of the nuclear receptor superfamily that functions as a ligand-activated transcription factor (Mangelsdorf et al. 1995; Baker 1997; Laudet 1997; Thornton and Kelley 1998). Thus, it provides a direct link between the signaling molecules controlling the processes of sex characteristics development by transcriptional responses. Based on molecular developmental analyses of secondary sex characteristics of cartilaginous fish, teleosts, and the mouse, the genes involved in the signaling pathways of Sonic hedgehog (Shh), Bone morphogenetic protein (Bmp), and Wnt-β/catenin were identified as effector genes that can interact with and/or function downstream of the androgen-AR pathway (Ogino et al. 2004, 2011, 2014; Miyagawa et al. 2009; O'Shaughnessy et al. 2015). Molecular evolution of AR gene might have provided the important contribution for the evolutionary divergence of the secondary sex characteristics, possibly affecting the expression of such effector genes. In fact, shark AR activates the target gene via androgen response element by classical androgens (Ogino et al. 2009, 2011). Based on currently available information, the most ancient type of AR activated by the classical androgens as ligands emerged before the Chondrichthyes-Osteichthyes split (Ogino et al. 2009, 2011) (Fig. 7.1).

Gene duplication may lead to the establishment of lineage-specific traits and to the development of novel biological functions (Ohno 1970; Hughes 2002; Lynch and Katju 2004). The contribution of duplicated genes to these evolutionary novelties has been explained by the duplication–degeneration–complementation model (Force et al. 1999). In teleosts, TSGD occurred approximately 350 Ma, after the split of non-teleost actinopterygian lineages (namely, bichir, sturgeon, gar, and bowfin) from the teleost lineage but before the divergence of Osteoglossomorpha (Chiu et al. 2004; Hoegg et al. 2004; Jaillon et al. 2004; Brunet et al. 2006). This TSGD may have facilitated the morphological diversification and evolutionary radiation of teleosts (Miya et al. 2001; Volff 2005). As a result of this TSGD, additional copies of ARs compared with the gene repertoire in other jawed vertebrates have been found in a number of teleosts (Fig. 7.1) (Ikeuchi et al. 1999; Sperry and Thomas 1999; Hawkins et al. 2000; Ogino et al. 2004). Medaka (*Oryzias latipes*) ARα and ARβ were mapped on chromosome 10 and 14, respectively. Flanking regions of AR genes on medaka chromosomes 10 and 14 contain genes orthologous to those located in syntenic regions on human chromosome X on which the AR is located, indicating that the teleost AR gene duplication has been associated with the duplication between chromosomes 10 and 14. Such retention of both duplicated copies has been thought

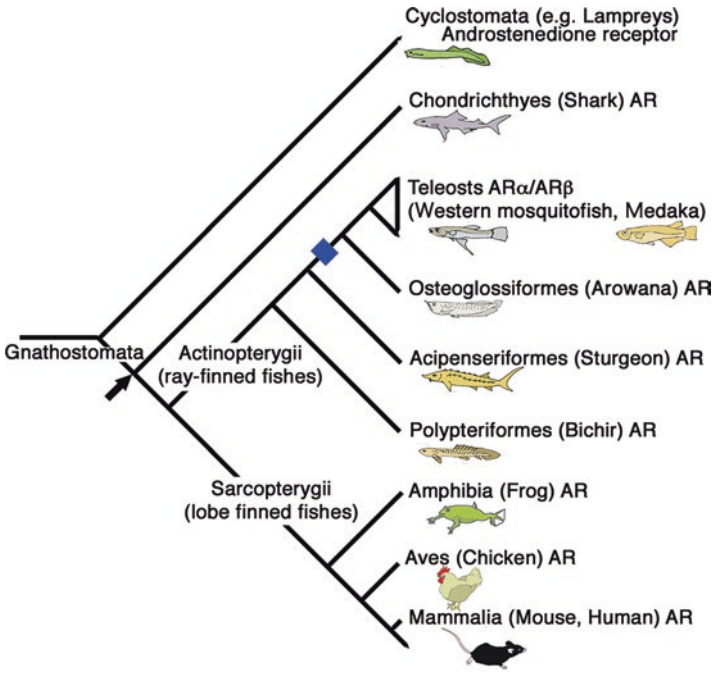

Fig. 7.1 Composite phylogeny for vertebrates with the hypothesized scenario of AR evolution in vertebrates. The evolutionary tree illustrates that the most ancient type of AR, as activated by the classical androgens as ligands, emerged before the Chondrichthyes-Osteichthyes split (shown by arrow) and TSGD event that gave rise to two different teleost ARs, ARα and ARβ (indicated by blue square). (Adapted from Douard et al. 2008; Ogino et al. 2009)

to have conferred an advantage through neofunctionalization and/or subfunctionalization (Prince and Pickett 2002). This chapter focuses on the functional innovation of AR gene and the interaction of androgen and growth factor pathways that promote the sexual differentiation of reproductive organs in vertebrates.

7.2 Molecular Evolution of Androgen Receptor Gene After TSGD

The steroid hormone receptor (SR) family provides an example of evolution of diverse transcription factors through WGD. Evolution of novel traits following duplication of SR genes has been considered to provide the evolutionary innovations in vertebrate lineage. Teleosts present an excellent model to investigate an accurate evolutionary history of protein function of SRs after WGD, because TSGD resulted in a variety of duplicated SR genes in modern fishes.

Many teleosts have two paralogus copies of AR (ARα and ARβ), whereas only one ortholog is present in tetrapods (Fig. 7.1). We recently compared the transactivation property of medaka and Western mosquitofish (*Gambusia affinis*) ARs with other vertebrates ARs (Ogino et al. 2009, 2011). We found that both ARα and ARβ of Western mosquitofish and medaka are activated by various androgens as ligands. However, ARα showed a unique intracellular localization and significantly higher transactivating response than that of ARβ and tetrapod and cartilaginous fish ARs (Fig. 7.2a) (Ogino et al. 2009, 2011). In agreement with the transcriptional properties, the structural analysis by constructing the 3D models of ligand-binding domains (LBDs) of ARs revealed that the interaction energy of 11-ketotestosterone (11KT)-ARα complex is lower than that of ARβ complexed with 11KT, indicating more stable binding of 11KT to ARα (Fig. 7.2b) (Ogino et al. 2016). A comparison of the deduced amino acid sequences of teleost ARs with ARs of tetrapods and cartilaginous fish, a common ancestor for tetrapods and teleost fishes, indicates that teleost ARα accumulated novel substitutions at a greater rate than those of teleost ARβ after the duplication that gave rise to ARα and ARβ (Ogino et al. 2016).

The availability of the numerous sequences of AR genes and a reliable basis of species phylogeny among diverse lineages of teleost fishes (Inoue et al. 2003; Kikugawa et al. 2004; Volff 2005; Sato and Nisida 2010) enables us to infer a potential genomic event which drove evolutionary novelty of AR genes in the teleost lineage. Indeed, we succeeded in identifying two key amino acid replacements that generate ARα-specific hyper-transactivation and constitutive nuclear localization in the ligand-binding domain and hinge region, respectively (Fig. 7.2b) (Ogino et al. 2016). Interestingly, such substitutions have been highly conserved in spiny-rayed

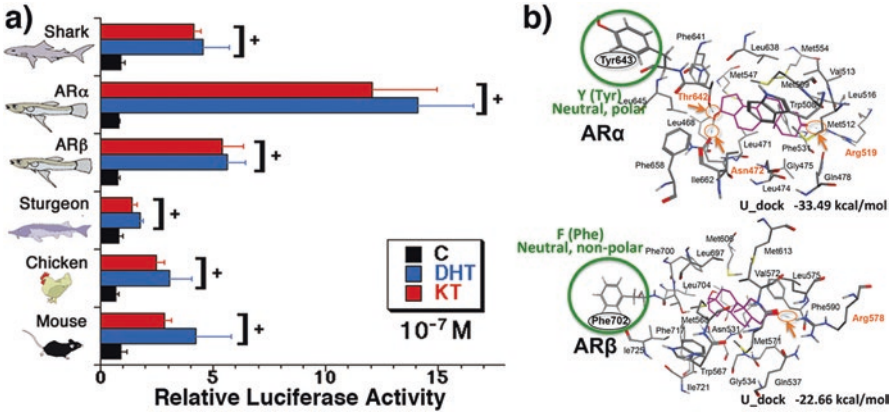

Fig. 7.2 Functional analysis of AR genes in COS-7 cells. (**a**) Ligand-dependent transactivation profiles of vertebrate ARs (Adapted from Ogino et al. 2009, 2011). (**b**) Predicted binding modes obtained from the docking simulation analysis of 11KT for the medaka ARα- and ARβ-LBD. Orange arrows indicate the predicted hydrogen bonds between 11KT and amino acid residues of LBD. The key residues regulating the transactivation capacity of medaka ARs, ARα Y643, and ARβ F702 are not directly implicated in 11KT binding. (Adapted from Ogino et al. 2016)

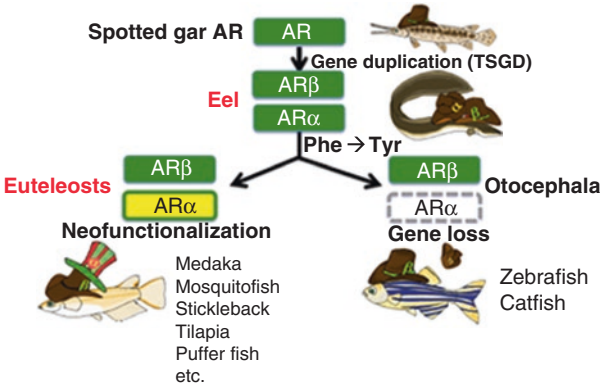

Fig. 7.3 Evolutionary scenario of AR genes in teleost lineage. The hypothesized timing of key substitution in the LBD of ARα genes was indicated. The ARα gene has been lost in some fishes in Otocephala lineage, but has been retained in euteleostes

fish (Acanthomorpha) ARα, but not in an earlier branching Elopomorpha lineage among teleosts, such as Japanese eel (Fig. 7.3). Insertion of these substitutions into ARs from Japanese eel recapitulates the evolutionary novelty of spiny-rayed fish ARα, indicating the substitutions generating a new functionality of teleost ARα were fixed in the teleost genome after the divergence of the Elopomorpha lineage (Ogino et al. 2016).

In the history of AR gene evolution, it is likely that the secondary loss of the ARα gene occurred independently in Cypriniformes (e.g., zebrafish *Danio rerio*, gold fish *Carassius auratus*, and fathead minnow *Pimephales promelas*) and Siluriformes (e.g., southern catfish *Silurus meridionalis*) (Fig. 7.3) (Douard et al. 2008; Hossain et al. 2008; Ogino et al. 2009; Huang et al. 2011). In Salmoniformes, whose lineage diverged early in euteleost evolution (Near et al. 2012), two AR subtypes were identified (Takeo and Yamashita 1999). However, these AR subtypes were categorized into the ARβ cluster, indicating that the duplication of the salmonid AR gene had occurred by lineage-specific gene duplication in the recent salmonid tetraploid event estimated to have taken place 100–50 Ma (Allendorf and Thorgaard 1984). The ARα might have been lost before this lineage-specific gene duplication. Such evolutionary novelty of protein function in ARα and lineage-specific gene loss of ARα genes might be related to the emergence of divergent sex characteristics in teleost lineage.

7.3 Secondary Sex Characteristics Development in Teleost Fishes

Vertebrates exhibit diverse masculine phenotypes in reproductive organs and sex attractive organs. External sexual characteristics, which often appear in sexually differentiated reproductive organs, have evolved in each species presumably for

survival and/or reproduction. In amniotes and also in some fishes, several types of copulatory organs have been developed for sperm transport. All elasmobranchs and holocephalans perform internal fertilization, and the medial border of the pelvic fin of male elasmobranchs is modified to form a tubular structure, termed the clasper.

In teleost fishes, male secondary sex characteristics appear as an elongation of the fin ray, kidney hypertrophy, increased skin thickness, an appearance of breeding colors (Borg 1994), and a transition of anal fin to copulatory organ (Kuntz 1914; Turner 1941a, b; Rosa-Molinar and Burke 2002; Ogino et al. 2004; Sone et al. 2005). The Western mosquitofish, a species of the family Poeciliidae, shows a prominent masculine sexual character for appendage development, the anal fin to gonopodium (GP) transition (Fig. 7.4a, b) (Kuntz 1914; Turner 1941a, b; Rosa-Molinar and Burke 2002; Ogino et al. 2004; Sone et al. 2005) and its appendicular supportive skeletal elements (Turner 1942a, b; Rosa-Molinar et al. 1994, 1996). The GP serves to transfer sperm bundles into the urogenital sinus of the female (Fig. 7.4c) (Rosa-Molinar et al. 1996; Rosen and Gordon 1953; Peden 1972). Such morphological diversification of copulatory organs has evolved as a phenotypic adaptation for developing external to internal fertilization under various environmental influences. The copulatory organ developments commonly involve a process of androgen-dependent organogenesis as a secondary sexual character.

Medaka offers a clue about sexual differentiation. They show a prominent masculine sexual character for appendage development, the formation of papillary processes in the anal fin (Fig. 7.4d). The papillary processes develop as the outgrowing bone nodules from each bone segment in posterior anal fin rays (Fig. 7.4e, compare with (f). Mating males embrace the posterior part of the female's body with the anal fin for efficient external fertilization (Fig. 7.4g) (Yamamoto and Egami 1974).

The male sex characteristics driven by androgens become apparent concomitantly with the sex differentiation of the testis. Evidence supporting the crucial role of androgen on the sex characteristic developments is based on pharmacological data. It is known that the androgens, especially 11KT that is considered an important androgen in fish, are present at higher levels in the blood plasma of mature males than in females and could stimulate male secondary sex characters in teleost fishes (Miura et al. 1991; Kime 1993; Angus et al. 2001). The development of both GP and papillary processes shows a strong response to the treatment of 11KT (Angus et al. 2001; Hishida and Kawamoto 1970), and also synthetic androgens such as ethynyltestosterone (ET) (Turner 1941a, b, 1942a, b; Ogino et al. 2004), trenbolone (Brockmeier et al. 2013), and 17α-methyltestosterone (MT) (Sone et al. 2005; Ogino et al. 2014). Castration causes regression of papillary processes, and transplantation of a testis to an adult female or administration of androgens to females induces papillary processes formation on anal fin rays (Okada and Yamashita 1994) (Hishida and Kawamoto 1970). Therefore, the number and size of papillary processes and the size of the GP are known as the main indicative phenotypes for exposure of androgenic and/or antiandrogenic chemicals (OECD 2004). The reduction in size of the GP (Batty and Lim 1999; Toft et al. 2003) and masculinization of females (Howell et al. 1980) (Parks et al. 2001; Orlando et al. 2002) have been reported in several countries.

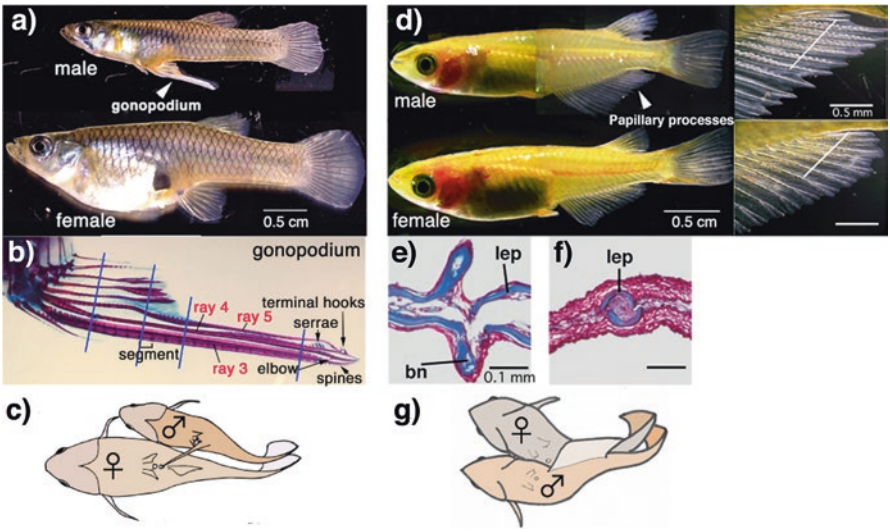

Fig. 7.4 Androgen-dependent sex characteristics development in Western mosquitofish *(Gambusia affinis)* and medaka (*Oryzias latipes*). (**a**) Mature male and female of Western mosquitofish. (**b**) Bone staining of gonopodium (GP). The distal portion of the GP is composed of the third, fourth, and fifth fin rays and the distal tip is equipped with spines, serrae, an elbow, and hooks. The third fin ray, as the axial center of rotation for the GP, is prominently thickened. (**c**) For copulation, the GP swings forward and sperm bundles, spermatozeugmata, are directly transported into the female urogenital sinus (the illustration modified from Rosen and Gordon 1953 and Peden 1972). (**d**) Mature male and female of medaka. Anal fins of male and female are shown. The papillary processes develop on the posterior anal fin rays in males. White lines indicate the plane of sections shown in panels e and f. (**e**, **f**) Masson trichrome staining of anal fins (e: male; f: female). The collagen and bone were stained blue and the cytoplasm was stained purple. bn: bone nodule of papillary processes; lep: lepidotrichia. (**g**) Mating male embraces the posterior part of the female's body with the anal fin for efficient external fertilization. (Figures were modified from Ogino et al. 2004, 2014)

7.4 Western Mosquitofish and Medaka as Models to Understand Molecular Mechanisms of Androgen-Dependent Sex Characteristics Development

Androgens are essential for the development of male sex characteristics evolved in each species for efficient fertilization. Understanding the process of such sexually dimorphic expression, which is to understand the mechanisms of sex hormone–dependent organogenesis underlying such reproductive diversity among species, is one of the central problems in biology. However, the molecular developmental mechanisms underlying androgenic functions remain largely unclear.

The GP and papillary processes present excellent models to understand the molecular mechanisms of androgen-dependent sex characteristics development, because these masculine phenotypes can be rapidly induced by the treatment of synthetic androgens in juvenile fry and adult females (Turner 1941a, b, 1942a, b;

Hishida and Kawamoto 1970; Ogino et al. 2004, 2014; Sone et al. 2005; Brockmeier et al. 2013). The outgrowth of the anal fin rays in Western mosquitofish and the branching bone nodule in medaka are clearly observed within a 10-day androgen treatment (Fig. 7.5a, b) (Ogino et al. 2004, 2014). Such inductivity of masculine phenotypes by androgen enables us to understand the molecular events leading to the development of secondary sex characteristics.

Interestingly, similar phenotypic alterations are detected in these sex characteristics developments. In the distal part of the outgrowing anal fin rays in Western mosquitofish, mesenchymal cells condense prominently, in which cells are highly proliferative (Ogino et al. 2004). Each bone nodule branched from anal fin rays in

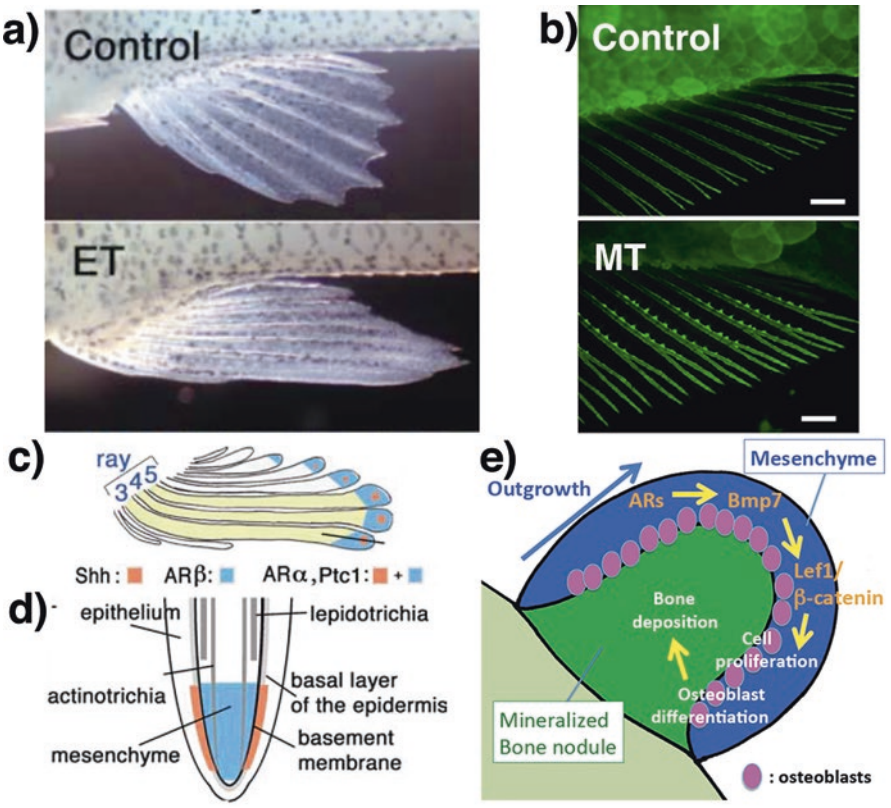

Fig. 7.5 Induction of sex characteristics by androgen treatment. (**a**) Anal fins of control, 3.2 nM ET-treated juvenile fry of Western mosquitofish (9 days after the administration). GP outgrowth is induced by ET. (**b**) Anal fins of control and 32 nM MT-treated mature female medaka (10 days after the administration). Scale bars in A, and B represent 0.5 mm. (**c**, **d**) Schematic representation of developing GP, in which anterior third to fifth fin rays are prospective intromittent fin rays. The black line in (c) indicates the plane of the sections shown in (d). (**e**) Scheme of papillary processes formation. Androgen-dependent Bmp7 signaling and Wnt/β-catenin signaling regulate cell proliferation and osteoblast differentiation. This contributes to the development of the outgrowth of the bone nodule in developing papillary processes. (Figures were modified from Ogino et al. 2004, 2014)

medaka is covered with thickened proliferating mesenchyme (Ogino et al. 2014). Responsiveness to androgens requires expression of functional AR. Western mosquitofish *ARβ* was predominantly expressed in the distal mesenchyme of anal fin rays, while the expression of *ARα* was observed in both epithelial and mesenchymal regions of the anal fin, indicating that the distal region of the anal fin is sensitive to the actions of androgen (Fig. 7.5c, d) (Ogino et al. 2004). In medaka, both *ARα and ARβ* were predominantly expressed in the mesenchyme surrounding the developing bone nodule, suggesting that these mesenchymal cells are sensitive to androgen (Fig. 7.5e) (Ogino et al. 2014). However, the sensitivity to androgen is not solely attributed to *AR* expression levels, because *AR* expressions were observed not only in the developing GP, but also in other fins in mosquitofish (Ogino et al. 2004). Both *AR*s were detected in the posterior- and anterior-anal fin rays of medaka (Ogino et al. 2014). Mechanisms responsible for tissue-specific AR pathways are largely unknown. Recently, the tissue-specific collaborating factors that are capable of binding to chromatin prior to AR loading were identified in mammals (Pihlajamaa et al. 2014). Further identification of such pioneer factors that modulate the AR function may be necessary to obtain new insights into the regulation of tissue-specific function of ARs.

7.5 Downstream Effector Genes of Androgen Signaling That Lead the Morphological Changes of Sex Characteristics Development

Sexual characteristics development contains the remarkably complex processes that depend on the orchestration of signaling networks, including the growth factor signaling and retinoic acid signaling.

Several growth factors are categorized as the effectors that regulate sex characteristics development associated with androgen signals in vertebrates (Ogino et al. 2004, 2011, 2014; Pu et al. 2007; Miyagawa et al. 2009; Brockmeier et al. 2013; O'Shaughnessy et al. 2015).

Expression of *Sonic hedgehog* (*shh*) induced by androgen is required for the formation of the GP in Western mosquitofish (Ogino et al. 2004) and in the clasper in cartilaginous fishes (O'Shaughnessy et al. 2015). During the androgen-induced anal fin to GP transition, *shh* expression is induced in the basal layer of epidermis of the distal anal fin rays (Fig. 7.5c, d). Flutamide (AR-antagonist) treatment reduces cell proliferation in distal anal fin regions accompanied by a reduced level of *shh* expression (Ogino et al. 2004). These results suggested that AR signaling, relaying to Shh signaling, regulates cell proliferation and contributes to the anal fin outgrowth leading to GP formation (Ogino et al. 2004). The Shh signaling is also known to be required for the formation of fin skeleton at the larval stage of zebrafish (Neumann et al. 1999). The *shh* expression was observed in the basal layer of epidermis adjacent to the developing anal fin rays during the larval stages of Western mosquitofish (Fig. 7.5c, d). Thus, the Shh signaling may be re-expressed in the

developing GP in response to AR signaling. The processes of secondary sex characteristics development may be including the androgen-induced heterochronic event, a change in developmental timing, known as an important mechanism of evolutionary change.

Not only the *shh*, but also several genes involved in the fin ray growth and regeneration were identified as the effector genes that regulate sex characteristics development associated with androgen signals, such as *Fibroblast growth factor receptor 1* (*Fgfr1*) (Offen et al. 2008) (Brockmeier et al. 2013), *bone morphogenic protein 7* (*Bmp7*), *lymphoid enhancer-binding factor-1* (*Lef1*) (Ogino et al. 2014), MsxC (Zauner et al. 2003), and aldh1a2, a retinoic acid synthesizing enzyme (Offen et al. 2013). For instances, the development of papillary processes is promoted by androgen-dependent augmentation of *Bmp7*. The Wnt/β-catenin signaling pathway has been identified as a masculine effector of androgen signaling in both medaka (Fig. 7.5e) (Ogino et al. 2014) and mouse (Miyagawa et al. 2009). Similar genotypic changes may result in similar phenotypic alterations, even across a wide range of species. Activation of Wnt/β-catenin signaling is, in fact, indispensable in masculinization of the external genitalia in mouse (Miyagawa et al. 2009) and of the anal fin in medaka (Ogino et al. 2014).

7.6 Conclusion

To understand the biological importance of the AR gene duplication in the teleost lineage, the functional analysis of these AR genes in vivo is necessary. Recent knockout (KO) study of AR gene in the zebrafish revealed that AR is indispensable for masculinization in teleost fishes (doi: https://doi.org/10.1101/159848) (doi: https://doi.org/10.1101/159848, 28620015). But the functional differences of two distinct paralogs of the AR (ARα and ARβ) in vivo are still unclear, because zebrafish have lost the ARα gene. To understand the contribution of two distinct paralogs of AR genes in diversified sex characteristics development in teleost fishes, we are currently developing ARα and ARβ KO medaka. The evolutionary occurrence of two functionally distinct AR proteins might have facilitated the phenotypic diversification of sex characteristics in the euteleost fishes. The evolutionary processes of AR gene loss and retention in teleosts illustrate that teleosts represent an excellent model system to study phenotypic effects of changes in gene repertoire.

Acknowledgments This study was supported by Grants-in-Aid for Scientific Research (KAKENHI) [15K07138 (Y.O.), 15H04395 (Y.O.), 15H04396 (Y.O., T.I.)] from the Japan Society for the Promotion of Science (JSPS); UK-Japan Research Collaboration Grants (T.I.) from the Ministry of the Environment, Japan, and the Department for Environment, Food and Rural Affairs (DEFRA), UK; the NIBB Cooperative Research Program (Y.O.) from National Institute for Basic Biology; The 2nd Women Researchers Promotion Program (Y.O.), Support for childbirth and childcare in Women Researchers Promotion Program (Y.O.) and Support for Women Returning from Maternity and Parental Leave from Kyushu University (Y.O.); The Naito Foundation (Y.O.). We thank Dr. Mike Roberts, DEFRA, UK, for his critical reading of this manuscript.

References

Allendorf FW, Thorgaard GH (1984) Tetraploidy and the evolution of Salmonid fishes. In: Turner JB (ed) Evolutionary genetics of fishes. Plenum Publishing Corp., New York, pp 1–53

Angus RA, McNatt HB, Howell WM, Peoples SD (2001) Gonopodium development in normal male and 11-ketotestosterone-treated female mosquitofish (*Gambusia affinis*): A quantitative study using computer image analysis. Gen Comp Endocrinol 123(2):222–234

Baker ME (1997) Steroid receptor phylogeny and vertebrate origins. Mol Cell Endocrinol 135(2):101–107

Batty J, Lim R (1999) Morphological and reproductive characteristics of male mosquitofish (*Gambusia affinis holbrooki*) inhabiting sewage-contaminated waters in New South Wales, Australia. Arch Environ Contam Toxicol 36(3):301–307

Borg B (1994) Androgens in teleost fishes. Comp Biochem Physiol 109C(3):219–245

Brockmeier EK, Ogino Y, Iguchi T, Barber DS, Denslow ND (2013) Effects of 17β-trenbolone on Eastern and Western mosquitofish (*Gambusia holbrooki* and *G. affinis*) anal fin growth and gene expression patterns. Aquat Toxicol 128-129:163–170

Brunet FG, Roest Crollius H, Paris M, Aury JM, Gibert P, Jaillon O, Laudet V, Robinson-Rechavi M (2006) Gene loss and evolutionary rates following whole-genome duplication in teleost fishes. Mol Biol Evol 23(9):1808–1816

Chiu CH, Dewar K, Wagner GP, Takahashi K, Ruddle F, Ledje C, Bartsch P, Scemama JL, Stellwag E, Fried C, Prohaska SJ, Stadler PF, Amemiya CT (2004) Bichir HoxA cluster sequence reveals surprising trends in ray-finned fish genomic evolution. Genome Res 14(1):11–17

Douard V, Brunet F, Boussau B, Ahrens I, Vlaeminck-Guillem V, Haendler B, Laudet V, Guiguen Y (2008) The fate of the duplicated androgen receptor in fishes: a late neofunctionalization event? BMC Evol Biol 8(1):336

Force A, Lynch M, Pickett FB, Amores A, Yan YL, Postlethwait J (1999) Preservation of duplicate genes by complementary, degenerative mutations. Genetics 151(4):1531–1545

Hawkins MB, Thornton JW, Crews D, Skipper JK, Dotte A, Thomas P (2000) Identification of a third distinct estrogen receptor and reclassification of estrogen receptors in teleosts. Proc Natl Acad Sci U S A 97(20):10751–10756

Hishida T-O, Kawamoto N (1970) Androgenic and male Inducing effects of 11 ketotestosterone on a teleost the medaka *Oryzias-latipes*. J Exp Zool 173(3):279–284

Hoegg S, Brinkmann H, Taylor JS, Meyer A (2004) Phylogenetic timing of the fish-specific genome duplication correlates with the diversification of teleost fish. J Mol Evol 59(2):190–203

Hossain MS, Larsson A, Scherbak N, Olsson PE, Orban L (2008) Zebrafish androgen receptor: isolation, molecular, and biochemical characterization. Biol Reprod 78(2):361–369

Howell WM, Black DA, Bortone SA (1980) Abnormal expression of secondary sex characters in a population of mosquitofish, *Gambusia affinis holbrooki*: Evidence for environmentally-induced masculinization. Copeia 4:676–681

Huang BF, Sun YL, Wu FR, Liu ZH, Wang ZJ, Luo LF, Zhang YG, Wang DS (2011) Isolation, sequence analysis, and characterization of androgen receptor in Southern catfish, *Silurus meridionalis*. Fish Physiol Biochem 37(3):593–601

Hughes AL (2002) Adaptive evolution after gene duplication. Trends Genet 18(9):433–434

Ikeuchi T, Todo T, Kobayashi T, Nagahama Y (1999) cDNA cloning of a novel androgen receptor subtype. J Biol Chem 274(36):25205–25209

Inoue JG, Miya M, Tsukamoto K, Nishida M (2003) Basal actinopterygian relationships: a mitogenomic perspective on the phylogeny of the "ancient fish". Mol Phylogenet Evol 26(1):110–120

Jaillon O, Aury JM, Brunet F, Petit JL, Stange-Thomann N, Mauceli E, Bouneau L, Fischer C, Ozouf-Costaz C, Bernot A, Nicaud S, Jaffe D, Fisher S, Lutfalla G, Dossat C, Segurens B, Dasilva C, Salanoubat M, Levy M, Boudet N, Castellano S, Anthouard V, Jubin C, Castelli V, Katinka M, Vacherie B, Biemont C, Skalli Z, Cattolico L, Poulain J, De Berardinis V, Cruaud C, Duprat S, Brottier P, Coutanceau JP, Gouzy J, Parra G, Lardier G, Chapple C, McKernan KJ, McEwan P, Bosak S, Kellis M, Volff JN, Guigo R, Zody MC, Mesirov J, Lindblad-Toh K,

Birren B, Nusbaum C, Kahn D, Robinson-Rechavi M, Laudet V, Schachter V, Quetier F, Saurin W, Scarpelli C, Wincker P, Lander ES, Weissenbach J, Roest Crollius H (2004) Genome duplication in the teleost fish *Tetraodon nigroviridis* reveals the early vertebrate proto-karyotype. Nature 431(7011):946–957

Kikugawa K, Katoh K, Kuraku S, Sakurai H, Ishida O, Iwabe N, Miyata T (2004) Basal jawed vertebrate phylogeny inferred from multiple nuclear DNA-coded genes. BMC Biol 2(1):3

Kime DE (1993) 'Classical' and 'non-classical' reproductive steroids in fish. Rev Fish Biol Fish 3:160–180

Kuntz A (1914) Notes on the habits, morphology of the reproductive organs, and embryology of the viviparous fish *Gambusia affinis*. Bull US Bur Fish 33:177–190

Laudet V (1997) Evolution of the nuclear receptor superfamily: early diversification from an ancestral orphan receptor. J Mol Endocrinol 19(3):207–226

Lynch M, Katju V (2004) The altered evolutionary trajectories of gene duplicates. Trends Genet 20(11):544–549

Mangelsdorf DJ, Thummel C, Beato M, Herrlich P, Schutz G, Umesono K, Blumberg B, Kastner P, Mark M, Chambon P, Evans RM (1995) The nuclear receptor superfamily: the second decade. Cell 83(6):835–839

Miura T, Yamauchi K, Takahashi H, Nagahama Y (1991) Hormonal induction of all stages of spermatogenesis in vitro in the male Japanese eel (*Anguilla japonica*). Proc Natl Acad Sci U S A 88(13):5774–5778

Miya M, Kawaguchi A, Nishida M (2001) Mitogenomic exploration of higher teleostean phylogenies: a case study for moderate-scale evolutionary genomics with 38 newly determined complete mitochondrial DNA sequences. Mol Biol Evol 18(11):1993–2009

Miyagawa S, Satoh Y, Haraguchi R, Suzuki K, Iguchi T, Taketo MM, Nakagata N, Matsumoto T, Takeyama K, Kato S, Yamada G (2009) Genetic interactions of the androgen and Wnt/β-catenin pathways for the masculinization of external genitalia. Mol Endocrinol 23(6):871–880

Near TJ, Eytan RI, Dornburg A, Kuhn KL, Moore JA, Davis MP, Wainwright PC, Friedman M, Smith WL (2012) Resolution of ray-finned fish phylogeny and timing of diversification. Proc Natl Acad Sci U S A 109(34):13698–13703

Neumann CJ, Grandel H, Gaffield W, Schulte-Merker S, Nusslein-Volhard C (1999) Transient establishment of anteroposterior polarity in the zebrafish pectoral fin bud in the absence of sonic hedgehog activity. Development 126(21):4817–4826

O'Shaughnessy KL, Dahn RD, Cohn MJ (2015) Molecular development of chondrichthyan claspers and the evolution of copulatory organs. Nat Commun 6:6698

OECD (2004) OECD draft report of the initial work towards the validation of the fish screening assay for the detection of endocrine active substances: Phase 1A. OECD, Paris

Offen N, Blum N, Meyer A, Begemann G (2008) Fgfr1 signalling in the development of a sexually selected trait in vertebrates, the sword of swordtail fish. BMC Dev Biol 8:98

Offen N, Kang JH, Meyer A, Begemann G (2013) Retinoic acid is involved in the metamorphosis of the anal fin into an intromittent organ, the gonopodium, in the green swordtail (*Xiphophorus hellerii*). PLoS One 8(10):e77580

Ogino Y, Katoh H, Yamada G (2004) Androgen dependent development of a modified anal fin, gonopodium, as a model to understand the mechanism of secondary sexual character expression in vertebrates. FEBS Lett 575(1–3):119–126

Ogino Y, Katoh H, Kuraku S, Yamada G (2009) Evolutionary history and functional characterization of androgen receptor genes in jawed vertebrates. Endocrinology 150(12):5415–5427

Ogino Y, Miyagawa S, Katoh H, Prins GS, Iguchi T, Yamada G (2011) Essential functions of androgen signaling emerged through the developmental analysis of vertebrate sex characteristics. Evol Dev 13(3):315–325

Ogino Y, Hirakawa I, Inohaya K, Sumiya E, Miyagawa S, Denslow N, Yamada G, Tatarazako N, Iguchi T (2014) Bmp7 and Lef1 are the downstream effectors of androgen signaling in androgen-induced sex characteristics development in medaka. Endocrinology 155(2):449–462

Ogino Y, Kuraku S, Ishibashi H, Miyakawa H, Sumiya E, Miyagawa S, Matsubara H, Yamada G, Baker ME, Iguchi T (2016) Neofunctionalization of androgen receptor by gain-of-function mutations in teleost fish lineage. Mol Biol Evol 33(1):228–244

Ohno S (1970) Evolution of gene duplication. Springer, New York

Okada YK, Yamashita H (1994) Experimental investigation of the manifestation of secondary sexual characters in fish, using the medaka, *Oryzias latipes* (Temmick and Schlegel) as material. J Fac Sci Tokyo Imp Univ Sec IV Zool 6:383–437

Orlando EF, Davis WP, Guillette LJ Jr (2002) Aromatase activity in the ovary and brain of the eastern mosquitofish (*Gambusia holbrooki*) exposed to paper mill effluent. Environ Health Perspect 110(Suppl 3):429–433

Parks LG, Lambright CS, Orlando EF, Guillette LJ Jr, Ankley GT, Gray LE Jr (2001) Masculinization of female mosquitofish in Kraft mill effluent-contaminated Fenholloway River water is associated with androgen receptor agonist activity. Toxicol Sci 62(2):257–267

Peden AE (1972) The function of gonopodial parts and behavioral pattern during copulation by *Gambusia* (Poeciliidae). Can J Zool 50:955–967

Pihlajamaa P, Sahu B, Lyly L, Aittomaki V, Hautaniemi S, Janne OA (2014) Tissue-specific pioneer factors associate with androgen receptor cistromes and transcription programs. EMBO J 33(4):312–326

Prince VE, Pickett FB (2002) Splitting pairs: the diverging fates of duplicated genes. Nat Rev Genet 3(11):827–837

Pu Y, Huang L, Birch L, Prins GS (2007) Androgen regulation of prostate morphoregulatory gene expression: Fgf10-dependent and -independent pathways. Endocrinology 148(4):1697–1706

Rosa-Molinar E, Burke AC (2002) Starting from fins: parallelism in the evolution of limbs and genitalia: the fin-to-genitalia transition. Evol Dev 4(2):124–126

Rosa-Molinar E, Hendricks SE, Rodriguez-Sierra JF, Fritzsch B (1994) Development of the anal fin appendicular support in the western mosquitofish, *Gambusia affinis affinis* (Baird and Girard, 1854): a reinvestigation and reinterpretation. Acta Anat (Basel) 151(1):20–35

Rosa-Molinar E, Fritzsch B, Hendricks SE (1996) Organizational-activational concept revisited: sexual differentiation in an atherinomorph teleost. Horm Behav 30(4):563–575

Rosen DE, Gordon M (1953) Functional anatomy and evolution of male genitalia in poeciliid fishes. Zoologica 38:1–52

Sato Y, Nisida M (2010) Teleost fish with specific genome duplication as unique models of vertebrate evolution. Environ Biol Fish 88:169–188

Sone K, Hinago M, Itamoto M, Katsu Y, Watanabe H, Urushitani H, Tooi O, Guillette LJ Jr, Iguchi T (2005) Effects of an androgenic growth promoter 17β-trenbolone on masculinization of Mosquitofish (*Gambusia affinis affinis*). Gen Comp Endocrinol 143(2):151–160

Sperry TS, Thomas P (1999) Identification of two nuclear androgen receptors in kelp bass (*Paralabrax clathratus*) and their binding affinities for xenobiotics: comparison with Atlantic croaker (*Micropogonias undulatus*) androgen receptors. Biol Reprod 61(4):1152–1161

Takeo J, Yamashita S (1999) Two distinct isoforms of cDNA encoding rainbow trout androgen receptors. J Biol Chem 274(9):5674–5680

Thornton JW, Kelley DB (1998) Evolution of the androgen receptor: structure-function implications. BioEssays 20(10):860–869

Toft G, Edwards TM, Baatrup E, Guillette LJ Jr (2003) Disturbed sexual characteristics in male mosquitofish (*Gambusia holbrooki*) from a lake contaminated with endocrine disruptors. Environ Health Perspect 111(5):695–701

Turner CL (1941a) Gonopodial characteristics produced in the anal fins of females of *Gambusia affinis affinis* by treatment with ethynyl testosterone. Biol Bull 30:371–383

Turner CL (1941b) Morphognesis of the gonopodium in *Gambusia affinis affinis*. J Morphol 69:161–185

Turner CL (1942a) Morphogenesis of the gonopodium suspensorium in *Gambusia affinis affinis* and the induction of male suspensorial characters in the female by androgenic hormones. J Exp Zool 91:167–193

Turner CL (1942b) A quantitative study of the effects of different concentrations of ethynyl testosterone and methyl testosterone in the production of gonopodia in females of *Gambusia affinis*. Physiol Zool 15(3):263–281

Volff JN (2005) Genome evolution and biodiversity in teleost fish. Heredity 94(3):280–294

Yamamoto M, Egami N (1974) Fine structure of the surface of the anal fin and the processes on its fin rays of male *Oryzias latipes*. Copeia 1974(1):262–265

Zauner H, Begemann G, Mari-Beffa M, Meyer A (2003) Differential regulation of msx genes in the development of the gonopodium, an intromittent organ, and of the "sword", a sexually selected trait of swordtail fishes (*Xiphophorus*). Evol Dev 5(5):466–477

Part III
Clinical Models

Chapter 8
Zebrafish Angiogenesis and Valve Morphogenesis: Insights from Development and Disease Models

Matina Katraki-Pavlou and Dimitris Beis

Abstract Research on zebrafish embryonic development has already contributed to major breakthroughs in our understanding of how the cardiovascular system forms and functions. Zebrafish embryos are transparent, allowing noninvasive in vivo imaging. The advancements of high-resolution imaging and image analysis software, combined with the generation of tissue-specific transgenic lines and forward genetic screens, enabled the study of endothelial development at cellular resolution. Also, zebrafish embryos are not fully dependent on a functional cardiovascular system during the first few days of development since they get enough oxygen by passive diffusion. This advantage allowed the deciphering of the interplay between cardiac form and function as well as the identification of severe mutations of the heart and vessels. In this chapter, we highlight the experimental approaches and disease models used in zebrafish to study different aspects of the cardiovascular system.

Keywords Angiogenesis · Lymphangiogenesis · Cardiac valve · Hemodynamics · Blood-brain barrier

8.1 Overview of Angiogenesis

Angiogenesis is the biological process by which new blood vessels are generated from preexisting ones. It is important for embryonic development, reproduction, and wound repair but is also involved in a variety of pathologies such as cancer, diabetic retinopathy, and rheumatoid arthritis (Risau 1997). Through the years, numerous studies in cancer angiogenesis have contributed to a better understanding of the molecular mechanisms of angiogenesis also in nonneoplastic diseases (Folkman 1995). Proper angiogenesis depends on a balance between inducers and inhibitors of cell proliferation and migration. The identification of some important

M. Katraki-Pavlou · D. Beis (✉)
Zebrafish Disease Models Laboratory, Biomedical Research Foundation, Academy of Athens, Athens, Greece
e-mail: dbeis@bioacademy.gr

H. Hirata, A. Iida (eds.), *Zebrafish, Medaka, and Other Small Fishes*,
https://doi.org/10.1007/978-981-13-1879-5_8

molecules of angiogenesis such as the vascular endothelial growth factor (VEGF) has been pivotal in elucidating the mechanism of angiogenesis in both normal and pathological conditions (Ferrara and Davis-Smyth 1997; Carmeliet and Collen 2000). In addition, other important inducers have been found, including angiopoietins (Fagiani and Christofori 2013), transforming growth factors (TGF) (van den Driesche et al. 2003), members of the fibroblast growth factor family (FGF) (Seghezzi et al. 1998; Cross and Claesson-Welsh 2001), platelet-derived growth factor (Battegay et al. 1994), tumor necrosis factor-α (Fajardo et al. 1992), the secreted heparin-binding growth factor pleiotrophin (Papadimitriou et al. 2016), and interleukins (Yang et al. 2014; Pan et al. 2015). Many factors including membrane-bound proteins, soluble growth factors, vascular-specific integrins, plasminogen activators, and matrix metalloproteases have been identified as key players of the interaction between endothelial cells (ECs).

The molecular mechanisms and the way that endothelial development occurs in the zebrafish are remarkably analogous to that of other vertebrates (Weinstein 2002). Also, the anatomical structures of embryonic blood vessels are well conserved between zebrafish and humans. This conservation of the main outline of the circulation system validates the zebrafish as a suitable model for studying the development and the anatomy of the vascular system (Isogai et al. 2001; Weinstein 2002). Zebrafish has several features that facilitate the analysis of early vascular development. These include the optical transparency, the ability to survive and develop for the first 3–4 days without blood circulation by passive diffusion, and the existence of different transgenic lines that allow real-time in vivo analysis at cellular resolution (Jin et al. 2005). Furthermore, zebrafish has evolved as an excellent model for high-throughput drug screening and has been widely used to identify compounds that regulate angiogenesis under physiological conditions or disease (Serbedzija et al. 1999; Papakyriakou et al. 2014; Merrigan and Kennedy 2017).

8.2 Vascular Morphogenesis

The development of embryonic blood vessels occurs by two distinct morphogenetic mechanisms, termed vasculogenesis and angiogenesis. During vasculogenesis a primary vascular network is formed in different domains of the body, and shortly after that, further blood vessels are generated via angiogenesis, progressively forming a fully functional circulation system (Coffin and Poole 1991; Risau and Flamme 1995; Weinstein 1999). During early vascular development in zebrafish, free angioblast progenitor cells form the first major blood vessels. These cells derive from the lateral plate mesoderm, migrate individually to the midline, and differentiate to ECs (Stainier et al. 1995; Weinstein 1999; Jin et al. 2005). The first wave of angioblast migration happens at the 14–17-somite stage, where cells reach the embryonic midline and contribute to the dorsal aorta (DA), while a second wave of cells forms the posterior cardinal vein (PCV). The primitive arterial and venous angioblasts aggregate to make a midline endothelial cord. DA is lumenized at around 23 hours post

fertilization (hpf), whereas PCV is not patent until the circulation loop is established. At approximately 26hpf the primitive cells of PCV enter the circulation, and until 28hpf both blood vessels are fully formed (Jin et al. 2005) (Fig. 8.1a).

Live imaging using transgenic reporter fish lines, such as the *Tg(fli1a:EGFP)*, *Tg(kdrl:EGFP)*, and derivatives of those with different fluorophores, revealed that precursor cells migrate as individual cells and express several arteriovenous differentiation markers including vascular endothelial growth factor receptor (*vegfr4/kdrl*), *fli1a*, and *ephrin-b2a* (Lawson et al. 2002; Herbert et al. 2009; Kohli et al. 2013). Arterial and venous endothelial cells are different at a functional and molecular level, and the specification of these two cell types, in early development, is driven by different genetic mechanisms (Swift and Weinstein 2009). *Ephrins* were identified as markers for the molecular distinction between arterial and venous endothelial cells (Wang et al. 1998). Ephrin-B2 (*efnb2)*, a member of tyrosine kinase receptor ligands, is expressed in arteries, in contrast with *EphB4*, an ephrin-B2 receptor, which is specifically expressed in venous cells (Adams et al. 1999). Studies in mice and zebrafish have shown that forward and reverse Ephrin-B2 signaling plays a critical role in vascular morphogenesis and that repulsive Ephb4a-Efnb2a signaling regulates the directional control of angioblast sprouting behavior (Adams et al. 2001; Herbert et al. 2009; Wang et al. 1998). Further data support that arterial/venous tubulogenesis is a result of coordinated regulation of Notch, VEGF, and Ephb4a/Efnb2a signaling.

Studies in zebrafish have helped to elucidate the interactions between these signaling pathways and understand their role in vascular development. Notch signaling

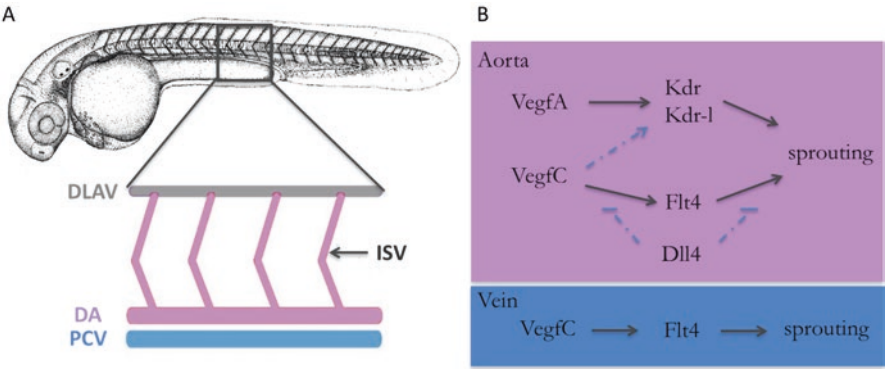

Fig. 8.1 Angiogenic sprouting in the zebrafish: (**a**) schematic overview of arterial and venous development. In embryonic trunk development, angiogenesis takes place in two distinct stages where arteries and veins arise from preexisitng vessels. ISVs and DA are formed during the first angiogenic sprouting, whereas during the secondary wave sprouts form from the PCV and give rise to a venous angiogenic process DA, dorsal aorta; PCV, posterior cardinal vein; ISV, intersegmental vessel v(venous) and a(arterial); DLAV, dorsal longitudinal anastomosing vessel. (**b**) Vegfa acts through kdrl and kdr and plays a dominant role in aISV sprouting. Vegfc also influences (dashed line) ISA (intersegmental artery) development and it is regulated by DII4. Sprouting of vISV is dependent on Vegfc/Flt4 signaling in venous angiogenesis

genes, which are expressed in arterial ECs, promote differentiation in arteries and not in venous endothelium (Lawson and Weinstein 2002; Siekmann and Lawson 2007). Based on in vivo analysis experiments, Notch is activated in endothelial progenitor cells during early stages of development. Later during the vascular formation, activation of Notch is restricted in arterial endothelial cells and determines their dorsal aorta fate (Quillien et al. 2014). In mice and zebrafish, *notch1a*, *notch1b*, and *notch3* receptors show restricted expression pattern in arterial endothelial cells, in contrast to Delta-like 4 (Dll4), Jagged1, and Jagged2 ligands (Lawson et al. 2001; Geudens et al. 2010). Defects in Notch signaling lead to several phenotypes, including arteriovenous shunts and reduction of arterial gene expression which leads to dysregulation of artery differentiation (Quillien et al. 2014).

The RBPJ/Notch intracellular domain together with the SOXF transcription factors (SOX7 and SOX18) regulates early vascular development by binding the arterial-specific enhancers of the Notch ligand dll4 (Sacilotto et al. 2013). Sox17 functions upstream of Notch and plays an essential role in endoderm formation and possession of arterial identity (Kanai-Azuma et al. 2002; Corada et al. 2013), while Sox18 is necessary for the differentiation of ECs in lymphatic cells (François et al. 2008). Recent works in zebrafish have shown that Sox18 and Sox7 are involved in arteriovenous specification (Herpers et al. 2008; Cermenati et al. 2008; Pendeville et al. 2008). In addition, it is suggested that Sox7 acts upstream of Notch signaling pathway controlling the expression arteriovenous patterning genes and regulates arteriovenous specification in a coordination with *Hey2* and *Efnb2* genes (Hermkens et al. 2015). Vascular endothelial growth factor (VEGF), a selective mitogen for endothelial cells, and its receptor (VEGF-R2/Flk-1/kdrl) are the major players for the formation and sprouting of blood vessels. In a subset of angioblasts, the transcriptional activation of several factors, such as Notch, is induced by Vegf, via the VEGF-receptor-2/Flk-1/kdrl (Lawson et al. 2002). Vegf in terms, through the induction of PLCγ/Mek/Erk pathway, activates the Notch signaling pathway in ECs and promotes arterial differentiation (Lawson et al. 2003) (Fig. 8.1b).

The formation of secondary endothelial vessels takes place in two distinct waves of vascular sprouting (Isogai et al. 2003). During the first angiogenic process, tip cells sprout from the dorsal part of DA and around 30hpf form the segmental arteries (aISVs). The newly formed ISVs start to make new boundaries with their neighbors' segments, giving eventually rise to the dorsal longitudinal anastomotic vessel (DLAV). By this time, the heart has already started beating and blood flow is established. The second angiogenic wave starts around 32 hpf where new ECs sprouts emerge from PCV and CV, anastomose with the ISVs and form segmental veins (vISVs) (Yaniv et al. 2006; Betz et al. 2016). By the time aISVs, DLAV, and vISVs have fully formed, the lumen becomes apparent and blood flow through the ISVs begins (Kamei et al. 2006). During these processes, Vegfa and Vegfc have a dominant role. Vegfa act via kdr and kdr-l receptors and is necessary for artery formation. Vegfc/Flt4 signaling mainly determinates normal venous sprouting but when Dll4 is not active leads to artery formation as well (Hogan et al. 2009) (Fig. 8.1b).

Sprouting angiogenesis is a process guiding two different populations of ECs, whose genetic profile is critical for vessel growth in the developing vascular system. The endothelial cells located at the terminal part of the sprouts, termed as tip cells, migrate extending long filopodia and lead the vascular sprout. The stalk endothelial cells are located behind the tip cells, proliferate, and maintain the structure of the lumen (Siekmann and Lawson 2007). Based on recent studies, cell elongation and cell rearrangements are important components of stalk elongation (Sauteur et al. 2014). Both migration of tip cell and proliferation of stalk cells are tightly regulated by vascular endothelial growth factor (VEGF) signaling (Benjamin et al. 1998). Tip cell sprouting behavior is induced by VEGFA and VEGFC signaling via VEGFR2 and VEGFR3 activation. The induction of VEGFR2 expression leads to upregulation of Notch receptor Delta-like 4 (DLL4) in tip cells, which activates Notch on adjacent stalk cells. Notch signaling in stalk cells downregulates the VEGFR3 and increases the expression of VEGFR1, limiting the ability of ECs to respond to pro-angiogenic Vegf signals (Herbert and Stainier 2011). *Vegfr1*, known as *flt1*, is a negative regulator of tip cell formation and migration in the zebrafish embryo. In *flt1* morphants, the tip cell number is increased, and new filopodia extensions form connections between vessels, while Notch signaling is lost (Krueger et al. 2011). Recent studies showed that expression of *flt4* gene is regulated by ERK activation, in late stages of zebrafish vasculogenesis (Shin et al. 2016), and during tip cell formation, inhibition of ERK blocks ISV sprouting but does not affect artery differentiation. Also, ERK activity is required for the specialized cells to emerge and form new vessels, making ERK a new marker for monitoring the emergence of cells in angiogenesis (Nagasawa-Masuda and Terai 2016).

In vivo time-lapse analysis reveals that in the absence of Notch, most of the sprouting endothelial cells gain a tip cell fate, leading to hyperbranching of segmental arteries (Siekmann and Lawson 2007). Thus, angiogenesis is regulated by the modulation of tip cell behavior in a Notch-independent manner, and several signaling pathways and molecules mediate these processes. BMP signaling promotes stalk tall behavior increasing Notch expression through the activation of ALK1 (Larrivée et al. 2012). Activation of Notch in stalk cells decreases the expression of neuropilin-1 (NRP1), which is highly expressed in tip cells (Aspalter et al. 2015). A recent study elucidated cAMP-dependent protein kinase A (PKA) as a regulator of angiogenesis in a Notch-independent manner. Inhibition of endothelial PKA, in both mouse and zebrafish, results in an increase of cell migration and vascular hypersprouting, and this signaling process seems to be autonomous and independent from Notch-induced sprouting (Nedvetsky et al. 2016). Furthermore, the current idea that Dll4/Notch-dependent lateral inhibition is the only exclusive way of tip/stalk identity specification has started to be reconsidered. Recent data support that asymmetric cell division plays a major role in the control of collective cell migration in angiogenesis (Costa et al. 2016). In vivo experiment in zebrafish and computational approaches have proposed that pro-migratory Vegfr signaling drives self-organization of daughter cells into leading/trailing cells after asymmetric endothelial tip cell division, in a Dll4/Notch-independent manner. Thus, asymmetric

divisions coordinate collective cell migration and probably assist the growth of multiple tissues during embryonic development, wound healing, and cancer invasion.

The pattern of arterial and venous vessels is crucial for the formation of a functional network. Isogai and colleagues suggested that the pattern of junctions between the first and second sprouting vessels is affected by the blood circulation (Isogai et al. 2003). Recent studies show that remodeling events during early development are regulated by circulatory flow dynamics (Kochhan et al. 2013). Differences in blood flow fusion influence the establishment of the newly formed vessel, with the strongly perfused vessels prevailing over the low perfused and less-functional vessels (Franco et al. 2015). Thus, hemodynamic forces contribute to the formation and the expansion of a new vascular tube. Lumen formation also depends on a balance between the circulation of dynamic forces, which are applied and shape the endothelial cell membrane and the local contractile responses from the endothelial cells (Gebala et al. 2016).

During development, endothelial and endocardial cells are exposed to different hemodynamic forces including blood flow, environmental and mechanical stresses, pressure, strain, and shear stress. Several genes are identified to respond to blood flow dynamics, with *klf2* being the best characterized. *Klf2* gene encodes the zinc finger transcription factor Krüppel-like factor 2 (Klf2) (Novodvorsky and Chico 2014), a shear stress-responsive promotor element. In human and zebrafish, *klf2a* expression is increased by high oscillatory flow and is required for cardiac valve formation (Vermot et al. 2009; Heckel et al. 2015). Within developing zebrafish aortic arch blood vessels, Klf2a promotes the expression of the endothelial-specific microRNA, miR-126, whose expression activates VEGF signaling, implying the essential role of blood flow in vasculature angiogenesis (Nicoli et al. 2010). In *gridlock* mutants, for example, the loss of *hey2* gene leads to reduction of arterial gene expression and suppression of DA specification (Zhong et al. 2000), while in *cloche* mutants, the lack of endocardium can affect the intracellular signaling within the myocardium leading to trabeculation defects (Peshkovsky et al. 2011).

Klf2 induction is also regulated by the cerebral cavernous malformation (CCM) complex in mice and zebrafish (Zhou et al. 2015; Renz et al. 2015). CCMs are prevalent vascular abnormalities characterized by dilated, thin-walled vascular vessels, which are prone to cerebral hemorrhages and can lead to stroke, seizures, and death. So far, three CCM proteins have been identified in heritable disorders: CCM1/KRIT1 (Laberge-le Couteulx et al. 1999), CCM2/malcavernin (Denier et al. 2004), and CCM3/programmed cell death 10 (PDCD10) (Bergametti et al. 2005). In zebrafish, loss of *ccm1* or *ccm2* genes (*santa* and *valentine* mutants) does not have any impact on EC differentiation but causes a cardiovascular phenotype demonstrated by the dilation of the heart and of the major blood vessels including subintestinal vessels and posterior cardinal vein (Mably et al. 2006; Hogan et al. 2008). In addition, vascular defects are the same in single and double mutants, confirming that Ccm1 and Ccm2 function in the same physical complex (Mably et al. 2006), while Ccm3 seems to have an independent role (Yoruk et al. 2012). A recent study showed that CCM complex is the main regulator of a β1 integrin-Klf2-Egfl7

pathway in zebrafish. In ccm2^{m201} mutants, klf2 expression induced by β1 integrin leads to aberrant angiogenesis (Renz et al. 2015).

8.3 Cardiac Valve Development

Cardiac valve development is the biological system where the interplay between biophysical forces, mechanotransduction, and heart morphogenesis can be best appreciated. Cardiac valves arise from endocardial cells after the heart starts beating and function to ensure unidirectional flow of the blood. However, at the first stages of cardiac morphogenesis and following the initiation of circulation, there is significant retrograde flow through the atrioventricular (AV) canal, where the valves will emerge. This intracardiac flow pattern triggers a Klf2-mediated signaling cascade that promotes valve development to establish unidirectional flow (Vermot et al. 2009; Renz et al. 2015) (Fig. 8.2). Taking advantage of surgical and pharmacological manipulations, as well as of mutants with defective myocardial contractility (*silent heart*, *weak atrium*) and altered intracardiac flow dynamic due to changes in heart geometry (*southpaw*), zebrafish has been pivotal in studying these interactions in vivo (Hove et al. 2003; Bartman et al. 2004; Vermot et al. 2009; Kalogirou et al. 2014; Pestel et al. 2016). These studies are largely facilitated by the ability to do high-resolution imaging at the cellular level, using high-speed cameras and/or

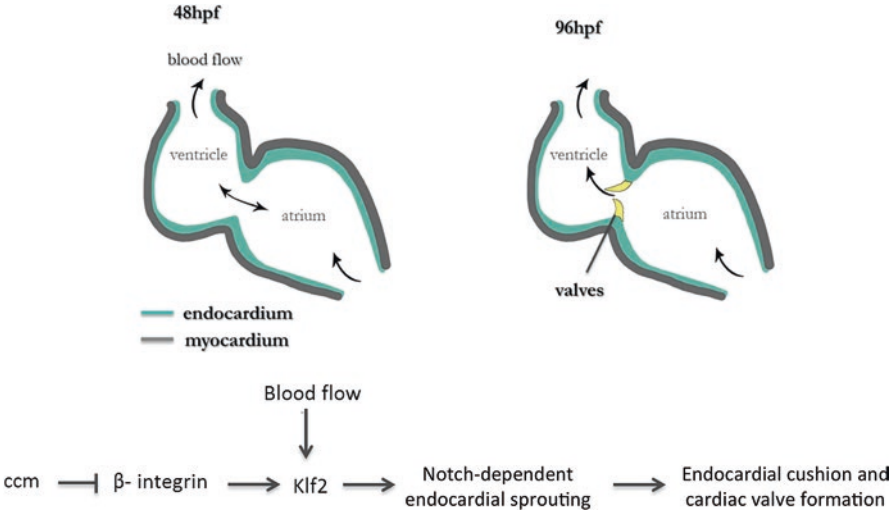

Fig. 8.2 The process of valvulogenesis depends on the biophysical stimulus of blood flow. At the atrioventricular canal where reverse intracardiac flow patterns occur, CCM proteins inhibit β-integrin, providing a bias in Klf2a expression levels. CCM complex is a key regulator of a β1 integrin-Klf2-Egfl7 pathway in zebrafish, and klf2a regulates Notch signaling and endocardial cushion and valve formation

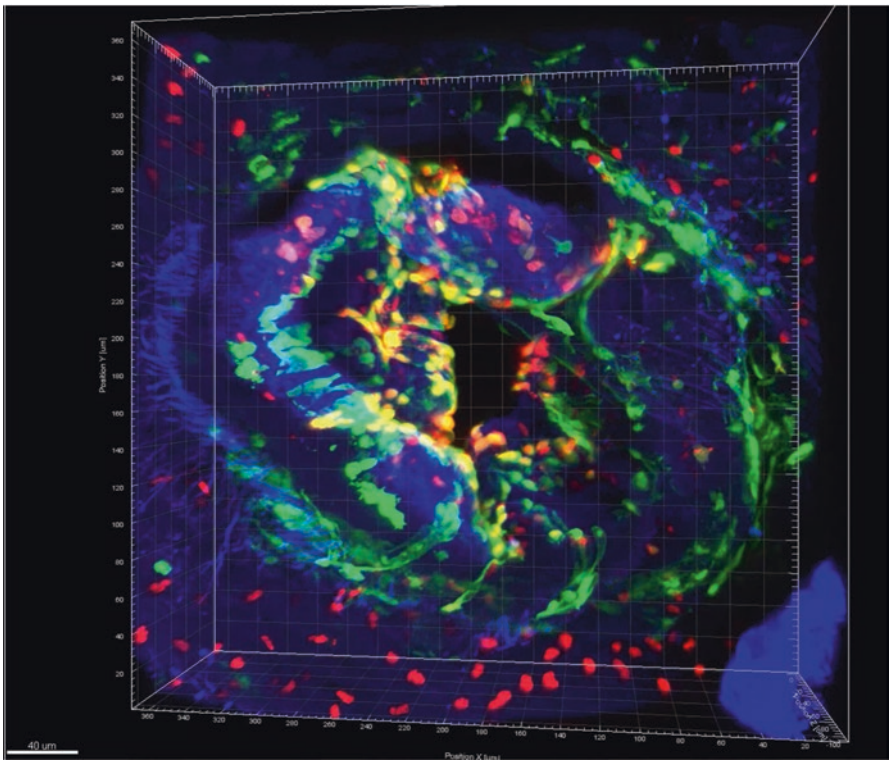

Fig. 8.3 A 3D projection of an adult atrioventricular valve showing the expression pattern of a valve-specific GAL4 driver line (green) and a Notch reporter line (red). The valve-specific GAL4 line allows the tissue-specific expression of any gene of interest. In this way, nitroreductase can be also expressed in a valve-specific pattern, and when metronidazole is added in the water, the expressing cells will be ablated enabling valve regeneration studies. Elastin2-positive cells are labeled in blue

selective plane illumination microscopy (SPIM) imaging and image reconstruction (Mickoleit et al. 2014; Pestel et al. 2016) (Fig. 8.3).

Notch signaling and Egfl7 have been identified as key downstream targets of Klf2, while the CCM proteins appear to function antagonistically to the activation of β1 integrin by shear stress (Macek Jilkova et al. 2014). Knockdown of β1 integrin suppresses the cardiovascular defects of CCM mutant embryos (Renz et al. 2015) (Fig. 8.2). In addition to the intracardiac flow dynamics and endocardial/myocardial interactions at the valve-forming region, it is worth noticing that there are extensive extracellular matrix components, also known as cardiac jelly. One of its major components is hyaluronic acid, produced by the Has2 enzyme, that is tightly regulated during AV development to restrict the AV region via the BMP signaling pathway (Smith et al. 2009), as well as mir23 (Lagendijk et al. 2011). Wnt signaling is also required for cardiac valve development (Hurlstone et al. 2003) and the specification of the mesenchymal, interstitial valve cells (Moro et al. 2012). Ectopic activation of Wnt results in ectopic Has2 expression and defects in valve morphogenesis. Finally,

fibronectin synthesis has been shown to be flow dependent and downstream of Klf2a, coupling the mechanosensory system to ECM composition (Steed et al. 2016).

8.4 Lymphangiogenesis

The lymphatic system is a second vascular system, structurally and functionally related with the blood vascular system. Lymphatic vessels derive from preexisting vessels via a dynamic process, termed lymphangiogenesis. Lymphatic vasculature is necessary for the maintenance of tissue fluid homeostasis, fat absorption, and normal immune surveillance (Tammela and Alitalo 2010) and also plays an important role in the existence and development of many pathological conditions including cancer metastasis, lymphedema, and chronic inflammation (Saaristo et al. 2002; Yaniv et al. 2006; Schulte-Merker et al. 2011; Alitalo 2011). Despite having such important functions, lymphangiogenesis has been less studied compared to angiogenesis, mainly because of the difficulty in identifying and visualizing lymphatic vessels in vivo. However, the identification of several transcription factors and markers, which highlight the lymphatic endothelium, has contributed to a better understanding of lymphatic vessel formation. These molecular tools have helped to give answers to many questions regarding lymphatic vessel formation and the origin of the first lymphatic endothelial cells. The mechanism underlying the development of lymphatic vascular system revealed many morphological and molecular features that are common between higher organisms (Yaniv et al. 2006; Semo et al. 2016). During the last years, forward genetic analysis, high-resolution in vivo imaging, and availability of specific transgenic lines for lymphatic endothelial cells highlighted zebrafish as an excellent model organism for studying lymphangiogenesis.

Analysis of *Prox1* gene (prospero-related homeobox gene 1), an essential marker for proper lymphatic system development (Wigle and Oliver 1999), elucidated the dual origin of lymphatic vessels in *Xenopus* tadpole and chick embryo (Ny et al. 2005; Wilting et al. 2006). The early lymphatic development consists of two main processes: commitment of cells in a lymphatic fate and formation of lymph sacs from migrating lymphatic progenitors. In zebrafish, the first specified lymphatic progenitors are detected between 24 and 36 hpf in the PCV. These Prox1-positive cells, known as parachordal lymphangioblasts (PLs), sprout from PCV at around 36 hpf, migrate dorsally, and align along the myoseptum giving rise to parachordal vessels (PACs) (Yaniv et al. 2006; Gore et al. 2012; Koltowska et al. 2015). Just after that lymphangioblasts, which are now referred as lymphatic endothelial cells (LECs), start to migrate dorsally or ventrally along the arterial intersegmental vessels in order to form a fully lymphatic network (Yaniv et al. 2006). Dorsal migration of lymphatic prosecutors depends on the specific guidance of arterial intersegmental vessel, while deletion of aISVs sprouting has a negative effect in dorsal LEC sprouting (Bussmann et al. 2010). At approximately 4 days post fertilization (dpf), LECs remodel three distinct types of vessels: the thoracic duct (TD) that runs between the dorsal aorta and the posterior cardinal vein (PCV), the intersegmental lymphatic vessels (ISLVs) which connects the TD to the dorsal longitudinal lymphatic vessel, and the dorsal

longitudinal lymphatic vessel (DLLV) (Hogan et al. 2009; Koltowska et al. 2013). Using in vivo imaging and photoconvertible lineage tracing tools during zebrafish development, a specialized population of angioblasts, within the PCV which are not fully differentiated and give rise to the PACs, was characterized, and Wnt5b was identified as a major inducer of LEC specification (Nicenboim et al. 2015).

The basic molecular mechanisms regulating the development of lymphatic system are highly similar between vertebrates. *Lyve1* (lymphatic vessel endothelial hyaluronan receptor 1) is a specific marker for LECs (Banerji et al. 1999), and its early expression indicates the begging of lymphatic formation (Wigle et al. 2002; Okuda et al. 2012). Further studies in mice suggest that the biased expression of transcription factor Sox18 is necessary for the induction of prospero-related homeobox gene 1 (*Prox1*). *Prox1* is required for specification of LEC progenitors at the venous endothelial cells (Wigle et al. 2002; François et al. 2008), and lack of *Prox1* in blood vessels leads to lymphatic hypoplasia (Srinivasan et al. 2007). Recent studies demonstrate that expression of Prox1 in zebrafish trunk is Vegfc/Flt4-dependent (Koltowska et al. 2015; Shin et al. 2017), while in facial lymphatic network, deletion of Flt4 signaling does not influence Prox1 induction (Shin et al. 2017), suggesting that facial and trunk lymphangiogenesis is regulated by different signaling pathways. Vascular endothelial growth factor (VEGF) appears to be the major regulator of these processes during lymphatic development. VEGFC/VEGFR-3 (Flt4) signaling induces the proliferation and budding of the Prox1-positive LEC progenitors and promotes their migration and survival, leading to the formation of the lymph sacs. Loss of *vegfc* and also loss of *vegfr3* result in failure of secondary lymphatic sprouting and thoracic duct formation (Küchler et al. 2006; Yaniv et al. 2006), without affecting blood vessel sprouting (Le Guen et al. 2014). Recent evidence supports that ERK act downstream of Vegfc/Flt4 signaling and its activation is necessary for the early steps in lymphatic formation (Shin et al. 2017). Additionally, collagen and calcium-binding EGF domain 1 (CCBE1) protein interact with both *vegfc* and *vegfr3* playing an essential role in lymphatic development (Hogan et al. 2009; Le Guen et al. 2014). CCBE1 orthologs are highly conserved between zebrafish, mice, and humans, and mutations in CCBE1 are associated with Hennekam syndrome (generalized lymphatic dysplasia) and lymphedema (Alders et al. 2009; Connell et al. 2010). *Ccbe1* morpholino injection in zebrafish transgenic line (hsp70l:GAL4; UAS:vegfc), which produces hyperbranched intersegmental vessels, blocked the enormous venous sprouting. Ccbe1 suppresses the Vegfc- and Vegfr3-driven venous phenotype, implying that it is a fundamental component of the Vegfc/Vegfr3 pathway in the embryo (Le Guen et al. 2014).

8.5 Retinal Angiogenesis

Functional damage of existing blood vessels and formation of new blood vessels in the adult retina constitute the main irreversible causes of blindness at all ages. Diabetic retinopathy (DR), age-related macular degeneration (AMD), and retinopathy of

prematurity (ROP), a major cause of acquired blindness at young ages, are the most known ocular diseases caused by inappropriate development of new blood vessels, a process called neovascularization (Frank 2004; Jager et al. 2008; Chen et al. 2011). Therapeutic perspectives for retinal diseases focus on the development of compounds that inhibit ocular neovascularization. The growing number of patients with ocular disorders emphasizes the imperative need to extend our understanding of blood vessel growth and pathological neovascularization in the retina. Thus, development of animal models with clinically relevant retinopathies, suitable for drug screening and validating antiangiogenic therapy, could offer important clinical improvements.

The retinal vasculature network of zebrafish has many common morphological features with human retinal vasculature, and numerous genetic approaches, as well as pharmacological screens, have been conducted in order to identify the molecular mechanisms of the hyaloid and retinal vasculature in development and disease (Alvarez et al. 2007). Development of clinically relevant and hypoxia-induced retinopathy zebrafish models gave rise to understanding the mechanisms of hypoxia-induced angiogenesis in vivo, to study vascular remodeling and vessel formation under pathological conditions correlating the vascular changes with disease development (Cao et al. 2010). The retina is a highly metabolically active organ that demands substantial oxygen and nutrients. Normal retinal development depends on nourishment by a vascular network. In zebrafish, there are two distinct vascular networks: the hyaloid vasculature, located at the anterior of the eye, between the retina and lens, and the choroidal, located at the posterior of the eye, surrounding the optic cup (Saint-Geniez and D'amore 2004).

The generation of specific transgenic fish lines, such as the *Tg(fli1a:EGFP)* and *Tg(kdrl:EGFP),* had a major impact on the characterization of the hyaloid retinal vasculature development. Data from live imaging studies suggest that hyaloid formation occurs in three distinct steps. During the first step, around 48 hpf, endothelial precursor cells are present between the lens and the retina, giving rise to the hyaloid loop at the posterior of the lens. In the second step, the newly formed hyaloid system develops into a primary vasculature hyaloid network which is tightly attached to the lens. Throughout the last step, a progressive reduction in hyaloid network branches takes place, vessels are organized in a hemispherical basket, and finally the system becomes fully enclosed. Around 19 dpf an intricate network has formed. Detailed in vivo analysis showed that over time, thin junctions between hyaloid vessels increased significantly in width, the connections break, and the two vessels remain separated, reducing the complexity of the network (Alvarez et al. 2007; Hartsock et al. 2014). Choroidal vasculature, on the other hand, is not as extensively studied. The choroidal system is necessary to provide blood supplies to the superficial part of the eye during development. During the first 2 days of embryo's life, a simple and highly stereotypic array of vessels develops on the surface of the eye, so-called superficial system (Isogai et al. 2001; Alvarez et al. 2007). The superficial system consists of the nasal radial vessel (NRV), the dorsal radial vessel (DRV), and ventral radial vessel (VRV) (Kitambi et al. 2009). This system is formed by angiogenesis sprouting progressed from a venous origin, finally leading to the development of choroidal vasculature at 9 dpf (Kitambi et al. 2009; Kaufman

et al. 2015). Recent data showed that nasal radial vessel upregulates Notch pathway activity, suggesting that these vessels have arterial identity (Kaufman et al. 2015).

Numerous factors are involved in developmental and pathological changes in vascular formation, with VEGF being the most studied over the years. VEGF is crucial for the survival of blood vessels during maturation and remodeling formation (Benjamin et al. 1999). VEGF-A guides filopodia extension from endothelial cell, controlling angiogenic sprouting in zebrafish embryo retinal system (Shui et al. 2003). In 1995, Alon et al. showed that VEGF is necessary for the protection of retinal vessels under hyperoxia conditions (Alon et al. 1995), but later studies found that VEGF is also the primary molecule responsible for abnormalities in the retina caused by several diseases (Gerhardt et al. 2003; Cao et al. 2008). The proangiogenic activity of VEGF in proliferative retinopathies has led to the development of alternative approaches in retinovascular therapies (Cai et al. 2012; Kwong and Mohamed 2014). However, therapies with anti-VEGF agents and blockers target only one part of the complex mechanism of angiogenesis. Thus, new approaches have been established to identify novel antiangiogenic strategies for other angiogenesis-regulated pathways (Ferrara and Kerbel 2005; Rezzola et al. 2016). In hypoxia, HIF upregulates VEGF transcription, but hypoxia-inducible expression of the Flt-1 receptor and posttranscriptional regulation of the Kdr receptor lead to inhibition of VEGF action (Pugh and Ratcliffe 2003). Several different compounds that cause either decrease or loss of retinal vessels or induction of length widening have been identified (Kitambi et al. 2009). Many of these drugs appear to affect hyaloid-retinal angiogenesis without having any impact on the vasculature of the trunk, implying the heterogeneity in the molecular mechanisms under angiogenesis. Studies with *Tg(fli1:EGFP)* zebrafish embryos show that SU5416, a tyrosine kinase VEGFR2 inhibitor, affects only hyaloid-retinal angiogenesis, and the LY294002, a broad-spectrum inhibitor of phosphoinositide 3-kinases (PI3K), is a selective inhibitor of intraocular angiogenesis, regulating retinal morphology and visual function in zebrafish embryos (Alvarez et al. 2009). Additionally, in vivo analysis demonstrated that several molecules, such as *laminin alpha 1,* are required specifically for hyaloid and retinal vascular development, while syndecan 2, plexin D1, and others are required for vascular development in general, including hyaloid (Alvarez et al. 2007). Recently, screening of chemical libraries for specific inhibition of HV angiogenesis identified that vitamin D receptor agonists act via the induction of miRNA der-miR-21 (Merrigan and Kennedy 2017).

8.6 Cancer Angiogenesis

In many neoplastic abnormalities, angiogenesis is required for the formation and the extensions of new vessels. In cancer, angiogenesis occurs to provide nutrients and oxygen supplies to the growing tumor. Thus, tumor angiogenesis is essential for the growth of primary tumors and metastasis (Ellis et al. 2001; Nishida et al. 2006). Neovascularization, in both physiological and tumor angiogenesis, depends on a network of regulating mechanisms, including VEGF, FGF, TGF-α, and matrix

metalloproteinases (MMPs). Angiogenic factors can be produced and secreted by the tumor cells as well as by the surrounding cells (Hanahan and Folkman 1996; Rosen 2002). Considering the importance of angiogenic inducers in the growth and spread of tumors, new therapeutic opportunities opened in the field of neoplastic vascularization (Folkman 1971; Ferrara and Alitalo 1999; Crawford and Ferrara 2009). Inhibition of angiogenesis is one of the possible effective therapeutic choices, as already proven by its application in various types of cancer and macular degeneration (Yoo and Kwon 2013). Several antiangiogenic molecules have been tested as anticancer agents, with VEGF signaling being the most common drug target (Crawford and Ferrara 2009; Potente et al. 2011). Even though antiangiogenic approaches have many clinical benefits, it has been observed that treatment with VEGFR inhibitors is transient, a fraction of patients are refractory, and in some cases their condition seems to deteriorate or the tumor becomes resistant to drugs (Bergers and Hanahan 2008; Goel et al. 2011; Giuliano and Pagès 2013). These data demonstrate that there is a constant need for identification of new targets for the development of drugs that could increase the effectiveness of the existing antiangiogenic approaches.

Zebrafish has emerged as a novel model in cancer research, offering several advantages compared to other vertebrate models. These include the feasibility of xenotransplantations, the generation of transgenic lines using mutant allele information from human oncogenes, in vivo imaging, and the feasibility to apply high-throughput chemical screens (White et al. 2013). Several forward genetic screens and transient or permanent gene inactivation have been used to identify genetic mutants in organs and cell types, helping to utilize fish as a promising alternative human disease model system (Lam et al. 2006). Zebrafish can spontaneously develop almost any type of neoplasms, including tumors in the testis, gut, thyroid, liver, peripheral nerve, connective tissue, and ultimobranchial gland (Spitsbergen et al. 2000; Lam et al. 2006; Feitsma and Cuppen 2008; Yen et al. 2014). Additionally, several technologies for studying cancer throughout the life of the animal similar to rodent models have been also established in fish. The tumor xenotransplantation is a major tool to trigger host angiogenesis (Jensen et al. 2009; Taylor and Zon 2009). Tumor cell engrafting can be performed at adult, juvenile, and embryonic stages, representing different advantages and disadvantages. Transplantation of primary tumor cells into an irradiated, immunocompromised adult casper or wild-type recipient can offer in vivo monitoring of tumor growth and metastasis at single-cell resolution. This provides a valuable, efficient, and low-cost system to evaluate the metastatic potential of human cancer cells (Teng et al. 2013; Heilmann et al. 2015). In this case, the use of in vivo imaging techniques, such as green fluorescent protein (GFP)-labeling, and the availability of transparent casper zebrafish allow the four dimensional analysis of single cells and readouts of cross talk between tumor cells and the "environment" of the embryo providing a quantitative analysis of tumor engraftment (White et al. 2008). Zebrafish embryos do not have a fully functional immune system, so they have the additional advantage that no xenograft rejection can occur at this stage (Taylor and Zon 2009). Thus, thousands of fish embryos can be transplanted in this way, which also can be easily used for high-throughput chemical screening approaches.

8.7 Blood-Brain Barrier

The central nervous system (CNS) has developed specific barriers for the maintenance of a stable environment. These barriers are vital for neurological functions, as they have an essential role in regulation of ionic balance, nutrient transport, and obstruction of toxic molecules. There are two types of barriers: the endothelial and the epithelial. The endothelial barrier is composed from the blood-brain barrier (BBB) and the blood-spinal cord barrier, while the choroid plexus is formed by the epithelial cells (Abbott et al. 2006; Neuwelt et al. 2008). CNS barriers have tight protein junctions blocking paracellular diffusion of water-soluble molecules but also express transporters regulating the access of molecules in the brain. Each blood-brain barrier has different classes of transporters, with BBB's transporter being the best characterized (Dejana et al. 2009). BBB disruption is associated with many CNS diseases. Although the proper function of BBB is vital, it also restricts the insertion of therapeutic compounds to the brain, being an obstacle in brain drug development. So the delivery of therapeutic compounds into the CNS for brain tumors, stroke, trauma, multiple sclerosis, and neurodegenerative disease faces an additional challenge (Erickson et al. 2007; Zlokovic 2008). Thus, there is a great need to develop new approaches using animal models to investigate in vivo the development and regulation of BBB aiming for new neurotherapeutics.

In zebrafish, BBB is established at 3 dpf and shares histological and ultrastructural characteristics with other vertebrates (Jeong et al. 2008; Bundgaard and Abbott 2008; Eliceiri et al. 2011). Several tracer molecules, including Evans blue, indocyanine green (ICG), and fluorescent dextran (Nishimura et al. 2013), and transgenic fish like Tg(l-fabp:DBP-EGFP) (Xie et al. 2010) enabled the study of BBB development in vivo. In addition, a good correlation of the permeability of small molecules between zebrafish and mice has been reported (Kim et al. 2017), indicating that new drugs can be tested also in these zebrafish models. This is very encouraging given the ability to do high-throughput screening assays in fish, as well as testing novel delivery methods that cross the BBB such as exosomes (Yang et al. 2015) or biocompatible nanogels (Kalaiarasi et al. 2016). It is therefore certain that zebrafish will also contribute to the development of CNS drugs that reach the brain.

8.8 Prospectives

In summary, zebrafish research has contributed significantly to our understanding of the development and function of the cardiovascular system. Forward genetic screens, initiated by the groups in Boston and Tubingen in the 1990s, have been pivotal in identifying the key signaling pathways that form the cardiovascular system. Similar efforts, as well as more focused forward genetic screens using transgenic lines, furthered our understanding of organogenesis. Lately zebrafish became notorious for its regenerating potential, and the cardiovascular system is not an

exception. Although the focus has been on myocardial regeneration using both surgical and genetic approaches, induction of angiogenesis is a crucial component of the regenerative response (not covered in this chapter). It is expected that the CRISPR technology in combination with the accumulation of Human Genetic Data will further boost zebrafish research. This combination will provide the ability to do knock-ins and transgenic disease models, based on human sequence information. Considering that zebrafish embryos are amenable to in vivo high-resolution imaging and high-throughput chemical screens, the zebrafish toolbox has now all the tools to accelerate the drug discovery process.

References

Abbott NJ, Rönnbäck L, Hansson E (2006) Astrocyte-endothelial interactions at the blood-brain barrier. Nat Rev Neurosci 7:41–53. https://doi.org/10.1038/nrn1824

Adams RH, Wilkinson GA, Weiss C et al (1999) Roles of ephrinB ligands and EphB receptors in cardiovascular development: demarcation of arterial/venous domains, vascular morphogenesis, and sprouting angiogenesis. Genes Dev 13:295–306

Adams RH, Diella F, Hennig S et al (2001) The cytoplasmic domain of the ligand ephrinB2 is required for vascular morphogenesis but not cranial neural crest migration. Cell 104:57–69

Alders M, Hogan BM, Gjini E et al (2009) Mutations in CCBE1 cause generalized lymph vessel dysplasia in humans. Nat Genet 41:1272–1274. https://doi.org/10.1038/ng.484

Alitalo K (2011) The lymphatic vasculature in disease. Nat Med 17:1371–1380. https://doi.org/10.1038/nm.2545

Alon T, Hemo I, Itin A et al (1995) Vascular endothelial growth factor acts as a survival factor for newly formed retinal vessels and has implications for retinopathy of prematurity. Nat Med 1:1024–1028

Alvarez Y, Cederlund ML, Cottell DC et al (2007) Genetic determinants of hyaloid and retinal vasculature in zebrafish. BMC Dev Biol 7:114. https://doi.org/10.1186/1471-213X-7-114

Alvarez Y, Astudillo O, Jensen L et al (2009) Selective Inhibition of Retinal Angiogenesis by Targeting PI3 Kinase. PLoS One 4:e7867. https://doi.org/10.1371/journal.pone.0007867

Aspalter IM, Gordon E, Dubrac A et al (2015) Alk1 and Alk5 inhibition by Nrp1 controls vascular sprouting downstream of Notch. Nat Commun 6:8264. https://doi.org/10.1038/ncomms8264

Banerji S, Ni J, Wang S-X et al (1999) LYVE-1, a new homologue of the CD44 glycoprotein, is a lymph-specific receptor for hyaluronan. J Cell Biol 144:789–801

Bartman T, Walsh EC, Wen K-K et al (2004) Early myocardial function affects endocardial cushion development in Zebrafish. PLoS Biol 2:e129. https://doi.org/10.1371/journal.pbio.0020129

Battegay EJ, Rupp J, Iruela-Arispe L et al (1994) PDGF-BB modulates endothelial proliferation and angiogenesis in vitro via PDGF beta-receptors. J Cell Biol 125:917–928

Benjamin LE, Hemo I, Keshet E (1998) A plasticity window for blood vessel remodelling is defined by pericyte coverage of the preformed endothelial network and is regulated by PDGF-B and VEGF. Dev Camb Engl 125:1591–1598

Benjamin LE, Golijanin D, Itin A et al (1999) Selective ablation of immature blood vessels in established human tumors follows vascular endothelial growth factor withdrawal. J Clin Invest 103:159–165. https://doi.org/10.1172/JCI5028

Bergametti F, Denier C, Labauge P et al (2005) Mutations within the Programmed Cell Death 10 Gene Cause Cerebral Cavernous Malformations. Am J Hum Genet 76:42–51

Bergers G, Hanahan D (2008) Modes of resistance to anti-angiogenic therapy. Nat Rev Cancer 8:592–603. https://doi.org/10.1038/nrc2442

Betz C, Lenard A, Belting H-G, Affolter M (2016) Cell behaviors and dynamics during angiogenesis. Development 143:2249–2260. https://doi.org/10.1242/dev.135616
Bundgaard M, Abbott NJ (2008) All vertebrates started out with a glial blood-brain barrier 4-500 million years ago. Glia 56:699–708. https://doi.org/10.1002/glia.20642
Bussmann J, Bos FL, Urasaki A et al (2010) Arteries provide essential guidance cues for lymphatic endothelial cells in the zebrafish trunk. Development 137:2653–2657. https://doi.org/10.1242/dev.048207
Cai X, Sezate SA, McGinnis JF (2012) Neovascularization: ocular diseases, animal models and therapies. Adv Exp Med Biol 723:245–252. https://doi.org/10.1007/978-1-4614-0631-0_32
Cao R, Jensen LDE, Söll I et al (2008) Hypoxia-induced retinal angiogenesis in Zebrafish as a model to study retinopathy. PLoS One 3:e2748. https://doi.org/10.1371/journal.pone.0002748
Cao Z, Jensen LD, Rouhi P et al (2010) Hypoxia-induced retinopathy model in adult zebrafish. Nat Protoc 5:1903–1910. https://doi.org/10.1038/nprot.2010.149
Carmeliet P, Collen D (2000) Transgenic mouse models in angiogenesis and cardiovascular disease. J Pathol 190:387–405
Cermenati S, Moleri S, Cimbro S et al (2008) Sox18 and Sox7 play redundant roles in vascular development. Blood 111:2657–2666. https://doi.org/10.1182/blood-2007-07-100412
Chen J, Stahl A, Hellstrom A, Smith LE (2011) Current update on retinopathy of prematurity: screening and treatment. Curr Opin Pediatr 23:173–178. https://doi.org/10.1097/MOP.0b013e3283423f35
Coffin JD, Poole TJ (1991) Endothelial cell origin and migration in embryonic heart and cranial blood vessel development. Anat Rec 231:383–395. https://doi.org/10.1002/ar.1092310312
Connell F, Kalidas K, Ostergaard P et al (2010) Linkage and sequence analysis indicate that CCBE1 is mutated in recessively inherited generalised lymphatic dysplasia. Hum Genet 127:231–241. https://doi.org/10.1007/s00439-009-0766-y
Corada M, Orsenigo F, Morini MF et al (2013) Sox17 is indispensable for acquisition and maintenance of arterial identity. Nat Commun 4:2609. https://doi.org/10.1038/ncomms3609
Costa G, Harrington KI, Lovegrove HE et al (2016) Asymmetric division coordinates collective cell migration in angiogenesis. Nat Cell Biol 18:1292–1301. https://doi.org/10.1038/ncb3443
Crawford Y, Ferrara N (2009) Tumor and stromal pathways mediating refractoriness/resistance to anti-angiogenic therapies. Trends Pharmacol Sci 30:624–630. https://doi.org/10.1016/j.tips.2009.09.004
Cross MJ, Claesson-Welsh L (2001) FGF and VEGF function in angiogenesis: signalling pathways, biological responses and therapeutic inhibition. Trends Pharmacol Sci 22:201–207
Dejana E, Tournier-Lasserve E, Weinstein BM (2009) The control of vascular integrity by endothelial cell junctions: molecular basis and pathological implications. Dev Cell 16:209–221. https://doi.org/10.1016/j.devcel.2009.01.004
Denier C, Goutagny S, Labauge P et al (2004) Mutations within the MGC4607 Gene Cause Cerebral Cavernous Malformations. Am J Hum Genet 74:326–337
Eliceiri BP, Gonzalez AM, Baird A (2011) Zebrafish Model of the Blood-Brain Barrier: Morphological and Permeability Studies. Methods Mol Biol Clifton NJ 686:371–378. https://doi.org/10.1007/978-1-60761-938-3_18
Ellis LM, Liu W, Ahmad SA, et al (2001) Overview of angiogenesis: biologic implications for antiangiogenic therapy. In: Seminars in oncology. Elsevier, pp 94–104
Erickson KK, Sundstrom JM, Antonetti DA (2007) Vascular permeability in ocular disease and the role of tight junctions. Angiogenesis 10:103–117. https://doi.org/10.1007/s10456-007-9067-z
Fagiani E, Christofori G (2013) Angiopoietins in angiogenesis. Cancer Lett 328:18–26. https://doi.org/10.1016/j.canlet.2012.08.018
Fajardo LF, Kwan HH, Kowalski J et al (1992) Dual role of tumor necrosis factor-alpha in angiogenesis. Am J Pathol 140:539
Feitsma H, Cuppen E (2008) Zebrafish as a Cancer Model. Mol Cancer Res 6:685–694. https://doi.org/10.1158/1541-7786.MCR-07-2167

Ferrara N, Alitalo K (1999) Clinical applications of angiogenic growth factors and their inhibitors. Nat Med 5:1359–1364. https://doi.org/10.1038/70928

Ferrara N, Davis-Smyth T (1997) The biology of vascular endothelial growth factor. Endocr Rev 18:4–25

Ferrara N, Kerbel RS (2005) Angiogenesis as a therapeutic target. Nature 438:967–974. https://doi.org/10.1038/nature04483

Folkman J (1971) Tumor angiogenesis: therapeutic implications. N Engl J Med 285:1182–1186. https://doi.org/10.1056/NEJM197111182852108

Folkman J (1995) Angiogenesis in cancer, vascular, rheumatoid and other disease. Nat Med 1:27–31

Franco CA, Jones ML, Bernabeu MO et al (2015) Dynamic endothelial cell rearrangements drive developmental vessel regression. PLoS Biol 13:e1002125. https://doi.org/10.1371/journal.pbio.1002125

François M, Caprini A, Hosking B et al (2008) Sox18 induces development of the lymphatic vasculature in mice. Nature 456:643–647. https://doi.org/10.1038/nature07391

Frank RN (2004) Diabetic retinopathy. N Engl J Med 350:48–58. https://doi.org/10.1056/NEJMra021678

Gebala V, Collins R, Geudens I et al (2016) Blood flow drives lumen formation by inverse membrane blebbing during angiogenesis in vivo. Nat Cell Biol 18:443–450. https://doi.org/10.1038/ncb3320

Gerhardt H, Golding M, Fruttiger M et al (2003) VEGF guides angiogenic sprouting utilizing endothelial tip cell filopodia. J Cell Biol 161:1163–1177. https://doi.org/10.1083/jcb.200302047

Geudens I, Herpers R, Hermans K et al (2010) Role of delta-like-4/Notch in the formation and wiring of the lymphatic network in zebrafish. Arterioscler Thromb Vasc Biol 30:1695–1702

Giuliano S, Pagès G (2013) Mechanisms of resistance to anti-angiogenesis therapies. Biochimie 95:1110–1119. https://doi.org/10.1016/j.biochi.2013.03.002

Goel S, Duda DG, Xu L et al (2011) Normalization of the vasculature for treatment of cancer and other diseases. Physiol Rev 91:1071–1121. https://doi.org/10.1152/physrev.00038.2010

Gore AV, Monzo K, Cha YR et al (2012) Vascular development in the zebrafish. Cold Spring Harb Perspect Med 2:a006684. https://doi.org/10.1101/cshperspect.a006684

Hanahan D, Folkman J (1996) Patterns and emerging mechanisms of the angiogenic switch during tumorigenesis. Cell 86:353–364

Hartsock A, Lee C, Arnold V, Gross JM (2014) In vivo analysis of hyaloid vasculature morphogenesis in zebrafish: A role for the lens in maturation and maintenance of the hyaloid. Dev Biol 394:327–339. https://doi.org/10.1016/j.ydbio.2014.07.024

Heckel E, Boselli F, Roth S et al (2015) Oscillatory flow modulates mechanosensitive klf2a expression through trpv4 and trpp2 during Heart Valve Development. Curr Biol CB 25:1354–1361. https://doi.org/10.1016/j.cub.2015.03.038

Heilmann S, Ratnakumar K, Langdon E et al (2015) A quantitative system for studying metastasis using transparent Zebrafish. Cancer Res 75:4272–4282. https://doi.org/10.1158/0008-5472.CAN-14-3319

Herbert SP, Stainier DYR (2011) Molecular control of endothelial cell behaviour during blood vessel morphogenesis. Nat Rev Mol Cell Biol 12:551–564. https://doi.org/10.1038/nrm3176

Herbert SP, Huisken J, Kim TN et al (2009) Arterial-venous segregation by selective cell sprouting: an alternative mode of blood vessel formation. Science 326:294–298. https://doi.org/10.1126/science.1178577

Hermkens DMA, van Impel A, Urasaki A et al (2015) Sox7 controls arterial specification in conjunction with hey2 and efnb2 function. Development 142:1695–1704. https://doi.org/10.1242/dev.117275

Herpers R, van de Kamp E, Duckers HJ, Schulte-Merker S (2008) Redundant roles for sox7 and sox18 in arteriovenous specification in zebrafish. Circ Res 102:12–15. https://doi.org/10.1161/CIRCRESAHA.107.166066

Hogan BM, Bussmann J, Wolburg H, Schulte-Merker S (2008) ccm1 cell autonomously regulates endothelial cellular morphogenesis and vascular tubulogenesis in zebrafish. Hum Mol Genet 17:2424–2432. https://doi.org/10.1093/hmg/ddn142

Hogan BM, Herpers R, Witte M et al (2009) Vegfc/Flt4 signalling is suppressed by Dll4 in developing zebrafish intersegmental arteries. Dev Camb Engl 136:4001–4009. https://doi.org/10.1242/dev.039990

Hove JR, Köster RW, Forouhar AS et al (2003) Intracardiac fluid forces are an essential epigenetic factor for embryonic cardiogenesis. Nature 421:172–177. https://doi.org/10.1038/nature01282

Hurlstone AFL, Haramis A-PG, Wienholds E et al (2003) The Wnt/beta-catenin pathway regulates cardiac valve formation. Nature 425:633–637. https://doi.org/10.1038/nature02028

Isogai S, Horiguchi M, Weinstein BM (2001) The vascular anatomy of the developing zebrafish: an atlas of embryonic and early larval development. Dev Biol 230:278–301. https://doi.org/10.1006/dbio.2000.9995

Isogai S, Lawson ND, Torrealday S et al (2003) Angiogenic network formation in the developing vertebrate trunk. Dev Camb Engl 130:5281–5290. https://doi.org/10.1242/dev.00733

Jager RD, Mieler WF, Miller JW (2008) Age-related macular degeneration. N Engl J Med 358:2606–2617. https://doi.org/10.1056/NEJMra0801537

Jensen LD, Cao R, Cao Y (2009) In vivo angiogenesis and lymphangiogenesis models. Curr Mol Med 9:982–991

Jeong J-Y, Kwon H-B, Ahn J-C et al (2008) Functional and developmental analysis of the blood–brain barrier in zebrafish. Brain Res Bull 75:619–628. https://doi.org/10.1016/j.brainresbull.2007.10.043

Jin S-W, Beis D, Mitchell T et al (2005) Cellular and molecular analyses of vascular tube and lumen formation in zebrafish. Development 132:5199–5209. https://doi.org/10.1242/dev.02087

Kalaiarasi S, Arjun P, Nandhagopal S et al (2016) Development of biocompatible nanogel for sustained drug release by overcoming the blood brain barrier in zebrafish model. J Appl Biomed 14:157–169. https://doi.org/10.1016/j.jab.2016.01.004

Kalogirou S, Malissovas N, Moro E et al (2014) Intracardiac flow dynamics regulate atrioventricular valve morphogenesis. Cardiovasc Res 104:49–60. https://doi.org/10.1093/cvr/cvu186

Kamei M, Brian Saunders W, Bayless KJ et al (2006) Endothelial tubes assemble from intracellular vacuoles in vivo. Nature 442:453–456. https://doi.org/10.1038/nature04923

Kanai-Azuma M, Kanai Y, Gad JM et al (2002) Depletion of definitive gut endoderm in Sox17-null mutant mice. Dev Camb Engl 129:2367–2379

Kaufman R, Weiss O, Sebbagh M et al (2015) Development and origins of Zebrafish ocular vasculature. BMC Dev Biol 15:18. https://doi.org/10.1186/s12861-015-0066-9

Kim SS, Im SH, Yang JY et al (2017) Zebrafish as a screening model for testing the permeability of blood–brain barrier to small molecules. Zebrafish 14:322–330. https://doi.org/10.1089/zeb.2016.1392

Kitambi SS, McCulloch KJ, Peterson RT, Malicki JJ (2009) Small molecule screen for compounds that affect vascular development in the zebrafish retina. Mech Dev 126:464–477. https://doi.org/10.1016/j.mod.2009.01.002

Kochhan E, Lenard A, Ellertsdottir E et al (2013) Blood flow changes coincide with cellular rearrangements during blood vessel pruning in zebrafish embryos. PLoS One 8:e75060. https://doi.org/10.1371/journal.pone.0075060

Kohli V, Schumacher JA, Desai SP et al (2013) Arterial and venous progenitors of the major axial vessels originate at distinct locations. Dev Cell 25:196–206. https://doi.org/10.1016/j.devcel.2013.03.017

Koltowska K, Betterman KL, Harvey NL, Hogan BM (2013) Getting out and about: the emergence and morphogenesis of the vertebrate lymphatic vasculature. Development 140:1857–1870. https://doi.org/10.1242/dev.089565

Koltowska K, Lagendijk AK, Pichol-Thievend C et al (2015) Vegfc regulates bipotential precursor division and Prox1 expression to promote lymphatic identity in zebrafish. Cell Rep 13:1828–1841. https://doi.org/10.1016/j.celrep.2015.10.055

Krueger J, Liu D, Scholz K et al (2011) Flt1 acts as a negative regulator of tip cell formation and branching morphogenesis in the zebrafish embryo. Dev Camb Engl 138:2111–2120. https://doi.org/10.1242/dev.063933

Küchler AM, Gjini E, Peterson-Maduro J et al (2006) Development of the zebrafish lymphatic system requires Vegfc signaling. Curr Biol 16:1244–1248. https://doi.org/10.1016/j.cub.2006.05.026

Kwong TQ, Mohamed M (2014) Anti-vascular endothelial growth factor therapies in ophthalmology: current use, controversies and the future: anti-vascular endothelial growth factor therapies. Br J Clin Pharmacol 78:699–706. https://doi.org/10.1111/bcp.12371

Laberge-le Couteulx S, Jung HH, Labauge P et al (1999) Truncating mutations in CCM1, encoding KRIT1, cause hereditary cavernous angiomas. Nat Genet 23:189–193. https://doi.org/10.1038/13815

Lagendijk AK, Goumans MJ, Burkhard SB, Bakkers J (2011) MicroRNA-23 restricts cardiac valve formation by inhibiting Has2 and extracellular hyaluronic acid production. Circ Res 109:649–657. https://doi.org/10.1161/CIRCRESAHA.111.247635

Lam SH, Wu YL, Vega VB et al (2006) Conservation of gene expression signatures between zebrafish and human liver tumors and tumor progression. Nat Biotechnol 24:73–75. https://doi.org/10.1038/nbt1169

Larrivée B, Prahst C, Gordon E et al (2012) ALK1 signaling inhibits angiogenesis by cooperating with the notch pathway. Dev Cell 22:489–500. https://doi.org/10.1016/j.devcel.2012.02.005

Lawson ND, Weinstein BM (2002) In vivo imaging of embryonic vascular development using transgenic zebrafish. Dev Biol 248:307–318. https://doi.org/10.1006/dbio.2002.0711

Lawson ND, Scheer N, Pham VN et al (2001) Notch signaling is required for arterial-venous differentiation during embryonic vascular development. Development 128:3675–3683

Lawson ND, Vogel AM, Weinstein BM (2002) sonic hedgehog and vascular endothelial growth factor act upstream of the Notch pathway during arterial endothelial differentiation. Dev Cell 3:127–136

Lawson ND, Mugford JW, Diamond BA, Weinstein BM (2003) phospholipase C gamma-1 is required downstream of vascular endothelial growth factor during arterial development. Genes Dev 17:1346–1351

Le Guen L, Karpanen T, Schulte D et al (2014) Ccbe1 regulates Vegfc-mediated induction of Vegfr3 signaling during embryonic lymphangiogenesis. Development 141:1239–1249. https://doi.org/10.1242/dev.100495

Mably JD, Chuang LP, Serluca FC et al (2006) Santa and valentine pattern concentric growth of cardiac myocardium in the zebrafish. Dev Camb Engl 133:3139–3146. https://doi.org/10.1242/dev.02469

Macek Jilkova Z, Lisowska J, Manet S et al (2014) CCM proteins control endothelial β1 integrin dependent response to shear stress. Biol Open 3:1228–1235. https://doi.org/10.1242/bio.201410132

Merrigan SL, Kennedy BN (2017) Vitamin D receptor agonists regulate ocular developmental angiogenesis and modulate expression of dre-miR-21 and VEGF. Br J Pharmacol 174:2636–2651. https://doi.org/10.1111/bph.13875

Mickoleit M, Schmid B, Weber M et al (2014) High-resolution reconstruction of the beating zebrafish heart. Nat Methods 11:919–922. https://doi.org/10.1038/nmeth.3037

Moro E, Ozhan-Kizil G, Mongera A et al (2012) In vivo Wnt signaling tracing through a transgenic biosensor fish reveals novel activity domains. Dev Biol 366:327–340. https://doi.org/10.1016/j.ydbio.2012.03.023

Nagasawa-Masuda A, Terai K (2016) ERK activation in endothelial cells is a novel marker during neovasculogenesis. Genes Cells 21:1164–1175. https://doi.org/10.1111/gtc.12438

Nedvetsky PI, Zhao X, Mathivet T et al (2016) cAMP-dependent protein kinase A (PKA) regulates angiogenesis by modulating tip cell behavior in a Notch-independent manner. Development 143:3582–3590. https://doi.org/10.1242/dev.134767

Neuwelt E, Abbott NJ, Abrey L et al (2008) Strategies to advance translational research into brain barriers. Lancet Neurol 7:84–96. https://doi.org/10.1016/S1474-4422(07)70326-5

Nicenboim J, Malkinson G, Lupo T et al (2015) Lymphatic vessels arise from specialized angioblasts within a venous niche. Nature 522:56–61. https://doi.org/10.1038/nature14425

Nicoli S, Standley C, Walker P et al (2010) MicroRNA-mediated integration of haemodynamics and Vegf signalling during angiogenesis. Nature 464:1196–1200. https://doi.org/10.1038/nature08889

Nishida N, Yano H, Nishida T et al (2006) Angiogenesis in Cancer. Vasc Health Risk Manag 2:213–219

Nishimura Y, Yata K, Nomoto T et al (2013) Identification of a novel indoline derivative for in vivo fluorescent imaging of blood-brain barrier disruption in animal models. ACS Chem Neurosci 4:1183–1193. https://doi.org/10.1021/cn400010t

Novodvorsky P, Chico TJA (2014) The role of the transcription factor KLF2 in vascular development and disease. Prog Mol Biol Transl Sci 124:155–188. https://doi.org/10.1016/B978-0-12-386930-2.00007-0

Ny A, Koch M, Schneider M et al (2005) A genetic Xenopus laevis tadpole model to study lymphangiogenesis. Nat Med 11:998. https://doi.org/10.1038/nm1285

Okuda KS, Astin JW, Misa JP et al (2012) lyve1 expression reveals novel lymphatic vessels and new mechanisms for lymphatic vessel development in zebrafish. Development 139:2381–2391. https://doi.org/10.1242/dev.077701

Pan B, Shen J, Cao J et al (2015) Interleukin-17 promotes angiogenesis by stimulating VEGF production of cancer cells via the STAT3/GIV signaling pathway in non-small-cell lung cancer. Sci Rep 5. https://doi.org/10.1038/srep16053

Papadimitriou E, Pantazaka E, Castana P et al (2016) Pleiotrophin and its receptor protein tyrosine phosphatase beta/zeta as regulators of angiogenesis and cancer. Biochim Biophys Acta 1866:252–265. https://doi.org/10.1016/j.bbcan.2016.09.007

Papakyriakou A, Kefalos P, Sarantis P et al (2014) A zebrafish in vivo phenotypic assay to identify 3-aminothiophene-2-carboxylic acid-based angiogenesis inhibitors. Assay Drug Dev Technol 12:527–535. https://doi.org/10.1089/adt.2014.606

Pendeville H, Winandy M, Manfroid I et al (2008) Zebrafish Sox7 and Sox18 function together to control arterial-venous identity. Dev Biol 317:405–416. https://doi.org/10.1016/j.ydbio.2008.01.028

Peshkovsky C, Totong R, Yelon D (2011) Dependence of cardiac trabeculation on neuregulin signaling and blood flow in zebrafish. Dev Dyn 240:446–456. https://doi.org/10.1002/dvdy.22526

Pestel J, Ramadass R, Gauvrit S et al (2016) Real-time 3D visualization of cellular rearrangements during cardiac valve formation. Development 143:2217–2227. https://doi.org/10.1242/dev.133272

Potente M, Gerhardt H, Carmeliet P (2011) Basic and therapeutic aspects of angiogenesis. Cell 146:873–887. https://doi.org/10.1016/j.cell.2011.08.039

Pugh CW, Ratcliffe PJ (2003) Regulation of angiogenesis by hypoxia: role of the HIF system. Nat Med 9:677–684. https://doi.org/10.1038/nm0603-677

Quillien A, Moore JC, Shin M et al (2014) Distinct Notch signaling outputs pattern the developing arterial system. Dev Camb Engl 141:1544–1552. https://doi.org/10.1242/dev.099986

Renz M, Otten C, Faurobert E et al (2015) Regulation of β1 integrin-Klf2-mediated angiogenesis by CCM proteins. Dev Cell 32:181–190. https://doi.org/10.1016/j.devcel.2014.12.016

Rezzola S, Paganini G, Semeraro F et al (2016) Zebrafish (Danio rerio) embryo as a platform for the identification of novel angiogenesis inhibitors of retinal vascular diseases. Biochim Biophys Acta (BBA) – Mol Basis Dis 1862:1291–1296. https://doi.org/10.1016/j.bbadis.2016.04.009

Risau W (1997) Mechanisms of angiogenesis. Nature 386:671–674. https://doi.org/10.1038/386671a0

Risau W, Flamme I (1995) Vasculogenesis. Annu Rev Cell Dev Biol 11:73–91. https://doi.org/10.1146/annurev.cb.11.110195.000445

Rosen LS (2002) Clinical experience with angiogenesis signaling inhibitors: focus on vascular endothelial growth factor (VEGF) blockers. Cancer Control J Moffitt Cancer Cent 9:36–44
Saaristo A, Karkkainen MJ, Alitalo K (2002) Insights into the molecular pathogenesis and targeted treatment of lymphedema. Ann N Y Acad Sci 979:94–110
Sacilotto N, Monteiro R, Fritzsche M et al (2013) Analysis of Dll4 regulation reveals a combinatorial role for Sox and Notch in arterial development. Proc Natl Acad Sci 110:11893–11898. https://doi.org/10.1073/pnas.1300805110
Saint-Geniez M, D'amore PA (2004) Development and pathology of the hyaloid, choroidal and retinal vasculature. Int J Dev Biol 48:1045–1058. https://doi.org/10.1387/ijdb.041895ms
Sauteur L, Krudewig A, Herwig L et al (2014) Cdh5/VE-cadherin promotes endothelial cell interface elongation via cortical actin polymerization during angiogenic sprouting. Cell Rep 9:504–513. https://doi.org/10.1016/j.celrep.2014.09.024
Schulte-Merker S, Sabine A, Petrova TV (2011) Lymphatic vascular morphogenesis in development, physiology, and disease. J Cell Biol 193:607–618. https://doi.org/10.1083/jcb.201012094
Seghezzi G, Patel S, Ren CJ et al (1998) Fibroblast Growth Factor-2 (FGF-2) induces Vascular Endothelial Growth Factor (VEGF) expression in the endothelial cells of forming capillaries: an autocrine mechanism contributing to angiogenesis. J Cell Biol 141:1659–1673
Semo J, Nicenboim J, Yaniv K (2016) Development of the lymphatic system: new questions and paradigms. Development 143:924–935. https://doi.org/10.1242/dev.132431
Serbedzija GN, Flynn E, Willett CE (1999) Zebrafish angiogenesis: a new model for drug screening. Angiogenesis 3:353–359
Shin M, Beane TJ, Quillien A et al (2016) Vegfa signals through ERK to promote angiogenesis, but not artery differentiation. Development 143:3796–3805. https://doi.org/10.1242/dev.137919
Shin M, Male I, Beane TJ et al (2017) Correction: Vegfc acts through ERK to induce sprouting and differentiation of trunk lymphatic progenitors. Development 144:531–531. https://doi.org/10.1242/dev.148569
Shui Y-B, Wang X, Hu JS et al (2003) Vascular endothelial growth factor expression and signaling in the lens. Investig opthalmology. Vis Sci 44:3911. https://doi.org/10.1167/iovs.02-1226
Siekmann AF, Lawson ND (2007) Notch signalling limits angiogenic cell behaviour in developing zebrafish arteries. Nature 445:781–784. https://doi.org/10.1038/nature05577
Smith KA, Joziasse IC, Chocron S et al (2009) Dominant-negative *ALK2* allele associates with congenital heart defects. Circulation 119:3062–3069. https://doi.org/10.1161/CIRCULATIONAHA.108.843714
Spitsbergen JM, Tsai HW, Reddy A et al (2000) Neoplasia in zebrafish (Danio rerio) treated with N-methyl-N'-nitro-N-nitrosoguanidine by three exposure routes at different developmental stages. Toxicol Pathol 28:716–725. https://doi.org/10.1177/019262330002800512
Srinivasan RS, Dillard ME, Lagutin OV et al (2007) Lineage tracing demonstrates the venous origin of the mammalian lymphatic vasculature. Genes Amp Dev 21:2422–2432. https://doi.org/10.1101/gad.1588407
Stainier DY, Weinstein BM, Detrich H 3rd et al (1995) Cloche, an early acting zebrafish gene, is required by both the endothelial and hematopoietic lineages. Development 121:3141–3150
Steed E, Faggianelli N, Roth S et al (2016) *klf2a* couples mechanotransduction and zebrafish valve morphogenesis through fibronectin synthesis. Nat Commun 7:11646. https://doi.org/10.1038/ncomms11646
Swift MR, Weinstein BM (2009) Arterial-venous specification during development. Circ Res 104:576–588. https://doi.org/10.1161/CIRCRESAHA.108.188805
Tammela T, Alitalo K (2010) Lymphangiogenesis: molecular mechanisms and future promise. Cell 140:460–476. https://doi.org/10.1016/j.cell.2010.01.045
Taylor AM, Zon LI (2009) Zebrafish tumor assays: the state of transplantation. Zebrafish 6:339–346. https://doi.org/10.1089/zeb.2009.0607
Teng Y, Xie X, Walker S et al (2013) Evaluating human cancer cell metastasis in zebrafish. BMC Cancer 13:453. https://doi.org/10.1186/1471-2407-13-453

van den Driesche S, Mummery CL, Westermann CJ (2003) Hereditary hemorrhagic telangiectasia: an update on transforming growth factor β signaling in vasculogenesis and angiogenesis. Cardiovasc Res 58:20–31

Vermot J, Forouhar AS, Liebling M et al (2009) Reversing Blood Flows Act through klf2a to ensure normal valvulogenesis in the developing heart. PLoS Biol 7:e1000246. https://doi.org/10.1371/journal.pbio.1000246

Wang HU, Chen Z-F, Anderson DJ (1998) Molecular distinction and angiogenic interaction between embryonic arteries and veins revealed by ephrin-B2 and its receptor Eph-B4. Cell 93:741–753

Weinstein BM (1999) What guides early embryonic blood vessel formation? Dev Dyn 215:2–11. https://doi.org/10.1002/(SICI)1097-0177(199905)215:1<2::AID-DVDY2>3.0.CO;2-U

Weinstein BM (2002) Vascular cell biology in vivo: a new piscine paradigm? Trends Cell Biol 12:439–445

White RM, Sessa A, Burke C et al (2008) Transparent adult zebrafish as a tool for in vivo transplantation analysis. Cell Stem Cell 2:183–189. https://doi.org/10.1016/j.stem.2007.11.002

White R, Rose K, Zon L (2013) Zebrafish cancer: the state of the art and the path forward. Nat Rev Cancer 13:624–636. https://doi.org/10.1038/nrc3589

Wigle JT, Oliver G (1999) Prox1 function is required for the development of the murine lymphatic system. Cell 98:769–778

Wigle JT, Harvey N, Detmar M et al (2002) An essential role for Prox1 in the induction of the lymphatic endothelial cell phenotype. EMBO J 21:1505–1513

Wilting J, Aref Y, Huang R et al (2006) Dual origin of avian lymphatics. Dev Biol 292:165–173. https://doi.org/10.1016/j.ydbio.2005.12.043

Xie J, Farage E, Sugimoto M, Anand-Apte B (2010) A novel transgenic zebrafish model for blood-brain and blood-retinal barrier development. BMC Dev Biol 10:76. https://doi.org/10.1186/1471-213X-10-76

Yang B, Kang H, Fung A et al (2014) The role of interleukin 17 in tumour proliferation, angiogenesis, and metastasis. Mediat Inflamm 2014:1–12. https://doi.org/10.1155/2014/623759

Yang T, Martin P, Fogarty B et al (2015) Exosome delivered anticancer drugs across the blood-brain barrier for brain cancer therapy in Danio rerio. Pharm Res 32:2003–2014. https://doi.org/10.1007/s11095-014-1593-y

Yaniv K, Isogai S, Castranova D et al (2006) Live imaging of lymphatic development in the zebrafish. Nat Med 12:711–716. https://doi.org/10.1038/nm1427

Yen J, White RM, Stemple DL (2014) Zebrafish models of cancer: progress and future challenges. Curr Opin Genet Dev 24:38–45. https://doi.org/10.1016/j.gde.2013.11.003

Yoo SY, Kwon SM (2013) Angiogenesis and its therapeutic opportunities. Mediat Inflamm 2013:127170. https://doi.org/10.1155/2013/127170

Yoruk B, Gillers BS, Chi NC, Scott IC (2012) Ccm3 functions in a manner distinct from Ccm1 and Ccm2 in a zebrafish model of CCM vascular disease. Dev Biol 362:121–131. https://doi.org/10.1016/j.ydbio.2011.12.006

Zhong TP, Rosenberg M, Mohideen MA et al (2000) gridlock, an HLH gene required for assembly of the aorta in zebrafish. Science 287:1820–1824

Zhou Z, Rawnsley DR, Goddard LM et al (2015) The cerebral cavernous malformation pathway controls cardiac development via regulation of endocardial MEKK3 signaling and KLF expression. Dev Cell 32:168–180. https://doi.org/10.1016/j.devcel.2014.12.009

Zlokovic BV (2008) The blood-brain barrier in health and chronic neurodegenerative disorders. Neuron 57:178–201. https://doi.org/10.1016/j.neuron.2008.01.003

Chapter 9
Advances in the Understanding of Skeletal Myopathies from Zebrafish Models

Emily Claire Baxter and Robert J. Bryson-Richardson

Abstract Skeletal muscle diseases, or myopathies, are a diverse group of disorders that range in severity from mild muscle weakness to lethality and in onset from in utero to late adulthood. Whilst in some cases the genetic basis of these diseases is known, understanding of the mechanism underlying muscle weakness is often lacking, and there are no effective treatments for these diseases. Zebrafish (*Danio rerio)* are well established as a model system and offer many advantages in terms of time, cost and ease of experimental manipulation, and in vivo tracking of pathology, for the study of muscle. Both the process of muscle development and muscle function are highly conserved throughout evolution, and, as such, zebrafish muscle has remarkable structural and molecular similarities to that of human and is highly suited to the investigation of skeletal myopathies.

Zebrafish models have been widely applied to the evaluation of potential myopathy disease variants, meeting a growing need for rapid functional analysis given the increasing application of high-throughput sequencing. Many of the models that have been generated, across the range of myopathy subtypes, have been characterised in detail and present pathologies that are strikingly similar to those observed in patients. Research using these models has resulted in significant contributions to our understanding of disease biology and has identified potential therapies. Here we provide a review of zebrafish skeletal myopathy models, detail the advances they have made to the field and highlight areas where they are poised to significantly contribute in the future.

Keywords Zebrafish · Myopathy · Muscular dystrophy · Drug screening · Model organism · Muscle · Treatment

E. C. Baxter · R. J. Bryson-Richardson (✉)
School of Biological Sciences, Monash University, Melbourne, Australia
e-mail: emily.baxter@monash.edu; robert.bryson-richardson@monash.edu

H. Hirata, A. Iida (eds.), *Zebrafish, Medaka, and Other Small Fishes*,
https://doi.org/10.1007/978-981-13-1879-5_9

9.1 Introduction

Myopathies are diseases of muscle and are known to be caused by mutations in many genes or triggered by an environmental stimulus. Norwood et al. (2009) surveyed 1105 cases of myopathies in Northern England and found that Duchenne muscular dystrophy (DMD) was the most prevalent affecting approximately 1 in 12,000 individuals. However, when the prevalence of heritable myopathies was summed together, they affect approximately 1 in 2000 individuals, and, with the addition of acquired myopathies, the total prevalence was estimated as 1 in 1150. As a point of reference, it is currently estimated that 1 in 2000 people will be diagnosed with melanoma skin cancer (Australian Institute of Health and Welfare (AIHW) 2017b) and 1 in 1560 with breast cancer (AIHW 2017a) in 2017 in Australia. Therefore, although subtypes may be rare, myopathies as a group are not.

Zebrafish (*Danio rerio*) are well established as a good model organism for the study of human development and disease. In addition to the rapid external development, high fecundity, optical transparency and wide range of genetic tools available, zebrafish have a number of significant advantages for myopathy research. Skeletal muscle makes up a considerable portion of the zebrafish trunk and has an exceptionally high degree of similarity to human muscle both molecularly and histologically. The disruption of muscle structure can be easily, and noninvasively, assessed via a birefringence assay, which examines changes in the polarity of light as it travels through the highly ordered muscle structure. Zebrafish can also readily absorb drugs added to their water and have been successfully utilised for large-scale drug screens (Kawahara et al. 2011a, 2014; Waugh et al. 2014). Finally, it is possible to assess muscle function through analysis of swimming performance (Sztal et al. 2016).

The first zebrafish model for skeletal muscle disease was described by Parsons et al. (2002) who used a morpholino oligonucleotide (MO) to knock-down dystroglycan which caused a muscular dystrophy phenotype. In the following year, Bassett et al. (2003) established the first zebrafish mutant as a model for skeletal muscle disease: the *sapje*^{t222a} (herein referred to as *sap*) mutant as a model for DMD. Since the discovery of *sap*, zebrafish studies have led to many valuable insights in relation to the cause of muscle disease, disease progression and potential treatments. Whilst the largest volume of skeletal myopathy research utilising zebrafish is in relation to DMD, there have also been significant advances in our understanding regarding a wide range of other muscle diseases, as detailed below.

9.2 Muscular Dystrophies

9.2.1 Dystrophinopathies

The initial zebrafish model for DMD, *sap*, provided the first in vivo evidence of fibre attachment failure in a dystrophin-deficient vertebrate organism (Bassett et al. 2003). Analysis of the *sap* mutant also demonstrated loss of integrity of the sarcolemma

and cell death prior to detachment (Bassett et al. 2003). Since the discovery of *sap*, additional mutant lines (Guyon et al. 2009; Berger et al. 2011), MO and siRNA knock-down (Bassett et al. 2003; Guyon et al. 2003; Dodd et al. 2004; Johnson et al. 2013) and endogenous gene tagging (Ruf-Zamojski et al. 2015) approaches have been employed to model DMD. The latter mentioned gene tag line is a recently established DMD model, and in vivo analysis has revealed spatio-temporal differences between *dmd* mRNA and dmd protein localisation during embryogenesis (Ruf-Zamojski et al. 2015). The dmd protein localises to the myosepta from the onset of its expression at 18 hours-post-fertilisation (hpf), but *dmd* mRNA is not predominately concentrated at the myosepta until 22.5 hpf (Ruf-Zamojski et al. 2015). There appears to be some delay between activation of transcription and presence of mature protein; however, the localisation of dmd protein to the myosepta coincides with the onset of myotube differentiation (Ruf-Zamojski et al. 2015). This gene tag line has since been studied with improved fluorescence recovery after photo-bleaching (FRAP) analysis to reveal that there are in fact three populations of dystrophin in skeletal muscle (Bajanca et al. 2015). There is an enduring, tightly bound membrane population that exists at muscle fibre tips, a smaller population of cytoplasmic dystrophin, and a pool of dystrophin that can be exchanged between membrane-bound and cytoplasmic populations rapidly (Bajanca et al. 2015).

In addition to increasing understanding that defects in dystrophin primarily cause, the effect on secondary signalling pathways has also been investigated in the zebrafish. Alexander et al. (2013) identified microRNAs (miRNAs) that are uniquely dysregulated in dystrophic muscle, which they later demonstrated in both mice and human muscle biopsies. One of the miRNAs they identified, miR-199a-5p, is induced in dystrophic muscle, and its overexpression in zebrafish resembles some of the features of s*ap*: disruption of myofibres, pericardial oedema and premature death (Alexander et al. 2013). With the increase of miR-199a-5p expression, there was a reciprocal decrease in WNT-signalling factors: WNT2, FZD4 and JAG1 (Alexander et al. 2013). These genes had previously been determined to be important in myogenic cell proliferation and differentiation (Polesskaya et al. 2003; Kozopas and Nusse 2002; Wang et al. 2007; Lindsell et al. 1995; Gnocchi et al. 2009), and it was therefore proposed that induction of miR-199a-5p in dystrophic muscle causes suppression of WNT-signalling factors and thus affects proliferation and differentiation (Alexander et al. 2013).

There has been substantial research into the discovery and evaluation of DMD therapies using the *sap* model. From two large-scale screens, Kawahara et al. identified 15 drugs capable of improving muscle structure in dystrophin-null fish (Kawahara et al. 2011a, 2014). The drug aminophylline, most commonly used to treat lung diseases, was highlighted in particular as it was able to increase survival of *sap* fish when treatment commenced after the onset of the skeletal muscle phenotype at 4dpf (Kawahara et al. 2011a). Aminophylline is a non-selective phosphodiesterase (PDE) inhibitor which causes activation of the PKA pathway, and PKA phosphorylation of calcium channels is essential for excitation-contraction coupling (Reiken et al. 2003). Selective PDE4 and PDE5 inhibitors are also effective in *sap* (Kawahara et al. 2011a) and the latter in the *mdx* mouse as well (Asai et al. 2007; Khairallah et al. 2008; Kobayashi et al. 2008). Unfortunately, although earlier stage

testing showed promise (Nelson et al. 2014; Martin et al. 2012), the most recent phase 3 clinical trials for use of PDE5 inhibitors have been discontinued as patients failed to show significant improvements (ClinicalTrials.gov identifier: NCT01865084; Guiraud and Davies 2017). Another screen carried out by Waugh et al. (2014) identified four drugs, ergotamine, pergolide, fluoxetine and ropinirole, all monoamine agonists, also capable of reducing abnormal birefringence in *sap*. Fluoxetine was further examined as it caused the greatest reduction and this led Waugh et al. (2014) to propose it improves membrane integrity related to calcium homeostasis; however, it is unable to completely restore stability and only yields positive results when commenced presymptomatically. Although the results of these screens have not translated into therapies as yet, they have demonstrated the capacity of zebrafish for drug screening and have provided leads for further research.

Zebrafish DMD models have also been used to evaluate therapeutic exon-skipping strategies (Berger et al. 2011), read-through of stop codons via ataluren (Li et al. 2014) and dasatinib treatment (Lipscomb et al. 2016). Given that large regions of dystrophin may be deleted with the function remaining largely intact, it was proposed that the mutation-harbouring exons could be skipped to restore functional dystrophin in patients (Hoffman et al. 1988; Klein et al. 1992; Harper et al. 2002; Aartsma-Rus et al. 2009). It has been estimated that between 60% and 83% of DMD patients may benefit from skipping of either a single or multiple exons (Aartsma-Rus et al. 2009; Flanigan et al. 2009). Berger et al. (2011) used a zebrafish *dmd* model to determine that restoration of dystrophin to 30–40% of the normal level was needed to rescue the DMD pathology, but benefits were observed from 10% to 20% restoration. Recently one drug that induces skipping of dystrophin exon 51, eteplirsen, was FDA approved, making it the first drug specifically approved for the treatment of DMD. The clinical trial results of eteplirsen documented dystrophin levels increasing to as high as 18% in patients (Cirak et al. 2011) although the effectiveness of eteplirsen at slowing disease progression is still unclear (Lim et al. 2017). Going forward zebrafish could be used to determine the level of efficacy that may be therapeutically useful in advance of extensive clinical trials.

Ataluren (PTC124) is reported to promote read-through of premature stop codons, a treatment option that may be applicable for about 10–15% of DMD patients (Aartsma-Rus et al. 2006). Research in zebrafish has demonstrated a bell-shaped dose-dependent effect of ataluren, with negative effects at high dose, similar to those described in trials (Pichavant et al. 2011), but at the optimal dose *sap* demonstrated a significant improvement in muscle function (Li et al. 2014). Studies in mice (Welch et al. 2007) and patients (Finkel et al. 2013; Bushby et al. 2014) have similarly reported that at the optimal dose, ataluren is well tolerated, results in recovered dystrophin expression and slows the progression of DMD. A recent phase 3 clinical trial found significant improvement only in a sub-group of patients that were more functionally capable at the beginning of the study (Bushby et al. 2016). Ataluren treatment may therefore be less effective when commenced at later stages of the disease and/or become less effective as disease progresses. Both these questions could be readily and rapidly assessed in zebrafish.

The most recently investigated therapy utilising *sap* fish has involved the use of dasatinib to stabilise the dystrophin-associated glycoprotein complex (DGC) (Lipscomb et al. 2016). Loss of dystrophin has been theorised to lead to increased phosphorylation of β-dystroglycan, a major component of the DGC, causing its internalisation and degradation via the proteasome, and thus lead to loss of the DGC from the sarcolemma (Ilsley et al. 2001; James et al. 2000; Sotgia et al. 2003). Lipscomb et al. (2016) recently showed that treatment of the *sap* zebrafish with a specific Src tyrosine kinase inhibitor, dasatinib, increased the non-phosphorylated form of β-dystroglycan, resulting in a significant improvement in muscle structure and function. Mutations in other components of the DGC are also known to cause its instability and lead to muscular dystrophies, and therefore, with the exception of *dystroglycan 1* (*DAG1)* mutations, this treatment may be applicable to other muscular dystrophies.

9.2.2 Facioscapulohumeral Muscular Dystrophy

Facioscapulohumeral muscular dystrophy (FSHD) is linked to contraction of D4Z4 tandem repeats on chromosome 4 (Wijmenga et al. 1992; Deutekom et al. 1993). Initial investigation identified possible involvement of a D4Z4-localised retro-gene *DUX4* (Hewitt et al. 1994; Lyle et al. 1995); however, the level of DUX4 expression in FSHD biopsies is very low (Dixit et al. 2007; Snider et al. 2010). Zebrafish lack a DUX4 orthologue, with DUX4 present only in primates and Afrotheria (Clapp et al. 2007). However, overexpression of human *DUX4* in zebrafish, even at low levels, results in a muscular dystrophy phenotype with hallmark features of FSHD, and analysis of DUX4 deletion constructs further demonstrated that DUX4-DNA binding is required for its toxicity (Wallace et al. 2011; Mitsuhashi et al. 2013). These findings support the prior, and currently prevailing, theory that deletions of D4Z4 repeats cause insufficient epigenetic repression of *DUX4* and its expression in skeletal muscle induces aberrant gene expression culminating in FSHD (Tawil et al. 2014).

9.2.3 Limb-Girdle Muscular Dystrophy

Zebrafish have also been successfully utilised to further understanding of limb-girdle muscular dystrophies (LGMDs), a group of disorders that are estimated to be nearly as prevalent as DMD (Norwood et al. 2009). Mutations in the gene *Titin* (*TTN*) result in numerous presentations of muscle disease including LGMD (Chauveau et al. 2014). The gene encodes a protein of monumental size with numerous isoforms and key roles in striated muscle including sarcomeric scaffolding and maintenance (Chauveau et al. 2014). Zebrafish have a duplication of the *titin* gene, but mutants have been identified for both *ttna* (*herzschlag/hel*) (Myhre et al. 2014b)

and *ttnb* (*runzel/ruz*) (Steffen et al. 2007) which both show progressive myopathy. Steffen et al. (2007) showed for the first time that titin isoforms are modified throughout embryonic development and that the *ruz* mutation specifically affects particular isoforms of *ttnb*. Over time *ruz* mutants displayed an aberrant and progressive decrease of the largest *ttnb* isoform which correlated to a progressive loss of sarcomeric organisation but did not affect the capacity to undergo sarcomerogenesis. Study of *hel* mutants has since shown that truncation of *ttna* similarly allows for sarcomere assembly, but myofibril disintegration occurs with the onset of contraction (Myhre et al. 2014b). Most recently zebrafish have been used to resolve why, contrary to expectation, C-terminal mutations in *TTN* result in a more severe myopathic phenotype than N-terminal mutations (Chauveau et al. 2014; Zou et al. 2015). Zou et al. (2015) uncovered an internal promoter that produces a C-terminal isoform, *Cronos*. During zebrafish development, *Cronos* is more highly expressed in skeletal than cardiac muscle which explains why zebrafish embryos with N-terminal mutations displayed similar cardiac defects to embryos with C-terminal mutations but lacked the severe skeletal muscle phenotype (Zou et al. 2015). The internal promoter and *Cronos* isoform are also found in humans, and if levels of *Cronos* could be increased, this may therapeutically benefit titinopathy patients (Zou et al. 2015).

As described for mutations in *TTN*, mutations in titin-cap/telethonin (*TCAP*) cause LGMD but do not impact sarcomerogenesis despite the known structural role of TCAP (Zhang et al. 2009). TCAP is chiefly known for its role to 'glue' two adjacent TTN molecules together and thereby create a rigid and essential anchor for TTN filaments at the Z-disk (Zou et al. 2006). Examination of morpholino-injected zebrafish (morphants) showed for the first time that TCAP is necessary for formation of transverse tubules (T-tubules) and attachment of T-tubules to Z-disks (Zhang et al. 2009). Thus, TCAP mutations result in LGMD by disruption of sarcomere-sarcolemma interaction (Zhang et al. 2009). Defects in T-tubule formation and organisation have also been documented in LGMD patients with mutations of caveolin-3 (*CAV3*) (Minetti et al. 2002) and in corresponding zebrafish (Nixon et al. 2005) and mouse (Galbiati et al. 2001) models. In muscle, CAVIN1 associates with CAV3 to form caveolae, invaginations of the plasma membrane (Hill et al. 2008). Analysis of zebrafish *cav3* and *cavin1* morphants and fish over-expressing human $CAV3^{P104L}$ has implicated membrane fragility as a major contributor to disease pathology as fish showed sarcolemmal lesions without fibre detachment (Lo et al. 2015). Lesions of the sarcolemma can occur from mechanical stress under normal physiological conditions but are normally rapidly repaired to avoid cell death (Bansal et al. 2003; Cooper and McNeil 2015). Mutations in *dysferlin* (*DYSF*) cause LGMD and Miyoshi myopathy (Bashir et al. 1998; Liu et al. 1998) due to defective membrane repair (Bansal et al. 2003). Zebrafish studies utilising high-resolution in vivo imaging have shown that dysf is an essential, early-recruited component of membrane 'repair patches' (Roostalu and Strähle 2012) that mediates the accumulation of phosphatidylserine (PS) (Middel et al. 2016), an 'eat-me' signal for macrophages (Fadok et al. 1992). Depending on the lesion size, macrophages then facilitate removal of the repair patch, and thus restoration of membrane integrity, or

devour entire myofibres (Middel et al. 2016). A previously unrecognised arginine-rich motif in DYSF was also identified in zebrafish which matches the mutation site of some dysferlinopathy patients (Bashir et al. 1998; Liu et al. 1998), and modifications to this motif reduced DYSF and PS accumulation at the repair patch in zebrafish and human cells (Middel et al. 2016). Zebrafish have therefore contributed many significant advances to our understanding of LGMDs.

9.3 Congenital Muscular Dystrophies

9.3.1 Dystroglycanopathies

Disruption of α-dystroglycan glycosylation results in a group of myopathies, collectively termed dystroglycanopathies, with a spectrum of presentations from LGMD to severe congenital muscular dystrophy including muscle-eye-brain disease (MEB) and Walker-Warburg syndrome (WWS) (Bouchet-Séraphin et al. 2015). Mutations that cause dystroglycanopathies have been identified in 19 genes which encode glycosyltransferases or are otherwise involved in the glycosylation of α-dystroglycan and in d*ystroglycan 1 (dag1*), which encodes for both α- and ß-dystroglycan, itself (Bouchet-Séraphin et al. 2015; Osborn et al. 2017). Many of these genes have been modelled in zebrafish and recapitulate the phenotypes seen in patients, although they are generally on the more severe side of the spectrum. The zebrafish *patchytail* mutant has a missense mutation in *dag1* that causes loss of both dystroglycans (Gupta et al. 2011). At the time, mutations in *DAG1* had not been found in patients although the authors noted the similarities in the fish phenotype to MEB and WWS. Within a month of the publication, patients were identified with *DAG1* mutations that resulted in LGMD (Hara et al. 2011) and in subsequent years with MEB (Geis et al. 2013) highlighting once again the suitability of zebrafish to model myopathies and identify novel disease genes.

There are two classes of dystroglycanopathies, primary (i.e. caused by mutations in *dag1*) and secondary (i.e. caused by mutations in genes other than *dag1*). Lin et al. (2011) demonstrated that there were differences in muscle pathology between fish models of primary and secondary dystroglycanopathies. *Fukutin* (*fktn*) or *fukutin-related protein* (*fkrp*) morphants had deficient differentiation of notochord cells prior to muscle degeneration as well as ER stress and activation of the unfolded protein response, whereas *dag1* mutant and morphant models lacked these phenotypes. A shared feature among dystroglycanopathies, however, is the degeneration of muscle fibres due to detachment from the extracellular matrix (ECM) and loss of connection to adjacent fibres (Gupta et al. 2011; Osborn et al. 2017; Stevens et al. 2013; Buysse et al. 2013; Thornhill et al. 2008; Lin et al. 2011; Carss et al. 2013; Roscioli et al. 2012; Praissman et al. 2016). From the study of *patchytail* mutants, it was also identified that loss of dystroglycan causes abnormalities to T-tubules which was thought to be a primary defect as in this study, it was also found that dystrogly-

can ordinarily localises to T-tubules (Gupta et al. 2011). Recently mutations in *INPPK* were found to cause dystroglycanopathy, and this was supported by generation of zebrafish *inpp5ka* morphants which also showed T-tubule abnormalities (Wiessner et al. 2017). The contribution of T-tubule abnormalities to pathogenesis of dystroglycanopathies has yet to be further investigated. Vascular defects have also been identified in some dystroglycanopathy patients (Sugino et al. 1991; Hoang et al. 2011; Zervos et al. 2001), and from study of *dag1*, *fktn* and *fkrp* morphants, it was revealed that these defects were not a consequence of muscle damage or antecedent to it but rather a separate aspect of pathology (Wood et al. 2011). As with T-tubule abnormalities, the level to which vascular defects contribute to dystroglycanopathy remains to be determined.

9.3.2 Merosin-Deficient Congenital Muscular Dystrophy

The most common form of congenital muscular dystrophy, merosin-deficient congenital muscular dystrophy (MDC1A), is modelled by the *candyfloss* (*caf*) mutant which contains a mutation in the gene encoding the laminin alpha 2 subunit (LAMA2, formerly known as merosin) (Hall et al. 2007; Gupta et al. 2012). *caf* mutants display fibre detachment, as seen in *sap*, but unlike *sap* loss of sarcolemmal integrity is not observed (Hall et al. 2007). Laminin is composed of multiple subunits and is adhered to the ECM by the DGC (Ervasti and Campbell 1993) and integrin α7-β1 heterodimer receptor complexes (Danen and Sonnenberg 2003). Utilising *caf* zebrafish it was determined that other laminins are secreted from surrounding non-muscle tissues and localise to the fibre attachment site to reinforce attachment but cannot completely compensate for loss of lama2 (Sztal et al. 2012). Supplementation with coenzyme nicotinamide adenine dinucleotide (NAD+), or a vitamin precursor of NAD+, vitamin B3/niacin, was shown to improve laminin attachment to the basement membrane of fish with knock-down of either *dag1* or *integrin α7* (*itga7*) or both (Goody et al. 2012). This study supports increasing fibre-ECM attachment as a therapeutic avenue and documented a treatment that is cost-effective and readily available.

9.4 Congenital Myopathies

9.4.1 Centronuclear Myopathy

As is seen with mutations causing muscular dystrophies and congenital muscular dystrophies, there are multiple presentations of myopathy that can result from mutation of the same gene. Mutations in *dynamin-2* (*DNM2*), for example, cause congenital muscular dystrophy and centronuclear myopathy (CNM) (Böhm et al. 2012; Bitoun et al. 2005). In zebrafish, overexpression of human *DNM2* harbouring a mutation that causes CNM results in functional and structural abnormalities

including impairment to T-tubules and thus disruption of excitation-contraction coupling (Gibbs et al. 2013, 2014). CNMs due to mutations in other gene have also been modelled in zebrafish, including *ryanodine receptor* (*RYR1*) (Hirata et al. 2007; Jurynec et al. 2008), *selenoprotein N* (*SELENON*) (Deniziak et al. 2007; Jurynec et al. 2008), *bridging integrator 1* (*BIN1*) (Smith et al. 2014) and *myotubularin* (*MTM1*), and have similarly shown impairment of excitation-contraction coupling. Study of one of these, the *ryr1b* mutant *relatively relaxed* (*ryr*) (Hirata et al. 2007), was the first indication that oxidative stress also contributed to pathology of *RYR1*-related myopathies (Dowling et al. 2012). Oxidative stress is known to increase muscle fatigue and decreased endurance (Powers and Jackson 2008) and has been observed in cultured fibroblasts and myoblasts from *RYR1*- and *SEPN1*-related myopathy patients (Arbogast et al. 2009; Dowling et al. 2012). Treatment with an antioxidant, *N*-acetylcysteine (NAC), leads to improvements in both patient myoblasts and the in vivo zebrafish model for *RYR1*-related myopathies including reduction of structural abnormalities, functional improvement and reduced susceptibility to cell death (Dowling et al. 2012; Hirata et al. 2007). NAC is one of only a few antioxidant drugs approved for human use, and the positive functional and morphological findings in *ryr*-treated fish were cited in support of a clinical trial for NAC use in *RYR1*-related myopathies (ClinicalTrials.gov identifier: NCT02362425). Clinical trials for use of NAC in patients with *RYR1*- and *SEPN1*-related myopathy are currently underway (ClinicalTrials.gov identifiers: NCT02362425, and NCT02505087, respectively).

Study of zebrafish CNM models has also demonstrated other drugs that are useful for treatment of such diseases. From study of zebrafish *mtm1* mutants, three drugs that inhibit PIK3C2B, a class II kinase involved in the generation of phosphoinositide-3-phosphate (PI3P), lead to improvements in muscle histopathology, muscle function and survival (Sabha et al. 2016). Some CNM patients have also showed improved strength when treated with acetylcholinesterase (AChE) inhibitors, pyridostigmine or neostigmine (Robb et al. 2011), which are antioxidants and act to increase both the level and duration of acetylcholine neurotransmitter action (Pope et al. 2005). Investigation in zebrafish has similarly shown that AChE inhibitors result in functional improvement in zebrafish models of *DNM2*- and *MTM1*-related CNM (Gibbs et al. 2013; Robb et al. 2011). Recently, pyridostigmine treatment was also documented to be beneficial in a nemaline myopathy (NEM) patient carrying a mutation in *KLHL40* (Natera-de Benito et al. 2016) which could be further investigated in the zebrafish *KLHL40* model (Ravenscroft et al. 2013) in the future.

9.4.2 Nemaline Myopathy

Nemaline myopathies (NEMs) share the hallmark feature of rod-shaped (nemaline) bodies in skeletal muscles and are known to be caused by mutations in 11 genes: *ACTA1* (Nowak et al. 1999), *CFL2* (Agrawal et al. 2007), *KBTBD13* (Sambuughin et al. 2012), *KLHL40* (Ravenscroft et al. 2013), *KLHL41* (Gupta et al. 2013b),

LMOD3 (Yuen et al. 2014), *MYO18B* (Alazami et al. 2015; Malfatti et al. 2015), *NEB* (Pelin et al. 1999), *TNNT1* (Johnston et al. 2000), *TPM3* (Laing et al. 1995) and *TPM2* (Donner et al. 2002). The majority of NEMs occur due to mutations in *nebulin* (*NEB*) or skeletal muscle *actin* (*ACTA1*) (Wallgren-Pettersson et al. 2011), the latter accounting for approximately 50% of the most severe presentations (Agrawal et al. 2004). Study of zebrafish models of ACTA1 and NEB NEMs identified that there is more than one type of nemaline body and they have different origins and dynamics in vivo (Sztal et al. 2015). The same study confirmed the presence of nemaline bodies that differ in immunoreactivity in biopsies (Sztal et al. 2015). Formation of actin-containing aggregates was observed in the ACTA1 overexpression and knock-down models and the NEB knock-down model (Sztal et al. 2015). An observation also made upon examination of samples from *CFL2* (Agrawal et al. 2007) and *KLHL40* (Ravenscroft et al. 2013) patients, indicating this may be a common feature of NEMs (Sztal et al. 2015). In patients the frequency of nemaline bodies does not correlate with disease severity (Malfatti et al. 2014); however, electron microscopy did show that nemaline bodies aligned with regions of myofibrillar disarray in zebrafish (Sztal et al. 2015), and patient analysis has indicated that fibre disorganisation and dissociation correlate with the severity of muscle weakness (Malfatti et al. 2014).

Two recent studies have associated mutations of human *myosin XVIIIB* (*MYO18B*) with formation of nemaline bodies, variation in fibre size and loss of filament assembly (Alazami et al. 2015; Malfatti et al. 2015). Three zebrafish mutants, showing different levels of severity due to complete or partial loss of function (LOF), have subsequently been identified (Berger et al. 2017; Gurung et al. 2017). Although nemaline bodies were not identified in the zebrafish mutants, analysis revealed that *myo18b* is specifically expressed in, and affects only, fast muscle fibres (Berger et al. 2017; Gurung et al. 2017). In fast fibres, Z-disks, thin and thick filaments form, despite *myo18b* mutations, but are not properly assembled into myofibrils (Berger et al. 2017; Gurung et al. 2017) resulting in an overall reduction in force generation in zebrafish (Berger et al. 2017). The pathology in patients shows there is some retained capacity to assemble sarcomeres (Alazami et al. 2015), similar to the partial-LOF zebrafish mutant (Berger et al. 2017). Going forward zebrafish NEM models could be utilised to determine how the MYO18B mutations seen in patients result in nemaline bodies and a fantastic tool for the discovery and development of NEM treatments, for which there are currently none.

9.5 Other Myopathies

9.5.1 Myofibrillar Myopathy

When grouped by disease classification, myofibrillar myopathies (MFMs) have the highest coverage of zebrafish models. To date there are zebrafish models to study MFMs related to mutations in ten of the thirteen identified genes (~77%).

MFM-causative mutations all affect proteins localised to the Z-disk, the structure that links sarcomeres together to form myofibrils, thus allowing for the transmission of contractile force. Such mutations result in the two hallmark features of MFMs, disintegration of myofibrils and formation of protein aggregates. Bührdel et al. (2015) used MOs to knock down all of the MFM genes known at the time and showed that knock-down of each gene caused disruption of muscle structure, thus demonstrating the suitability of zebrafish to model MFMs.

Study of MFMs caused by mutations in *filamin C* (*FLNC*), *bcl-2-associated athanogene 3* (*BAG3*) and *desmin* (*DES*) in zebrafish has yielded many significant insights into this class of myopathy. Study of zebrafish *FLNC*- and *BAG3*-related MFM models has shown that loss of either FLNC or BAG3 impacts fibre integrity causing susceptibility to fibre disintegration following muscle contraction without aggregate formation (Ruparelia et al. 2012). Similarly, reduction or loss of DES causes myofibril disorganisation, abnormal interfilamentous spacing and reduction in active force generation, indicating muscle weakness, as well as vulnerability to muscle damage due to eccentric muscle contraction (Li et al. 2013b; Ramspacher et al. 2015). Expression of human FLNC^{W2710X}, the most prevalent FLNC mutation that results in MFM (Vorgerd et al. 2005), or human BAG3^{P209L}, which causes severe childhood-onset MFM (Selcen et al. 2009), however, results in aggregate formation in zebrafish (Ruparelia et al. 2016, 2014). Such findings have significantly contributed to the current understanding that aggregates form due to toxic gain of function (GOF), whilst myofibrillar disintegration is the result of LOF (Ruparelia et al. 2014; Maerkens et al. 2016). Remarkably, FLNC^{W2710X} and BAG3^{P209L} localise correctly to the Z-disk, and their expression rescues myofibril disintegration caused by knock-down of their respective wild-type orthologues in zebrafish (Ruparelia et al. 2014, 2016). This indicates that these MFM-causing mutations do not abolish Z-disk function but result in dominant negative GOF, and thus abrogation of these acquired functions would be the best treatment avenue.

Inroads to treatments have been made utilising zebrafish MFM models. Induction of autophagy reduces the number of aggregates in FLNC^{W2710X} and BAG3^{P209L}-expressing fish (Ruparelia et al. 2014, 2016). Normally FLNC is continually removed and replaced at the Z-disk, as repeated contraction-relaxation causes damage to the protein, and one of the mechanisms by which FLNC is degraded is via the chaperone-assisted selective autophagy (CASA) pathway (Arndt et al. 2010; Ulbricht et al. 2013a, b). BAG3 is a key component of the CASA complex and binds directly to FLNC to target it for degradation (Ulbricht et al. 2013a, b; Arndt et al. 2010). Bag3 is present in aggregates of FLNC^{W2710X}-expressing fish, but surprisingly, reduction of Bag3 is effective in reducing the number of aggregates in these fish suggesting that the presence of Bag3 in aggregates prevents their clearance via CASA and other autophagic pathways (Ruparelia et al. 2016). In the *DES*-related MFM model, treatment with the antibiotic doxycycline also showed effectiveness at reducing the size and number of DES aggregates and the severity of the skeletal muscle phenotype (Ramspacher et al. 2015). Zebrafish have therefore provided multiple leads for clinical exploration.

9.6 Acquired Myopathies

Zebrafish myopathy studies have predominately focused on inherited myopathies; however, they have also been used to study acquired myopathies. Statins inhibit 3-hydroxy-3-methyl-glutaryl-coenzyme A reductase (HMG-CoA reductase/HMGCR), a rate-limiting enzyme of the mevalonate pathway, and are commonly prescribed to treat cardiovascular disease (Shepherd et al. 1995; Ludman et al. 2009). Their use can cause adverse side effects in skeletal muscle including pain, weakness, cell damage and, in more extreme cases, induction of rhabdomyolysis which can be fatal (Staffa et al. 2002; Rosenson 2004; Thompson et al. 2003). In zebrafish treatment with lovastatin or knock-down of the *HMGCR* gene causes thinner myofibrils, irregularities in myofibril spacing, disruption of somitic boundaries, shortened sarcomeres and myofibril disintegration (Hanai et al. 2007; Huang et al. 2011). Hanai et al. (2007) theorised that statin-induced myopathy may share common features with other muscle wasting diseases. They showed that expression of the *F-box protein 32* (*FBXO32*, formerly known as *atrogin-1*), previously known to be induced prior to atrophy (Sandri et al. 2004; Gomes et al. 2001), was expressed at significantly higher levels in zebrafish and cultured myotubes treated with lovastatin as well as in muscle biopsies of statin myopathy patients. Knock-down of *FBXO32* prevented muscle defects in zebrafish with concurrent *HMGCR* knock-down or lovastatin treatment (Hanai et al. 2007). Subsequent work utilising zebrafish and cultured mouse myotubes identified that inhibition of the mevalonate pathway by statins results in downstream inhibition of geranylgeranyl pyrophosphate and thus affects the post-translational modification geranylgeranylation (Cao et al. 2009). In lovastatin-treated fish, reduction of geranylgeranylation results in *FBXO32* induction and subsequently muscle damage; however, supplementation with geranylgeraniol partially rescues the myopathy phenotype (Cao et al. 2009). Differing levels of *FBXO32* expression have thus been suggested to explain differences in susceptibility to, and severity of, statin myopathy, and *FBXO32* is therefore a therapeutic target for reduction in patients (Cao et al. 2009; Hanai et al. 2007).

Zebrafish have also been utilised to investigate myopathy caused by vitamin deficiency. Deficiency of α-tocopherol, the favoured form of vitamin E that is absorbed (Rigotti 2007), results in myopathic lesions and ataxia (Guggenheim et al. 1982). Supplementation of vitamin E is known to prevent further deterioration or even reverse the neuromuscular pathology (Guggenheim et al. 1982; Nelson 2009; Kleopa et al. 2005); however, the mechanism behind how vitamin E deficiency results in these defects is not fully understood. Vitamin E and vitamin C/ascorbic acid have an essential nutrient-nutrient interaction (Hamilton et al. 2000; Bendich et al. 1984), and in vitro it has been shown that vitamin C is involved in recycling the α-tocopheroxyl radical (Buettner 1993). As in humans, but not mice, teleost fish, such as zebrafish, cannot synthesise their own vitamin C and thus require it from a dietary source (Dabrowski 1990; Touhata et al. 1995; Toyohara et al. 1996). Zebrafish raised on a vitamin E-deficient diet showed concomitant depletion of vita-

min C as well as myofibre degeneration and functional impairment (Lebold et al. 2013; Miller et al. 2012). Examination of muscle tissue indicated that vitamin E/C deficiency caused increased oxidative stress and consequently muscle tissue damage (Lebold et al. 2013). It is estimated that the prevalence of acquired myopathies is comparable to heritable myopathies (Norwood et al. 2009). Acquired myopathies are therefore currently underexplored and are an area of research that could be more thoroughly investigated using zebrafish in the future.

9.7 Gene Discovery

In addition to the modelling of existing myopathies, zebrafish have rapidly become established as the model of choice for the investigation of potential disease-causing variants. With the increasing use of exome and whole-genome sequencing, there has been a dramatic increase in the rate of disease gene discovery, and we found 26 examples of zebrafish being used to validate myopathic mutations in the past 5 years: *ADSSL1* (Park et al. 2016), *B3GALNT2* (Stevens et al. 2013), *B4GAT1* (Buysse et al. 2013), *BIN1* (Smith et al. 2014), *BVES* (Schindler et al. 2016), *CCDC78* (Majczenko et al. 2012), *DNAJB6* (Sarparanta et al. 2012; Nam et al. 2015), *DPM1* (Marchese et al. 2016), *DPM2 (Marchese et al.* 2016*)*, *DPM3* (Marchese et al. 2016), *GMPPB* (Carss et al. 2013), *GOLGA2* (Shamseldin et al. 2016a), *HNRNPDL* (Vieira et al. 2014), *INPP5K* (Wiessner et al. 2017; Osborn et al. 2017), *ISPD* (Roscioli et al. 2012), *KLHL40* (Ravenscroft et al. 2013), *KLHL41* (Gupta et al. 2013b), *LMOD3* (Yuen et al. 2014), *MEGF10* (Boyden et al. 2012), *POMGNT2* (Manzini et al. 2012), *POMK* (DiCostanzo et al. 2014), *POMT1* (Avşar-Ban et al. 2010), *POMT2* (Avşar-Ban et al. 2010), *PYROXD1* (O'Grady et al. 2016), *SLC25A42* (Shamseldin et al. 2016b) and *TMEM5* (Praissman et al. 2016).

Whilst zebrafish have been used extensively to confirm variants identified in patients, and even findings from golden retriever muscular dystrophy dogs (Vieira et al. 2015, 2017), causative gene identification has also occurred the other way around. For example, *dag1* mutations (discussed above) were initially identified in the zebrafish, prior to identification of affected patients. More recently, mutations in *STAC3* were identified to cause Native American myopathy (NAM) after discovery in zebrafish (Horstick et al. 2013). Zebrafish with locomotor impairment and defective excitation-contraction coupling were identified, and the causative mutation was mapped to the gene *stac3*. Stac3 co-localised and co-immunoprecipitated with RYR1 and dihydropyridine receptor (DHPR) (Horstick et al. 2013) which form essential calcium channels and mutations in the encoding genes are implicated in congenital muscular dystrophies (Marty and Fauré 2016). A homologue for *stac3* was identified in humans, which matched a previously identified locus for NAM (Stamm et al. 2008a, b), and sequencing confirmed *STAC3* was mutated in patients (Horstick et al. 2013). There are many other cases in which myopathy phenotypes

have been observed in zebrafish, but mutations in the orthologues have not yet been identified in patients. We identified 18 applicable genes from zebrafish studies; their human homologues are known as *ANXA6* (Roostalu and Strähle 2012), *APOBEC2* (Etard et al. 2010), *CAVIN4* (Housley et al. 2016), *COL15A1* (Pagnon-Minot et al. 2008; Bretaud et al. 2011), *COL22A1* (Charvet et al. 2013), *COL6A4* (Ramanoudjame et al. 2015), *CTSD* (Follo et al. 2013), *HSP90AA1* (Hawkins et al. 2008; Du et al. 2008), *ILK* (Postel et al. 2008), *MBNL2* (Machuca-Tzili et al. 2011), *MTMR12* (Gupta et al. 2013a), *MYBPC2* (Li et al. 2016), *RIPOR2* (Balasubramanian et al. 2014), *SMYD1* (Just et al. 2011; Prill et al. 2015; Tan et al. 2006; Li et al. 2013a), *TMEM2* (Ryckebüsch et al. 2016), *TMOD4* (Berger et al. 2014), *UNC45A* (Comyn and Pilgrim 2012) *and UNC45B* (Etard et al. 2007; Myhre et al. 2014a; Comyn and Pilgrim 2012; Wohlgemuth et al. 2007; Bernick et al. 2010). Given the track record of zebrafish to accurately model human myopathies, such genes are promising candidates for genetically unresolved myopathies.

9.8 Conclusion

Zebrafish models have made many significant contributions to our understanding of myopathies, from the identification of disease-causing genes to the mechanistic basis of disease and the identification of potential therapies. These models are not even limited to genes for which a zebrafish orthologue exists; the DUX4-overexpressing zebrafish model, for example, has provided valuable insights into FSHD (Mitsuhashi et al. 2013). In total we found zebrafish models for 75 out of 121 known skeletal myopathy-associated genes (Table 9.1). Whilst there are many more myopathy-associated genes to be identified, a process in which zebrafish will play a key role, it means to date models currently exist for 62% of identified genes. In many cases the description of the model has been the extent of the research, and therefore there is great potential to further utilise these existing models to investigate disease biology and potential therapeutics. In other cases, there have been significant improvements in our understanding of disease, with many of the findings subsequently being confirmed in patients, once again validating the use of the zebrafish models.

Whilst the evaluation and identification of therapies for skeletal myopathy have not yet translated into routine clinical use, they have identified leads, provided preclinical data to support trials and have had immediate impacts on diagnosis, through the identification of novel disease genes. In the future, the generation of models, not just for each disease, but for specific mutations, will allow the investigation of the biology behind differing presentations and severity, and evaluation of alternative therapeutic approaches, tailoring the treatment to the mutation. Further research in zebrafish will therefore contribute greatly to realising the potential of personalised medicine.

Table 9.1 Zebrafish skeletal myopathy models

Mutated gene/protein encoded	Skeletal muscle disease phenotypes	Zebrafish model/s
ACTA1, skeletal muscle alpha actin	Nemaline myopathy	Overexpression (Sztal et al. 2015), MO (Sztal et al. 2015)
ACVR1, activin A receptor type 1	Fibrodysplasia ossificans progressiva	Mutant (*lost-a-fin*) (Bauer et al. 2001; Mintzer et al. 2001), Overexpression (Shen et al. 2009), MO (Bauer et al. 2001)
ADSSL1, adenylosuccinate synthase like 1	Adolescent-onset distal myopathy	Overexpression (Park et al. 2016), MO (Park et al. 2016)
ATP2A1, ATPase sarcoplasmic/endoplasmic reticulum Ca2+ transporting 1	Brody disease	Mutant (*accordion*) (Hirata et al. 2004; Hirata et al. 2007)
B3GALNT2, beta-1,3-N-acetylgalactosaminyltransferase 2	Dystroglycanopathy	MO (Stevens et al. 2013)
B4GAT1, beta-1,4-glucuronyltransferase 1	Walker-Warburg syndrome	MO (Buysse et al. 2013)
BAG3, BCL2-associated athanogene 3	Myofibrillar myopathy	Overexpression (Ruparelia et al. 2014), MO (Ruparelia et al. 2014; Bührdel et al. 2015)
BIN1, bridging integrator 1	Centronuclear myopathy	MO (Smith et al. 2014)
BVES, blood vessel epicardial substance	Limb-girdle muscular dystrophy	Mutant (*popdc1*^{S191F}) (Schindler et al. 2016), MO (Schindler et al. 2016)
CAVIN1, caveolae-associated protein	Muscular dystrophy with generalised lipodystrophy	MO (Lo et al. 2015)
CAV3, caveolin-3	Limb-girdle muscular dystrophy	Overexpression (Nixon et al. 2005; Lo et al. 2015), MO (Nixon et al. 2005)
CCDC78, coiled-coil domain containing 78	Congenital myopathy with internal nuclei and atypical cores	MO (Majczenko et al. 2012)
CLCN1, chloride voltage-gated channel 1	Myotonia, dominant (Thomsen disease); myotonia, recessive (Becker disease)	Overexpression (Cheng et al. 2014)
COL6A1, collagen type VI alpha 1 chain	Bethlem myopathy, Ullrich syndrome	Mutant (Radev et al. 2015), MO (Telfer et al. 2010)
COL6A2, collagen type VI alpha 2 chain	Bethlem myopathy, Ullrich syndrome, myosclerosis	MO (Ramanoudjame et al. 2015)

(continued)

Table 9.1 (continued)

Mutated gene/protein encoded	Skeletal muscle disease phenotypes	Zebrafish model/s
COL6A3, collagen type VI alpha 3 chain	Bethlem myopathy, Ullrich syndrome	MO (Telfer et al. 2010)
CRYAB, alpha B crystallin	Myofibrillar myopathy	MO (Bührdel et al. 2015)
DAG1, dystroglycan 1	Muscle-eye-brain disease	Mutant (*patchytail*) (Gupta et al. 2011) and (*dag1*^{hu3072}) (Lin et al. 2011), MO (Parsons et al. 2002)
DES, desmin	Myofibrillar myopathy	Mutant (*desma*^{sa5}) (Ramspacher et al. 2015), Transgenic (*Gt(desma)*$^{ct122a/Ct122aRGt}$) (Ramspacher et al. 2015; Trinh et al. 2011), MO (Bührdel et al. 2015; Li et al. 2013b)
DMD, dystrophin	Duchenne/Becker muscular dystrophies	Mutant (*sapje/dmd*) (Bassett et al. 2003; Guyon et al. 2009; Berger et al. 2011), Transgenic (*Gt(dmd)*^{ct90a}) (Ruf-Zamojski et al. 2015), MO (Guyon et al. 2003; Johnson et al. 2013; Bassett et al. 2003), siRNA (Dodd et al. 2004)
DMPK, DM1 protein kinase	Myotonic dystrophy (Steinert)	Overexpression (Todd et al. 2013)
DNAJB6, DnaJ heat shock protein family (Hsp40) member B6	Limb-girdle muscular dystrophy	Overexpression (Sarparanta et al. 2012; Nam et al. 2015), MO (Sarparanta et al. 2012; Bührdel et al. 2015)
DNM2, dynamin 2	Congenital muscular dystrophy, centronuclear myopathy	MO (Koutsopoulos et al. 2013; Gibbs et al. 2013; Bragato et al. 2016), Overexpression (Gibbs et al. 2013)
DPM1, dolichyl-phosphate mannosyltransferase catalytic subunit 1	Dystroglycanopathy	MO (Marchese et al. 2016)
DPM2, dolichyl-phosphate mannosyltransferase regulatory subunit 2	Dystroglycanopathy with severe epilepsy	MO (Marchese et al. 2016)

(continued)

Table 9.1 (continued)

Mutated gene/protein encoded	Skeletal muscle disease phenotypes	Zebrafish model/s
DPM3, dolichyl-phosphate mannosyltransferase subunit 3	Dystroglycanopathy	MO (Marchese et al. 2016)
DUX4, double homeobox 4	Facio-scapulo-humeral muscular dystrophy	Overexpression (Wallace et al. 2011; Mitsuhashi et al. 2013)
DYSF, dysferlin	Limb-girdle muscular dystrophy	MO (Kawahara et al. 2011b; Roostalu and Strähle 2012)
FHL1, four and a half LIM domain 1	Myofibrillar myopathy	MO (Bührdel et al. 2015)
FKRP, fukutin-related protein	Walker-Warburg syndrome, muscle-eye-brain disease, dystroglycanopathy	MO (Thornhill et al. 2008; Kawahara et al. 2009; Wood et al. 2011; Lin et al. 2011)
FKTN, fukutin	Fukuyama congenital muscular dystrophy, Walker-Warburg syndrome	MO (Lin et al. 2011; Wood et al. 2011)
FLNC, filamin C	Myofibrillar myopathy	Mutant (*stretched-out*) (Ruparelia et al. 2012), MO (Ruparelia et al. 2012; Bührdel et al. 2015), Overexpression (Ruparelia et al. 2016)
GMPPB, GDP-mannose pyrophosphorylase B	Limb-girdle muscular dystrophy, muscle-eye-brain disease	MO (Carss et al. 2013)
GNE, UDP-N-acetylglucosamine-2-epimerase/N-acetylmannosamine kinase	Distal myopathy with rimmed vacuoles, inclusion body myopathy; Nonaka myopathy	MO (Daya et al. 2014)
GOLGA2, golgin A2	Congenital muscle dystrophy with brain involvement	MO (Shamseldin et al. 2016a)
HNRNPDL, heterogeneous nuclear ribonucleoprotein D-like	Limb-girdle muscular dystrophy	MO (Vieira et al. 2014)

(continued)

Table 9.1 (continued)

Mutated gene/protein encoded	Skeletal muscle disease phenotypes	Zebrafish model/s
HSPG2, heparan sulphate proteoglycan 2	Schwartz-Jampel syndrome	MO (Zoeller et al. 2008)
INPP5K, inositol polyphosphate-5-phosphatase K	Dystroglycanopathy, Marinesco-Sjögren syndrome	MO (Wiessner et al. 2017; Osborn et al. 2017)
ISPD, isoprenoid synthase domain containing	Walker-Warburg syndrome	MO (Roscioli et al. 2012)
ITGA7, integrin subunit alpha 7	Congenital muscular dystrophy	MO (Postel et al. 2008; Seger et al. 2011)
KCNJ2, potassium voltage-gated channel subfamily J member 2	Andersen-Tawil syndrome	Overexpression (Leong et al. 2014)
KLHL40, kelch-like family member 40	Nemaline myopathy	MO (Ravenscroft et al. 2013)
KLHL41, kelch-like family member 41	Nemaline myopathy	MO (Gupta et al. 2013b)
LAMA2, laminin subunit alpha 2	Congenital muscular dystrophy	Mutant (*candyfloss/lama2* (Hall et al. 2007; Gupta et al. 2012)
LDB3, LIM domain binding 3	Myofibrillar myopathy	MO (Bührdel et al. 2015)
LMNA, lamin A/C	Congenital muscular dystrophy	MO (Koshimizu et al. 2011)
LMOD3, leiomodin 3	Nemaline myopathy	Morpholino (Yuen et al. 2014)
MEGF10, multiple EGF-like domains 10	Early-onset myopathy, areflexia, respiratory distress, and dysphagia; Minicore myopathy	Morpholino (Boyden et al. 2012)
MSTN, myostatin	Muscle hypertrophy	MO (*mstn1*) (Amali et al. 2004), Overexpression (*mstn2*) (Amali et al. 2008)
MTM1, myotubularin	Myotubular myopathy	MO (Dowling et al. 2009; Gibbs et al. 2010)
MYO18B, myosin XVIIIB	Nemaline myopathy	Mutant (*frozen/fro*) (Gurung et al. 2017) , (*schläfrig/sig/myo18b*^{sig}) (Berger et al. 2017) and (*myo18b*$^{-9+3}$) (Berger et al. 2017)

(continued)

Table 9.1 (continued)

Mutated gene/protein encoded	Skeletal muscle disease phenotypes	Zebrafish model/s
MYOT, myotilin	Myopathy myofibrillar, spheroid body myopathy	MO (Bührdel et al. 2015)
NEB, nebulin	Nemaline myopathy	Mutant (*neb*) (Telfer et al. 2012), MO (Sztal et al. 2015)
ORAI1, ORAI calcium release-activated calcium modulator 1	Tubular aggregate myopathy	MO (Völkers et al. 2012)
PLEC, plectin	Late-onset muscular dystrophy associated with epidermolysis bullosa simplex	MO (Bührdel et al. 2015)
POMGNT2, protein O-linked mannose N-acetylglucosaminyltransferase 2	Congenital muscular dystrophy with brain and eye anomalies, Walker-Warburg syndrome	MO (Manzini et al. 2012)
POMK, protein-O-mannose kinase	Dystroglycanopathy, Walker-Warburg syndrome	MO (DiCostanzo et al. 2014)
POMT1, protein-O-mannosyltransferase 1	Walker-Warburg syndrome	MO (Avşar-Ban et al. 2010)
POMT2, protein-O-mannosyltransferase 2	Walker-Warburg syndrome, muscle-eye-brain disease	MO (Avşar-Ban et al. 2010)
PYROXD1, pyridine nucleotide-disulphide oxidoreductase domain 1	Early-onset myopathy with internalised nuclei and myofibrillar disorganisation	Overexpression (O'Grady et al. 2016), MO (O'Grady et al. 2016)
RYR1, ryanodine receptor 1	Congenital fibre-type disproportion myopathy, centronuclear myopathy, multiminicore myopathy	Mutant (*relatively relaxed*) (Hirata et al. 2007), MO (Jurynec et al. 2008)
SELENON, selenoprotein N	Congenital fibre-type disproportion myopathy	MO (Deniziak et al. 2007; Jurynec et al. 2008)
SGCD, sarcoglycan delta	Limb-girdle muscular dystrophy	MO (Guyon et al. 2005), and (Cheng et al. 2006)
SLC25A42, solute carrier family 25 member 42	Mitochondrial myopathy	MO (Shamseldin et al. 2016b)

(continued)

Table 9.1 (continued)

Mutated gene/protein encoded	Skeletal muscle disease phenotypes	Zebrafish model/s
STAC3, SH3- and cysteine-rich domain 3	Native American myopathy	Mutant (*stac3*) (Linsley et al. 2017), Overexpression (*Tg: muscle actin:stac3^{NAM}-EGFP*) (Linsley et al. 2017)
TCAP, titin-cap	Limb-girdle muscular dystrophy	Overexpression (Zhang et al. 2009), MO (Zhang et al. 2009)
TMEM5, transmembrane protein 5	Dystroglycanopathy	MO (Praissman et al. 2016)
TPM2, tropomyosin 2	Nemaline myopathy, cap myopathy	Overexpression (Davidson et al. 2013)
TTN, titin	Limb-girdle muscular dystrophy, congenital myopathy with fatal cardiomyopathy, tibial muscular dystrophy (Udd myopathy)	Mutant (*runzel*) (Steffen et al. 2007), Mutant (*herzschlag*) (Myhre et al. 2014b), MO (Steffen et al. 2007)
VCP, valosin-containing protein	Myofibrillar myopathy	MO (Bührdel et al. 2015)

References

Aartsma-Rus A, Fokkema I, Verschuuren J, Ginjaar I, Van Deutekom J, van Ommen GJ, Den Dunnen JT (2009) Theoretic applicability of antisense-mediated exon skipping for Duchenne muscular dystrophy mutations. Hum Mutat 30(3):293–299

Aartsma-Rus A, Van Deutekom JC, Fokkema IF, Van Ommen GJB, Den Dunnen JT (2006) Entries in the Leiden Duchenne muscular dystrophy mutation database: An overview of mutation types and paradoxical cases that confirm the reading-frame rule. Muscle Nerve 34(2):135–144

Agrawal PB, Greenleaf RS, Tomczak KK, Lehtokari V-L, Wallgren-Pettersson C, Wallefeld W, Laing NG, Darras BT, Maciver SK, Dormitzer PR (2007) Nemaline myopathy with minicores caused by mutation of the CFL2 gene encoding the skeletal muscle actin–binding protein, cofilin-2. Am J Hum Genet 80(1):162–167

Agrawal PB, Strickland CD, Midgett C, Morales A, Newburger DE, Poulos MA, Tomczak KK, Ryan MM, Iannaccone ST, Crawford TO (2004) Heterogeneity of nemaline myopathy cases with skeletal muscle α-actin gene mutations. Ann Neurol 56(1):86–96

Alazami AM, Kentab AY, Faqeih E, Mohamed JY, Alkhalidi H, Hijazi H, Alkuraya FS (2015) A novel syndrome of Klippel-Feil anomaly, myopathy, and characteristic facies is linked to a null mutation in MYO18B. J Med Genet 52(6):400–404

Alexander M, Kawahara G, Motohashi N, Casar J, Eisenberg I, Myers J, Gasperini M, Estrella E, Kho A, Mitsuhashi S (2013) MicroRNA-199a is induced in dystrophic muscle and affects WNT signaling, cell proliferation, and myogenic differentiation. Cell Death Differ 20(9):1194–1208

Amali AA, Lin CJ-F, Chen Y-H, Wang W-L, Gong H-Y, Rekha RD, Lu J-K, Chen TT, Wu J-L (2008) Overexpression of Myostatin2 in zebrafish reduces the expression of dystrophin associated protein complex (DAPC) which leads to muscle dystrophy. J Biomed Sci 15(5):595–604

Amali AA, Lin CJF, Chen YH, Wang WL, Gong HY, Lee CY, Ko YL, Lu JK, Her GM, Chen TT (2004) Up-regulation of muscle-specific transcription factors during embryonic somitogenesis of zebrafish (Danio rerio) by knock-down of myostatin-1. Dev Dyn 229(4):847–856

Arbogast S, Beuvin M, Fraysse B, Zhou H, Muntoni F, Ferreiro A (2009) Oxidative stress in SEPN1-related myopathy: From pathophysiology to treatment. Ann Neurol 65(6):677–686

Arndt V, Dick N, Tawo R, Dreiseidler M, Wenzel D, Hesse M, Fürst DO, Saftig P, Saint R, Fleischmann BK (2010) Chaperone-assisted selective autophagy is essential for muscle maintenance. Curr Biol 20(2):143–148

Asai A, Sahani N, Kaneki M, Ouchi Y, Martyn JJ, Yasuhara SE (2007) Primary role of functional ischemia, quantitative evidence for the two-hit mechanism, and phosphodiesterase-5 inhibitor therapy in mouse muscular dystrophy. PLoS One 2(8):e806

Australian Institute of Health and Welfare (AIHW) (2017a) Australian Cancer Incidence and Mortality (ACIM) books: Breast cancer. AIHW, Canberra. http://www.aihw.gov.au/acim-books

Australian Institute of Health and Welfare (AIHW) (2017b) Australian Cancer Incidence and Mortality (ACIM) books: Melanoma of the skin. AIHW, Canberra. http://www.aihw.gov.au/acim-books

Avşar-Ban E, Ishikawa H, Manya H, Watanabe M, Akiyama S, Miyake H, Endo T, Tamaru Y (2010) Protein O-mannosylation is necessary for normal embryonic development in zebrafish. Glycobiology 20(9):1089–1102

Bajanca F, Gonzalez-Perez V, Gillespie SJ, Beley C, Garcia L, Theveneau E, Sear RP, Hughes SM (2015) In vivo dynamics of skeletal muscle Dystrophin in zebrafish embryos revealed by improved FRAP analysis. elife 4:e06541

Balasubramanian A, Kawahara G, Gupta VA, Rozkalne A, Beauvais A, Kunkel LM, Gussoni E (2014) Fam65b is important for formation of the HDAC6-dysferlin protein complex during myogenic cell differentiation. FASEB J 28(7):2955–2969

Bansal D, Miyake K, Vogel SS, Groh S, Chen C-C, Williamson R, McNeil PL, Campbell KP (2003) Defective membrane repair in dysferlin-deficient muscular dystrophy. Nature 423(6936):168–172

Bashir R, Britton S, Strachan T, Keers S, Vafiadaki E, Lako M, Richard I, Marchand S, Bourg N, Argov Z (1998) A gene related to Caenorhabditis elegans spermatogenesis factor fer-1 is mutated in limb-girdle muscular dystrophy type 2B. Nat Genet 20(1):37–42

Bassett DI, Bryson-Richardson RJ, Daggett DF, Gautier P, Keenan DG, Currie PD (2003) Dystrophin is required for the formation of stable muscle attachments in the zebrafish embryo. Development 130(23):5851–5860

Bauer H, Lele Z, Rauch G-J, Geisler R, Hammerschmidt M (2001) The type I serine/threonine kinase receptor Alk8/Lost-a-fin is required for Bmp2b/7 signal transduction during dorsoventral patterning of the zebrafish embryo. Development 128(6):849–858

Bendich A, D'Apolito P, Gabriel E, Machlin LJ (1984) Interaction of dietary vitamin C and vitamin E on guinea pig immune responses to mitogens. J Nutr 114(9):1588–1593

Berger J, Berger S, Jacoby AS, Wilton SD, Currie PD (2011) Evaluation of exon-skipping strategies for Duchenne muscular dystrophy utilizing dystrophin-deficient zebrafish. J Cell Mol Med 15(12):2643–2651

Berger J, Berger S, Li M, Currie PD (2017) Myo18b is essential for sarcomere assembly in fast skeletal muscle. Hum Mol Genet 26(6):1146–1156

Berger J, Tarakci H, Berger S, Li M, Hall TE, Arner A, Currie PD (2014) Loss of Tropomodulin4 in the zebrafish mutant träge causes cytoplasmic rod formation and muscle weakness reminiscent of nemaline myopathy. Dis Model Mech 7(12):1407–1415

Bernick EP, Zhang P-J, Du S (2010) Knockdown and overexpression of Unc-45b result in defective myofibril organization in skeletal muscles of zebrafish embryos. BMC Cell Biol 11(1):70

Bitoun M, Maugenre S, Jeannet P-Y, Lacene E, Ferrer X, Laforet P, Martin J-J, Laporte J, Lochmüller H, Beggs AH (2005) Mutations in dynamin 2 cause dominant centronuclear myopathy. Nat Genet 37(11):1207–1209

Böhm J, Biancalana V, DeChene ET, Bitoun M, Pierson CR, Schaefer E, Karasoy H, Dempsey MA, Klein F, Dondaine N (2012) Mutation spectrum in the large GTPase dynamin 2, and genotype–phenotype correlation in autosomal dominant centronuclear myopathy. Hum Mutat 33(6):949–959

Bouchet-Séraphin C, Vuillaumier-Barrot S, Seta N (2015) Dystroglycanopathies: About numerous genes involved in glycosylation of one single glycoprotein. J Neuromus Dis 2(1):27–38

Boyden SE, Mahoney LJ, Kawahara G, Myers JA, Mitsuhashi S, Estrella EA, Duncan AR, Dey F, DeChene ET, Blasko-Goehringer JM (2012) Mutations in the satellite cell gene MEGF10 cause a recessive congenital myopathy with minicores. Neurogenetics 13(2):115–124

Bragato C, Gaudenzi G, Blasevich F, Pavesi G, Maggi L, Giunta M, Cotelli F, Mora M (2016) Zebrafish as a model to investigate dynamin 2-related diseases. Sci Rep 6

Bretaud S, Pagnon-Minot A, Guillon E, Ruggiero F, Le Guellec D (2011) Characterization of spatial and temporal expression pattern of Col15a1b during zebrafish development. Gene Expr Patterns 11(1):129–134

Buettner GR (1993) The pecking order of free radicals and antioxidants: lipid peroxidation, α-tocopherol, and ascorbate. Arch Biochem Biophys 300(2):535–543

Bührdel JB, Hirth S, Keßler M, Westphal S, Forster M, Manta L, Wiche G, Schoser B, Schessl J, Schröder R (2015) In vivo characterization of human myofibrillar myopathy genes in zebrafish. Biochem Biophys Res Commun 461(2):217–223

Bushby K, Finkel R, Wong B, Barohn R, Campbell C, Comi GP, Connolly AM, Day JW, Flanigan KM, Goemans N (2014) Ataluren treatment of patients with nonsense mutation dystrophinopathy. Muscle Nerve 50(4):477–487

Bushby K, Kirschner J, Luo X, Elfring G, Kroger H, Riebling P, Ong T, Spiegel R, Peltz S, Muntoni F (2016) Results of North Star Ambulatory Assessments (NSAA) in the Phase 3 Ataluren Confirmatory Trial in Patients with Nonsense Mutation Duchenne Muscular Dystrophy (ACT DMD)(I15. 008). Neurology 86(16 Supplement):I15. 008

Buysse K, Riemersma M, Powell G, van Reeuwijk J, Chitayat D, Roscioli T, Kamsteeg E-J, van den Elzen C, van Beusekom E, Blaser S (2013) Missense mutations in β-1, 3-N-acetylglucosaminyltransferase 1 (B3GNT1) cause Walker–Warburg syndrome. Hum Mol Genet 22(9):1746–1754

Cao P, Hanai J-i, Tanksale P, Imamura S, Sukhatme VP, Lecker SH (2009) Statin-induced muscle damage and atrogin-1 induction is the result of a geranylgeranylation defect. FASEB J 23(9):2844–2854

Carss KJ, Stevens E, Foley AR, Cirak S, Riemersma M, Torelli S, Hoischen A, Willer T, Van Scherpenzeel M, Moore SA (2013) Mutations in GDP-mannose pyrophosphorylase B cause congenital and limb-girdle muscular dystrophies associated with hypoglycosylation of α-dystroglycan. Am J Hum Genet 93(1):29–41

Charvet B, Guiraud A, Malbouyres M, Zwolanek D, Guillon E, Bretaud S, Monnot C, Schulze J, Bader HL, Allard B (2013) Knockdown of col22a1 gene in zebrafish induces a muscular dystrophy by disruption of the myotendinous junction. Development 140(22):4602–4613

Chauveau C, Rowell J, Ferreiro A (2014) A rising titan: TTN review and mutation update. Hum Mutat 35(9):1046–1059

Cheng L, Guo X-f, Yang X-y, Chong M, Cheng J, Li G, Y-h G, Lu D-r (2006) δ-Sarcoglycan is necessary for early heart and muscle development in zebrafish. Biochem Biophys Res Commun 344(4):1290–1299

Cheng W, Tian J, Burgunder J-M, Hunziker W, Eng H-L (2014) Myotonia congenita-associated mutations in chloride channel-1 affect zebrafish body wave swimming kinematics. PLoS One 9(8):e103445

Cirak S, Arechavala-Gomeza V, Guglieri M, Feng L, Torelli S, Anthony K, Abbs S, Garralda ME, Bourke J, Wells DJ (2011) Exon skipping and dystrophin restoration in patients with Duchenne muscular dystrophy after systemic phosphorodiamidate morpholino oligomer treatment: an open-label, phase 2, dose-escalation study. Lancet 378(9791):595–605

Clapp J, Mitchell LM, Bolland DJ, Fantes J, Corcoran AE, Scotting PJ, Armour JA, Hewitt JE (2007) Evolutionary conservation of a coding function for D4Z4, the tandem DNA repeat mutated in facioscapulohumeral muscular dystrophy. Am J Hum Genet 81(2):264–279

Comyn SA, Pilgrim D (2012) Lack of developmental redundancy between Unc45 proteins in zebrafish muscle development. PLoS One 7(11):e48861

Cooper ST, McNeil PL (2015) Membrane repair: mechanisms and pathophysiology. Physiol Rev 95(4):1205–1240

Dabrowski K (1990) Gulonolactone oxidase is missing in teleost fish. The direct spectrophotometric assay. Biol Chem Hoppe Seyler 371(1):207–214

Danen EH, Sonnenberg A (2003) Erratum: Integrins in regulation of tissue development and function. J Pathol; 200: 471–480. J Pathol 201(4):632–641

Davidson AE, Siddiqui FM, Lopez MA, Lunt P, Carlson HA, Moore BE, Love S, Born DE, Roper H, Majumdar A (2013) Novel deletion of lysine 7 expands the clinical, histopathological and genetic spectrum of TPM2-related myopathies. Brain 136(2):508–521

Daya A, Vatine GD, Becker-Cohen M, Tal-Goldberg T, Friedmann A, Gothilf Y, Du SJ, Mitrani-Rosenbaum S (2014) Gne depletion during zebrafish development impairs skeletal muscle structure and function. Hum Mol Genet 23(13):3349–3361

Deniziak M, Thisse C, Rederstorff M, Hindelang C, Thisse B, Lescure A (2007) Loss of selenoprotein N function causes disruption of muscle architecture in the zebrafish embryo. Exp Cell Res 313(1):156–167

Deutekom JCV, Wljmenga C, Tlenhoven EAV, Gruter A-M, Hewitt JE, Padberg GW, G-JBv O, Hofker MH, Fronts RR (1993) FSHD associated DNA rearrangements are due to deletions of integral copies of a 3.2 kb tandemly repeated unit. Hum Mol Genet 2(12):2037–2042

DiCostanzo S, Balasubramanian A, Pond HL, Rozkalne A, Pantaleoni C, Saredi S, Gupta VA, Sunu CM, Timothy WY, Kang PB (2014) POMK mutations disrupt muscle development leading to a spectrum of neuromuscular presentations. Hum Mol Genet ddu296

Dixit M, Ansseau E, Tassin A, Winokur S, Shi R, Qian H, Sauvage S, Mattéotti C, van Acker AM, Leo O (2007) DUX4, a candidate gene of facioscapulohumeral muscular dystrophy, encodes a transcriptional activator of PITX1. Proc Natl Acad Sci 104(46):18157–18162

Dodd A, Chambers SP, Love DR (2004) Short interfering RNA-mediated gene targeting in the zebrafish. FEBS Lett 561(1-3):89–93

Donner K, Ollikainen M, Ridanpää M, Christen H-J, Goebel HH, de Visser M, Pelin K, Wallgren-Pettersson C (2002) Mutations in the β-tropomyosin (TPM2) gene–a rare cause of nemaline myopathy. Neuromuscul Disord 12(2):151–158

Dowling JJ, Arbogast S, Hur J, Nelson DD, McEvoy A, Waugh T, Marty I, Lunardi J, Brooks SV, Kuwada JY (2012) Oxidative stress and successful antioxidant treatment in models of RYR1-related myopathy. Brain 135(4):1115–1127

Dowling JJ, Vreede AP, Low SE, Gibbs EM, Kuwada JY, Bonnemann CG, Feldman EL (2009) Loss of myotubularin function results in T-tubule disorganization in zebrafish and human myotubular myopathy. PLoS Genet 5(2):e1000372

Du SJ, Li H, Bian Y, Zhong Y (2008) Heat-shock protein 90α1 is required for organized myofibril assembly in skeletal muscles of zebrafish embryos. Proc Natl Acad Sci 105(2):554–559

Ervasti JM, Campbell KP (1993) A role for the dystrophin-glycoprotein complex as a transmembrane linker between laminin and actin. J Cell Biol 122:809–809

Etard C, Behra M, Fischer N, Hutcheson D, Geisler R, Strähle U (2007) The UCS factor Steif/Unc-45b interacts with the heat shock protein Hsp90a during myofibrillogenesis. Dev Biol 308(1):133–143

Etard C, Roostalu U, Strähle U (2010) Lack of Apobec2-related proteins causes a dystrophic muscle phenotype in zebrafish embryos. J Cell Biol 189(3):527–539

Fadok V, Voelker D, Campbell P, Cohen J, Bratton D, Henson P (1992) Exposure of phosphatidylserine on the surface of apoptotic lymphocytes triggers specific recognition and removal by macrophages. J Immunol 148(7):2207–2216

Finkel RS, Flanigan KM, Wong B, Bönnemann C, Sampson J, Sweeney HL, Reha A, Northcutt VJ, Elfring G, Barth J (2013) Phase 2a study of ataluren-mediated dystrophin production in patients with nonsense mutation Duchenne muscular dystrophy. PLoS One 8(12):e81302

Flanigan KM, Dunn DM, Von Niederhausern A, Soltanzadeh P, Gappmaier E, Howard MT, Sampson JB, Mendell JR, Wall C, King WM (2009) Mutational spectrum of DMD mutations in dystrophinopathy patients: application of modern diagnostic techniques to a large cohort. Hum Mutat 30(12):1657–1666

Follo C, Ozzano M, Montalenti C, Santoro MM, Isidoro C (2013) Knockdown of cathepsin D in zebrafish fertilized eggs determines congenital myopathy. Biosci Rep 33(2):e00034

Galbiati F, Engelman JA, Volonte D, Zhang XL, Minetti C, Li M, Hou H, Kneitz B, Edelmann W, Lisanti MP (2001) Caveolin-3 null mice show a loss of caveolae, changes in the microdomain distribution of the dystrophin-glycoprotein complex, and t-tubule abnormalities. J Biol Chem 276(24):21425–21433

Geis T, Marquard K, Rödl T, Reihle C, Schirmer S, von Kalle T, Bornemann A, Hehr U, Blankenburg M (2013) Homozygous dystroglycan mutation associated with a novel muscle-eye-brain disease-like phenotype with multicystic leucodystrophy. Neurogenetics 14(3-4):205

Gibbs EM, Clarke NF, Rose K, Oates EC, Webster R, Feldman EL, Dowling JJ (2013) Neuromuscular junction abnormalities in DNM2-related centronuclear myopathy. J Mol Med 91(6):727–737

Gibbs EM, Davidson AE, Telfer WR, Feldman EL, Dowling JJ (2014) The myopathy-causing mutation DNM2-S619L leads to defective tubulation in vitro and in developing zebrafish. Dis Model Mech 7(1):157–161

Gibbs EM, Feldman EL, Dowling JJ (2010) The role of MTMR14 in autophagy and in muscle disease. Autophagy 6(6):819–820

Gnocchi VF, White RB, Ono Y, Ellis JA, Zammit PS (2009) Further characterisation of the molecular signature of quiescent and activated mouse muscle satellite cells. PLoS One 4(4):e5205

Gomes MD, Lecker SH, Jagoe RT, Navon A, Goldberg AL (2001) Atrogin-1, a muscle-specific F-box protein highly expressed during muscle atrophy. Proc Natl Acad Sci 98(25):14440–14445

Goody MF, Kelly MW, Reynolds CJ, Khalil A, Crawford BD, Henry CA (2012) NAD+ biosynthesis ameliorates a zebrafish model of muscular dystrophy. PLoS Biol 10(10):e1001409

Guggenheim MA, Ringel SP, Silverman A, Grabert BE (1982) Progressive neuromuscular disease in children with chronic cholestasis and vitamin E deficiency: diagnosis and treatment with alpha tocopherol. J Pediatr 100(1):51–58

Guiraud S, Davies KE (2017) Pharmacological advances for treatment in Duchenne muscular dystrophy. Curr Opin Pharmacol 34:36–48

Gupta V, Kawahara G, Gundry SR, Chen AT, Lencer WI, Zhou Y, Zon LI, Kunkel LM, Beggs AH (2011) The zebrafish dag1 mutant: a novel genetic model for dystroglycanopathies. Hum Mol Genet 20(9):1712–1725

Gupta VA, Hnia K, Smith LL, Gundry SR, McIntire JE, Shimazu J, Bass JR, Talbot EA, Amoasii L, Goldman NE (2013a) Loss of catalytically inactive lipid phosphatase myotubularin-related protein 12 impairs myotubularin stability and promotes centronuclear myopathy in zebrafish. PLoS Genet 9(6):e1003583

Gupta VA, Kawahara G, Myers JA, Chen AT, Hall TE, Manzini MC, Currie PD, Zhou Y, Zon LI, Kunkel LM (2012) A splice site mutation in laminin-α2 results in a severe muscular dystrophy and growth abnormalities in zebrafish. PLoS One 7(8):e43794

Gupta VA, Ravenscroft G, Shaheen R, Todd EJ, Swanson LC, Shiina M, Ogata K, Hsu C, Clarke NF, Darras BT (2013b) Identification of KLHL41 mutations implicates BTB-Kelch-mediated ubiquitination as an alternate pathway to myofibrillar disruption in nemaline myopathy. Am J Hum Genet 93(6):1108–1117

Gurung R, Ono Y, Baxendale S, Lee SLC, Moore S, Calvert M, Ingham PW (2017) A Zebrafish Model for a Human Myopathy Associated with Mutation of the Unconventional Myosin MYO18B. Genetics 205(2):725–735

Guyon J, Mosley A, Zhou Y, O'brien K, Sheng X, Chiang K, Davidson A, Volinski J, Zon L, Kunkel L (2003) The dystrophin associated protein complex in zebrafish. Hum Mol Genet 12(6):601–615

Guyon JR, Goswami J, Jun SJ, Thorne M, Howell M, Pusack T, Kawahara G, Steffen LS, Galdzicki M, Kunkel LM (2009) Genetic isolation and characterization of a splicing mutant of zebrafish dystrophin. Hum Mol Genet 18(1):202–211

Guyon JR, Mosley AN, Jun SJ, Montanaro F, Steffen LS, Zhou Y, Nigro V, Zon LI, Kunkel LM (2005) δ-sarcoglycan is required for early zebrafish muscle organization. Exp Cell Res 304(1):105–115

Hall TE, Bryson-Richardson RJ, Berger S, Jacoby AS, Cole NJ, Hollway GE, Berger J, Currie PD (2007) The zebrafish candyfloss mutant implicates extracellular matrix adhesion failure in laminin α2-deficient congenital muscular dystrophy. Proc Natl Acad Sci 104(17):7092–7097

Hamilton IM, Gilmore WS, Benzie IF, Mulholland CW, Strain J (2000) Interactions between vitamins C and E in human subjects. Br J Nutr 84(3):261–267

Hanai J-i, Cao P, Tanksale P, Imamura S, Koshimizu E, Zhao J, Kishi S, Yamashita M, Phillips PS, Sukhatme VP (2007) The muscle-specific ubiquitin ligase atrogin-1/MAFbx mediates statin-induced muscle toxicity. J Clin Invest 117(12):3940

Hara Y, Balci-Hayta B, Yoshida-Moriguchi T, Kanagawa M, Beltrán-Valero de Bernabé D, Gündeşli H, Willer T, Satz JS, Crawford RW, Burden SJ (2011) A dystroglycan mutation associated with limb-girdle muscular dystrophy. N Engl J Med 364(10):939–946

Harper SQ, Hauser MA, DelloRusso C, Duan D, Crawford RW, Phelps SF, Harper HA, Robinson AS, Engelhardt JF, Brooks SV (2002) Modular flexibility of dystrophin: implications for gene therapy of Duchenne muscular dystrophy. Nat Med 8(3):253–261

Hawkins TA, Haramis A-P, Etard C, Prodromou C, Vaughan CK, Ashworth R, Ray S, Behra M, Holder N, Talbot WS (2008) The ATPase-dependent chaperoning activity of Hsp90a regulates thick filament formation and integration during skeletal muscle myofibrillogenesis. Development 135(6):1147–1156

Hewitt JE, Lyle R, Clark LN, Valleley EM, Wright TJ, Wijmenga C, van Deutekom JC, Francis F, Sharpe PT, Hofker M (1994) Analysis of the tandem repeat locus D4Z4 associated with facioscapulohumeral muscular dystropothhy. Hum Mol Genet 3(8):1287–1295

Hill MM, Bastiani M, Luetterforst R, Kirkham M, Kirkham A, Nixon SJ, Walser P, Abankwa D, Oorschot VM, Martin S (2008) PTRF-Cavin, a conserved cytoplasmic protein required for caveola formation and function. Cell 132(1):113–124

Hirata H, Saint-Amant L, Waterbury J, Cui W, Zhou W, Li Q, Goldman D, Granato M, Kuwada JY (2004) accordion, a zebrafish behavioral mutant, has a muscle relaxation defect due to a mutation in the ATPase Ca2+ pump SERCA1. Development 131(21):5457–5468

Hirata H, Watanabe T, Hatakeyama J, Sprague SM, Saint-Amant L, Nagashima A, Cui WW, Zhou W, Kuwada JY (2007) Zebrafish relatively relaxed mutants have a ryanodine receptor defect, show slow swimming and provide a model of multi-minicore disease. Development 134(15):2771–2781

Hoang QV, Blair MP, Rahmani B, Galasso JM, Shapiro MJ (2011) Multiple retinal holes and peripheral nonperfusion in muscle-eye-brain disease. Arch Ophthalmol 129(3):373–379

Hoffman EP, Fischbeck KH, Brown RH, Johnson M, Medori R, Loire JD, Harris JB, Waterston R, Brooke M, Specht L (1988) Characterization of dystrophin in muscle-biopsy specimens from patients with Duchenne's or Becker's muscular dystrophy. N Engl J Med 318(21):1363–1368

Horstick EJ, Linsley JW, Dowling JJ, Hauser MA, McDonald KK, Ashley-Koch A, Saint-Amant L, Satish A, Cui WW, Zhou W (2013) Stac3 is a component of the excitation-contraction coupling machinery and mutated in Native American myopathy. Nat Commun 4:1952

Housley MP, Njaine B, Ricciardi F, Stone OA, Hölper S, Krüger M, Kostin S, Stainier DY (2016) Cavin4b/Murcb Is Required for Skeletal Muscle Development and Function in Zebrafish. PLoS Genet 12(6):e1006099

Huang S-H, Hsiao C-D, Lin D-S, Chow C-Y, Chang C-J, Liau I (2011) Imaging of zebrafish in vivo with second-harmonic generation reveals shortened sarcomeres associated with myopathy induced by statin. PLoS One 6(9):e24764

Ilsley J, Sudol M, Winder S (2001) The interaction of dystrophin with β-dystroglycan is regulated by tyrosine phosphorylation. Cell Signal 13(9):625–632

James M, Nuttall A, Ilsley J, Ottersbach K, Tinsley J, Sudol M, Winder S (2000) Adhesion-dependent tyrosine phosphorylation of (beta)-dystroglycan regulates its interaction with utrophin. J Cell Sci 113(10):1717–1726

Johnson NM, Farr GH III, Maves L (2013) The HDAC Inhibitor TSA Ameliorates a zebrafish model of duchenne muscular dystrophy. PLOS Curr Musc Dyst

Johnston JJ, Kelley RI, Crawford TO, Morton DH, Agarwala R, Koch T, Schäffer AA, Francomano CA, Biesecker LG (2000) A novel nemaline myopathy in the Amish caused by a mutation in troponin T1. Am J Hum Genet 67(4):814–821

Jurynec MJ, Xia R, Mackrill JJ, Gunther D, Crawford T, Flanigan KM, Abramson JJ, Howard MT, Grunwald DJ (2008) Selenoprotein N is required for ryanodine receptor calcium release channel activity in human and zebrafish muscle. Proc Natl Acad Sci 105(34):12485–12490

Just S, Meder B, Berger IM, Etard C, Trano N, Patzel E, Hassel D, Marquart S, Dahme T, Vogel B (2011) The myosin-interacting protein SMYD1 is essential for sarcomere organization. J Cell Sci 124(18):3127–3136

Kawahara G, Gasperini MJ, Myers JA, Widrick JJ, Eran A, Serafini PR, Alexander MS, Pletcher MT, Morris CA, Kunkel LM (2014) Dystrophic muscle improvement in zebrafish via increased heme oxygenase signaling. Hum Mol Genet 23(7):1869–1878

Kawahara G, Guyon JR, Nakamura Y, Kunkel LM (2009) Zebrafish models for human FKRP muscular dystrophies. Hum Mol Genet ddp528

Kawahara G, Karpf JA, Myers JA, Alexander MS, Guyon JR, Kunkel LM (2011a) Drug screening in a zebrafish model of Duchenne muscular dystrophy. Proc Natl Acad Sci 108(13):5331–5336

Kawahara G, Serafini PR, Myers JA, Alexander MS, Kunkel LM (2011b) Characterization of zebrafish dysferlin by morpholino knockdown. Biochem Biophys Res Commun 413(2):358–363

Khairallah M, Khairallah R, Young M, Allen B, Gillis M, Danialou G, Deschepper C, Petrof B, Des Rosiers C (2008) Sildenafil and cardiomyocyte-specific cGMP signaling prevent cardiomyopathic changes associated with dystrophin deficiency. Proc Natl Acad Sci 105(19):7028–7033

Klein CJ, Coovert DD, Bulman DE, Ray PN, Mendell JR, Burghes A (1992) Somatic reversion/suppression in Duchenne muscular dystrophy (DMD): evidence supporting a frame-restoring mechanism in rare dystrophin-positive fibers. Am J Hum Genet 50(5):950

Kleopa KA, Kyriacou K, Zamba-Papanicolaou E, Kyriakides T (2005) Reversible inflammatory and vacuolar myopathy with vitamin E deficiency in celiac disease. Muscle Nerve 31(2):260–265

Kobayashi YM, Rader EP, Crawford RW, Iyengar NK, Thedens DR, Faulkner JA, Parikh SV, Weiss RM, Chamberlain JS, Moore SA (2008) Sarcolemma-localized nNOS is required to maintain activity after mild exercise. Nature 456(7221):511–515

Koshimizu E, Imamura S, Qi J, Toure J, Valdez DM Jr, Carr CE, Hanai J-i, Kishi S (2011) Embryonic senescence and laminopathies in a progeroid zebrafish model. PLoS One 6(3):e17688

Koutsopoulos OS, Kretz C, Weller CM, Roux A, Mojzisova H, Böhm J, Koch C, Toussaint A, Heckel E, Stemkens D (2013) Dynamin 2 homozygous mutation in humans with a lethal congenital syndrome. Eur J Hum Genet 21(6):637–642

Kozopas KM, Nusse R (2002) Direct flight muscles in Drosophila develop from cells with characteristics of founders and depend on DWnt-2 for their correct patterning. Dev Biol 243(2):312–325

Laing N, Wilton S, Akkari P, Dorosz S, Boundy K, Kneebone C, Blumbergs P, White S, Watkins H, Love D (1995) A mutation in the alpha tropomyosin gene TPM3 associated with autosomal dominant nemaline myopathy NEM1. Nat Genet 10(2):249–249

Lebold KM, Löhr CV, Barton CL, Miller GW, Labut EM, Tanguay RL, Traber MG (2013) Chronic vitamin E deficiency promotes vitamin C deficiency in zebrafish leading to degenerative myop-

athy and impaired swimming behavior. Comp Biochem Physiol Part C Toxicol Pharmacol 157(4):382–389
Leong IU, Skinner JR, Shelling AN, Love DR (2014) Expression of a mutant kcnj2 gene transcript in zebrafish. ISRN Mol Biol 2014
Li H, Zhong Y, Wang Z, Gao J, Xu J, Chu W, Zhang J, Fang S, Du SJ (2013a) Smyd1b is required for skeletal and cardiac muscle function in zebrafish. Mol Biol Cell 24(22):3511–3521
Li M, Andersson-Lendahl M, Sejersen T, Arner A (2013b) Knockdown of desmin in zebrafish larvae affects interfilament spacing and mechanical properties of skeletal muscle. J Gen Physiol 141(3):335–345
Li M, Andersson-Lendahl M, Sejersen T, Arner A (2014) Muscle dysfunction and structural defects of dystrophin-null sapje mutant zebrafish larvae are rescued by ataluren treatment. FASEB J 28(4):1593–1599
Li M, Andersson-Lendahl M, Sejersen T, Arner A (2016) Knockdown of fast skeletal myosin-binding protein C in zebrafish results in a severe skeletal myopathy. J Gen Physiol 147(4):309–322
Lim KRQ, Maruyama R, Yokota T (2017) Eteplirsen in the treatment of Duchenne muscular dystrophy. Drug Des Devel Ther 11:533
Lin Y-Y, White RJ, Torelli S, Cirak S, Muntoni F, Stemple DL (2011) Zebrafish Fukutin family proteins link the unfolded protein response with dystroglycanopathies. Hum Mol Genet ddr059
Lindsell CE, Shawber CJ, Boulter J, Weinmaster G (1995) Jagged: a mammalian ligand that activates Notch1. Cell 80(6):909–917
Linsley JW, Hsu I-U, Groom L, Yarotskyy V, Lavorato M, Horstick EJ, Linsley D, Wang W, Franzini-Armstrong C, Dirksen RT (2017) Congenital myopathy results from misregulation of a muscle Ca2+ channel by mutant Stac3. Proc Natl Acad Sci 114(2):E228–E236
Lipscomb L, Piggott RW, Emmerson T, Winder SJ (2016) Dasatinib as a treatment for Duchenne muscular dystrophy. Hum Mol Genet 25(2):266–274
Liu J, Aoki M, Illa I, Wu C, Fardeau M, Angelini C, Serrano C, Urtizberea JA, Hentati F, Hamida MB (1998) Dysferlin, a novel skeletal muscle gene, is mutated in Miyoshi myopathy and limb girdle muscular dystrophy. Nat Genet 20(1):31–36
Lo HP, Nixon SJ, Hall TE, Cowling BS, Ferguson C, Morgan GP, Schieber NL, Fernandez-Rojo MA, Bastiani M, Floetenmeyer M, Martel N, Laporte J, Pilch PF, Parton RG (2015) The caveolin–cavin system plays a conserved and critical role in mechanoprotection of skeletal muscle. J Cell Biol 210(5):833–849
Ludman A, Venugopal V, Yellon DM, Hausenloy DJ (2009) Statins and cardioprotection—more than just lipid lowering? Pharmacol Ther 122(1):30–43
Lyle R, Wright TJ, Clark LN, Hewitt JE (1995) The FSHD-associated repeat, D4Z4, is a member of a dispersed family of homeobox-containing repeats, subsets of which are clustered on the short arms of the acrocentric chromosomes. Genomics 28(3):389–397
Machuca-Tzili LE, Buxton S, Thorpe A, Timson CM, Wigmore P, Luther PK, Brook JD (2011) Zebrafish deficient for Muscleblind-like 2 exhibit features of myotonic dystrophy. Dis Model Mech 4(3):381–392
Maerkens A, Olivé M, Schreiner A, Feldkirchner S, Schessl J, Uszkoreit J, Barkovits K, Güttsches A, Theis V, Eisenacher M (2016) New insights into the protein aggregation pathology in myotilinopathy by combined proteomic and immunolocalization analyses. Acta Neuropathol Commun 4(1):8
Majczenko K, Davidson AE, Camelo-Piragua S, Agrawal PB, Manfready RA, Li X, Joshi S, Xu J, Peng W, Beggs AH (2012) Dominant mutation of CCDC78 in a unique congenital myopathy with prominent internal nuclei and atypical cores. Am J Hum Genet 91(2):365–371
Malfatti E, Böhm J, Lacène E, Beuvin M, Brochier G, Romero NB, Laporte J (2015) A premature stop codon in MYO18B is associated with severe nemaline myopathy with cardiomyopathy. J Neuromu Dis 2(3):219–227
Malfatti E, Lehtokari V-L, Böhm J, De Winter JM, Schäffer U, Estournet B, Quijano-Roy S, Monges S, Lubieniecki F, Bellance R (2014) Muscle histopathology in nebulin-related nema-

line myopathy: ultrastrastructural findings correlated to disease severity and genotype. Acta Neuropathol Commun 2(1):44

Manzini MC, Tambunan DE, Hill RS, Tim WY, Maynard TM, Heinzen EL, Shianna KV, Stevens CR, Partlow JN, Barry BJ (2012) Exome sequencing and functional validation in zebrafish identify GTDC2 mutations as a cause of Walker-Warburg syndrome. Am J Hum Genet 91(3):541–547

Marchese M, Pappalardo A, Baldacci J, Verri T, Doccini S, Cassandrini D, Bruno C, Fiorillo C, Garcia-Gil M, Bertini E (2016) Dolichol-phosphate mannose synthase depletion in zebrafish leads to dystrophic muscle with hypoglycosylated α-dystroglycan. Biochem Biophys Res Commun 477(1):137–143

Martin EA, Barresi R, Byrne BJ, Tsimerinov EI, Scott BL, Walker AE, Gurudevan SV, Anene F, Elashoff RM, Thomas GD (2012) Tadalafil alleviates muscle ischemia in patients with Becker muscular dystrophy. Sci Transl Med 4(162):162ra155–162ra155

Marty I, Fauré J (2016) Excitation-Contraction Coupling Alterations in Myopathies. J Neuromu Dis 3(4):443–453

Middel V, Zhou L, Takamiya M, Beil T, Shahid M, Roostalu U, Grabher C, Rastegar S, Reischl M, Nienhaus GU (2016) Dysferlin-mediated phosphatidylserine sorting engages macrophages in sarcolemma repair. Nat Commun 7:12875

Miller GW, Labut EM, Lebold KM, Floeter A, Tanguay RL, Traber MG (2012) Zebrafish (Danio rerio) fed vitamin E-deficient diets produce embryos with increased morphologic abnormalities and mortality. J Nutr Biochem 23(5):478–486

Minetti C, Bado M, Broda P, Sotgia F, Bruno C, Galbiati F, Volonte D, Lucania G, Pavan A, Bonilla E (2002) Impairment of caveolae formation and T-system disorganization in human muscular dystrophy with caveolin-3 deficiency. Am J Pathol 160(1):265–270

Mintzer KA, Lee MA, Runke G, Trout J, Whitman M, Mullins MC (2001) Lost-a-fin encodes a type I BMP receptor, Alk8, acting maternally and zygotically in dorsoventral pattern formation. Development 128(6):859–869

Mitsuhashi H, Mitsuhashi S, Lynn-Jones T, Kawahara G, Kunkel LM (2013) Expression of DUX4 in zebrafish development recapitulates facioscapulohumeral muscular dystrophy. Hum Mol Genet 22(3):568–577

Myhre JL, Hills JA, Jean F, Pilgrim DB (2014a) Unc45b is essential for early myofibrillogenesis and costamere formation in zebrafish. Dev Biol 390(1):26–40

Myhre JL, Hills JA, Prill K, Wohlgemuth SL, Pilgrim DB (2014b) The titin A-band rod domain is dispensable for initial thick filament assembly in zebrafish. Dev Biol 387(1):93–108

Nam T-S, Li W, Heo S-H, Lee K-H, Cho A, Shin J-H, Kim YO, Chae J-H, Kim D-S, Kim M-K (2015) A novel mutation in DNAJB6, p.(Phe91Leu), in childhood-onset LGMD1D with a severe phenotype. Neuromuscul Disord 25(11):843–851

Natera-de Benito D, Nascimento A, Abicht A, Ortez C, Jou C, Müller J, Evangelista T, Töpf A, Thompson R, Jimenez-Mallebrera C (2016) KLHL40-related nemaline myopathy with a sustained, positive response to treatment with acetylcholinesterase inhibitors. J Neurol 263(3):517–523

Nelson JS (2009) Neuropathological studies of chronic vitamin E deficiency in mammals including humans. Biol Vit E 845:92

Nelson MD, Rader F, Tang X, Tavyev J, Nelson SF, Miceli MC, Elashoff RM, Sweeney HL, Victor RG (2014) PDE5 inhibition alleviates functional muscle ischemia in boys with Duchenne muscular dystrophy. Neurology 82(23):2085–2091

Nixon SJ, Wegner J, Ferguson C, Mery P-F, Hancock JF, Currie PD, Key B, Westerfield M, Parton RG (2005) Zebrafish as a model for caveolin-associated muscle disease; caveolin-3 is required for myofibril organization and muscle cell patterning. Hum Mol Genet 14(13):1727–1743

Norwood FL, Harling C, Chinnery PF, Eagle M, Bushby K, Straub V (2009) Prevalence of genetic muscle disease in Northern England: in-depth analysis of a muscle clinic population. Brain awp236

Nowak KJ, Wattanasirichaigoon D, Goebel HH, Wilce M, Pelin K, Donner K, Jacob RL, Hübner C, Oexle K, Anderson JR (1999) Mutations in the skeletal muscle α-actin gene in patients with actin myopathy and nemaline myopathy. Nat Genet 23(2):208–212

O'Grady GL, Best HA, Sztal TE, Schartner V, Sanjuan-Vazquez M, Donkervoort S, Neto OA, Sutton RB, Ilkovski B, Romero NB (2016) Variants in the Oxidoreductase PYROXD1 Cause Early-Onset Myopathy with Internalized Nuclei and Myofibrillar Disorganization. Am J Hum Genet 99(5):1086–1105

Osborn DP, Pond HL, Mazaheri N, Dejardin J, Munn CJ, Mushref K, Cauley ES, Moroni I, Pasanisi MB, Sellars EA (2017) Mutations in INPP5K Cause a Form of Congenital Muscular Dystrophy Overlapping Marinesco-Sjögren Syndrome and Dystroglycanopathy. Am J Hum Genet 100(3):537–545

Pagnon-Minot A, Malbouyres M, Haftek-Terreau Z, Kim HR, Sasaki T, Thisse C, Thisse B, Ingham PW, Ruggiero F, Le Guellec D (2008) Collagen XV, a novel factor in zebrafish notochord differentiation and muscle development. Dev Biol 316(1):21–35

Park HJ, Hong YB, Choi YC, Lee J, Kim EJ, Lee JS, Mo WM, Ki SM, Kim HI, Kim HJ (2016) ADSSL1 mutation relevant to autosomal recessive adolescent onset distal myopathy. Ann Neurol 79(2):231–243

Parsons MJ, Campos I, Hirst EM, Stemple DL (2002) Removal of dystroglycan causes severe muscular dystrophy in zebrafish embryos. Development 129(14):3505–3512

Pelin K, Hilpelä P, Donner K, Sewry C, Akkari PA, Wilton SD, Wattanasirichaigoon D, Bang M-L, Centner T, Hanefeld F (1999) Mutations in the nebulin gene associated with autosomal recessive nemaline myopathy. Proc Natl Acad Sci 96(5):2305–2310

Pichavant C, Aartsma-Rus A, Clemens PR, Davies KE, Dickson G, Si T, Wilton SD, Wolff JA, Wooddell CI, Xiao X (2011) Current status of pharmaceutical and genetic therapeutic approaches to treat DMD. Mol Ther 19(5):830–840

Polesskaya A, Seale P, Rudnicki MA (2003) Wnt signaling induces the myogenic specification of resident CD45+ adult stem cells during muscle regeneration. Cell 113(7):841–852

Pope C, Karanth S, Liu J (2005) Pharmacology and toxicology of cholinesterase inhibitors: uses and misuses of a common mechanism of action. Environ Toxicol Pharmacol 19(3):433–446

Postel R, Vakeel P, Topczewski J, Knöll R, Bakkers J (2008) Zebrafish integrin-linked kinase is required in skeletal muscles for strengthening the integrin–ECM adhesion complex. Dev Biol 318(1):92–101

Powers SK, Jackson MJ (2008) Exercise-induced oxidative stress: cellular mechanisms and impact on muscle force production. Physiol Rev 88(4):1243–1276

Praissman JL, Willer T, Sheikh MO, Toi A, Chitayat D, Lin Y-Y, Lee H, Stalnaker SH, Wang S, Prabhakar PK (2016) The functional O-mannose glycan on α-dystroglycan contains a phosphoribitol primed for matriglycan addition. elife 5:e14473

Prill K, Reid PW, Wohlgemuth SL, Pilgrim DB (2015) Still heart encodes a structural HMT, SMYD1b, with chaperone-like function during fast muscle sarcomere assembly. PLoS One 10(11):e0142528

Radev Z, Hermel J-M, Elipot Y, Bretaud S, Arnould S, Duchateau P, Ruggiero F, Joly J-S, Sohm F (2015) A TALEN-Exon skipping design for a Bethlem Myopathy model in zebrafish. PLoS One 10(7):e0133986

Ramanoudjame L, Rocancourt C, Lainé J, Klein A, Joassard L, Gartioux C, Fleury M, Lyphout L, Kabashi E, Ciura S (2015) Two novel COLVI long chains in zebrafish that are essential for muscle development. Hum Mol Genet ddv368

Ramspacher C, Steed E, Boselli F, Ferreira R, Faggianelli N, Roth S, Spiegelhalter C, Messaddeq N, Trinh L, Liebling M (2015) Developmental alterations in heart biomechanics and skeletal muscle function in desmin mutants suggest an early pathological root for desminopathies. Cell Rep 11(10):1564–1576

Ravenscroft G, Miyatake S, Lehtokari V-L, Todd EJ, Vornanen P, Yau KS, Hayashi YK, Miyake N, Tsurusaki Y, Doi H (2013) Mutations in KLHL40 are a frequent cause of severe autosomal-recessive nemaline myopathy. Am J Hum Genet 93(1):6–18

Reiken S, Lacampagne A, Zhou H, Kherani A, Lehnart SE, Ward C, Huang F, Gaburjakova M, Gaburjakova J, Rosemblit N (2003) PKA phosphorylation activates the calcium release channel (ryanodine receptor) in skeletal muscle. J Cell Biol 160(6):919–928

Rigotti A (2007) Absorption, transport, and tissue delivery of vitamin E. Mol Asp Med 28(5):423–436

Robb SA, Sewry CA, Dowling JJ, Feng L, Cullup T, Lillis S, Abbs S, Lees MM, Laporte J, Manzur AY (2011) Impaired neuromuscular transmission and response to acetylcholinesterase inhibitors in centronuclear myopathies. Neuromuscul Disord 21(6):379–386

Roostalu U, Strähle U (2012) In vivo imaging of molecular interactions at damaged sarcolemma. Dev Cell 22(3):515–529

Roscioli T, Kamsteeg E-J, Buysse K, Maystadt I, van Reeuwijk J, van den Elzen C, van Beusekom E, Riemersma M, Pfundt R, Vissers LE (2012) Mutations in ISPD cause Walker-Warburg syndrome and defective glycosylation of [alpha]-dystroglycan. Nat Genet 44(5):581–585

Rosenson RS (2004) Current overview of statin-induced myopathy. Am J Med 116(6):408–416

Ruf-Zamojski F, Trivedi V, Fraser SE, Trinh LA (2015) Spatio-temporal differences in dystrophin dynamics at mRNA and protein levels revealed by a novel FlipTrap line. PLoS One 10(6):e0128944

Ruparelia AA, Oorschot V, Ramm G, Bryson-Richardson RJ (2016) FLNC myofibrillar myopathy results from impaired autophagy and protein insufficiency. Hum Mol Genet ddw080

Ruparelia AA, Oorschot V, Vaz R, Ramm G, Bryson-Richardson RJ (2014) Zebrafish models of BAG3 myofibrillar myopathy suggest a toxic gain of function leading to BAG3 insufficiency. Acta Neuropathol 128(6):821–833

Ruparelia AA, Zhao M, Currie PD, Bryson-Richardson RJ (2012) Characterization and investigation of zebrafish models of filamin-related myofibrillar myopathy. Hum Mol Genet 21(18):4073–4083

Ryckebüsch L, Hernandez L, Wang C, Phan J, Yelon D (2016) Tmem2 regulates cell-matrix interactions that are essential for muscle fiber attachment. Development 143(16):2965–2972

Sabha N, Volpatti JR, Gonorazky H, Reifler A, Davidson AE, Li X, Eltayeb NM, Dall'Armi C, Di Paolo G, Brooks SV (2016) PIK3C2B inhibition improves function and prolongs survival in myotubular myopathy animal models. J Clin Invest 126(9):3613

Sambuughin N, Swietnicki W, Techtmann S, Matrosova V, Wallace T, Goldfarb L, Maynard E (2012) KBTBD13 interacts with Cullin 3 to form a functional ubiquitin ligase. Biochem Biophys Res Commun 421(4):743–749

Sandri M, Sandri C, Gilbert A, Skurk C, Calabria E, Picard A, Walsh K, Schiaffino S, Lecker SH, Goldberg AL (2004) Foxo transcription factors induce the atrophy-related ubiquitin ligase atrogin-1 and cause skeletal muscle atrophy. Cell 117(3):399–412

Sarparanta J, Jonson PH, Golzio C, Sandell S, Luque H, Screen M, McDonald K, Stajich JM, Mahjneh I, Vihola A (2012) Mutations affecting the cytoplasmic functions of the co-chaperone DNAJB6 cause limb-girdle muscular dystrophy. Nat Genet 44(4):450–455

Schindler RF, Scotton C, Zhang J, Passarelli C, Ortiz-Bonnin B, Simrick S, Schwerte T, Poon K-L, Fang M, Rinné S (2016) POPDC1S201F causes muscular dystrophy and arrhythmia by affecting protein trafficking. J Clin Invest 126(1):239

Seger C, Hargrave M, Wang X, Chai RJ, Elworthy S, Ingham PW (2011) Analysis of Pax7 expressing myogenic cells in zebrafish muscle development, injury, and models of disease. Dev Dyn 240(11):2440–2451

Selcen D, Muntoni F, Burton BK, Pegoraro E, Sewry C, Bite AV, Engel AG (2009) Mutation in BAG3 causes severe dominant childhood muscular dystrophy. Ann Neurol 65(1):83–89

Shamseldin HE, Bennett AH, Alfadhel M, Gupta V, Alkuraya FS (2016a) GOLGA2, encoding a master regulator of golgi apparatus, is mutated in a patient with a neuromuscular disorder. Hum Genet 135(2):245–251

Shamseldin HE, Smith LL, Kentab A, Alkhalidi H, Summers B, Alsedairy H, Xiong Y, Gupta VA, Alkuraya FS (2016b) Mutation of the mitochondrial carrier SLC25A42 causes a novel form of mitochondrial myopathy in humans. Hum Genet 135(1):21–30

Shen Q, Little SC, Xu M, Haupt J, Ast C, Katagiri T, Mundlos S, Seemann P, Kaplan FS, Mullins MC (2009) The fibrodysplasia ossificans progressiva R206H ACVR1 mutation activates BMP-independent chondrogenesis and zebrafish embryo ventralization. J Clin Invest 119(11):3462–3472

Shepherd J, Cobbe SM, Ford I, Isles CG, Lorimer AR, Macfarlane PW, McKillop JH, Packard CJ (1995) Prevention of coronary heart disease with pravastatin in men with hypercholesterolemia. N Engl J Med 333(20):1301–1308

Smith LL, Gupta VA, Beggs AH (2014) Bridging integrator 1 (Bin1) deficiency in zebrafish results in centronuclear myopathy. Hum Mol Genet ddu067

Snider L, Geng LN, Lemmers RJ, Kyba M, Ware CB, Nelson AM, Tawil R, Filippova GN, van der Maarel SM, Tapscott SJ (2010) Facioscapulohumeral dystrophy: incomplete suppression of a retrotransposed gene. PLoS Genet 6(10):e1001181

Sotgia F, Bonuccelli G, Bedford M, Brancaccio A, Mayer U, Wilson MT, Campos-Gonzalez R, Brooks JW, Sudol M, Lisanti MP (2003) Localization of phospho-β-dystroglycan (pY892) to an intracellular vesicular compartment in cultured cells and skeletal muscle fibers in vivo. Biochemistry 42(23):7110–7123

Staffa JA, Chang J, Green L (2002) Cerivastatin and reports of fatal rhabdomyolysis. N Engl J Med 346(7):539–540

Stamm D, Powell C, Stajich J, Zismann V, Stephan D, Chesnut B, Aylsworth A, Kahler S, Deak K, Gilbert J (2008a) Novel congenital myopathy locus identified in Native American Indians at 12q13. 13-14.1. Neurology 71(22):1764–1769

Stamm DS, Aylsworth AS, Stajich JM, Kahler SG, Thorne LB, Speer MC, Powell CM (2008b) Native American myopathy: congenital myopathy with cleft palate, skeletal anomalies, and susceptibility to malignant hyperthermia. Am J Med Genet A 146(14):1832–1841

Steffen LS, Guyon JR, Vogel ED, Howell MH, Zhou Y, Weber GJ, Zon LI, Kunkel LM (2007) The zebrafish runzel muscular dystrophy is linked to the titin gene. Dev Biol 309(2):180–192

Stevens E, Carss KJ, Cirak S, Foley AR, Torelli S, Willer T, Tambunan DE, Yau S, Brodd L, Sewry CA (2013) Mutations in B3GALNT2 cause congenital muscular dystrophy and hypoglycosylation of α-dystroglycan. Am J Hum Genet 92(3):354–365

Sugino S, Miyatake M, Ohtani Y, Yoshioka K, Miike T, Uchino M (1991) Vascular alterations in Fukuyama type congenital muscular dystrophy. Brain Dev 13(2):77–81

Sztal TE, Ruparelia AA, Williams C, Bryson-Richardson RJ (2016) Using Touch-evoked Response and Locomotion Assays to Assess Muscle Performance and Function in Zebrafish. JoVE 116

Sztal TE, Sonntag C, Hall TE, Currie PD (2012) Epistatic dissection of laminin–receptor interactions in dystrophic zebrafish muscle. Hum Mol Genet 21(21):4718–4731

Sztal TE, Zhao M, Williams C, Oorschot V, Parslow AC, Giousoh A, Yuen M, Hall TE, Costin A, Ramm G, Bird P, Busch-Nentwich E, Stemple DL, Currie PD, Cooper ST, Laing NG, Nowak KJ, Bryson-Richardson RJ (2015) Zebrafish models for nemaline myopathy reveal a spectrum of nemaline bodies contributing to reduced muscle function. Acta Neuropathol 130(3):389–406

Tan X, Rotllant J, Li H, DeDeyne P, Du SJ (2006) SmyD1, a histone methyltransferase, is required for myofibril organization and muscle contraction in zebrafish embryos. Proc Natl Acad Sci U S A 103(8):2713–2718

Tawil R, van der Maarel SM, Tapscott SJ (2014) Facioscapulohumeral dystrophy: the path to consensus on pathophysiology. Skelet Muscle 4(1):12

Telfer W, Busta A, Bonnemann C, Feldman E, Dowling J (2010) Zebrafish models of collagen VI-related myopathies. Hum Mol Genet 19(12):2433–2444

Telfer WR, Nelson DD, Waugh T, Brooks SV, Dowling JJ (2012) Neb: a zebrafish model of nemaline myopathy due to nebulin mutation. Dis Model Mech 5(3):389–396

Thompson PD, Clarkson P, Karas RH (2003) Statin-associated myopathy. JAMA 289(13):1681–1690

Thornhill P, Bassett D, Lochmüller H, Bushby K, Straub V (2008) Developmental defects in a zebrafish model for muscular dystrophies associated with the loss of fukutin-related protein (FKRP). Brain 131(6):1551–1561

Todd PK, Ackall FY, Hur J, Sharma K, Paulson HL, Dowling JJ (2013) Transcriptional changes and developmental abnormalities in a zebrafish model of myotonic dystrophy type 1. DMM 012427

Touhata K, Toyohara H, Mitani T, Kinoshita M, Satou M, Sakaguchi M (1995) Distribution of L-gulono-1, 4-lactone oxidase among fishes. Fish Sci 61(4):729–730

Toyohara H, Nakata T, Touhata K, Hashimoto H, Kinoshita M, Sakaguchi M, Nishikimi M, Yagi K, Wakamatsu Y, Ozato K (1996) Transgenic Expression ofl-Gulono-γ-lactone Oxidase in Medaka (Oryzias latipes), a Teleost Fish That Lacks This Enzyme Necessary forl-Ascorbic Acid Biosynthesis. Biochem Biophys Res Commun 223(3):650–653

Trinh LA, Hochgreb T, Graham M, Wu D, Ruf-Zamojski F, Jayasena CS, Saxena A, Hawk R, Gonzalez-Serricchio A, Dixson A (2011) A versatile gene trap to visualize and interrogate the function of the vertebrate proteome. Genes Dev 25(21):2306–2320

Ulbricht A, Arndt V, Höhfeld J (2013a) Chaperone-assisted proteostasis is essential for mechanotransduction in mammalian cells. Comm Int Biol 6(4):e24925

Ulbricht A, Eppler FJ, Tapia VE, van der Ven PF, Hampe N, Hersch N, Vakeel P, Stadel D, Haas A, Saftig P (2013b) Cellular mechanotransduction relies on tension-induced and chaperone-assisted autophagy. Curr Biol 23(5):430–435

Vieira NM, Elvers I, Alexander MS, Moreira YB, Eran A, Gomes JP, Marshall JL, Karlsson EK, Verjovski-Almeida S, Lindblad-Toh K (2015) Jagged 1 rescues the duchenne muscular dystrophy phenotype. Cell 163(5):1204–1213

Vieira NM, Naslavsky MS, Licinio L, Kok F, Schlesinger D, Vainzof M, Sanchez N, Kitajima JP, Gal L, Cavaçana N (2014) A defect in the RNA-processing protein HNRPDL causes limb-girdle muscular dystrophy 1G (LGMD1G). Hum Mol Genet ddu127

Vieira NM, Spinazzola JM, Alexander MS, Moreira YB, Kawahara G, Gibbs DE, Mead LC, Verjovski-Almeida S, Zatz M, Kunkel LM (2017) Repression of phosphatidylinositol transfer protein α ameliorates the pathology of Duchenne muscular dystrophy. Proc Natl Acad Sci 114(23):6080–6085

Völkers M, Dolatabadi N, Gude N, Most P, Sussman MA, Hassel D (2012) Orai1 deficiency leads to heart failure and skeletal myopathy in zebrafish. J Cell Sci 125(2):287–294

Vorgerd M, van der Ven PF, Bruchertseifer V, Löwe T, Kley RA, Schröder R, Lochmüller H, Himmel M, Koehler K, Fürst DO (2005) A mutation in the dimerization domain of filamin c causes a novel type of autosomal dominant myofibrillar myopathy. Am J Hum Genet 77(2):297–304

Wallace LM, Garwick SE, Mei W, Belayew A, Coppee F, Ladner KJ, Guttridge D, Yang J, Harper SQ (2011) DUX4, a candidate gene for facioscapulohumeral muscular dystrophy, causes p53-dependent myopathy in vivo. Ann Neurol 69(3):540–552

Wallgren-Pettersson C, Sewry CA, Nowak KJ, Laing NG (2011) Nemaline myopathies. Semin Pediatr Neurol 4:230–238

Wang H, Gilner JB, Bautch VL, Wang D-Z, Wainwright BJ, Kirby SL, Patterson C (2007) Wnt2 coordinates the commitment of mesoderm to hematopoietic, endothelial, and cardiac lineages in embryoid bodies. J Biol Chem 282(1):782–791

Waugh TA, Horstick E, Hur J, Jackson SW, Davidson AE, Li X, Dowling JJ (2014) Fluoxetine prevents dystrophic changes in a zebrafish model of Duchenne muscular dystrophy. Hum Mol Genet ddu185

Welch EM, Barton ER, Zhuo J, Tomizawa Y, Friesen WJ, Trifillis P, Paushkin S, Patel M, Trotta CR, Hwang S (2007) PTC124 targets genetic disorders caused by nonsense mutations. Nature 447(7140):87–91

Wiessner M, Roos A, Munn CJ, Viswanathan R, Whyte T, Cox D, Schoser B, Sewry C, Roper H, Phadke R (2017) Mutations in INPP5K, Encoding a Phosphoinositide 5-Phosphatase, Cause Congenital Muscular Dystrophy with Cataracts and Mild Cognitive Impairment. Am J Hum Genet 100(3):523–536

Wijmenga C, Hewitt JE, Sandkuijl LA, Clark LN, Wright TJ, Dauwerse HG, Gruter A-M, Hofker MH, Moerer P, Williamson R (1992) Chromosome 4q DNA rearrangements associated with facioscapulohumeral muscular dystrophy. Nat Genet 2(1):26–30

Wohlgemuth SL, Crawford BD, Pilgrim DB (2007) The myosin co-chaperone UNC-45 is required for skeletal and cardiac muscle function in zebrafish. Dev Biol 303(2):483–492

Wood AJ, Müller JS, Jepson CD, Laval SH, Lochmüller H, Bushby K, Barresi R, Straub V (2011) Abnormal vascular development in zebrafish models for fukutin and FKRP deficiency. Hum Mol Genet ddr426

Yuen M, Sandaradura SA, Dowling JJ, Kostyukova AS, Moroz N, Quinlan KG, Lehtokari V-L, Ravenscroft G, Todd EJ, Ceyhan-Birsoy O (2014) Leiomodin-3 dysfunction results in thin filament disorganization and nemaline myopathy. J Clin Invest 124(11):4693–4708

Zervos A, Hunt K, Tong H, Avallone J, Morales J, Friedman N, Cohen B, Clark B, Guo S, Gazda H (2001) Clinical, genetic and histopathologic findings in two siblings with muscle-eye-brain disease. Eur J Ophthalmol 12(4):253–261

Zhang R, Yang J, Zhu J, Xu X (2009) Depletion of zebrafish Tcap leads to muscular dystrophy via disrupting sarcomere–membrane interaction, not sarcomere assembly. Hum Mol Genet 18(21):4130–4140

Zoeller JJ, McQuillan A, Whitelock J, Ho S-Y, Iozzo RV (2008) A central function for perlecan in skeletal muscle and cardiovascular development. J Cell Biol 181(2):381–394

Zou J, Tran D, Baalbaki M, Tang LF, Poon A, Pelonero A, Titus EW, Yuan C, Shi C, Patchava S (2015) An internal promoter underlies the difference in disease severity between N-and C-terminal truncation mutations of Titin in zebrafish. elife 4:e09406

Zou P, Pinotsis N, Lange S, Song Y-H, Popov A, Mavridis I, Mayans OM, Gautel M, Wilmanns M (2006) Palindromic assembly of the giant muscle protein titin in the sarcomeric Z-disk. Nature 439(7073):229–233

Chapter 10
Zebrafish Models of Muscular Dystrophies and Congenital Myopathies

Hiroaki Mitsuhashi

Abstract Muscular dystrophies and congenital myopathies are genetic disorders that affect skeletal muscle. Mice have been widely used as animal models of the diseases; however, the zebrafish has recently received much attention as a new model system complementary to mammalian models. The basic structure of zebrafish skeletal muscle is similar to that of humans, and approximately 70% of human genes correspond to at least one ortholog in the zebrafish genome. Furthermore, various attributes make zebrafish suited for the inherited muscular disorders, for example, ease of genetic manipulation by microinjection, rapid external development, reproducible motor behavior from 24 h postfertilization, in vivo imaging based on the transparency of embryos, and mutant resource generated by a forward genetic approach. This review highlights key studies using zebrafish as a model of inherited muscular disorders, focusing on disease mutants identified from forward genetic screening, causative gene discovery by reverse genetic approach, and drug screening to develop novel therapeutic strategies.

Keywords Zebrafish · Muscular dystrophy · Congenital myopathy · Skeletal muscle · Disease model

10.1 Muscular Dystrophy and Congenital Myopathy

Muscular dystrophy and congenital myopathy are two major categories of inherited muscle diseases. Both are heterogeneous groups of genetic diseases that affect skeletal muscle, leading to muscle weakness.

Muscular dystrophies are a group of degenerative diseases, in which muscle forms normally at first but the muscle cells or muscle fibers gradually degenerate. Patients with muscular dystrophy develop progressive muscle weakness and muscle

H. Mitsuhashi (✉)
Department of Applied Biochemistry, School of Engineering, Tokai University, Kanagawa, Japan
e-mail: hmitsuhashi@tsc.u-tokai.ac.jp

H. Hirata, A. Iida (eds.), *Zebrafish, Medaka, and Other Small Fishes*,
https://doi.org/10.1007/978-981-13-1879-5_10

atrophy. Disease onset varies from severe forms in which the symptoms become apparent at birth or infancy (congenital muscular dystrophy) to relatively mild adult-onset muscular dystrophy. A number of studies have proposed that the pathomechanism of muscular dystrophies compromises the integrity of the muscle cell plasma membrane, or sarcolemma. The sarcolemma is stabilized by the submembranous actin cytoskeleton and the basal lamina consisting of the extracellular matrix (ECM) so that it maintains the integrity against mechanical stress induced by muscle contraction (Cohn and Campbell 2000; Nowak and Davies 2004; Ozawa et al. 1995; Rahimov and Kunkel 2013). Muscle fibers express the dystrophin-associated glycoprotein complex (DGC) that links the actin cytoskeleton with the basal lamina and consequently protects the sarcolemma from mechanical stress. Mutations in genes associated with DGC or basal lamina cause muscular dystrophies. Muscle creatine kinase, which is an abundant enzyme in the muscle fiber, is abnormally elevated in the serum of muscular dystrophy patients, suggesting leakage of the enzyme through the fragile sarcolemma.

In contrast, congenital myopathy is a group of developmental disorder in which muscle formation is affected. Patients with congenital myopathy usually present hypotonia and muscle weakness at birth or in childhood (Nance et al. 2012; Sewry et al. 2008). Skeletal muscle fibers have two fundamental structures, excitation–contraction (E–C) coupling machinery and contractile apparatus, which are essential for muscle contraction. Briefly, an action potential in muscle fiber is conducted into the interior of muscle fibers along transverse tubules (T-tubules), which are invaginations of the sarcolemma, and induces the release of Ca^{2+} from the sarcoplasmic reticulum (SR). The SR is a modified endoplasmic reticulum that stores Ca^{2+} in muscle cells. The T-tubules tightly associate with two portions of SRs to form a structure called a triad. The released Ca^{2+} binds to troponin C in the contractile apparatus and triggers the interaction between actin thin filaments and myosin thick filaments. Mutations in the genes associated with the E–C coupling machinery or the contractile apparatus cause congenital myopathies (Al-Qusairi and Laporte 2011; de Winter and Ottenheijm 2017; Dowling et al. 2014).

Both muscular dystrophies and congenital myopathies are very rare. To the best of our knowledge, over 80 causative genes have been identified in muscular dystrophies and congenital myopathies (Kaplan and Hamroun 2015) since the discovery of the *DMD* gene as a causative for Duchenne muscular dystrophy (DMD) (Koenig et al. 1987). Despite considerable efforts in molecular genetic studies, it is still difficult to identify causative mutations in more than half of patients (Nishikawa et al. 2017). Further development of genetic and functional analysis is required to decipher the mechanism of the disease. As there is no available cure for any form of muscular dystrophy or congenital myopathy, a variety of therapeutic approaches has been extensively studied. Identifying causative genes in patients could lead to a better understanding of the molecular basis of the pathology of these diseases and development of therapies.

10.2 Advantages of Zebrafish for Research into Inherited Muscular Disorders

Numerous studies on muscular dystrophies and congenital myopathies using patient samples, cultured cell systems, and mouse models have contributed to the identification of causative genes and an understanding of their pathomechanisms.

Cultured cell systems, where gene expression can be easily manipulated by RNAi or introduction of cloned cDNA of a gene of interest, allow us to investigate the effect of loss-of-function or gain-of-function mutations on muscle cells. They are also suited to drug screening assays because they are inexpensive, easy to grow, and reproducible. However, cultured cell systems have limitations owing to the difficulties to recapitulate the nerve–muscle interaction which is essential for muscle fiber maturation and muscle contraction. Thus, muscle contraction, which is considered an important factor in the pathomechanism of muscular dystrophies, does not occur in the cellular system. In addition, it is difficult to analyze the effect of gene mutations on the sites of connection between muscle and other tissues, such as neuromuscular junctions (NMJs) or myotendinous junctions (MTJs), which are often compromised in inherited muscular disorders.

The mouse is an excellent mammalian model with a similar anatomy and physiology to humans. Mouse models are widely used; however, it is expensive to maintain large numbers of laboratory animals and generate genetically engineered mouse strains. A large-scale drug screening or forward genetic approach is not feasible in mouse models due to the cost and time required. In addition, mice have a much higher capacity of muscle regeneration than humans (Dangain and Vrbova 1984; Turk et al. 2005). Therefore, mice are not an entirely desirable disease model for muscular dystrophy.

Zebrafish have several desirable attributes that complement these models. First, the basic structure of zebrafish skeletal muscle is similar to that of humans (Fig. 10.1). Furthermore, their large clutch size, rapid development, and relatively small genome size (approximately 60% of the mouse genome) make zebrafish suitable for large-scale mutagenesis (Howe et al. 2013). Several zebrafish mutants with myopathic phenotypes, such as *sapje* and *candyfloss*, were identified using a forward genetic approach (Granato et al. 1996). The transparency of the embryos enables us to visualize skeletal muscle in live animals. In particular, the muscle birefringence assay is useful for muscle disease research (Berger et al. 2012; Felsenfeld et al. 1990; Granato et al. 1996). Under polarized light zebrafish muscle can be detected as a bright area, whereas affected muscle appears dark (Fig. 10.2). This noninvasive, readily accessible assay was used to identify myopathic mutants in forward genetic screening or drug screening assays as a simple readout. In addition, a number of transgenic zebrafish expressing fluorescent markers driven by muscle-specific promoters were created (Fig. 10.3) (Elworthy et al. 2008; Higashijima et al. 1997; Seger et al. 2011). Transgenic zebrafish enable visualization of the dynamic physiological processes such as sarcolemmal repair or calcium influx in muscle fibers (Horstick et al. 2013; Roostalu and Strähle 2012). Moreover,

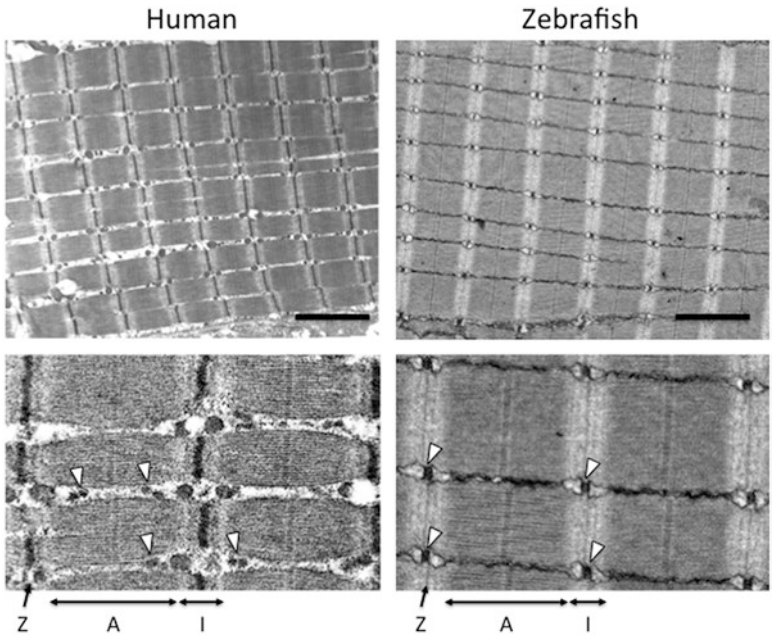

Fig. 10.1 Ultrastructure of human skeletal muscle and zebrafish skeletal muscle**.** Longitudinal section of human skeletal muscle (left panels) and zebrafish skeletal muscle (right panels). Basic structure including well-aligned sarcomeres and triads are conserved between human and zebrafish. *Z* Z-disc, *A* A band, *I* I band. Arrowheads indicate triads. Scale bar, 2 μm

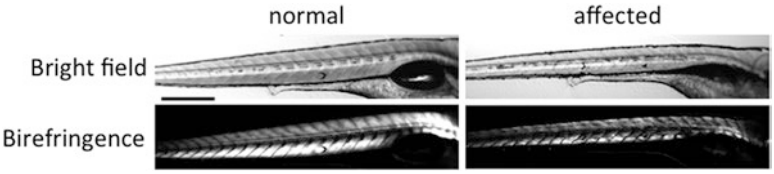

Fig. 10.2 Muscle birefringence
Muscle birefringence is a light effect that results from the diffraction of polarized light through the pseudo-crystalline array of the muscle sarcomeres. Muscle degeneration is detected as a dark area under polarized light. Upper panel: birefringence of normal trunk muscle. Lower panel: birefringence of affected trunk muscle. 4 dpf zebrafish embryos. Rostral is to the right. Scale bar, 400 μm

developing zebrafish embryos display stereotyped motor behavior within 48 hours postfertilization (hpf). They show spontaneous alternating contractions called spontaneous coiling at around 19 hpf and then develop a touch-evoked escape response at around 48 hpf (Saint-Amant and Drapeau 1998). These motor behaviors provide simple measures of locomotor activity and can be utilized to detect muscle weakness. Microinjection of antisense morpholinos (AMOs) or mRNA allows manipulation of gene expression in zebrafish in a quick and easy way. Zebrafish embryos

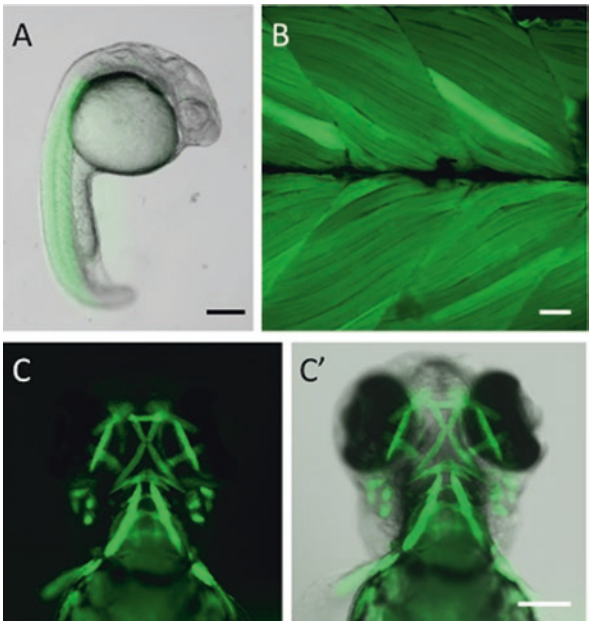

Fig. 10.3 Transgenic zebrafish with muscle-specific fluorescent reporter
Muscle-specific reporter zebrafish line. Transgenic zebrafish [Tg(α-actin–GFP)] expressing green fluorescent protein (GFP) driven by skeletal muscle actin (α-actin) promoter. (**a**) Image of GFP fluorescence merged with bright-field image at 1 dpf. Scale bar, 200 μm. (**b**) Confocal laser scanning microscopy of trunk muscle of [Tg(α-actin–GFP)] at 3 dpf, visualizing muscle fibers aligned orderly. Rostral is to the right. Scale bar, 20 μm. (**c**, **c'**) Facial musculature visualized by GFP at 3 dpf. (**c**) GFP fluorescence. (**c'**) Merged image. Ventral view. Rostral is to the top. Scale bar, 200 μm

with morpholino-mediated knockdown, or "morphants," have been widely used as models of loss-of-function mutations. Furthermore, zebrafish embryos readily absorb small compounds. Thus, zebrafish have great potential as a platform for high-throughput drug screening. Recently, genome editing technologies have been applied to zebrafish (Hwang et al. 2013). It would be straightforward to create zebrafish models of inherited muscular disorders that harbor mutations in specific genes.

10.3 Zebrafish Mutant Models of Muscular Dystrophies

In 1996, Granato et al. first suggested the potential of zebrafish as a model for muscle disease (Granato et al. 1996). They reported zebrafish motility mutants obtained from a forward genetic approach. They described four mutants (*sapje*, *softy*, *runzel*, and *schwammerl*) characterized by initially normal muscle formation

but reduced muscle birefringence and slow swimming around 96 hpf. The observed phenotypes were similar to the condition of human muscular dystrophy characterized by progressive muscle weakness and muscle degeneration. In 2003, Guyon et al. demonstrated that injection of AMOs against the zebrafish ortholog of the *DMD* gene, encoding dystrophin, into zebrafish embryos caused a curved or bent body phenotype after hatching out of the chorion (Guyon et al. 2003). The dystrophin morphants were less active than control embryos, lying on the bottom of the culture dish. Immunohistochemistry revealed that dystrophin predominantly expressed in myosepta, a tendon-like structure of fish, and that two DGC components, β- and γ-sarcoglycan, were colocalized with dystrophin. Importantly, the dystrophin morphants showed reduction of the sarcoglycans as well as dystrophin, suggesting that dystrophin forms the DGC with sarcoglycans in zebrafish as in mammals. Concurrent reduction of dystrophin and sarcoglycans is frequently observed in human DMD patients.

In addition, Bassett et al. revealed that *sapje*^{ta222a} mutants carry a nonsense mutation in the zebrafish dystrophin gene (Bassett et al. 2003). It implied that the function of genes associated with muscle integrity may be conserved between human and zebrafish. Of note, Bassett et al. found that the progressive muscle degeneration of *sapje* is caused by the separation of muscle fibers from their attachment points on the myosepta. Given that the myosepta is analogous to mammalian tendon, the junctional areas between muscle fibers and the myosepta would correspond to MTJs. In previous studies with mouse models of muscular dystrophies, most attention focused on the role of DGC in maintaining the integrity of non-junctional sarcolemma. However, studies of dystrophin morphants and *sapje* mutants in zebrafish have suggested a novel pathomechanism of DMD and a potential role of DGC in maintaining the integrity of MTJs. Another important point is that *sapje* mutants recapitulate the human DMD condition better than mouse models in terms of severity. *Sapje* mutants did not display recovery of muscle degeneration and died after several weeks postfertilization (wpf) (Bassett et al. 2003). In contrast, dystrophin-deficient mdx mice show much milder muscle degeneration and do not show decreased survival rate, probably because of the high regenerative capacity of murine skeletal muscle. Furthermore, Berger et al. observed mononucleated cell infiltration, variation in fiber size, fibrosis, and active proliferation of Pax7-positive muscle progenitor cells in sapje mutants, demonstrating that sapje mutants closely resemble the human DMD muscle pathology (Berger et al. 2010).

10.3.1 Zebrafish Models of DGC Deficiency

In mammals, dystrophin is associated with the glycoproteins α-, β-, γ-, and δ-sarcoglycan and α- and β-dystroglycan (Ozawa et al. 1995). Mutations in these dystrophin-associated glycoproteins cause muscular dystrophies (Bonnemann et al. 1995; Hara et al. 2011; Lim et al. 1995; Nigro et al. 1996; Noguchi et al. 1995; Roberds et al. 1994). The importance of δ-sarcoglycan in zebrafish was investigated

by antisense morpholino injection targeting zebrafish δ-sarcoglycan. The morphants showed abnormal phenotypes similar to dystrophin morphants, curved body shape, reduced activity, and concurrent reduction of γ-sarcoglycan at myosepta (Cheng et al. 2006; Guyon et al. 2005), suggesting a conserved role of sarcoglycans in muscle integrity in zebrafish.

Dystroglycan is a central component of the DGC that directly binds to dystrophin. Both α- and β-dystroglycans are encoded by a single gene, *DAG1,* and each protein is generated by proteolytic processing of a precursor protein (Ibraghimov-Beskrovnaya et al. 1992). α-Dystroglycan is an extracellular subunit that binds to laminin α2, which is an ECM protein in the basal lamina. *O*-linked glycosylation of α-dystroglycan is critical for its binding to laminin. β-Dystroglycan is an integral membrane protein that binds to dystrophin via the C-terminal region. Overall, dystroglycan links the cytoplasmic actin filament network with the ECM. Dystroglycan is essential for mammalian embryogenesis. *Dag1* null mice are embryonic lethal due to failure to form the rodent-specific basement membrane known as Reichert's membrane (Williamson et al. 1997). To examine the role of dystroglycan in vertebrate skeletal muscle, Parsons et al. knocked down dystroglycan with AMO against zebrafish *dag1*. The *dag1* morphants survived and appeared normal prior to 24 hpf, suggesting that *dag1* is not necessary for external development of zebrafish embryos. The knockdown of *dag1* caused necrosis and disorganization of the sarcomere and SR, suggesting that *dag1* is required for maintenance of muscle fibers rather than muscle formation (Parsons et al. 2002). Two *dag1* mutants were later reported, *patchytail* and *dag1*^{hu3072} (Gupta et al. 2011; Lin et al. 2011). *Patchytail* mutants contain a point mutation resulting in a p.V567D substitution in the C-terminal domain of α-dystroglycan that interacts with β-dystroglycan. *Patchytail* mutants showed progressive reduction of muscle birefringence, implicating progressive muscle degeneration. Structural abnormality of the myosepta was observed under an electron microscope, further suggesting an important role of DGCs in the MTJs. Interestingly, this mutant showed structural abnormalities in the triads, as irregular-shaped T-tubules and disorganized SR. These findings suggest an unexpected role of dystroglycan in E–C coupling (Gupta et al. 2011). In addition to skeletal muscle abnormalities, *patchytail* mutants showed eye structure abnormalities and brain abnormalities. The cells within the ganglion layers were loosely packed in the posterior chamber, and the cells with inclusion bodies were present in the lens. The tectal cells were less organized in the midbrain and granular cell layer in the cerebellum. These phenotypes are quite similar to the phenotypes of human muscle–eye–brain disease (MEB) and Walker–Warburg syndrome (WWS), known as α-dystroglycanopathy associated with reduced *O*-linked glycosylation of α-dystroglycan. Because dystroglycan is strongly expressed in the eyes and central nervous system (CNS) in addition to skeletal muscle, it is rational that a deficiency of dystroglycan affects these organs. Thus, zebrafish *dag1* mutants suggest that mutations in *dag1* might cause MEB or WWS in humans.

Another *dag1* mutant fish, *dag1*^{hu3072}, has a nonsense mutation p.R398*, predicting a truncation of α-dystroglycan within the mucin domain. Antibodies against α- and β-dystroglycan did not detect endogenous dystroglycans in the homozygous

embryos, indicating that the *dag1*^{hu3072} mutant is a complete loss-of-function model (Lin et al. 2011). This mutant showed a more severe phenotype than the *patchytail* mutant and exhibited severe muscular dystrophy with muscle fiber detachment and loss of dystrophin at the vertical myosepta. In the same year, the first limb-girdle muscular dystrophy (LGMD) patient with *DAG1* mutation (p.T192M) was reported (Hara et al. 2011). This patient had accompanied mental retardation with muscular dystrophy. Biochemical analysis in vitro revealed that the p.T192M mutation affected the affinity of α-dystroglycan to laminin. Recently, other patients with DAG1 mutations were reported (Dong et al. 2015; Geis et al. 2013). Two Libyan patients with p.C669F mutations in β-dystroglycan presented more severe phenotypes similar to MEB disease with multicystic leukodystrophy. Given that *patchytail* mutants showed abnormalities in their muscle, eyes, and brain, the *dag1* mutant zebrafish would be a useful animal model for further analysis of the molecular mechanism of *DAG1*-related muscular dystrophy and to study a therapeutic approach.

10.3.2 Zebrafish Model of Laminin Deficiency

Laminins are major structural components of the basal lamina. There are three laminin subunits, α-, β-, and γ-chains, which form heterotrimers. Laminin-2 is the major laminin isoform in skeletal muscle that consists of α2, β1, and γ1 chains. As mentioned above, laminin binds to the DGC through α-dystroglycan. The resulting linkage between the subsarcolemmal actin cytoskeleton and the basal lamina stabilizes the sarcolemma against mechanical stress. Mutations in the laminin α2 (*LAMA2*) gene cause severe congenital muscular dystrophy with merosin deficiency (MDC1A) (Helbling-Leclerc et al. 1995). Studies using mouse models of laminin α2 deficiency suggested that apoptosis may contribute to the pathology (Gawlik and Durbeej 2011). Three zebrafish lines with *lama2* mutations were isolated using a forward genetic approach. Among these, *candyfloss* mutant strains (*caf*^{teg15a} and *caf*^{tk209}) have nonsense mutations that add a premature stop codon within the C-terminal globular domain in laminin α2 protein (Hall et al. 2007). This domain is essential for the binding of laminin α2 to dystroglycan, and the mutations are located in close proximity to human MDC1A mutations. In *caf* mutants, initial formation of muscle fibers appeared normal, but a dystrophic phenotype was observed by 72 hpf, and most mutants died around 2 weeks. As seen in dystrophin-deficient zebrafish, fiber detachment from vertical myosepta occurred in *caf* mutants. Immunohistochemical analysis showed that dystrophin, β-dystroglycan, and laminin 1 were detectable at the MTJs in *caf* mutants, indicating that fiber attachment failure occurred within the ECM rather than at the sarcolemma.

Gupta et al. reported another laminin mutant, *lama2*$^{cl501/cl501}$, with RNA missplicing of the *lama2* transcript (Gupta et al. 2012). This mutant developed progressive muscle degeneration and died at around 1–2 weeks. This *lama2*$^{cl501/cl501}$ strain showed growth defects in the brain and eyes. Growth retardation is also reported in

laminin α2-deficient mice (Miyagoe et al. 1997). Hall et al. examined whether muscle damage in *candyfloss* mutants was related to muscle contraction. Mutant embryos raised under anesthesia did not develop muscle degeneration up to 72 hpf. In contrast, mutants raised in viscous media (0.6% methylcellulose), which put an increased mechanical load on muscle, showed more severe muscle damage than those in normal media (Hall et al. 2007). A protective effect of immobilization on muscle damage was also observed in *sapje* mutants (Li and Arner 2015), suggesting that zebrafish dystrophic mutants recapitulate the pathomechanism of muscular dystrophy, that is, muscle degeneration caused by contraction-induced mechanical stress. This strengthens the relevance of zebrafish as a model of muscular dystrophy.

10.4 Zebrafish Mutant Models of Congenital Myopathies

10.4.1 Zebrafish Model of E–C Coupling Defect

The E–C coupling machinery mediates the action potential transmitted by the motor neuron into intracellular Ca^{2+} release and muscle contraction. Membrane depolarization spreads down into the muscle fiber via T-tubules and activates the dihydropyridine receptor (DHPR) in the T-tubules, triggering the opening of the ryanodine receptor 1 (RyR1) in the adjacent SR. Activation of the RyR induces release of Ca^{2+} from the SR into the cytosol of the muscle fiber, allowing the interaction between actin and myosin in the contractile apparatus. It is known that mutations in genes associated with E–C coupling cause a variety of myopathies.

Hirata et al. reported that the zebrafish *relatively relaxed* (*ryr*^{mi340}) mutant carries a mutation in the *ryr1b* gene (Hirata et al. 2007). This mutation causes aberrant splicing, resulting in a premature stop codon in the middle of the ryr1b protein. The homozygous *ryr* mutant showed slow swimming after 36 hpf, although electrophysiological tests indicated that the CNS and NMJs are not affected. Live imaging techniques using a Ca^{2+} indicator dye revealed that the Ca^{2+} transients in fast muscle were compromised in the homozygous *ryr* mutants, suggesting a defect in E–C coupling in fast muscle. Immunohistochemistry showed that RyRs, DHPRα1, DHPRα2, and DHPRβ were not localized in the junctions between the T-tubule and SR in fast muscle in homozygous *ryr* mutants. *RYR1* mutations in humans cause a wide variety of congenital myopathies including central core disease and multi-minicore disease (Hwang et al. 2012). Ultrastructural analysis of the homozygous *ryr* mutants revealed small amorphous cores that were similar to the minicores observed in multi-minicore disease patients. Furthermore, Hirata et al. demonstrated that normal swimming was recovered in the homozygous *ryr* mutants by the introduction of AMO to restore splicing of the *ryr1b* transcript. These results suggested that *ryr* mutants could serve as a useful animal model of multi-minicore disease.

Recently, Horstick et al. identified mi34 zebrafish mutants that show defective motor behavior such as spontaneous coiling, touch-induced escape contractions, and touch-induced swimming. Live imaging of Ca^{2+} transients with GCaMP3 Ca^{2+} indicator revealed greatly reduced Ca^{2+} transients in skeletal muscles in the mi34 mutants, suggesting a defect in the E–C coupling. The gene responsible for the mi34 phenotype was identified as *stac3*, encoding an adaptor-like protein of unknown function (Horstick et al. 2013). mi34 mutants have a point mutation that disrupts a splice donor site, resulting in no Stac3 protein. Immunohistochemical analysis revealed that Stac3 is specifically expressed in skeletal muscles and colocalizes with DHPRα1 and presumably RyR1. Immunoprecipitation assays indicated that Stac3 is associated with both DHPRα1 and RyR1 in wild-type adult muscle. These results suggest that Stac3 is a novel essential component of the E–C coupling machinery. In addition, the authors identified mutations in the human *STAC3* gene in a cohort of congenital Native American myopathy families. Native American myopathy is an autosomal recessive disorder found within the Lumbee Native American population, characterized by muscle weakness, susceptibility to malignant hyperthermia, multiple joint contractures, and dysmorphic facial features. In the cohort, a c. G1046C point mutation was identified, resulting in p.W284A substitution in the first SH3 domain of the STAC3 protein. The effect of the p.W284S mutation on STAC3 protein function was investigated using zebrafish mi34 mutants. A phenotypic rescue experiment showed that expression of wild-type zebrafish stac3 rescued touch-induced swimming in mi34 mutants, whereas expression of zebrafish stac3 with an analogous W-to-S substitution failed to rescue the phenotype. STAC3 mutations were first identified in the zebrafish mutant, shedding light on the molecular cause of the myopathy. This study emphasizes the value of zebrafish in medical research into human genetic disorders.

10.4.2 Zebrafish Model of Contractile Apparatus Defect

Contractile apparatus is a specialized structure for muscle contraction. It consists of basic units called sarcomeres that are mainly composed of myosin thick filaments and actin thin filaments. Mutations in human genes associated with the actin thin filaments cause nemaline myopathy, one of the most common forms of congenital myopathies characterized by neonatal hypotonia, severe weakness, facial and respiratory muscle involvement, and abnormal rodlike structures (nemaline rods) on muscle pathology (Nance et al. 2012; Sewry et al. 2008). *NEB*, encoding nebulin, is a known causative gene of nemaline myopathy. Nebulin is believed to work as a "molecular ruler" for actin filament assembly and regulates the length of the thin filaments.

Telfer et al. utilized publicly available zebrafish mutants (hu2849, termed *neb*) with a nebulin gene mutation generated by ENU mutagenesis at the Sanger Institute Zebrafish Mutant Resource (http://www.sanger.ac.uk/resources/zebrafish/zmp/) (Telfer et al. 2012). *neb* mutants have a mutation in the splice donor site that leads

to exon 43 exclusion. *neb* homozygous mutants showed an impaired touch-induced escape response and reduced muscle birefringence and died by 7 days postfertilization (dpf). The authors developed a method to measure peak force and kinetics of force generation of zebrafish larvae and revealed impaired force generation in *neb* mutants. Electron microscopy and immunofluorescence showed short length of thin filaments and abnormal aggregates with filamentous material containing α-actinin and actin, mirroring the muscle pathology of nemaline myopathy patients. This study suggests the great potential of the public mutant library to find a zebrafish model for other myopathies.

10.5 Transient Models by Antisense Morpholino-Mediated Knockdown

Morpholino-mediated knockdown is a useful technology to investigate the effect of loss-of-function of genes of interest in a whole organism. It has potential to rapidly create disease models of autosomal recessive disorders. To date, a number of muscle disease models have been created by morpholino injection (summarized in Table 10.1) (Avsar-Ban et al. 2010; Bragato et al. 2016; Dowling et al. 2009; Jurynec et al. 2008; Kawahara et al. 2010; Koshimizu et al. 2011; Li et al. 2013; Lin et al. 2011; Lo et al. 2015; Nixon et al. 2005; Postel et al. 2008; Smith et al. 2014; Sztal et al. 2015; Telfer et al. 2010; Thornhill et al. 2008; Vieira et al. 2014; Vogel et al. 2009; Wood et al. 2011; Zhang et al. 2009). This review will focus on the study by Roostalu and Strähle that highlights the power of zebrafish to elucidate molecular mechanisms underlying muscular dystrophy associated with *DYSF* mutation.

Mutations in the human *DYSF* gene cause LGMD type 2B or Miyoshi myopathy. *DYSF* encodes a large transmembrane protein, dysferlin, which has been proposed to be involved in plasma membrane repair (Bansal et al. 2003). The importance of dysferlin in muscle integrity was demonstrated by two independent AMO-mediated knockdown experiments where *dysf* morphants showed reduction of muscle birefringence and disorganization of myofibrils (Kawahara et al. 2011b; Roostalu and Strähle 2012). Roostalu and Strähle expressed fluorescent-tagged dysferlin (Dysf-mTFP1) in zebrafish muscle to monitor dysferlin localization and generated small sarcolemmal ruptures in live zebrafish embryos with two-photon laser pulses (Roostalu and Strähle 2012). In this system, they observed a rapid Dysf-mTFP1 accumulation at the sarcolemmal lesion. Their high-resolution imaging visualized real-time membrane resealing in myofibers in live animals and revealed that annexins participate in the resealing process. Annexin A6 (Anxa6) simultaneously accumulated with dysferlin at the lesion and formed a repair patch. Subsequently, annexin A2a (Anxa2a) was recruited to the site followed by annexin A1a (Anxa1a). Knockdown of dysferlin or Anxa6 perturbed Anxa1a and Anxa2a accumulation at the lesion. Moreover, knockdown of both dysferlin and Anxa6 caused failure to generate a dense repair patch. This elegant optical assay would be difficult in mam-

Table 10.1 Zebrafish models of human muscular dystrophies and congenital myopathies

Categories	Human gene	Zebrafish gene	Human disease	Model type	Reference
Muscular dystrophy	*DMD*	*dmd*	Duchenne muscular dystrophy (DMD)	Morpholino	Guyon et al. (2003)
				Mutant (*sapje*)	Bassett et al. (2003)
				Mutant (*sapje-like*)	Guyon et al. (2009)
	LMNA	*lmna*	Limb-girdle muscular dystrophy type 1B (LGMD1B)	Morpholino	Vogel et al. (2009) and Koshimizu et al. (2011)
	DUX4		Facioscapulohumeral muscular dystrophy (FSHD)	mRNA injection	Wallace et al. (2011) and Mitsuhashi et al. (2013)
	PTRF	*ptrfa*	Muscular dystrophy with lipodystrophy	Morpholino	Lo et al. (2015)
	CAV3	*cav3*	Limb-girdle muscular dystrophy type 1C (LGMD1C)	Morpholino	Nixon et al. (2005)
				Overexpression (Transgenic)	Lo et al. (2015)
	DNAJB6	*dnajb6b*	Limb-girdle muscular dystrophy type 1D (LGMD1D)	mRNA injection / Morpholino	Sarparanta et al. (2012)
	DES	*desma*	Limb-girdle muscular dystrophy type 1E (LGMD1E)	Morpholino	Vogel et al. (2009)and Li et al. (2013)
	HNRPDL	*hnrpdl*	Limb-girdle muscular dystrophy type 1G (LGMD1G)	Morpholino	Vieira et al. (2014)
	DYSF	*dysf*	Limb-girdle muscular dystrophy type 2B (LGMD2B)	Morpholino	Kawahara et al. (2011a, b) and Roostalu and Strähle (2012)
	SGCD	*sgcd*	Limb-girdle muscular dystrophy type 2F (LGMD2F)	Morpholino	Guyon et al. (2005) and Cheng et al. (2006)
	TCAP	*tcap*	Limb-girdle muscular dystrophy type 2G (LGMD2G)	Morpholino	Vogel et al. (2009) and Zhang et al. (2009)

	TTN	*ttn1, ttn2*	Limb-girdle muscular dystrophy type 2J (LGMD2J)	Mutant (*runzel*)	Steffen et al. (2007)
				Genome editing (TALEN)	Shih et al. (2016)
	DAG1	*dag1*	Limb-girdle muscular dystrophy	Morpholino	Parsons et al. (2002)
				Mutant (*patchytail*)	Gupta et al. (2011)
				Mutant (*dag1hu3072*)	Lin et al. (2011)
	POPDC1	*popdc1*	Limb-girdle muscular dystrophy and cardiac arrhythmia	Morpholino, Genome editing (TALEN)	Schindler et al. (2016)
Congenital muscular dystrophy	*LAMA2*	*lama2*	Congenital muscular dystrophy with merosin deficiency (MDC1A)	Mutant (*candyfloss*)	Hall et al. (2007)and Smith et al. (2017)
				(*lama2 cl501/cl501*)	Gupta et al. (2012)
	COL6A1	*col6a1*	Ullrich congenital muscular dystrophy, Bethlem myopathy	Morpholino	Telfer et al. (2010)
			Bethlem myopathy	Genome editing (TALEN)	Radev et al. (2015)
	COL6A3	*col6a3*	Ullrich congenital muscular dystrophy	Morpholino	Telfer et al. (2010)
	ITGA7	*itga7*	Congenital muscular dystrophy	Morpholino	Postel et al. (2008)
α-dystroglycanopathy	*FKTN*	*fktn*	Fukuyama congenital muscular dystrophy, Walker-Warburg syndrome (WWS), Limb-girdle muscular dystrophy (LGMD)	Morpholino	Lin et al. (2011) and Wood et al. (2011)
	FKRP	*fkrp*	Congenital muscular dystrophy, Walker-Warburg syndrome (WWS), Muscle-Eye-Brain disease (MEB), Limb-girdle muscular dystrophy (LGMD)	Morpholino	Thornhill et al. (2008), Kawahara et al. (2010), Lin et al. (2011), and Wood et al. (2011)

(continued)

Table 10.1 (continued)

Categories	Human gene	Zebrafish gene	Human disease	Model type	Reference
	POMT1	*pomt1*	Walker-Warburg syndrome (WWS), Limb-girdle muscular dystrophy (LGMD)	Morpholino	Avsar-Ban et al. (2010)
	POMT2	*pomt2*	Walker-Warburg syndrome (WWS), Muscle-Eye-Brain disease (MEB), Limb-girdle muscular dystrophy (LGMD)	Morpholino	Avsar-Ban et al. (2010)
	ISPD	*ispd*	Walker-Warburg syndrome (WWS), Limb-girdle muscular dystrophy (LGMD)	Morpholino	Roscioli et al. (2012)
	GTDC2 (POMGNT2)	*gfdc2*	Walker-Warburg syndrome (WWS)	Morpholino	Manzini et al. (2012)
	B3GNT1	*b3gnt1*	Walker-Warburg syndrome (WWS)	Morpholino	Buysse et al. (2013)
	GMPPB	*gmppb*	Congenital muscular dystrophy, Walker-Warburg syndrome (WWS), Limb-girdle muscular dystrophy (LGMD)	Morpholino	Carss et al. (2013)
	DPM1	*dpm1*	Congenital muscular dystrophy	Morpholino	Ardiccioni et al. (2016) and Marchese et al. (2016)
	DPM2	*dpm2*	Congenital muscular dystrophy	Morpholino	Marchese et al. (2016)
	DPM3	*dpm3*	Limb-girdle muscular dystophy	Morpholino	Marchese et al. (2016)
	B3GALNT2	*b3galnt2*	Congenital muscular dystrophy	Morpholino	Stevens et al. (2013)
	TMEM5	*tmem5*	Congenital muscular dystrophy	Morpholino	Praissman et al. (2016)
	POMK (SGK196)	*pomk*	Congenital muscular dystrophy	Morpholino	Di Costanzo et al. (2014)

Congenital myopathy	*NEB*	*neb*	Nemalin myopathy	Mutant (*neb*)	Telfer et al. (2012)
				Morpholino	Sztal et al. (2015)
	ACTA1	*acta1a, acta1b*	Nemalin myopathy	Overexpression (Transgenic)	Sztal et al. (2015)
	TPM2	*tpm2*	Nemalin myopathy	Overexpression (Transgenic)	Davidson et al. (2013)
	KLHL40	*klhl40a, klhl40b*	Nemalin myopathy	Morpholino	Ravenscroft et al. (2013)
	KLHL41	*klhl41a, klhl41b*	Nemalin myopathy	Morpholino	Gupta et al. (2013)
	LMOD3	*lmod3*	Nemalin myopathy	Morpholino	Yuen et al. (2014)
	MTM1	*mtm1*	Myotubular myopathy	Morpholino	Dowling et al. (2009)
	DNM2	*dnm2a*	Centronuclear myopathy	Morpholino, mRNA injection	Bragato et al. (2016)
	BIN1	*bin1*	Centronuclear myopathy	Morpholino	Smith et al. (2014)
	STAC3	*stac3*	Native American myopathy	Mutant (*mi34*)	Horstick et al. (2013)
	RYR1	*ryr1b*	Multiple forms of congenital myopathy	mutant (*relatively relaxed*)	Hirata et al. (2007)
	SEPN1	*sepn1*	Multiple forms of congenital myopathy	Morpholino	Jurynec et al. (2008)

malian system, and this study highlights the great potential of zebrafish to visualize the dynamic processes associated with muscle disease pathology.

10.6 Zebrafish Models for Identification of Novel Causative Genes

Despite the extensive effort to search for a genetic cause, approximately 70% of inherited muscular disease patients remain undiagnosed (Nishikawa et al. 2017). It is important to give a precise molecular diagnosis to the patient for genetic counseling, prognosis, and choice of treatment. Recently, whole-exome sequencing with a next-generation sequencer (NGS) has been widely used for gene discovery in genetically unsolved diseases. NGS allows rapid, cost-effective screening of large regions of the genome. However, it can also reveal numerous unreported variants of unclear biological significance. To identify true pathogenic variants, functional analysis of genetic variants is required. However, it is time-consuming to verify the pathogenicity of genetic variations using conventionally used mouse models. Currently, zebrafish have been recognized as an ideal model system to validate novel variants identified in patients because of their rapid development and the ease of genetic manipulation. The following are notable examples that the zebrafish aided in the identification of novel causative genes of inherited muscular disorders.

10.6.1 Identification of Novel Causative Genes of α-Dystroglycanopathies

As described above, dystroglycan is a central component of the DGC, and α-dystroglycan requires *O*-mannose-type glycosylation for binding to laminin. Defects of *O*-linked glycosylation of α-dystroglycan cause a clinically and genetically heterogeneous group of disorders called α-dystroglycanopathies (Yoshida-Moriguchi and Campbell 2015). Phenotypes of α-dystroglycanopathies range from severe forms of congenital muscular dystrophy with eye and brain abnormalities, including Fukuyama congenital muscular dystrophy, WWS, and MEB, to relatively mild adult-onset LGMDs. Prior to the advent of NGS, it was discovered that mutations in six genes, *POMT1*, *POMT2*, *POMGNT1*, *FKTN*, *FKRP*, and *LARGE*, all of which are involved in the glycosylation of α-dystroglycan, cause α-dystroglycanopathies. However, mutations in these genes represent only 35% of WWS incidence, suggesting the existence of additional causative genes. Roscioli et al. searched for a novel causative gene involved in WWS. Using a combination of single-nucleotide polymorphism haplotyping and whole-exome sequencing, they identified homozygous or compound heterozygous mutations in the *ISPD* gene, all of which were predicted to cause loss-of-function of the protein. As the function of

ISPD in vertebrates was unknown, they knocked down the *ispd* ortholog in zebrafish by injecting antisense morpholinos. The *ispd* morphants showed reduced eye size, hydrocephalus, brain folding abnormalities, muscle fiber degeneration, compromised sarcolemmal integrity, and reduced glycosylation of α-dystroglycan, recapitulating the major aspects of WWS patients. From these results, the authors concluded that *ISPD* is a novel causative gene for WWS (Roscioli et al. 2012). More recently, mutations in eight additional genes, *GTDC2*, *B3GNT1*, *GMPPB*, *B3GALNT2*, *DPM1*, *DPM2*, *ALG13*, *TMEM5*, and *POMK*, were identified as causative for α-dystroglycanopathies. Except for *ALG13*, morpholino-mediated knockdown in zebrafish was used to determine whether these genes were involved in the pathology of the disease. Each zebrafish morphant displayed muscle, eye, and/or brain defects with reduced glycosylation of α-dystroglycan (Ardiccioni et al. 2016; Buysse et al. 2013; Carss et al. 2013; Di Costanzo et al. 2014; Manzini et al. 2012; Marchese et al. 2016; Praissman et al. 2016; Stevens et al. 2013). These results suggested that all the novel causative genes are involved in posttranslational modification of α-dystroglycan and highlighted zebrafish as a remarkably useful model for the study of α-dystroglycanopathies.

10.6.2 Identification of Novel Causative Genes of Nemaline Myopathies

In addition to *NEB*, it is known that mutations in *ACTA1*, *TPM2*, *TPM3*, *TNNT1*, and *CFL2* cause nemaline myopathy. These six genes encode the components of actin thin filaments in the contractile apparatus or the regulators of thin filament assembly. However, a substantial number of patients do not have any mutations in these known causative genes, suggesting additional causes of nemaline myopathy. Recently, whole-exome sequencing of genetically undiagnosed patients identified *KBTBD13*, *KLHL40* (*KBTBD5*), *KLHL41* (*KBTBD10*), and *LMOD3* as new causative genes of nemaline myopathies. Among these, a morpholino-mediated knockdown in zebrafish system was used for the functional analysis of *KLHL40*, *KLHL41*, and *LMOD3* genes. In 2013, Ravenscroft et al. used whole-exome sequencing to identify homozygous or compound heterozygous mutations in the *KLHL40* (kelch-like family member 40) gene in a severe form of nemaline myopathy patients (Ravenscroft et al. 2013). Subsequently, Gupta et al. used whole-exome sequencing and identified seven homozygous or compound heterozygous mutations in the *KLHL41* (kelch-like family member 41) gene in cohorts of typical to severe forms of nemaline myopathy patients (Gupta et al. 2013). In mammals, both *KLHL40* and *KLHL41* proteins are abundant in muscle. The zebrafish genome contains two orthologous genes for each human gene: *klhl40a* and *klhl40b* for human *KLHL40* and *klhl41a* and *klhl41b* for human *KLHL41*, respectively. Whole-mount in situ hybridization of zebrafish orthologs showed that *klhl40a* and *klhl41b* are abundant in skeletal muscle and heart, *klhl40b* is abundant in skeletal muscle, and *klhl41a* is expressed ubiquitously during

early development but is diminished in skeletal muscle by 2 dpf. Most of the mutations identified in the patients are located in the conserved BTB-BACK domains or kelch repeats, and the proteins are barely detectable in the patient muscle, suggesting loss of function of *KLHL40* or *KLHL41* proteins. To investigate the role of *KLHL40* and *KLHL41* in muscle development, morpholino-mediated knockdown in zebrafish was performed. Single knockdown of *klhl40a* or *klhl40b* resulted in reduced birefringence and muscle fiber disorganization with small head phenotype. Double morphants of *klhl40a* and *klhl40b* showed more severe phenotypes than single morphants (Ravenscroft et al. 2013). Knockdown of *klhl41* led to similar phenotypes, with reduced birefringence and muscle fiber disorganization. Double *klhl41* morphants showed a curved body and died by 3 dpf (Gupta et al. 2013). Of note, nemaline-like structures were observed in the skeletal muscle of the morphants in both studies. Given that many members of the kelch-like family are involved in the ubiquitin-proteasome pathway (Gupta and Beggs 2014), *KLHL40* and *KLHL41* may be involved in surveillance and protein turnover of thin filament components. Mutations in additional genes related to this pathway may be found in the idiopathic nemaline myopathy in the future. Zebrafish could aid the validation of the pathogenicity of the mutations in novel types of nemaline myopathy.

More recently, *LMOD3* mutations were identified in a cohort of severe, usually lethal, nemaline myopathy (Yuen et al. 2014). *LMOD3*, encoding leiomodin-3, is a member of the tropomodulin protein family, which is characterized by an N-terminal tropomyosin-binding domain and an actin-binding domain with a leucine-rich repeat domain. Leiomodin-3 binds to actin monomers to form a polymerization nucleus. Western blot analysis revealed complete loss or expression of truncated proteins in the patient muscles. Knockdown of zebrafish ortholog, *lmod3*, caused reduced birefringence, disorganized muscle fibers, and aberrant accumulation of α-actinin which frequently accumulates in nemaline rods. The N-terminus of leiomodins is homologous to tropomodulins (TMODs) that cap the pointed ends of actin thin filament and regulate the length and stability of the actin thin filament in contractile apparatus. Berger et al. reported the zebrafish mutant *träge*, which has nonsense mutation in *tmod4* gene (Berger et al. 2014) and shows severe muscle weakness, disorganized muscle fibers, and nemaline-like rod structure in the muscle. Although mutations in *TMOD4* in humans have not been identified in any muscle diseases so far, studies of the zebrafish *träge* mutant have implicated *TMOD4* as a candidate for congenital myopathy of unknown cause.

10.6.3 Identification of DNAJB6 as a Causative Gene of LGMD1D

Zebrafish can be utilized for the validation of dominant mutations. Limb-girdle muscular dystrophy type 1D (LGMD1D) is a muscular dystrophy showing autosomal dominant inheritance. The disease is linked to 7q36, but the causative gene had not yet been determined. Sarparanta et al. identified four heterozygous mutations in

DNAJB6 gene that lead to a p.F89I or p.F93L substitution, in LGMD1D patients (Sarparanta et al. 2012). LGMD1D is characterized by myofibrillar disintegration at Z-discs, abnormal protein accumulations, and autophagic vacuoles on muscle pathology. To validate the pathogenicity of these mutations, human *DNAJB6* mRNAs with patient mutations were injected into zebrafish embryos. Expression of the mutant DNAJB6 resulted in muscle fiber detachment from the vertical myosepta, whereas expression of wild-type DNAJB6 yielded no appreciable defects. Coinjection of wild-type and mutant mRNAs showed enhanced severity of the phenotype, suggesting a dominant toxic function of the mutant protein. DNAJB6 is a cochaperone belonging to the heat-shock protein 40 family and is involved in autophagic and proteasomal protein turnover. The authors hypothesized that DNAJB6 may interact with BAG3, another cochaperone protein that is important for Z-disc maintenance, and tested the hypothesis with the zebrafish system. Coinjection of DNAJB6 mutant and BAG3 mRNAs accentuated the muscle defect compared with a single DNAJB6 mutant injection, suggesting a role for BAG3 in the pathomechanism of LGMD1D. Nam et al. reported severe childhood-onset LGMD1D cases and identified the p.F91L mutation in *DNAJB6* in the patients (Nam et al. 2015). They also utilized zebrafish for functional analysis, and injection of mutant *DNAJB6* mRNA caused detachment of muscle fibers as seen in the previous study. They compared the effect of each mutation identified in the LGMD1D patients and showed that p.F89I or p.F91L mutations caused more severe muscle defects than the p.F93L mutation.

10.6.4 Evaluation of the Pathogenicity of DUX4: A Candidate Gene for FSHD

Facioscapulohumeral muscular dystrophy (FSHD) is a unique autosomal dominant muscular dystrophy characterized by asymmetric muscle weakness and atrophy in the face, shoulders, and upper arms. In addition to muscle involvement, FSHD is frequently accompanied by retinal vasculopathy and/or hearing loss. The genetic cause of FSHD is known to be the contraction of tandemly arrayed macrosatellite repeats, named D4Z4 repeats, on chromosome 4q35. The D4Z4 array usually consists of 11–100 repeats in healthy individuals, whereas it consists of 1–10 repeats in most of the FSHD patients. It remained unclear how the reduction in D4Z4 copy number causes the autosomal dominant disorder. The epigenetic mechanism was recently discovered showing how contraction of D4Z4 repeats leads to depletion of heterochromatic feature of the region allowing misexpression of the *DUX4* gene located within the last D4Z4 unit. DUX4 protein is a transcription factor with double homeobox domains. Overexpression of a full-length isoform of DUX4 (DUX4-fl) in a cell culture system induces apoptosis and activates hundreds of genes involved in early embryogenesis, stem cell program, and germline cells (Bosnakovski et al. 2008; Geng et al. 2012; Kowaljow et al. 2007). Therefore,

DUX4 was proposed as a candidate gene of FSHD. However, this hypothesis was controversial because the level of DUX4-fl expression in FSHD muscle is extremely low. In addition, at that time no animal models expressed the relevant level of DUX4-fl because the DUX4-fl transgenic mouse was embryonic lethal due to its high toxicity. To generate an animal model that matched the low level of DUX4-fl expression, human DUX4-fl mRNA was injected into zebrafish embryos. Because of the high productivity of zebrafish, the dose of the mRNA could easily be titrated. Although injection of 10 pg of DUX4-fl mRNA was lethal, injection of 0.1 pg of the mRNA recapitulated several human phenotypes, including muscle degeneration, and the non-muscle phenotypes such as eye and ear abnormalities and asymmetric involvement of affected organs (Mitsuhashi et al. 2013). Facial muscle disorganization and mislocalization of myogenic cells during development were demonstrated using transgenic zebrafish that express enhanced green fluorescent protein (EGFP) under muscle-specific promoter. These results support the hypothesis for a role of DUX4-fl in FSHD pathogenesis.

10.7 Zebrafish Models Created by Genome Editing Technologies

A method for targeted mutagenesis in zebrafish has long been sought. However, recent advances in genome editing technologies such as zinc finger nucleases (ZFNs), transcription activator-like effector nucleases (TALENs), and clustered regularly interspaced short palindromic repeats (CRISPR)/Cas9 system enable us to induce lesions in a targeted gene (knockout) in zebrafish. In addition, several studies have shown that targeted gene replacement (knockin) can be carried out (Auer et al. 2014; Hisano et al. 2015; Kimura et al. 2014). Thus, zebrafish have become an unexemplified vertebrate model where both forward and reverse genetic approaches can be utilized. To date, there are still a few reports on muscle disease models using genome editing technologies. However, these new technologies will certainly accelerate the generation of zebrafish models for inherited muscular disorders.

Radev et al. generated a zebrafish model of Bethlem myopathy by disrupting an essential splice site in *col6a1* gene by TALEN, resulting in an in-frame skipping of exon 14 (Radev et al. 2015). The skipping of exon 14 of *COL6A1*, encoding collagen type VI alpha-1 chain, is frequently found in Bethlem myopathy patients and prevents the assembly of collagen VI and inhibits the secretion of tetramers into the ECM. The established zebrafish mutant line, $col6a1^{ama605003}$, showed no apparent phenotype in muscle birefringence or locomotor activity within 4 dpf. However, abnormal intracellular vacuoles, disorganized myofibrils, enlarged SR, and altered mitochondrial morphology were observed in the mutants at 3 wpf. These phenotypes worsened with aging and were more severe in homozygotes than heterozygotes. Thus, the progressive muscle alteration and codominant character were reproduced in the $col6a1^{ama605003}$ mutants. This stable mutant line is expected to serve as a platform for drug discovery assay for Bethlem myopathy in the future.

Mutations in the *POPDC1* gene were identified in three patients with LGMD and cardiac arrhythmia in a family originating from a small isolated region in Italy. Whole-exome sequencing identified the p.S201F variation in POPDC1 in this family, but the same variation was not detected in another 104 patients with similar symptoms, suggesting the variation to be very rare. *POPDC1* encodes a plasma membrane-localized cAMP-binding protein, and p.S201F substitution is located within the Popeye domain which functions as a cAMP-binding domain. To elucidate the role of *POPDC1* in the disease, Schindler et al. first knocked down *popdc1* in zebrafish using antisense morpholino (Schindler et al. 2016). The *popdc1* morphants displayed atrioventricular block, muscle fiber detachment, and malformed MTJs. Next, to directly test the pathogenicity of the p.S201F substitution, they introduced a corresponding mutation (p.S191F) into the zebrafish *popdc1* gene using TALEN-mediated genome editing. Homozygous *popdc1*^{S191F} embryos displayed cardiac edema and abnormalities in trunk muscle. However, these phenotypes showed a reduced penetrance of approximately one-third of the embryos. Electron microscopy and immunofluorescence revealed muscle fiber detachment and aberrant formation of MTJs with various degrees of severity at 5 dpf. The mutants also reproduced cardiac phenotypes such as cardiac arrhythmia and reduced heart rate although the penetrance was approximately 5–10%. Analysis of adult homozygous mutants revealed that Popdc1 and Popdc2 proteins were diminished in the plasma membrane and an increased number of intracellular vesicles with Popdc1 were detected in the mutant skeletal muscle, mirroring the phenotype observed in patients. Generating knockin zebrafish using genome editing technologies would allow us to validate the pathogenicity of the mutations more precisely and provide disease models for longer-term study.

10.8 Drug Screening in Zebrafish Models

There is currently no cure for any forms of muscular dystrophy or congenital myopathy. A model system that is suitable for large-scale drug screening is required to search for new therapeutic pathways or lead compounds that could ameliorate the symptoms. The zebrafish is an ideal animal model to this end because of its small size, rapid development, large numbers of offspring, and conserved function of disease causative genes. The ability of zebrafish embryos to absorb small compounds is also a great advantage for chemical screening. To date, a couple of studies where non-biased chemical libraries were screened with zebrafish models of muscular dystrophy have been published. These studies identified attractive target pathways for the development of therapies in the future.

Kawahara et al. performed a large-scale drug screening using dystrophin-deficient zebrafish, *sapje* and *sapje-like* (Kawahara et al. 2011a). As described above, these mutants show reduced muscle birefringence after 3 dpf. They obtained zebrafish embryos from matings of heterozygous dystrophin mutant pairs, expecting that approximately 25% of embryos would show reduced muscle birefringence.

The resulting embryos were treated in multi-well plates with 140 chemical pools from non-biased 1120 chemicals and observed muscle birefringence at 4 dpf. In the first screen, six chemical pools reduced the numbers of embryos with abnormal birefringence to less than 7.5%. In the second screening, the selected pools were separated into 48 individual chemicals, and seven chemicals were identified as effective for preservation of muscle integrity. These seven chemicals were classified as anti-inflammatory agent, anti-allergic agent, phosphodiesterase (PDE) inhibitor, estradiol steroid, chelating agent, and cardiotonic glycoside. These chemicals did not restore dystrophin expression in the mutant embryos, suggesting a dystrophin-independent mechanism for muscle preservation. In addition, a long-term study where the affected embryos were treated with the seven individual chemicals for 26 days (from 4 to 30 dpf) demonstrated that the PDE inhibitor, aminophylline, extends survival of the affected embryos. The surviving dystrophin-deficient embryos showed a normal muscle structure similar to wild type even at 30 dpf. A series of PDE inhibitors was tested, and sildenafil citrate, a PDE5 inhibitor, was found to have a similar effect to aminophylline. As aminophylline is known to increase the levels of intracellular cAMP and activate protein kinase A (PKA), PKA phosphorylation and activity were examined in aminophylline-treated mutant embryos. Both PKA phosphorylation and the activity were increased in treated embryos, suggesting a role for the PKA pathway in the restoration of muscle integrity. Of note, sildenafil was shown to ameliorate the symptoms in the mouse model of DMD. Therefore, this study provided us with important evidence that zebrafish are suitable for drug screening for inherited muscular disorders.

Another drug screening for DMD treatment using *sapje* zebrafish mutants was performed by Wauch et al. (2014). Their strategy was almost the same as that described above. A total of 640 compounds were screened, and muscle birefringence was measured at 4 dpf as readout. Of note, their screening also identified aminophylline as a positive hit compound, supporting the previous finding. Additionally, they found that monoamine agonists, pergolide, ergotamine, and fluoxetine, had a positive effect on the *sapje* mutant embryos. They further tested a broad class of monoamine agonists and concluded that the serotonin pathway was a common element among the positive hit compounds. To confirm this, they knocked down *slc6a4a* and *slc6a4b*, encoding serotonin transporters, with antisense morpholinos. The *slc6a4b* morphants showed reduced numbers of embryos with abnormal birefringence. Transcriptome analysis of fluoxetine-treated *sapje* mutants revealed gene expression changes involved in calcium homeostasis, suggesting a potential mechanism of action for fluoxetine.

Apart from drug screening with disease models, Xu et al. searched for chemicals that could promote muscle stem cell expansion. They used *myf5* and *mylz2* as markers of muscle cell differentiation since *myf5* is expressed in the earliest myogenic precursors and *mylz2* is expressed in terminally differentiated muscle cells. The embryos of double transgenic zebrafish with *myf5*-GFP and *mylz2*-mCherry were disassociated at the oblong stage, and blastomere cells were cultured in 384-well

plates. A total of 2400 chemicals were screened in this system, and GSK3b inhibitors, calpain inhibitors, and the cAMP activator, forskolin, were identified to increase the signals of myf5-GFP and mylz2-mCherry (Xu et al. 2013). These chemicals were further tested with mouse muscle stem cells (or satellite cells) and human-induced pluripotent stem cells (iPSCs). Among the chemicals, only forskolin triggered the expansion of satellite cell cultures. However, a cocktail of basic fibroblast growth factor (bFGF), GSK3b inhibitor BIO, and forskolin upregulated mesodermal marker genes and promoted myogenic specification of iPSCs. The iPSC-derived cells treated with the "triple cocktail" of the bFGF/BIO/forskolin differentiated into multinucleated myotubes and formed sarcomere structures after 36 days. Transplantation of the "triple cocktail"-treated cells into immunodeficient mouse muscles preinjured by cardiotoxin injection revealed that the iPSC-derived cells engrafted into mouse skeletal muscle and contributed to muscle regeneration in vivo. Therefore, these chemicals might have the potential to promote iPSC-derived regenerative cell therapy for inherited muscular disorders in the future. In addition to non-biased large-scale chemical screening, zebrafish myopathic mutants have been used for pathway-based therapies or gene manipulation therapy (Berger et al. 2011; Dowling et al. 2012; Goody et al. 2012; Li et al. 2014; Lipscomb et al. 2016; Winder et al. 2011). Taken together, zebrafish could be extensively used as a desirable platform for drug screening or testing rational approaches to therapies.

10.9 Concluding Remarks

Accumulating evidence, including extensive use of forward genetics and morpholino knockdown, has demonstrated that zebrafish can be a suitable model for the inherited muscular disorders. Zebrafish is now recognized as an established in vivo model for muscle disease research by taking advantage of the recent developments in genome engineering, live imaging, and drug screening. Combined with the advancement of NGS and genome editing, which are outstanding technologies that have revolutionized current biology, zebrafish will continue to play a pivotal role in this research field. However, we must recognize its capabilities and limitations, as there are biological differences between zebrafish and mammals. In addition, several techniques such as tissue-specific or inducible knockouts are still not common in zebrafish compared to mouse models although they are under development (Ablain et al. 2015; Giacomotto et al. 2015; Kobayashi et al. 2014). We believe that our continuous efforts will establish these techniques in zebrafish in the near future, just like many other techniques that are currently available in zebrafish. We hope to accelerate muscle disease research by using zebrafish to deepen our understanding of the pathomechanisms of diseases, which could eventually lead to the development of new therapies.

References

Ablain J, Durand EM, Yang S, Zhou Y, Zon LI (2015) A CRISPR/Cas9 vector system for tissue-specific gene disruption in zebrafish. Dev Cell 32:756–764. https://doi.org/10.1016/j.devcel.2015.01.032

Al-Qusairi L, Laporte J (2011) T-tubule biogenesis and triad formation in skeletal muscle and implication in human diseases. Skelet Muscle 1:26. https://doi.org/10.1186/2044-5040-1-26

Ardiccioni C, Clarke OB, Tomasek D, Issa HA, von Alpen DC, Pond HL, Banerjee S, Rajashankar KR, Liu Q, Guan Z, Li C, Kloss B, Bruni R, Kloppmann E, Rost B, Manzini MC, Shapiro L, Mancia F (2016) Structure of the polyisoprenyl-phosphate glycosyltransferase GtrB and insights into the mechanism of catalysis. Nat Commun 7:10175. https://doi.org/10.1038/ncomms10175

Auer TO, Duroure K, De Cian A, Concordet JP, Del Bene F (2014) Highly efficient CRISPR/Cas9-mediated knock-in in zebrafish by homology-independent DNA repair. Genome Res 24:142–153. https://doi.org/10.1101/gr.161638.113

Avsar-Ban E, Ishikawa H, Manya H, Watanabe M, Akiyama S, Miyake H, Endo T, Tamaru Y (2010) Protein O-mannosylation is necessary for normal embryonic development in zebrafish. Glycobiology 20:1089–1102. https://doi.org/10.1093/glycob/cwq069

Bansal D, Miyake K, Vogel SS, Groh S, Chen CC, Williamson R, McNeil PL, Campbell KP (2003) Defective membrane repair in dysferlin-deficient muscular dystrophy. Nature 423:168–172. https://doi.org/10.1038/nature01573

Bassett DI, Bryson-Richardson RJ, Daggett DF, Gautier P, Keenan DG, Currie PD (2003) Dystrophin is required for the formation of stable muscle attachments in the zebrafish embryo. Development 130:5851–5860. https://doi.org/10.1242/dev.00799

Berger J, Berger S, Hall TE, Lieschke GJ, Currie PD (2010) Dystrophin-deficient zebrafish feature aspects of the Duchenne muscular dystrophy pathology. Neuromuscul Disord 20:826–832. https://doi.org/10.1016/j.nmd.2010.08.004

Berger J, Berger S, Jacoby AS, Wilton SD, Currie PD (2011) Evaluation of exon-skipping strategies for Duchenne muscular dystrophy utilizing dystrophin-deficient zebrafish. J Cell Mol Med 15:2643–2651. https://doi.org/10.1111/j.1582-4934.2011.01260.x

Berger J, Sztal T, Currie PD (2012) Quantification of birefringence readily measures the level of muscle damage in zebrafish. Biochem Biophys Res Commun 423:785–788. https://doi.org/10.1016/j.bbrc.2012.06.040

Berger J, Tarakci H, Berger S, Li M, Hall TE, Arner A, Currie PD (2014) Loss of Tropomodulin4 in the zebrafish mutant trage causes cytoplasmic rod formation and muscle weakness reminiscent of nemaline myopathy. Dis Model Mech 7:1407–1415. https://doi.org/10.1242/dmm.017376

Bonnemann CG, Modi R, Noguchi S, Mizuno Y, Yoshida M, Gussoni E, McNally EM, Duggan DJ, Angelini C, Hoffman EP (1995) Beta-sarcoglycan (A3b) mutations cause autosomal recessive muscular dystrophy with loss of the sarcoglycan complex. Nat Genet 11:266–273. https://doi.org/10.1038/ng1195-266

Bosnakovski D, Xu Z, Gang EJ, Galindo CL, Liu M, Simsek T, Garner HR, Agha-Mohammadi S, Tassin A, Coppee F, Belayew A, Perlingeiro RR, Kyba M (2008) An isogenetic myoblast expression screen identifies DUX4-mediated FSHD-associated molecular pathologies. EMBO J 27:2766–2779. https://doi.org/10.1038/emboj.2008.201

Bragato C, Gaudenzi G, Blasevich F, Pavesi G, Maggi L, Giunta M, Cotelli F, Mora M (2016) Zebrafish as a model to investigate dynamin 2-related diseases. Sci Rep 6:20466. https://doi.org/10.1038/srep20466

Buysse K, Riemersma M, Powell G, van Reeuwijk J, Chitayat D, Roscioli T, Kamsteeg EJ, van den Elzen C, van Beusekom E, Blaser S, Babul-Hirji R, Halliday W, Wright GJ, Stemple DL, Lin YY, Lefeber DJ, van Bokhoven H (2013) Missense mutations in beta-1,3-N-acetylglucosaminyltransferase 1 (B3GNT1) cause Walker-Warburg syndrome. Hum Mol Genet 22:1746–1754. https://doi.org/10.1093/hmg/ddt021

Carss KJ, Stevens E, Foley AR, Cirak S, Riemersma M, Torelli S, Hoischen A, Willer T, van Scherpenzeel M, Moore SA, Messina S, Bertini E, Bonnemann CG, Abdenur JE, Grosmann CM, Kesari A, Punetha J, Quinlivan R, Waddell LB, Young HK, Wraige E, Yau S, Brodd L, Feng L, Sewry C, MacArthur DG, North KN, Hoffman E, Stemple DL, Hurles ME, van Bokhoven H, Campbell KP, Lefeber DJ, Consortium UK, Lin YY, Muntoni F (2013) Mutations in GDP-mannose pyrophosphorylase B cause congenital and limb-girdle muscular dystrophies associated with hypoglycosylation of alpha-dystroglycan. Am J Hum Genet 93:29–41. https://doi.org/10.1016/j.ajhg.2013.05.009

Cheng L, Guo XF, Yang XY, Chong M, Cheng J, Li G, Gui YH, Lu DR (2006) Delta-sarcoglycan is necessary for early heart and muscle development in zebrafish. Biochem Biophys Res Commun 344:1290–1299. https://doi.org/10.1016/j.bbrc.2006.03.234

Cohn RD, Campbell KP (2000) Molecular basis of muscular dystrophies. Muscle Nerve 23:1456–1471

Dangain J, Vrbova G (1984) Muscle development in mdx mutant mice. Muscle Nerve 7:700–704. https://doi.org/10.1002/mus.880070903

Davidson AE, Siddiqui FM, Lopez MA, Lunt P, Carlson HA, Moore BE, Love S, Born DE, Roper H, Majumdar A, Jayadev S, Underhill HR, Smith CO, von der Hagen M, Hubner A, Jardine P, Merrison A, Curtis E, Cullup T, Jungbluth H, Cox MO, Winder TL, Abdel Salam H, Li JZ, Moore SA, Dowling JJ (2013) Novel deletion of lysine 7 expands the clinical, histopathological and genetic spectrum of TPM2-related myopathies. Brain 136:508–521. https://doi.org/10.1093/brain/aws344

de Winter JM, Ottenheijm CAC (2017) Sarcomere dysfunction in nemaline myopathy. J Neuromuscul Dis 4:99–113. https://doi.org/10.3233/JND-160200

Di Costanzo S, Balasubramanian A, Pond HL, Rozkalne A, Pantaleoni C, Saredi S, Gupta VA, Sunu CM, Yu TW, Kang PB, Salih MA, Mora M, Gussoni E, Walsh CA, Manzini MC (2014) POMK mutations disrupt muscle development leading to a spectrum of neuromuscular presentations. Hum Mol Genet 23:5781–5792. https://doi.org/10.1093/hmg/ddu296

Dong M, Noguchi S, Endo Y, Hayashi YK, Yoshida S, Nonaka I, Nishino I (2015) DAG1 mutations associated with asymptomatic hyperCKemia and hypoglycosylation of alpha-dystroglycan. Neurology 84:273–279. https://doi.org/10.1212/WNL.0000000000001162

Dowling JJ, Vreede AP, Low SE, Gibbs EM, Kuwada JY, Bonnemann CG, Feldman EL (2009) Loss of myotubularin function results in T-tubule disorganization in zebrafish and human myotubular myopathy. PLoS Genet 5:e1000372. https://doi.org/10.1371/journal.pgen.1000372

Dowling JJ, Arbogast S, Hur J, Nelson DD, McEvoy A, Waugh T, Marty I, Lunardi J, Brooks SV, Kuwada JY, Ferreiro A (2012) Oxidative stress and successful antioxidant treatment in models of RYR1-related myopathy. Brain 135:1115–1127. https://doi.org/10.1093/brain/aws036

Dowling JJ, Lawlor MW, Dirksen RT (2014) Triadopathies: an emerging class of skeletal muscle diseases. Neurotherapeutics 11:773–785. https://doi.org/10.1007/s13311-014-0300-3

Elworthy S, Hargrave M, Knight R, Mebus K, Ingham PW (2008) Expression of multiple slow myosin heavy chain genes reveals a diversity of zebrafish slow twitch muscle fibres with differing requirements for Hedgehog and Prdm1 activity. Development 135:2115–2126. https://doi.org/10.1242/dev.015719

Felsenfeld AL, Walker C, Westerfield M, Kimmel C, Streisinger G (1990) Mutations affecting skeletal muscle myofibril structure in the zebrafish. Development 108:443–459

Gawlik KI, Durbeej M (2011) Skeletal muscle laminin and MDC1A: pathogenesis and treatment strategies. Skelet Muscle 1:9. https://doi.org/10.1186/2044-5040-1-9

Geis T, Marquard K, Rodl T, Reihle C, Schirmer S, von Kalle T, Bornemann A, Hehr U, Blankenburg M (2013) Homozygous dystroglycan mutation associated with a novel muscle-eye-brain disease-like phenotype with multicystic leucodystrophy. Neurogenetics 14:205–213. https://doi.org/10.1007/s10048-013-0374-9

Geng LN, Yao Z, Snider L, Fong AP, Cech JN, Young JM, van der Maarel SM, Ruzzo WL, Gentleman RC, Tawil R, Tapscott SJ (2012) DUX4 activates germline genes, retroelements,

and immune mediators: implications for facioscapulohumeral dystrophy. Dev Cell 22:38–51. https://doi.org/10.1016/j.devcel.2011.11.013

Giacomotto J, Rinkwitz S, Becker TS (2015) Effective heritable gene knockdown in zebrafish using synthetic microRNAs. Nat Commun 6:7378. https://doi.org/10.1038/ncomms8378

Goody MF, Kelly MW, Reynolds CJ, Khalil A, Crawford BD, Henry CA (2012) NAD+ biosynthesis ameliorates a zebrafish model of muscular dystrophy. PLoS Biol 10:e1001409. https://doi.org/10.1371/journal.pbio.1001409

Granato M, van Eeden FJ, Schach U, Trowe T, Brand M, Furutani-Seiki M, Haffter P, Hammerschmidt M, Heisenberg CP, Jiang YJ, Kane DA, Kelsh RN, Mullins MC, Odenthal J, Nusslein-Volhard C (1996) Genes controlling and mediating locomotion behavior of the zebrafish embryo and larva. Development 123:399–413

Gupta VA, Beggs AH (2014) Kelch proteins: emerging roles in skeletal muscle development and diseases. Skelet Muscle 4:11. https://doi.org/10.1186/2044-5040-4-11

Gupta V, Kawahara G, Gundry SR, Chen AT, Lencer WI, Zhou Y, Zon LI, Kunkel LM, Beggs AH (2011) The zebrafish dag1 mutant: a novel genetic model for dystroglycanopathies. Hum Mol Genet 20:1712–1725. https://doi.org/10.1093/hmg/ddr047

Gupta VA, Kawahara G, Myers JA, Chen AT, Hall TE, Manzini MC, Currie PD, Zhou Y, Zon LI, Kunkel LM, Beggs AH (2012) A splice site mutation in laminin-alpha2 results in a severe muscular dystrophy and growth abnormalities in zebrafish. PLoS One 7:e43794. https://doi.org/10.1371/journal.pone.0043794

Gupta VA, Ravenscroft G, Shaheen R, Todd EJ, Swanson LC, Shiina M, Ogata K, Hsu C, Clarke NF, Darras BT, Farrar MA, Hashem A, Manton ND, Muntoni F, North KN, Sandaradura SA, Nishino I, Hayashi YK, Sewry CA, Thompson EM, Yau KS, Brownstein CA, Yu TW, Allcock RJ, Davis MR, Wallgren-Pettersson C, Matsumoto N, Alkuraya FS, Laing NG, Beggs AH (2013) Identification of KLHL41 mutations implicates BTB-Kelch-mediated ubiquitination as an alternate pathway to myofibrillar disruption in nemaline myopathy. Am J Hum Genet 93:1108–1117. https://doi.org/10.1016/j.ajhg.2013.10.020

Guyon JR, Mosley AN, Zhou Y, O'Brien KF, Sheng X, Chiang K, Davidson AJ, Volinski JM, Zon LI, Kunkel LM (2003) The dystrophin associated protein complex in zebrafish. Hum Mol Genet 12:601–615. https://doi.org/10.1093/hmg/ddg071

Guyon JR, Mosley AN, Jun SJ, Montanaro F, Steffen LS, Zhou Y, Nigro V, Zon LI, Kunkel LM (2005) Delta-sarcoglycan is required for early zebrafish muscle organization. Exp Cell Res 304:105–115. https://doi.org/10.1016/j.yexcr.2004.10.032

Guyon JR, Goswami J, Jun SJ, Thorne M, Howell M, Pusack T, Kawahara G, Steffen LS, Galdzicki M, Kunkel LM (2009) Genetic isolation and characterization of a splicing mutant of zebrafish dystrophin. Hum Mol Genet 18:202–211. https://doi.org/10.1093/hmg/ddn337

Hall TE, Bryson-Richardson RJ, Berger S, Jacoby AS, Cole NJ, Hollway GE, Berger J, Currie PD (2007) The zebrafish candyfloss mutant implicates extracellular matrix adhesion failure in laminin alpha2-deficient congenital muscular dystrophy. Proc Natl Acad Sci USA 104:7092–7097. https://doi.org/10.1073/pnas.0700942104

Hara Y, Balci-Hayta B, Yoshida-Moriguchi T, Kanagawa M, Beltran-Valero de Bernabe D, Gundesli H, Willer T, Satz JS, Crawford RW, Burden SJ, Kunz S, Oldstone MB, Accardi A, Talim B, Muntoni F, Topaloglu H, Dincer P, Campbell KP (2011) A dystroglycan mutation associated with limb-girdle muscular dystrophy. N Engl J Med 364:939–946. https://doi.org/10.1056/NEJMoa1006939

Helbling-Leclerc A, Zhang X, Topaloglu H, Cruaud C, Tesson F, Weissenbach J, Tome FM, Schwartz K, Fardeau M, Tryggvason K et al (1995) Mutations in the laminin alpha 2-chain gene (LAMA2) cause merosin-deficient congenital muscular dystrophy. Nat Genet 11:216–218. https://doi.org/10.1038/ng1095-216

Higashijima S, Okamoto H, Ueno N, Hotta Y, Eguchi G (1997) High-frequency generation of transgenic zebrafish which reliably express GFP in whole muscles or the whole body by using promoters of zebrafish origin. Dev Biol 192:289–299

Hirata H, Watanabe T, Hatakeyama J, Sprague SM, Saint-Amant L, Nagashima A, Cui WW, Zhou W, Kuwada JY (2007) Zebrafish relatively relaxed mutants have a ryanodine receptor defect, show slow swimming and provide a model of multi-minicore disease. Development 134:2771–2781. https://doi.org/10.1242/dev.004531

Hisano Y, Sakuma T, Nakade S, Ohga R, Ota S, Okamoto H, Yamamoto T, Kawahara A (2015) Precise in-frame integration of exogenous DNA mediated by CRISPR/Cas9 system in zebrafish. Sci Rep 5:8841. https://doi.org/10.1038/srep08841

Horstick EJ, Linsley JW, Dowling JJ, Hauser MA, McDonald KK, Ashley-Koch A, Saint-Amant L, Satish A, Cui WW, Zhou W, Sprague SM, Stamm DS, Powell CM, Speer MC, Franzini-Armstrong C, Hirata H, Kuwada JY (2013) Stac3 is a component of the excitation-contraction coupling machinery and mutated in Native American myopathy. Nat Commun 4:1952. https://doi.org/10.1038/ncomms2952

Howe K, Clark MD, Torroja CF, Torrance J, Berthelot C, Muffato M, Collins JE, Humphray S, McLaren K, Matthews L, McLaren S, Sealy I, Caccamo M, Churcher C, Scott C, Barrett JC, Koch R, Rauch GJ, White S, Chow W, Kilian B, Quintais LT, Guerra-Assuncao JA, Zhou Y, Gu Y, Yen J, Vogel JH, Eyre T, Redmond S, Banerjee R, Chi J, Fu B, Langley E, Maguire SF, Laird GK, Lloyd D, Kenyon E, Donaldson S, Sehra H, Almeida-King J, Loveland J, Trevanion S, Jones M, Quail M, Willey D, Hunt A, Burton J, Sims S, McLay K, Plumb B, Davis J, Clee C, Oliver K, Clark R, Riddle C, Elliot D, Threadgold G, Harden G, Ware D, Begum S, Mortimore B, Kerry G, Heath P, Phillimore B, Tracey A, Corby N, Dunn M, Johnson C, Wood J, Clark S, Pelan S, Griffiths G, Smith M, Glithero R, Howden P, Barker N, Lloyd C, Stevens C, Harley J, Holt K, Panagiotidis G, Lovell J, Beasley H, Henderson C, Gordon D, Auger K, Wright D, Collins J, Raisen C, Dyer L, Leung K, Robertson L, Ambridge K, Leongamornlert D, McGuire S, Gilderthorp R, Griffiths C, Manthravadi D, Nichol S, Barker G et al (2013) The zebrafish reference genome sequence and its relationship to the human genome. Nature 496:498–503. https://doi.org/10.1038/nature12111

Hwang JH, Zorzato F, Clarke NF, Treves S (2012) Mapping domains and mutations on the skeletal muscle ryanodine receptor channel. Trends Mol Med 18:644–657. https://doi.org/10.1016/j.molmed.2012.09.006

Hwang WY, Fu Y, Reyon D, Maeder ML, Tsai SQ, Sander JD, Peterson RT, Yeh JR, Joung JK (2013) Efficient genome editing in zebrafish using a CRISPR-Cas system. Nat Biotechnol 31:227–229. https://doi.org/10.1038/nbt.2501

Ibraghimov-Beskrovnaya O, Ervasti JM, Leveille CJ, Slaughter CA, Sernett SW, Campbell KP (1992) Primary structure of dystrophin-associated glycoproteins linking dystrophin to the extracellular matrix. Nature 355:696–702. https://doi.org/10.1038/355696a0

Jurynec MJ, Xia R, Mackrill JJ, Gunther D, Crawford T, Flanigan KM, Abramson JJ, Howard MT, Grunwald DJ (2008) Selenoprotein N is required for ryanodine receptor calcium release channel activity in human and zebrafish muscle. Proc Natl Acad Sci USA 105:12485–12490. https://doi.org/10.1073/pnas.0806015105

Kaplan JC, Hamroun D (2015) The 2016 version of the gene table of monogenic neuromuscular disorders (nuclear genome). Neuromuscul Disord 25:991–1020. https://doi.org/10.1016/j.nmd.2015.10.010

Kawahara G, Guyon JR, Nakamura Y, Kunkel LM (2010) Zebrafish models for human FKRP muscular dystrophies. Hum Mol Genet 19:623–633. https://doi.org/10.1093/hmg/ddp528

Kawahara G, Karpf JA, Myers JA, Alexander MS, Guyon JR, Kunkel LM (2011a) Drug screening in a zebrafish model of Duchenne muscular dystrophy. Proc Natl Acad Sci USA 108:5331–5336. https://doi.org/10.1073/pnas.1102116108

Kawahara G, Serafini PR, Myers JA, Alexander MS, Kunkel LM (2011b) Characterization of zebrafish dysferlin by morpholino knockdown. Biochem Biophys Res Commun 413:358–363. https://doi.org/10.1016/j.bbrc.2011.08.105

Kimura Y, Hisano Y, Kawahara A, Higashijima S (2014) Efficient generation of knock-in transgenic zebrafish carrying reporter/driver genes by CRISPR/Cas9-mediated genome engineering. Sci Rep 4:6545. https://doi.org/10.1038/srep06545

Kobayashi I, Kobayashi-Sun J, Kim AD, Pouget C, Fujita N, Suda T, Traver D (2014) Jam1a-Jam2a interactions regulate haematopoietic stem cell fate through Notch signalling. Nature 512:319–323. https://doi.org/10.1038/nature13623

Koenig M, Hoffman EP, Bertelson CJ, Monaco AP, Feener C, Kunkel LM (1987) Complete cloning of the Duchenne muscular dystrophy (DMD) cDNA and preliminary genomic organization of the DMD gene in normal and affected individuals. Cell 50:509–517

Koshimizu E, Imamura S, Qi J, Toure J, Valdez DM Jr, Carr CE, Hanai J, Kishi S (2011) Embryonic senescence and laminopathies in a progeroid zebrafish model. PLoS One 6:e17688. https://doi.org/10.1371/journal.pone.0017688

Kowaljow V, Marcowycz A, Ansseau E, Conde CB, Sauvage S, Matteotti C, Arias C, Corona ED, Nunez NG, Leo O, Wattiez R, Figlewicz D, Laoudj-Chenivesse D, Belayew A, Coppee F, Rosa AL (2007) The DUX4 gene at the FSHD1A locus encodes a pro-apoptotic protein. Neuromuscul Disord 17:611–623. https://doi.org/10.1016/j.nmd.2007.04.002

Li M, Arner A (2015) Immobilization of Dystrophin and Laminin alpha2-Chain Deficient Zebrafish Larvae In Vivo Prevents the Development of Muscular Dystrophy. PLoS One 10:e0139483. https://doi.org/10.1371/journal.pone.0139483

Li M, Andersson-Lendahl M, Sejersen T, Arner A (2013) Knockdown of desmin in zebrafish larvae affects interfilament spacing and mechanical properties of skeletal muscle. J Gen Physiol 141:335–345. https://doi.org/10.1085/jgp.201210915

Li M, Andersson-Lendahl M, Sejersen T, Arner A (2014) Muscle dysfunction and structural defects of dystrophin-null sapje mutant zebrafish larvae are rescued by ataluren treatment. FASEB J 28:1593–1599. https://doi.org/10.1096/fj.13-240044

Lim LE, Duclos F, Broux O, Bourg N, Sunada Y, Allamand V, Meyer J, Richard I, Moomaw C, Slaughter C et al (1995) Beta-sarcoglycan: characterization and role in limb-girdle muscular dystrophy linked to 4q12. Nat Genet 11:257–265. https://doi.org/10.1038/ng1195-257

Lin YY, White RJ, Torelli S, Cirak S, Muntoni F, Stemple DL (2011) Zebrafish Fukutin family proteins link the unfolded protein response with dystroglycanopathies. Hum Mol Genet 20:1763–1775. https://doi.org/10.1093/hmg/ddr059

Lipscomb L, Piggott RW, Emmerson T, Winder SJ (2016) Dasatinib as a treatment for Duchenne muscular dystrophy. Hum Mol Genet 25:266–274. https://doi.org/10.1093/hmg/ddv469

Lo HP, Nixon SJ, Hall TE, Cowling BS, Ferguson C, Morgan GP, Schieber NL, Fernandez-Rojo MA, Bastiani M, Floetenmeyer M, Martel N, Laporte J, Pilch PF, Parton RG (2015) The caveolin-cavin system plays a conserved and critical role in mechanoprotection of skeletal muscle. J Cell Biol 210:833–849. https://doi.org/10.1083/jcb.201501046

Manzini MC, Tambunan DE, Hill RS, Yu TW, Maynard TM, Heinzen EL, Shianna KV, Stevens CR, Partlow JN, Barry BJ, Rodriguez J, Gupta VA, Al-Qudah AK, Eyaid WM, Friedman JM, Salih MA, Clark R, Moroni I, Mora M, Beggs AH, Gabriel SB, Walsh CA (2012) Exome sequencing and functional validation in zebrafish identify GTDC2 mutations as a cause of Walker-Warburg syndrome. Am J Hum Genet 91:541–547. https://doi.org/10.1016/j.ajhg.2012.07.009

Marchese M, Pappalardo A, Baldacci J, Verri T, Doccini S, Cassandrini D, Bruno C, Fiorillo C, Garcia-Gil M, Bertini E, Pitto L, Santorelli FM (2016) Dolichol-phosphate mannose synthase depletion in zebrafish leads to dystrophic muscle with hypoglycosylated alpha-dystroglycan. Biochem Biophys Res Commun 477:137–143. https://doi.org/10.1016/j.bbrc.2016.06.033

Mitsuhashi H, Mitsuhashi S, Lynn-Jones T, Kawahara G, Kunkel LM (2013) Expression of DUX4 in zebrafish development recapitulates facioscapulohumeral muscular dystrophy. Hum Mol Genet 22:568–577. https://doi.org/10.1093/hmg/dds467

Miyagoe Y, Hanaoka K, Nonaka I, Hayasaka M, Nabeshima Y, Arahata K, Nabeshima Y, Takeda S (1997) Laminin alpha2 chain-null mutant mice by targeted disruption of the Lama2 gene: a new model of merosin (laminin 2)-deficient congenital muscular dystrophy. FEBS Lett 415:33–39

Nam TS, Li W, Heo SH, Lee KH, Cho A, Shin JH, Kim YO, Chae JH, Kim DS, Kim MK, Choi SY (2015) A novel mutation in DNAJB6, p.(Phe91Leu), in childhood-onset LGMD1D with a severe phenotype. Neuromuscul Disord 25:843–851. https://doi.org/10.1016/j.nmd.2015.08.002

Nance JR, Dowling JJ, Gibbs EM, Bonnemann CG (2012) Congenital myopathies: an update. Curr Neurol Neurosci Rep 12:165–174. https://doi.org/10.1007/s11910-012-0255-x

Nigro V, de Sa ME, Piluso G, Vainzof M, Belsito A, Politano L, Puca AA, Passos-Bueno MR, Zatz M (1996) Autosomal recessive limb-girdle muscular dystrophy, LGMD2F, is caused by a mutation in the delta-sarcoglycan gene. Nat Genet 14:195–198. https://doi.org/10.1038/ng1096-195

Nishikawa A, Mitsuhashi S, Miyata N, Nishino I (2017) Targeted massively parallel sequencing and histological assessment of skeletal muscles for the molecular diagnosis of inherited muscle disorders. J Med Genet 54:104–110. https://doi.org/10.1136/jmedgenet-2016-104073

Nixon SJ, Wegner J, Ferguson C, Mery PF, Hancock JF, Currie PD, Key B, Westerfield M, Parton RG (2005) Zebrafish as a model for caveolin-associated muscle disease; caveolin-3 is required for myofibril organization and muscle cell patterning. Hum Mol Genet 14:1727–1743. https://doi.org/10.1093/hmg/ddi179

Noguchi S, McNally EM, Ben Othmane K, Hagiwara Y, Mizuno Y, Yoshida M, Yamamoto H, Bonnemann CG, Gussoni E, Denton PH, Kyriakides T, Middleton L, Hentati F, Ben Hamida M, Nonaka I, Vance JM, Kunkel LM, Ozawa E (1995) Mutations in the dystrophin-associated protein gamma-sarcoglycan in chromosome 13 muscular dystrophy. Science 270:819–822

Nowak KJ, Davies KE (2004) Duchenne muscular dystrophy and dystrophin: pathogenesis and opportunities for treatment. EMBO Rep 5:872–876. https://doi.org/10.1038/sj.embor.7400221

Ozawa E, Yoshida M, Suzuki A, Mizuno Y, Hagiwara Y, Noguchi S (1995) Dystrophin-associated proteins in muscular dystrophy. Hum Mol Genet 4:1711–1716

Parsons MJ, Campos I, Hirst EM, Stemple DL (2002) Removal of dystroglycan causes severe muscular dystrophy in zebrafish embryos. Development 129:3505–3512

Postel R, Vakeel P, Topczewski J, Knoll R, Bakkers J (2008) Zebrafish integrin-linked kinase is required in skeletal muscles for strengthening the integrin-ECM adhesion complex. Dev Biol 318:92–101. https://doi.org/10.1016/j.ydbio.2008.03.024

Praissman JL, Willer T, Sheikh MO, Toi A, Chitayat D, Lin YY, Lee H, Stalnaker SH, Wang S, Prabhakar PK, Nelson SF, Stemple DL, Moore SA, Moremen KW, Campbell KP, Wells L (2016) The functional O-mannose glycan on alpha-dystroglycan contains a phospho-ribitol primed for matriglycan addition. Elife:5. https://doi.org/10.7554/eLife.14473

Radev Z, Hermel JM, Elipot Y, Bretaud S, Arnould S, Duchateau P, Ruggiero F, Joly JS, Sohm F (2015) A TALEN-Exon Skipping Design for a Bethlem Myopathy Model in Zebrafish. PLoS One 10:e0133986. https://doi.org/10.1371/journal.pone.0133986

Rahimov F, Kunkel LM (2013) The cell biology of disease: cellular and molecular mechanisms underlying muscular dystrophy. J Cell Biol 201:499–510. https://doi.org/10.1083/jcb.201212142

Ravenscroft G, Miyatake S, Lehtokari VL, Todd EJ, Vornanen P, Yau KS, Hayashi YK, Miyake N, Tsurusaki Y, Doi H, Saitsu H, Osaka H, Yamashita S, Ohya T, Sakamoto Y, Koshimizu E, Imamura S, Yamashita M, Ogata K, Shiina M, Bryson-Richardson RJ, Vaz R, Ceyhan O, Brownstein CA, Swanson LC, Monnot S, Romero NB, Amthor H, Kresoje N, Sivadorai P, Kiraly-Borri C, Haliloglu G, Talim B, Orhan D, Kale G, Charles AK, Fabian VA, Davis MR, Lammens M, Sewry CA, Manzur A, Muntoni F, Clarke NF, North KN, Bertini E, Nevo Y, Willichowski E, Silberg IE, Topaloglu H, Beggs AH, Allcock RJ, Nishino I, Wallgren-Pettersson C, Matsumoto N, Laing NG (2013) Mutations in KLHL40 are a frequent cause of severe autosomal-recessive nemaline myopathy. Am J Hum Genet 93:6–18. https://doi.org/10.1016/j.ajhg.2013.05.004

Roberds SL, Leturcq F, Allamand V, Piccolo F, Jeanpierre M, Anderson RD, Lim LE, Lee JC, Tome FM, Romero NB et al (1994) Missense mutations in the adhalin gene linked to autosomal recessive muscular dystrophy. Cell 78:625–633

Roostalu U, Strähle U (2012) In vivo imaging of molecular interactions at damaged sarcolemma. Dev Cell 22:515–529. https://doi.org/10.1016/j.devcel.2011.12.008

Roscioli T, Kamsteeg EJ, Buysse K, Maystadt I, van Reeuwijk J, van den Elzen C, van Beusekom E, Riemersma M, Pfundt R, Vissers LE, Schraders M, Altunoglu U, Buckley MF, Brunner HG, Grisart B, Zhou H, Veltman JA, Gilissen C, Mancini GM, Delree P, Willemsen MA, Ramadza

DP, Chitayat D, Bennett C, Sheridan E, Peeters EA, Tan-Sindhunata GM, de Die-Smulders CE, Devriendt K, Kayserili H, El-Hashash OA, Stemple DL, Lefeber DJ, Lin YY, van Bokhoven H (2012) Mutations in ISPD cause Walker-Warburg syndrome and defective glycosylation of alpha-dystroglycan. Nat Genet 44:581–585. https://doi.org/10.1038/ng.2253

Saint-Amant L, Drapeau P (1998) Time course of the development of motor behaviors in the zebrafish embryo. J Neurobiol 37:622–632

Sarparanta J, Jonson PH, Golzio C, Sandell S, Luque H, Screen M, McDonald K, Stajich JM, Mahjneh I, Vihola A, Raheem O, Penttila S, Lehtinen S, Huovinen S, Palmio J, Tasca G, Ricci E, Hackman P, Hauser M, Katsanis N, Udd B (2012) Mutations affecting the cytoplasmic functions of the co-chaperone DNAJB6 cause limb-girdle muscular dystrophy. Nat Genet 44(450-5):S1–S2. https://doi.org/10.1038/ng.1103

Schindler RF, Scotton C, Zhang J, Passarelli C, Ortiz-Bonnin B, Simrick S, Schwerte T, Poon KL, Fang M, Rinne S, Froese A, Nikolaev VO, Grunert C, Muller T, Tasca G, Sarathchandra P, Drago F, Dallapiccola B, Rapezzi C, Arbustini E, Di Raimo FR, Neri M, Selvatici R, Gualandi F, Fattori F, Pietrangelo A, Li W, Jiang H, Xu X, Bertini E, Decher N, Wang J, Brand T, Ferlini A (2016) POPDC1(S201F) causes muscular dystrophy and arrhythmia by affecting protein trafficking. J Clin Invest 126:239–253. https://doi.org/10.1172/JCI79562

Seger C, Hargrave M, Wang X, Chai RJ, Elworthy S, Ingham PW (2011) Analysis of Pax7 expressing myogenic cells in zebrafish muscle development, injury, and models of disease. Dev Dyn 240:2440–2451. https://doi.org/10.1002/dvdy.22745

Sewry CA, Jimenez-Mallebrera C, Muntoni F (2008) Congenital myopathies. Curr Opin Neurol 21:569–575. https://doi.org/10.1097/WCO.0b013e32830f93c7

Shih YH, Dvornikov AV, Zhu P, Ma X, Kim M, Ding Y, Xu X (2016) Exon- and contraction-dependent functions of titin in sarcomere assembly. Development 143:4713–4722. https://doi.org/10.1242/dev.139246

Smith LL, Gupta VA, Beggs AH (2014) Bridging integrator 1 (Bin1) deficiency in zebrafish results in centronuclear myopathy. Hum Mol Genet 23:3566–3578. https://doi.org/10.1093/hmg/ddu067

Smith SJ, Wang JC, Gupta VA, Dowling JJ (2017) A novel early onset phenotype in a zebrafish model of merosin deficient congenital muscular dystrophy. PLoS One 12:e0172648. https://doi.org/10.1371/journal.pone.0172648

Steffen LS, Guyon JR, Vogel ED, Howell MH, Zhou Y, Weber GJ, Zon LI, Kunkel LM (2007) The zebrafish runzel muscular dystrophy is linked to the titin gene. Dev Biol 309:180–192. https://doi.org/10.1016/j.ydbio.2007.06.015

Stevens E, Carss KJ, Cirak S, Foley AR, Torelli S, Willer T, Tambunan DE, Yau S, Brodd L, Sewry CA, Feng L, Haliloglu G, Orhan D, Dobyns WB, Enns GM, Manning M, Krause A, Salih MA, Walsh CA, Hurles M, Campbell KP, Manzini MC, Consortium UK, Stemple D, Lin YY, Muntoni F (2013) Mutations in B3GALNT2 cause congenital muscular dystrophy and hypoglycosylation of alpha-dystroglycan. Am J Hum Genet 92:354–365. https://doi.org/10.1016/j.ajhg.2013.01.016

Sztal TE, Zhao M, Williams C, Oorschot V, Parslow AC, Giousoh A, Yuen M, Hall TE, Costin A, Ramm G, Bird PI, Busch-Nentwich EM, Stemple DL, Currie PD, Cooper ST, Laing NG, Nowak KJ, Bryson-Richardson RJ (2015) Zebrafish models for nemaline myopathy reveal a spectrum of nemaline bodies contributing to reduced muscle function. Acta Neuropathol 130:389–406. https://doi.org/10.1007/s00401-015-1430-3

Telfer WR, Busta AS, Bonnemann CG, Feldman EL, Dowling JJ (2010) Zebrafish models of collagen VI-related myopathies. Hum Mol Genet 19:2433–2444. https://doi.org/10.1093/hmg/ddq126

Telfer WR, Nelson DD, Waugh T, Brooks SV, Dowling JJ (2012) Neb: a zebrafish model of nemaline myopathy due to nebulin mutation. Dis Model Mech 5:389–396. https://doi.org/10.1242/dmm.008631

Thornhill P, Bassett D, Lochmuller H, Bushby K, Straub V (2008) Developmental defects in a zebrafish model for muscular dystrophies associated with the loss of fukutin-related protein (FKRP). Brain 131:1551–1561. https://doi.org/10.1093/brain/awn078

Turk R, Sterrenburg E, de Meijer EJ, van Ommen GJ, den Dunnen JT, t Hoen PA (2005) Muscle regeneration in dystrophin-deficient mdx mice studied by gene expression profiling. BMC Genomics 6:98. https://doi.org/10.1186/1471-2164-6-98

Vieira NM, Naslavsky MS, Licinio L, Kok F, Schlesinger D, Vainzof M, Sanchez N, Kitajima JP, Gal L, Cavacana N, Serafini PR, Chuartzman S, Vasquez C, Mimbacas A, Nigro V, Pavanello RC, Schuldiner M, Kunkel LM, Zatz M (2014) A defect in the RNA-processing protein HNRPDL causes limb-girdle muscular dystrophy 1G (LGMD1G). Hum Mol Genet 23:4103–4110. https://doi.org/10.1093/hmg/ddu127

Vogel B, Meder B, Just S, Laufer C, Berger I, Weber S, Katus HA, Rottbauer W (2009) In-vivo characterization of human dilated cardiomyopathy genes in zebrafish. Biochem Biophys Res Commun 390:516–522. https://doi.org/10.1016/j.bbrc.2009.09.129

Wallace LM, Garwick SE, Mei W, Belayew A, Coppee F, Ladner KJ, Guttridge D, Yang J, Harper SQ (2011) DUX4, a candidate gene for facioscapulohumeral muscular dystrophy, causes p53-dependent myopathy in vivo. Ann Neurol 69:540–552. https://doi.org/10.1002/ana.22275

Waugh TA, Horstick E, Hur J, Jackson SW, Davidson AE, Li X, Dowling JJ (2014) Fluoxetine prevents dystrophic changes in a zebrafish model of Duchenne muscular dystrophy. Hum Mol Genet 23:4651–4662. https://doi.org/10.1093/hmg/ddu185

Williamson RA, Henry MD, Daniels KJ, Hrstka RF, Lee JC, Sunada Y, Ibraghimov-Beskrovnaya O, Campbell KP (1997) Dystroglycan is essential for early embryonic development: disruption of Reichert's membrane in Dag1-null mice. Hum Mol Genet 6:831–841

Winder SJ, Lipscomb L, Angela Parkin C, Juusola M (2011) The proteasomal inhibitor MG132 prevents muscular dystrophy in zebrafish. PLoS Curr 3:RRN1286. https://doi.org/10.1371/currents.RRN1286

Wood AJ, Muller JS, Jepson CD, Laval SH, Lochmuller H, Bushby K, Barresi R, Straub V (2011) Abnormal vascular development in zebrafish models for fukutin and FKRP deficiency. Hum Mol Genet 20:4879–4890. https://doi.org/10.1093/hmg/ddr426

Xu C, Tabebordbar M, Iovino S, Ciarlo C, Liu J, Castiglioni A, Price E, Liu M, Barton ER, Kahn CR, Wagers AJ, Zon LI (2013) A zebrafish embryo culture system defines factors that promote vertebrate myogenesis across species. Cell 155:909–921. https://doi.org/10.1016/j.cell.2013.10.023

Yoshida-Moriguchi T, Campbell KP (2015) Matriglycan: a novel polysaccharide that links dystroglycan to the basement membrane. Glycobiology 25:702–713. https://doi.org/10.1093/glycob/cwv021

Yuen M, Sandaradura SA, Dowling JJ, Kostyukova AS, Moroz N, Quinlan KG, Lehtokari VL, Ravenscroft G, Todd EJ, Ceyhan-Birsoy O, Gokhin DS, Maluenda J, Lek M, Nolent F, Pappas CT, Novak SM, D'Amico A, Malfatti E, Thomas BP, Gabriel SB, Gupta N, Daly MJ, Ilkovski B, Houweling PJ, Davidson AE, Swanson LC, Brownstein CA, Gupta VA, Medne L, Shannon P, Martin N, Bick DP, Flisberg A, Holmberg E, Van den Bergh P, Lapunzina P, Waddell LB, Sloboda DD, Bertini E, Chitayat D, Telfer WR, Laquerriere A, Gregorio CC, Ottenheijm CA, Bonnemann CG, Pelin K, Beggs AH, Hayashi YK, Romero NB, Laing NG, Nishino I, Wallgren-Pettersson C, Melki J, Fowler VM, MacArthur DG, North KN, Clarke NF (2014) Leiomodin-3 dysfunction results in thin filament disorganization and nemaline myopathy. J Clin Invest 124:4693–4708. https://doi.org/10.1172/JCI75199

Zhang R, Yang J, Zhu J, Xu X (2009) Depletion of zebrafish Tcap leads to muscular dystrophy via disrupting sarcomere-membrane interaction, not sarcomere assembly. Hum Mol Genet 18:4130–4140. https://doi.org/10.1093/hmg/ddp362

Chapter 11
Emergence of Zebrafish as a Model System for Understanding Human Scoliosis

Long Guo, Shiro Ikegawa, and Chisa Shukunami

Abstract Scoliosis is a three-dimensional rotation of the spine that is defined as lateral curvature with a Cobb angle greater than 10 degrees. About 2–3% of the global population is affected by scoliosis, and more than 80% of scoliosis are caused by unknown factors (idiopathic). Adolescent idiopathic scoliosis is the most common type of scoliosis and occurs in children over 10 years, showing a female predominance. Of scoliosis patients, 10% have curve progression requiring medical interventions such as bracing and surgery. Scoliosis research has been delayed due to the genetic complexity and a lack of relevant animal models for functional studies; however, significant breakthroughs of scoliosis study have recently been made using zebrafish. The zebrafish is a powerful tool, owing to easy genetic manipulation and a natural susceptibility to spinal curvature. Here, we summarize the utility of zebrafish as a model system for human scoliosis.

Keywords Scoliosis · Polygenic disease · Vertebral column · Notochord

11.1 Anatomy and Histology of the Human and Zebrafish Spine

The spine is part of the axial skeleton that is also called the backbone, the spinal column, or the vertebral column. The basic structure of the spine is very similar in all vertebrates. It elongates from the skull base to the pelvis and serves as a pillar to support the body weight and to enclose the spinal cord connecting the brain with nerves in the rest of the body. The spine is made up of a series of stacking bones

L. Guo · S. Ikegawa
Laboratory of Bone and Joint Diseases, RIKEN Center for Integrative Medical Sciences, Tokyo, Japan
e-mail: long.guo@riken.jp; sikegawa@ims.u-tokyo.ac.jp

C. Shukunami (✉)
Department of Molecular Biology and Biochemistry, Division of Dental Sciences, Graduate School of Biomedical & Health Sciences, Hiroshima University, Hiroshima, Japan
e-mail: shukunam@hiroshima-u.ac.jp

H. Hirata, A. Iida (eds.), *Zebrafish, Medaka, and Other Small Fishes*,
https://doi.org/10.1007/978-981-13-1879-5_11

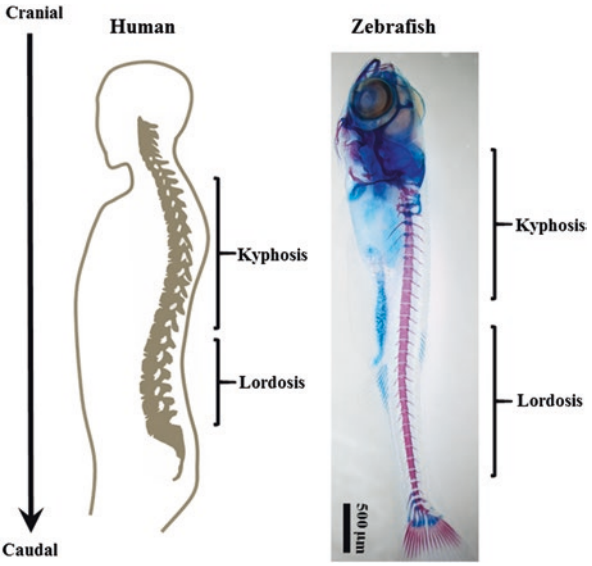

Fig. 11.1 Structure of human and zebrafish spine The lateral view of zebrafish backbone (21 dpf) stained by alcian blue and alizarin red shows obvious similarities to that of human. Zebrafish presents two main physiological curvatures in the pre-caudal spine (kyphosis) and the caudal spine (lordosis), which have analogy to kyphosis and lordosis in the human thoracic and lumbar spine, respectively. dpf, days post-fertilization

called vertebrae and the intervertebral discs between adjacent vertebral bodies supported by spinal ligaments, tendons, and muscles. The human spine includes five major regions: cervical, thoracic, lumbar, sacral, and coccygeal from top to bottom. The normal human spine has naturally occurring curves termed lordosis in the cervical and the lumbar spine and kyphosis in the thoracic and the sacral spine, looking at the spine from the lateral (Fig. 11.1). Such curves give the spine an "S" shape that helps to distribute the body weight more evenly and absorb force or jarring during activity, thus allowing a range of bodily motions and balance maintenance which is crucial for bipedalism.

Zebrafish has the similar spinal column architecture and vertebral structure to those of humans (Fig. 11.1). Like humans, the vertebral column in zebrafish is composed of alternating bony vertebrae and intervertebral discs (Fig. 11.2). The spinal cord passes between neural arches (Fleming et al. 2004). Comparable with the human thoracic vertebrae and rib cage, zebrafish pre-caudal vertebrae are also associated with the rib segments. The pre-caudal spine in zebrafish also presents a natural kyphosis similar to human thoracic spine (Fig. 11.1).

Both the human and zebrafish vertebral column are developed from axial and paraxial mesodermal lineages, although the process of ossification is different (Stickney et al. 2000; Brent and Tabin 2002). Paraxial mesoderm gives rise to the somite that is subdivided into the sclerotome, the myotome, and the dermatome. Compared with mammalian somites, teleosts have the somite with the smaller sclerotome and the larger myotome (Fig. 11.3). Zebrafish vertebrae arise by direct ossification of the notochord sheath followed by intramembranous bone formation around the notochord (Fleming et al. 2004). On the other hand, human vertebrae are formed through a process called endochondral ossification by which a cartilaginous intermediate derived from the sclerotome is replaced by the bone and bone marrows

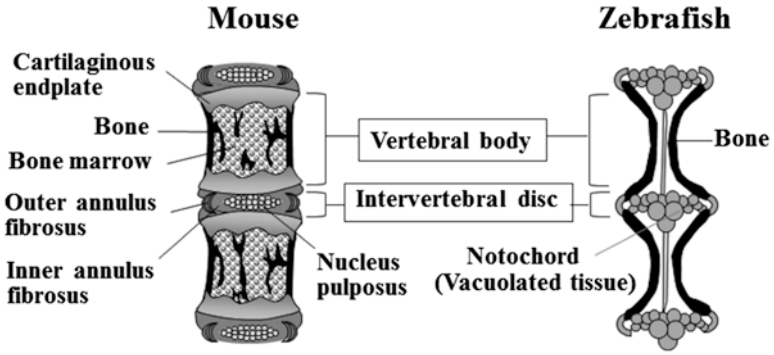

Fig. 11.2 Histology of vertebral bodies in mouse and zebrafish
Schematic sagittal section of mouse (left) and zebrafish (right) vertebrae. In mice, intervertebral discs between vertebral bodies consist of nucleus pulposus and annulus fibrosus. Hyaline cartilaginous endplates are strongly bound to the intervertebral disc. Mouse vertebral bodies are filled with spongiosa. In zebrafish, intervertebral discs composed of vacuolated tissues are located between lumen surrounded by the bone

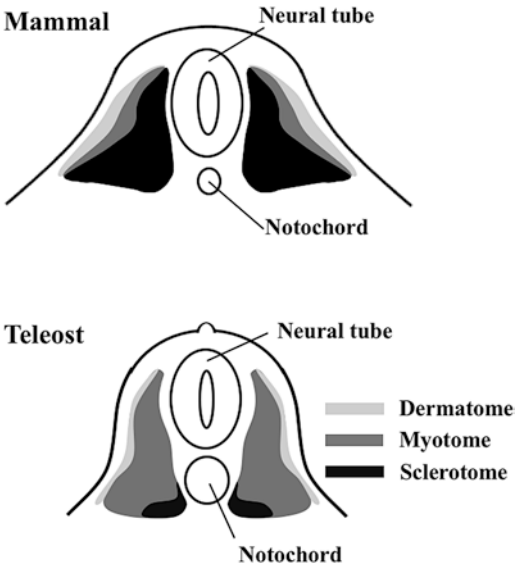

Fig. 11.3 Comparison of mammalian and teleost somite structure
Schematic cross section of mammalian and teleost embryos at the segmentation stage. Mesoderm mainly consists of notochord and somites. Somites are bilaterally paired blocks of paraxial mesoderm that are formed along the head-to-tail axis of the developing embryo. In both mammalian and teleost, somites are subdivided into the sclerotomes, myotomes, and dermatomes. Compared with mammalian, teleost has somites with smaller sclerotomes and larger myotomes

(Brent and Tabin 2002). Zebrafish do not have hematopoietic tissue inside the bone marrow (Fig. 11.2) because hematopoiesis takes place in their kidneys, analogous to the mammalian bone marrow (Witten and Huysseune 2009).

Although these developmental differences must be considered when modeling vertebral column formation, the high conservation and similarities in the fundamental architecture and developmental origins of the spine between human and zebrafish suggest zebrafish could be an ideal model for studying human spinal deformities.

11.2 Scoliosis

Human spinal deformities are defined as the abnormality of the formation, alignment, and/or shape of the vertebral column. Scoliosis is a common spinal deformity. It refers to lateral spinal curvature with a Cobb angle greater than 10 degrees, often accompanied by a rotational defect. Scoliosis is classified clinically into congenital scoliosis (CS), idiopathic scoliosis (IS), and secondary scoliosis (Pourquie 2011). Secondary scoliosis is attributed to a wide variety of primary causes. These causes include neuropathy such as cerebral palsy, muscular defects such as Duchenne muscular dystrophy, and connective tissue disorders such as Marfan syndrome. Relative to the wide complications in secondary scoliosis, CS, in a narrow sense, is solely caused by embryonic vertebral malformation that results in deviation of the normal spinal alignment (Hedequist and Emans 2007). An estimated prevalence of CS is 0.5–1 per 1000 persons (Shands and Bundens 1956). Vertebral malformations such as hemi-vertebrae and wedge-shaped vertebrae occur during somitogenesis, resulting in imbalanced vertebral growth and scoliosis. As the origin of CS, somitogenesis defects that could be induced by either genetic or environmental factors have been studied intensively in the past decades (Pourquie 2011).

However, most of human scoliosis arises without apparent anatomical and physiological defects. This type of scoliosis is clinically described to be "idiopathic" that means the cause is unknown. IS is further categorized into infantile, juvenile, and adolescent types by age of onset. Among the three types, adolescent IS (AIS) accounts for 80% of all human scoliosis and develops in 2–4% of children aged between 10 and 16 years across all racial groups (Konieczny et al. 2013). AIS has a significant female preference. The change of the body figure by AIS leads to profound physiopsychologic problems. Although most AIS are mild and without the need for specific medical intervention, the risk of the curve progression makes the frequent radiological check necessary, thus bringing a heavy physical and mental burden to patients. Indeed, better understanding the etiology and pathology of IS is imperious for the development of the preventive and therapeutic intervention.

As with humans, the vertebral column in teleost fish is naturally susceptible to axial mechanical stress. A mutant guppy strain, *curveback*, develops non-induced spinal deformity that is similar to human scoliosis (Gorman et al. 2007). Sporadic spinal deformity has also been noted in other teleosts, including medaka and swordtail. Zebrafish also frequently develop curvature without vertebral malformation.

11.3 Genetic Studies of IS

IS is considered as a polygenic disease controlled by genetic and environmental factors. The familial aggregation and concordance among monozygotic twins support a strong genetic cause of IS (Cheng et al. 2015; Wang et al. 2011). Early studies searching for genetic factors of IS using linkage and association analyses have

reported some susceptibility genes in the past decades. With the advent of genome-wide association study (GWAS) and whole exome/genome sequencing (WES/WGS), studies on IS have progressed dramatically, and many convincing IS loci have been identified. These loci refer to *LBX1* (Takahashi et al. 2011), *GPR126* (Kou et al. 2013), *BNC2* (Ogura et al. 2015), *PAX1* (Sharma et al. 2015), *POC5* (Patten et al. 2015), and so on. Although the identified IS loci only explain a fraction of the total genetic variance in IS (the missing heritability problem), a broad genetic landscape for IS has been established by GWAS and WES/WGS.

11.3.1 Linkage Studies

The familial aggregation and concordance among monozygotic twins strongly support a genetic cause of IS (Cheng et al. 2015; Wang et al. 2011). Early pedigree-based linkage studies reported several susceptibility loci (Gorman et al. 2012). A genome-wide linkage analysis of seven IS families found linkage (P-value = 0.002) in a 3.5-Mb region on 5p13.3 (Gorman et al. 2012). However, most of linkage studies failed to address the precise causal/susceptibility genes due to the poor resolution of the method.

11.3.2 Genome-Wide Association Study

With the development of the gene chip technology, genetic researches on human common disease came into the age of GWAS. In this decade, GWAS has identified many loci associated with IS. Many of the top variants in these loci have been replicated across multiple racial groups. These findings allow us to come close to the mystery of IS for the first time.

Sharma et al. conducted GWAS on IS (Sharma et al. 2011) using the transmission disequilibrium test and identified AIS-susceptible single nucleotide polymorphisms (SNPs) in regions near *CHL1*, *DSCAM*, and *CNTNAP2*, all of which are involved in axon guidance pathways. The subsequent GWAS by our group on a Japanese population using the case-control design identified three loci associated with AIS (Ikegawa 2016).

The first locus was on chromosome 10q24 and had a high genome-wide significance level (Takahashi et al. 2011). The most significantly associated SNP was rs11190970. The P-value reached 1.24×10^{-19} with odds ratio (OR) of 1.56 (95% confidence interval (CI) = 1.41–1.71). An international meta-analysis using a total of ~24,000 subjects showed that rs11190870 is a global AIS susceptibility SNP ($P = 1.22 \times 10^{-45}$; OR = 1.60) (Londono et al. 2014). rs11190870 is in an 80-kb linkage disequilibrium (LD) block containing two genes, *LBX1* and *FLJ41350*, which exist head to head closely. *FLJ41350* is a hypothetical gene without known function. *LBX1* is a transcriptional factor specifically expressed during embryogenesis

in mouse, with restricted expression to the developing central nervous system and muscles (Londono et al. 2014).

The second locus identified in our GWAS was on chromosome 6q24.1 (Kou et al. 2013). The combined *P*-value of the GWAS and the replication study in Chinese for the most significantly associated SNP, rs6570507, was 6.96×10^{-10} (OR = 1.28). A further international meta-analysis using 6873 cases and 38,916 controls showed that rs6570507 is also a global AIS susceptibility SNP ($P = 2.95 \times 10^{-20}$; OR = 1.22) (Kou et al. 2018). The most significantly associated SNPs were in intron 2 of *GPR126* (*G protein-coupled receptor 126*).

The third locus identified in our GWAS was on chromosome 9p22.2 represented by a SNP, rs3904778 (Ogura et al. 2015). Its *P*-value was 3.50×10^{-11} (OR = 1.21). A further international meta-analysis confirmed its global association ($P = 3.28 \times 10^{-18}$; OR = 1.19) (Ogura et al. 2018). The most significantly associated SNPs were in intron 3 of *BNC2* that encodes a zinc-finger transcription factor, basonuclin 2.

Additional GWAS in US Caucasian found significant associations of IS with chromosome 20p11.22 SNPs for females ($P = 6.89 \times 10^{-9}$) but not males ($P = 0.71$). This association was replicated in independent female cohorts from the US Caucasian and Japanese (overall $P = 2.15 \times 10^{-10}$; OR = 1.30) (Sharma et al. 2015). The 174-kb- associated locus is distal to *PAX1*, which encodes paired box 1, a transcription factor involved in spine development. GWAS in Chinese identified three new AIS susceptibility loci at 1p36.32 (rs241215, $P = 2.95 \times 10^{-9}$), 2q36.1 (rs13398147, $P = 7.59 \times 10^{-13}$), and 18q21.33 (rs4940576, $P = 2.22 \times 10^{-12}$) (Zhu et al. 2015). The association has not been replicated.

11.3.3 Next-Generation Sequencing-Based Study

Next-generation sequencing (NGS) technology is another revolution in the modern genetic study. WES and WGS realized the nucleotide level resolution in pedigree-based studies in a cost-effective manner, thus leading to the more precise identification of the associated variants in familial cases of IS than ever. Indeed, WES and WGS have identified several IS-associated rare variants in genes encoding extracellular matrix components such as *HSPG2* (Baschal et al. 2014) and *FBN1/2* (Buchan et al. 2014) and genes encoding other proteins including the centriolar protein *POC5* (Patten et al. 2015), the cytoskeleton protein *AKAP2* (Li et al. 2016), and the planar cell polarity component *VANGL1* (Andersen et al. 2017). These genes are waiting for replication.

11.4 Animal Models for IS

Despite recent rapid advances in molecular genetic technology, studies elucidating the etiology and pathology of scoliosis have been hampered due to the lack of suitable experimental animal models. Scoliosis has long been considered to be exclusive to bipedal vertebrates, especially in human (Ouellet and Odent 2013). It has been proposed that the unique human upright posture generates a specific cranial-to-caudal spine load and causes altered biomechanics contributing to eventual development of scoliosis (Castelein et al. 2005). Other bipedal animals except for human carry their trunk in front of their pelvis. In contrast to the high incidence of scoliosis in human, naturally occurring scoliosis is quite rare in quadrupedal vertebrates such as rats and mice (Ouellet and Odent 2013). Indeed, in mice, their spinal structure, gravity center, and spinal loading are quite different from those of humans. While quadrupedal rodents are refractory to the developing scoliosis, the bipedal rodents generated by amputation of forelimb and tail frequently develop the IS-like spinal deformity (Bobyn et al. 2015). Pinealectomy of bipedal rodents and chickens causes severe scoliosis (Bobyn et al. 2015), implicating the combined effects of the endocrine signaling and specific biomechanics of the upright posture could be involved in the etiopathogenesis of IS. However, it remains unclear whether these models recapitulate the pathogenic state of human IS. So far, the endocrine signaling hypothesis has not been supported by clinical and genetic evidence. Moreover, as these models are either time-consuming or difficult to manipulate genetically, their broad application to the IS study is hampered.

In contrast, a natural susceptibility to spinal curvatures is observed in teleosts, including zebrafish, medaka, and swordtail. IS-like scoliosis has been reported across many laboratory and aquaculture species (Gorman and Breden 2009; Gorman et al. 2007). Similar to human, fish naturally develop scoliosis with age (Hayes et al. 2013). Some argue that the spinal load of fish acts along the cranial-to-caudal axis similar to humans, because the activity of swimming forward is driven by a couple of forces, the resistant force from water, and the propulsion from caudal tail (Gorman and Breden 2009). As a teleost, zebrafish has been a widely used vertebrate model organism in developmental biology. Well-developed zebrafish genetic resources including abundant mutant lines are available to the researchers. Besides, it is easy to manipulate zebrafish genetically by injection of fertilized eggs on a large scale. Zebrafish embryos are transparent, thus allowing scientists to directly monitor sequential processes of axial development, which is considered to be associated closely with the pathogenesis of human scoliosis. Thus, zebrafish has emerged as the first-line tool for *in vivo* studies of scoliosis.

11.5 Emergence of Zebrafish as a New Tool for Studying IS

The utilization of zebrafish in modeling human scoliosis has been reported in a number of studies. These studies can be classified into two types according to their starting point. One starts from human; its basis is the findings obtained by the human genetic studies for IS summarized above (susceptibility gene-based approach). The IS loci identified by the human genetic studies usually contain several candidate susceptibility genes. In these studies, zebrafish has been used to clarify the roles of these candidate genes and/or the variants in the etiology and/or pathogenesis of IS. The other starts from zebrafish; its basis is the unexpected phenotypes in zebrafish mutant lines showing the phenotype similar to human IS (phenotype-based approach). The study identifies the mutated gene and clarifies its function related to IS.

11.5.1 Susceptibility Gene-Based Approach

As noted previously, several susceptibility genes for IS have been identified by the genetic studies. We summarized the utilization of zebrafish in the functional analysis of these genes in Table 11.1.

The most significantly associated AIS SNP is rs11190870 (Takahashi et al. 2011). It is located in the intergenic region, and the nearest genes are *LBX1* and *FLJ41350*, which are 7.5 kb upstream and 8.1 kb downstream of rs11190870, respectively. The chromosome conformation capture assay reveals that rs11190870 could contribute to AIS susceptibility by affecting the transcriptional activity of *LBX1* (Guo et al. 2016). The evidence from *Lbx1*-null mice indicated that *Lbx1* is involved in heart development, migration of limb muscle precursors, and dorsal-ventral patterning of the spinal cord (Brohmann et al. 2000; Gross et al. 2002; Schäfer et al. 2003). The potential effect of altered *LBX1* expression on the pathogenesis of AIS is demonstrated by a series of experiments using zebrafish (Guo et al. 2016). Overexpressing *lbx1b* transiently or stably in zebrafish caused body axial deformity, while loss-of-function (LOF) mutants of *lbx1a*, *lbx1b*, and *lbx2* did not show significant phenotypes. Some transiently transgenic fishes with mild body axial deformity could live until adults and develop late-onset scoliosis with or without vertebral malformation (Fig. 11.4). The presented scoliosis phenotypes also showed female preference similar to that of human AIS. However, a heritable IS model was not established due to the early lethality in the transgenic zebrafish. The deformation of the embryonic body axis by *lbx1b* overexpression was associated with defects in convergent extension, which is a component of the main axis-elongation machinery in gastrulating embryos. Non-canonical Wnt/planar cell polarity (PCP) pathway is a known main mechanism regulating the movement of convergent extension. Further study indicates *lbx1b* overexpression caused defects in convergent extension by decreasing the expression of *wnt5b*, a ligand of the non-canonical Wnt/PCP pathway. The study demonstrates a novel pathological feature

Table 11.1 Utilization of zebrafish in human IS study

Type	Gene	Scoliosis-associated human variant, method	Variant locus	Zebrafish assay	Phenotype	Heritable IS model	Ref.
Susceptibility gene-based approach	*LBX1*	rs11190870, GWAS	Intergenic	*lbx1b*^{ko10} and *lbx2*^{ko11} LOF mutants by TALENs	No scoliosis-related phenotype	No	Guo et al. (2016)
				Overexpression through transient and stable transgenesis and mRNA injection	Embryonic axial defects, late-onset scoliosis with or without vertebral malformations	No	
	PAX1	rs169311, GWAS	Intergenic	Allele-specific enhancer activity assay by reporter gene transient transgenesis	Abolished enhancer activity by IS-associated haplotype	No	Sharma et al. (2015)
	POC5	p.A429V	Coding region	Overexpression via mutant mRNA injection	Embryonic axial defects, late-onset scoliosis without vertebral malformations	No	Patten et al. (2015)
		p.A446T					
		p.A455P					
		Linkage analysis		Embryonic rescue of MO phenotypes by WT or mutant mRNA injection	Mutant mRNA fails to rescue MO phenotype	No	
		+WES					
	GPR126	rs6570507, GWAS	Intronic	Knockdown by MO injection	Bone mineralization delay	No	Kou et al. (2013)
				gpr126^{st49} and *gpr126*^{st86} LOF mutants by ENU mutagenesis	Myelination defects, no scoliosis-related phenotype	No	
	BNC2	rs10738445, GWAS	Intronic	Overexpression via transient transgenesis and mRNA injection	Embryonic axial defects	No	Ogura et al. (2015)
	IRX1/2/4	Linkage analysis	Intergenic	Allele-specific enhancer activity assay by reporter gene stable transgenesis	Inconclusive	No	Justice et al. (2016)

(continued)

Table 11.1 (continued)

Type	Gene	Scoliosis-associated human variant, method	Variant locus	Zebrafish assay	Phenotype	Heritable IS model	Ref.
Phenotype-based approach	*PTK7*	p.P545A, identified in a single patient and his non-penetrant father by sequencing	Coding region	Zygotic *Ptk7*^{hsc9} LOF mutant	Late-onset scoliosis without vertebral malformations	Yes	Hayes et al. (2014)
				Maternal-zygotic *Ptk7*^{hsc9} LOF mutant	Scoliosis with vertebral malformations	No	
				Embryonic rescue of maternal-zygotic *Ptk7*^{hsc9} mutant phenotypes by WT or mutant mRNA injection	Mutant mRNA fails to rescue the mutant phenotypes	No	
	KIF6	None	N/A	*kif6*^{gw326} LOF mutant by ENU mutagenesis; *kif6*^{gw327}, *kif6*^{gw328}, *kif6*^{gw329} mutants by TALENs	Late-onset scoliosis without vertebral malformations	Yes	Buchan et al. (2014)
	STAT3	None	N/A	*stat3*^{stl27} and *stat3*^{stl28} LOF mutants by TALENs	Mild embryonic axial defects, scoliosis with variable vertebral malformations	No	Liu et al. (2017)

LOF loss of function; *LBX1* ladybird homeobox 1; *PAX1* paired box 1; *POC5* proteome of centriole 5; *GPR126* G protein-coupled receptor 126; *BNC2* basonuclin-2; *IRX1/2/4* iroquois homeobox; *PTK7* protein tyrosine kinase 7; *KIF6* kinesin family member 6; *STAT3* signal transducer and activator of transcription 3; WES whole exome sequencing

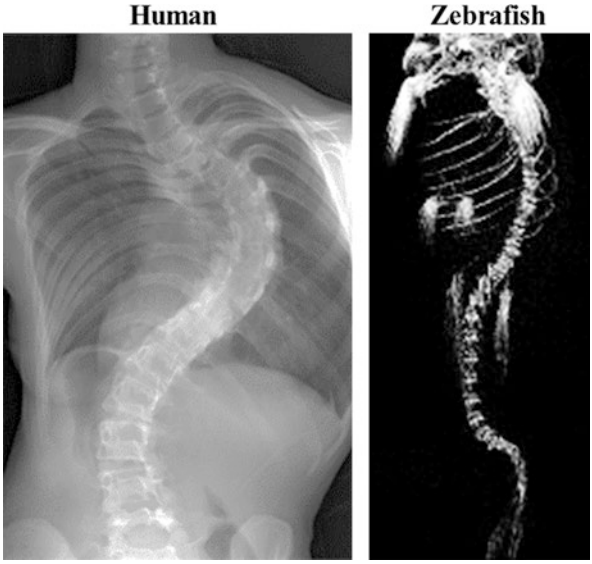

Fig. 11.4 Modeling human scoliosis in zebrafish
Micro-computed tomography (micro-CT) of zebrafish with transient *lbx1b* overexpression shows spinal curvature mimicking human adolescent idiopathic scoliosis (AIS) demonstrated by X-ray

of *LBX1* and its zebrafish homologs in body axis deformation at various stages of embryonic and subsequent growth in zebrafish, suggesting involvement of the non-canonical Wnt/PCP in the pathogenesis of AIS.

Another AIS-associated GWAS locus is distal to *PAX1* (Sharma et al. 2015). Pax1 is a member of the paired box (Pax) family of transcription factors containing a paired box domain and a paired-type homeodomain (Dahl et al. 1997). The Pax1/Pax9 subfamily regulates development of the axial skeleton (Peters et al. 1999). *Pax1* mouse mutants recapitulate human spinal anomalies including CS (Adham et al. 2005). Sharma et al. hypothesized that *Pax1* could contribute to the pathogenesis of IS by its roles in the post-somitogenesis development (Sharma et al. 2015). They found that a *PAX1* enhancer locus is associated with susceptibility to IS in females. The allele-specific transcriptional activity of a candidate enhancer named PEC7 was detected by transgenesis in zebrafish, although the reporter activity was detected in the somatic muscle. PEC7 contains a haplotype of five variants including the top-associated SNP rs169311. The risk haplotype completely abolished its enhancer activity. This finding suggests that the IS susceptibility haplotype confers a loss of function for an enhancer of *PAX1*.

Patten et al. examined six IS families with possible monogenic transmission by genetic linkage analyses combined with WES and identified a rare missense variant (p.A446T) of POC5 in a family (Patten et al. 2015). Then, two additional rare missense variants (p.A455P and p.A429V) were found in several families and individuals. POC5, a centrin-binding protein, is localized to the distal portion of human centrioles and is recruited to procentrioles for full centriolar maturation and normal cell cycle processing (Azimzadeh et al. 2009). Injection of the three variant POC5 mRNAs resulted in the embryonic body axis defects and scoliosis without vertebral malformations (Patten et al. 2015). Given that *poc5* is ubiquitously expressed during somitogenesis and that Poc5 functions as a centrosomal protein involved in cell

division, polarity, and motility, POC5 could play an important role in the early phase of body axis development. The left-right axis determination affected by primary cilia assembled by centrosomal proteins such as POC5 may underlie the pathogenesis of IS.

Zebrafish is also used in the functional analysis of several other IS susceptibility genes including *GPR126*, *BNC2*, and *IRX1/2/4*. *Gpr126* was found to be expressed in the cartilage. The knockdown of *gpr126* in zebrafish by injection of a morpholino antisense oligomer caused delayed ossification of the developing spine (Kou et al. 2013). Combined with the recent report that chondrocyte-specific conditional knockout lacking *Gpr126* in the *Col2a1*-expressing region mice develops IS-like spinal deformity at the thoracic level (Karner et al. 2015), *GPR126* is considered to contribute to the etiology of IS by its unknown roles in cartilage formation and/or function.

BNC2 was another susceptibility gene identified by GWAS (Yoji Ogura et al. 2015). While knockout mice and knockdown zebrafish did not exhibit scoliosis-associated phenotypes, ubiquitous overexpression of *BNC2* by tol2-mediated transient transgenesis in zebrafish causes severe body axial curvature and somite malformation (Yoji Ogura et al. 2015). The dose-dependent effects of *BNC2* were confirmed by *BNC2* mRNA injection into the fertilized zebrafish embryos. Abnormal somite formation of *BNC2* mRNA injected embryos was evident when 13–20 somites were present. Thus, increased *BNC2* expression would be implicated in the etiology of AIS, although the mechanism behind how *BNC2* causes AIS remains to be examined.

Genome-wide linkage identified a 3.5-Mb region on 5p13.3 containing three known genes, *IRX1*, *IRX2*, and *IRX4* (Justice et al. 2016). rs117273909 was located in a conserved intergenic region that is conserved among diverse species and is known to function as an enhancer in mice (Visel et al. 2007). To evaluate allelic difference of the enhancer activity of rs117273909 in zebrafish, transgenesis was performed using zebrafish enhancer detection (ZED) vector with fragments containing either allele of rs117273909 (Bessa et al. 2009; Justice et al. 2016). There were differences in the level of expression and the timing of GFP expression between the risk and non-risk alleles of rs117273909, although possibility of the positional effects cannot be excluded due to a large variation of expression pattern among multiple transgenic lines.

11.5.2 Phenotype-Based Approach

In the recent decade, the zebrafish has emerged as a popular model system among scientists, especially developmental biologists. Several projects were launched to generate the large scale of mutant libraries by forward genetic approaches determining the genetic basis responsible for a phenotype produced by artificial (random) mutagenesis such as chemical, radiation-induced, or insertional mutagenesis (Patton and Zon 2001). Compared with the traditional screening for mutants with visible

embryonic and larval phenotypes within the first 5 days of life, recent studies started to focus on the late-onset phenotypes such as neurodegenerative diseases and IS. On the other hand, recent progress in reverse genetic approaches analyzing the phenotypic effects of specific engineered gene sequences, especially the newly developed genome editing technologies, has made it much more efficient and affordable to generate mutant lines for genes of interests. Novel zebrafish mutant lines are being established much faster than ever before by lots of researchers with different interests. In these novel lines, unexpected phenotypes including IS have been found.

One of them is *Ptk7* mutant. Ptk7 is known as a regulator of both canonical Wnt/β-catenin and non-canonical Wnt/PCP signaling pathways and is required for vertebrate embryonic patterning and morphogenesis (Lu et al. 2004). Hayes et al. reported that maternal-zygotic $Ptk7^{hsc9}$ generated by using zinc-finger nuclease (ZFN) shows defects in axial convergence and extension and neural tube morphogenesis, which are related to the disruption of noncanonical Wnt/PCP signaling pathway (Hayes et al. 2013). Chimeric maternal-zygotic $Ptk7^{hsc9}$ mutant can survive to adult and display scoliosis with vertebral malformations that mimic human CS (Hayes et al. 2014). To some extent, these phenotypes overlap with those of transgenic zebrafish with *lbx1b* up-regulation (Guo et al. 2016). However, zygotic *ptk7* mutant zebrafish develop spinal curvatures that progress rapidly during late larval and early juvenile stages, without showing evident embryonic deformities and significant vertebral malformations due to maternal effects (Hayes et al. 2014). Such a spinal deformity also presents female preference, thus perfectly recapitulating the phenotype of human IS.

A further study using the *ptk7* mutant line found motile cilia defects in ependymal cell (EC) (Grimes et al. 2016). Motile cilia are microtubule-based organelles that project from the cell surface and function in generating the polarized flow of extracellular fluid. Cerebrospinal fluid (CSF) within the brain and spinal cord is generated by EC cilia motility (Ohata and Alvarez-Buylla 2016). Wnt signaling pathway has a known role in ciliogenesis (Choksi et al. 2014). *ptk7* zebrafish mutant exhibited gross disorganization of EC motile cilia in their brains, hydrocephalus, and severe deficiencies in CSF flow. Motile-ciliated cell-specific *pkt7* expression rescued the IS phenotype in the *ptk7* mutant zebrafish (Grimes et al. 2016). These studies on the *pkt7* mutant zebrafish implicate irregularities in CSF flow as an underlying biological cause of IS.

Based on the strong evidence from the zebrafish study, 96 IS patients were screened for *PTK7* mutations (Hayes et al. 2014). A novel heterozygous missense variant (p.P545A) was found in one IS patient and his non-penetrant father. Although the variant was determined to be a LOF mutation in zebrafish functional assays, the association of *PTK7* with IS in human was not established. Further study on the mutational burden of *PTK7* in a large population is necessary.

A forward mutagenesis screen using an N-ethyl-N-nitrosourea identified a zebrafish mutant with recessively inherited scoliosis similar to human IS (Buchan et al. 2014). The mutant line named *skolios* develops a complex, three-dimensional spinal curvature. It develops juvenile scoliosis without an increased frequency of

structural vertebral malformations. However, in contrast to the female preference in human AIS, *skolios* developed more severe spinal curves in male.

Using meiotic mapping and whole genome sequencing, a nonsense mutation (Tyr53*: gw326) in *kif6* was identified as the disease gene for the IS-like phenotype. Either homozygous *kif6*^{gw327} or compound heterozygous *kif6*$^{gw328/gw329}$ frameshift mutants generated with transcription activator-like effector nucleases (TALENs) recapitulated both the embryonic and post-embryonic *skolios* phenotypes, confirming that the loss of *kif6* is a cause of *skolios*. The known association of *kif6* with cilia suggests a possible involvement of ciliogenesis in the scoliosis formation, although no evidence for cilia dysfunction was seen in *kif6*^{gw326} mutants. The mechanism that LOF of *kif6* causes IS-like phenotypes in zebrafish remains unknown; these mutant lines would be valuable tools for understanding the etiology and pathogenesis of human IS.

STAT3 is an essential mediator of cytokine and growth factor signaling (Levy and Darnell 2002). Knockdown studies using morpholino in zebrafish revealed a requirement for stat3 in PCP signaling and gastrulation movements (Yamashita et al. 2002; Miyagi et al. 2004). *Stat3* knockout mice is lethal prior to gastrulation (Takeda et al. 1997). However, in zebrafish with null *stat3* mutations, both maternal and zygotic *stat3* mutants of zebrafish show nearly normal embryogenesis except for mild delay in extension movements during gastrulation due to the defects in cell proliferation and survival (Liu et al. 2017). Later, the zebrafish mutants present excessive inflammation and die by 1.5–2 months of age, which mimic multiple human syndromes such as hyper-IgE recurrent infection syndrome caused by *STAT3* mutations (Holland et al. 2007). Interestingly, the *stat3* mutants also show scoliotic phenotypes with variable structural abnormalities in the vertebrae (Liu et al. 2017). Although the pathology and etiology of syndromic scoliosis are usually considered to be greatly different from that of IS and CS, the mechanism of STAT3 in scoliosis formation is worth studying further.

11.6 Conclusions

Zebrafish model for scoliosis has just begun. Generally, the susceptibility gene-based approach in zebrafish has provided good support for their genetic association with scoliosis, especially AIS. The problem is that the majority of SNPs is not within a coding region but in non-coding or intergenic region. Even though the associated SNPs are mapped in the gene, establishing an AIS model is difficult due to polygenic inheritance of AIS. On the other hand, the phenotype-based approach found some good heritable IS in zebrafish mutants; however, most of them lack human counterparts. Nevertheless, findings from both types of approaches have converged to suggest that Wnt signaling pathway involved in the embryonic axial patterning and ciliogenesis could play a crucial role in the etiology and pathogenesis of IS, highlighting the advantage of the zebrafish system for understanding and modeling human scoliosis. With the advent of large-scale phenotype screening

system focusing on the late-onset diseases, more zebrafish IS models are expected to be generated. Much larger scale of GWAS and NGS-based genetic studies will no doubt identify more susceptibility genes which need to be investigated using *in vivo* models. The precise genome editing technology will allow us to establish more accurate zebrafish IS models. Coupled with the known advantage of the zebrafish system in high-throughput small molecule screens, zebrafish will give us hopes for the discovery and development of new drugs for treating IS.

References

Adham IM, Gille M, Gamel AJ, Reis A, Dressel R, Steding G et al (2005) The scoliosis (sco) mouse: a new allele of Pax1. Cytogenet Genome Res 111:16–26. https://doi.org/10.1159/000085665

Andersen MR, Farooq M, Koefoed K, Kjaer KW, Simony A, Christensen ST et al (2017) Mutation of the planar cell polarity gene VANGL1 in adolescent idiopathic scoliosis. Spine 42:E702–E707. https://doi.org/10.1097/BRS.0000000000001927

Azimzadeh J, Hergert P, Delouvee A, Euteneuer U, Formstecher E, Khodjakov A et al (2009) hPOC5 is a centrin-binding protein required for assembly of full-length centrioles. J Cell Biol 185(1):101–114. https://doi.org/10.1083/jcb.200808082

Baschal EE, Wethey CI, Swindle K, Baschal RM, Gowan K, Tang NLS et al (2014) Exome sequencing identifies a rare HSPG2 variant associated with familial idiopathic scoliosis. *G3 (Bethesda, Md.) 5*:167–174. https://doi.org/10.1534/g3.114.015669

Bessa J, Tena JJ, de la Calle-Mustienes E, Fernandez-Minan A, Naranjo S, Fernandez A et al (2009) Zebrafish enhancer detection (ZED) vector: a new tool to facilitate transgenesis and the functional analysis of cis-regulatory regions in zebrafish. Dev Dyn 238(9):2409–2417. https://doi.org/10.1002/dvdy.22051

Bobyn JD, Little DG, Gray R, Schindeler A (2015) Animal models of scoliosis. J Orthop Res: Official Publication of the Orthopaedic Research Society 33:458–467. https://doi.org/10.1002/jor.22797

Brent AE, Tabin CJ (2002) Developmental regulation of somite derivatives: muscle, cartilage and tendon. Curr Opin Genet Dev 12(5):548–557

Brohmann H, Jagla K, Birchmeier C (2000) The role of Lbx1 in migration of muscle precursor cells. Development (Cambridge, England) *127*:437–445

Buchan JG, Alvarado DM, Haller GE, Cruchaga C, Harms MB, Zhang T et al (2014) Rare variants in FBN1 and FBN2 are associated with severe adolescent idiopathic scoliosis. Hum Mol Genet 23:5271–5282. https://doi.org/10.1093/hmg/ddu224

Castelein RM, van Dieën JH, Smit TH (2005) The role of dorsal shear forces in the pathogenesis of adolescent idiopathic scoliosis – a hypothesis. Med Hypotheses 65:501–508. https://doi.org/10.1016/j.mehy.2005.03.025

Cheng JC, Castelein RM, Chu WC, Danielsson AJ, Dobbs MB, Grivas TB et al (2015) Adolescent idiopathic scoliosis. Nat Rev Dis Primers 1:15030. https://doi.org/10.1038/nrdp.2015.30

Choksi SP, Lauter G, Swoboda P, Roy S (2014) Switching on cilia: transcriptional networks regulating ciliogenesis. Development 141:1427–1441. https://doi.org/10.1242/dev.074666

Dahl E, Koseki H, Balling R (1997) Pax genes and organogenesis. BioEssays 19(9):755–765. https://doi.org/10.1002/bies.950190905

Fleming A, Keynes R, Tannahill D (2004) A central role for the notochord in vertebral patterning. Development 131(4):873–880. https://doi.org/10.1242/dev.00952

Gorman KF, Breden F (2009) Idiopathic-type scoliosis is not exclusive to bipedalism. Med Hypotheses 72:348–352. https://doi.org/10.1016/j.mehy.2008.09.052

Gorman KF, Tredwell SJ, Breden F (2007) The mutant guppy syndrome curveback as a model for human heritable spinal curvature. Spine 32:735–741. https://doi.org/10.1097/01.brs.0000259081.40354.e2

Gorman KF, Julien C d, Moreau A (2012) The genetic epidemiology of idiopathic scoliosis. Eur Spine J 21:1905–1919. https://doi.org/10.1007/s00586-012-2389-6

Grimes DT, Boswell CW, Morante NFC, Henkelman RM, Burdine RD, Ciruna B (2016) Zebrafish models of idiopathic scoliosis link cerebrospinal fluid flow defects to spine curvature. Science 352:1341–1344. https://doi.org/10.1126/science.aaf6419

Gross MK, Dottori M, Goulding M (2002) Lbx1 specifies somatosensory association interneurons in the dorsal spinal cord. Neuron 34:535–549

Guo L, Yamashita H, Kou I, Takimoto A, Meguro-Horike M, Horike S-i et al (2016) Functional investigation of a non-coding variant associated with adolescent idiopathic scoliosis in zebrafish: elevated expression of the ladybird Homeobox gene causes body axis deformation. PLoS Genet 12:e1005802. https://doi.org/10.1371/journal.pgen.1005802

Hayes M, Naito M, Daulat A, Angers S, Ciruna B (2013) Ptk7 promotes non-canonical Wnt/PCP-mediated morphogenesis and inhibits Wnt/β-catenin-dependent cell fate decisions during vertebrate development. Development (Cambridge, England) 140:1807–1818. https://doi.org/10.1242/dev.090183

Hayes M, Gao X, Yu LX, Paria N, Henkelman RM, Wise CA et al (2014) ptk7 mutant zebrafish models of congenital and idiopathic scoliosis implicate dysregulated Wnt signalling in disease. Nat Commun *5*:4777. https://doi.org/10.1038/ncomms5777

Hedequist D, Emans J (2007) Congenital scoliosis: a review and update. J Pediatr Orthop 27(1):106–116. https://doi.org/10.1097/BPO.0b013e31802b4993

Holland SM, DeLeo FR, Elloumi HZ, Hsu AP, Uzel G, Brodsky N et al (2007) STAT3 mutations in the hyper-IgE syndrome. N Engl J Med 357(16):1608–1619. https://doi.org/10.1056/NEJMoa073687

Ikegawa S (2016) Genomic study of adolescent idiopathic scoliosis in Japan. Scoliosis Spinal Disord 11:5. https://doi.org/10.1186/s13013-016-0067-x

Justice CM, Bishop K, Carrington B, Mullikin JC, Swindle K, Marosy B et al (2016) Evaluation of IRX genes and conserved noncoding elements in a region on 5p13.3 linked to families with familial idiopathic scoliosis and kyphosis. G3 (Bethesda, Md.) 6:1707–1712. https://doi.org/10.1534/g3.116.029975

Karner CM, Long F, Solnica-Krezel L, Monk KR, Gray RS (2015) Gpr126/Adgrg6 deletion in cartilage models idiopathic scoliosis and pectus excavatum in mice. Hum Mol Genet 24(15):4365–4373. https://doi.org/10.1093/hmg/ddv170

Konieczny MR, Senyurt H, Krauspe R (2013) Epidemiology of adolescent idiopathic scoliosis. J Child Orthop 7:3–9. https://doi.org/10.1007/s11832-012-0457-4

Kou I, Takahashi Y, Johnson TA, Takahashi A, Guo L, Dai J et al (2013) Genetic variants in GPR126 are associated with adolescent idiopathic scoliosis. Nat Genet 45(6):676–679. https://doi.org/10.1038/ng.2639

Kou I, Watanabe K, Takahashi Y, Momozawa Y, Khanshour A, Grauers A, Zhou H, Liu G, Fan Y-H, Takeda K, Ogura Y, Zhou T, Iwasaki Y, Kubo M, Wu Z, Matsumoto M, Einarsdottir E, Kere J, Huang D, Qiu G, Qiu Y, Wise CA, Song Y-Q, Wu N, Su P, Gerdhem P, Ikegawa S (2018) A multi-ethnic metaanalysis confirms the association of rs6570507 with adolescent idiopathic scoliosis. Sci Rep 8(1)

Levy DE, Darnell JE Jr (2002) Stats: transcriptional control and biological impact. Nat Rev Mol Cell Biol 3(9):651–662. https://doi.org/10.1038/nrm909

Li W, Li Y, Zhang L, Guo H, Tian D, Li Y et al (2016) AKAP2 identified as a novel gene mutated in a Chinese family with adolescent idiopathic scoliosis. J Med Genet 53:488–493. https://doi.org/10.1136/jmedgenet-2015-103684

Liu Y, Sepich DS, Solnica-Krezel L (2017) Stat3/Cdc25a-dependent cell proliferation promotes embryonic axis extension during zebrafish gastrulation. PLoS Genet 13(2):e1006564. https://doi.org/10.1371/journal.pgen.1006564

Londono D, Kou I, Johnson TA, Sharma S, Ogura Y, Tsunoda T et al (2014) A meta-analysis identifies adolescent idiopathic scoliosis association with *LBX1* locus in multiple ethnic groups. J Med Genet 51:401–406. https://doi.org/10.1136/jmedgenet-2013-102067

Lu X, Borchers AGM, Jolicoeur C, Rayburn H, Baker JC, Tessier-Lavigne M (2004) PTK7/CCK-4 is a novel regulator of planar cell polarity in vertebrates. Nature 430:93–98. https://doi.org/10.1038/nature02677

Miyagi C, Yamashita S, Ohba Y, Yoshizaki H, Matsuda M, Hirano T (2004) STAT3 noncell-autonomously controls planar cell polarity during zebrafish convergence and extension. J Cell Biol 166(7):975–981. https://doi.org/10.1083/jcb.200403110

Ogura Y, Kou I, Miura S, Takahashi A, Xu L, Takeda K et al (2015) A functional SNP in BNC2 is associated with adolescent idiopathic scoliosis. Am J Hum Genet 97(2):337–342. https://doi.org/10.1016/j.ajhg.2015.06.012

Ogura Y, Takeda K, Kou I, Khanshour A, Grauers A, Zhou H, Liu G, Fan Y-H, Zhou T, Wu Z, Takahashi Y, Matsumoto M, Einarsdottir E, Kere J, Huang D, Qiu G, Xu L, Qiu Y, Wise CA, Song Y-Q, Wu N, Su P, Gerdhem P, Watanabe K, Ikegawa S (2018) An international meta-analysis confirms the association of BNC2 with adolescent idiopathic scoliosis. Sci Rep 8(1)

Ohata S, Alvarez-Buylla A (2016) Planar organization of multiciliated ependymal (E1) cells in the brain ventricular epithelium. Trends Neurosci 39:543–551. https://doi.org/10.1016/j.tins.2016.05.004

Ouellet J, Odent T (2013) Animal models for scoliosis research: state of the art, current concepts and future perspective applications. Eur Spine J: Official Publication of the European Spine Society, the European Spinal Deformity Society, and the European Section of the Cervical Spine Research Society 22(Suppl 2):S81–S95. https://doi.org/10.1007/s00586-012-2396-7

Patten SA, Margaritte-Jeannin P, Bernard J-C, Alix E, Labalme A, Besson A et al (2015) Functional variants of POC5 identified in patients with idiopathic scoliosis. J Clin Invest 125:1124–1128. https://doi.org/10.1172/JCI77262

Patton EE, Zon LI (2001) The art and design of genetic screens: zebrafish. Nat Rev Genet 2:956–966. https://doi.org/10.1038/35103567

Peters H, Wilm B, Sakai N, Imai K, Maas R, Balling R (1999) Pax1 and Pax9 synergistically regulate vertebral column development. Development 126(23):5399–5408

Pourquie O (2011) Vertebrate segmentation: from cyclic gene networks to scoliosis. Cell 145(5):650–663. https://doi.org/10.1016/j.cell.2011.05.011

Schäfer K, Neuhaus P, Kruse J, Braun T (2003) The homeobox gene Lbx1 specifies a subpopulation of cardiac neural crest necessary for normal heart development. Circ Res 92:73–80

Shands AR Jr, Bundens WD (1956) Congenital deformities of the spine; an analysis of the roentgenograms of 700 children. Bull Hosp Joint Dis 17(2):110–133

Sharma S, Gao X, Londono D, Devroy SE, Mauldin KN, Frankel JT et al (2011) Genome-wide association studies of adolescent idiopathic scoliosis suggest candidate susceptibility genes. Hum Mol Genet 20:1456–1466. https://doi.org/10.1093/hmg/ddq571

Sharma S, Londono D, Eckalbar WL, Gao X, Zhang D, Mauldin K et al (2015) A PAX1 enhancer locus is associated with susceptibility to idiopathic scoliosis in females. Nat Commun 6:6452. https://doi.org/10.1038/ncomms7452

Stickney HL, Barresi MJ, Devoto SH (2000) Somite development in zebrafish. Dev Dyn 219(3):287–303. https://doi.org/10.1002/1097-0177(2000)9999:9999<::AID-DVDY1065>3.0.CO;2-A

Takahashi Y, Kou I, Takahashi A, Johnson TA, Kono K, Kawakami N et al (2011) A genome-wide association study identifies common variants near LBX1 associated with adolescent idiopathic scoliosis. Nat Genet 43(12):1237–1240. https://doi.org/10.1038/ng.974

Takeda K, Noguchi K, Shi W, Tanaka T, Matsumoto M, Yoshida N et al (1997) Targeted disruption of the mouse Stat3 gene leads to early embryonic lethality. Proc Natl Acad Sci U S A 94(8):3801–3804

Visel A, Minovitsky S, Dubchak I, Pennacchio LA (2007) VISTA enhancer browser – a database of tissue-specific human enhancers. Nucleic Acids Res 35:D88–D92. https://doi.org/10.1093/nar/gkl822

Wang WJ, Yeung HY, Chu WC-W, Tang NL-S, Lee KM, Qiu Y et al (2011) Top theories for the etiopathogenesis of adolescent idiopathic scoliosis. J Pediatr Orthop 31:S14–S27. https://doi.org/10.1097/BPO.0b013e3181f73c12

Witten PE, Huysseune A (2009) A comparative view on mechanisms and functions of skeletal remodelling in teleost fish, with special emphasis on osteoclasts and their function. Biol Rev Camb Philos Soc 84(2):315–346. https://doi.org/10.1111/j.1469-185X.2009.00077.x

Yamashita S, Miyagi C, Carmany-Rampey A, Shimizu T, Fujii R, Schier AF et al (2002) Stat3 controls cell movements during zebrafish gastrulation. Dev Cell 2(3):363–375

Zhu Z, Tang NL-S, Xu L, Qin X, Mao S, Song Y et al (2015) Genome-wide association study identifies new susceptibility loci for adolescent idiopathic scoliosis in Chinese girls. Nat Commun 6:8355. https://doi.org/10.1038/ncomms9355

Chapter 12
Medaka Fish Model of Parkinson's Disease

Norihito Uemura and Ryosuke Takahashi

Abstract Parkinson's disease (PD) is the most common neurodegenerative movement disorder. PD is pathologically characterized by dopamine (DA) neuron loss in the substantia nigra pars compacta (SNpc), accompanied by α-synuclein aggregates known as Lewy bodies. Animal models are indispensable for elucidating the pathological mechanisms of diseases and developing new treatments. However, a lack of animal model that faithfully replicates PD has been a major barrier to overcoming this disease. Here, we present novel animal models of PD in medaka fish. Teleost fish have DA neurons that correspond to those observed in humans within the SNpc, allowing us to evaluate their phenotypes as PD models. We have developed several animal models of PD in medaka fish via toxin or genetic modification. In our models, we found that dopaminergic neurotoxins caused DA neuron loss and a reduction of spontaneous swimming movement, suggesting the potential utility of medaka fish as an animal model of PD. Administration of proteasome or lysosome inhibitors resulted in DA neuron loss accompanied by ubiquitin-positive cytosolic inclusion bodies, suggesting that DA neurons are vulnerable to proteasome or lysosome dysfunction. Several lines of medaka fish with mutations in the causative genes of rare familial PD demonstrated that mitochondrial dysfunction and impairment of the autophagy–lysosome pathway are involved in the development of PD. In this review, we outline PD medaka models we have developed and discuss future perspectives on medaka fish as a PD model.

Keywords Parkinson's disease · Dopamine neuron · Animal model · Neurotoxin · Genetics · Medaka

N. Uemura (✉) · R. Takahashi
Department of Neurology, Kyoto University Graduate School of Medicine, Kyoto, Japan
e-mail: nuemura@kuhp.kyoto-u.ac.jp; ryosuket@kuhp.kyoto-u.ac.jp

H. Hirata, A. Iida (eds.), *Zebrafish, Medaka, and Other Small Fishes*,
https://doi.org/10.1007/978-981-13-1879-5_12

12.1 Introduction

Parkinson's disease (PD) was first described by James Parkinson in 1817. Today, this disease is the second most common neurodegenerative disorder after Alzheimer's disease, affecting ~1% of the population aged >60 years (de Lau and Breteler 2006). Clinically, PD is characterized by four cardinal motor manifestations: bradykinesia, muscular rigidity, resting tremor, and postural instability (Kalia and Lang 2015). Other symptoms may include various non-motor features such as smell loss, constipation, anxiety, depression, and cognitive dysfunction. Pathologically, the diagnostic criteria of PD include dopamine (DA) neuron loss in the substantia nigra pars compacta (SNpc) and the presence of α-synuclein (α-Syn) aggregates in the form of Lewy bodies and neurites (Dickson et al. 2009) (Fig. 12.1). The resulting DA deficiency in the basal ganglia leads to parkinsonian motor symptoms. DA replacement therapy is available for motor symptoms, but no treatments have been shown to halt or even slow the neurodegenerative process. In addition, non-motor symptoms are frequently difficult to control and lead to distress among patients and caregivers. Therefore, there is a strong demand for the elucidation of the pathological mechanisms of this disease and the development of new treatments.

Most cases of PD are sporadic, but a subset (5–10%) of them is familial. Various environmental and genetic factors are thought to be associated with the development of sporadic PD. Environmental factors include aging, smoking, coffee consumption, dietary habits, physical activity, exposure to heavy metals, head trauma, and exposure to pesticides (de Lau and Breteler 2006; Petzinger et al. 2013). Genome-wide association studies have demonstrated that single nucleotide

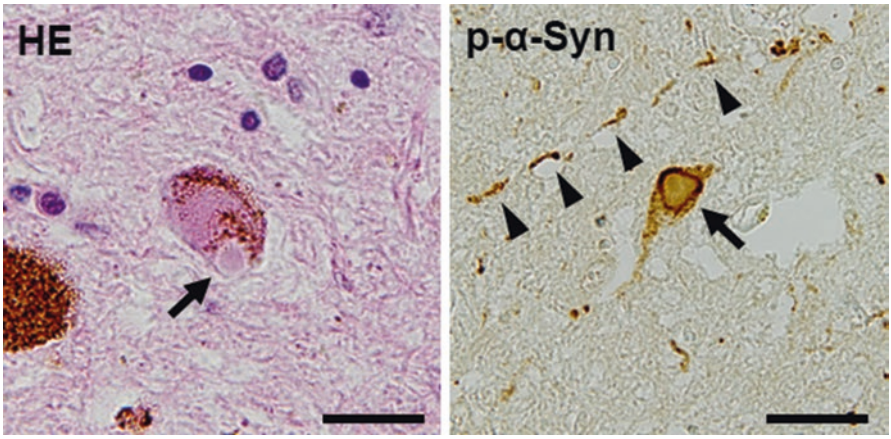

Fig. 12.1 Lewy pathology in the substantia nigra pars compacta of a patient with Parkinson's disease (PD). Left panel: hematoxylin and eosin (HE) staining. In humans, dopamine neurons in the substantia nigra pars compacta contain the pigment neuromelanin. Right panel: phosphorylated alpha-synuclein (p-α-Syn) immunohistochemistry. Lewy bodies (arrows) and Lewy neurites (arrowheads). Scale bar, 20 μm

Table 12.1 Classification of familial PD

Symbol	Loci	Gene	Inheritance
PARK1	4q21-22	SNCA	AD
PARK2	6q25-27	Parkin	AR
PARK3	2p13	?	AD
PARK4	4q21-22	SNCA	AD
PARK5	4p14	UCH-L1	AD (?)
PARK6	1p35-36	PINK1	AR
PARK7	1p36	DJ-1	AR
PARK8	12q12	LRRK2	AD
PARK9	1p36	ATP13A2	AR
PARK10	1p32	?	Susceptibility locus
PARK11	2q36-37	GIGYF2	Susceptibility locus (?)
PARK12	Xq21-q25	?	Susceptibility locus
PARK13	2p12	Omi/HtrA2	Susceptibility locus
PARK14	22q13	PLA2G6	AR
PARK15	22q12-13	FBX07	AR
PARK16	1q32	RAB7L1	Susceptibility locus
PARK17	16q12	VPS35	AD
PARK18	3q27	EIF4G1	AD
GBA	1q21-22	GBA	Susceptibility locus

AD autosomal dominant, *AR* autosomal recessive

polymorphisms in several genes are potential risk factors for sporadic PD (Satake et al. 2009). In addition, heterozygous mutations in *GBA* gene were recently identified as the strongest risk factors for sporadic PD (Sidransky et al. 2009). Meanwhile, to date, approximately 20 genes have been implicated in the familial forms of PD. They include PARK1 [mutation of *alpha-synuclein* (*SNCA*)], PARK2 (mutation of *Parkin*), PARK4 (triplication of *SNCA*), PARK6 [mutation of *PTEN-induced putative kinase 1* (*PINK1*)], and PARK9 (mutation of *ATP13A2*) (Table 12.1).

Animal models are quite instructive in understanding the pathophysiology of brain diseases; they provide the means to study a cellular process in the context of functional neuronal circuits and a complex system of neurons and glia. Moreover, animal models can be used to develop new therapeutic strategies for treating human diseases, including identification and validation of candidate compounds and assessment of toxicity and safety. Animals ranging from invertebrates (e.g., nematodes, flies) to vertebrates (e.g., rodents, monkeys) have been used as PD models. However, there are still no animal models that faithfully recapitulate the clinical and pathological features of PD (Dawson et al. 2010). Notably, even *Parkin*/*PINK1*/*DJ-1* triple-knockout mice do not show DA neuron loss in the SNpc (Kitada et al. 2009). To overcome this limitation, we have aimed to develop a novel animal model of PD using medaka fish.

12.2 Catecholamine Systems in Mammals and Teleost Fish

The mammalian catecholamine (CA) neuron groups in the central nervous system are numbered in a caudo-rostral order (Kastenhuber et al. 2010; Bjorklund and Dunnett 2007). The mammalian noradrenaline (NA) groups A1, A2, and A4–A7 are located in the hindbrain. Among them, NA neurons in the locus coeruleus (LC, A6) are the most prominent and have both ascending and descending projections to widespread brain regions. Mammalian DA neurons are categorized into A8–A17. The major mammalian DA neuron groups are located in the midbrain and include the retrorubral area (A8), SNpc (A9), and ventral tegmental area (VTA, A10). These midbrain DA neurons project to the striatum and to the limbic/cerebral cortical regions (Bjorklund and Dunnett 2007). A9 neurons of the SNpc project to the striatum along the mesostriatal pathway, whereas A10 neurons of the VTA project to the limbic/cortical areas along the mesolimbic and mesocortical pathways. A8 neurons, forming a dorsal and caudal extension of the A9 cell group, project to both the striatum and the limbic/cortical areas. DA neurons are also located in the diencephalon (A11–A15), olfactory bulb (A16), and inner nuclear layer of the retina (A17).

In PD, DA neurons in the SNpc (A9) are particularly vulnerable compared with other DA groups and are implicated in the expression of parkinsonian motor symptoms. However, Lewy pathology is not only observed in the SNpc but also more widely within the central nervous system (Braak et al. 2003). Systematic pathological analysis of PD patients and incidental cases suggest that Lewy pathology initially develops in the olfactory bulb and dorsal motor nucleus of the vagal nerve (dmX) and spreads in the brain in a stereotypical fashion. In particular, Lewy pathology in the dmX proceeds mainly in a caudo-rostral direction, involving the LC (A6), before reaching the SNpc. Severe NA neuron loss in the LC as well as DA neuron loss in the SNpc is observed in patients with PD (Del Tredici and Braak 2013).

The CA neuron system of teleost fish has been thoroughly investigated in zebrafish. NA neurons have been located and described in the medulla oblongata and LC and as well as DA cell groups in the olfactory bulb, subpallium (ventral telencephalon), retina, preoptic region, pretectum, and ventral diencephalon. DA neurons in the ventral diencephalon (DC) have been assigned numbers (DC1–DC7) based on their morphology and position along the rostro-caudal axis (Rink and Wullimann 2002). Unlike mammals, teleost fish lack DA neurons in the mesencephalon. However, some DA neurons located in the posterior tuberculum (DC2 and DC4) have been shown to project to the subpallium, indicating that these neurons are equivalent to mammalian midbrain DA neurons (Tay et al. 2011; Rink and Wullimann 2001).

To assess the potential for a teleost fish model of PD, we first evaluated the distribution of DA neurons in the medaka fish via tyrosine hydroxylase (TH) immunohistochemistry and DA transporter (DAT) in situ hybridization (unpublished data). Anatomically, the DA system of the medaka fish is almost identical to that of zebrafish (Matsui et al. 2009). Therefore, we were able to count the number of DA neurons in the ventral diencephalon (including DC2/DC4 of the posterior tuberculum) and NA neurons in the LC to evaluate our experimental PD models in the medaka fish (Fig. 12.2).

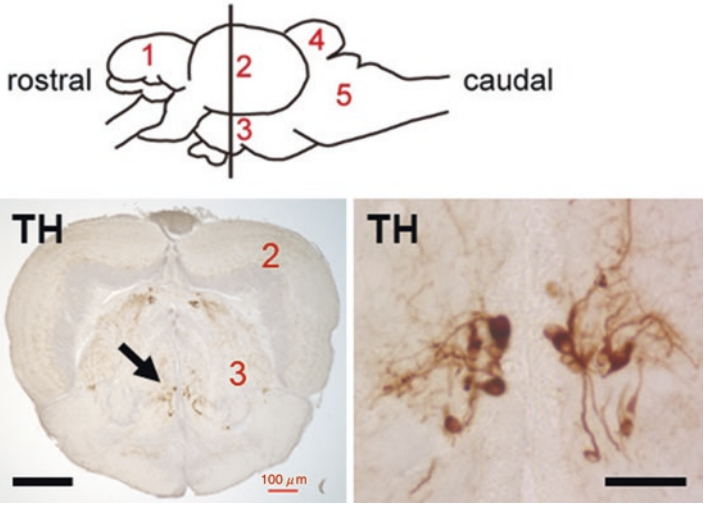

Fig. 12.2 Dopamine neurons in the diencephalon of the medaka fish. Upper panel: schematic of a lateral view of the medaka fish brain. Each number signifies a part of the brain: 1, telencephalon; 2, optic tectum; 3, diencephalon; 4, cerebellum; 5, medulla oblongata. Lower left panel: low-magnification image of tyrosine hydroxylase (TH) immunohistochemistry. This section is illustrated by the vertical line in the upper panel and contains the optic tectum (2) and diencephalon (3). TH-positive neurons in the ventral diencephalon (arrow). Scale bar, 200 μm. Lower right panel: high-magnification image of the TH-positive neurons in the ventral diencephalon. Scale bar, 40 μm

12.3 Toxin-Induced Models

12.3.1 MPTP and 6-OHDA Models

A couple of neurotoxins have been used to induce PD-like phenotypes in animal models. One such neurotoxin is 1-methyl-4-phenyl-1,2,3,6-tetrahydropyridine (MPTP), an accidentally produced analog of the narcotic drug meperidine. MPTP was initially discovered as a parkinsonism-inducing neurotoxin in the 1980s (Przedborski et al. 2001). MPTP crosses the blood–brain barrier and is metabolized into MPP+ and is then taken up by DAT. Once inside DA neurons, MPP+ impairs mitochondrial respiration by inhibiting complex I of the electron transport chain, resulting in increased production of free radicals and induction of DA neuron death (Vila and Przedborski 2003). MPTP is frequently used to replicate DA neuron loss and resulting motor deficit in animal models. To explore our medaka model of PD induced by MPTP, we kept the medaka fish in water containing MPTP (Matsui et al. 2009). For the measurement of spontaneous swimming movement, medaka fish treated with or without MPTP were kept in the circular water tanks, and their images were collected by a video camera positioned above the water tanks. We found that treatment of medaka larva with MPTP for 2 days induced DA neuron loss in the diencephalon and decreased spontaneous swimming movement in a concentration-dependent manner. Interestingly, among TH-positive neurons in the medaka brain,

a specific cluster in the paraventricular area of the middle diencephalon was particularly vulnerable to MPTP toxicity. This finding led us to speculate that this middle diencephalic cluster shares a similar vulnerability to the mammalian SNpc.

Another neurotoxin, 6-hydroxydopamine (6-OHDA), has also been used to induce PD-like phenotypes in animal models. Given that 6-OHDA does not easily cross the blood–brain barrier, 6-OHDA should be directly injected into areas of the rodent brain, such as the SNpc, medial forebrain bundle, or striatum (Blum et al. 2001). Following its injection, 6-OHDA is taken up into DA neurons via DAT and gains access to the cytosol, where it generates oxidative stress, leading to DA neuron loss. For the treatment of adult medaka fish with 6-OHDA, we developed a method using a glass micropipette coupled with a Hamilton syringe. This method allows us to deliver the chemicals directly into the cerebrospinal fluid (CSF) space of the medaka fish without damaging the brain parenchyma (Matsui et al. 2010a). Three days after administration of 6-OHDA using this method, we observed selective DA neuron loss in the diencephalon and decreased spontaneous swimming movement.

Collectively, we found that classical dopaminergic neurotoxins (MPTP and 6-OHDA) successfully induced PD-like phenotypes in the medaka fish, indicating the potential for the medaka fish to serve as an animal model of PD.

12.3.2 Proteasome or Lysosome Inhibitor Models

The pathological hallmark of PD is α-Syn aggregates, referred to as Lewy bodies. Several lines of experimental evidence show that clearance of α-Syn involves ubiquitin–proteasome and autophagy–lysosome systems. Elevated expression level of α-Syn or impairment of these degradation systems leads to aggregation of α-Syn (Ebrahimi-Fakhari et al. 2012). In support of this notion, Lewy bodies are immunopositive for ubiquitin, LC3, and p62/SQSTM1 as well as α-Syn. Both LC3 and p62/SQSTM1 participate in autophagy. Moreover, recent genetic studies revealed that PARK9, a type of autosomal recessive familial PD, is caused by mutations of *ATP13A2*, which encodes a cation transporter-like membrane protein localized in the lysosome (Ramirez et al. 2006). More recently, mutations in *GBA*, which encodes the lysosomal enzyme glucocerebrosidase, were reported to be the strongest genetic risk factors for sporadic PD (Sidransky et al. 2009). These genetic findings also suggest that lysosomal dysfunction participates in the development of PD.

To examine the effects of dysfunction in these degradation systems on DA neurons, we first injected proteasome inhibitors, lactacystin or epoxomicin, into the CSF space of the medaka fish (Matsui et al. 2010a). A single injection of each proteasome inhibitor successfully inhibited proteasome activity in the brain after 1 day postinjection. Histological analysis performed 3 days postinjection revealed ubiquitin-positive aggregates throughout the brain. TH-positive neurons also contained cytoplasmic ubiquitin-positive inclusions. Surprisingly, although inclusion body formation was not specific to DA/NA neurons, neuronal loss was observed

predominantly in DA/NA neurons. Moreover, DA/NA levels were reduced in the medaka fish treated with lactacystin without any changes in the levels of serotonin, another monoamine. These fish showed decreased spontaneous swimming movement, which may reflect PD-like motor deficits.

Next, we administered a lysosome inhibitor, ammonium chloride, into the CSF space of the medaka fish (Matsui et al. 2010b). Similarly, although ubiquitin-positive aggregates were observed throughout the brain, neuron loss was observed specifically in DA/NA neurons. Interestingly, in this model, we also found that synuclein accumulated and co-localized with ubiquitin in the brain.

In summary, these results indicate that DA/NA neurons are particularly vulnerable to proteasome and lysosome dysfunction. Administration of inhibitors of these systems into the CSF space may recapitulate part of the PD phenotype in medaka fish.

12.4 Genetic Models

12.4.1 Parkin and PINK1 Mutant Model

Mutations in *Parkin* were first identified as the genetic cause of autosomal recessive juvenile parkinsonism among Japanese families (Kitada et al. 1998). More than 100 mutations in *Parkin* have subsequently been reported, accounting for 50% of familial PD cases and at least 20% of early-onset PD (Lucking et al. 2000). Mutations in *PINK1*, the second most common autosomal recessive mutation following *Parkin*, contribute to almost 2–4% of early-onset PD (Samaranch et al. 2010). Unlike sporadic PD, most autopsy cases with homozygous *Parkin* mutations have revealed DA neuron loss in the SNpc, with absent Lewy body pathology (Schneider and Alcalay 2017). In terms of *PINK1*, a brain autopsy was available for only one patient with compound heterozygous mutations in *PINK1*. In contrast to cases with *Parkin* mutations, this autopsy case revealed classical Lewy body pathology.

Parkin functions as an E3 ubiquitin ligase in the cytoplasm and participates in the ubiquitin–proteasome system. PINK1 is a serine/threonine kinase localized to the mitochondria. *Drosophila* greatly contributed to clarifying the molecular mechanisms of Parkin and PINK1 (Park et al. 2006; Clark et al. 2006). Knockout of Parkin in *Drosophila* led to muscle degeneration accompanied by morphological abnormality of mitochondria and to infertility due to abnormality of sperm. Interestingly, the phenotype of *Drosophila* lacking PINK1 was similar to that observed in Parkin knockouts, and this phenotype was ameliorated by transgenic expression of Parkin. However, transgenic expression of PINK1 had no effect on Parkin knockout phenotypes. This led to the hypothesis that Parkin and PINK1 function in a common pathway, in which PINK1 is upstream of Parkin. In line with this notion, additional cellular studies showed that Parkin accumulates in damaged mitochondria and promotes autophagic clearance of mitochondria (i.e., mitophagy), together with PINK, to maintain mitochondria homeostasis and function (Narendra et al. 2010). On the other hand, as mentioned above, even *Parkin*/*PINK1*/*DJ-1* triple-knockout mice do

not show any apparent phenotypes, suggesting that mice have some compensatory mechanisms for loss of function of these genes (Kitada et al. 2009).

We generated Parkin nonsense (Y320X) mutant and PINK1 nonsense (Q178X) mutant medaka fish by screening the Targeting Induced Local Lesions In Genomes (TILLING) library (Matsui et al. 2010c, 2013a). Y320X mutation in Parkin resulted in the deletion of IBR and RING2 domains, whereas Q178X mutation in PINK1 resulted in disruption of the kinase domain. This suggests that both gene mutations result in a loss of function. However, even 12-month-old medaka fish with homozygous Parkin or PINK1 mutations show minimal motor deficits and no DA/NA neuron loss. Surprisingly, however, homozygous Parkin/PINK1 double mutant medaka fish showed PD-like phenotypes, age-dependent DA/NA neuron loss, and decreased spontaneous swimming movement. In addition, homozygous Parkin/PINK1 double mutant medaka fish showed decreased activity in mitochondrial complexes and morphological abnormality of mitochondria. These results were reproduced with mammalian cells—mouse embryonic fibroblasts (MEF). In particular, Parkin/PINK1 double-deficient MEF showed a further decrease in mitochondrial membrane potential and mitochondrial complex I activity, as well as higher rates of apoptosis than Parkin or PINK1 single-deficient MEF. Interestingly, the mitochondrial abnormalities observed in Parkin-deficient MEF were compensated by exogenously expressed PINK1, but not by disease-related mutants. Based on these results, we hypothesized that Parkin and PINK1 in vertebrates work not only in a single pathway but also in independent parallel pathways to protect DA neurons by maintaining mitochondrial quality. In initial support of our hypothesis, a recent study reported that mitophagy can be initiated by PINK1 alone even if the cells lack Parkin and that Parkin acts to amplify this process (Lazarou et al. 2015).

12.4.2 ATP13A2 Mutant Model

ATP13A2 mutations have been linked to an autosomal recessive juvenile form of parkinsonism called Kufor–Rakeb syndrome. This atypical parkinsonism includes pyramidal signs, supranuclear gaze palsy, and cognitive decline (Williams et al. 2005). Brain pathology is not available from any patient diagnosed with Kufor–Rakeb syndrome. However, homozygous *ATP13A2* mutations were identified in a family diagnosed with juvenile neuronal ceroid lipofuscinosis, whose brain pathology is available. Pathology showed abundant neuronal and glial lipofuscinosis throughout the brain and no visible Lewy bodies (Schneider and Alcalay 2017; Bras et al. 2012).

ATP13A2 is an ATPase belonging to the type 5 P-type family. This protein is localized to the endo−/lysosome and putatively functions as a cation transporter. Several cellular experiments have demonstrated that overexpression of ATP13A2 rendered cells more resistant to Mn^{2+} cytotoxicity, indicating a protective role of ATP13A2 against elevated concentrations of Mn^{2+} (Gitler et al. 2009). In contrast, other cellular studies have reported that ATP13A2 acts as a transporter of Zn^{2+} and relieves Zn^{2+} cytotoxicity (Tsunemi and Krainc 2014). Thus, the true function of ATP13A2 remains elusive.

We found *ATP13A2* splicing mutant (IVS13, T-C, +2) medaka in the TILLING library (Matsui et al. 2013b). Homozygous *ATP13A2* mutant medaka showed a reduction in expression levels of *ATP13A2* mRNA in the brain to ~20%. Although homozygous *ATP13A2* mutant medaka fish did not show motor deficits, they did show DA/NA neuron loss at 12 months of age. In addition, we observed decreased cathepsin D activity in the brains and fingerprint-like structures in the neurons of homozygous *ATP13A2* mutant medaka fish. These features (i.e., decreased cathepsin D activity and fingerprint-like structures) were replicated using ATP13A2-knockdown cultured cells. Interestingly, fingerprint-like structures have also been described in the neurons of cathepsin D-deficient mice and in human patients with neuronal ceroid lipofuscinosis or with sphingolipidoses. These results indicated that decreased expression of ATP13A2 results in lysosomal dysfunction. Although cathepsin D is known to degrade α-Syn, we did not find any α-Syn accumulation in the brains of homozygous *ATP13A2* mutant medaka.

Recent research with *ATP13A2* knockout mice demonstrated lysosomal abnormalities in neurons, lipofuscin deposition, and progressive motor symptoms (Kett et al. 2015). Interestingly, however, DA neuron loss and α-Syn accumulation were not observed in these mice. Furthermore, α-Syn depletion did not ameliorate the phenotypes of *ATP13A2* knockout mice, indicating that α-Syn is not involved in the pathogenesis of ATP13A2 deficiency.

12.4.3 GBA Mutant Model

Gaucher disease (GD) is the most common lysosomal storage disease caused by homozygous mutations in *GBA*. *GBA* encodes glucocerebrosidase, a lysosomal protein, and mutations in *GBA* lead to decreased enzymatic activity of glucocerebrosidase (GCase) and result in the accumulation of its substrates, glucocerebroside and glucosylsphingosine (Grabowski 2008). GD is classically divided into three subtypes: a non-neuronopathic form (type 1), an acute neuronopathic form (type 2), and a subacute neuronopathic form (type 3). Visceral manifestations of all forms are characterized by hepatosplenomegaly, cytopenia, and skeletal disease. Pathologically, the accumulation of lipid-laden macrophages, known as Gaucher cells, is observed in the affected organs. Neurological manifestations of neuronopathic forms of GD include brain stem dysfunction, intellectual disability, seizures, and myoclonic movement. Pathological features of neuronopathic forms include neuronal loss, astrogliosis, microgliosis, and perivascular accumulation of Gaucher cells (Wong et al. 2004). The most severe neuronopathic form is known as the perinatal lethal type (Eblan et al. 2005). Common presentations of patients with the perinatal lethal type include hydrops fetalis and congenital ichthyosis. Almost no residual GCase enzymatic activity is found in these cases. Given that currently available therapies are ineffective for neurological manifestations, there is a critical need to elucidate pathological mechanisms and develop novel therapies.

Recognition of the association between *GBA* mutations and PD began in the clinic with the identification of some patients with type 1 GD who also showed

parkinsonian symptoms (Neudorfer et al. 1996). Subsequent pedigree analyses revealed that relatives of patients with GD, many of whom were obligate heterozygotes (i.e., GD carriers), had an increased incidence of PD (Goker-Alpan et al. 2004). Recently, a large-scale genetic study revealed a strong association between *GBA* mutations and PD (odds ratio for PD patients vs. controls, 5.43) (Sidransky et al. 2009). In addition, patients with type 1 GD have been shown to have an increased lifetime risk of developing PD (Bultron et al. 2010). In particular, the adjusted lifetime risk ratio of PD among patients with type 1 GD was reported to be 21.4. PD patients carrying *GBA* mutations show intraneuronal accumulation of α-Syn (i.e., Lewy bodies), the pathological hallmark of sporadic PD (Wong et al. 2004). Based on these findings, *GBA* is recognized as one of the most important clues to clarify the pathogenesis of sporadic PD.

Several cellular, animal, and postmortem studies have indicated an association between *GBA* mutations and α-Syn accumulation. Deficiency in GCase enzymatic activity causes lysosomal dysfunction and α-Syn accumulation (Mazzulli et al. 2011). Increase in α-Syn, in turn, induces a vicious cycle by inhibiting the trafficking of GCase to lysosomes, thus leading to further decrease in GCase activity in lysosomes. Consistent with this notion, mouse models overexpressing α-Syn and postmortem tissue from patients with PD show reduced GCase activity in the brain (Gegg et al. 2012; Sardi et al. 2013).

We generated *GBA* nonsense (W337X) mutant medaka fish that are completely deficient in GCase activity (Uemura et al. 2015). In contrast to the perinatal death observed in both humans and mice lacking GCase activity, homozygous *GBA* mutant medaka fish survived for months, enabling analysis of the pathological progression. Homozygous *GBA* mutant medaka fish displayed abnormal rotating swimming movement at 2 months of age, as well pathological phenotypes resembling human neuronopathic GD including infiltration of Gaucher cell-like cells into the brains, progressive neuronal loss, and microgliosis. This neuron loss was observed not only in DA/NA neurons but also in tryptophan hydroxylase-positive serotonin neurons of the raphe nuclei. Detailed pathological findings showed decreased cathepsin D staining, morphological abnormality in lysosomes, and p62/ubiquitin-positive aggregates in the perikarya, indicating impairment of the autophagy–lysosome system. Furthermore, α-Syn accumulation was observed in axonal swellings containing autophagosomes. To examine the pathological role of α-Syn accumulation in this model, we subsequently generated *α-Syn* deletion mutant medaka fish by TALEN and crossed them with *GBA* mutant medaka fish. Unexpectedly, disruption of α-Syn did not improve the life span, formation of axonal swellings, neuronal loss, or neuroinflammation in homozygous *GBA* mutant medaka fish.

Taken together, these data suggest that homozygous *GBA* mutant medaka are a novel viable neuronopathic model of GD with α-Syn accumulation. α-Syn accumulated in their brains presumably due to an impairment in the autophagy–lysosome pathway. However, α-Syn accumulation has minimal contribution to the pathophysiology in this model.

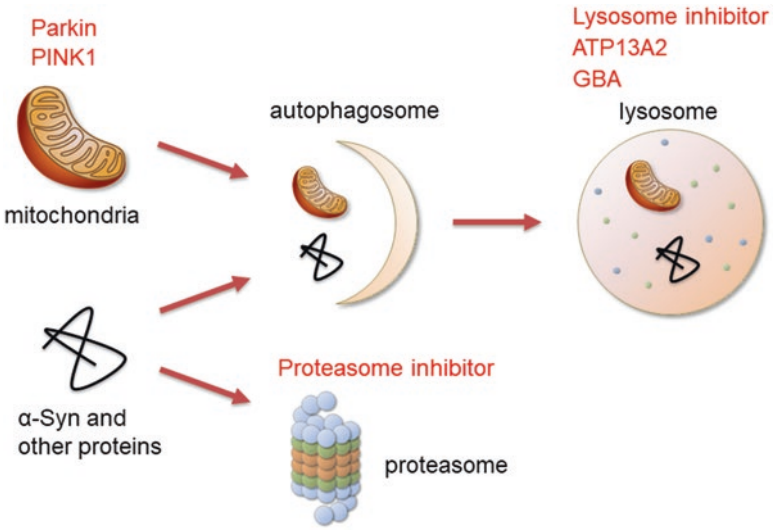

Fig. 12.3 Schematic summary of the pathological mechanisms involved in Parkinson's disease (PD)

12.5 Conclusions

Here, we summarized findings obtained from toxin-induced and genetic mutant medaka fish (Fig. 12.3). Despite in-depth research on PD using various cellular and animal models, the pathological mechanisms of PD remain largely unknown. Recent development of gene manipulation techniques, such as TALENs and CRISPR/CAS9, allows us to generate genetic mutant medaka fish more easily. Medaka fish are vertebrate and possess almost all causative genes of familial PD in contrast to the invertebrates (i.e., nematodes, flies). In addition, considering the fertility and ease of handling of medaka fish, we assert that medaka models can be a powerful tool for genetic studies of PD, such as the studies reviewed here. We hope that the medaka fish will contribute to further elucidation of the pathological mechanisms of PD and to the development of new treatments.

Acknowledgment These works were mainly supported by the Core Research for Evolutional Science and Technology (CREST) of the Japan Science and Technology Agency (JST); by Grant-in-Aid for Specially Promoted Research and Scientific Research on Innovative Areas "Brain Environment" from the Ministry of Education, Culture, Sports, Science and Technology of Japan; and by JSPS KAKENHI Grant Number JP15H02540. We thank Dr. Hideaki Matsui, who conducted many of the studies introduced here. We also thank Drs. Masato Kinoshita, Tomoko Ishikawa-Fujiwara, Takeshi Todo, and Shunichi Takeda for their excellent collaborations.

References

Bjorklund A, Dunnett SB (2007) Dopamine neuron systems in the brain: an update. Trends Neurosci 30(5):194–202. https://doi.org/10.1016/j.tins.2007.03.006 PubMed PMID: 17408759

Blum D, Torch S, Lambeng N, Nissou M, Benabid AL, Sadoul R et al (2001) Molecular pathways involved in the neurotoxicity of 6-OHDA, dopamine and MPTP: contribution to the apoptotic theory in Parkinson's disease. Prog Neurobiol 65(2):135–172 Epub 2001/06/19. PubMed PMID: 11403877

Braak H, Del Tredici K, Rub U, de Vos RA, Jansen Steur EN, Braak E (2003) Staging of brain pathology related to sporadic Parkinson's disease. Neurobiol Aging 24(2):197–211 Epub 2002/12/25. PubMed PMID: 12498954

Bras J, Verloes A, Schneider SA, Mole SE, Guerreiro RJ (2012) Mutation of the parkinsonism gene ATP13A2 causes neuronal ceroid-lipofuscinosis. Hum Mol Genet 21(12):2646–2650. https://doi.org/10.1093/hmg/dds089 PubMed PMID: 22388936; PubMed Central PMCID: PMCPMC3363329

Bultron G, Kacena K, Pearson D, Boxer M, Yang R, Sathe S et al (2010) The risk of Parkinson's disease in type 1 Gaucher disease. J Inherit Metab Dis. 33(2):167–173. Epub 2010/02/24. https://doi.org/10.1007/s10545-010-9055-0 PubMed PMID: 20177787

Clark IE, Dodson MW, Jiang C, Cao JH, Huh JR, Seol JH et al (2006) Drosophila pink1 is required for mitochondrial function and interacts genetically with parkin. Nature 441(7097):1162–1166. https://doi.org/10.1038/nature04779 PubMed PMID: 16672981

Dawson TM, Ko HS, Dawson VL (2010) Genetic animal models of Parkinson's disease. Neuron 66(5):646–661 Epub 2010/06/16. doi: S0896-6273(10)00327-2 [pii]1016/j.neuron.2010.04.034 [doi]. PubMed PMID: 20547124

de Lau LML, Breteler MMB (2006) Epidemiology of Parkinson's disease. Lancet Neurol 5(6):525–535. https://doi.org/10.1016/s1474-4422(06)70471-9

Del Tredici K, Braak H (2013) Dysfunction of the locus coeruleus-norepinephrine system and related circuitry in Parkinson's disease-related dementia. J Neurol Neurosurg Psychiatry 84(7):774–783. https://doi.org/10.1136/jnnp-2011-301817 PubMed PMID: 23064099

Dickson DW, Braak H, Duda JE, Duyckaerts C, Gasser T, Halliday GM et al (2009) Neuropathological assessment of Parkinson's disease: refining the diagnostic criteria. Lancet Neurol 8(12):1150–1157. https://doi.org/10.1016/s1474-4422(09)70238-8

Eblan MJ, Goker-Alpan O, Sidransky E (2005) Perinatal lethal Gaucher disease: a distinct phenotype along the neuronopathic continuum. Fetal Pediatr Pathol 24(4–5):205–222 Epub 2006/01/07. doi: JW22511415K11678 [pii] 49.1080/15227950500405296 [doi]. PubMed PMID: 16396828

Ebrahimi-Fakhari D, Wahlster L, McLean PJ (2012) Protein degradation pathways in Parkinson's disease: curse or blessing. Acta Neuropathol. 124(2):153–172. Epub 2012/06/30. https://doi.org/10.1007/s00401-012-1004-6. PubMed PMID: 22744791

Gegg ME, Burke D, Heales SJ, Cooper JM, Hardy J, Wood NW et al (2012) Glucocerebrosidase deficiency in substantia nigra of parkinson disease brains. Ann Neurol. 72(3):455–463. Epub 2012/10/05. https://doi.org/10.1002/ana.23614 [doi]. PubMed PMID: 23034917

Gitler AD, Chesi A, Geddie ML, Strathearn KE, Hamamichi S, Hill KJ et al (2009) Alpha-synuclein is part of a diverse and highly conserved interaction network that includes PARK9 and manganese toxicity. Nat Genet 41(3):308–315. https://doi.org/10.1038/ng.300 PubMed PMID: 19182805; PubMed Central PMCID: PMCPMC2683786

Goker-Alpan O, Schiffmann R, LaMarca ME, Nussbaum RL, McInerney-Leo A, Sidransky E (2004) Parkinsonism among Gaucher disease carriers. J Med Genet 41(12):937–940. https://doi.org/10.1136/jmg.2004.024455 PubMed PMID: 15591280; PubMed Central PMCID: PMCPMC1735652

Grabowski GA (2008) Phenotype, diagnosis, and treatment of Gaucher's disease. Lancet 372(9645):1263–1271 Epub 2008/12/20. doi: S0140-6736(08)61522-6 [pii] 45.1016/S0140-6736(08)61522-6 [doi]. PubMed PMID: 19094956

Kalia LV, Lang AE (2015) Parkinson's disease. Lancet 386(9996):896–912. https://doi.org/10.1016/s0140-6736(14)61393-3

Kastenhuber E, Kratochwil CF, Ryu S, Schweitzer J, Driever W (2010) Genetic dissection of dopaminergic and noradrenergic contributions to catecholaminergic tracts in early larval zebrafish. J Comp Neurol 518(4):439–458. https://doi.org/10.1002/cne.22214 PubMed PMID: 20017210; PubMed Central PMCID: PMCPMC2841826

Kett LR, Stiller B, Bernath MM, Tasset I, Blesa J, Jackson-Lewis V et al (2015) alpha-Synuclein-independent histopathological and motor deficits in mice lacking the endolysosomal Parkinsonism protein Atp13a2. J Neurosci 35(14):5724–5742. https://doi.org/10.1523/JNEUROSCI.0632-14.2015 PubMed PMID: 25855184; PubMed Central PMCID: PMCPMC4388928

Kitada T, Asakawa S, Hattori N, Matsumine H, Yamamura Y, Minoshima S et al (1998) Mutations in the parkin gene cause autosomal recessive juvenile parkinsonism. Nature. 392(6676):605–608. Epub 1998/04/29. https://doi.org/10.1038/33416. PubMed PMID: 9560156

Kitada T, Tong Y, Gautier CA, Shen J (2009) Absence of nigral degeneration in aged parkin/DJ-1/PINK1 triple knockout mice. J Neurochem 111(3):696–702. https://doi.org/10.1111/j.1471-4159.2009.06350.x PubMed PMID: 19694908; PubMed Central PMCID: PMC2952933

Lazarou M, Sliter DA, Kane LA, Sarraf SA, Wang C, Burman JL et al (2015) The ubiquitin kinase PINK1 recruits autophagy receptors to induce mitophagy. Nature 524(7565):309–314. https://doi.org/10.1038/nature14893 PubMed PMID: 26266977; PubMed Central PMCID: PMCPMC5018156

Lucking CB, Durr A, Bonifati V, Vaughan J, De Michele G, Gasser T et al (2000) Association between early-onset Parkinson's disease and mutations in the parkin gene. N Engl J Med. 342(21):1560–1567. Epub 2000/05/29. https://doi.org/10.1056/nejm200005253422103. PubMed PMID: 10824074

Matsui H, Taniguchi Y, Inoue H, Uemura K, Takeda S, Takahashi R (2009) A chemical neurotoxin, MPTP induces Parkinson's disease like phenotype, movement disorders and persistent loss of dopamine neurons in medaka fish. Neurosci Res. 65(3):263–271. https://doi.org/10.1016/j.neures.2009.07.010. PubMed PMID: 19665499

Matsui H, Ito H, Taniguchi Y, Inoue H, Takeda S, Takahashi R (2010a) Proteasome inhibition in medaka brain induces the features of Parkinson's disease. J Neurochem 115(1):178–187. Epub 2010/07/24. doi: JNC6918 [pii] 1111/j.1471-4159.2010.06918.x [doi]. PubMed PMID: 20649841

Matsui H, Ito H, Taniguchi Y, Takeda S, Takahashi R (2010b) Ammonium chloride and tunicamycin are novel toxins for dopaminergic neurons and induce Parkinson's disease-like phenotypes in medaka fish. J Neurochem. 115(5):1150–1160. https://doi.org/10.1111/j.1471-4159.2010.07012.x. PubMed PMID: 21219329

Matsui H, Taniguchi Y, Inoue H, Kobayashi Y, Sakaki Y, Toyoda A et al (2010c) Loss of PINK1 in medaka fish (Oryzias latipes) causes late-onset decrease in spontaneous movement. Neurosci Res 66(2):151–161. Epub 2009/11/10. doi: S0168-0102(09)02015-X [pii] https://doi.org/10.1016/j.neures.2009.33.010 [doi]. PubMed PMID: 19895857

Matsui H, Gavinio R, Asano T, Uemura N, Ito H, Taniguchi Y et al (2013a) PINK1 and Parkin complementarily protect dopaminergic neurons in vertebrates. Hum Mol Genet 22(12):2423–2434. Epub 2013/03/02. doi: ddt095 [pii] 35.1093/hmg/ddt095 [doi]. PubMed PMID: 23449626

Matsui H, Sato F, Sato S, Koike M, Taruno Y, Saiki S et al (2013b) ATP13A2 deficiency induces a decrease in cathepsin D activity, fingerprint-like inclusion body formation, and selective degeneration of dopaminergic neurons. FEBS Lett 587(9):1316–1325. Epub 2013/03/19. doi: S0014-5793(13)00192-0 [pii] 42.1016/j.febslet.2013.02.046 [doi]. PubMed PMID: 23499937

Mazzulli JR, Xu YH, Sun Y, Knight AL, McLean PJ, Caldwell GA et al (2011) Gaucher disease glucocerebrosidase and alpha-synuclein form a bidirectional pathogenic loop in synucleinopathies. Cell 146(1):37–52. Epub 2011/06/28. doi: S0092-8674(11)00601-5 [pii] 54.1016/j.cell.2011.06.001 [doi]. PubMed PMID: 21700325

Narendra DP, Jin SM, Tanaka A, Suen DF, Gautier CA, Shen J et al (2010) PINK1 is selectively stabilized on impaired mitochondria to activate Parkin. PLoS Biol. 8(1):e1000298. doi: https://doi.org/10.1371/journal.pbio.1000298. PubMed PMID: 20126261; PubMed Central PMCID: PMCPMC2811155

Neudorfer O, Giladi N, Elstein D, Abrahamov A, Turezkite T, Aghai E et al (1996) Occurrence of Parkinson's syndrome in type I Gaucher disease. QJM : Monthly J Assoc Physicians 89(9):691–694. Epub 1996/09/01. PubMed PMID: 8917744.

Park J, Lee SB, Lee S, Kim Y, Song S, Kim S et al (2006) Mitochondrial dysfunction in Drosophila PINK1 mutants is complemented by parkin. Nature. 441(7097):1157–1161. https://doi.org/10.1038/nature04788. PubMed PMID: 16672980

Petzinger GM, Fisher BE, McEwen S, Beeler JA, Walsh JP, Jakowec MW (2013) Exercise-enhanced neuroplasticity targeting motor and cognitive circuitry in Parkinson's disease. Lancet Neurol 12(7):716–726. https://doi.org/10.1016/s1474-4422(13)70123-6

Przedborski S, Jackson-Lewis V, Naini AB, Jakowec M, Petzinger G, Miller R et al (2001) The parkinsonian toxin 1-methyl-4-phenyl-1,2,3,6-tetrahydropyridine (MPTP): a technical review of its utility and safety. J Neurochem 76(5):1265–1274. Epub 2001/03/10 PubMed PMID: 11238711

Ramirez A, Heimbach A, Grundemann J, Stiller B, Hampshire D, Cid LP et al (2006) Hereditary parkinsonism with dementia is caused by mutations in ATP13A2, encoding a lysosomal type 5 P-type ATPase. Nat Genet. 38(10):1184–1191. https://doi.org/10.1038/ng1884. PubMed PMID: 16964263

Rink E, Wullimann MF (2001) The teleostean (zebrafish) dopaminergic system ascending to the subpallium (striatum) is located in the basal diencephalon (posterior tuberculum). Brain Res 889(1–2):316–330. Epub 2001/02/13. doi: S0006-8993(00)03174-7 [pii]. PubMed PMID: 11166725

Rink E, Wullimann MF (2002) Development of the catecholaminergic system in the early zebrafish brain: an immunohistochemical study. Brain Res Dev Brain Res 137(1):89–100. Epub 2002/07/20. PubMed PMID: 12128258

Samaranch L, Lorenzo-Betancor O, Arbelo JM, Ferrer I, Lorenzo E, Irigoyen J et al (2010) PINK1-linked parkinsonism is associated with Lewy body pathology. Brain. 133(Pt 4):1128–1142. https://doi.org/10.1093/brain/awq051. PubMed PMID: 20356854

Sardi SP, Clarke J, Viel C, Chan M, Tamsett TJ, Treleaven CM et al (2013) Augmenting CNS glucocerebrosidase activity as a therapeutic strategy for parkinsonism and other Gaucher-related synucleinopathies. Proc Natl Acad Sci U S A. 110(9):3537–3542. doi: https://doi.org/10.1073/pnas.1220464110. PubMed PMID: 23297226; PubMed Central PMCID: PMCPMC3587272

Satake W, Nakabayashi Y, Mizuta I, Hirota Y, Ito C, Kubo M et al (2009) Genome-wide association study identifies common variants at four loci as genetic risk factors for Parkinson's disease. Nat Genet. 41(12):1303–1307. https://doi.org/10.1038/ng.485 PubMed PMID: 19915576

Schneider SA, Alcalay RN (2017) Neuropathology of genetic synucleinopathies with parkinsonism: review of the literature. Mov Disord..32(11):1504–1523. https://doi.org/10.1002/mds.27193. PubMed PMID: 29124790

Sidransky E, Nalls MA, Aasly JO, Aharon-Peretz J, Annesi G, Barbosa ER et al (2009) Multicenter analysis of glucocerebrosidase mutations in Parkinson's disease. New Engl J Med 361(17):1651–1661. Epub 2009/10/23. doi: 361/17/1651 [pii] 1056/NEJMoa0901281 [doi]. PubMed PMID: 19846850

Tay TL, Ronneberger O, Ryu S, Nitschke R, Driever W (2011) Comprehensive catecholaminergic projectome analysis reveals single-neuron integration of zebrafish ascending and descending dopaminergic systems. Nat Commun. 2:171. https://doi.org/10.1038/ncomms1171. PubMed PMID: 21266970; PubMed Central PMCID: PMCPMC3105308

Tsunemi T, Krainc D (2014) Zn(2)(+) dyshomeostasis caused by loss of ATP13A2/PARK9 leads to lysosomal dysfunction and alpha-synuclein accumulation. Hum Mol Genet. 23(11):2791–2801. https://doi.org/10.1093/hmg/ddt572. PubMed PMID: 24334770; PubMed Central PMCID: PMCPMC4014186

Uemura N, Koike M, Ansai S, Kinoshita M, Ishikawa-Fujiwara T, Matsui H et al (2015) Viable neuronopathic Gaucher disease model in Medaka (Oryzias latipes) displays axonal accumulation of alpha-synuclein. PLoS Genet. 11(4):e1005065. https://doi.org/10.1371/journal.pgen.1005065. PubMed PMID: 25835295; PubMed Central PMCID: PMCPMC4383526

Vila M, Przedborski S (2003) Targeting programmed cell death in neurodegenerative diseases. Nat Rev Neurosci ;4(5):365–375. doi: https://doi.org/10.1038/nrn1100. PubMed PMID: 12728264

Williams DR, Hadeed A, al-Din AS, Wreikat AL, Lees AJ (2005) Kufor Rakeb disease: autosomal recessive, levodopa-responsive parkinsonism with pyramidal degeneration, supranuclear gaze palsy, and dementia. Mov Disord. 20(10):1264–1271. https://doi.org/10.1002/mds.20511. PubMed PMID: 15986421

Wong K, Sidransky E, Verma A, Mixon T, Sandberg GD, Wakefield LK et al (2004) Neuropathology provides clues to the pathophysiology of Gaucher disease. Mol Genet Metab 82(3):192–207. Epub 2004/07/06. https://doi.org/10.1016/j.ymgme.2004.04.011 [doi] S1096719204001179 [pii]. PubMed PMID: 15234332

Part IV
Eccentric Fish

Chapter 13
"Out of the Dark" Cavefish Are Entering Biomedical Research

Nicolas Rohner

Abstract The emergence of cheaper sequencing platforms and more widely applicable genome editing techniques is empowering new model organisms to emerge in the field of biomedical science. A promising branch of such organisms are the so-called evolutionary mutant models. To be covered by this definition, an animal must display phenotypes reminiscent of human pathologies, but these phenotypes must be part of the animal's natural condition. In other words, these animals are not considered sick, but rather they have evolved disease-like traits as part of their strategy to survive in the wild. The cavefish *Astyanax mexicanus* is such an animal species. *A. mexicanus* displays many traits resembling a variety of human pathologies including retinal degenerations, diabetes-like phenotypes, and even psychiatric diseases. The study of evolutionary mutant models, such as the cavefish, promises to provide important new insights into human pathologies by offering a different perspective compared to the classical model systems. Here, I introduce the cavefish model system *Astyanax mexicanus* to the reader and provide an overview of the latest efforts to establish this species as a valid member of animal models that are successfully used in biomedical research.

Keywords Cavefish · Astyanax mexicanus · Adaptation · Evolutionary mutant models · Albinism · Blindness · Asymmetry · Autism · Sleep loss · Circadian rhythm · Regeneration · Obesity

N. Rohner (✉)
Stowers Institute for Medical Research, Kansas City, MO, USA

Department of Molecular & Integrative Physiology, KU Medical Center, Kansas City, KS, USA
e-mail: nro@stowers.org

H. Hirata, A. Iida (eds.), *Zebrafish, Medaka, and Other Small Fishes*,
https://doi.org/10.1007/978-981-13-1879-5_13

13.1 Introduction

Most biomedical science relies on only a handful of well-established model organisms, which receive the bulk of biomedical funding (Lauer 2016). There is no doubt that classical model organisms are and have been tremendously important for biomedical research. Focusing on a few well-established model systems allows efforts and resources from many labs and disciplines to be combined. This has substantially accelerated the development of molecular tools in these organisms. However, focusing on just a tiny fraction of the diversity in nature (the most commonly used model organisms represent only 0.0005% of described animal species in the world) does have limitations. In contrast to what one may expect, the classical model organisms have not been selected because they present good models for human disease or physiology. They were mainly chosen for their rapid generation time and the ease of propagation in the laboratory (Perlman 2016). However, evolutionary selection for rapid and robust development does favor stronger genetic control during development and impedes environmental phenotypic plasticity (Bolker 2012). While this is important for reproducibility and the ability to compare results across different laboratories, it may not necessarily reflect the situation in human diseases. Many human diseases, especially the ones with a more complex genetic basis, are often dependent on environmental contributions. In addition, most research in classical model organisms uses highly inbred lines which again increases robustness of the results but disregards a large portion of the genetic and phenotypic repertoire present in natural populations. This is relevant to the study of human disease as natural variations between human populations are known to significantly influence disease prevalence, susceptibility, and treatment options (Lu et al. 2014). Thus, there have been recent pleas for harvesting more of this natural variation by extending the repertoire of animal model systems (Bolker 2012; Goldstein and King 2016) Given new and affordable technologies, such as next-gen sequencing (Goodwin et al. 2016) and CRISPR/Cas9 (Cong et al. 2013) it is now achievable to cross the barrier between classical and emerging model systems (Goldstein and King 2016). New model systems will not only increase the genetic and phenotypic space that can be explored but will also allow for the development of new strategies to model and study disease. The main approach to artificially model human disease in classical model organisms is to make the animal sick. Undoubtedly, this approach has been useful and has provided generations of scientists with great insights into human pathology (Fox et al. 2007). A complementary approach, however, is to take advantage of naturally occurring phenotypes that resemble disease phenotypes but are part of the animal's adaptive strategy. Animals that have such traits have recently been defined as "evolutionary mutant models." It has been proposed that studying these animals could provide fresh new insights into many human diseases (Albertson et al. 2009). Of course, this assumes that the mode of action in natural selection is similar to the one that contributes to human disease. If true, it would allow not only for the identification of novel genes and gene-by-environment interactions implicated in human disease but also for the identification of strategies to dodge the negative effects associated with diseases in humans. A unique advantage of using natural animal

models is that, by default, more regulatory mutations affecting multiple different loci in the genome will be uncovered, as this is the route evolution preferably uses (Wray 2007). Likewise, the genetic architecture of many complex human diseases, such as diabetes, is polygenic and driven by regulatory mutations (i.e., a large fraction of the GWAS hits map to noncoding regions (Maurano et al. 2012; Gusev et al. 2014)). Not surprisingly, as many diseases, diabetes just being one of many examples, are closely linked to our own evolutionary history. It has been argued that the large incidences of certain diseases in modern civilizations are due to a mismatch between the current environment and the environment we have adapted to as a species (Lieberman 2014). Such diseases are also called "mismatch diseases." Because genes responsible for disease progression were originally under natural selection, evolutionary models have the chance of uncovering such evolutionary relevant changes by focusing on loci under selection. There are many promising examples of such evolutionary model systems. Among them, giraffes have been proposed as a model for hypertension, (Zhang 2006) and hibernating animals could serve as a natural model for insulin resistance (Wu et al. 2013). However, there are obvious practical limitations to studying bears and giraffes. Fish, on the other hand, can often be studied more easily. With over 30,000 different species adapted to a wide variety of different and extreme environments, fish represent the most diverse class of vertebrates. Consequently, fish have been explored as evolutionary model systems. A famous example is the Antarctic icefish. Living in ice-cold (and oxygen-rich) water, they have eliminated the need for red blood cells in their circulatory system. Having this unique feature makes them a promising model for anemia (Braasch et al. 2015). In addition, Antarctic fish may be valuable for the study of other diseases as well. Icefish, like many fish adapted to the bottom of the ocean, have reduced their swim bladder during evolution. When new environments became available and ice fish wanted to explore these niches, they had to find other strategies to float. To accomplish this, Antarctic icefish reduced their bone density in a similar fashion as is seen in many osteoporosis patients (Braasch et al. 2015).

13.2 Cavefish: *Astyanax mexicanus*

Cavefishes are another important evolutionary fish model system entering the arena of biomedical research. Cave animals are an interesting evolutionary phenomenon. Living their entire lives underground in complete darkness, they have drastically changed their morphology, physiology, and behavior compared to their surface ancestors. There are many different cave animals across many phyla, but other than the occasional salamander or snake, it is again fishes that dominate the cave vertebrate fauna. Worldwide, more than 150 known obligate cavefish species are found on every continent, except Antarctica (Behrmann-Godel et al. 2017). Only a few, however, possess all the advantages of *Astyanax mexicanus,* a small tetra species (Gross et al. 2015). Most research on cavefish, therefore, has focused on this species, and they will also be the focus of this chapter. The most common form of *A. mexicanus* can be found in rivers from Texas to South America and is not built to impress. Small,

slender, and not especially colorful or flavorful, the fish do not stand out as particularly interesting for research or trade. But deep inside certain caves in the Sierra del Abra, in Northeastern Mexico, some populations of this species have acquired the typical cave traits that have fascinated layman and scientists alike (Fig. 13.1).

The most obvious cave traits are the loss of eyes and the reduction in body pigmentation. However, cavefish have changed many other morphological, behavioral, and physiological traits (Keene et al. 2016). Many of these traits are relevant to biomedical research and will be discussed throughout this chapter. The time of separation between the cave and surface forms has been long enough for the cave forms to adapt to the extreme environment by acquiring drastic phenotypic changes but not yet long enough to separate them into different species. Consequently, the surface and cave populations remain accessible for comparative studies and more importantly are interfertile. The latter means that they can generate fertile offspring in the laboratory, which is imperative when studying the genetic basis of the cave traits using quantitative trait loci (QTL) analysis. QTL analysis is a useful method for model systems with fertile hybrids and permits identification of genetic regions linked to the phenotypes under study. Not only is it possible to identify these genetic intervals, it is also possible to dissect the influence of different genetic factors (multiple genes, epistasis). And when used in different populations, information about genetic convergence of the traits can be obtained.

Another advantage of *Astyanax mexicanus* is that the direction of evolution is known (i.e., from surface to cave) and the cave populations can be regarded as natural mutants of the ancestral surface forms. Importantly, this has happened in at least five independently derived populations known within the region (Gross 2012). Such repeatability of evolution is an important aspect of the model system. Many natural model systems lack this repeatability, but it is an important feature for rigorous scientific study.

The ability to maintain and propagate these fish with relative ease in the laboratory is, however, the main reason these fish are so successfully used as a model system (Fig. 13.1d). Both fortunately and unfortunately, this has led to the fact that many researchers working on these fish never encounter their natural habitat. Fortunate, because climbing down the caves, dealing with venomous snakes, scorpions, killer bees, and disease carrying bats can be quite challenging. Unfortunate, because the research gets uncoupled from the ecological conditions in the natural environment, something that has happened extensively for most classical model systems. To avoid this, the community of *Astyanax* researchers make an effort to meet at least once every other year in Mexico to discuss the latest scientific advances but most importantly to visit a cave or two.

Fig. 13.1 (continued) (**b**) A researcher staring into the abyss of one of the cave entrances in the area. Some of the cave entrance pits can be 100 m deep and the cave systems several kilometers long. (Picture: Nicolas Rohner). (**c**) Surface population (top) and four different cave populations of *Astyanax mexicanus*. (**d**) Cave and surface populations can be maintained with relative ease in the laboratory (depicted is the aquatic facility at the Stowers Institute for Medical Research) which makes them a useful system for biomedical research. (Pictures, Zachary Zakibe, Nicolas Rohner)

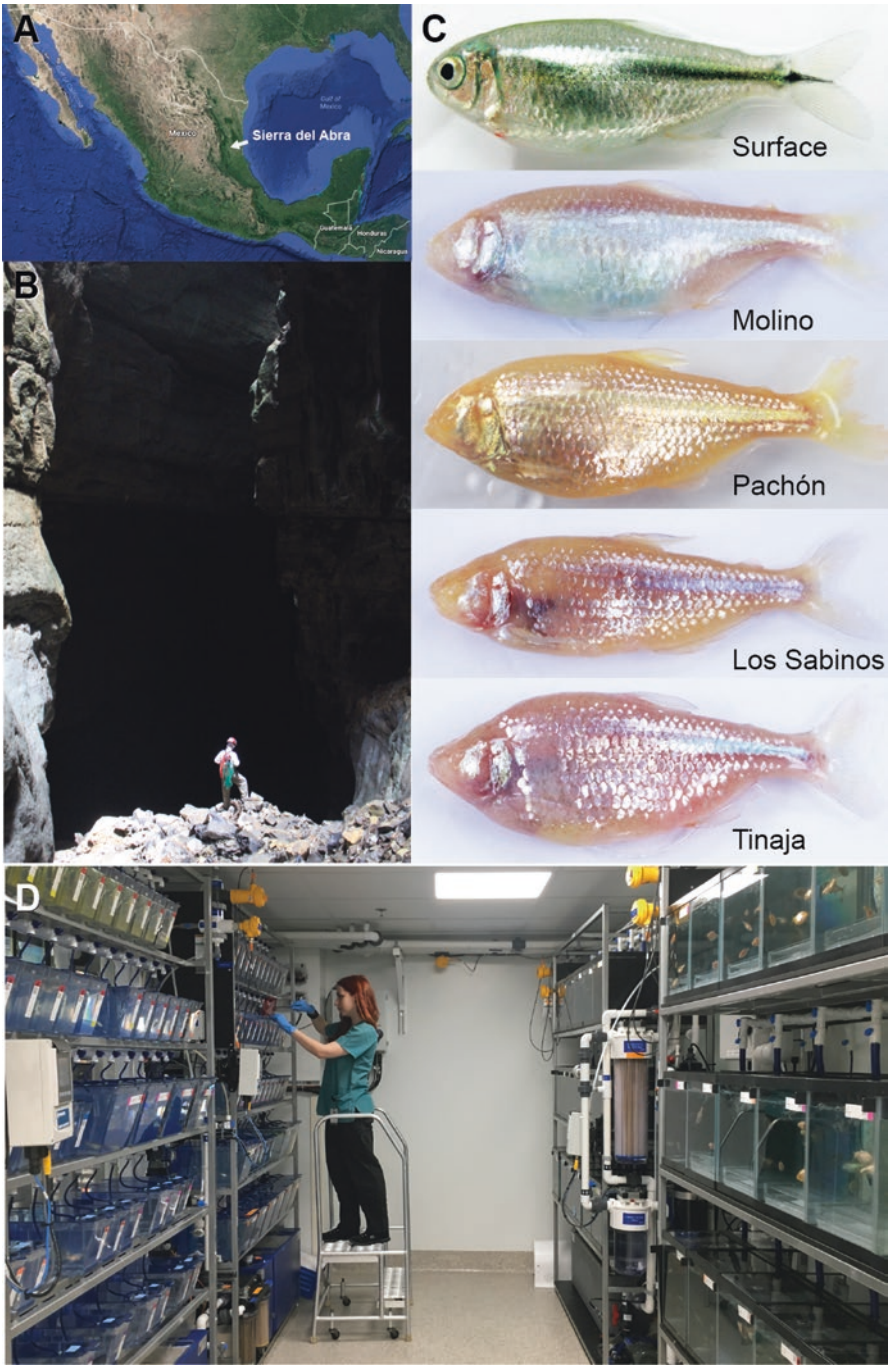

Fig. 13.1 *Astyanax mexicanus* as an emerging model system for biomedical research (**a**) Map of Mexico highlighting the area where the cave populations of *Astyanax mexicanus* are endemic. The surface populations can be found throughout Mexico. (Imagery ©2017 Data SIO, NOAA, U.S. Navy, NGA, GEBCO, Landsat/Copernicus, Map data ©2017 Google, INEGI).

The *Astyanax* model system can compete with other model organisms from a technical perspective as well. A fully annotated genome (McGaugh et al. 2014) and a large array of other genomic resources and genetic maps are available (Di Palma et al. 2007; Gross et al. 2008; O'Quin et al. 2013) Compared to most other vertebrate model organisms, the generation time (5 months) may be a bit longer; however, once sexually mature, a single female can produce more than 1000 eggs per week and remains fertile for over 10 years. As the eggs are externally fertilized, common gene perturbation and editing techniques (such as morpholinos (Ma et al. 2014), TALEN (Ma et al. 2015), CRISPR (Kowalko et al. in preparation), RNA injection (Yamamoto et al. 2004), and transgenesis (Elipot et al. 2014)) are applicable.

13.2.1 Albinism

Next to eye loss, the loss of pigmentation is the most obvious morphological difference between cave and surface fish. Almost all obligate cavefish have lost their dark pigmentation to some extent. Traditionally, changes in pigmentation is a well-studied trait in evolutionary genetic model systems, and the genetic basis of altered levels of pigmentation is well-defined in many animal systems (Hubbard et al. 2010; Massey and Wittkopp 2016). Classical examples include beach mice that evolved a lighter coat color to better camouflage on the sandy ground compared to their forest living relatives (Mullen et al. 2009). Another famous example is the increase in melanin in the black jaguar that allows them to better blend in with the shapes of the jungle (Schneider et al. 2015). The genetic basis of these, and many other examples, has been identified and often can be explained by mutations in a handful of typical pigmentation genes such as OCA2, MC1R, tyrosinase, or agouti (Reissmann and Ludwig 2013). In cavefish, the genetic basis of pigmentation loss has been studied extensively, and mutations in the genes *oca2* and *mc1r* have been identified to contribute to the phenotype (Protas et al. 2006; Gross et al. 2009; Stahl and Gross 2015). Importantly, these are the same genes that are mutated in cases of human albinism (oculocutaneous albinism – Genetics Home Reference). As these genetic disorders in humans have a simple and well-defined genetic basis, there are likely better systems than cavefish as a model for human albinism. However, given that the genetic basis underlying the similar pigmentation phenotypes in cavefish and in human albinism is the same, it may indeed be reasonable to assume that there are more cavefish phenotypes that share their genetic basis with human diseases.

13.2.2 Eye Loss

Eye loss is probably the most striking phenotype of cavefish and has fascinated scientists and layman alike. As such, eye loss has been studied extensively in *Astyanax mexicanus (Krishnan and Rohner* 2017*)*. Cavefish start out with relatively

normal eye development during the first hours of their life. However, soon afterward, the eye and retina rapidly arrest, degenerate, and sink into the surrounding orbit. Cavefish eye degeneration has been proposed as a model for human retinal degeneration diseases and for blindness in general. Retinal degeneration is a complex disease caused and affected by many environmental and genetic factors. The most common inherited form is retinitis pigmentosa (RP). RP affects 1 in 3000 Americans at some point of their life (Bravo-Gil et al. 2017). So far, over 70 genes linked to the development of RP have been identified. However, in more than one third of the cases, the underlying genetic cause remains unsolved (Daiger et al. 2013). Identifying the exact genetic basis of a disease is important. Besides giving the patient the comfort of knowing what causes her/his disease, it also opens potentially new therapeutic avenues. In contrast to studies using human patients or artificially created mouse models, using naturally blind model systems will tap into a completely different and new reservoir of genetic variation underlying retinal degeneration. Again, *Astyanax mexicanus* is a promising system to study retinal diseases as the retinal degeneration phenotype in the cavefish mimics some of the patient’s symptoms (O’Quin et al. 2013). Like mammalian models of RP, cavefish are born with eyes, and the degeneration occurs during early development. Importantly, the availability of interpopulation crosses and genomic resources makes it a suitable genetic model fully capable of identifying new genetic loci and pathways underlying retinal degeneration. These can serve as blueprints in the search for the missing heritable link in human RP. For people that are born blind or have lost their eyesight through different means, *Astyanax* cavefish may be a helpful model for better understanding sensory substitution and compensatory mechanisms that develop after vision loss. Cavefish present a unique scenario in which sensory substitution has naturally evolved, and methods applicable to study neuronal circuits in vivo are in principal like the ones developed for zebrafish. Using these methods, it is possible to observe and trace the activity of individual neurons with unprecedented precision. Of course, human and fish brains differ in many aspects, but the basic concepts of neuronal integration, connectivity, and plasticity are surprisingly conserved in vertebrates (Joshua and Lisberger 2015), making cavefish a promising model to study certain aspects of human blindness.

13.2.3 Craniofacial Changes

Cavefish display multiple craniofacial alterations compared to their surface cousins. For example, their lower jaw protrudes, they have a larger opercula bone, and generally two or more maxillary teeth, while a single tooth suffices for surface fish (Keene et al. 2016). Their orbital bones display many fusions and fragmentations, many of which are likely related to eye regression. However, some of these morphological modifications, such as the fragmentation of the third suborbital bone, have evolved separately from eye loss (Gross et al. 2014). Many of the craniofacial traits in cavefish have been mapped to genomic regions using quantitative trait loci analysis

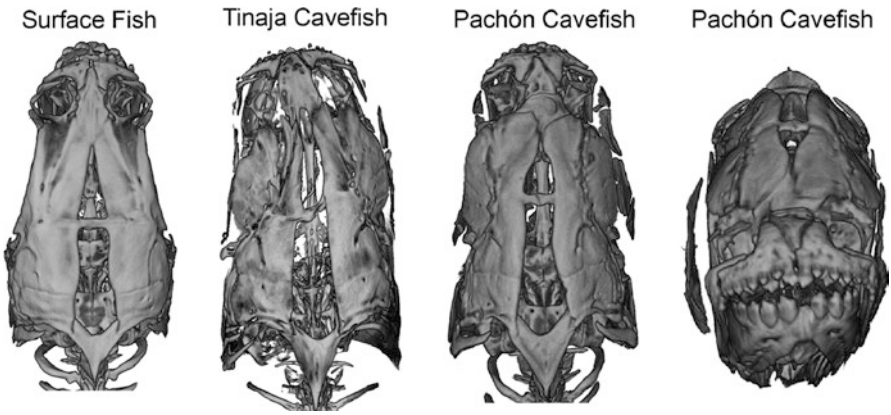

Fig. 13.2 Cavefish skulls are asymmetric. Surface-rendered microCT images of *Astyanax mexicanus* skulls. From left to right: surface fish, dorsal view; Tinaja cavefish, dorsal view; Pachón cavefish, dorsal view; Pachón cavefish, frontal view. Note the left side bias in the cavefish skull. (Adapted from Powers et al. 2017)

(Gross et al. 2014; Protas et al. 2008). A better understanding of the genetic architecture of these phenotypes may well provide better insights into human syndromes. For example, a protruding lower jaw (prognathism) in humans can affect speech or proper mastication, while a cleft palate, one of the most common types of birth defects in the USA, stems from a failure to fuse bones during craniofacial development. Another rather surprising observation that has come out of morphological studies in cavefish is that many cave adapted populations display a substantial degree of asymmetry in their skull shape (Gross et al. 2016) (Fig. 13.2). Facial symmetry is under strong selection in most species, including strong sexual selection in humans as a universal measure of attractiveness. Despite this strong selection, perfect facial symmetry is almost never achieved in humans. Craniofacial asymmetries underlie a variety of different syndromes that can affect dental function and proper joint function and, in extreme cases, even lead to life-threatening breathing impairments. Despite the prevalence of craniofacial asymmetry in humans, very little is known about the underlying genetic basis. *Astyanax mexicanu*s, with their strong heritable differences in craniofacial asymmetry between surface and cave forms, present a unique model system to uncover the genetic basis of facial symmetry and the processes that can go wrong while building it (Powers et al. 2017).

13.2.4 Autism

While at first sight fish may not be considered ideal models for psychosomatic diseases, Masato Yoshizawa, a cavefish researcher from Hawaii, noticed that some of the behavioral repertoire in cavefish displays similarities to patients suffering from

neurological disorders such as autism. He originally aimed to understand brain evolution by investigating the effects of natural selection on behavior, when he noticed that cavefish displayed certain "symptoms" of autism, such as sleeplessness, hyperactivity, and asocial behavior compared to surface fish (Yoshizawa 2015). Altered behaviors such as a solitary live and constant movement in search for food may be the best strategy for cavefish to survive in a nutrient-deprived world free of predators. However, the study of these behaviors in cavefish could provide avenues into understanding the molecular underpinnings and how these behaviors are connected to each other. In preliminary experiments, Yoshizawa found 90% of the 101 classic risk factor genes for human psychiatric diseases to be present in the cavefish genome and a large portion of them to be differentially regulated between cavefish and surface fish. In a first step toward validating these findings, Yoshizawa treated cavefish with several psychiatric drugs. An earlier study by another research team showed that the antidepressant fluoxetine (commonly known as Prozac) reversed some of the cavefish-specific behavioral phenotypes. Yoshizawa then could show that the antipsychotic clozapine has the same effect (Pennisi 2016). Overall, these drug responses in cavefish are very similar to those in human patients and could indicate similar mechanistic bases. Despite these findings, there is still a long way to go before cavefish will be accepted as a good model for human psychiatric disease.

13.2.5 Sleep

Sleep is a universal trait. Almost all animals sleep, but the amount of sleep individual species need can vary dramatically. Some, such as bats, sleep 20 hours a day, while others, such as elephants, only need a few hours of sleep (Gravett et al. 2017). Likewise, there is considerable variation in sleep times in humans. Some individuals sleep for only 5 hours per night, while others regularly need 9 hours or more of sleep to perform. The evolutionary reason for these intra- and interspecies differences is still subject to debate, but it is known that the amount of sleep can be modulated by environmental changes. For example, most animals will increase their sleep as a response to limited food availability (Masek et al. 2014). One thing all animals have in common is that forfeiting sleep results in illness and the emergence of cognitive and behavioral deficits during their waking hours (Rechtschaffen et al. 1983). Humans are no exception to this rule, as we have probably all experienced at some point. Indeed, studies have shown that sleep deprivation is linked to many metabolic and cardiovascular diseases and an increased mortality rate (Itani et al. 2017). Studying the effects of sleep deprivation in animal model systems is difficult, as only few exist that show strong intraspecies differences in sleep pattern and are amenable to genetic approaches. *Astyanax mexicanus* therefore is an excellent model to study differences in sleep needs as some cavefish populations have decreased their amount of sleep dramatically compared to their surface cousins (Duboue et al. 2011). While adult surface fish sleep about 8 hours per day, Pachón cavefish sleep only 2 hours per day. Notably, these differences persist even in the

laboratory where both populations are kept under the same conditions, which suggests that these differences are hardwired. Sleep is a complex phenotype and can be difficult to assess in animals that cannot close their eyes (or even lack them entirely), especially as electrophysiological studies are difficult to perform in small animals. Studies in *Astyanax mexicanus*, like studies in zebrafish, have therefore focused on behavioral markers of sleep such as prolonged periods of inactivity or elevated arousal thresholds (Jaggard et al. 2017). Sleep studies carried out that way in cavefish revealed that the sleep phenotype is a convergent trait for most, but not all, cave populations (Yoshizawa et al. 2015). Importantly, these genetic studies calculated that only a handful of genes with large effect sizes are responsible for the sleep phenotype, which makes functional studies of identified candidate genes possible. Starvation promotes sleep loss in Pachón cavefish which indicates that, like in other species, sleep loss in cavefish is linked to their metabolic state (Yoshizawa et al. 2015). It has been hypothesized that sleep loss represents a mechanism to increase foraging time, which could be a potential explanation for why cavefish have lost sleep (Yoshizawa et al. 2015). Another possibility is that sleep has evolved to avoid predation and having no known predators, cavefish may as a consequence need less sleep. Future studies will be needed to uncover the ecological reason for sleep loss in these fish. The neuronal basis controlling sleep homeostasis is conserved between fish and humans. Therefore, cavefish represent a unique system for studying the molecular mechanism of sleep loss and may lead to the discovery of potential parallels in humans. For example, in a small screen of commonly associated sleep- or wake-promoting drugs, it was found that inhibition of noradrenergic signaling and glutamate signaling enhanced sleep in cavefish, but not in surface fish (Yoshizawa et al. 2015; Duboue et al. 2012). This suggests an involvement of these signaling pathways in the sleep loss of cavefish. Taken together, these findings make *Astyanax mexicanus* an exciting model system to study naturally occurring sleep differences. Their accessibility also allows for pharmaceutical compound screens to identify potential mechanisms that can be substituted for sleep deprivation in other species.

13.2.6 Circadian Rhythm

Sleep is tightly linked to circadian rhythm, which when disrupted can have a substantial impact on our well-being including long-term effect on our health. Everyone who has experienced jet lag will easily agree. Organisms that live in constant darkness are of particular interest to circadian researchers. As such, *Astyanax mexicanus* has been a prime candidate for the study of the biological clock. As expected, cavefish do not show any sign of circadian activity in their natural habitat due to the lack of a zeitgeber (the environmental cue that can set the internal body clock) (Beale et al. 2013). Using the expression pattern of key circadian genes as a marker for circadian periodicity, researchers found that, in a laboratory setting, the cavefish populations do not entirely lose their ability to generate a circadian rhythm. Their clock still oscillates, but with a rhythm lower in amplitude than the surface fish,

which suggests differences in the core oscillator of the biological clock (Beale et al. 2013). Expression analysis of genes known to be under tight control of the circadian rhythm points toward a rather unexpected result. The data, at least from a molecular point of view, is consistent with the fish being in constant light rather than in constant darkness. Consequently, cavefish show an increased expression of DNA repair genes, which are usually turned on during the day where there is a high chance of UV-induced DNA damage. As this was observed both in the laboratory and in the wild, it was speculated that an enhanced ability to repair DNA changes could help fish survive the harsh cave conditions (i.e., different pH or low oxygen levels could induce DNA damage) (Beale et al. 2013). As such, *Astyanax* cavefish can be considered a natural overexpression mutant of enhanced DNA repair, a feature that could be important to exploit in future cancer studies.

13.2.7 Regeneration

Fish models have traditionally been strong in the field of regeneration research because of their natural ability to regenerate many of their organs and body parts. Most fish can regenerate their fins or scales when lost or amputated. Even entire organs can regenerate in fish. For example, adult zebrafish can regenerate a heart to nearly full function when up to one third is amputated (Arnaout et al. 2014). It did therefore not come as a surprise, when British researchers found that the surface form of *Astyanax mexicanus* has similar regeneration capacities. The surprise came when the scientists tested the cavefish populations and found that their hearts did not regenerate. Instead scar tissues formed, as would in human hearts damaged by a heart attack. Studying the molecular mechanisms underlying the cellular environment favoring heart regeneration over scarring could help millions of patients suffering from heart disease. Cavefish are a powerful and potentially unique model because individuals of a single species show differences in their heart regeneration capacity. This allows for the use of quantitative trait loci analysis to link the ability for heart regeneration directly to the genome. Preliminary results indicate that this ability for heart regeneration can be linked to a small number of loci containing a limited number of genes (Mommersteeg 2015) making cavefish a novel and extremely exciting model for heart disease studies.

13.2.8 Metabolism

Caves are dark and as such lack photosynthesis-driven primary production. Therefore, most cave environments rely exclusively on food chains originating outside of the cave. This is also true for the caves of *Astyanax mexicanus* in which most of the energy resources stem from bats or floods during the rainy season that bring in organic matter. As these floods occur only a few times in the summer months,

cavefish have had to find other means to survive when resources are lacking. Cavefish have found several ways to deal with such dire conditions. For one, they save energy by exhibiting a lower standard metabolic rate (Hervant and Malard 2012). Up to one third of their daily energy use is also saved by eliminating a circadian rhythm in their metabolic activity (Moran et al. 2014). A second strategy is to eat more when food is available. It has been shown that food restriction increases orexin mRNA transcription levels in cavefish brain (Wall and Volkoff 2013), which leads to increased food consumption (Penney and Volkoff 2014). Furthermore, we found in a recent study that cavefish tend to binge eat when food is available, a behavior that is hardwired and can be observed even under ad libitum feedings in the laboratory (Aspiras et al. 2015). We showed that mutations in MC4R, a master regulator of appetite control, partly contribute to the overeating phenotype. Interestingly, these same coding mutations cause extreme cases of obesity in humans, further highlighting the relevance of using evolutionary model systems to study human disease. As a consequence of this mutation and other changes to the genome, the cavefish acquire much higher levels of body fat than the surface fish. We measured up to ten times more body fat depending on the populations (Aspiras et al. 2015; Salin et al. 2010, PMID: 29883659). Acquiring body fat allows the cavefish to sustain leaner times much better than surface fish pointing to the fact that this is presumably an adaptive physiological response and not a pathological one. Indeed, when cavefish were starved for 2 months, they only lost a fraction of the body weight that surface fish lost on the same diet (Aspiras et al. 2015). In part, this can be explained by a decrease in locomotor activity of cavefish during fasting, a behavior not present in surface fish (Salin et al. 2010) or may simply be explained by the fact that fat tissues can store a higher energy density. This raises the intriguing question whether a lifestyle of overeating and fasting has any health consequences on the cavefish, especially as cavefish display phenotypes usually associated with the negative health effects of overeating in humans, such as fatty liver and diabetes-like conditions (Aspiras et al. in preparation, PMID: 29555241) (Fig. 13.3). Yet, cavefish live as long as surface fish and molecular markers of disease are not elevated. Possibly, these fish have coevolved factors that mitigate the negative health effects typically associated with such phenotypes. More detailed genetic studies of metabolism in cavefish will give insight into the regulatory pathways underlying their unique (protective) physiological adaptations. This could have great potential in providing a better basis for therapeutic interventions into metabolic disorders in the future.

13.3 Concluding Remarks

While these studies are all still in their infancies, the *Astyanax mexicanus* model system will help in elucidating important pathways involved in human disease. As a genetic system, the power relies on the feasibility of QTL studies. The prospects of functional validation in vivo, in these exciting times of gene editing through CRISPR, further substantiate the validity of the system for biomedical research. Another important feature, the cavefish system shares with other fish systems, is

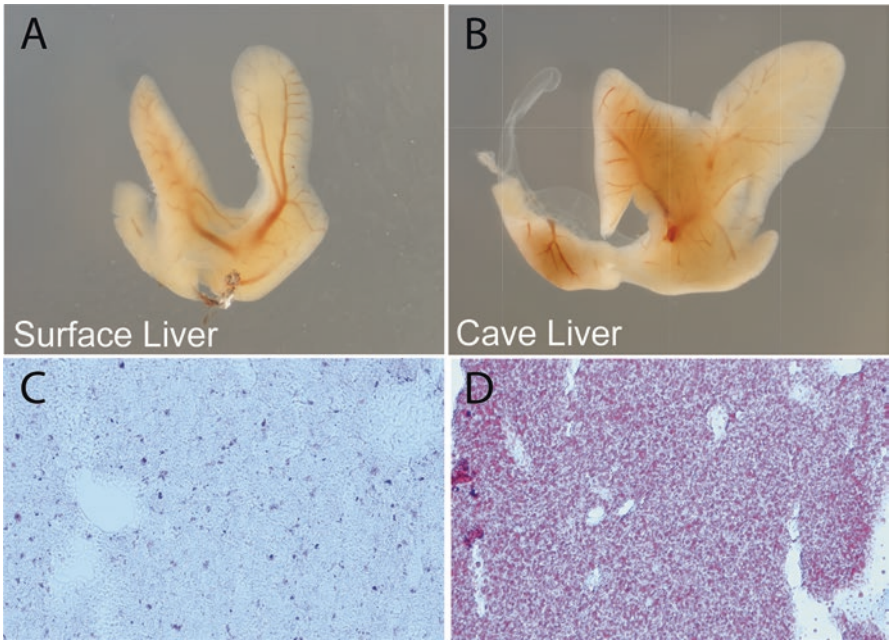

Fig. 13.3 Cavefish have fatty and enlarged livers. (**a**) Surface fish liver. (**b**) Tinaja cavefish liver (enlarged). (**c**) Oil red O staining (stains lipids red) of surface fish liver section. (**d**) Oil red O staining of Tinaja cavefish liver section (displaying much elevated fat levels compared to the surface fish liver)

that it is amenable to large-scale pharmacological screens, which makes gene and drug discovery cheaper and easier than in most mammalian systems. Therefore, I predict that the emergence of “out of the box organisms,” such as cavefish, has the potential to provide novel and exciting insights into biomedical research. The general idea follows the so-called Krogh principle, which was famously named after the Danish physiologist August Krogh (1874–1949) and states that: “for a large number of problems there will be some animal of choice […] on which it can be most conveniently studied” (Krogh 1929). For many problems, the animal of choice seems to be the cavefish *Astyanax mexicanus*.

References

Albertson RC, Cresko W, Detrich HW 3rd, Postlethwait JH (2009) Evolutionary mutant models for human disease. Trends Genet 25(2):74–81

Arnaout R, Reischauer S, Stainier DY (2014) Recovery of adult zebrafish hearts for high-throughput applications. J Vis Exp 94

Aspiras AC, Rohner N, Martineau B, Borowsky RL, Tabin CJ (2015) Melanocortin 4 receptor mutations contribute to the adaptation of cavefish to nutrient-poor conditions. Proc Natl Acad Sci U S A 112(31):9668–9673

Beale A, Guibal C, Tamai TK, Klotz L, Cowen S, Peyric E, Reynoso VH, Yamamoto Y, Whitmore D (2013) Circadian rhythms in Mexican blind cavefish Astyanax mexicanus in the lab and in the field. Nat Commun 4:2769

Behrmann-Godel J, Nolte AW, Kreiselmaier J, Berka R, Freyhof J (2017) The first European cave fish. Curr Biol 27(7):R257–R258

Bolker J (2012) Model organisms: there's more to life than rats and flies. Nature 491(7422):31–33

Braasch I, Peterson SM, Desvignes T, McCluskey BM, Batzel P, Postlethwait JH (2015) A new model army: emerging fish models to study the genomics of vertebrate Evo-devo. J Exp Zool B Mol Dev Evol 324(4):316–341

Bravo-Gil N, Gonzalez-Del Pozo M, Martin-Sanchez M, Mendez-Vidal C, Rodriguez-de la Rua E, Borrego S, Antinolo G (2017) Unravelling the genetic basis of simplex retinitis Pigmentosa cases. Sci Rep 7:41937

Cong L, Ran FA, Cox D, Lin S, Barretto R, Habib N, Hsu PD, Wu X, Jiang W, Marraffini LA, Zhang F (2013) Multiplex genome engineering using CRISPR/Cas systems. Science 339(6121):819–823

Daiger SP, Sullivan LS, Bowne SJ (2013) Genes and mutations causing retinitis pigmentosa. Clin Genet 84(2):132–141

Di Palma F, Kidd C, Borowsky R, Kocher TD (2007) Construction of bacterial artificial chromosome libraries for the Lake Malawi cichlid (Metriaclima zebra), and the blind cavefish (Astyanax mexicanus). Zebrafish 4(1):41–47

Duboue ER, Keene AC, Borowsky RL (2011) Evolutionary convergence on sleep loss in cavefish populations. Curr Biol 21(8):671–676

Duboue ER, Borowsky RL, Keene AC (2012) Beta-adrenergic signaling regulates evolutionarily derived sleep loss in the Mexican cavefish. Brain Behav Evol 80(4):233–243

Elipot Y, Legendre L, Pere S, Sohm F, Retaux S (2014) Astyanax transgenesis and husbandry: how cavefish enters the laboratory. Zebrafish 11(4):291–299

Fox JG, Barthold SW, Davisson MT (2007) The mouse in biomedical research. Elsevier, Amsterdam. ISBN: 9780123694584

Goldstein B, King N (2016) The future of cell biology: emerging model organisms. Trends Cell Biol 26(11):818–824

Goodwin S, McPherson JD, McCombie WR (2016) Coming of age: ten years of next-generation sequencing technologies. Nat Rev Genet 17(6):333–351

Gravett N, Bhagwandin A, Sutcliffe R, Landen K, Chase MJ, Lyamin OI, Siegel JM, Manger PR (2017) Inactivity/sleep in two wild free-roaming African elephant matriarchs - does large body size make elephants the shortest mammalian sleepers? PLoS One 12(3):e0171903

Gross JB (2012) The complex origin of Astyanax cavefish. BMC Evol Biol 12:105

Gross JB, Protas M, Conrad M, Scheid PE, Vidal O, Jeffery WR, Borowsky R, Tabin CJ (2008) Synteny and candidate gene prediction using an anchored linkage map of Astyanax mexicanus. Proc Natl Acad Sci U S A 105(51):20106–20111

Gross JB, Borowsky R, Tabin CJ (2009) A novel role for Mc1r in the parallel evolution of depigmentation in independent populations of the cavefish Astyanax mexicanus. PLoS Genet 5(1):e1000326

Gross JB, Krutzler AJ, Carlson BM (2014) Complex craniofacial changes in blind cave-dwelling fish are mediated by genetically symmetric and asymmetric loci. Genetics 196(4):1303–1319

Gross JB, Meyer B, Perkins M (2015) The rise of Astyanax cavefish. Dev Dyn 244(9):1031–1038

Gross JB, Gangidine A, Powers AK (2016) Asymmetric facial bone fragmentation mirrors asymmetric distribution of cranial Neuromasts in blind Mexican cavefish, Symmetry (Basel) 8(11)

Gusev A, Lee SH, Trynka G, Finucane H, Vilhjalmsson BJ, Xu H, Zang C, Ripke S, Bulik-Sullivan B, Stahl E, Kahler AK, Hultman CM, Purcell SM, McCarroll SA, Daly M, Pasaniuc B, Sullivan PF, Neale BM, Wray NR, Raychaudhuri S, Price AL (2014) Partitioning heritability of regulatory and cell-type-specific variants across 11 common diseases. Am J Hum Genet 95(5):535–552

Hervant F, Malard F (2012) Responses to low oxygen. In: Encyclopedia of caves, Second edn. Academic Press, United Kingdom, pp 651–658. ISBN: 978-0-12-383832-2
Hubbard JK, Uy JA, Hauber ME, Hoekstra HE, Safran RJ (2010) Vertebrate pigmentation: from underlying genes to adaptive function. Trends Genet 26(5):231–239
Itani O, Jike M, Watanabe N, Kaneita Y (2017) Short sleep duration and health outcomes: a systematic review, meta-analysis, and meta-regression. Sleep Med 32:246–256
Jaggard J, Robinson BG, Stahl BA, Oh I, Masek P, Yoshizawa M, Keene AC (2017) The lateral line confers evolutionarily derived sleep loss in the Mexican cavefish. J Exp Biol 220(Pt 2):284–293
Joshua M, Lisberger SG (2015) A tale of two species: neural integration in zebrafish and monkeys. Neuroscience 296:80–91
Keene A, Yoshizawa M, McGaugh S (2016) Biology and evolution of the Mexican cavefish. Elsevier Inc, New York. ISBN: 9780128021484
Krishnan J, Rohner N (2017) Cavefish and the basis for eye loss. Philos Trans R Soc Lond Ser B Biol Sci 372(1713)
Krogh (1929) The progress of physiology. Am J Phys 90(2):243–251
Lauer M (2016) A look at NIH support for model organisms, NIH office of extramural research – extramural nexus. https://nexus.od.nih.gov/all/2016/08/03/model-organisms-part-two/
Lieberman D (2014) The story of the human body: evolution, health, and disease. First Vintage Books Edition. ISBN: 978-0307741806
Lu YF, Goldstein DB, Angrist M, Cavalleri G (2014) Personalized medicine and human genetic diversity. Cold Spring Harb Perspect Med 4(9):a008581
Ma L, Parkhurst A, Jeffery WR (2014) The role of a lens survival pathway including sox2 and alphaA-crystallin in the evolution of cavefish eye degeneration. EvoDevo 5:28
Ma L, Jeffery WR, Essner JJ, Kowalko JE (2015) Genome editing using TALENs in blind Mexican cavefish, Astyanax mexicanus. PLoS One 10(3):e0119370
Masek P, Reynolds LA, Bollinger WL, Moody C, Mehta A, Murakami K, Yoshizawa M, Gibbs AG, Keene AC (2014) Altered regulation of sleep and feeding contributes to starvation resistance in Drosophila melanogaster. J Exp Biol 217(Pt 17):3122–3132
Massey JH, Wittkopp PJ (2016) The genetic basis of pigmentation differences within and between Drosophila species. Curr Top Dev Biol 119:27–61
Maurano MT, Humbert R, Rynes E, Thurman RE, Haugen E, Wang H, Reynolds AP, Sandstrom R, Qu H, Brody J, Shafer A, Neri F, Lee K, Kutyavin T, Stehling-Sun S, Johnson AK, Canfield TK, Giste E, Diegel M, Bates D, Hansen RS, Neph S, Sabo PJ, Heimfeld S, Raubitschek A, Ziegler S, Cotsapas C, Sotoodehnia N, Glass I, Sunyaev SR, Kaul R, Stamatoyannopoulos JA (2012) Systematic localization of common disease-associated variation in regulatory DNA. Science 337(6099):1190–1195
McGaugh SE, Gross JB, Aken B, Blin M, Borowsky R, Chalopin D, Hinaux H, Jeffery WR, Keene A, Ma L, Minx P, Murphy D, O’Quin KE, Retaux S, Rohner N, Searle SM, Stahl BA, Tabin C, Volff JN, Yoshizawa M, Warren WC (2014) The cavefish genome reveals candidate genes for eye loss. Nat Commun 5:5307
Mommersteeg T (2015) The blind cavefish: unravelling the mechanisms underlying heart regeneration. In: Noujaim S (ed) Oxford Talks. https://talks.ox.ac.uk/talks/id/bc3fb05d-2e63-448f-a1eb-caa367afa4e1/
Moran D, Softley R, Warrant EJ (2014) Eyeless Mexican cavefish save energy by eliminating the circadian rhythm in metabolism. PLoS One 9(9):e107877
Mullen LM, Vignieri SN, Gore JA, Hoekstra HE (2009) Adaptive basis of geographic variation: genetic, phenotypic and environmental differences among beach mouse populations. Proc Biol Sci 276(1674):3809–3818
O’Quin KE, Yoshizawa M, Doshi P, Jeffery WR (2013) Quantitative genetic analysis of retinal degeneration in the blind cavefish Astyanax mexicanus. PLoS One 8(2):e57281
Penney CC, Volkoff H (2014) Peripheral injections of cholecystokinin, apelin, ghrelin and orexin in cavefish (Astyanax fasciatus mexicanus): effects on feeding and on the brain expression levels of tyrosine hydroxylase, mechanistic target of rapamycin and appetite-related hormones. Gen Comp Endocrinol 196:34–40

Pennisi E (2016) Antisocial cave fish may hold clues to schizophrenia, autism. Science. (Magazine Health, Plants & Animals). https://doi.org/10.1126/science.aaf5813
Perlman RL (2016) Mouse models of human disease: an evolutionary perspective. Evol Med Public Health 2016(1):170–176
Powers AK, Davis EM, Kaplan SA, Gross JB (2017) Cranial asymmetry arises later in the life history of the blind Mexican cavefish, Astyanax mexicanus. PLoS One 12(5):e0177419
Protas ME, Hersey C, Kochanek D, Zhou Y, Wilkens H, Jeffery WR, Zon LI, Borowsky R, Tabin CJ (2006) Genetic analysis of cavefish reveals molecular convergence in the evolution of albinism. Nat Genet 38(1):107–111
Protas M, Tabansky I, Conrad M, Gross JB, Vidal O, Tabin CJ, Borowsky R (2008) Multi-trait evolution in a cave fish Astyanax mexicanus. Evol Dev 10(2):196–209
Rechtschaffen A, Gilliland MA, Bergmann BM, Winter JB (1983) Physiological correlates of prolonged sleep deprivation in rats. Science 221(4606):182–184
Reissmann M, Ludwig A (2013) Pleiotropic effects of coat colour-associated mutations in humans, mice and other mammals. Semin Cell Dev Biol 24(6–7):576–586
Salin K, Voituron Y, Mourin J, Hervant F (2010) Cave colonization without fasting capacities: an example with the fish Astyanax fasciatus mexicanus. Comp Biochem Physiol A Mol Integr Physiol 156(4):451–457
Schneider A, Henegar C, Day K, Absher D, Napolitano C, Silveira L, David VA, O'Brien SJ, Menotti-Raymond M, Barsh GS, Eizirik E (2015) Recurrent evolution of melanism in South American felids. PLoS Genet 11(2):e1004892
Stahl BA, Gross JB (2015) Alterations in Mc1r gene expression are associated with regressive pigmentation in Astyanax cavefish. Dev Genes Evol 225(6):367–375
Wall A, Volkoff H (2013) Effects of fasting and feeding on the brain mRNA expressions of orexin, tyrosine hydroxylase (TH), PYY and CCK in the Mexican blind cavefish (Astyanax fasciatus mexicanus). Gen Comp Endocrinol 183:44–52
Wray GA (2007) The evolutionary significance of cis-regulatory mutations. Nat Rev Genet 8(3):206–216
Wu CW, Biggar KK, Storey KB (2013) Biochemical adaptations of mammalian hibernation: exploring squirrels as a perspective model for naturally induced reversible insulin resistance. Braz J Med Biol Res 46(1):1–13
Yamamoto Y, Stock DW, Jeffery WR (2004) Hedgehog signalling controls eye degeneration in blind cavefish. Nature 431(7010):844–847
Yoshizawa M (2015) Behaviors of cavefish offer insight into developmental evolution. Mol Reprod Dev 82(4):268–280
Yoshizawa M, Robinson BG, Duboue ER, Masek P, Jaggard JB, O'Quin KE, Borowsky RL, Jeffery WR, Keene AC (2015) Distinct genetic architecture underlies the emergence of sleep loss and prey-seeking behavior in the Mexican cavefish. BMC Biol 13:15
Zhang QG (2006) Hypertension and counter-hypertension mechanisms in giraffes. Cardiovasc Hematol Disord Drug Targets 6(1):63–67

Chapter 14
Xenotoca eiseni, a Viviparous Teleost, Possesses a Trophotaenial Placenta for Maternal Nutrient Intake

Atsuo Iida

Abstract Over 500 species of teleost fish have been identified as live-bearers. These fish breed by internal fertilization, and, in some species, the embryo weight increases during pregnancy. This indicates that these fish likely possess the specific machinery required to absorb maternally derived nutrients. Approximately 170 viviparous species are included in the order Cyprinodontiformes. This chapter focuses on a viviparous teleost species, *Xenotoca eiseni*, which belongs to the family Goodeidae. Members of the family Goodeidae have a unique structure called the "trophotaenial placenta," which is a branching, ribbonlike structure that extends from the perianal region of the goodeid embryo. The trophotaenial placenta is a hindgut-derived pseudoplacenta that allows the absorption of maternal nutrients during the prenatal stage. The trophotaeniae preliminarily regress when the embryo is born. Because the offspring can ingest food orally soon after birth, the trophotaeniae become unnecessary. Immunohistochemistry indicates that caspase-3-activated cells with fragmented nuclei are present in the regressed processes of the fry immediately after birth. This finding suggests that the trophotaeniae are rapidly resorbed by apoptosis during the last phase of the pregnancy. Such prenatal regression of pseudoplacentae has not been reported in other viviparous vertebrates. Therefore, the small teleost might be a convenient model for understanding the diversity of viviparity in vertebrates.

Keywords Goodeidae · *Xenotoca eiseni* · Viviparity · Pseudoplacenta · Apoptosis

A. Iida (✉)
Department of Regeneration Science and Engineering, Institute for Frontier Life and Medical Sciences, Kyoto University, Kyoto, Japan

H. Hirata, A. Iida (eds.), *Zebrafish, Medaka, and Other Small Fishes*,
https://doi.org/10.1007/978-981-13-1879-5_14

14.1 Introduction: Viviparity in Vertebrates

14.1.1 Mammal

Many viviparous animals exist among the extant vertebrates (Blackburn 2014). In all species of mammals, excluding the monotremes, embryonic growth and development happen within the female body, supported by the provision of maternally derived nutrients. For nutrient absorption, mammals have a placenta and umbilical cord fused to the mother's body. It is suggested that the common ancestor of the extant viviparous mammals obtained the placenta by acquiring the retrotransposon-derived *Peg10* gene, which is essential for placental formation (Kaneko-Ishino and Ishino 2012). The gestation period from the implantation of the fertilized egg to delivery is exactly regulated by the endocrine secretion of estrogen, progestin, and other sex hormones. Furthermore, a current study reported that a particular stem cell regulates interfollicular epidermal expansion corresponding to the baby's growth during the pregnancy (Ichijo et al. 2017). Mammalian viviparity is well understood as described above in terms of morphology, genetics, endocrinology, and the underlying molecular mechanisms from knowledge acquired in rodents, a convenient experimental model.

14.1.2 Nonmammal

Among the nonmammalian vertebrates, viviparous reptiles, amphibians, and fish have been identified; viviparous reptiles have morphological homologs to the mammalian placenta and umbilical cord (Blackburn and Flemming 2012). There have been no reports on nonmammalian animals performing implantation and possessing placenta and umbilical cords during viviparous development similar to that in mammals; their fertilized eggs are presumed to progress through embryonic development and hatch similar to oviparous or ovoviviparous animals and subsequently build a specific compartment for growth in the mother's body. Various forms of pseudoplacenta or hypertrophied hindgut have been reported by morphological studies of viviparous fish (Castro 2009; Wourms 1981). In some viviparous amphibians and cartilaginous fish, cannibalism has been reported during embryonic growth in the mother's body (Wourms 1981; Buckley et al. 2007). The genetic background or molecular mechanisms underlying viviparous systems in nonmammalian vertebrates are poorly understood. In mammals, the origin of the viviparity is presumed to be a genetic modification that occurred in common ancestor of extant marsupials and eutherians; thus, the genomes of monotremes, who are ovoviviparous and form an out-group of them, do not include the *Peg10* gene. Nonmammalian animals possess no *peg10* orthologous genes, but viviparous species have appeared in several phyletic groups. Therefore, diverse viviparous reproduction systems have likely evolved independently.

14.1.3 Teleost

In teleosts, the eggs are commonly thought to be externally fertilized and developed outside the mother's body. However, over 500 live-bearing teleost species are distributed throughout 14 orders and 118 genera (Wourms 1981), and these live-bearing species include both ovoviviparous and viviparous species. In the ovoviviparous species, fertilization occurs internally and embryos hatch in the mother's body. Furthermore, the offspring do not increase their body weight before delivery, and thus, it is deemed that the embryos use nutrients only from their own yolk sacs during the development and do not receive external nutrients. Such a reproduction system involving internal fertilization without nutritional contribution from the mother to offspring is similar to oviparity reported in birds or most reptiles. In contrast, some teleost species are viviparous and perform internal fertilization, and their embryos increase in body weight throughout development similar to that in most mammals. Embryo of nonmammalian viviparous species possesses specific conduits to absorb maternal nutrients, similar to the placenta or umbilical cords in viviparous mammals. In viviparous species of the family Clinidae or Embiotocidae, it is thought that the embryo absorbs maternal nutrients via the skin epithelium. Viviparous species of the order Cyprinodontiformes are reported to possess specific structures for nutrient absorption, such as a follicular pseudoplacenta, hypertrophied hindgut, or trophotaeniae (Wourms 1981). The diversity of the reproductive system in teleosts is notable for further study of their morphology or evolution.

14.1.4 The Family Goodeidae

In particular, the order Cyprinodontiformes includes approximately 170 live-bearing species in 3 families: Poeciliidae, Anablepidae, and Goodeidae (Turner 1933, 1938, 1940a, b). This chapter focuses on a viviparous teleost species belonging to the family Goodeidae that is a freshwater fish found in the lakes and rivers of the Central Plateau of Mexico. Approximately 40 species are included in the family Goodeidae, all of which have been identified as viviparous species. These species likely acquired their viviparous traits independently from mammals and other viviparous vertebrates. The goodeid fish have a unique structure, "trophotaenial placenta," which is a pseudoplacenta that functions to absorb maternally derived nutrients (Lombardi and Wourms 1985a; Mendoza 1972). Other viviparous species belonging to the family Poeciliidae or Anablepidae possess no structures corresponding to the trophotaeniae (Turner 1933, 1938, 1940a). A previous study indicated that all viviparous species that belong to the family Goodeidae, excluding *Ataeniobius toweri*, possess a trophotaenial placenta during their development (Turner 1937; Schindler and Hamlett 1993). This chapter describes a morphological change in the pseudoplacenta during pregnancy using a goodeid species, *Xenotoca eiseni*.

14.2 *Xenotoca eiseni*: An Experimental Model for the Viviparous Teleost

14.2.1 Maintenance and Breeding

The viviparous species, *X. eiseni*, belongs to the family Goodeidae and was used as a model for my research regarding the trophotaenial placenta (Fig. 14.1a). *X. eiseni* is a popular aquarium fish that is easily obtained from commercial suppliers. Adult fish were maintained in freshwater at 27 °C under a 14:10-h light-dark photoperiod cycle. Fish were bred in a mass-mating design. The juveniles were fed live brine shrimp larvae and a small pellet food, and the adults were fed only a pellet food. To accurately track the pregnancy period, the laboratory-born fish were crossed in a pair-mating design and the mating behavior was recorded. The duration of pregnancy in *X. eiseni* was approximately 5 weeks (34–39 days) under these breeding conditions.

14.2.2 Development and Growth in the Mother's Body

In the goodeid species, including *X. eiseni*, eggs hatch in the ovary of the mother's body, where the embryos develop until birth (Fig. 14.1b). During early development, the embryos absorb nutrients from their own yolk sacs, similar to oviparity fish. After depletion of the yolk nutrients, the trophotaeniae develop to allow the absorption of extra nutrients for further embryonic growth. This absorption of

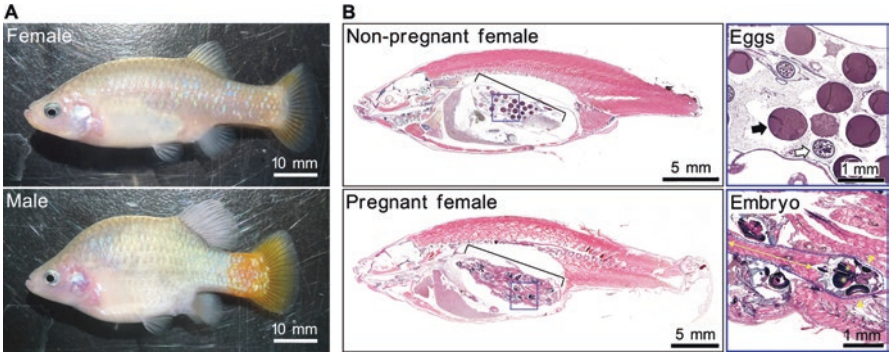

Fig. 14.1 Morphological overview of the viviparous teleost *X. eiseni*
(**a**) Morphological comparison of adult female and male *X. eiseni*. The adult male fish exhibits sex-specific characteristics, such as a high arch body and red color in the tail. (**b**) Sagittal sections of pregnant and nonpregnant female fish. The pregnant fish maintains the embryo in the ovary (brackets). The blue squares indicate larger images for the unfertilized eggs in the nonpregnant fish and the embryo at approximately 3 weeks in the pregnant fish. White arrow, growing follicle; black arrow, matured follicle; dashed line, embryo shape; double-headed arrow, body trunk; asterisks, brain; arrowheads, eyes

nutrients via the trophotaeniae allows the offspring to be born at a more advanced stage relative to that observed in oviparous and ovoviviparous fish. Figure 14.2a shows *X. eiseni* embryos obtained from females at the 2nd, 3rd, and fourth week after mating. The embryos have different degrees of trophotaeniae elongation from the perianal region, depending on the stage of embryonic development. The trophotaeniae were not fused to the maternal tissues, and no decidual-like structure was observed on the ovarian lumen. In past studies using other Goodeid species, these trophotaeniae were also reported as hindgut-derived ribbonlike structures that extended from the perianal region of the embryo (Turner 1940a). Given that the trophotaenia is not fused to the mother's body, these goodeid embryos likely receive maternally derived nutrients provided from the ovarian lumen in a secreted form (Lombardi and Wourms 1985b; Schindler 2014). Therefore, my observations indicated that the *X. eiseni* embryo possesses a typical trophotaenial placenta that is similar to that of other viviparous species belonging to the family Goodeidae (Lombardi and Wourms 1985b; Schindler 2014).

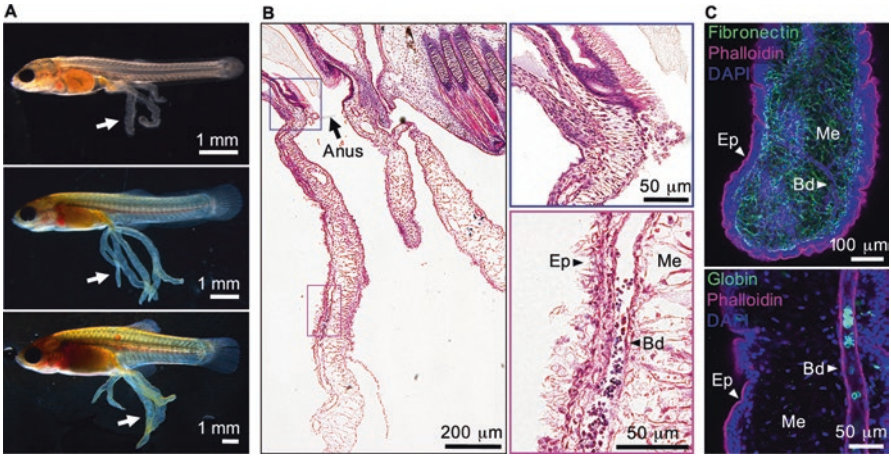

Fig. 14.2 Structure of the trophotaenial placenta
(**a**) The *X. eiseni* embryo extracted from the ovaries at the 2nd (top), 3rd (middle), and fourth week (bottom). The arrows indicate trophotaenial placenta. (**b**) Hematoxylin-eosin-stained section of the trophotaeniae of a fourth-week embryo. The blue square indicates an enlarged image of the basal portion of the trophotaeniae developed from the perianal region. The magenta square indicates vasculature and circulated blood cells in the trophotaeniae. (**c**) Fluorescent immunochemistry to visualize the structure of the trophotaeniae in the fourth-week embryo. The panels indicate an overview of the terminal structure (top) and an enlarged image focused on the vasculature (bottom). *Bd* Blood vessel, *Ep* Epidermal cell layer, *Me* Mesenchyme

14.3 Trophotaenial Placenta

14.3.1 Structure

Histological analyses of sections of the fourth-week embryos stained using hematoxylin-eosin (HE) indicated that the trophotaeniae have a complicated structure, consisting of an epidermal cell layer, mesenchyme, vasculature, and blood cells (Fig. 14.2b). The processes were continuous with the gastrointestinal submucosa or epidermis of the fry. Furthermore, fluorescent microscopy indicated that the epidermal cell layer could be labeled using a fluorescent-conjugated phalloidin marker, which was found to be associated with filamentous actins. The fibronectin-rich mesenchyme was surrounded by the epithelial-like component. Globin-positive erythrocytes were detected in the lumen of the phalloidin-associated vasculature walls (Fig. 14.2c). Live observations indicated that the blood cells and the plasma component were circulating in the processes throughout the embryonic body. A previous study indicated that the secreted nutrients were absorbed from the epithelial surface of the trophotaenia and supplied to the embryonic body via the blood circulation (Hollenberg and Worums 1994). These results indicate that this structure is not an organ homologous to the mammalian placenta and umbilical cord, neither anatomically nor functionally.

14.3.2 Prenatal Regression

The role of the trophotaenial placenta indicates that it is only transiently required for absorption of maternally derived nutrients during embryonic development in the ovary. Because the offspring can ingest food orally soon after birth, the trophotaeniae become unnecessary. In fact, the trophotaeniae of goodeid embryos start to regress at birth and then disappear within a few days (Turner 1933; Mendoza 1965). Therefore, the removal machinery for the trophotaeniae begins to function at the prenatal stage. Figure 14.3a shows shrunken processes at the perianal region of the fry immediately after birth. These are residues of the trophotaeniae. Histological observations indicate that the epidermal cell layer and mesenchymal structures are lost in the regressed processes. The vasculature displays a snaking pattern and blood cells are observed in the vascular lumen (Fig. 14.3b and c). The developmental stage of the fry is estimated to begin at approximately the fifth week after fertilization. Conversely, fourth-week embryos still have complete processes with no signs of regression (Fig. 14.2a). These observations suggest that the trophotaeniae undergo rapid regression in the mother's body during the last phase of pregnancy. Because of the important role that the trophotaenial placenta plays for uptake of maternally derived nutrients during embryonic development in the mother's body, prenatal regression is likely controlled under a firm regulatory mechanism.

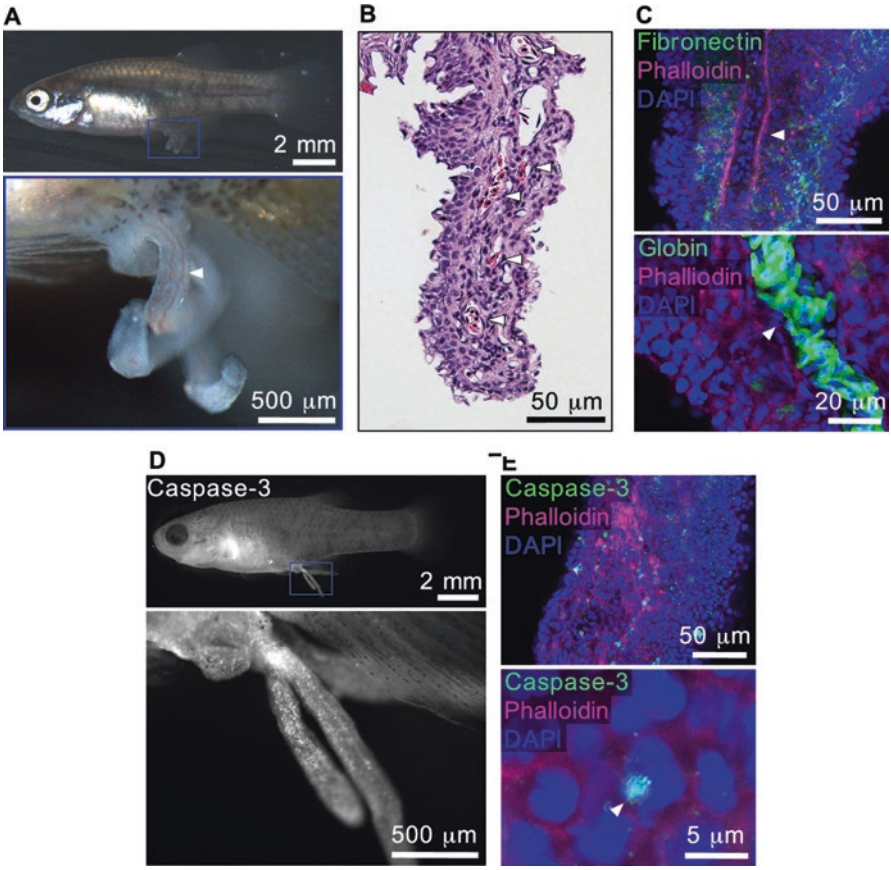

Fig. 14.3 Apoptotic regression of the trophotaenial placenta
(**a**) Full image of a fry immediately after birth. The blue square indicates an enlarged image of the regressed process, a vestige of the trophotaenia in the fry. The white arrowhead indicates circulated blood cells. (**b**) Hematoxylin-eosin-stained section of the regressed processes in the fry. The white arrowheads indicate snaking vasculature and blood cells. (**c**) Confocal microscopy of the fluorescent immunochemistry to visualize the structure of the regressed processes. The white arrowheads indicate snaking vasculature and blood cells. (**d**) Fluorescent immunochemistry to detect the apoptotic cells in the regressed processes. The blue square indicates an enlarged image for apoptotic signals visualized by the caspase-3 antibody. (**e**) Confocal microscopy of fluorescent immunochemistry to detect the apoptotic cells in the regressed processes (top). The white arrowhead indicates the apoptotic cells defined by the caspase-3 antibody and fragmented nuclei (bottom)

14.3.3 Apoptosis

Apoptosis, the process of programmed cell death involving nucleus fragmentation, widely contributes to disease development, physiological tissue turnover, and morphogenesis during development (Jacobson et al. 1997; Yaron and Hermann 2011). Caspase-3 activation is a major marker of apoptosis-related cell death (Sakahira et al.

1998). Fluorescent microscopy showed positive active caspase-3 immunoreactivity with fragmented nuclei in the regressed processes, indicating the presence of some apoptotic cells in the regressed processes of the fry (Fig. 14.3d and e). These cells were not detected in the elongated trophotaeniae of the 2nd- or fourth-week embryos (Iida et al. 2015). These observations indicate that the trophotaenial placenta of *X. eiseni* prenatally regresses by a process of apoptotic cell death. Conversely, these apoptotic cells are not observed in the blood vessels of the trophotaeniae, which suggests that the vasculature and blood cells are less sensitive or more resistant to these apoptotic cell death signals than the other types of cells (Iida et al. 2015).

14.3.4 Biological Significance

What is significance of the fact that the blood circulation system of the trophotaeniae survives and maintains its function during the regression process? This could be a mechanism for hemorrhage prevention during the regression process, which would prevent the possibility of necrotic cell death or starvation due to arrest of the circulation and nutrient transport. Another possibility is that the surviving cells contribute to vascular rearrangement during the regression process. A previous study indicated that vascular networks at the perianal region of a different goodeid fish, *Skiffia bilineata*, were dramatically rearranged during the perinatal stage (Mendoza 1937). Therefore, our findings suggest that prenatal regression involves not only tissue-specific apoptotic disruption of the unnecessary processes but also serves to help remodel the vascular networks to form an alternate circulatory pathway at the perianal region. However, the specific upstream pathway responsible for apoptosis activation has not been identified. One possibility is that an extrinsic signal is transmitted from the mother to the embryo. In this scenario, a direct trigger for apoptosis activation is provided in the form of maternal elements. Alternatively, the embryo might autonomously regulate apoptosis through an intrinsic and/or extrinsic pathway. One such candidate is the thyroid hormone (TH), which contributes to amphibian metamorphosis and induces apoptosis in the larval intestine (Ishizuya-Oka et al. 2010). TH and its receptors are conserved in teleosts, expressed in the embryonic stage, and contribute to developmental changes in the gut and other organs (Power et al. 2001; Specker 1988). Therefore, these molecules are potent candidates to be embryo-autonomous factors of apoptosis induction. However, this hypothesis does not rule out the possibility of a maternal contribution. Further studies are required to determine the factors that regulate this apoptosis and whether any maternal factors are involved.

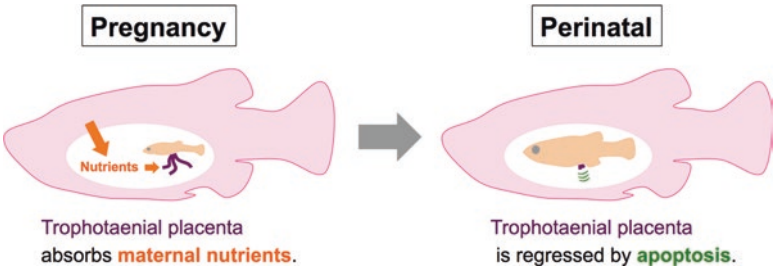

Fig. 14.4 A graphical abstract summarizing the embryonic growth of the goodeid fish Schematic illustration summarizing the model of trophotaenial placenta changes during development. The *X. eiseni* embryo in the mother's body absorbs maternal nutrients via the trophotaeniae (purple). The absorptive tissue begins to disappear at the last stage of pregnancy before birth. This "prenatal regression" process is regulated by apoptosis

14.4 Conclusion

In this study, we presented the goodeid fish species *X. eiseni* as a small fish model for understanding nonmammalian viviparity and elucidated the apoptotic regression process for the postnatal removal of the trophotaenial placenta, which is used for nutritional absorption in their embryos (Fig. 14.4). To the best of our knowledge about vertebrates, including humans, there are no previous reports regarding such regression or any positive roles of apoptotic cell death, excluding pathological process that could result in placental disorders, in placentae or pseudoplacentae that function to absorb maternally derived nutrients (Smith et al. 1997; Sharp et al. 2010). Therefore, the small teleost fish has an organ that is neither anatomically nor functionally homologous to that of the mammalian placenta and umbilical cord and might be a good model for deepening the understanding of the diversity of reproduction systems in vertebrates.

References

Blackburn DG (2014) Evolution of vertebrate viviparity and specializations for fetal nutrition: A quantitative and qualitative analysis. J Morphol. https://doi.org/10.1002/jmor.20272

Blackburn DG, Flemming AF (2012) Invasive implantation and intimate placental associations in a placentotrophic African lizard, Trachylepis ivensii (Scincidae). J Morphol 273:137–159

Buckley D, Alcobendas M, García-París M, Wake MH (2007) Heterochrony, cannibalism, and the evolution of viviparity in *Salamandra salamandra*. Evol Dev 9:105–115

Castro JI (2009) Observations on the reproductive cycles of some viviparous north American sharks. Aqua 15:4–15

Hollenberg F, Worums JP (1994) Ultrastructure and protein uptake of the embryonic trophotaeniae of four species of goodeid fishes (Teleostei: Atheriniformes). J Morphol 219:105–129
Ichijo R, Kobayashi H, Yoneda S, Iizuka Y, Kubo H, Matsumura S, Kitano S, Miyachi H, Honda T, Toyoshima F (2017) Tbx3-dependent amplifying stem cell progeny drives interfollicular epidermal expansion during pregnancy and regeneration. Nat Commun 8:508
Iida A, Nishimaki T, Sehara-Fujisawa A (2015) Prenatal regression of the trophotaenial placenta in a viviparous fish, *Xenotoca eiseni*. Sci Rep 5:7855
Ishizuya-Oka A, Hasebe T, Shi YB (2010) Apoptosis in amphibian organs during metamorphosis. Apoptosis 15:350–364
Jacobson MD, Weil M, Raff MC (1997) Programmed cell death in animal development. Cell 88:347–354
Kaneko-Ishino T, Ishino F (2012) The role of genes domesticated from LTR retrotransposons and retroviruses in mammals. Front Microbiol 3:262
Lombardi J, Wourms JP (1985a) The trophotaenial placenta of a viviparous goodeid fish. II. Ultrastructure of trophotaeniae, the embryonic component. J Morphol 184:293–309
Lombardi J, Wourms JP (1985b) The trophotaenial placenta of a viviparous goodeid fish. III: Protein uptake by trophotaeniae, the embryonic component. J Exp Zool 236:165–179
Mendoza G (1937) Structural and vascular changes accompanying the resorption of the proctodaeal processes after birth in the embryos of the Goodeidae, a family of viviparous fishes. J Morphol 61:95–125
Mendoza G (1965) The ovary and anal processes of "Characodon" eiseni, a viviparous cyprinodont teleost from Mexico. Biol Bull 129:303–315
Mendoza G (1972) The fine structure of an absorptive epithelium in a viviparous teleost. J Morphol 136:109–130
Power DM et al (2001) Thyroid hormones in growth and development of fish. Comp Biochem Physiol C Pharmacol Toxicol Endocrinol 130:447–459
Sakahira H, Enari M, Nagata S (1998) Cleavage of CAD inhibitor in CAD activation and DNA degradation during apoptosis. Nature 391:96–99
Schindler JF (2014) Structure and function of placental exchange surfaces in goodeid fishes (Teleostei: Atheriniformes). J Morphol. https://doi.org/10.1002/jmor.20292
Schindler JF, Hamlett WC (1993) Maternal-embryonic relations in viviparous teleosts. J Exp Zool 266:378–393
Sharp AN, Heazell AE, Crocker IP, Mor G (2010) Placental apoptosis in health and disease. Am J Reprod Immunol 64:159–169
Smith SC, Baker PN, Symonds EM (1997) Placental apoptosis in normal human pregnancy. Am J Obstet Gynecol 177:57–65
Specker JL (1988) Preadaptive role of thyroid hormones in larval and juvenile salmon: growth, the gut and evolutionary considerations. Am Zool 28:337–349
Turner CL (1933) Viviparity superimposed upon ovo-viviparity in the goodeidae, a family of cyprinodont teleost fishes of the Mexican plateau. J Morphol 55:207–251
Turner CL (1937) The trophotaeniae of the goodeidae, a family of viviparous cyprinodont fishes. J Morphol 61:495–523
Turner CL (1938) Adaptations for viviparity in embryos and ovary of Anableps anableps. J Morphol 62:323–349
Turner CL (1940a) Pseudoamnion, pseudochorion, and follicular pseudoplacenta in poeciliid fishes. J Morphol 67:59–89
Turner CL (1940b) Adaptations for viviparity in jenynsiid fishes. J Morphol 67:291–297
Wourms JP (1981) Viviparity: the maternal-fetal relationship in fishes. Am Zool 21:473–515
Yaron F, Hermann S (2011) Programmed cell death in animal development and disease. Cell 147:742–758

Chapter 15
Mormyrid Electric Fish as a Model to Study Cellular and Molecular Basis of Temporal Processing in the Brain

Tsunehiko Kohashi

Abstract The nervous system must deal with the temporal dynamics of sensory inputs to allow animals to adapt and anticipate events happening in the world. The mechanisms underlying neural processing of temporal patterns of sensory inputs have been difficult to uncover at the subcellular level, primarily due to the lack of an in vitro reduced preparation method in which the mechanisms are readily accessible yet behaviorally relevant network activity is preserved. In this chapter, I introduce the electrosensory pathway of the African mormyrid electric fish as a powerful model system enabling us to overcome this difficulty. Mormyrid electric fish communicate by varying the intervals between electric pulses (interpulse intervals, or IPI) generated in the tail. The timing of each pulse from a neighboring fish is coded by peripheral electroreceptors into precisely timed action potentials. Within the midbrain posterior exterolateral nucleus (ELp), the temporal patterns of afferent spike trains are filtered to establish selectivity to IPI (IPI tuning) at the level of single neurons. Recent studies have developed a series of in vitro preparations of this pathway in which IPI tuning of ELp neurons can be reproduced by direct stimulation of afferent inputs with behaviorally relevant temporal patterns. By taking advantage of this striking possibility, studies have revealed some of the key mechanisms that shape IPI tuning of the ELp circuit, such as temporal dynamics of excitatory and inhibitory synaptic inputs, neuronal microcircuits, and membrane excitability.

Keywords Animal communication · Temporal interval · Timing · Electrosensation · Sensory coding · Temporal coding · Membrane excitability · Synaptic response · Electrophysiology

T. Kohashi (✉)
Neuroscience Institute, Division of Biological Science, Graduate School of Science, Nagoya University, Nagoya, Japan
e-mail: kohashi-t@bio.nagoya-u.ac.jp

H. Hirata, A. Iida (eds.), *Zebrafish, Medaka, and Other Small Fishes*,
https://doi.org/10.1007/978-981-13-1879-5_15

15.1 Introduction

The dynamic nature of our external environment combined with the temporal nature of animal communication has provided strong evolutionary and ecological pressure for the nervous system to process temporal information (Goel and Buonomano 2014). Many sensory circuits in the central nervous system contain neurons that exhibit selective responses to particular temporal structures in sensory stimuli (Baker et al. 2013; Edwards et al. 2002; Edwards and Rose 2003; Goel and Buonomano 2014; Grothe 1994; Huetz et al. 2011; Kostarakos and Hedwig 2012; Pluta and Kawasaki 2010; Rose and Fortune 1999).

A variety of synaptic mechanisms have been suggested to be involved in this selectivity (Baker and Carlson 2014; Baker et al. 2013; Edwards et al. 2007, 2008; Fortune and Rose 2001; George et al. 2011; Goel and Buonomano 2014; Grothe 1994; Klyachko and Stevens 2006; Rose et al. 2011; Schoneich et al. 2015; Zucker and Regehr 2002). Intrinsic properties of postsynaptic membranes can also contribute to temporal filtering of synaptic inputs (Ashida and Carr 2011; Carlson and Kawasaki 2006; Ellis et al. 2007; Fortune and Rose 1997, 2003; Golding 2012; Hutcheon and Yarom 2000; Mehaffey et al. 2008; O'Donnell and Nolan 2011; Ponnath and Farris 2010; Trussell 1999).

In vitro slice preparations are particularly suitable for investigating the mechanisms of these temporal processing circuits in detail. For instance, fewer physical obstacles and exposed recording sites in these slice preparations greatly help in performing dual-cell recording, or even in accurately positioning multiple electrodes at different locations in a single cell. Rapid and precisely located drug delivery to the slice at an accurate concentration allows finely designed pharmacological experiments as well. However, it is quite challenging to link information processing occurring in vivo with the synaptic and cellular mechanisms revealed in vitro (Abbott and Regehr 2004). This is because of the preparation method's fundamental inability to reveal whether the network activities observed within the reduced network in vitro are the same as, or at least similar to, those occurring in the intact circuit in vivo. To this end, we first need to ensure that the direct, artificial activation of presynaptic inputs to the recorded neurons in vitro successfully replicates the temporal patterns of the inputs evoked by sensory stimulation in vivo.

In this chapter, I introduce the midbrain circuit of pulse-type weakly electric mormyrid fish from Africa (Fig. 15.1) as a powerful model system enabling us to overcome this difficulty and thus progress further in our understanding of the cellular mechanisms underlying temporal pattern processing in the central nervous system. The precise timing of the patterns in mormyrids' electric communication signals is preserved by afferent spike trains along the central electrosensory pathway until a midbrain nucleus where neurons exhibit temporal selectivity to the pattern (Baker et al. 2013). This unique feature of the mormyrid electrosensory pathway allows us to reproduce neuronal temporal selectivity in a behaviorally relevant manner, even using in vitro preparations, and thus to directly relate cellular mechanisms revealed in vitro to the temporal filtering performed by the intact circuit in vivo.

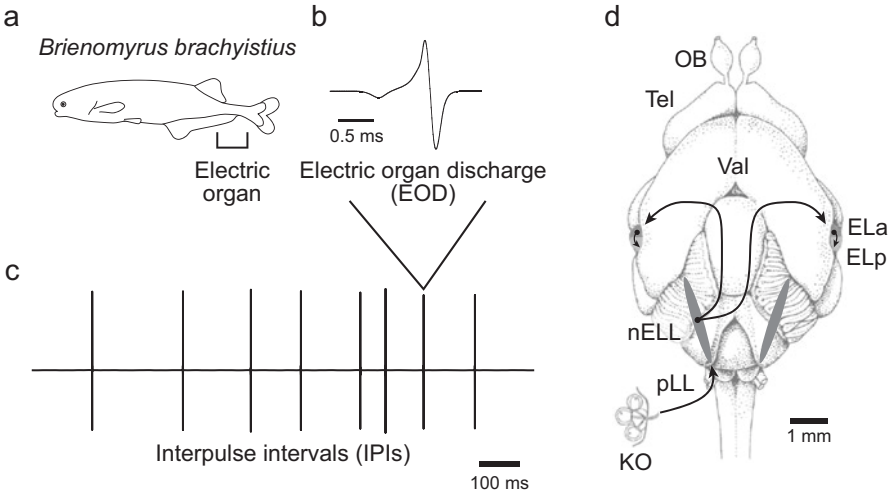

Fig. 15.1 Electric signaling behavior and the sensory pathway for electric communication in weakly electric mormyrid fish
(**a**) *Brienomyrus brachyistius*, a model mormyrid species used to study temporal processing of communication signals in the brain. Mormyrids generate electric communication signals from an electric organ located at the base of the tail. (**b**, **c**) The two basic components of electric communication are the waveform of the electric organ discharge (EOD) (**b**) and interpulse intervals (IPIs) (**c**). Signals are recoded with a pair of electrodes placed near the fish in the aquarium tank. The EOD waveform is displayed in the head-positive polarity. (**d**) Dorsal view of the brain of *B. brachyistius*. Knollenorgan (KO) primary afferents project ipsilaterally to the nucleus of the electrosensory lateral lone lobe (nELL) in the hindbrain via the posterior lateral line nerve (pLL). Neurons in the nELL project bilaterally to the anterior exterolateral nucleus (ELa) in the midbrain, which projects ipsilaterally to the adjacent posterior exterolateral nucleus (ELp). Note that the ELa and ELp are exposed on the side of the brain so that the structures are easily accessible for recording. Val, valvula of the cerebellum; Tel, telencephalon; OB, olfactory bulb.

15.2 Sensory Pathway Dedicated to Electric Communication

Mormyrids produce weak electric organ discharges (EODs) to communicate and actively sense their environment (Carlson 2006; von der Emde 2006). Communication in mormyrids involves two primary components: the waveform of each pulse of EOD (Fig. 15.1b) and interpulse intervals (IPIs) (Fig. 15.1c). The EOD waveform is species-specific, and in some species, it provides additional information about identity such as sex, maturity, and dominance status (Carlson 2002). EOD waveform can vary in polarity, number of phases, duration, and overall shape across closely related species (Hopkins 1999). Signaling fish also vary their IPIs, ranging from slightly under 10 ms to several seconds, to communicate their behavioral state, such as dominance, submission, aggression, and courtship (Carlson 2002; Hopkins 1986). Several patterns of IPI sequences are identified across species: irregular random patterns, regularized patterns, pauses in discharging called cessations, and bursts of short-interval pulses (Carlson 2002).

To detect electric signals, mormyrids have three types of electroreceptors in their skin: mormyromasts are used for active sensing that relies on reception of the fish's own EOD (von der Emde 2006), ampullary receptors for passive electroreception that respond to low-frequency signals originating from animate and inanimate objects (Wilkens and Hofmann 2005), and knollenorgans (KOs) for communication (Xu-Friedman and Hopkins 1999). In the following, I will review studies on KO electroreceptors and their downstream sensory pathway called the KO pathway. I will specifically focus on studies from one mormyrid lineage known as "clade A" (Carlson et al. 2011), which constitutes most of one of the two subfamilies (Mormyrinae) in the family Mormyridae. This is worth noting because recent studies have found that species from the other subfamily, the Petrocephalinae, show striking differences in KO pathway anatomy and physiology, even from the level of KOs (Baker et al. 2015; Carlson et al. 2011; Velez and Carlson 2016).

Figure 15.1d illustrates the schematic overview of the principal KO pathway. KO afferents project ipsilaterally to the hindbrain nucleus of the electrosensory lateral line lobe (nELL), where corollary discharge inhibition plays its role to block the pathway's response to the fish's own EOD (Bell and Grant 1989; Zipser and Bennett 1976). The axons of nELL neurons project bilaterally through the lateral lemniscus to the midbrain torus semicircularis (Szabo et al. 1983). The main projection from the nELL is the anterior exterolateral nucleus (ELa) within the torus, in which KO spike information from different parts of the body is first merged for processing the temporal structure of an EOD waveform (Xu-Friedman and Hopkins 1999). Output neurons in the ELa project exclusively to the adjacent posterior exterolateral nucleus (ELp) (Haugede-Carre 1979), in which processing for IPIs first takes place (Carlson 2009).

Three lines of evidence suggest that the KO pathway is used exclusively for communication. First, KOs have a high sensitivity, or low threshold, and their frequency response properties match the spectrums of the species' own EOD (Arnegard et al. 2006; Hopkins 1981; Lyons-Warren et al. 2012). Second, selective lesions of the exterolateral nucleus in the KO pathway abolish some communication behaviors (Moller and Szabo 1981). Finally, sensory response of the KO pathway is strongly inhibited, at the level of the hindbrain nELL, by the efference copy of the motor command for EOD (corollary discharge inhibition) (Bell and Grant 1989; Zipser and Bennett 1976). Thus, KOs and their primary afferents respond to the fish's own discharge, but this response can never pass the hindbrain, making the fish "deaf" to its own discharges while specializing the pathway for detecting and processing EOD signals from neighboring fish. These characteristics make the KO pathway an ideal model system to study sensory processing of communication signals because everything that occurs within this pathway can be directly associated with the fish's communication.

15.3 Physiology of Knollenorgan Sensory Pathway to Code Electrocommunication Signals

KO electroreceptors are scattered over the body surface (Carlson et al. 2011; Harder 1968). KOs in clade A species generate spike-like potentials in response to electrosensory stimuli. The response is unidirectional to the stimulus polarity: KOs only spike in response to positive changes in voltage across the skin, or inward current (Bennett 1965; Hopkins and Bass 1981; Lyons-Warren et al. 2012). Due to this rectification property, a brief pulse of electrical current, either an artificial square pulse or an EOD, activates KOs on one side of the body at the onset and activates those on the opposite side of the body at the offset. Therefore, fish can analyze the temporal structure of a stimulus by comparing the temporal pattern of spikes from KOs.

The ELa is the first step in EOD waveform analysis (Lyons-Warren et al. 2013; Xu-Friedman and Hopkins 1999). There are two distinct cell types within the ELa, small cells and large cells, and axons from the nELL terminate on both cell types with mixed chemical and electrical synapses (Mugnaini and Maler 1987). Small cells are excitatory projection neurons, and large cells are local, GABAergic inhibitory interneurons that synapse onto the small cells (Friedman and Hopkins 1998; Mugnaini and Maler 1987). The nELL axons synapse onto large cells shortly after entering the ELa, while the axons follow long winding paths before synapsing onto small cells (Friedman and Hopkins 1998). In a sharp contrast to nELL axons, large cell axons project fairly directly to small cells (Friedman and Hopkins 1998).

This circuit architecture inspired a computational model of ELa circuitry in which the small cell serves as a time comparator of KO spike times coming from different parts of the body to detect the duration of stimulus pulses (Friedman and Hopkins 1998; Xu-Friedman and Hopkins 1999): small cells receive delayed synaptic excitation due to the long winding nELL axons activated by stimulus onset, as well as non-delayed synaptic inhibition from the large cells activated by stimulus offset; thus, small cells fire upon excitation only with a delay which is long enough not to collide with the inhibition. This “delay-line anticoincidence” model predicts that small cells are “long-pass tuned” to pulse duration: individual small cells increase the number of spikes, which eventually reaches a plateau, as the duration of the stimulus pulse, i.e., the time difference between stimulus onset and offset, becomes longer than a certain length determined by the conduction delay of the nELL axon. This model was recently confirmed experimentally by extracellular single-unit recording from individual small cell axons: a majority of small cells are indeed long-pass tuned to pulse duration, as predicted (Lyons-Warren et al. 2013).

Small cells are the sole output neurons in the ELa and project only to adjacent ELp, so that all of the information processed within the ELa is transferred to the ELp. Extracellular single-unit recording suggested that stimulus pulse duration processed in the ELa is represented differently by two cell types within the ELp

(Amagai 1998). Type I cells are long-pass tuned to pulse duration. Type II cells, meanwhile, are band-pass tuned (or, they respond the best to pulses with an intermediate duration but less responsive to short or long pulses) and more sensitive to stimulus polarity and amplitude than type I cells are. The sensitivity of ELp neurons to stimulus pulse duration, amplitude, and polarity proves that the information for identifying as well as locating the signaling fish is sufficiently embedded in the spike timing of KOs.

In addition to the pulse waveform, most ELp neurons are also tuned to IPIs, as first reported by Carlson (2009) (Fig. 15.2). Low-pass ELp neurons respond selectively, with large synaptic depolarizations and resulting action potentials, to long intervals but are less responsive to short intervals (thus the neurons "pass" information to their postsynaptic neurons only when the pulse repetition rate is "low"). On the contrary, high-pass ELp neurons show preference to short intervals but not to long intervals (thus the neurons selectively "pass" the "high-frequency" information). Band-pass neurons exhibit preference to intermediate intervals and band-stop neurons to short and long but not intermediate intervals. In addition to their preference for a constant IPI sequence, ELp neurons are also responsive to the direction of IPI changes, resulting in selective responses to different burst patterns that are used in different behavioral contexts (Carlson 2009). Overall, the above in vivo

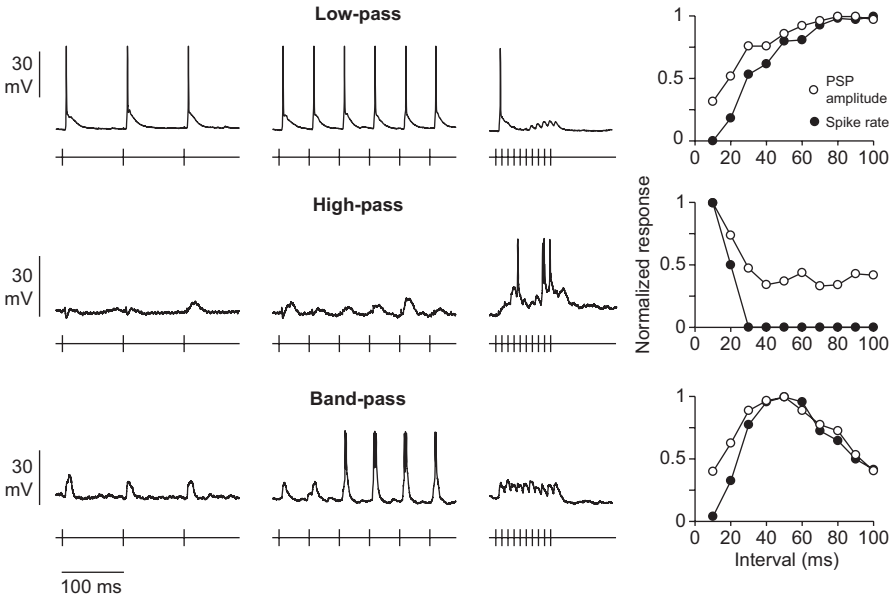

Fig. 15.2 ELp neurons exhibit selective response to pulse intervals
IPI tuning of three different ELp neurons (low-pass, high-pass, and band-stop neuron) in response to electrosensory stimulation in vivo. Intracellular recordings show responses to stimulus trains with 100, 50, and 10 ms IPIs (from left to right, bottom trace of each panel). On the far right, tuning curves show the normalized average spike rate and amplitude of postsynaptic potentials (PSPs) as a function of stimulus IPI. (Adapted from Baker et al. 2013)

studies have revealed that the population of ELp neurons carries information about both components of communication signals – EOD waveform and IPI sequence – at the same time, as a result of sequential conversion of KO spike times first by ELa circuitry and then by ELp circuitry (Baker et al. 2013).

15.4 In Vitro Preparation to Study Cellular Mechanisms of IPI Tuning in the ELp

ELp neurons are multipolar and exhibit large, spiny dendritic arborizations (up to 200 μm in diameter) that branch widely throughout the nucleus (George et al. 2011; Ma et al. 2013; Xu-Friedman and Hopkins 1999). In addition to their extrinsic projections, the axons of ELp neurons also branch extensively within the nucleus (George et al. 2011; Xu-Friedman and Hopkins 1999). Furthermore, the ELp contains a number of inhibitory GABAergic interneurons (George et al. 2011). These anatomical observations indicate that the ELp is the site of intense local processing within the nucleus.

Indeed, the IPI selectivity of the ELp essentially arises within the activity of the local ELp circuitry itself because sensory stimulation and direct electrical stimulation of the ELa with identical IPI patterns give rise to similar IPI tuning in the same ELp neuron (Carlson 2009). In other words, only the ELa, not any of the earlier steps in the KO pathway (Fig. 15.1d), is required to essentially reproduce IPI selectivity in the ELp. This finding encouraged the researchers to develop a series of in vitro reduced preparation to further investigate the synaptic and cellular mechanisms involved in the IPI tuning of ELp neurons (George et al. 2011; Kohashi and Carlson 2014; Ma et al. 2013), which I will review in the following sections. The technical advantages of in vitro preparations over in vivo preparations are as follows:

1. Freedom of physical access: In in vivo preparations, the arrangement of devices for purposes other than recording and stimulation (e.g., those for fixation and those for sustaining life) greatly limit the approach to the recording site. For instance, access to unexposed parts of the brain, multielectrode recording, and visually guided recording from subcellular structures with the aid of high-magnification optics, which are critical to study neuronal circuits at the subcellular level, are often limited.
2. Precisely and rapidly controlled pharmacology: Drug concentration is difficult to control in vivo due to diffusion into body fluids. In addition, difficulty in physically securing the brain may destabilize electrophysiological recordings during drug application.

Taking advantage of the technical superiority of in vitro preparations, a series of in vitro whole-cell recordings has revealed a generalized view about how IPI selectivity is established in ELp neurons: overall tuning category (high-pass, low-pass, band-pass, and band-stop) is largely determined by the temporal dynamics of excitatory and inhibitory synaptic responses, and the shape of the tuning curve is fine-tuned by intrinsic membrane properties.

15.5 Synaptic Mechanisms Underlying IPI Selectivity

A variety of synaptic mechanisms such as temporal summation of synaptic responses and short-term synaptic plasticity as well as relative timing of excitation and inhibition including time windows of post-inhibitory rebound excitation have been suggested to establish single-neuron selectivity for temporal intervals (Baker and Carlson 2014; Baker et al. 2013; Buonomano 2000; Edwards et al. 2007, 2008; Fortune and Rose 2001; George et al. 2011; Grothe 1994; Klyachko and Stevens 2006; Rose et al. 2011; Schoneich et al. 2015; Zucker and Regehr 2002). Temporal summation and short-term synaptic plasticity will give rise to a rate-dependent (i.e., inverse of intervals between synaptic inputs) increment or decrement of synaptic potentials during successive stimulations (see Fig. 15.3). These mechanisms by themselves could act as high-pass or low-pass filters for intervals. Integration of these responses, with their relative timing differences, would set a variety of interval-selectivity windows. However, even without rate-dependent changes in synaptic strength, timing differences in excitatory and inhibitory synaptic inputs could solely set an IPI selectivity by interference between synaptic responses evoked by preceding and following stimuli.

The first attempt to reveal the synaptic mechanisms underlying IPI selectivity of ELp neurons was performed by whole-cell membrane potential recordings of ELp

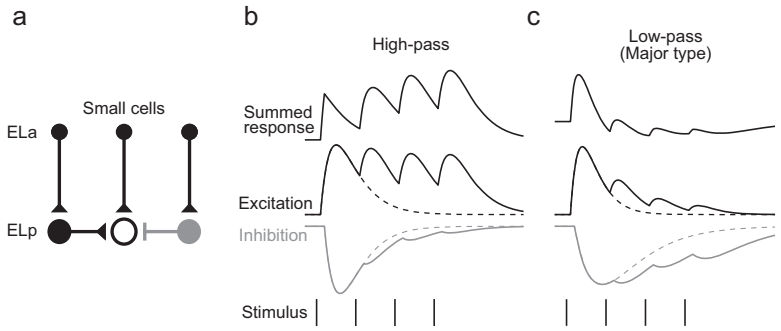

Fig. 15.3 Synaptic mechanisms contributing to interval tuning of ELp neurons (**a**) An ELp neuron (black empty circle) receives excitatory inputs (black) from ELa small cells and from other ELp neurons, as well as inhibitory inputs (gray) from other ELp neurons. (**b, c**) Schematic drawings of PSPs that create IPI tuning of ELp neurons. Up, depolarization; down, hyperpolarization. (**b**) High-pass tuning is associated with excitation (middle, black traces) which depresses less effectively than inhibition (middle, gray traces) does, leading to more temporal summation of excitation than inhibition. Responses elicited by the first stimulus pulse alone are indicated by dotted lines. The summed response (top) is the result of adding excitatory and inhibitory traces, showing a gradual increase in depolarization amplitude during high-frequency stimulus train (bottom). (**c**) The majority of low-pass neurons exhibit excitation which depresses more than inhibition does. In addition, onset inhibition lasts longer than onset excitation does. Thus, successive high-frequency stimuli do not elicit significant depolarization in the summed response. (Adapted from Baker and Carlson 2014. Reprinted with permission from the Society for Neuroscience)

neurons from an in vitro slice preparation in which synaptic inputs to ELp neurons were activated by direct stimulation of the ELa (George et al. 2011). By isolating excitatory synaptic responses with inhibitory neurotransmission blockers, temporal summation of excitation and inhibition was suggested to play a major role in establishing the IPI selectivity of ELp neurons (George et al. 2011): temporal summation of excitation can cause increased responses to short intervals, whereas temporal summation of inhibition can cause decreased responses to short intervals. In addition, computational modeling demonstrated that this one mechanism can establish all major classes of IPI tuning (George et al. 2011).

George et al. (2011) also revealed that a small subset of ELp neurons may be influenced by short-term synaptic depression. In a later study, however, this synaptic mechanism actually turned out to be more dominant in vivo (Baker and Carlson 2014). Instead of using a pharmacological agent to block excitatory or inhibitory neurotransmission, this in vivo study computationally estimated excitatory and inhibitory synaptic responses from whole-cell membrane potential recordings. The analysis suggested that, in addition to temporal summation of synaptic responses, short-term depression and a large synaptic inhibition at the onset of stimulus train (onset inhibition) are also prominent in establishing IPI tuning of ELp neurons (Fig. 15.3) (Baker and Carlson 2014).

Figure 15.3 depicts a model of how these multiple mechanisms interact in shaping two of the most major classes of IPI tuning, high-pass and low-pass (Baker and Carlson 2014). In either class, the difference in the amount of temporal summation between excitatory and inhibitory inputs, which results from the difference in the degree of short-term synaptic depression, serves as a key determinant. During high-frequency (or short-interval) stimulation, a high-pass neuron receives diminishing inhibition (due to strong synaptic depression) and summating excitation (but exhibits weak synaptic depression), which overall result in a gradually developing depolarization (Fig. 15.3b). In the majority of low-pass neurons, on the other hand, excitation and inhibition show reversed kinetics (Fig. 15.3c). A subset of low-pass neurons indeed exhibits less depression of excitation than inhibition (Baker and Carlson 2014). Even in this case, however, a long, large onset inhibition is suggested to effectively counteract the ongoing excitation (Baker and Carlson 2014).

The short-term synaptic depression revealed in vivo (Baker and Carlson 2014) comes at least partially from a local network among ELp neurons (Ma et al. 2013), and the disruption of this network could explain why this synaptic mechanism was not clearly observed in the slice preparation. This fundamental issue with the in vitro preparation was circumvented by the development of a novel whole-brain preparation in which the ELp circuitry remains intact (Ma et al. 2013).

The whole-brain preparation enables us to analyze the network structure of intact ELp circuitry. Dual whole-cell recording from neighboring (located within 50 μm between soma) ELp neurons revealed excitatory connections between as much as 17% of recorded pairs, and the excitatory connections exhibited clear short-term depression (Ma et al. 2013), suggesting that the extensive excitatory connections among ELp neurons could serve as one of the major sources of the synaptic depression that shapes IPI tuning as observed in vivo (Baker and Carlson 2014).

Interestingly, similarly tuned neurons share an excitatory synaptic connection more often and more strongly than differently tuned neurons do (Ma et al. 2013). This finding suggested a general model for the ELp local excitatory network (Ma et al. 2013): strong synaptic connections from similarly tuned neurons reinforce their own tuning type together but also contribute to variation in the shapes of tuning curves. Weak synaptic connections from differently tuned neurons modify the tuning curve shapes without changing the basic patterns of tuning.

15.6 Membrane Excitability Regulating IPI Tuning

ELp neurons recorded from whole-brain preparations often fire action potentials in response to ELa stimulation (Kohashi and Carlson 2014), unlike those recorded from slice preparations in which network connections are severely damaged by slicing. This fact provides an opportunity to investigate how synaptic filtering for IPI interacts with intrinsic properties of postsynaptic neurons to eventually generate IPI-selective spiking responses that are sent downstream of the sensory pathway.

In addition to the classes of IPI tuning, ELp neurons are classified into two types according to their firing properties in response to a prolonged suprathreshold depolarization (Kohashi and Carlson 2014). One type is named tonic neurons because they repetitively fire action potentials throughout depolarization. The other type is named phasic neurons and is characterized by a strong spike frequency adaptation to stop firing shortly after the onset of depolarization.

One major mechanism of spike frequency adaptation is Ca^{2+}-activated K^+ (K_{Ca}) channels expressed on the neuronal plasma membrane (Sah 1996; Sah and Faber 2002). These K^+ channels are opened by a rise in cytosolic Ca^{2+}, especially resulting from Ca^{2+} influx via voltage-gated Ca^{2+} (Ca_v) channels active during action potentials, and thus mediate outward, hyperpolarizing (or "inhibitory") K^+ currents. There are three broad families of K_{Ca} channels identified biophysically and pharmacologically. They are called, based on the single channel electrical conductance (i.e., ion permeability), SK (small conductance), IK (intermediate conductance), and BK (large conductance) channels (Sah and Faber 2002). Pharmacological manipulations during membrane potential or membrane current recording of ELp neurons suggested that, among the K_{Ca} subtypes, a fast BK current is more highly expressed in tonic neurons than in phasic neurons (Fig. 15.4a). Detailed analysis of the BK current and spike waveform further suggested that the current promotes tonic firing by accelerating action potential repolarization and indirectly slowing accumulation of inactivated Na^+ channels which cause spikes to adapt (Kohashi and Carlson 2014).

The above membrane model potentially explains observed relationships between firing pattern and IPI selectivity as well (Kohashi and Carlson 2014) (Fig. 15.4b). Postsynaptic potentials (PSPs), as a result of IPI filtering by synaptic mechanisms, should eventually be converted into spike outputs. This PSP-to-spike conversion is more faithful in tonic neurons than in phasic neurons; in other words, PSP amplitude

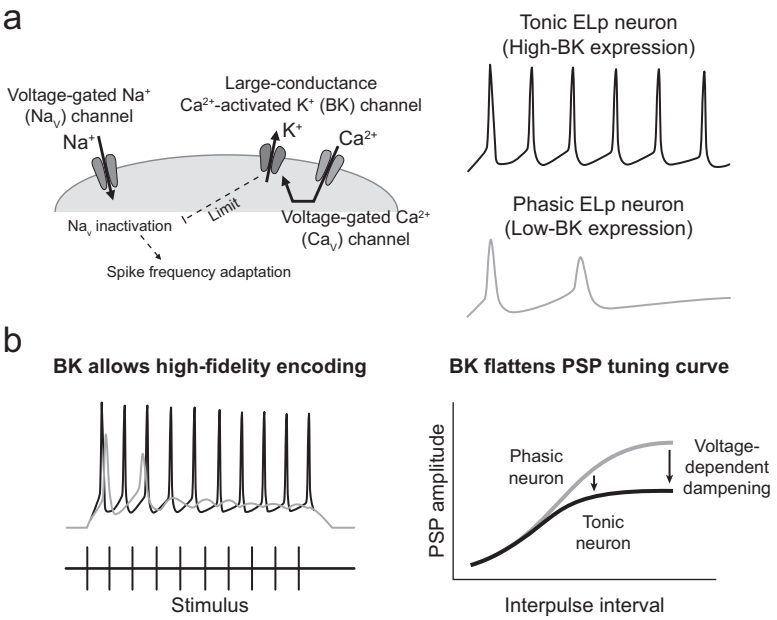

Fig. 15.4 Membrane model for the role of BK channels in shaping interval tuning (**a**) Left, ELp neurons express voltage-gated Ca^{2+} (Ca_v) channels and large-conductance Ca^{2+}-activated K^+ (BK) channels. The Ca^{2+} influx through the Ca_v channels in turn activates the BK channels (bent arrow). When the BK channels are highly expressed, the fast BK current activated during action potentials accelerates the membrane repolarization, limits inactivation of voltage-gated Na^+ (Na_v) channels, and thus suppresses spike frequency adaptation resulting from accumulation of inactivated Na_v channels (dotted lines). Right, tonic ELp neurons are able to fire action potentials continuously due to high BK current expression (top). On the other hand, phasic ELp neurons express only a low BK current density and show strong spike frequency adaptation that is characterized by diminishing action potentials (bottom). (**b**) BK current regulates IPI tuning. Left, large BK current allows tonic neurons (top, black trace) to follow stimulus trains (bottom) with spikes by suppressing spike frequency adaptation. Right, BK channels are activated even by subthreshold PSPs in a depolarization-dependent manner, due to Ca_v influx during synaptic depolarization as well as voltage-sensitivity of BK channels themselves. Thus, the larger the synaptic excitation is, the more the resulting PSP is attenuated by the BK current (arrows) so that the overall shape of the tuning curve is flattened. This effect is more prominent in tonic neurons (black curve) than in phasic neurons (gray curve)

correlates better with spike numbers in tonic neurons (Fig. 15.4b, left) (Kohashi and Carlson 2014). This effect is particularly prominent at short IPIs where PSPs easily summate and result in large prolonged depolarizations that cause strong spike adaptation in phasic neurons. Furthermore, the subthreshold BK current activated by excitatory PSP may also explain why phasic neurons are more sharply tuned to IPIs than tonic neurons are (Fig. 15.4b, right) (Kohashi and Carlson 2014). Pharmacological analysis also revealed that ELp neurons express a Ca_v current that can be activated even by synaptic depolarization below spike threshold. This Ca_v current is suggested to activate the BK current. The voltage-dependency of the subthreshold Ca^{2+} influx,

together with the voltage-sensitivity of the BK channels themselves, provides ELp neurons with a hyperpolarizing K^+ current that increases as the neurons become more depolarized by synaptic excitation. Thus, membrane depolarization is counteracted in a depolarization-dependent manner by the subthreshold BK activation. This voltage-dependent dampening effect could be strongest at the peak of IPI selectivity, giving the IPI tuning curves of tonic neurons a more flattened appearance compared to those of phasic neurons. Overall, tonic neurons can faithfully encode an incoming stimulus train but are not sharply tuned to IPIs. By contrast, phasic neurons are sharply tuned to IPIs but cannot encode long-lasting stimulus trains, particularly at short IPIs. Here is a systematic trade-off between accuracy of IPI detection and capability of long-term encoding. The heterogeneity of tonic and phasic neurons in the ELp may maximize mormyrids' capability of detecting complex EOD patterns that convey social context.

Among K_{Ca} channel subtypes, the function of SK channels has been extensively studied in temporal processing such as frequency tuning (Ellis et al. 2007; Mehaffey et al. 2008) and amplitude-modulation (AM) frequency tuning (Ponnath and Farris 2010). By contrast, this study was the first to suggest a role for BK channels in the temporal processing of sensory input at the levels of integrating synaptic inputs into PSPs and of the PSP-to-spike conversion. Subcellular localization of the BK channels is also of interest to further investigate this membrane model because, for instance, dendritic BK channels (Johnston and Narayanan 2008) can shape local dendritic computations, which in turn dramatically increases the degree of freedom for subcellular processing.

15.7 Future Directions

The unique features of the mormyrid KO pathway have made the ELp an excellent model system to study neuronal processing of temporal patterns seamlessly from the subcellular level to the behavioral level, i.e., the ultimate consequences of the circuit function. However, our current understanding of the ELp circuit is mostly limited to single-cell electrophysiology. Many basic questions about temporal processing within the ELp still remain to be elucidated. How does a population of ELp neurons with diverse filtering properties code for the variety of communication signals? How is local subcellular computation achieved for temporal filtering? What is the molecular basis underlying the computation?

Recently, Baker et al. (2016) demonstrated, by computationally pooling single-cell electrophysiological responses of ELp neurons obtained individually in vivo, that a population of ELp neurons can detect minute variation in EOD sequences with millisecond precision. Large-scale Ca^{2+} imaging of the neuronal population (Carrillo-Reid et al. 2017), in either in vivo or in vitro preparations, will be a promising way to further push this frontier forward. Cell assembly activated by different IPI patterns will be one immediate topic to investigate in this regard. Ca^{2+} imaging of subcellular structures (Grienberger and Konnerth 2012) such as presynaptic terminals,

dendrites, and dendritic spines will also provide essential information about how local computations are integrated to eventually establish single-neuron temporal filters.

The recent expansion of available genomic information about electric fish including mormyrids (Pitchers et al. 2016) should not only improve our understanding of the molecular basis of temporal processing but also expand our ability to dissect network functions. Especially, CRISPR/Cas9 (or simply CRISPR)-mediated genome editing has been performed successfully in a wide variety of animal species, including many teleost fishes (Barman et al. 2017; Ceasar et al. 2016). The generation of CRISPR-based transgenic mormyrids that express light-sensitive exogenous proteins in ELp neurons will allow researchers to use optical approaches in both monitoring (Knopfel 2012; Lin and Schnitzer 2016) and manipulating (Yizhar et al. 2011) network activities.

The development of mormyrid ELp preparations in which IPI tuning can be reproduced in vitro in behaviorally relevant ways has opened a wide range of possibilities for unveiling the cellular mechanisms of temporal pattern processing. Thanks to the direct link between the temporal patterns of sensory stimulus and those of presynaptic inputs from the ELa, data obtained in vivo are immediately testable in vitro or vice versa. This advantage allows researchers the freedom of comfortably switching between in vivo and in vitro preparations to investigate specific aspects of their questions. Combining this unique advantage of the ELp with the state-of-the art techniques that have been developed in other model organisms will accelerate our understanding of neuronal processing of temporal information.

References

Abbott LF, Regehr WG (2004) Synaptic computation. Nature 431:796–803

Amagai S (1998) Time coding in the midbrain of mormyrid electric fish. II. Stimulus selectivity in the nucleus exterolateralis pars posterior. J Comp Physiol A 182:131–143

Arnegard ME, Jackson BS, Hopkins CD (2006) Time-domain signal divergence and discrimination without receptor modification in sympatric morphs of electric fishes. J Exp Biol 209:2182–2198. https://doi.org/10.1242/jeb.02239

Ashida G, Carr CE (2011) Sound localization: Jeffress and beyond. Curr Opin Neurobiol 21:745–751. https://doi.org/10.1016/j.conb.2011.05.008

Baker CA, Carlson BA (2014) Short-term depression, temporal summation, and onset inhibition shape interval tuning in midbrain neurons. J Neurosci 34:14272–14287. https://doi.org/10.1523/JNEUROSCI.2299-14.2014

Baker CA, Kohashi T, Lyons-Warren AM, Ma X, Carlson BA (2013) Multiplexed temporal coding of electric communication signals in mormyrid fishes. J Exp Biol 216:2365–2379. https://doi.org/10.1242/jeb.082289

Baker CA, Huck KR, Carlson BA (2015) Peripheral sensory coding through oscillatory synchrony in weakly electric fish. elife 4:e08163. https://doi.org/10.7554/eLife.08163

Baker CA, Ma L, Casareale CR, Carlson BA (2016) Behavioral and single-neuron sensitivity to millisecond variations in temporally patterned communication signals. J Neurosci 36:8985–9000. https://doi.org/10.1523/JNEUROSCI.0648-16.2016

Barman HK et al (2017) Gene editing tools: state-of-the-art and the road ahead for the model and non-model fishes. Transgenic Res 26(5):577–589. https://doi.org/10.1007/s11248-017-0030-5
Bell CC, Grant K (1989) Corollary discharge inhibition and preservation of temporal information in a sensory nucleus of mormyrid electric fish. J Neurosci 9:1029–1044
Bennett MV (1965) Electroreceptors in mormyrids. Cold Spring Harb Symp Quant Biol 30:245–262
Buonomano DV (2000) Decoding temporal information: a model based on short-term synaptic plasticity. J Neurosci 20:1129–1141
Carlson BA (2002) Electric signaling behavior and the mechanisms of electric organ discharge production in mormyrid fish. J Physiol Paris 96:405–419
Carlson BA (2006) A neuroethology of electrocommunication: senders, receivers, and everything in between. In: Ladich F, Collin SP, Moller P, Kapoor BG (eds) Communication in fishes, vol 2. Science Publishers, Enfield, pp 805–848
Carlson BA (2009) Temporal-pattern recognition by single neurons in a sensory pathway devoted to social communication. Behav J Neurosci 29:9417–9428
Carlson BA, Kawasaki M (2006) Stimulus selectivity is enhanced by voltage-dependent conductances in combination-sensitive neurons. J Neurophysiol 96:3362–3377
Carlson BA, Hasan SM, Hollmann M, Miller DB, Harmon LJ, Arnegard ME (2011) Brain evolution triggers increased diversification of electric fishes. Science 332:583–586. https://doi.org/10.1126/science.1201524
Carrillo-Reid L, Yang W, Kang Miller JE, Peterka DS, Yuste R (2017) Imaging and optically manipulating neuronal ensembles. Annu Rev Biophys 46:271–293. https://doi.org/10.1146/annurev-biophys-070816-033647
Ceasar SA, Rajan V, Prykhozhij SV, Berman JN, Ignacimuthu S (2016) Insert, remove or replace: a highly advanced genome editing system using CRISPR/Cas9. Biochim Biophys Acta 1863:2333–2344. https://doi.org/10.1016/j.bbamcr.2016.06.009
Edwards CJ, Rose GJ (2003) Interval-integration underlies amplitude modulation band-suppression selectivity in the anuran midbrain. J Comp Physiol A Neuroethol Sens Neural Behav Physiol 189:907–914. https://doi.org/10.1007/s00359-003-0467-2
Edwards CJ, Alder TB, Rose GJ (2002) Auditory midbrain neurons that count. Nat Neurosci 5:934–936. https://doi.org/10.1038/nn916
Edwards CJ, Leary CJ, Rose GJ (2007) Counting on inhibition and rate-dependent excitation in the auditory system. J Neurosci 27:13384–13392. https://doi.org/10.1523/JNEUROSCI.2816-07.2007
Edwards CJ, Leary CJ, Rose GJ (2008) Mechanisms of long-interval selectivity in midbrain auditory neurons: roles of excitation, inhibition, and plasticity. J Neurophysiol 100:3407–3416. https://doi.org/10.1152/jn.90921.2008
Ellis LD, Mehaffey WH, Harvey-Girard E, Turner RW, Maler L, Dunn RJ (2007) SK channels provide a novel mechanism for the control of frequency tuning in electrosensory neurons. J Neurosci 27:9491–9502. https://doi.org/10.1523/JNEUROSCI.1106-07.2007
Fortune ES, Rose GJ (1997) Passive and active membrane properties contribute to the temporal filtering properties of midbrain neurons in vivo. J Neurosci 17:3815–3825
Fortune ES, Rose GJ (2001) Short-term synaptic plasticity as a temporal filter. Trends Neurosci 24:381–385
Fortune ES, Rose GJ (2003) Voltage-gated Na+ channels enhance the temporal filtering properties of electrosensory neurons in the torus. J Neurophysiol 90:924–929
Friedman MA, Hopkins CD (1998) Neural substrates for species recognition in the time-coding electrosensory pathway of mormyrid electric fish. J Neurosci 18:1171–1185
George AA, Lyons-Warren AM, Ma X, Carlson BA (2011) A diversity of synaptic filters are created by temporal summation of excitation and inhibition. J Neurosci 31:14721–14734. https://doi.org/10.1523/JNEUROSCI.1424-11.2011
Goel A, Buonomano DV (2014) Timing as an intrinsic property of neural networks: evidence from in vivo and in vitro experiments. Philos T R Soc B 369. https://doi.org/10.1098/Rstb.2012.0460 doi: Artn 20120460

Golding NL (2012) Neuronal response properties and voltage-gated ion channels in the auditory system. In: Trussell LO, Fay RR, Popper AN (eds) Synaptic mechanisms in the auditory system, Springer handbook of auditory research, vol 41. Springer, New York, pp 7–41. https://doi.org/10.1007/978-1-4419-9517-9_2

Grienberger C, Konnerth A (2012) Imaging calcium in neurons. Neuron 73:862–885. https://doi.org/10.1016/j.neuron.2012.02.011

Grothe B (1994) Interaction of excitation and inhibition in processing of pure tone and amplitude-modulated stimuli in the medial superior olive of the mustached bat. J Neurophysiol 71:706–721

Harder W (1968) Die beziehungen zwischen electrorezeptoren, elektrischem organ, seitenlinien-organen und nervensystem bei den Mormyridae (Teleostei, Pisces). Z Vgl Physiol 59:272–318

Haugede-Carre F (1979) The mesencephalic exterolateral posterior nucleus of the mormyrid fish Bryenomyrus niger: efferent connections studied by the HRP method. Brain Res 178:179–184

Hopkins CD (1981) On the diversity of electric signals in a community of mormyrid electric fish in West-Africa. Am Zool 21:211–222

Hopkins CD (1986) Behavior of Mormyridae. In: Bullock TH, Heiligenberg W (eds) Elecroreception. Wiley, New York, pp 527–576

Hopkins CD (1999) Design features for electric communication. J Exp Biol 202:1217–1228

Hopkins CD, Bass AH (1981) Temporal coding of species recognition signals in an electric fish. Science 212:85–87

Huetz C, Gourevitch B, Edeline JM (2011) Neural codes in the thalamocortical auditory system: from artificial stimuli to communication sounds. Hear Res 271:147–158. https://doi.org/10.1016/j.heares.2010.01.010

Hutcheon B, Yarom Y (2000) Resonance, oscillation and the intrinsic frequency preferences of neurons. Trends Neurosci 23:216–222

Johnston D, Narayanan R (2008) Active dendrites: colorful wings of the mysterious butterflies. Trends Neurosci 31:309–316. https://doi.org/10.1016/j.tins.2008.03.004

Klyachko VA, Stevens CF (2006) Excitatory and feed-forward inhibitory hippocampal synapses work synergistically as an adaptive filter of natural spike trains. PLoS Biol 4:e207. https://doi.org/10.1371/journal.pbio.0040207

Knopfel T (2012) Genetically encoded optical indicators for the analysis of neuronal circuits. Nat Rev Neurosci 13:687–700. https://doi.org/10.1038/nrn3293

Kohashi T, Carlson BA (2014) A fast BK-type KCa current acts as a postsynaptic modulator of temporal selectivity for communication signals. Front Cell Neurosci 8:286. https://doi.org/10.3389/fncel.2014.00286

Kostarakos K, Hedwig B (2012) Calling song recognition in female crickets: temporal tuning of identified brain neurons matches behavior. J Neurosci 32:9601–9612. https://doi.org/10.1523/JNEUROSCI.1170-12.2012

Lin MZ, Schnitzer MJ (2016) Genetically encoded indicators of neuronal activity. Nat Neurosci 19:1142–1153. https://doi.org/10.1038/nn.4359

Lyons-Warren AM, Hollmann M, Carlson BA (2012) Sensory receptor diversity establishes a peripheral population code for stimulus duration at low intensities. J Exp Biol 215:2586–2600. https://doi.org/10.1242/jeb.064733

Lyons-Warren AM, Kohashi T, Mennerick S, Carlson BA (2013) Detection of submillisecond spike timing differences based on delay-line anticoincidence detection. J Neurophysiol 110:2295–2311. https://doi.org/10.1152/jn.00444.2013

Ma X, Kohashi T, Carlson BA (2013) Extensive excitatory network interactions shape temporal processing of communication signals in a model sensory system. J Neurophysiol 110:456–469. https://doi.org/10.1152/jn.00145.2013

Mehaffey WH, Ellis LD, Krahe R, Dunn RJ, Chacron MJ (2008) Ionic and neuromodulatory regulation of burst discharge controls frequency tuning. J Physiol Paris 102:195–208. https://doi.org/10.1016/j.jphysparis.2008.10.019

Moller P, Szabo T (1981) Lesions in the nucleus mesencephali exterolateralis effects on electrocommunication in the mormyrid fish Gnathonemus petersii (Mormyriformes). J Comp Physiol 144:327–333

Mugnaini E, Maler L (1987) Cytology and immunocytochemistry of the nucleus extrolateralis anterior of the mormyrid brain: possible role of GABAergic synapses in temporal analysis. Anat Embryol (Berl) 176:313–336

O'Donnell C, Nolan MF (2011) Tuning of synaptic responses: an organizing principle for optimization of neural circuits. Trends Neurosci 34:51–60. https://doi.org/10.1016/j.tins.2010.10.003

Pitchers WR, Constantinou SJ, Losilla M, Gallant JR (2016) Electric fish genomics: progress, prospects, and new tools for neuroethology. J Physiol Paris 110:259–272. https://doi.org/10.1016/j.jphysparis.2016.10.003

Pluta SR, Kawasaki M (2010) Temporal selectivity in midbrain electrosensory neurons identified by modal variation in active sensing. J Neurophysiol 104:498–507. https://doi.org/10.1152/jn.00731.2009

Ponnath A, Farris HE (2010) Calcium-dependent control of temporal processing in an auditory interneuron: a computational analysis. J Comp Physiol A Neuroethol Sens Neural Behav Physiol 196:613–628. https://doi.org/10.1007/s00359-010-0547-z

Rose GJ, Fortune ES (1999) Mechanisms for generating temporal filters in the electrosensory system. J Exp Biol 202:1281–1289

Rose GJ, Leary CJ, Edwards CJ (2011) Interval-counting neurons in the anuran auditory midbrain: factors underlying diversity of interval tuning. J Comp Physiol A 197:97–108

Sah P (1996) Ca(2+)-activated K+ currents in neurons: types, physiological roles and modulation. Trends Neurosci 19:150–154

Sah P, Faber ES (2002) Channels underlying neuronal calcium-activated potassium currents. Prog Neurobiol 66:345–353

Schoneich S, Kostarakos K, Hedwig B (2015) An auditory feature detection circuit for sound pattern recognition. Sci Adv 1:e1500325. https://doi.org/10.1126/sciadv.1500325

Szabo T, Ravaille M, Libouban S, Enger PS (1983) The mormyrid rhombencephalon: I. Light and EM investigations on the structure and connections of the lateral line lobe nucleus with HRP labelling. Brain Res 266:1–19

Trussell LO (1999) Synaptic mechanisms for coding timing in auditory neurons. Annu Rev Physiol 61:477–496

Velez A, Carlson BA (2016) Detection of transient synchrony across oscillating receptors by the central electrosensory system of mormyrid fish. elife 5:e16851. https://doi.org/10.7554/eLife.16851

von der Emde G (2006) Non-visual environmental imaging and object detection through active electrolocation in weakly electric fish. J Comp Physiol A Neuroethol Sens Neural Behav Physiol 192:601–612. https://doi.org/10.1007/s00359-006-0096-7

Wilkens LA, Hofmann MH (2005) Behavior of animals with passive low-frequency electrosensory systems. In: Bullock TH, Hopkins CD, Popper AN, Fay RR (eds) Electroreception. Springer, New York, pp 229–263

Xu-Friedman MA, Hopkins CD (1999) Central mechanisms of temporal analysis in the knollenorgan pathway of mormyrid electric fish. J Exp Biol 202:1311–1318

Yizhar O, Fenno LE, Davidson TJ, Mogri M, Deisseroth K (2011) Optogenetics in neural systems. Neuron 71:9–34. https://doi.org/10.1016/j.neuron.2011.06.004

Zipser B, Bennett MV (1976) Interaction of electrosensory and electromotor signals in lateral line lobe of a mormyrid fish. J Neurophysiol 39:713–721

Zucker RS, Regehr WG (2002) Short-term synaptic plasticity. Annu Rev Physiol 64:355–405. https://doi.org/10.1146/annurev.physiol.64.092501.114547

Chapter 16
Chemosensory Systems in the Sea Catfish, *Plotosus japonicus*

Takanori Ikenaga and Sadao Kiyohara

Abstract The gustatory system of the Japanese sea catfish *Plotosus japonicus* is highly developed. *P. japonicus* has four pairs of barbels around its mouth that act as gustatory organs, and taste buds are distributed along the entire length of the barbels. The density of taste buds in barbels is higher at the tip than proximally and is also higher in rostral areas than in caudal areas. Taste bud-rich regions on barbels are more likely to come into frequent contact with environmental substrates, so uneven distribution of the taste buds would seem to benefit effective food searching. The taste buds are also distributed in the fins and trunk. The taste buds contain disk-shaped serotonin-immunopositive cells in their basal regions. The function of these basal cells and the associated serotonin regarding taste information transduction is currently unknown.

Gustatory information is transmitted from taste buds to the brain via one of the three cranial nerves, including the facial, glossopharyngeal, and vagus nerves. The facial nerve innervates taste buds of body surface and the rostral-most region of the mouth, whereas the other two nerves innervate those of the posterior oropharyngeal region. The primary gustatory center in the medulla protrudes dorsally as a pair of longitudinal columns, of which their anterior and posterior regions are termed the facial and vagal lobes. The facial lobe has five distinct lobules, four of which receive topographical inputs from facial nerve fibers innervating corresponding barbels.

Nerve fibers innervating barbels respond to some amino acids, including betaine, glycine, L-alanine, and L-proline; betaine has been shown to elicit feeding behavior. In addition to amino acid responses, nerve fibers innervating barbels also respond to slight ($\leqq 0.1$) transient declines in the pH of ambient seawater. Behavioral experiments suggest that *P. japonicus* can detect cryptic prey due to minute pH declines in the surrounding seawater that result from an accumulation of respiratory by products.

Olfactory neurons also respond to several amino acids, including L-leucine and L-methionine, which may serve as feeding cues. The formation of schools is

T. Ikenaga (✉) · S. Kiyohara
Department of Chemistry and Bioscience, Graduate School of Science and Engineering, Kagoshima University, Kagoshima-shi, Kagoshima, Japan
e-mail: ikenaga@sci.kagoshima-u.ac.jp; k3495884@kadai.jp

H. Hirata, A. Iida (eds.), *Zebrafish, Medaka, and Other Small Fishes*,
https://doi.org/10.1007/978-981-13-1879-5_16

mediated by the olfactory sense as well, and recognition of schooling odor is governed by the mixing pattern of the specific phosphatidylcholine molecular species.

Keywords Catfish · Gustatory sense · Taste bud · Barbel · Innervation · Facial lobe · pH sensing · Olfactory sense

16.1 Introduction

Catfish (order Siluriformes) are a diverse group of actinopterygians, or ray-finned fish, that comprise one of the largest orders with over 2800 species (Nelson 2006). Most catfish are freshwater fish; only about 117 species from the families Ariidae and Plotosidae are found in the ocean. Marine eeltail sea catfish are popular around the main island of Japan (Honshu Island) and are widely used in many physiological, behavioral, and anatomical studies. This Japanese eeltail catfish has been given the names *Plotosus anguillaris* or *Plotosus lineatus* in previous research articles. Eeltail sea catfish identified as *Plotosus anguillaris* or *Plotosus lineatus* originally were described from the Indian Ocean near mainland India (Yoshino and Kishimoto 2008). Recently, Yoshino and Kishimoto (2008) identified the eeltail sea catfish that is distributed from Honshu Island to the Ryukyu Islands in Japan as *Plotosus japonicus* and as a separate species from *Plotosus lineatus*, which is widely distributed in the Indo-West-Pacific region, including north to the Ryukyu Islands.

Adult *P. japonicus* are benthic nocturnal feeders (Kasai et al. 2009). These fish use a unique ball-shaped schooling behavior that begins at approximately 4 days after hatching (Moriuchi and Dotsu 1973). It is believed that this school organization is composed of brood fish (Kinoshita 1975). Adult fish do not form a ball-shaped school but still swim in a small group size.

P. japonicus has a depressed head with large mouth and an elongated and compressed body with a tapered tail. Two to three narrow yellow longitudinal stripes run along the length of the body, and two of the three extend all the way to the head (Fig. 16.1; Yoshino and Kishimoto 2008). This fish has a pair of pectoral fins and a single dorsal fin containing a sharp spine that is serrated with fine teeth on both edges. The caudal fin shows a lanceolate shape, extending rostrally in both dorsal and ventral sides, where it fuses with the anal fin, forming a continuous medial confluent fin. The body surface is covered with mucus and is without scales, except for a row of minute tubular scales that are embedded under the skin (Yoshino and Kishimoto 2008). *P. lineatus* also shows a similar morphology, so that these two species closely resemble; however, they can be distinguished because *P. japonicus* has fewer anal-fin rays, fewer dorsal procurrent caudal-fin rays, fewer total rays in the confluent median fin, fewer gill rakers, and fewer free vertebrae (Yoshino and Kishimoto 2008).

P. japonicus has four pairs of barbels around its mouth, as seen in other catfish species, such as the channel catfish (Fig. 16.1). As discussed later, these barbels function as a sensory organ, particularly for gustation. Since *P. japonicus* also has a sensitive olfactory system, this fish has been used for many studies regarding its

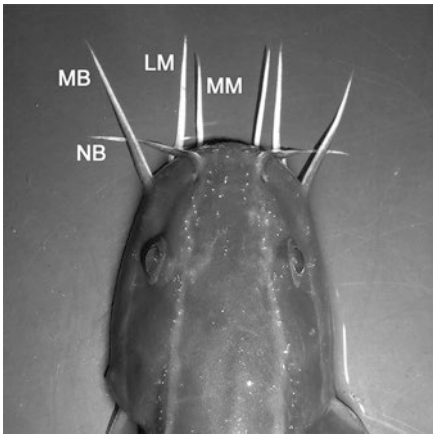

Fig. 16.1 Dorsal view of the head of *P. japonicus* showing the distribution of four pairs of barbels. *LM* lateral mandibular barbel, *MB* maxillary barbel, *MM* medial mandibular barbel, *NB* nasal barbel

chemical senses. In this chapter, we review the mechanisms of the gustatory and olfactory senses of *P. japonicus*, including its peripheral and central anatomy, physiology, and behavior.

16.2 Distribution of Taste Buds and Their Innervation

Taste buds, the sensory end organs for the gustatory sense, have been identified in all vertebrates except hagfishes, the most ancestral species of vertebrates (Northcutt 2004; Barreiro-Iglesias et al. 2008). Catfish have many taste buds, not only on the barbels and the mouth cavity but also across the entire body surface, from the lips to caudal fin (Atema 1971; Northcutt 2005). *P. japonicus* also has taste buds in many of its organs, a phenomenon seen in other types of catfish as well.

16.2.1 Barbel

P. japonicus has four pairs of barbels that are all roughly the same in length and structure (Kiyohara et al. 1996). They are referred to as the nasal, maxillary, lateral mandibular, and medial mandibular barbels (Sato 1937, Fig. 16.1). These barbels cannot be moved by the fish actively and are usually maintained passively extending forward during swimming, as they have no intrinsic musculature (Sakata et al. 2001). Taste buds are distributed throughout the epidermis of the barbels along their entire length and density, with higher concentrations in distal areas than in proximal areas (Sakata et al. 2001). The surface of the barbels is subdivided into three longitudinal parts, defined as the rostral, intermediate or lateral, and caudal regions. The rostral surface of each barbel faces the lips when the barbel is extended anteriorly away from the animal. The density of taste buds is higher in this rostral region and

moderately high in the caudal region, while the intermediate portion of a barbel has the lowest density of taste buds (Fig. 16.2a, b; Sakata et al. 2001). The taste bud-rich regions of the barbels are more likely to come into frequent contact with environmental substrates, including foods, so the uneven distribution of taste buds would seem to be beneficial for effective food searching.

The taste buds on barbels are innervated by peripheral rami, containing both the trigeminal and facial nerve fibers (Kiyohara et al. 1996). The ramus enters from the caudal region of each barbel at its base and sends many nerve bundles to the rostral side as it runs toward the barbel tip (Sakata et al. 2001). Distribution of these fibers was examined by a tract-tracing experiment with DiI (Sakata et al. 2001) and immunofluorescence with an anti-acetylated tubulin antibody (Nakamura et al. 2017). In both cases, the labeled nerve fibers within the bundles could be followed along the entire length of the barbel. These fibers form networks under the epidermis in a polygonal shape where the taste buds are distributed (Fig. 16.2c). Fascicles of these

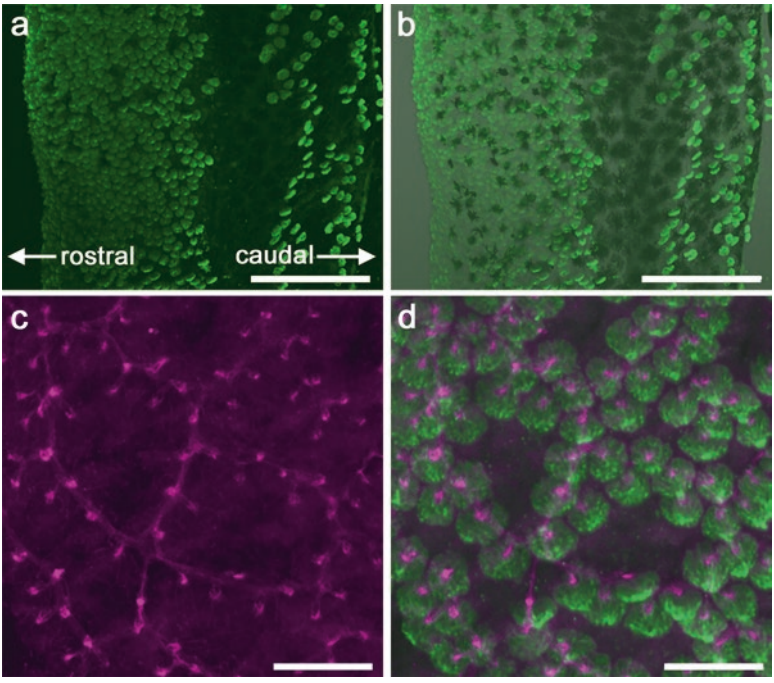

Fig. 16.2 Confocal microscopic images of the taste buds and nerve fibers in barbels, labeled by immunofluorescence. (**a**) Surface view of small area of the barbel with calretinin-immunoreactive taste buds (green). Left is rostral and right is caudal. (**b**) Merged image combining (**a**) with transmitted light. Note that more taste buds are distributed in the rostral area than caudal area. (**c**, **d**) Images showing the distribution of the neural fibers labeled with an anti-acetylated tubulin antibody (magenta, **c**) and its correlation with calretinin-immunoreactive taste buds (green, **d**). Swellings of acetylated tubulin-immunoreactive nerve terminals show bright signals, and all of them associate with taste buds. Scale bar, 500 μm (**a**, **b**), 100 μm (**c**, **d**). (Modified from Nakamura et al. 2017)

nerve fibers originate from the network extending toward the surface where they terminate as bushy swellings within the basal regions of the taste buds (Fig. 16.2d). Some single fibers or thin fiber bundles emerge from the networks and are distributed as extragemmal fibers that are not associated with the taste buds. The networks are most abundant in the rostral surfaces, moderate in the caudal surfaces, and sparse in the intermediate surfaces of the barbels, corresponding to the density of taste buds (Sakata et al. 2001).

16.2.2 Oral and Branchial Cavity

The surface morphologies of the upper oral cavity and branchial cavity of *P. japonicus* are different. The surface of the dorsal oral cavity is relatively smooth, while that of dorsal branchial cavity contains numerous bulges, similar to the palatal organ of goldfish and carp (cyprinid fish). The distribution and density of taste buds are different between these two cavities. The taste buds in the lateral region of oral cavity are aligned along the anterior-posterior axis (Fig. 16.3a). In contrast, taste bud distribution is more sparse in the medial region of the oral cavity. In the lateral region of the oral cavity, large nerve bundles are aligned under taste buds where they branch into 1–3 thinner fascicles (Fig. 16.3b). These fascicles then turn toward the surface and terminated within the taste buds (Fig. 16.3c). Free-nerve endings in the surrounding epithelium are distributed throughout the oral cavity. In the branchial cavity, some taste buds are localized on each epithelial bulge (Fig. 16.3d). The nerve bundles enter from the base of these bulges and ramify superficially into 2–3 separate branches, each with finely ramified tips (Fig. 16.3e). The taste buds are always situated at these ramified tips of nerve fascicles (Fig. 16.3f), meaning that each taste bud group on a single bulge is innervated by nerve strands that originate from a single large nerve bundle. This suggests that the taste bud cluster on each bulge forms a functional unit and a gustatory two-point discrimination threshold would be determined by the distance between neighboring bulges in the branchial cavity. Thinner nerve strands with free-nerve ending-like structures are also distributed in the bulges (Fig. 16.3f).

16.2.3 Fins and Trunk

In addition to the barbels and orobranchial cavity, typical gustatory organs, *P. japonicus* also possesses taste buds throughout the epithelium of the entire body, including the fins and trunk. Taste buds are aligned between fin rays of the pectoral, dorsal, and caudal fins (arrowheads in Fig. 16.4a, b, e, f). The density of taste buds is highest at the edges of these fins compared to other regions of them (arrows in Fig. 16.4a, b, e, f) because contact with food sources would be greater at these edges, similar to what has been observed with the barbels. Therefore, these patterns

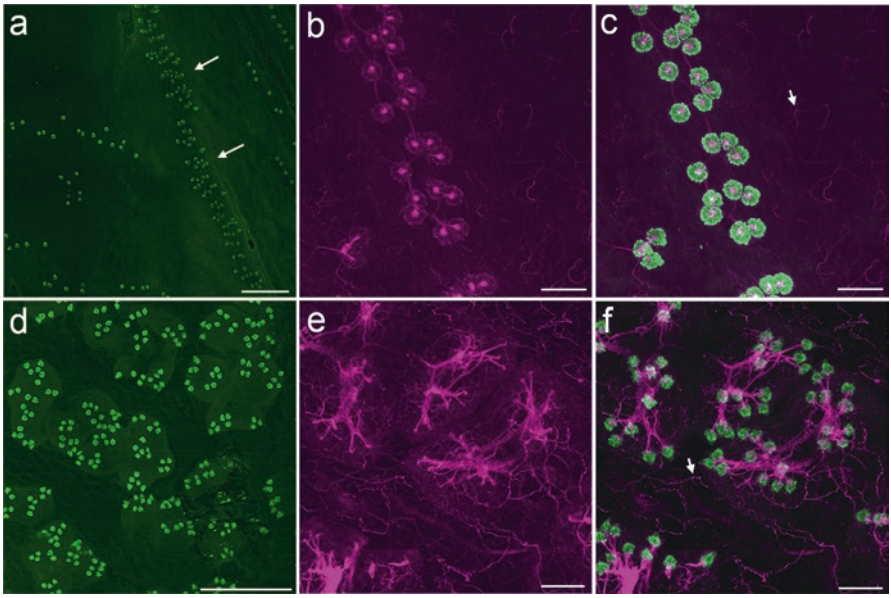

Fig. 16.3 Distribution of the taste buds and nerve fibers in the upper surface of the oral and branchial cavities. (**a**, **d**) Confocal microscopic images of the calretinin-immunoreactive taste buds (green) in oral cavity (**a**) and branchial cavity (**d**). White arrows in (**a**) indicate taste buds distributed longitudinally in the lateral region of the oral cavity. In the branchial cavity, clusters of some taste buds are situated on each epithelial bulge. Top, rostral; bottom, caudal; left, medial; right, lateral. (**b**, **c**, **e**, **f**) Confocal microscopic images showing neural innervation of taste buds in the oral cavity (**b**, **c**) and branchial cavity (**e**, **f**). (**b**, **e**) Images of the acetylated tubulin-immunopositive nerve fibers (magenta). (**c**, **f**) Images simultaneously showing nerve fibers in (**b** and **e**) and calretinin-immunoreactive taste buds (green), respectively. White arrows indicate examples of free-nerve ending-like structures. Scale bar, 500 μm (**a**, **d**), 100 μm (**b**, **c**), 200 μm (**e**, **f**). (Modified from Nakamura et al. 2017)

of distribution of the taste buds in the fins are also an adaptation for effective food-exploring behavior. In the pectoral fins, fiber bundles run parallel to the fin rays (Fig. 16.4a, b). Branches emerge from these fiber bundles to terminate near the surface with fine densely branched tufts. These tufts are located in the basal regions of the taste buds (Fig. 16.4c, d). In the dorsal and caudal fins, larger fiber bundles also run along the axis of the fin rays with short nerve strands branching from them. Tufted swellings are observed on the tips of these strands, where the taste buds are distributed. This distribution pattern of nerve fibers suggests that the aligned taste buds within the fins work as a functional unit.

In the trunk region, the taste buds are distributed without any regularity (Fig. 16.4i, j). Nerve fibers are observed in broad areas of the trunk region (Fig. 16.4k), including larger fiber bundles with terminal tufts with taste buds (Fig. 16.4l).

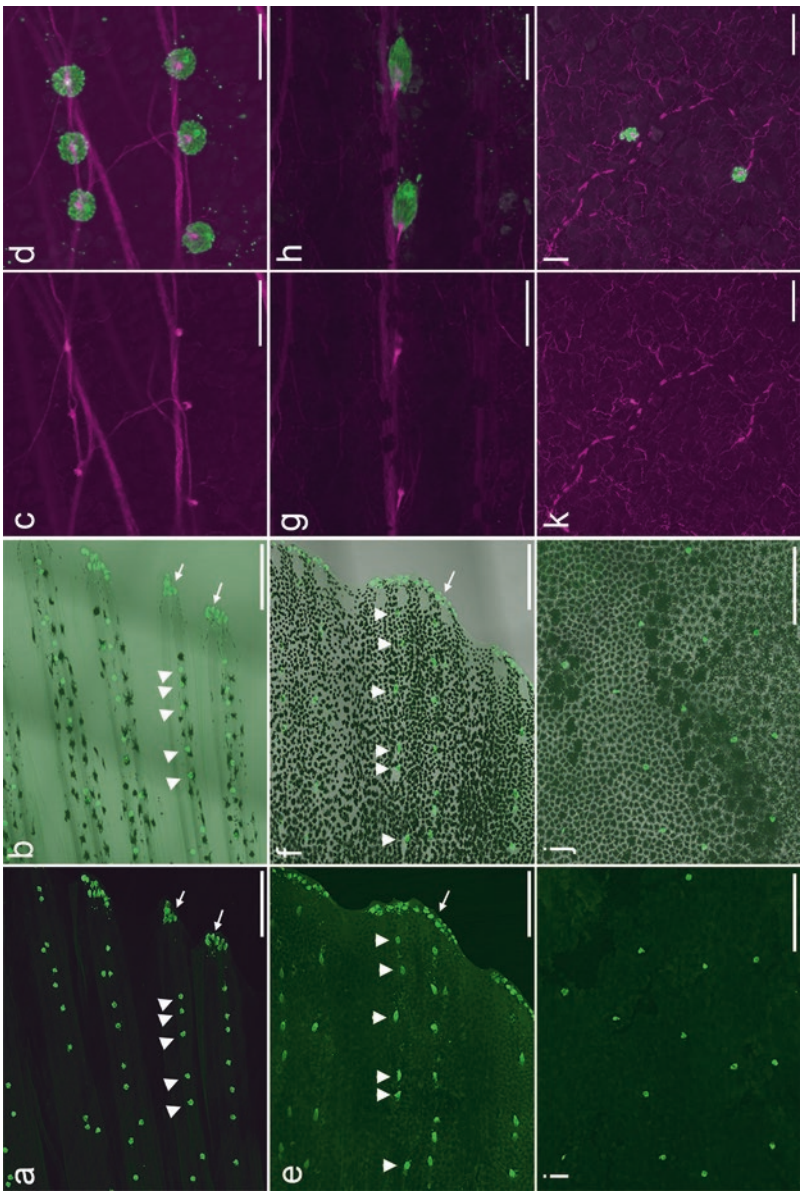

Fig. 16.4 Images of confocal microscopy showing the distribution of taste buds and neural fibers and their relations in the fins (**a–d**, pectoral fin; **e–h**, caudal fin) and trunk (**i–l**). (**a**, **e**, **i**). Single-channel confocal images of calretinin-immunoreactive taste buds (green). (**b**, **f**, **j**) Images combining fluorescent signals from (**a**, **e**, and **i**) with bright-field images. (**c**, **g**, **k**) Images of acetylated tubulin-immunoreactive nerve fibers (magenta). (**d**, **h**, **l**) Merged images of nerve fibers in (**c**, **g**, and **k**) with calretinin-immunoreactive taste buds (green), respectively. White arrowheads in (**a**, **b**, **e**, and **f**) indicate how taste buds are distributed parallel to the long axis of the fin rays. White arrows in (**a**, **b**, **e**, and **f**) indicate taste buds on the fin edge, and note that the density of taste buds is high at edges of the fins. Scale bar, 500 μm (**a**, **b**, **e**, **f**, **i**, **j**), 100 μm (**c**, **d**, **g**, **h**, **k**, **l**). (Modified from Nakamura et al. 2017)

16.3 The Structure and Synaptic Transmission of Taste Buds

Teleost fish, including *Plotosus*, have taste buds that are pear-shaped and organized from clusters of elongated cells that include supporting cells and gustatory cells. The supporting cells, or dark cells, have many small microvilli on their apex, while the gustatory cells, or light cells, have only one thick microvillus extending in the "taste pore" (Jakubowski and Whitear 1990; Reutter 1992; Reutter and Witt 1993; Hansen et al. 2002;). In addition to these elongated cells, disk-shaped cells lie along the basal regions of taste buds in teleost fish, and these cells are referred as basal cells (Toyoshima et al. 1984; Jakubowski and Whitear 1990; Reutter and Witt 1993). In mammals, immature cells are located in the basal regions of taste buds and are termed "basal cells" (Miura et al. 2014), but these are distinct from basal cells in teleosts. Teleostean basal cells are also referred as Merkel-like cells according to their morphology (Zachar and Jonz 2012). Antibody against serotonin labels basal cells in some teleost fish (Varatharasan et al. 2009; Zachar and Jonz 2012; Kirino et al. 2013). Recently, our study using a whole-mount immunofluorescence technique revealed that serotonin-immunopositive cells are distributed widely on the barbels of *P. japonicus* (Fig. 16.5a, b) and are associated with all taste buds (Fig. 16.5d, Nakamura et al. 2017). The shape of these cells from a surface view is irregular, being roundish but with some concavities (Fig. 16.5c). Each taste bud in the barbels contains only a single serotonin-immunoreactive cell (Fig. 16.5c). In the lateral view, the serotonin-immunopositive cells have an oval shape and are located in the basal portion of the taste buds (Fig. 16.5e, f).

Other parts of *P. japonicus*, including the oral and branchial cavities, pectoral fin, dorsal fin, caudal fin, and trunk, similarly contain serotonin-immunopositive basal cells in their taste buds. Figure 16.6a and c are representative images showing that taste buds and serotonin-immunopositive cells are colocalized in the oral and branchial cavities. The morphology of these serotonin-immunoreactive basal cells from a surface view is slightly different between organs. Serotonin-immunopositive cells of the oral and branchial cavities show similar morphologies to those in barbels, including irregular circumferences with multiple concavities (Fig. 16.6b, d). In the fins, the concavities are smaller, so the circumferences are smoother, compared with the above organs (Fig. 16.6e). Serotonin-immunopositive basal cells of the trunk region do not show significant concavities, so their morphology is nearly round (Fig. 16.6f). Except for the branchial cavity and trunk, all taste buds contain only a single serotonin-immunoreactive cell. Some taste buds in the branchial cavity have been observed with two serotonin-immunoreactive cells (Fig. 16.6d), while no serotonin-immunoreactive cells are seen in 20% of the taste buds in the trunk region (Nakamura et al. 2017).

An electron microscopic study showed that the basal cells in teleosts contain several vesicles (Toyoshima et al. 1984), suggesting that basal cells release serotonin as a neurotransmitter. This is also true for the basal cells in *Plotosus* (Reutter 1992). In amphibians, it has been suggested that Merkel-like basal cells release serotonin and modulate the responses of taste cells (Delay et al. 1997). In larval

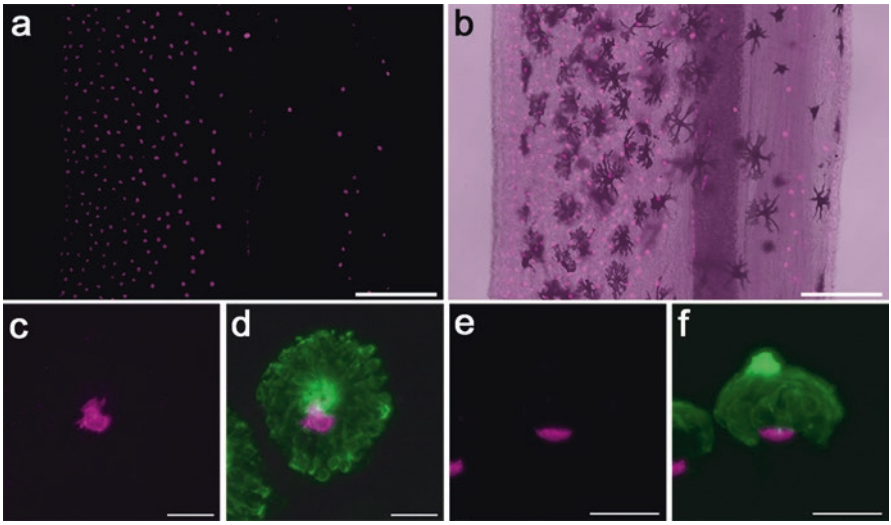

Fig. 16.5 Confocal microscopic images showing the distribution of serotonin-immunoreactive cells in the taste buds of the barbels. (**a**) Lower magnification image of serotonin-immunoreactive cells on the surface of barbel (magenta). (**b**) Image combining fluorescent signals in (**a**) and a bright-field image. Left is rostral and right is caudal. The density of serotonin-immunoreactive cells is higher at rostral. (**c**) Higher magnification image of the surface view of a serotonin-immunoreactive cell in a barbel. (**d**) Merged image of the surface view of calretinin-immunopositive taste bud (green) with (**c**). (**e**, **f**) Lateral view of a serotonin-immunoreactive cell from a histological section of a barbel. (**f**) is a merged image with (**e**) and a calretinin-immunopositive taste bud. Upper is surface of the barbel. Scale bar, 200 μm (**a**, **b**), 20 μm (**c–f**). (Modified from Nakamura et al. 2017)

zebrafish, serotonergic cells work to direct and maintain taste receptor cells during taste bud formation (Soulika et al. 2016); however, in adult teleost fish, the roles of basal cells and released serotonin in signal transduction remain unknown.

While serotonin-immunoreactive basal cells have been reported in teleostean and amphibian taste buds (Barlow et al. 1996; Zachar and Jonz 2012; Kirino et al. 2013), these types of cells have never been described in mammals; however, another class of serotonin-immunoreactive cells exists. Mammalian serotonin-immunoreactive cells are elongate taste cells, known as Type III cells, that form conventional synapses with the afferent nerves (Yee et al. 2001). Mammalian "basal cells" are immature, non-serotonergic cells situated in the basal region of the taste buds (Miura et al. 2014). Thus far, the existence of serotonin-immunoreactive cells in avian and reptilian taste buds is unknown. Among anamniote vertebrates, lampreys have no serotonin-immunopositive basal cells in their taste buds; however, elongated ciliated cells in lampreys show serotonin immunoreactivity, more similar to the mammalian situation (Barreiro-Iglesias et al. 2008). An electron microscopic study of elasmobranchs indicates the existence of basal cells in taste buds (Whitear and Moate 1994), but there have been no studies of serotonin immunohistochemistry for cartilaginous fishes. There is also no information available regarding

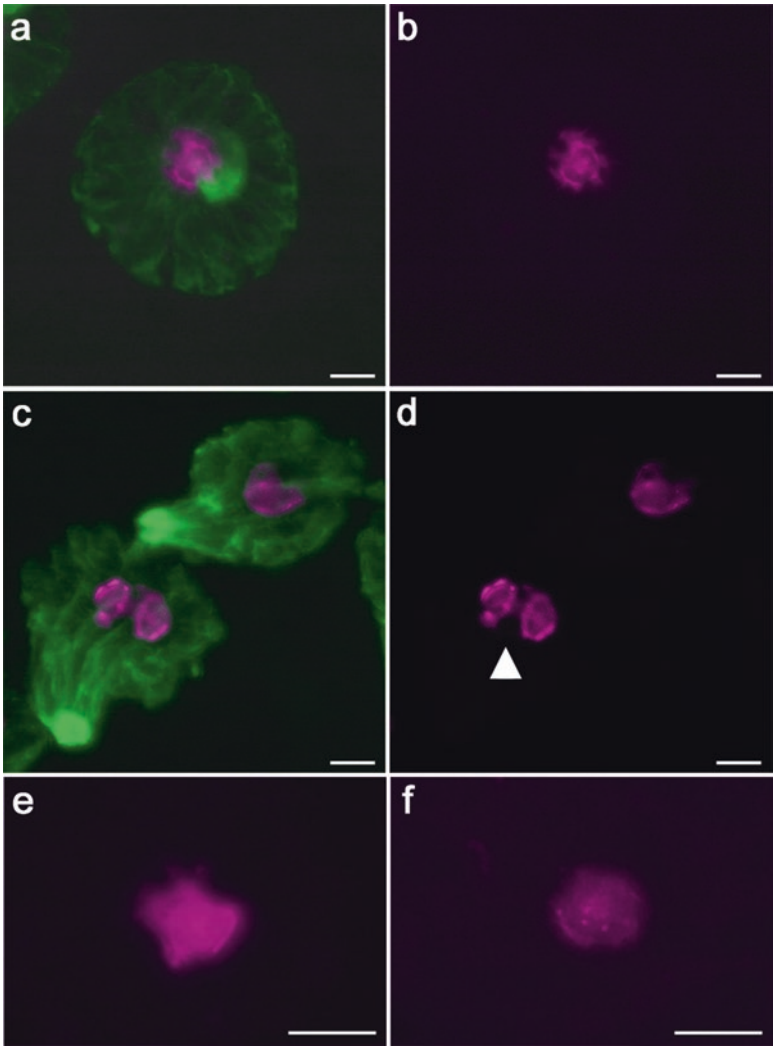

Fig. 16.6 Confocal microscopic pictures showing serotonin-immunoreactive cells in multiple organs. (**a**, **c**) A merged image of the surface view of calretinin-immunoreactive taste buds (green) and serotonin-immunoreactive cells (magenta) in the oral (**a**) and branchial cavities (**c**). (**b**, **d**) A single-channel image of the serotonin-immunoreactive cells in the same surface view as (**a** and **c**), respectively. The arrowhead in (**d**) indicates two serotonin-immunoreactive cells in a single taste bud. (**e**, **f**) Surface view of serotonin-ir cells in the pectoral fin (**e**) and trunk (**f**). Scale bar, 10 μm. (Modified from Nakamura et al. 2017)

serotonin-immunoreactive cells and basal cells in the taste buds of ancestral ray-finned fishes, including sturgeons and bichirs. Analysis of serotonin-immunoreactive cells in the taste buds of these taxa is necessary for understanding the diversity and origin of serotonergic taste bud basal cells in anamniotes.

Unlike olfactory receptor cells, vertebrate taste bud receptor cells have no axons and make synaptic connections with gustatory nerves via chemical neurotransmitters. It has been suggested that Type II receptor cells utilize ATP as a neurotransmitter in mammalian taste buds (Finger et al. 2005). An enzyme histochemical study to reveal ecto-ATPase activity in *P. japonicus* showed that synaptic transmission from the gustatory cells to the sensory nerves also is mediated by ATP (Kirino et al. 2013), as occurs in mammals (Finger et al. 2005).

16.4 Gustatory Sensory Nerves

The gustatory information detected by taste buds is transmitted to the medulla via one of the three gustatory nerves: the facial (VII), glossopharyngeal (IX), or vagus (X) nerves (Finger 1983). Peripheral distribution of the primary gustatory nerve terminals indicates specific topographical organization. The facial nerve innervates taste buds of the rostral area of the mouth and body surface, while the glossopharyngeal and vagus nerves innervate the branchial cavity and pharynx in a rostro-caudal manner (Finger 1997a). The cell bodies of these primary gustatory neurons are located in the peripheral ganglia of these cranial nerves.

As mentioned above, the facial nerve innervates taste buds in extra-oral regions, including the barbels, fins, and trunk, and it is separated into eight rami: superficial ophthalmic, palatine, upper lip, lower lip, maxillary barbel, mandibular barbel, hyomandibular, and recurrent (Fig. 16.7a). Six of the rami, not including palatine and recurrent, contain both the trigeminal and facial nerves and emerge from the anterior ganglion (Fig. 16.7b). This ganglion contains cell bodies of the trigeminal, facial, and lateral line neurons. The facial nerve innervating taste buds of the fins and trunk organizes the recurrent ramus. The ganglion of this ramus is known as the recurrent ganglion and is independent from the anterior ganglion (Fig. 16.7b). Sensory neurons of the recurrent ganglion show a typical bipolar morphology, where a thick process emerges from the caudal pole and a thin process emerges from the rostral pole of the cell bodies of recurrent facial neurons (Fig. 16.7c). Except for their initial segments, both types of processes are myelinated (Denil et al. 2013). The recurrent ramus has two major branches: the trunk branches to innervate taste buds along the whole trunk surface and the pectoral fin branches to innervate taste buds across the pectoral fin (Fig. 16.7a). When two neural tracers with different fluorescent dyes were applied simultaneously to the central stump of these two recurrent branches, retrograde-labeled cell bodies with different colors in the recurrent ganglion were not distributed into distinct topographical populations, meaning that no somatotopical organization was evident in this ganglion (Denil et al. 2013).

The glossopharyngeal and vagus nerves provide innervation for taste buds in the oropharyngeal region. In channel catfish, the glossopharyngeal nerve projects to the first gill arch and to the floor of the oral cavity (Kanwal and Caprio 1987). The vagus nerve innervates the second, third, and fourth gill arches and corresponding

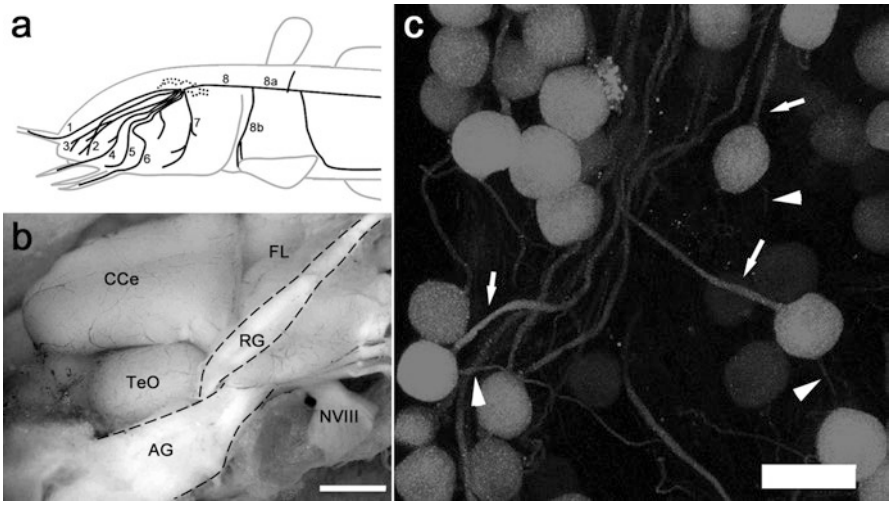

Fig. 16.7 (**a**) Lateral view of *P. japonicus* illustrating the distribution of facial lami. 1, superficial ophthalmic; 2, palatine; 3, upper lip; 4, maxillary barbel; 5, lower lip; 6, mandibular barbel; 7, hyomandibular; 8, whole recurrent; 8a, trunk recurrent; 8b, pectoral fin recurrent. (**b**) Enlarged photograph of dorsolateral view of the brain around the optic tectum (TeO), corpus cerebelli, (CCe), and facial lobe (FL) and showing the position of the anterior ganglion (AG) and the recurrent facial ganglion (RG). AG and RG are encircled with dotted lines. Left, rostral; right, caudal. NVIII, octaval nerve. (**c**) Neurons in the recurrent ganglion labeled by rhodamine-conjugated dextran amine. Arrows indicate thick peripheral fibers, and arrowheads indicate thin central fibers. Scale bar, 1 mm (**b**), 40 μm (**c**). (Modified from Denil et al. 2013)

portions of the oral cavity. Separated branches of the vagus nerve also innervate the palatal organ, the roof structure of the pharyngeal region. Posterior branches turn caudally to innervate visceral organs (Kanwal and Caprio 1987). Similar innervation patterns of the glossopharyngeal and vagus nerves can be seen in *P. japonicus* by anatomical observation.

16.5 Primary Gustatory Center

The three primary gustatory sensory nerves (facial, glossopharyngeal, and vagus) project to a pair of visceral sensory columns in the medulla in all vertebrates, including teleost fish (Finger 1983). In some teleost fish, including catfish and carp, the primary gustatory center extraordinarily protrudes dorsally and shows very distinct structure in the dorsal medulla. These large primary sensory centers for the facial and vagus nerves are known as the facial lobe and the vagal lobe, respectively. Some catfish species, including *P. japonicus*, possess both the facial and vagal lobes (Finger 1978; Kanwal and Caprio 1987; Hayama and Caprio 1989; Kiyohara et al. 1996; Fig. 16.8a). The facial lobe is larger than the vagal lobe in the catfish to reflect

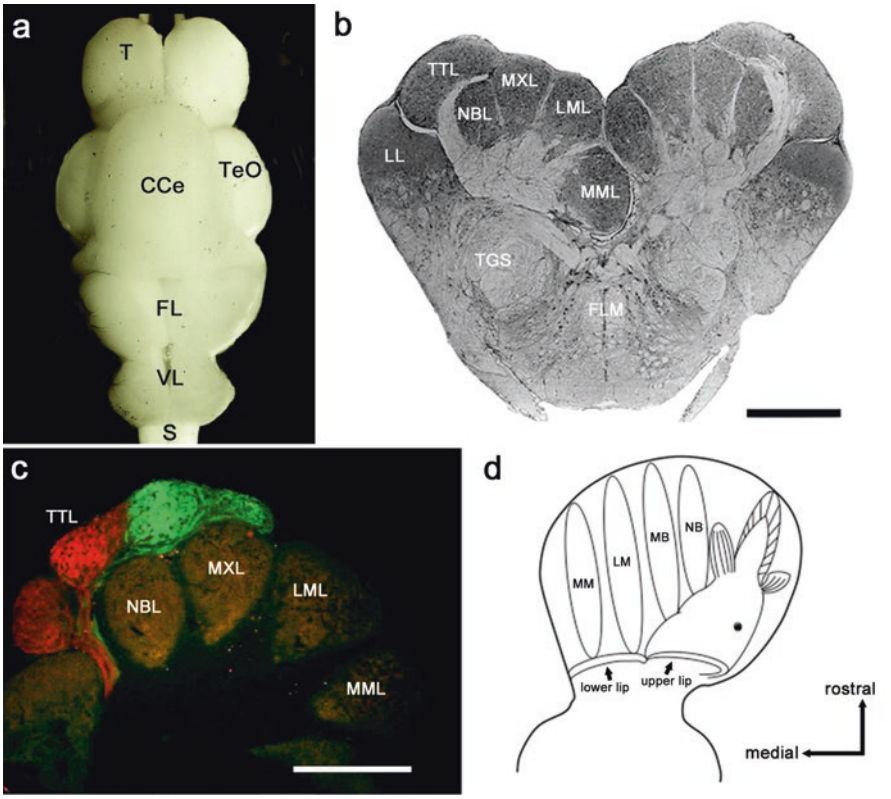

Fig. 16.8 (**a**) Dorsal view of the isolated brain of *P. japonicus*. Arrow indicates approximate level of the transverse section of facial lobe (FL) shown in (**b**). Top is rostral and bottom is caudal. Huge facial lobe is located in the caudal portion of the brain. The vagal lobe (VL) is situated in just caudal to the facial lobe. CCe, corpus cerebelli; S, spinal cord; T, telencephalon; TeO, optic tectum. (**b**) Image of a transverse section of the facial lobe. Facial lobe has five lobes: the medial mandibular barbel lobule (MML), the lateral mandibular barbel lobule (LML), the maxillary barbel lobule (MXL), the nasal barbel lobule (NBL), and the trunk-tail lobule (TTL). *FLM* medial longitudinal fascicule, *LL* lateral-line lobe, *TGS* ascending secondary gustatory tract. (**c**) Transverse section showing topographic projections of neural fibers of the trunk (red) and pectoral-fin branch (green) in the right TTL. Left is lateral and right is medial. (**d**) Schematic representation of the somatotopic map in the facial lobe. Top, rostral; bottom, caudal; left, medial; right, lateral. Scale bar, 1 mm (**b**), 500 μm (**c**). (**a–c**: Modified from Denil et al. 2013)

the morphological and functional significance of the facial gustatory system in the external peripheral organs including barbels. In contrast, goldfish and related carp have more hypertrophied vagal lobes. During feeding, these fish first scoop up materials, both food and mud, from the bottom substrates, which are transported to the oropharyngeal region and sorted there with the palatal organ and gill arches. Acceptable food particles are transferred toward the chewing organ for swallowing. Nonfood particles are ejected from the mouth. There are numerous taste buds around the palatal organ and gill arches that are innervated by the vagus nerve

(Lamb and Finger 1995; Finger 1997a). Reflecting the functional significance of oropharyngeal food-sorting behavior, the palatal organ and vagal lobe are well developed in goldfish and related carp. The vagal lobe of these fish has a complex laminated structure (Finger 1997a; Ikenaga et al. 2009).

The facial lobe of *P. japonicus* has five distinct lobules that are separated by fascicles of nerve fibers (Fig. 16.8b): the medial mandibular barbel lobule (MML), the lateral mandibular barbel lobule (LML), the maxillary barbel lobule (MXL), the nasal barbel lobule (NBL), and the trunk-tail lobule (TTL). These lobules are named based on both histological and electrophysiological evidences for topographical projections of nerve fibers from each barbel or other body surface. For example, when neural tracer is applied to one of the four barbel rami (Fig. 16.7a), the single corresponding barbel lobule is labeled (Kiyohara et al. 1996). Sensory fibers of the facial nerve enter the facial lobe from the rostral portion; therefore, labeled fibers of individual barbel rami are observed from the rostral tip of each barbel lobule to the caudal end, where the lobules become obscure. These barbel lobules extend rostrocaudally and occupy approximately the anterior two-thirds of the facial lobe (Kiyohara et al. 1996). Electrophysiological experiments indicate that the neurons in each barbel lobule respond to stimulation by corresponding barbels, and the proximal-distal axis of each lobule is represented in the posterior-anterior axis of each lobule (Marui et al. 1988). Another sea catfish, *Arius felis*, has three pairs of barbels with different lengths. Neural tracer application to the nerves of each barbel labeled fibers and terminals somatotopically in three distinct lobules (Kiyohara and Caprio 1996). In the channel catfish, *Ictalurus punctatus*, the facial lobe has four barbel lobules, each of which receives input from one of the four barbels, and the proximal-distal axis of each barbel is also represented in the posterior-anterior axis of the lobules (Hayama and Caprio 1989). The lengths of the four barbel lobules in *P. japonicus* are approximately equivalent, reflecting that the lengths of the four barbels are also nearly the same (Kiyohara et al. 1996). In *Ictalurus punctatus* and *Arius felis*, the lengths of the barbel lobules differ, correlating to the differences in the lengths of the barbels (Hayama and Caprio 1989; Kiyohara and Caprio 1996).

The terminal field of the recurrent ramus is distributed in the TTL (Denil et al. 2013). In contrast to the organization of the sensory ganglion, the trunk and pectoral fins in *P. japonicus* are represented separately in the TTL. For instance, simultaneous application of two different fluorescent dyes to the trunk and pectoral fin branches of the recurrent ramus shows that the fibers of the trunk branch are distributed in rostral and lateral regions of TTL and those of the pectoral-fin branch are distributed in the caudal and medial regions (Fig. 16.8c). Similar topography of TTL is observed in other catfish species as well (Hayama and Caprio 1989; Kiyohara and Caprio 1996). Branches of the facial nerve innervating taste buds in the upper lip and lower lip also project topographically to the most posterior areas of the facial lobe. This topographical representation of the facial lobe is shown in Fig. 16.8d.

As shown in Fig. 16.8a, the vagal lobe of *P. japonicus* is located caudally to the facial lobe. In contrast to the facial lobe, the vagal lobe has no obvious lobules. Both the glossopharyngeal and vagus nerves project to the vagal lobe. In channel catfish, *Ictalurus punctatus*, the sensory fibers of the glossopharyngeal nerve enter the

brainstem separately from the vagus nerve, and some of the fibers terminate in the anterior region of the ipsilateral vagal lobe (Kanwal and Caprio 1987). In addition, extra fibers project to the ipsilateral intermedius nucleus of facial and vagal lobes. These nuclei are situated ventrally to the facial and vagal lobes, respectively, along the fourth ventricle. The vagus nerve also may project to the brain stem, and branches of them innervating the gill arches and palatal organ terminate into the ipsilateral vagal lobe. Furthermore, terminals of the posterior branch of the vagus nerve innervating visceral organs may be distributed ipsilaterally in the nucleus intermedius of vagal lobe and bilaterally in the general visceral nucleus (Kanwal and Caprio 1987).

16.6 Chemosensation by the Gustatory System

The teleost fish uses multiple sensory systems, including vision, audition, mechanoreception, lateral line, electroreception, olfaction, and gustation, to locate and detect appropriate prey. As described above, large numbers of taste buds are distributed not only in the orobranchial cavity but also in extra-oral regions in *P. japonicus*; therefore, *P. japonicus* could detect and locate the prey using its gustatory senses. In behavioral experiments, *P. japonicus* spent more time in a partition of the aquarium containing a U tube that emanated a 10^{-6}–10^{-3} M betaine solution than when control seawater was released. *P. japonicus* often bit the tube, releasing the betaine solution (Caprio et al. 2015). Olfactory nerves of *Plotosus* also respond to betaine, but responsiveness to 10^{-4} M betaine is weaker compared to other amino acids, including L-alanine (Theisen et al. 1991). In behavioral experiments using other species of freshwater catfish, anosmic treatments did not affect behaviors regarding orientation to feeding cues (Bardach et al. 1967) and the threshold of behavioral responses to amino acids (Holland and Teeter 1981). Therefore, betaine-induced feeding behavior is likely mediated by the gustatory sense in *P. japonicus*, as well as in other catfish.

Nerve fibers teased from the facial/trigeminal complex that innervates the maxillary barbel respond not only to betaine but to other amino acids including glycine, L-alanine, and L-proline (Caprio et al. 2015). All four amino acids are found in relatively high concentrations in the tissues of many marine organisms (Carr et al. 1996), some of which are primary prey for sea catfish. According to the specificity of responses, nerve fibers can be classified into two types. The first nerve fiber is highly responsive to L-proline and betaine, while the other is most responsive to glycine and L-alanine. In both types of fibers, the L-isomers appear to be more stimulating than the D-enantiomers. Other amino acids (e.g., L-cysteine, L-glutamic acid, and L-histidine) do not seem to stimulate as well as the four amino acids discussed above (Caprio et al. 2015). Nerve fibers innervating the lips also respond to NaCl, quinine, and acid, but not to sucrose, and these fibers also do not respond to extracts from marine worms (Konishi et al. 1966). Therefore, the worm-sensitive fibers may respond to above amino acids and betaine. In addition to chemical

stimulation, some nerve fibers that innervate the barbels respond to tactile stimuli as well as passive bending of the barbel (Konishi et al. 1966).

16.7 Mechanisms of pH Sensing for Prey Detection

In addition to amino acids, recent studies with electrophysiological and behavioral experiments have revealed that *P. japonicus* can detect the respiration of cryptic prey (polychaetes) that results in a slight ($\leqq 0.1$) decline in pH due to the respiratory by products of ambient H^+/CO_2 occurring adjacent to the prey (Caprio et al. 2014). Extracellular recordings from the specific fibers of the facial or trigeminal nerve complexes that innervate the maxillary barbel reveal that slight transient declines in the pH of ambient seawater applied to the barbel elicit action potentials in these fibers. Although the decrease is less than 0.1 pH unit, responses of the nerve fibers are observed. Larger drops in pH also can elicit responses of these nerves. If the pH of seawater for bathing the barbels is lowered to <pH 8.0 and maintained at that level for several minutes, a greater drop in pH is required to activate the same fibers, or the fibers became inactivated (Caprio et al. 2014).

Because *P. japonicus* are nocturnal benthic feeders (Kasai et al. 2009) and their stomach contents typically contain polychaete worms (Clark et al. 2011), it could be expected that a function of their highly sensitive H^+/CO_2 systems is to detect polychaete worms which live in semipermanent U- or Y-shaped burrows in coastal marine sediments and release punctate amounts of H^+/CO_2 into surrounding waters during respiration. The pH measured by electrode at the outflow end of grass U tube containing a single worm is transiently lowered by 0.15–0.25 (Caprio et al. 2014). In behavioral experiment, *P. japonicus* spent significantly more time in the partition of aquariums containing U tubes that emitted seawater with lower pH (pH 7.8–7.9) than if U tubes released control seawater (pH 8.1–8.3). *P. japonicus* also would frequently bite the end of the U tubes releasing lower-pH seawater, and this behavior was never observed with the control seawater (Caprio et al. 2014). These results indicate clearly that an elevation in ambient H^+/CO_2 alone is sufficient for *P. japonicus* to detect the worm prey.

So far the receptor cells for this extraordinary sensitivity to lower pH are unknown, although some candidates exist. Taste bud cells innervated by the facial nerve are a potential option. The solitary chemosensory cells that are scattered across the surface of organs and are innervated by the trigeminal or facial nerve (Finger 1997b) and a free-nerve ending of the trigeminal nerve are also candidates. The facial nerve that innervates taste buds in the head makes a complex with the trigeminal nerve, and the current electrophysiological experiment could not determine whether recorded nerves responding to lower-pH stimulation were from the facial or trigeminal nerves. The receptor molecule for this pH-sensing activity and the manner in which the central nervous system corresponds to process and integrate such minute changes in the ambient seawater are also unclear.

16.8 Olfactory System

Olfaction is another chemosensory system in vertebrates. The pair of olfactory organs of *P. japonicus* is situated anteriorly in the snout, and each of them is associated with both the incurrent and excurrent nostrils. The incurrent nostril is situated in front of the nasal barbel, while the excurrent nostril is located posterolaterally to the nasal barbel (Fig. 16.9). Ambient water enters the incurrent nostril and exits the excurrent nostril through the nasal cavity. The olfactory rosette lies in the rostral area of the nasal cavity and consists of approximately ten lamellae arranged longitudinally (Theisen et al. 1991). Electron microscopy indicates that there are at least two kinds of receptor cells in *Plotosus* olfactory lamellae: microvillous and ciliated receptor cells (Theisen et al. 1991). The channel catfish, *Ictalurus punctatus*, not only has these two receptor cells, but crypt cells are present as well (Hansen et al. 2003). The olfactory nerve, a bundle of axons of the olfactory neuron, arises from lamellae and extends caudally to connect with the olfactory bulb. The olfactory bulb is not fused to the rostral tip of the forebrain, unlike in many teleost fish, and the olfactory tract, connecting the olfactory bulb and the forebrain, is long and anatomically visible. The olfactory tract is separated into medial and lateral tracts and enters the rostral forebrain from the ventral section.

Olfactory physiology has been well investigated in the channel catfish. Research has shown that they respond to various classes of olfactory stimuli, including amino acids, nucleotides, and bile salts (Nikonov and Caprio 2001; Hansen et al. 2003; Nikonov et al. 2005). There are clear odotopic maps in the olfactory bulb and the forebrain. Reponses to amino acids are recorded in the rostral, ventral, and dorsolateral regions of the olfactory bulb (Nikonov and Caprio 2001), where ciliated cells project predominantly (Hansen et al. 2003). In the lateral portions of the forebrain, amino acid-responsive neurons are situated (Nikonov et al. 2005). Nucleotide-responsive neurons are distributed in the caudo-lateral region of the dorsal olfactory bulb (Nikonov and Caprio 2001). In the telencephalon, nucleotide-responsive units are situated in the lateral half of it near the amino acid-response zone but lay more dorsal, caudal, and medial than the amino acid units (Nikonov et al. 2005). The

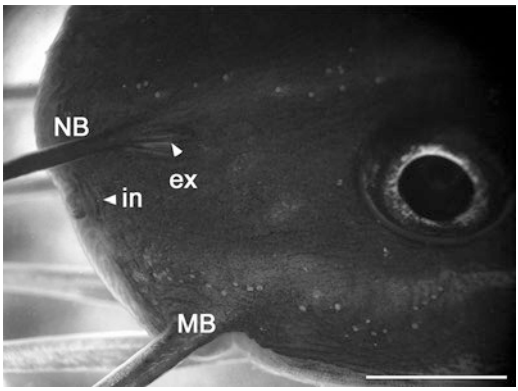

Fig. 16.9 Dorsolateral view of the rostral portion of the head showing the position of the incurrent nostril (in) and excurrent nostril (ex). *MB* maxillary barbel, *NB* nasal barbel. Scale bar, 5 mm

microvillous olfactory receptor cells project predominantly toward the nucleotide unit area in the olfactory bulb (Hansen et al. 2003). Responses to bile salts are recorded primarily from the medial area of both the ventral and dorsal olfactory bulb (Nikonov and Caprio 2001) and from the medial area of the forebrain (Nikonov et al. 2005). Electrophysiological experiments have indicated that the olfactory neurons of *Plotosus* also respond to several amino acids; L-leucine and L-methionine are most effective, while betaine and D-alanine are least effective (Theisen et al. 1991). Amino acid information via the olfactory system of *Plotosus* may be utilized as feeding cues as shown in the channel catfish (Valenticic et al. 1994).

One of the unique behaviors of *P. japonicus* is the formation of a ball-shaped school during their younger stages (Moriuchi and Dotsu 1973). *Plotosus* does not show this schooling behavior under dark conditions, suggesting importance of the visual sense for schooling (Sato 1937). Although typical *P. japonicus* are attracted to seawater holding their own school, as opposed to seawater of other schooling fish (Kinoshita 1975), anosmic fish cannot discriminate between the two (Hayashi et al. 1994), suggesting that the olfactory sense mediates this social behavior as well (Kinoshita 1975; Hayashi et al. 1994). Phosphatidylcholine from skin mucus has been identified as a signaling molecule for this schooling behavior (Matsumura et al. 2004, 2007). Each school of *Plotosus* contains the same set of phosphatidylcholine molecular species, but not the same specific phosphatidylcholine molecular species. The mixing pattern of these phosphatidylcholine molecular species is highly heterogeneous across different schools. These findings suggest that recognition of a specific school odor is governed by a pattern of mixed phosphatidylcholine molecular species (Matsumura et al. 2004, 2007).

16.9 Conclusion

Since the chemical senses and related organs of the catfish including *P. japonicus* are highly developed, many studies regarding the chemical senses are carried out with these fish. Some teleosts including catfish possess the taste buds in the fins and trunk in addition to the mouth. Such distribution of the taste buds is not observed in all teleost fish. As described in this review, structure of the central nervous system relating to the gustatory sense is also well specialized. The facial lobe which is the primary facial gustatory center has topographical map representing each peripheral organ. Detailed molecular mechanisms to organize such uncommon peripheral and central structures are unclear. To address these subjects will give us a piece of clue for understanding how sensory systems of animals are optimized to their own ecological niches. In addition, one remarkable feature of *P. japonicus* is an extraordinary sensitivity to pH decline of ambient seawater. As mentioned above, receptor cell and molecule for this pH sensing are unknown, and identifying them is important for a comprehensive understanding of this interesting sensory system of *P. japonicus*. Transcriptome analysis of the receptor molecules expressing on the receptor cells by next-generation sequencing must be effective to solve such

questions. Since this unique sensory system is observed only in the *P. japonicus* so far, this fish and its unique sensory system are good model for investigating the integration of different gustatory information in the vertebrate nervous systems.

References

Atema J (1971) Structures and functions of the sense of taste in the catfish, *Ictalurus natalis*. Brain Behav Evol 4:273–294

Bardach JE, Todd J, Crickmer R (1967) Orientation by taste in fish of the genus Ictalurus. Science 155:1276–1278

Barlow LA, Chien CB, Northcutt RG (1996) Embryonic taste buds develop in the absence of innervation. Development 122:1103–1111

Barreiro-Iglesias A, Villar-Cerviño V, Villar-Cheda B, Anadón R, Rodicio MC (2008) Neurochemical characterization of sea lamprey taste buds and afferent gustatory fibers: presence of serotonin, calretinin, and CGRP immunoreactivity in taste bud bi-ciliated cells of the earliest vertebrates. J Comp Neurol 511:438–453

Caprio J, Shimohara M, Marui T, Harada S, Kiyohara S (2014) Marine teleost locate live prey through pH sensing. Science 344:1154–1156

Caprio J, Shimohara M, Marui T, Kohbara J, Harada S, Kiyohara S (2015) Amino acid specificity of fibers of the facial/trigeminal complex innervating the maxillary barbel in the Japanese sea catfish, *Plotosus japonicus*. Physiol Behav 152:288–294

Carr WES, Netherton JC III, Gleeson RA, Derby CD (1996) Stimulants of feeding behavior in fish: analyses of tissues of diverse marine organisms. Biol Bull 190:149–160

Clark E, Nelson DR, Stoll MJ, Kobayashi Y (2011) Swarming, diel movements, feeding and cleaning behavior of juvenile venomous eeltail catfish, *Plotosus lineatus* and *P. japonicus* (Siluriformes: Plotosidae). Aqua 17:211–239

Delay RJ, Kinnamon SC, Roper SD (1997) Serotonin modulates voltage-dependent calcium current in taste cells. J Neurophysiol 77:2515–2524

Denil NA, Yamashita E, Kirino M, Kiyohara S (2013) Recurrent facial taste neurons of sea catfish *Plotosus japonicus*: morphology and organization in the ganglion. J Fish Biol 82:1773–1788

Finger TE (1978) Gustatory pathways in the bullhead catfish. I Connections of the anterior ganglion. J Comp Neurol 165:513–526

Finger TE (1983) The gustatory system in teleost fish. In: Northcutt RG, Davis RE (eds) Fish neurobiology, vol 1. University of Michigan Press, Ann Arbor, pp 285–309

Finger TE (1997a) Feeding patterns and brain evolution in ostariophysean fishes. Acta Physiol Scand 161:59–66

Finger TE (1997b) Evolution of taste and solitary chemoreceptor cell systems. Brain Behav Evol 50:234–243

Finger TE, Danilova V, Barrows J, Bartel DL, Vigers AJ, Stone L, Hellekant G, Kinnamon SC (2005) ATP signaling is crucial for communication from taste buds to gustatory nerves. Science 310:1495–1499

Hansen A, Reutter K, Zeiske E (2002) Tate bud development in the zebrafish, *Danio rerio*. Dev Dyn 223:483–496

Hansen A, Rolen SH, Anderson K, Morita Y, Caprio J, Finger TE (2003) Correlation between olfactory receptor cell type and function in the channel catfish. J Neurosci 23:9328–9339

Hayama T, Caprio J (1989) Lobule structure and somatotopic organization of the medullary facial lobe in the channel catfish *Ictalurus punctatus*. J Comp Neurol 285:9–17

Hayashi N, Nakamura S, Yoshikawa H, Abe T, Kobayashi H (1994) A role of olfaction in schooling of Japanese sea catfish, *Plotosus lineatus*. Jpn J Ichthyol 41:7–13 (in Japanese with English abstract)

Holland KN, Teeter JH (1981) Behavioral and Cardiac reflex assays of the chemosensory acuity of channel catfish to amino acids. Physiol Behav 27:699–707

Ikenaga T, Ogura T, Finger TE (2009) Vagal gustatory reflex circuits for intraoral food sorting behavior in the goldfish: cellular organization and neurotransmitters. J Comp Neurol 516:213–225

Jakubowski M, Whitear M (1990) Comparative morphology and cytology of taste buds in teleosts. Z Mikrosk Anat Forsch 104:529–560

Kanwal JS, Caprio J (1987) Central projections of the glossopharyngeal and vagal nerves in the channel catfish, *Ictalurus punctatus*: clues to differential processing of visceral inputs. J Comp Neurol 264:216–230

Kasai M, Yamamoto T, Kiyohara S (2009) Circadian locomotor activity in Japanese sea catfish *Plotosus lineatus*. Fish Sci 75:81–89

Kinoshita H (1975) Gonzui no murekodo. In: Okajma A, Maruyama K (eds) Undo to kodo, Gendai seibutsu kagaku, vol 9. Iwanami, Tokyo, pp 135–154 (in Japanese)

Kirino M, Parnes J, Hansen A, Kiyohara S, Finger TE (2013) Evolutionary origins of taste buds: phylogenetic analysis of purinergic neurotransmission in epithelial chemosensors. Open Biol 3:130015

Kiyohara S, Caprio J (1996) Somatotopic organization of the facial lobe of the sea catfish *Arius felis* studied by transganglionic transport of horseradish peroxidase. J Comp Neurol 368:121–135

Kiyohara S, Kitoh J, Shito A, Yamashita S (1996) Anatomical studies of the medullary facial lobe in the sea catfish *Plotosus lineatus*. Fish Sci 62:511–519

Konishi J, Uchida M, Mori Y (1966) Gustatory fibers in the sea catfish. Jpn J Physiol 16:194–204

Lamb CF, Finger TE (1995) Gustatory control of feeding behavior in goldfish. Physiol Behav 57:483–488

Marui T, Caprio J, Kiyohara S, Kasahara Y (1988) Topographical organization of taste and tactile neurons in the facial lobe of the sea catfish, *Plotosus lineatus*. Brain Res 446:178–182

Matsumura K, Matsunaga S, Fusetani N (2004) Possible involvement of phosphatidylcholine in school recognition in the catfish, *Plotosus lineatus*. Zool Sci 21:257–264

Matsumura K, Matsunaga S, Fusetani N (2007) Phosphatidylcholine profile-mediated group recognition in catfish. J Exp Biol 210:1992–1999

Miura H, Scott JK, Harada S, Barlow LA (2014) Sonic hedgehog-expressing basal cells are general post-mitotic precursors of functional taste receptor cells. Dev Dyn 243:1286–1297

Moriuchi S, Dotsu Y (1973) The spawning and the larva rearing of the sea catfish *Plotosus anguillaris*. Bull Fac Fish Nagasaki Univ 36:7–12 (in Japanese with English abstract)

Nakamura T, Matsuyama N, Kirino M, Kasai M, Kiyohara S, Ikenaga T (2017) Distribution, innervation, and cellular organization of taste buds in sea catfish, *Plotosus japonicus*. Brain Behav Evol 89:209–218

Nelson JS (2006) Fishes of the world. Wiley, Hoboken

Nikonov AA, Caprio J (2001) Electrophysiological evidence for a chemotopy of biologically relevant odors in the olfactory bulb of the channel catfish. J Neurophysiol 86:1869–1876

Nikonov AA, Finger TE, Caprio J (2005) Beyond the olfactory bulb: an odotopic map in the forebrain. Proc Natl Acad Sci U S A 102:18688–18693

Northcutt RG (2004) Taste buds: development and evolution. Brain Behav Evol 64:198–206

Northcutt RG (2005) Taste bud development in the channel catfish. J Comp Neurol 482:1–16

Reutter K (1992) Structure of the peripheral gustatory organ, presented by the siluroid fish *Plotosus lineatus* (Thunberg). In: Hara TJ (ed) Fish chemoreception. Chapman and Hall, London, pp 60–78

Reutter K, Witt M (1993) Morphology of vertebrate taste organs and their nerve supply. In: Simon SA, Roper SD (eds) Mechanisms of taste transduction. CRC Press, Boca Raton, pp 29–82

Sakata Y, Tsukahara J, Kiyohara S (2001) Distribution of nerve fibers in the barbels of sea catfish, *Plotosus lineatus*. Fish Sci 67:1136–1144

Sato M (1937) On the barbels of a Japanese sea catfish, *Plotosus anguillaris* (Aacepede). Sci Rep Tohoku Imp Univ Biol (Sendai, Japan) 11:323–332

Soulika M, Kaushik AL, Mathieu B, Lourenço R, Komisarczuk AZ, Romano SA, Jouary A, Lardennois A, Tissot N, Okada S, Abe K, Becker TS, Kapsimali M (2016) Diversity in cell motility reveals the dynamic nature of the formation of zebrafish taste sensory organs. Development 143:2012–2024

Theisen B, Zeiske E, Silver WL, Marui T, Caprio J (1991) Morphological and physiological studies on the olfactory organ of the striped eel catfish, *Plotosus lineatus*. Mar Biol 110:127–135

Toyoshima K, Nada O, Shimamura A (1984) Fine structure of monoamine-containing basal cells in the taste buds on the barbels of three species of teleost. Cell Tissue Res 235:479–484

Valenticic T, Wegert S, Caprio J (1994) Learned olfactory discrimination versus innate taste responses to amino acids in channel catfish (*Ictalurus punctatus*). Physiol Behav 55:865–873

Varatharasan N, Croll RP, Franz-Odendaal T (2009) Taste bud development and patterning in sighted and blind morphs of *Astyanax mexicanus*. Dev Dyn 238:3056–3064

Whitear M, Moate RM (1994) Microanatomy of taste buds in the dogfish, *Scyliorhinus canicula*. J Submicrosc Cytol Pathol 26:357–367

Yee CL, Yang C, Böttger B, Finger TT, Kinnamon JC (2001) "Type III" cells of rat taste buds: immunohistochemical and ultrastructural studies of neuron-specific enolase, protein gene product 9.5, and serotonin. J Comp Neurol 440:97–108

Yoshino T, Kishimoto H (2008) *Plotosus japonicus*, a new eeltail catfish (Siluriformes: Plotosidae) from Japan. Bull Natl Mus Nat Sci Ser A (Suppl 2):1–11

Zachar PC, Jonz MG (2012) Confocal imaging of Merkel-like basal cells in the taste buds of zebrafish. Acta Histochem 114:101–115